SYNTHESIS AND ANTI-VIRAL ACTIVITY OF NOVEL TRIPEPTIDYL COMPOUNDS, MODIFICATION OF GRAPHENE OXIDES, AND SYNTHESIS OF PEPTIDYL SUBSTRATES FOR USE IN AN ELECTROCHEMICAL BIOSENSOR DEVICE.

by

ALLAN MARK PRIOR

M.Sc., University of KwaZulu-Natal, South Africa, 2009

AN ABSTRACT OF A DISSERTATION

submitted in partial fulfillment of the requirements for the degree

DOCTOR OF PHILOSOPHY

Department of Chemistry
College of Arts and Sciences

KANSAS STATE UNIVERSITY
Manhattan, Kansas

2013

Abstract

Three research projects are described in this dissertation and they consist of the discovery of norovirus protease inhibitors, modification of graphene oxides (GO) for the detection of norovirus, and design and fabrication of nanoelectronic device based on nanocarbon fibers for the detection of breast cancer proteases, legumain and cathepsin B.

A novel class of tripeptidyl anti-noroviral compounds which strongly inhibit $NV3CL^{pro}$ in enzyme and cell based assays was discovered. An example of one of the most active compounds is (1-{3-methyl-1-[2-oxo-1-(2-oxo-pyrrolidin-3-ylmethyl)-ethylcarbamoyl]-butylcarbamoyl}-2-naphthalen-1-yl-ethyl)-carbamic acid benzyl ester, which showed an IC_{50} value of 0.14 ± 0.2 μM (enzyme assay) and EC_{50} value of 0.04 ± 0.02 μM (cell based assay). This compound has an aldehyde warhead, a P1 glutamine surrogate, a P2 leucine, a P3 L-1-napthylalanine and an *N*-terminal carboxybenzyl cap. The corresponding bisulfite adduct, 2-[2-(2-benzyloxycarbonylamino-3-naphthalen-1-yl-propionylamino)-4-methyl-pentanoylamino]-1-hydroxy-3-(2-oxo-pyrrolidin-3-yl)-propane-1-sulfonic acid monosodium salt, has a comparable activity in enzyme and cell based assays (IC_{50} 0.24 ± 0.1 μM; EC_{50} 0.04 ± 0.03 μM). (1-{3-methyl-1-[2-oxo-1-(2-oxo-pyrrolidin-3-ylmethyl)-ethylcarbamoyl]-butylcarbamoyl}-2-naphthalen-1-yl-ethyl)-carbamic acid benzyl ester and its ketoamide derivative, (1-{1-[2-isopropylcarbamoyl-2-oxo-1-(2-oxo-pyrrolidin-3-ylmethyl)-ethylcarbamoyl]-3-methyl-butylcarbamoyl}-2-naphthalen-1-yl-ethyl)-carbamic acid benzyl ester, exhibited very good broad spectrum anti-viral activity, especially in human rhino virus and severe acute respiratory syndrome bioassays.

We demonstrated that the surface of graphene oxide can be chemically modified with *t*-butylester and carboxylic acid functionalities. Fourier transform infrared spectroscopy, Raman spectroscopy and solid state nuclear magnetic resonance spectroscopy confirmed the presence of *t*-butylester and carboxylic acid functional groups. One sided oligonucleotide functionalized graphene oxide was synthesized using a solid state technique. A carboxylic acid functionalized graphene oxide was deposited onto the surface of electronic chips to bridge two gold electrodes, using a direct deposition technique. The carboxylic acid functionalized graphene oxide displayed semi-conductive properties and its use in an electronic biosensor device to detect noroviral RNA was investigated.

Novel redox-active protease substrate peptides H_2N-$(CH_2)_4$CO-Ala-Ala-Asn-Leu-$NHCH_2$-ferrocene and H_2N-$(CH_2)_4$CO-Leu-Arg-Phe-Gly-$NHCH_2$-ferrocene were synthesized successfully and used in an alternating current voltammetry technique to facilitate the detection of the cancer related protease enzymes legumain and cathepsin B. After attachment of these peptides to the tips of carbon nanofiber nanoelectrode arrays, the presence of active protease enzymes could be detected as manifest by an exponential decay in current signal detect when monitored by alternating current voltammetry, at initial enzyme concentrations of 80.1 nM (legumain) and 30.7 nM (cathepsin B). The peptide cleavage sites were confirmed by analyses of the cleaved fragments using high performance liquid chromatography and mass spectrometry. Results showed that the cleavage of H_2N-$(CH_2)_4$CO-Ala-Ala-Asn-Leu-$NHCH_2$-ferrocene at the *C*-terminal side of asparagine residues by legumain and cleavage of H_2N-$(CH_2)_4$CO-Leu-Arg-Phe-Gly-$NHCH_2$-ferrocene at the *C*-terminal side of arginine residues by cathepsin B. Legumain exhibited a specificity constant (k_{cat}/K_m) of 11.3 x 10^3 $M^{-1}S^{-1}$ while cathepsin B exhibited a higher value of specificity constant (4.3 x 10^4 $M^{-1}S^{-1}$) which agreed with the values obtained from fluorescence enzyme assay.

SYNTHESIS AND ANTI-VIRAL ACTIVITY OF NOVEL TRIPEPTIDYL COMPOUNDS, MODIFICATION OF GRAPHENE OXIDES, AND SYNTHESIS OF PEPTIDYL SUBSTRATES FOR USE IN AN ELECTROCHEMICAL BIOSENSOR DEVICE.

by

ALLAN MARK PRIOR

M.Sc., University of KwaZulu-Natal, South Africa, 2009

A DISSERTATION

submitted in partial fulfillment of the requirements for the degree

DOCTOR OF PHILOSOPHY

Department of Chemistry
College of Arts and Sciences

KANSAS STATE UNIVERSITY
Manhattan, Kansas

2013

Approved by:

Major Professor
Duy H Hua

Copyright

Abstract

Three research projects are described in this dissertation and they consist of the discovery of norovirus protease inhibitors, modification of graphene oxides (GO) for the detection of norovirus, and design and fabrication of nanoelectronic device based on nanocarbon fibers for the detection of breast cancer proteases, legumain and cathepsin B.

A novel class of tripeptidyl anti-noroviral compounds which strongly inhibit $NV3CL^{pro}$ in enzyme and cell based assays was discovered. An example of one of the most active compounds is (1-{3-methyl-1-[2-oxo-1-(2-oxo-pyrrolidin-3-ylmethyl)-ethylcarbamoyl]-butylcarbamoyl}-2-naphthalen-1-yl-ethyl)-carbamic acid benzyl ester, which showed an IC_{50} value of 0.14 ± 0.2 μM (enzyme assay) and EC_{50} value of 0.04 ± 0.02 μM (cell based assay). This compound has an aldehyde warhead, a P1 glutamine surrogate, a P2 leucine, a P3 L-1-napthylalanine and an *N*-terminal carboxybenzyl cap. The corresponding bisulfite adduct, 2-[2-(2-benzyloxycarbonylamino-3-naphthalen-1-yl-propionylamino)-4-methyl-pentanoylamino]-1-hydroxy-3-(2-oxo-pyrrolidin-3-yl)-propane-1-sulfonic acid monosodium salt, has a comparable activity in enzyme and cell based assays (IC_{50} 0.24 ± 0.1 μM; EC_{50} 0.04 ± 0.03 μM). (1-{3-methyl-1-[2-oxo-1-(2-oxo-pyrrolidin-3-ylmethyl)-ethylcarbamoyl]-butylcarbamoyl}-2-naphthalen-1-yl-ethyl)-carbamic acid benzyl ester and its ketoamide derivative, (1-{1-[2-isopropylcarbamoyl-2-oxo-1-(2-oxo-pyrrolidin-3-ylmethyl)-ethylcarbamoyl]-3-methyl-butylcarbamoyl}-2-naphthalen-1-yl-ethyl)-carbamic acid benzyl ester, exhibited very good broad spectrum anti-viral activity, especially in human rhino virus and severe acute respiratory syndrome bioassays.

We demonstrated that the surface of graphene oxide can be chemically modified with *t*-butylester and carboxylic acid functionalities. Fourier transform infrared spectroscopy, Raman spectroscopy and solid state nuclear magnetic resonance spectroscopy confirmed the presence of *t*-butylester and carboxylic acid functional groups. One sided oligonucleotide functionalized graphene oxide was synthesized using a solid state technique. A carboxylic acid functionalized graphene oxide was deposited onto the surface of electronic chips to bridge two gold electrodes, using a direct deposition technique. The carboxylic acid functionalized graphene oxide displayed semi-conductive properties and its use in an electronic biosensor device to detect noroviral RNA was investigated.

Novel redox-active protease substrate peptides H_2N-$(CH_2)_4$CO-Ala-Ala-Asn-Leu-$NHCH_2$-ferrocene and H_2N-$(CH_2)_4$CO-Leu-Arg-Phe-Gly-$NHCH_2$-ferrocene were synthesized successfully and used in an alternating current voltammetry technique to facilitate the detection of the cancer related protease enzymes legumain and cathepsin B. After attachment of these peptides to the tips of carbon nanofiber nanoelectrode arrays, the presence of active protease enzymes could be detected as manifest by an exponential decay in current signal detect when monitored by alternating current voltammetry, at initial enzyme concentrations of 80.1 nM (legumain) and 30.7 nM (cathepsin B). The peptide cleavage sites were confirmed by analyses of the cleaved fragments using high performance liquid chromatography and mass spectrometry. Results showed that the cleavage of H_2N-$(CH_2)_4$CO-Ala-Ala-Asn-Leu-$NHCH_2$-ferrocene at the *C*-terminal side of asparagine residues by legumain and cleavage of H_2N-$(CH_2)_4$CO-Leu-Arg-Phe-Gly-$NHCH_2$-ferrocene at the *C*-terminal side of arginine residues by cathepsin B. Legumain exhibited a specificity constant (k_{cat}/K_m) of 11.3 x 10^3 $M^{-1}S^{-1}$ while cathepsin B exhibited a higher value of specificity constant (4.3 x 10^4 $M^{-1}S^{-1}$) which agreed with the values obtained from fluorescence enzyme assay.

Table of Contents

TABLE OF CONTENTS……...viii

LIST OF FIGURES……...x

LIST OF TABLES……..xiv

LIST OF SCHEMES……...xv

LIST OF COMPOUNDS……..xvii

LIST OF ABBREVIATIONS…….xxvii

COPY WRITE CLEARANCES……...xxx

ACKNOWLEDGEMENTS xxxii

I. DESIGN, SYNTHESIS, AND BIOEVALUATION OF VIRAL CYSTEINE PROTEASE INHIBITORS. 1

I.I. INTRODUCTION 1

I.II. RESULTS AND DISCUSSION 7

I.III. SYNTHESIS OF NPI COMPOUNDS **1 - 48** 21

I.IV. CONCLUSION 38

II. FACIAL SURFACE MODIFICATION OF GRAPHENE OXIDES WITH TERT-BUTYL ESTER AND CARBOXYLIC ACID FUNCTIONALITY AND ITS USE IN A BIOELECTRONIC SENSOR DEVICE TO DETECT NOROVIRAL RNA. 39

II.I. INTRODUCTION 39

II.II. SYNTHESIS AND CHARACTERIZATION OF *T*-BUTYLESTER AND CARBOXYLIC ACID FUNCTIONALIZED GRAPHENE OXIDE 41

II.III. SOLID STATE SYNTHESIS OF DNA FUNCTIONALIZED GRAPHENE OXIDE 57

II.IV. Studies Towards the Development of a Novel Noroviral Bioelectronic Sensor Device using Carboxylic acid Functionalized Graphene Oxide **114**. 63
II.V. Conclusion 70

III. ELECTROCHEMICAL DETECTION OF THE BREAST CANCER RELATED PROTEASE ENZYMES LEGUMAIN AND CATHEPSIN B USING REDOX ACTIVE PEPTIDE SUBSTRATES ATTACHED TO CARBON NANOFIBRE NANOELECTRODE ARRAYS 71

III.I. Introduction 71
III.II. Results and Discussion 72
III.III. Synthesis of Peptide Substrates **119** and **120**. 83
III.IV. Conclusion 88

IV. EXPERIMENTAL SECTION 89

IV.I. General Experimental Procedures 89
IV.II. Experimental Procedures 93

V. REFERENCES 159

VI. APPENDICES: COMPOUND SPECTRAL DATA 170

List of Figures

Figure 1: The Norovirus Genome. 2

Figure 2: Replication of Norovirus. 3

Figure 3: Examples of Antiviral Drugs. 5

Figure 4: Dipeptidyl Compound, **GC373**. 7

Figure 5: Cleavage Sites Recognized by NV3CL Protease Enzymes. 8

Figure 6: Series of Synthesized P2 Alanine anti-NV Compounds for Structure Activity Relationship Studies to Evaluate P3 Residue. 9

Figure 7: Structures of Anti-NV Candidates with Modification of C-Terminal Warheads. 10

Figure 8: NPI Compounds Having Modification at the P2 Site. 12

Figure 9: Synthesized P2 Leucine NPI Candidates Having Modification at P3 Site. 13

Figure 10: Modification of C-terminal Warhead. 14

Figure 11: HPLC Data of Compounds **24** and **35** to Show Stability of Bisulfite Adduct **35** in PBS Buffer, pH 7.4. 16

Figure 12: Modification of *N*-Terminal Cap. 17

Figure 13: Macrocyclic anti-NV Candidates. 18

Figure 14: X-Ray Crystal structure of Compound **24** in Complex with SARS 3CLpro. . 20

Figure 15: Lithium Coordinated Transition State Proposed by Hanessian and Schaum[50] that Accounts for the High Asymmetric Induction Observed in the Synthesis of Compound **51**. 22

Figure 16: Structures of Graphene and Graphene Oxide 39

Figure 17: Raman Spectrum of Synthesized GO **108**. 42

Figure 18: AFM image of GO **108** Showing Cross Sectional Height. 43

Figure 19: Raman Spectrum of t-Butylester Functionalized Graphene Oxide **109** 45

Figure 20: Overlaid FTIR Spectra of GO 108 and t-Butyl Ester Functionalized GO **109**. 46

Figure 21: Solid State NMR Spectra for GO **108** and ^{13}C-t-Butyl ester Functionalized GO **113**. 48

FIGURE 22: MONITORING OF THE INTENSITY OF T-BUTANOL $(M+Na)^+$ PEAK IN MASS SPECTRUM OVER TIME DURING TFA HYDROLYSIS OF **109** TO FORM COMPOUND **114**. 50
FIGURE 23: TFA HYDROLYSIS OF T-BUTYLESTER **109** TO CARBOXYLIC ACID **114**. 51
FIGURE 24: OVERLAID FTIR SPECTRA OF T-BUTYLESTER **109** (TOP) AND CARBOXYLIC ACID **114** (BOTTOM) FUNCTIONALIZED GO. 52
FIGURE 25: RAMAN SPECTRUM OF CARBOXYLIC ACID FUNCTIONALIZED GRAPHENE OXIDE **114**. 53
FIGURE 26: OVERLAY OF SOLID STATE NMR SPECTRA OF GO (TOP), ^{13}C-T-BUTYLESTER (MIDDLE) AND ^{13}C-CARBOXYLIC ACID (BOTTOM) FUNCTIONALIZED GRAPHENE OXIDES. 54
FIGURE 27: STAGE MICROSCOPE IMAGES OF GOS. A) GO **108**, SCALE BAR = 10 μM; B) GO, SCALE BAR = 100 μM ; C) T-BUTYLESTER FUNCTIONALIZED GO **109**, SCALE BAR = 10 μM; D) T-BUTYLESTER FUNCTIONALIZED GO **109**, SCALE BAR = 50 μM ; E) CARBOXYLIC ACID FUNCTIONALIZED GO **114**, SCALE BAR = 10 μM ; F) CARBOXYLIC ACID FUNCTIONALIZED GO **114**, SCALE BAR = 100 μM. 55
FIGURE 28: MICROSCOPE IMAGES TAKEN AT DIFFERENT STAGES OF THE SOLID STATE SYNTHESIS OF OLIGONUCLEOTIDE FUNCTIONALIZED GO **118**. A) 2-CHLOROTRITYL RESIN AT 100X MAGNIFICATION (SCALE BAR = 100 μM); B) GO COATED RESIN **116** AT 100X MAGNIFICATION (SCALE BAR = 100 μM); C) GO COATED RESIN **116** AT 300X MAGNIFICATION (SCALE BAR = 100 μM); D) CRUDE MIXTURE OF RESIN AND OLIGO-GO **118** IN TRIFLUOROETHANOL AT 100X MAGNIFICATION; E) RESIN REMAINS AFTER CLEAVAGE AT 100X MAGNIFICATION; F) OLIGO-GO **118** AFTER CLEAVAGE FROM RESIN AT 1000X MAGNIFICATION (SCALE BAR = 10 μM). 59
FIGURE 29: OVERLAY OF FTIR SPECTRA OF GO-ACID **114** AND GO-DNA **118** (SCALE UNITS IN CM^{-1}). 60
FIGURE 30: FTIR OVERLAY SPECTRA OF FINGERPRINT REGIONS OF GO-ACID **114** AND GO-DNA **118** 61
FIGURE 31: RAMAN SPECTRUM OF CARBOXYLIC ACID FUNCTIONALIZED GRAPHENE OXIDE **114**. 62
FIGURE 32: DESIGN OF THE ELECTRONIC SENSOR DEVICE. 63
FIGURE 33: MICROSCOPE IMAGE OF ELECTRONIC CHIP AT 100X MAGNIFICATION (IMAGE MADE BY ALLAN PRIOR BUT HAS BEEN INCLUDED IN THE MSC THESIS OF DUY LE). 64
FIGURE 34: MICROSCOPE IMAGE AT 1000X MAGNIFICATION SHOWING A SHEET OF GO-CARBOXYLIC ACID **114** BRIDGING TWO GOLD ELECTRODES (SCALE BAR = 10 μM). 65

Figure 35: Hybridization and Dehybridization of Oligonucleotide Probe with ssRNA Target (Current values recorded at +4V). 66
Figure 36: Hybridization and Dehybridization of Oligonucleotide Probe with ssRNA Target (I/V data was recorded by sweeping the voltage from -4 to +4V)..... 67
Figure 37: Treatment of Oligonucleotide Probe with Non-Complementary ssRNA (Current values recorded at +4V). 68
Figure 38: Images of Chip After Treatment with Non-Complementary ssRNA and Complementary DNA-FAM. A) Bright field Image; B) Fluorescence Image (exposure time = 100 ms). 69
Figure 39: Field-emission scanning electron microscopy image of VACNFs coated with a SiO_2 matrix. Reprinted with permission from (Swisher et al., J. Phys. Chem. C: 2013, 117, 4268-4277). Copyright (2013) American Chemical Society. 73
Figure 40: Ferrocene labeled peptide substrates for legumain (left, compound **119**) and cathepsin B (right, compound **120**). 74
Figure 41: Expected cleavage sites for peptide **119** (legumain) and peptide **120** (cathepsin B). 75
Figure 42: HPLC data showing proteolytic activity of legumain. A: Compound **119** only in 50 mM MES buffer (pH 5.0) and 250 mM NaCl (no legumain). B: Compound **133** only (cleavage fragment) in 50 mM MES buffer (pH 5.0) and 250 mM NaCl. C: Compound **119** in 50 mM MES buffer (pH 5.0) and 250 mM NaCl incubated with 98.7 ng/μL (2.01 mM) legumain for 2 hours. Modified with permission from (Swisher *et al.*, *J. Phys. Chem. C:* 2013, *117*, 4268-4277). Copyright (2013) American Chemical Society. 76
Figure 43: HPLC data showing proteolytic activity of cathepsin B. A: Compound **120** only in 25 mM MES buffer (pH 5.0) (no cathepsin B). B: Compound **136** only in 25 mM MES buffer (pH 5.0). C: Compound **120** in 25 mM MES buffer (pH 5.0) incubated with 4.95 ng mL^{-1} (0.17 mM) cathepsin B for 2 hours. Modified with permission from (Swisher *et al.*, *J. Phys. Chem. C:* 2013, *117*, 4268-4277). Copyright (2013) American Chemical Society. 77
Figure 44: Three electrode ACV electrochemical cell containing covalently attached Fc-labeled tetrapeptide for legumain and cathepsin B detection. 78

FIGURE 45: CYCLIC VOLTAMMOGRAMS OF COMPOUND **119** IMMOBILIZED ON (A) GCE AND (B) VACNF ELECTRODE. REPRINTED WITH PERMISSION FROM (SWISHER *ET AL.*, *J. PHYS. CHEM. C:* 2013, *117*, 4268-4277). COPYRIGHT (2013) AMERICAN CHEMICAL SOCIETY. 79

FIGURE 46: PLOT OF PEAK CURRENT ($I_{P,ACV}$) VS TIME FOR COMPOUND **119** ON A VACNF ELECTRODE SHOWING CLEAVAGE OF PEPTIDE **119** BY LEGUMAIN STARTING AT ~20 MINUTES WITH [E_O] OF 80.1 NM. ADAPTED WITH PERMISSION FROM (SWISHER *ET AL.*, *J. PHYS. CHEM. C:* 2013, *117*, 4268-4277). COPYRIGHT (2013) AMERICAN CHEMICAL SOCIETY. 81

FIGURE 47: PLOT OF PEAK CURRENT ($I_{P,ACV}$) FOR COMPOUND **120** ON CNF ELECTRODE VS TIME. CATHEPSIN B WAS ADDED AT TIME 20 MINUTES WITH [E_O] OF 30.7 NM. ADAPTED WITH PERMISSION FROM (SWISHER *ET AL.*, *J. PHYS. CHEM. C:* 2013, *117*, 4268-4277). COPYRIGHT (2013) AMERICAN CHEMICAL SOCIETY. 82

List of Tables

TABLE 1: BIOACTIVITIES OF COMPOUNDS **1 - 23** IN NV3CLPRO (ENZYME) AND NV (CELL) ASSAYS. 11

TABLE 2: ACTIVITY DATA FOR COMPOUNDS **24 - 31** IN NV3CPRO (ENZYME) AND NV (CELL) ASSAYS. 13

TABLE 3: ACTIVITY DATA FOR COMPOUNDS **32 - 43** IN NV3CLPRO (ENZYME) AND NV (CELL) ASSAYS. 15

TABLE 4: ACTIVITY DATA FOR COMPOUNDS **44-46** IN NV3CLPRO (ENZYME) AND NV (CELL) ASSAYS. 17

TABLE 5: ACTIVITY DATA FOR COMPOUNDS **47-48** IN NV3CL^{PRO} (ENZYME) AND NV (CELL) ASSAYS. 18

TABLE 6: IC_{50} VALUES OF COMPOUNDS **24** AND **32** AGAINST OTHER VIRAL 3C^{PRO} AND 3CL^{PRO} IN ENZYME ASSAY. 19

TABLE 7: EC_{50} VALUES OF COMPOUNDS **24** AND **32** AGAINST OTHER VIRAL CELL LINES AND CC_{50} VALUES. 19

TABLE 8: CALCULATED KCAT/KM VALUES FOR THE COMMERCIAL LEGUMAIN SUBSTRATE (ALA-ALA-ASN-AMC) AND COMPOUND **119** FROM FLUORESCENCE AND ELECTROCHEMICAL DATA RESPECTIVELY. 81

TABLE 9: CALCULATED KCAT/KM VALUES FOR THE COMMERCIAL CATHEPSIN B SUBSTRATE (LEU-ARG-AMC) AND COMPOUND **120** FROM FLUORESCENCE AND ELECTROCHEMICAL DATA RESPECTIVELY 83

List of Schemes

SCHEME 1: SYNTHESIS OF GLUTAMINE SURROGATE METHYL ESTER 53 AND GLUTAMINE SURROGATE ALDEHYDE (**53A**). 21

SCHEME 2: SYNTHESIS OF DIPEPTIDYL ALDEHYDES **1** AND **2**. 23

SCHEME 3: SYNTHESIS OF PIPERIDINE-1,2-DICARBOXYLIC ACID 1-BENZYL ESTER (COMPOUND **A**). 23

SCHEME 4: SYNTHESIS OF TRIPEPTIDYL ALDEHYDES **3**, **5** AND **7**. 24

SCHEME 5: SYNTHESIS OF TRIPEPTIDYL FORMAMIDYL ALDEHYDE **4** AND CORRESPONDING KETOAMIDE **15**. 25

SCHEME 6: SYNTHESIS OF TRIPEPTIDYL ALDEHYDES **7 - 11** AND **24 - 31**. 27

SCHEME 7: SYNTHESIS OF CBZ PROTECTED AMINO ACIDS **86A - 91A**. 28

SCHEME 8: SYNTHESIS OF BIPHENYLALANINE **91D**. 28

SCHEME 9: SYNTHESIS OF KETOAMIDE **13**. 29

SCHEME 10: SYNTHESIS OF KETOAMIDES **14**, **16-20** AND **32-33**. 29

SCHEME 11: SYNTHESIS OF KETOAMIDE **34**. 30

SCHEME 12: SYNTHESIS OF TRIPEPTIDYL AMIDES **21-22**. 30

SCHEME 13: SYNTHESIS OF SODIUMBISULFITE ADDUCT **35**. 31

SCHEME 14: SYNTHESIS OF DIALKYLPHOSPHONATES **36 - 37** AND **42 - 43**. 31

SCHEME 15: SYNTHESIS OF TRIPEPTIDYL-NITRILE **38**. 32

SCHEME 16: SYNTHESIS OF TRIPEPTIDYL-THIOZOLE **39**. 32

SCHEME 17: SYNTHESIS OF TRIPEPTIDYL-EPOXYKETONES **40** AND **41**. 34

SCHEME 18: SYNTHESIS OF TRIPEPTIDES **44** AND **45** WITH DIFFERENT N-TERMINAL CAPS. 35

SCHEME 19: SYNTHESIS OF AMC CAP **104**. 36

SCHEME 20: SYNTHESIS OF MACROCYCLIC TRIPEPTIDYL ESTER **47** AND ALDEHYDE **48**. 37

SCHEME 21: SYNTHESIS OF GRAPHENE OXIDE USING A MODIFIED HUMMERS METHOD. 41

SCHEME 22: SYNTHESIS OF T-BUTYL ESTER FUNCTIONALIZED GRAPHENE OXIDE **109**. 44

SCHEME 23: SYNTHESIS OF ^{13}C LABELED T-BUTYL-BROMOACETATE **112**. 47

SCHEME 24: SYNTHESIS OF ^{13}C-LABELED T-BUTYL ESTER FUNCTIONALIZED GRAPHENE OXIDE **113**. 47

SCHEME 25: SYNTHESIS OF CARBOXYLIC ACID FUNCTIONALIZED GRAPHENE OXIDE **114**. 49

SCHEME 26: SYNTHESIS OF ^{13}C LABELED CARBOXYLIC ACID FUNCTIONALIZED GRAPHENE OXIDE **115**. 53
SCHEME 27: SOLID STATE SYNTHESIS OF OLIGONUCLEOTIDE FUNCTIONALIZED GO **118**. 58
SCHEME 28: EXPERIMENTAL DESIGN TO DETECT NOROVIRAL SSRNA. 65
SCHEME 29: SYNTHESIS OF LEGUMAIN SUBSTRATE **119**. 84
SCHEME 30: SYNTHESIS OF CATHEPSIN B SUBSTRATE **120**. 85
SCHEME 31: SYNTHESIS OF CATHEPSIN B NON-SUBSTRATE **131**. 86
SCHEME 32: SYNTHESIS OF LEGUMAIN SUBSTRATE FRAGMENT **133** FOR HPLC STUDY. 87
SCHEME 33: SYNTHESIS OF CATHEPSIN B SUBSTRATE FRAGMENT **136** FOR HPLC STUDY. 88

List of Compounds

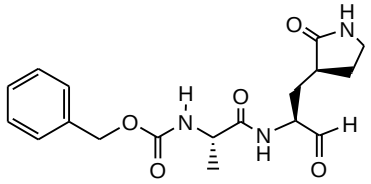

1

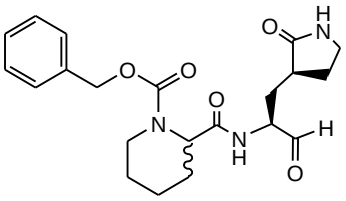

2

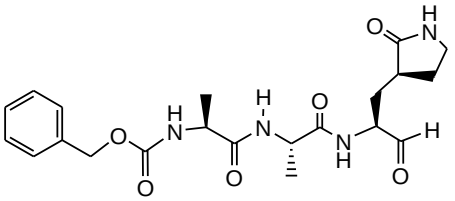

3

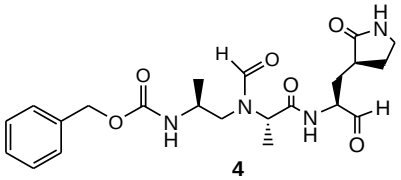

4

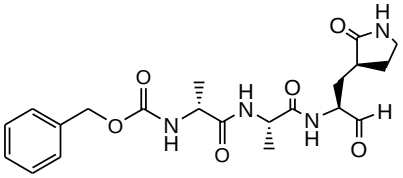

5

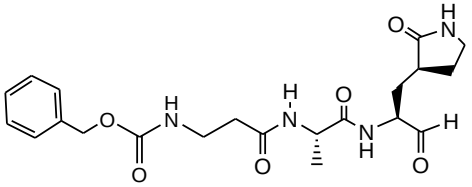

6

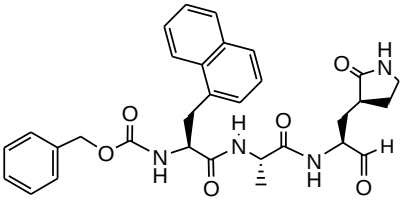

7

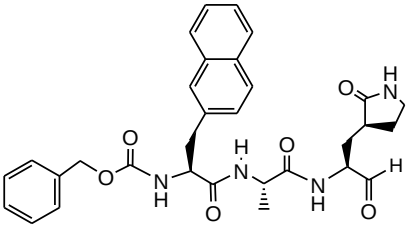

8

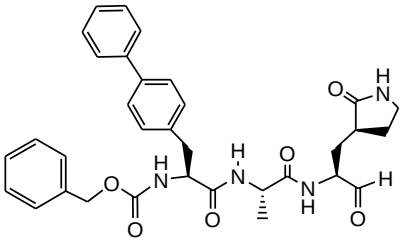

9

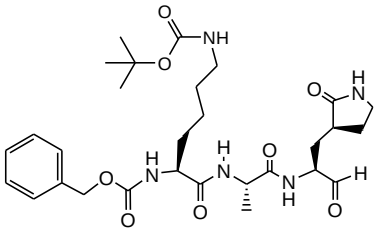

10

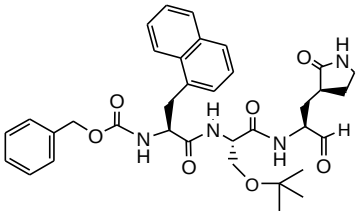

11

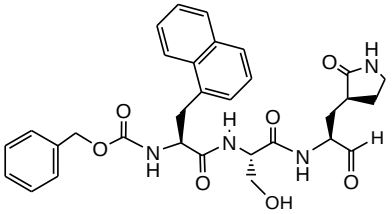

12

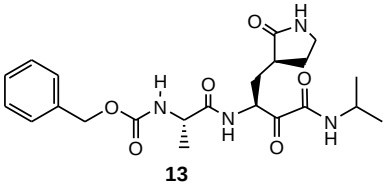

13

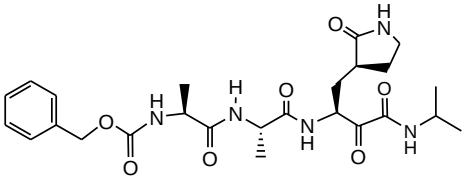

14

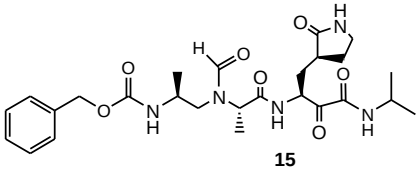

15

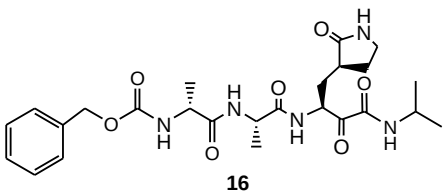

16

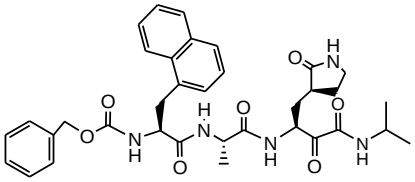

17

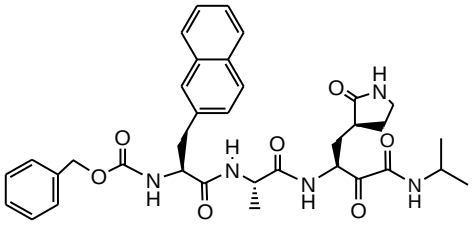

18

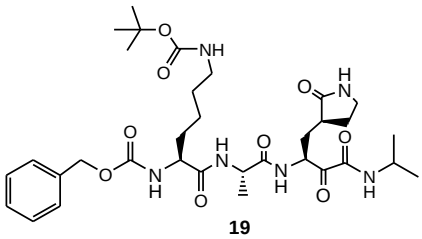

19

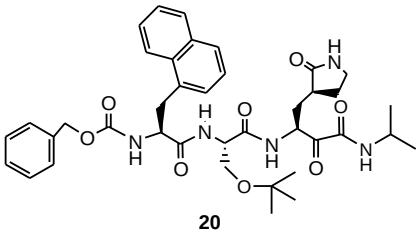

20

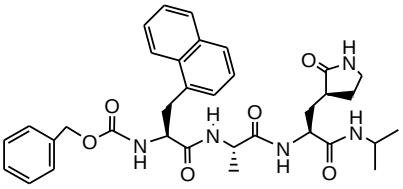

21

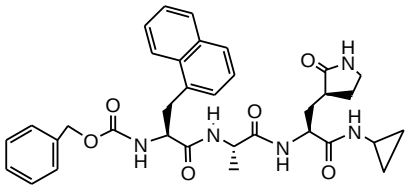

22

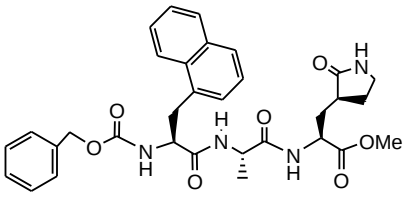

23

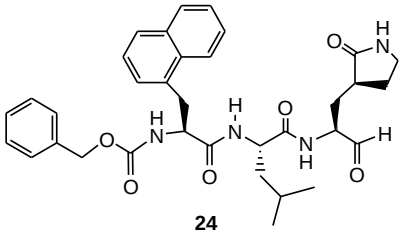

24

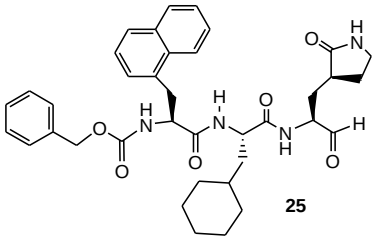

25

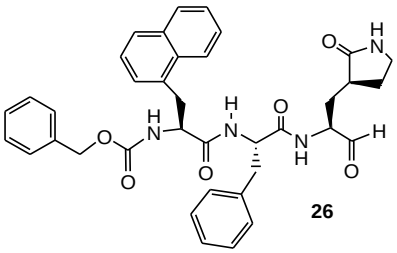

26

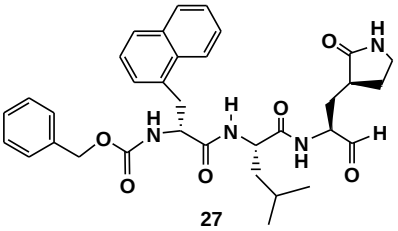

27

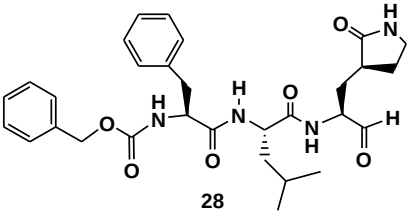

28

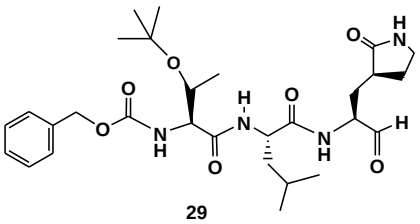

29

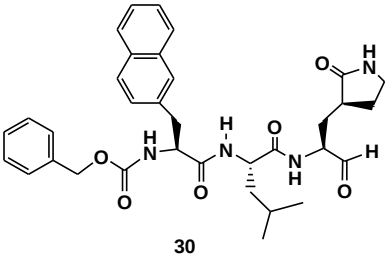

30

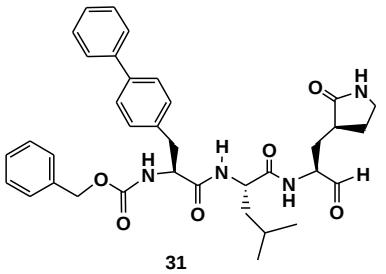

31

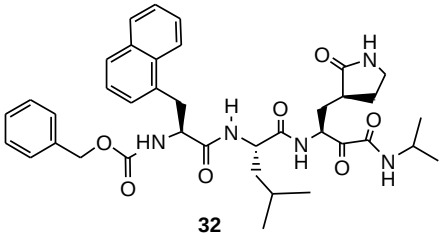

32

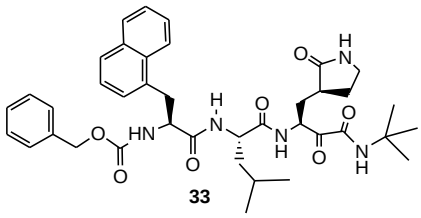

33

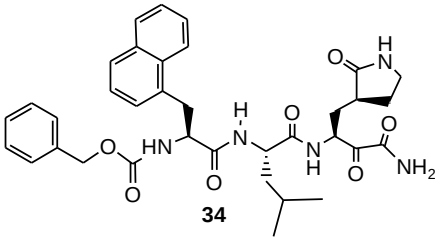

34

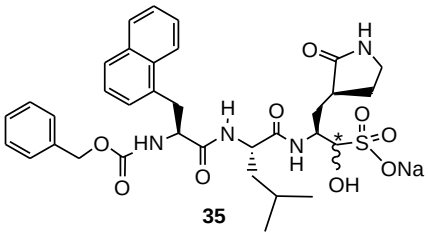

35

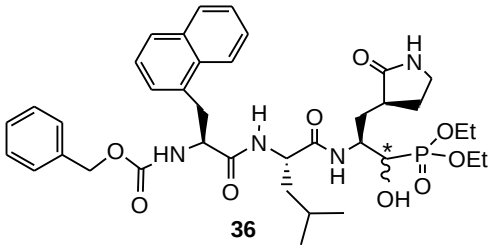

36

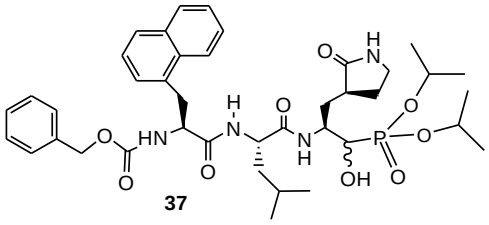

37

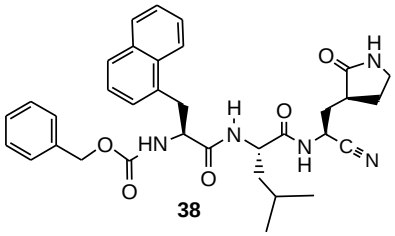

38

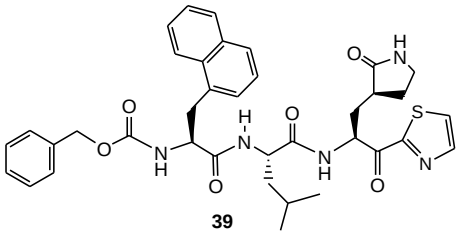

39

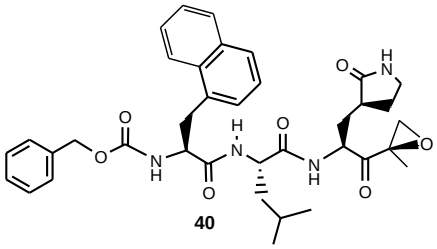

40

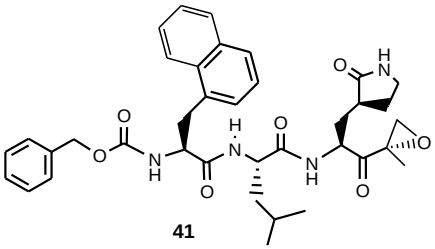

41

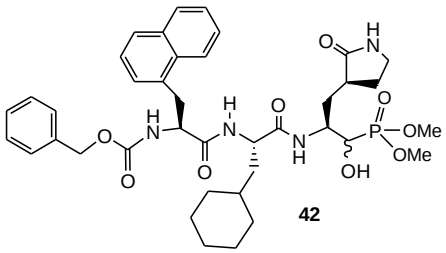

42

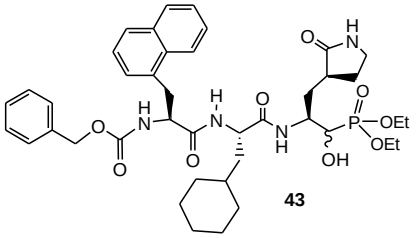

43

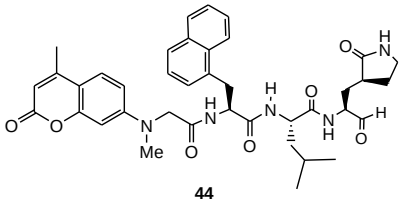

44

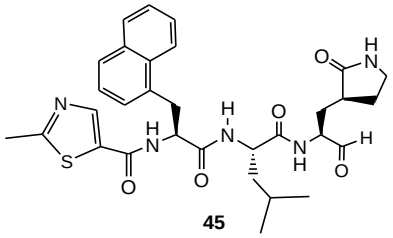

45

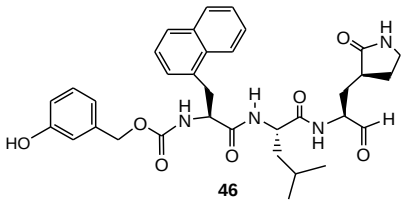

46

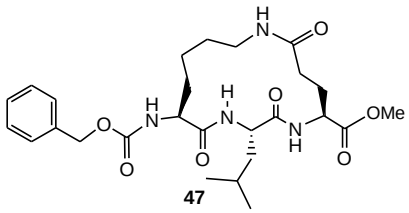

47

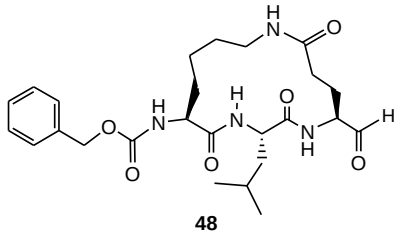

48

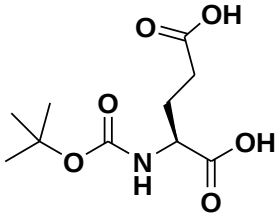

49

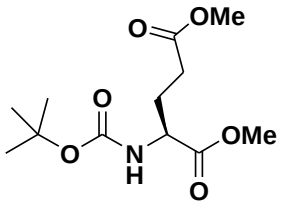

50

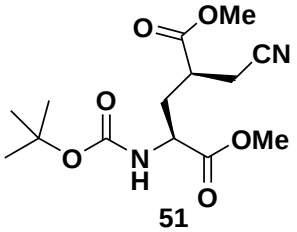

51

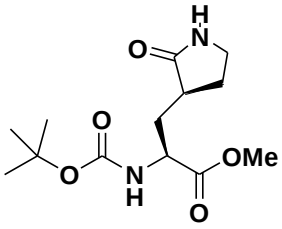

52

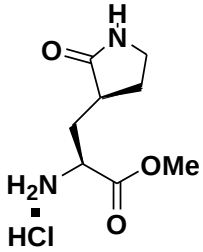

53

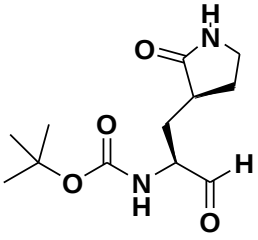

53a

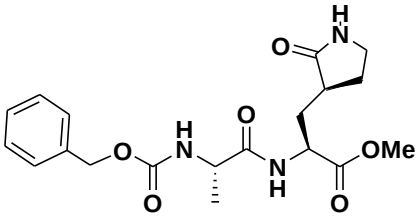

54

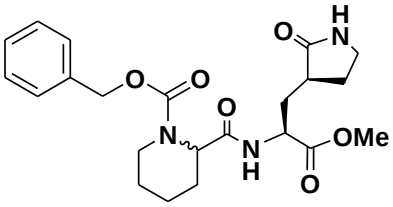

55

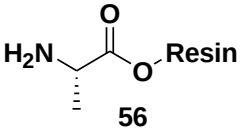

56

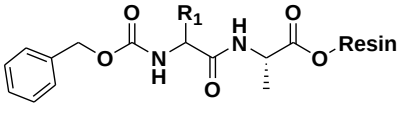

57, R_1 = L-methyl
58, R_1 = D-methyl
59, R_1 = L-1-napthyl

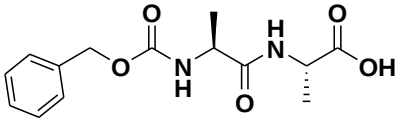

60

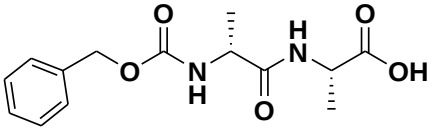

61

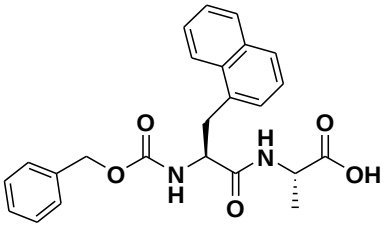

62

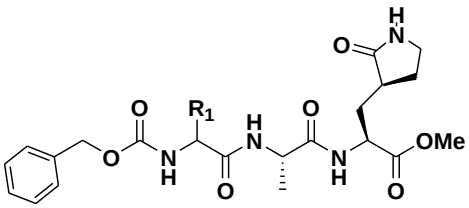

63, R_1 = L-methyl
64, R_1 = D-methyl

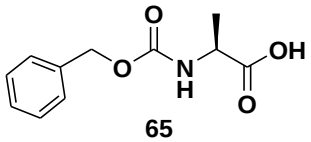

65

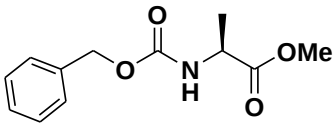

66

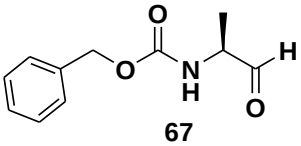

67

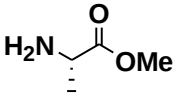

68

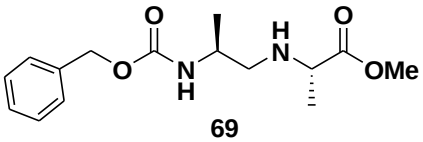

69

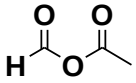

70

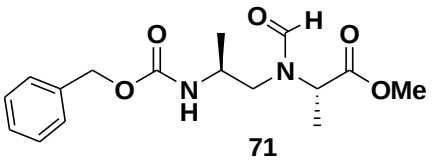

71

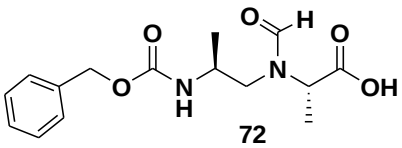

72

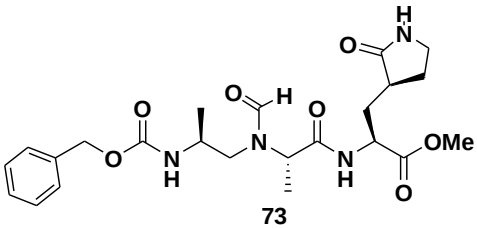

73

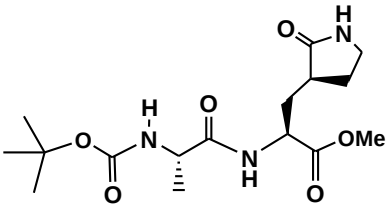

74

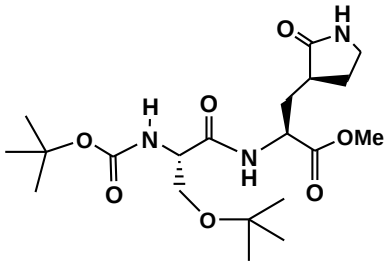

75

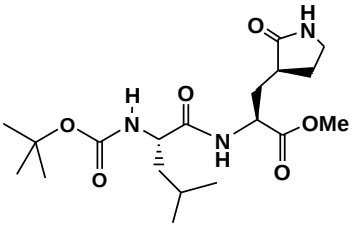

76

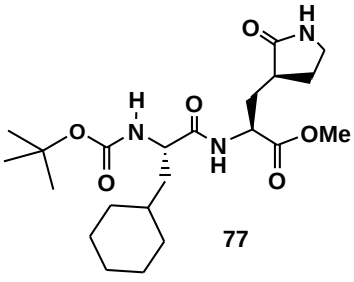

77

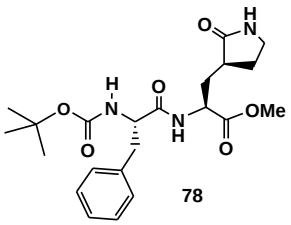

78

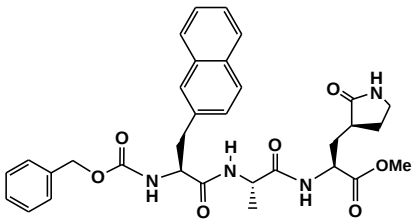

80

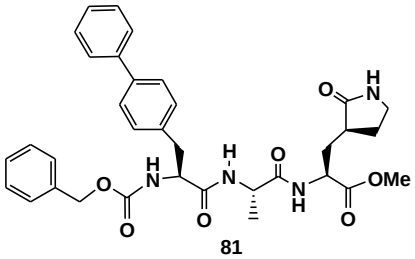

81

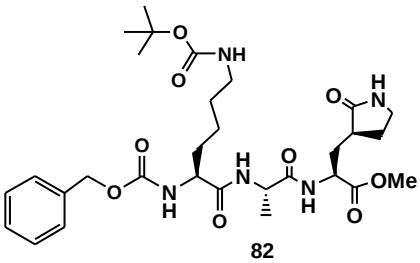

82

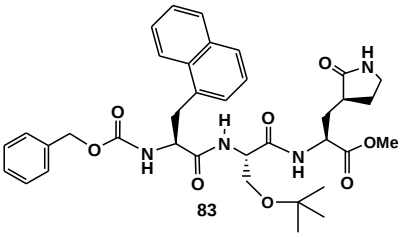

83

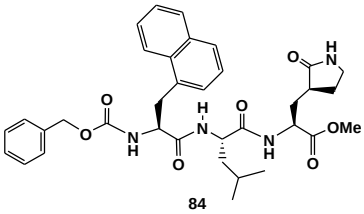

84

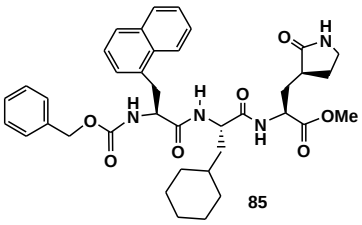

85

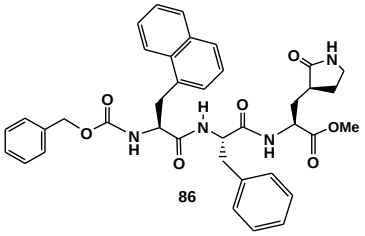

86

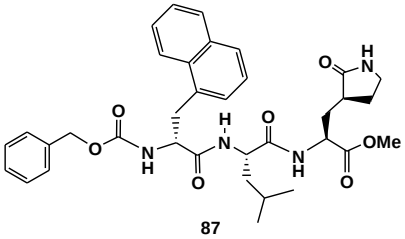

87

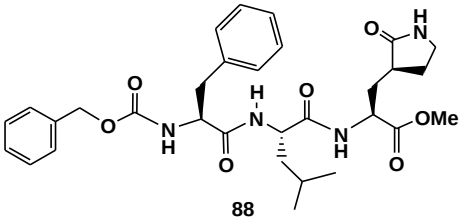

88

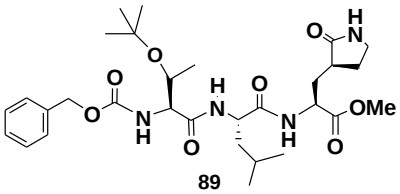

89

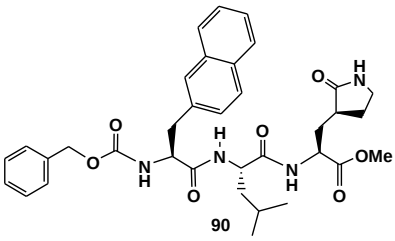

90

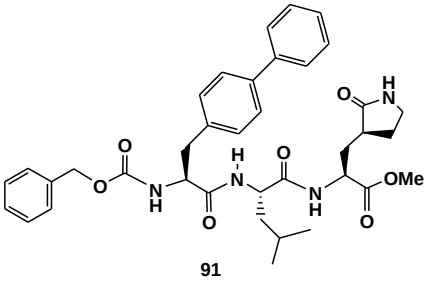

91

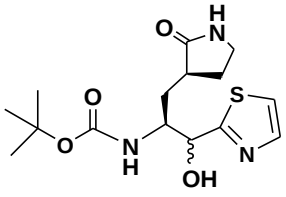

92

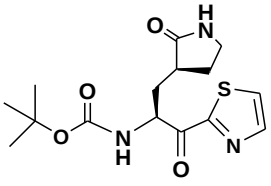

93

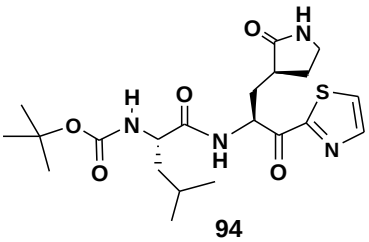

94

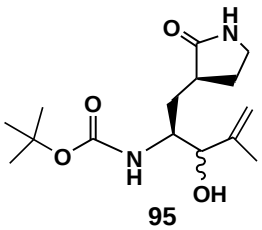

95

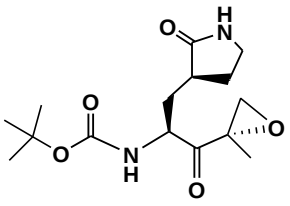

96-mp

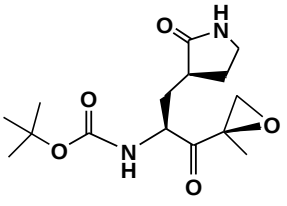

96-lp

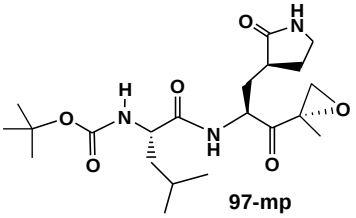

97-mp

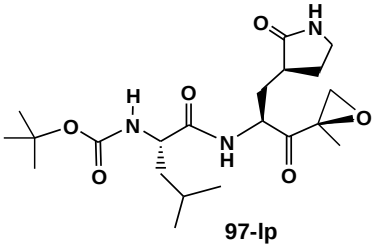

97-lp

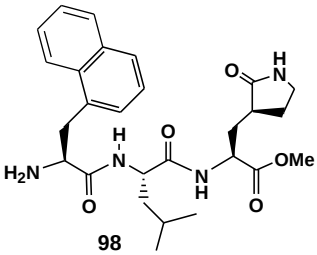

98

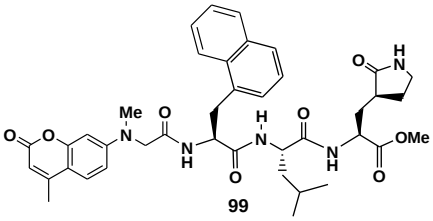

99

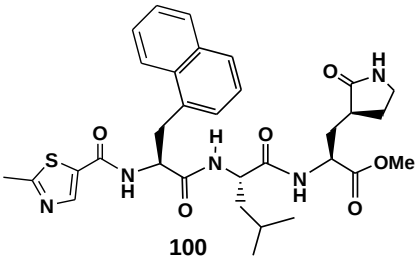

100

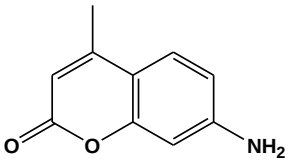

101

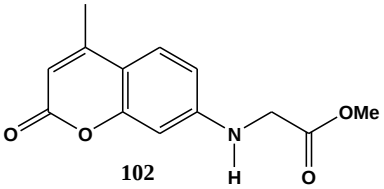

102

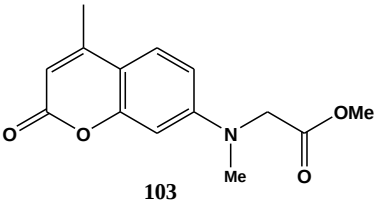

103

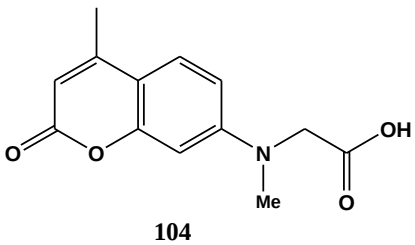

104

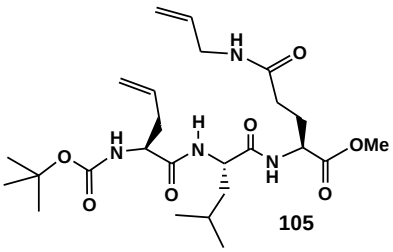

105

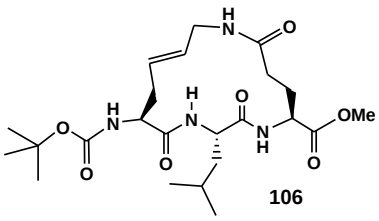

106

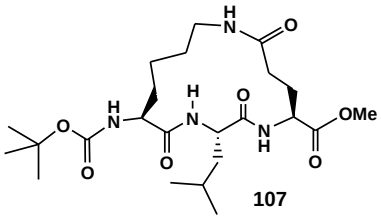

107

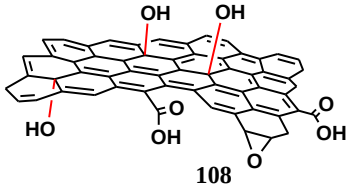

108

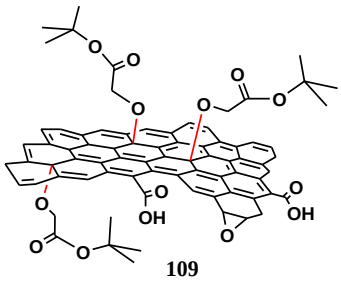

109

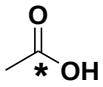

110

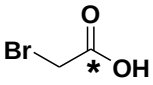

111

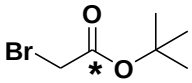

112

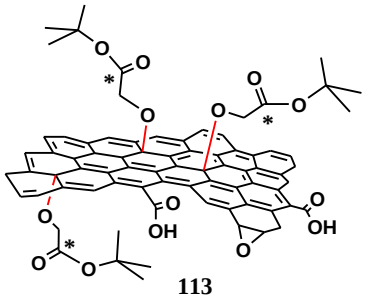

113

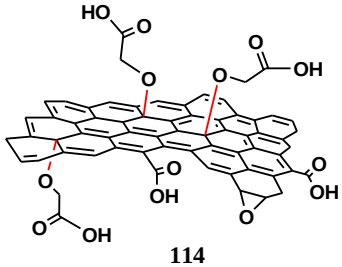

114

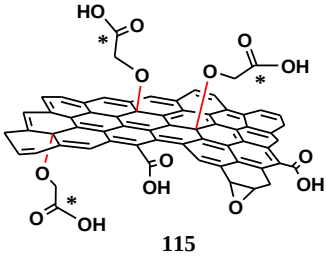

115

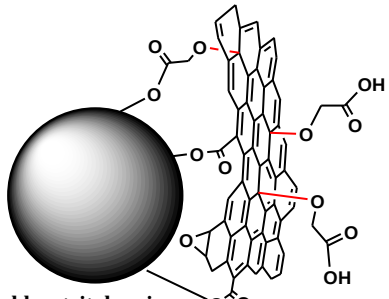

chlorotrityl-resin
(black)

116

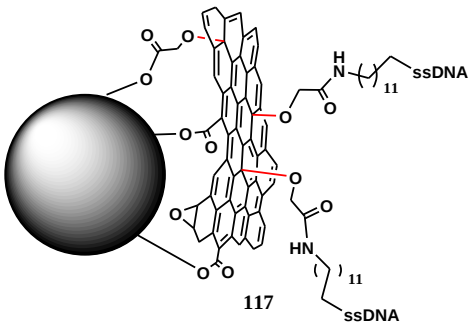

117

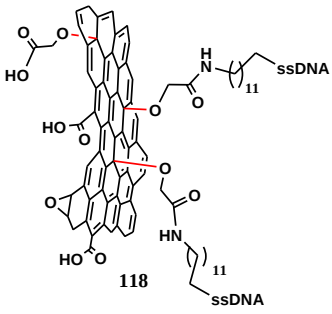

118

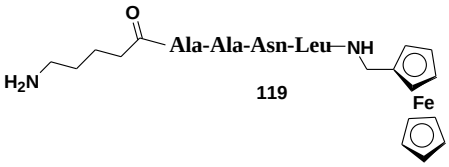

119

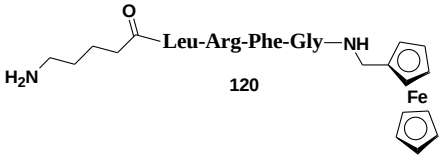

120

Ala-Ala-Asn-Leu-Resin

121

Ala-Ala-Asn-Leu

122

Boc-Ala-Ala-Asn-Leu

122a

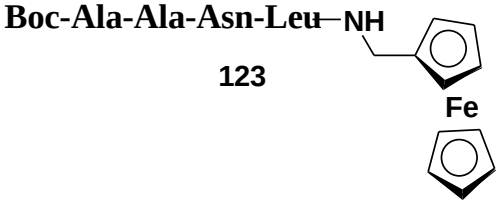

123

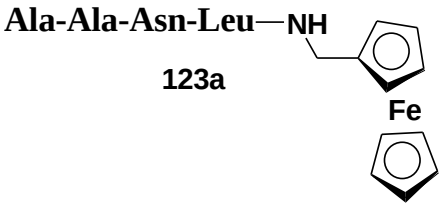

123a

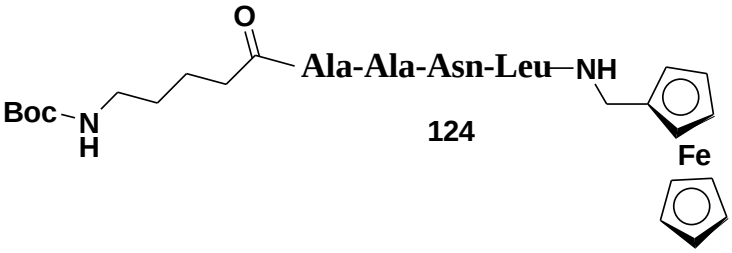

124

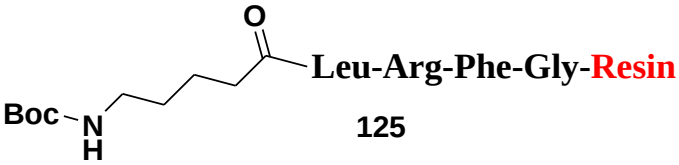

125

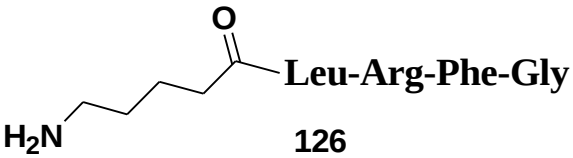

126

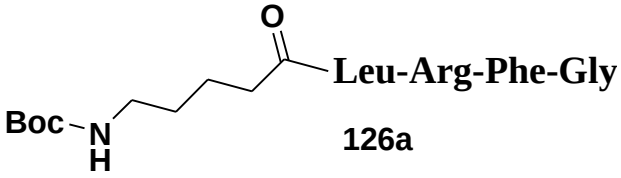

126a

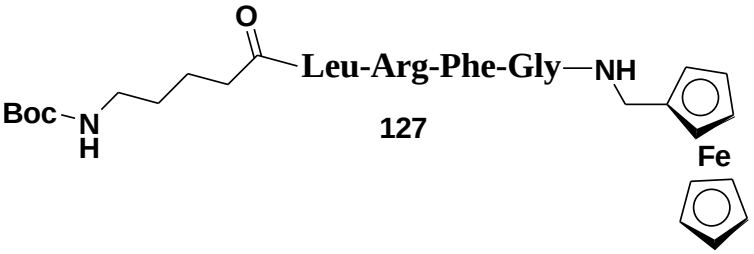

127

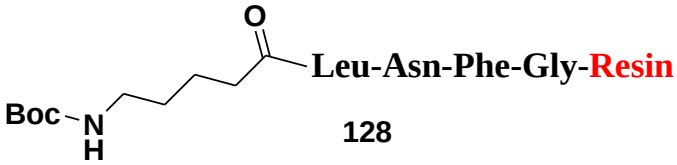

128

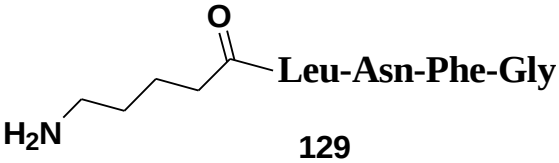

129

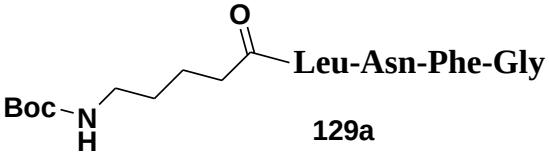

129a

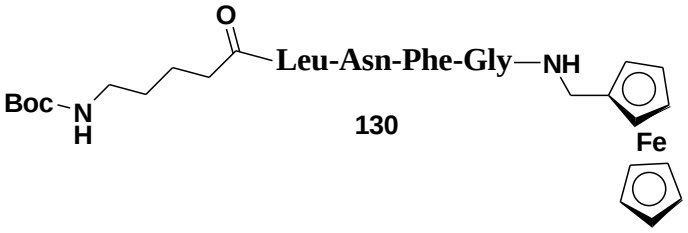

130

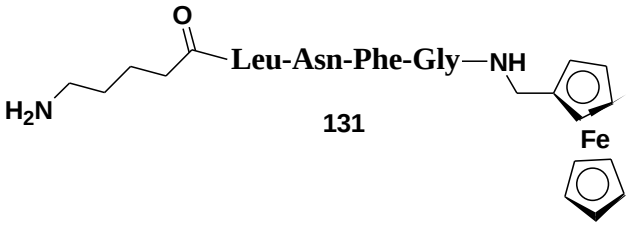

131

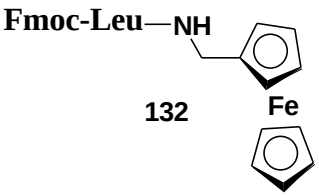

132

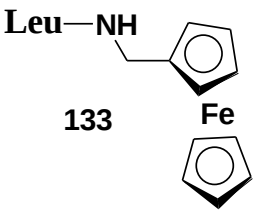

133

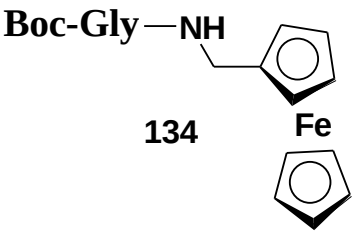

134

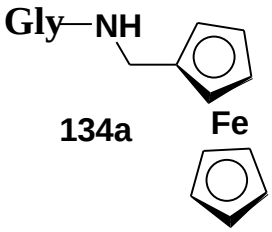

134a

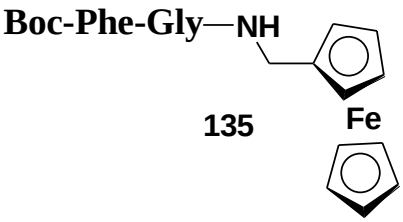

135

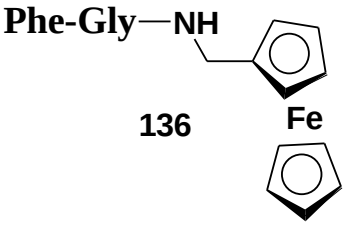

136

List of Abbreviations

ACV: alternating current voltammetry

AFM: atomic force microscopy

AMC: amino-4-methylcoumarin

Cbz: carboxybenzyl

CNF: carbon nanofiber

CoV: coronaviridae

CT: computed tomography

CV: caliciviridae

CV: cyclic voltammetry

DMAP: dimethylaminopyridine

DMF: dimethylformamide

DMP: Dess Martin periodinane

DMSO: dimethylsulfoxide

EDCI: 1-Ethyl-3-(3-dimethylaminopropyl)carbodiimide

ER: endoplasmic reticulum

ESI: electrospray ionization

ETR: electron transfer rate

eV: electron volts

EV: enteroviruses

Fc: ferrocene

FCV: feline calicivirus

FRET: fluorescence resonance energy transfer

FTIR: fourier transform infrared

GCE: glassy carbon electrode

GO: graphene oxide

HBGA: human histo-blood group antigen

HPLC: high performance liquid chromatography

HRV: human rhino virus

LiHMDS: lithium hexamethyldisilazane

MAVS: mitochondrial antiviral signaling protein

m-CPBA: *meta*-Chloroperoxybenzoic acid

MRI: magnetic resonance imaging

MS: mass spectrometry

NEA: nanoelectrode array

NMR: nuclear magnetic resonance

NPI: noroviral protease inhibitor

NTP: nucleoside triphosphatase

NV: noroviruses

$NV3CL^{pro}$: Norovirus 3C-like protease

ORF: open reading frame

PBS: phosphate buffered saline

PECVD: plasma enhanced chemical vapor deposition

PEG: polyethyleneglycol

PET: positron emission tomography

PV: picornavirus

RdRp: RNA-dependant RNA polymerase

RT-PCR: reverse-transcription polymerase chain reaction

RV: rhinoviruses

SAR: structure activity relationship

SARS: severe acute respiratory syndrome

SDS: sodium dodecyl sulfate

SEM: scanning electron microscopy

siRNA: small interfering RNA

TFA: trifluoroacetic acid

VACNF: vertically aligned carbon nanofiber

VPG: a viral genome protein

Copy write Clearances

(For Chapter I)

The structures, bioactivity data and synthesis of compounds **24**, **27-28**, **30-32** and **35-36** have been reported recently. (Prior, A.M., Kim, Y., Weerasekara, S., Moroze, M., Alliston, K.R., Uy, R.A.Z., Groutas,W.C., Chang, K-O., Hua, D.H., Design, Synthesis, and Bioevaluation of Viral 3C and 3C-Like Protease Inhibitors, *Bioorganic & Medicinal Chemistry Letters* 23 (2013) 6317–6320.

(For Chapter III)

Acknowledgements

I wish to thank my major professor Dr. Duy H. Hua for his support and guidance throughout my studies. I thank my wife Kirsty, for her love and support. I thank my advisory committee and lab mates, past and present for their support and valuable discussions. I would like to acknowledge the chemistry department at Kansas State University and the research support staff for invaluable technical assistance.

I. Design, Synthesis, and Bioevaluation of Viral Cysteine Protease Inhibitors.

I.I. Introduction

Noroviruses (NVs) are prevalent worldwide and are the leading cause (~90%) of severe gastroenteritis in children and adults [1] and is responsible for ~58% of all food borne illnesses.[2] Outbreaks usually occur in conditions where people are sharing living quarters or restrooms such as cruise ships, hospitals, nursing homes and dormitories where person to person transmission is more favorable.[1] It has been reported that NVs only need a few virions (~17 virus particles) to cause an infection and hence NV is highly infectious.[3] People don't develop a long lasting immunity against NVs due to the high NV mutation rate and existence of high genetic variation. Infection rates are amplified due the resistance of human NVs to common disinfection procedures such as hand sanitizers (ethanol) or quaternary ammonium compounds.[4, 5] NVs utilize a fecal-oral route for transmission and propagation and once the host has been infected the NV virion will make its way through the gut until it reaches the small intestine where is starts replication. After about 2 days in the small intestine, symptoms such as diarrhea, nausea, vomiting, abdominal pain, lethargy and headaches will occur, which are normally self limiting and last for about 24 to 60 hours. However many deaths are associated with NV infections especially among children, the elderly and people with compromised immune systems. It is estimated that 200,000 deaths per year occur in young children and infants in developing countires.[1] A common way that NVs can be introduced into the public is through fresh produce since farming practices make use of manure and bio-solid based fertilizers.[2] NVs can also contaminate produce at the farm through insects and animals, soil, dust and contaminated water used for irrigation.[2] A recent survey was conducted in Canada, Belgium and France that found NVs in packaged leafy greens in 28 to 50 % of samples as determined by real-time reverse-transcription polymerase chain reaction (RT-PCR).[2] Although the NVs that were detected have not associated with any severe outbreaks, the results suggest that packaged produce could be a viable route for NV transmission.[2]

NVs belong to the family of Calicivirdae (CV).[6] NVs are non-enveloped viruses containing a single stranded positive sense ~7.5-kb RNA genome that encodes for many important structural and non-structural proteins.[6] The genome contains three open reading frames (ORFs) as shown in Figure 1.

Figure 1: The Norovirus Genome.

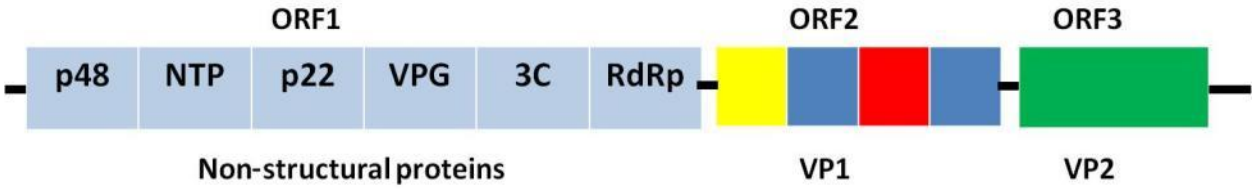

(p48): an amino-terminal protein (~48 kDa).
(NTP): nucleoside triphosphatase.
(p22): a 22 kDa 3A-like protein.
(VPG): a viral genome-linked protein to the 5′ end of the genome.
(3C): 3C-like protease.
(RdRp): RNA-dependant RNA polymerase, a 3D-like protein.

ORF1 encodes for six non-structural proteins, p48, nucleoside triphosphatase (NTP), p22, viral genome protein (VPG), 3C-like protease (3C) and RNA-dependant RNA polymerase (RdRp). ORF2 encodes the major capsid protein (VP1) while ORF3 encodes a minor (VP2) capsid protein.[1] NVs are grouped into five genogroups, GI, GII, GIII, GIV and GV and categorization is based on VP1 protein sequence similarity.[1] Viruses most commonly infecting humans belong to GI and GII and both of these genogroups can be further subdivided into different genetic clusters or genotypes. GII for example has 19 genotypes, of which genotype 4 (abbreviated GII.4) accounts for most of the adult NV outbreaks around the world.[1]

Figure 2 shows a scheme adapted from Rocha-Pereira *et al.*[3] and summarizes the mechanism of NV replication. The first step involves attachment of a virion to a carbohydrate receptor such as human histo-blood group antigen (HBGA), sialic acid or heparin sulfate present on a host cell surface. It has been reported that the virion-receptor binding makes use of the P2 domain of the VP1 structural protein of the virion.[3] The virion then enters the cell through a pH independent endocytic pathway that is not mediated by clathrin or caveolin, but rather by dynamin II and

cholesterol. Once inside the cell, a prepackaged non structural protein (VPG) initiates translation of ORF1 of the viral RNA genome into a long polyprotein, which, after the action of the 3C-like (3CL) protease, releases many nonstructural viral proteins such as p48, NTP, p22, VPG, 3C and RdRp.

Figure 2: Replication of Norovirus.

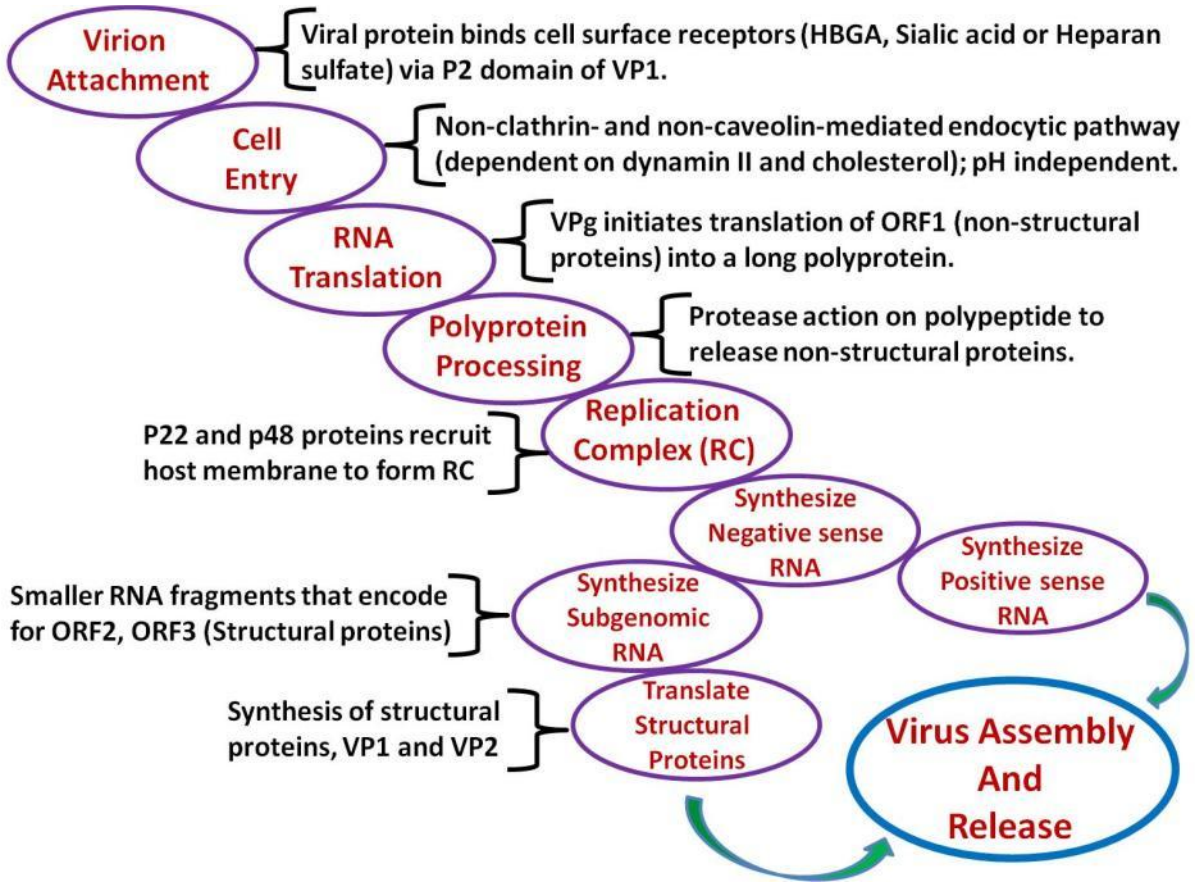

The proteins p48 and p22 recruit host membrane to form a replication complex, inside of which the replication of NV is believed to occur. The replication complex is a membranous structure that contains the viral nonstructural proteins, viral RNA genome and host proteins that will facilitate viral replication. After transcription of the positive sense RNA into negative sense RNA, the RdRp will transcribe many copies of the negative sense RNA back to the genomic positive sense RNA for packaging into new virion. Simultaneously the virus will synthesize shorter subgenomic RNA that contain ORF2 and ORF3. These are translated into the viral structural proteins VP1 and VP2 which assemble to form the new virion capsid. After assembly

of the structural proteins and packaging of new genomic RNA the mature virion can be released from the cell, a step that remains poorly understood.[3]

NV is receiving increasing attention each year due to the significant amount of morbidity and mortality and this has driven increasing drug discovery research efforts. Despite this however, no anti-noroviral drug or vaccine is available for treatment or for prophylactic purposes.[3] Although anti-noroviral research is in its infancy, researchers have identified possible targets situated at different stages of NV replication cycle that could be exploited for potential drug design. This information has been captured in a recent review article[3] and therefore will not be discussed in great length, however, a brief summary will be made to set the scene of this research.

The first step in the viral infection process is the attachment of virion to carbohydrates on the cellular surface (HBGA) and hence it has been suggested that drugs that target the HBGA binding domain on the virion capsid may be used for prophylactic purposes in the event of a NV outbreak.[7-9] It may also serve to lessen the severity of the infection in people that have already contracted it as it would hinder the NV propagation.[10] There are limitations to this however since there are a numerous other carbohydrates (e.g. sialic acid[11] or heparin sulfate[12]) that are said to be recognized by NVs and hence the pool of sugar residue structures that could interact with NVs is quite broad making drug development efforts very challenging. Moreover, viral capsid proteins can accommodate many structural changes without compromising viral vitality and therefore this class of drug would be easily susceptible to mutational drug resistance.[3]

The nonstructural proteins p48[13, 14] and p22[15] are believed to play a role in the formation of the replication complex (RC) and hence have been suggested as potential targets for drug development. The limitation however is that the function of these proteins in NVs is not well defined. The p22 protein, however, has a well conserved section that has been reported to inhibit protein trafficking from the endoplasmic reticulum (ER) to the Golgi body by mimicking the normal ER export signal.[16, 17] Although no inhibitors for these proteins have been reported in NV, enteroviruses (EVs) and rhinoviruses (RVs) have both experienced inhibition *in vitro* to their structurally similar protein (3A) by enviroxime[18] and TTP-8307[19] (Figure 3).

Small molecules targeting VPg (hippuristanol,[20] panteamine[21]) and NTP (TBZE-029, MRL-1237, HBB)[22-24] have come to light (Figure 3) and show *in vitro* inhibition to structurally

analogous proteins belonging to the feline calicivirus (FCV) and picornavirus (PV) families respectively. Drug development targeting these classes of proteins in NV could therefore be highly relevant.

Figure 3: Examples of Antiviral Drugs.

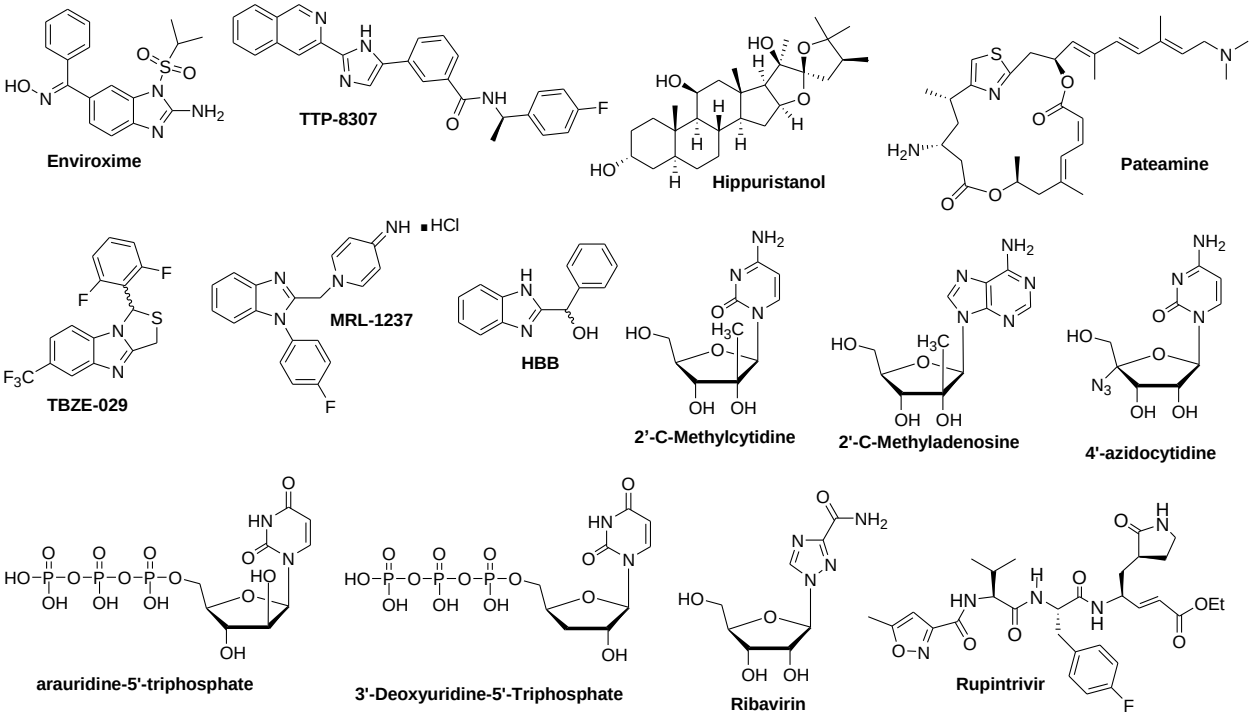

It has been stated that the two most promising nonstructural enzymes to focus drug discovery efforts on is the RdRp and 3C protease.[3] RdRp plays a crucial role in the synthesis of viral RNA and is thus central to viral propagation. It keeps a highly conserved catalytic site among all viral polymerases, which is an attractive feature when considering targets for drug development.[3] For example, 2'-C-methylcytidine, 2'-C-methyladenosine and 4-azidocytidine (Figure 3) have broad spectrum anti-RdRp activity against many positive strand RNA viruses.[25-27] Moreover, 2'-arauridine-5'-triphosphate and 3'-deoxyuridine-5'-triphosphate (Figure 3) have anti-RdRp activity in a NV assay.[28] The 3CL protease is another central enzyme essential for viral propagation since it is involved in polypeptide processing to release essential nonstructural viral proteins, but has been reported recently to have additional roles such as inactivation (cleavage) of mitochondrial antiviral signaling protein (MAVS).[15, 29] The 3C protease also has been shown to contain a highly conserved active site among all CVs.[13] It has been suggested that the 3C protease of NV may be the most promising target to aim drug development efforts due to its

important function as well as the availability of detailed structural information.[10] Rupintrivir[23, 30] (Figure 3) is an example of a 3CL protease inhibitors found active against PVs.

Although other strategies to tackle the problem of NV infection are being investigated such as small interfering RNAs (siRNAs)[31] and vaccine development,[1, 32-34] our efforts to discover a new anti-NV drug will focus primarily on targeting the NV 3C-like protease ($NV3CL^{pro}$).

$NV3CL^{pro}$ is "3C-like" because it contains chymotrypsin-like folds and belongs to the chymotrypsin-like protease family.[35] The $NV3CL^{pro}$ uses a cysteine (SH side chain) as the nucleophile to cleave the peptide substrate scissile bond, whereas, chymotrypsin uses a serine (OH side chain) to cleave the substrate. Studies have shown that His30, Glu54 and Cys139 are conserved in all $NV3CL^{pro}$ enzymes and the His30/Cys139 pair work as an acid-base dyad that is essential for protease activity.[35] Glu54 has been shown by mutagenesis studies to be important for protease activity because mutation of Glu54 to Ala resulted in loss of proteolytic activity.[36] X-ray crystal structures[35] and NMR solved solution structures[37] have been reported for $NV3CL^{pro}$ which give useful structural information. The substrate binding site of $NV3CL^{pro}$ contains substrate binding pockets (S1, S2, S3…) starting at the active site and labeled in an order moving away from the active site toward the bound substrates *N*-terminus end. The S1 pocket contains the important residues Thr134, His157 and Ala160[28] which can interact with the P1 Gln/Glu of the substrate.[37] The S2 pocket is hydrophobic in nature and encompasses Ile109, Arg112 and Val114 and can accommodate bulky hydrophobic P2 side chains such as Leu and Phe.[37]

A report of our intensive research efforts to discover new and potent anti-NV compounds will be discussed in the following section.

I.II. Results and Discussion

Groutas and coworkers were first to discover a "hit" dipepidyl compound GC373 (Figure 4) that showed micromolar inhibition (IC_{50} = 1.82 μM)[38] of NV3CL^{pro} *in vitro* using a fluorescence resonance energy transfer (FRET) enzyme assay[39, 40] and EC_{50} of 2.1 μM[38] in a NV cell based assay.[40, 41] In order to clearly distinguish between these activity data, IC_{50} values represent data obtained from a FRET enzyme assay, while EC_{50} values represent data obtained from the cell based assay. The bioactivity data of all synthesized compounds were evaluated by Dr. Kyeong-Ok Chang and Dr. Yunjeong Kim at the Department of Diagnostic Medicine and Pathobiology, Kansas State University. Experimental details describing the FRET enzyme assay[39, 40] and cell based assay[40, 41] have been previously reported.

Figure 4: Dipeptidyl Compound, GC373.

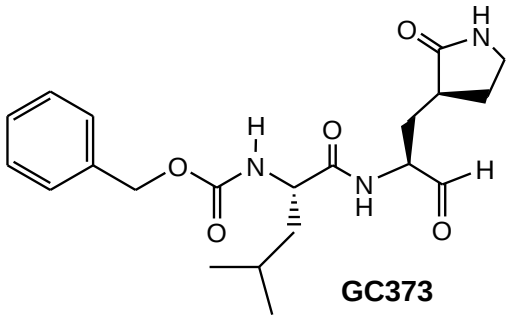

GC373

The Groutas group examined the cleavage sites recognized by NV (Figure 5), which helped in their discovery of compound GC373. The dashed line in Figure 5 represents the cleavage site (scissile bond) of cleavable peptide substrates. The letters represent amino acids that correspond to positions (P1, P2, P3…etc.) in the cleavable peptide substrate. The Groutas group used a *C*-terminal aldehyde "warhead", which acts as the electrophilic site for nucleophilic attack from Cys139, a P1 Gln "surrogate" that is recognized by the S1 enzyme pocket, a P2 Leu that will be recognized by the S2 pocket and a Cbz *N*-terminal cap.

Figure 5: Cleavage Sites Recognized by NV3CL Protease Enzymes.

	P5	P4	P3	P2	P1	P1’	P2’
Norovirus	D	F	H	L	Q	G	P
	E	Y	E	W	E	A	
		M	Q	Y			
			D	M			
			N	F			

NV proteases are quite specific to the identity of the substrate P1 amino acid side chain and require either a Gln (Q) of Glu (E), but higher tolerability is noticed for substrate P2 and P3. With knowledge of this, our initial research efforts focused on synthesizing a new class of NV protease inhibitors using a structure-activity relationship (SAR) approach.

First, we decided to keep P2 as alanine, and investigate how the nature of P3 affects activity. A series of *C*-terminal aldehyde compounds were synthesized (Figure 6) along with their corresponding *C*-terminal ketoamides (Figure 7). The structures of these compounds were influenced to some extent by a translational anti-viral research project in which a different viral protease enzyme was also targeted, however, the name of this enzyme or the bioactivities of compounds **1 - 23** against this enzyme are not discussed at this time due to its confidential nature.

Figure 6: Series of Synthesized P2 Alanine Anti-NV Compounds for Structure Activity Relationship Studies to Evaluate P3 Residue.

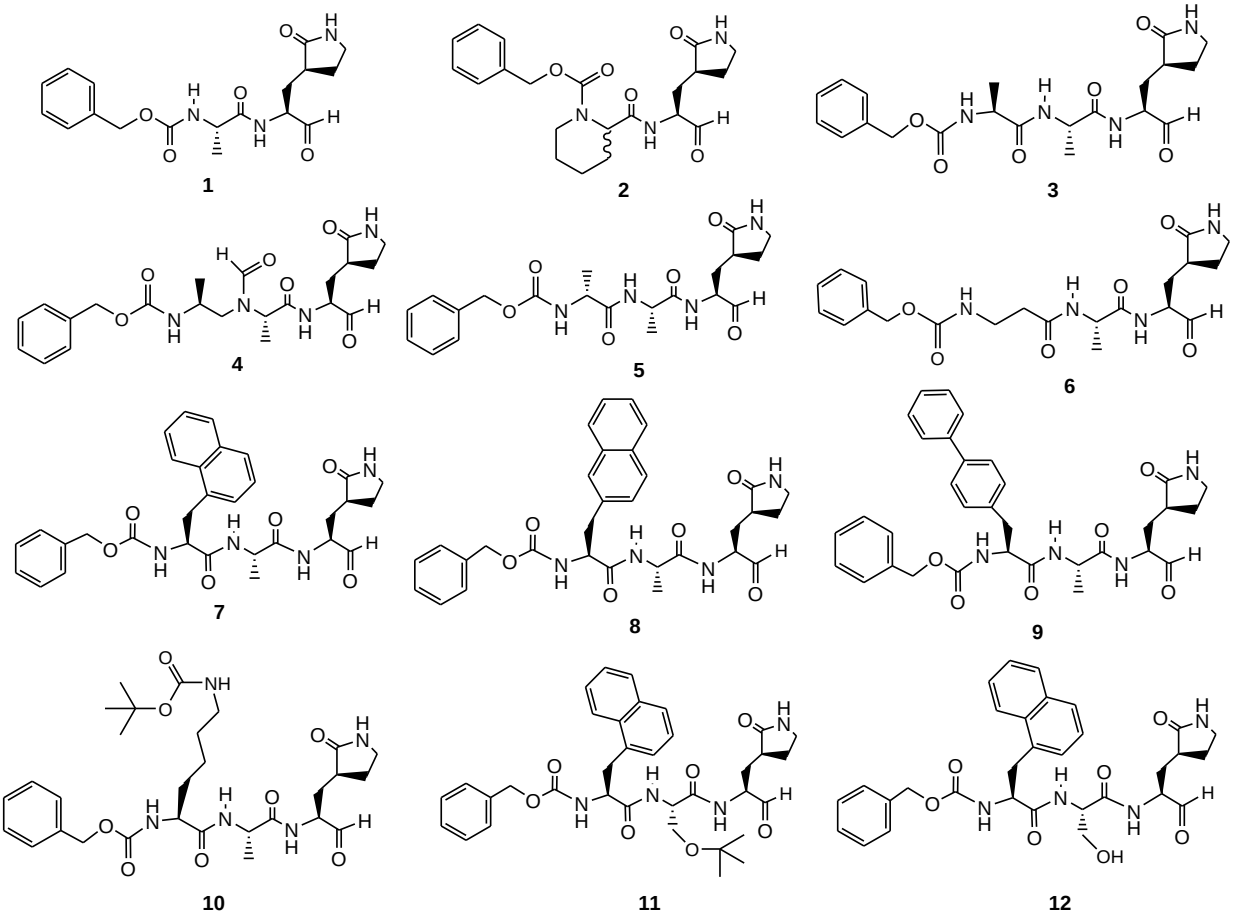

Figure 7: Structures of Anti-NV Candidates with Modification of C-Terminal Warheads.

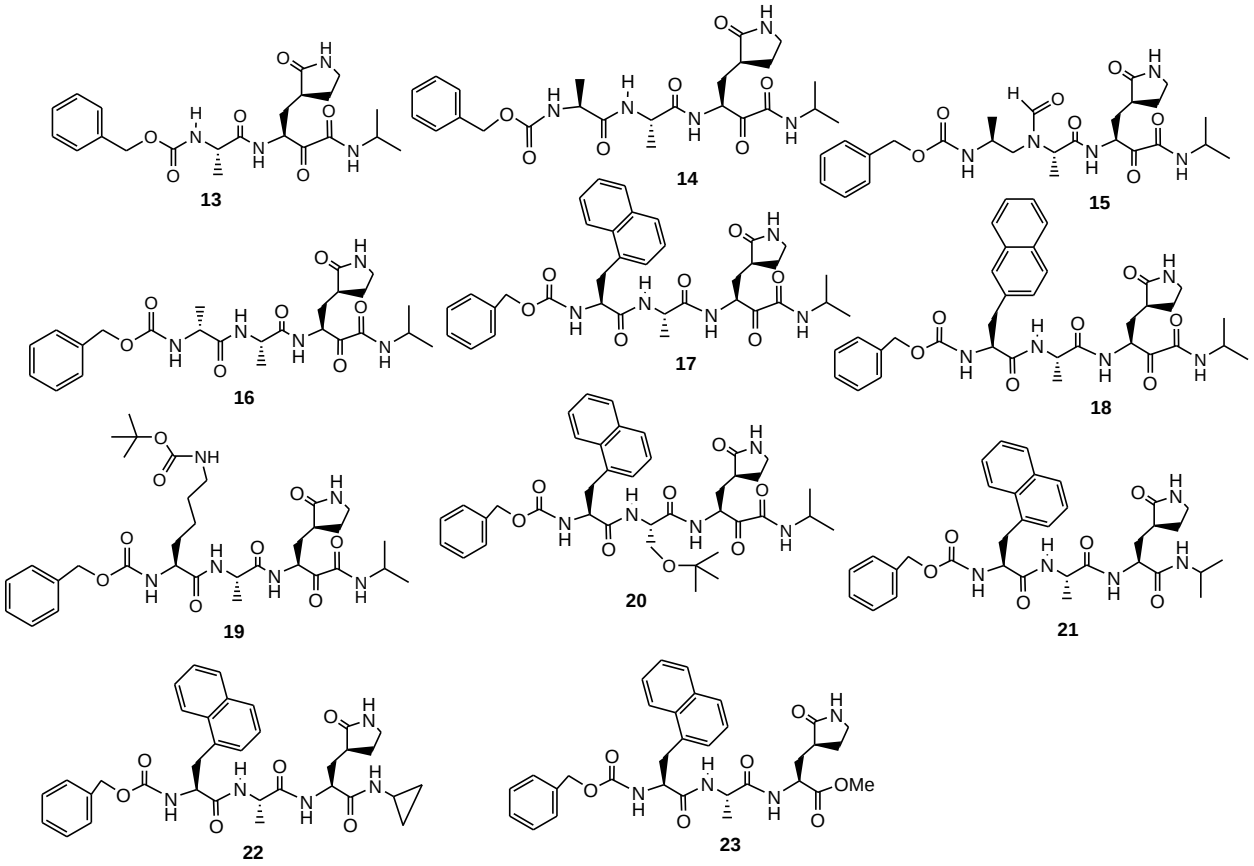

The inhibitory activities of all compounds against NV were evaluated using a FRET-based enzyme[39] and cell-based assays using the NV replicon cell system.[41] The activities for compounds **1 - 23** against NV enzyme and cell assays are shown in Table 1. The initial IC_{50} and EC_{50} data obtained by Dr. Kyeong-Ok Chang was for screening purposes only, and thus no error bars are available. Compounds that showed good activities in the initial screening were assayed again, in triplicate, by Dr. Chang, and these IC_{50} and EC_{50} values have error bars associated with them. Compounds **1 - 6** showed no inhibition in enzyme or cell based assays up to the highest concentration tested (50 μM and 10 μM, respectively) except for compound **3**, which showed inhibition in the enzyme assay only (IC_{50} 2.5 μM). Compounds **1**, **3**, **4** and **5** were converted into ketoamide derivatives to form compounds **13**, **14**, **15** and **16**, respectively of which only **16** showed inhibition in the enzyme assay (IC_{50} value of 4.6 μM).

Table 1: Bioactivities of Compounds 1 - 23 in NV3CLpro (enzyme) and NV (cell) Assays.

Compound	IC_{50} (Enzyme), µM	EC_{50} (Cell), µM	Compound (ketoamide)	IC_{50} (Enzyme), µM	EC_{50} (Cell), µM
1	> 50	> 10	**13**	> 50	> 10
2	> 50	> 10			
3	2.5	> 10	**14**	> 50	> 10
4	> 50	> 10	**15**	> 50	> 10
5	> 50	> 10	**16**	4.6	> 10
6	> 50	> 10			
7	1.8	5.6	**17**	5.1	> 10
8	2.3	7.6	**18**	5.3	> 10
9	ND	ND			
10	2.1	> 10	**19**	4.1	> 10
11	0.34	0.9	**20**	5.6	~9
12	7.0	8.6			
21	> 50	> 10			
22	> 50	> 10			
23	> 50	> 10			

All of the above mentioned compounds did not exhibit cell based inhibition activities, which suggests that these structures are not membrane permeable and/or are degraded too quickly by the cellular components of the cell based assay to be effective. Nevertheless, we continued with a structure-activity relationship study (SARS) to determine whether a lower IC_{50} and greater bioactivity (a lower the EC_{50}) could be achieved. A series of *C*-terminal aldehydes were synthesized having a hydrophobic, unnatural amino acid side chain at the P3 position as shown in compounds **7 - 12** (Figure 6). The activity data were obtained and the results showed a much improved inhibition of $NV3CL^{pro}$ in enzyme and cell based assays (Table 1). Interestingly, the compound that showed the strongest activity was compound **11**, which possessed an L-1-napthylalanine (P3) and an O-*t*-butyl-L-serine (P2). The hydrophobic nature of the 1-

napthylalanine and O-*t*-butyl-L-serine probably allows for enhanced cell membrane permeability and hence inhibition was also observed in the cell based assay. The P2 O-*t*-butyl group contained in compound **11** must fit the S2 pocket of NV3CL^{pro} much more favorably than a P2 methyl because compound **11** showed more than 5 fold stronger inhibitory activity in the enzyme assay over compound **7**, which has a P2 alanine. This confirms speculation in the literature which indicates that the S2 pocket is hydrophobic in nature and can accommodate bulky hydrophobic P2 side chains, such as Leu and Phe.[37] The *C*-terminal amides, compounds **21** and **22,** or the *C*-terminal ester, compound **23,** do not show inhibition up to the highest concentrations tested. This suggests that these warhead functionalities reduce the affinity of these compounds for the NV3CL^{pro} substrate binding site, probably due to the reduced electrophilicity of their carbonyl carbons, lowering the chance of nucleophilic attack from Cys139, as compared to a highly electrophilic aldehyde warhead.

The S2 pocket was probed by changing the side chain of P2 amino acid residue to have bigger, hydrophobic groups (compounds **24 - 26**) as shown in Figure 8. The activity data (Table 2) show that the P2 leucine gave the stronger activity, as suggested by the lowest IC_{50} value (0.14 µM) and EC_{50} value (0.04 µM). The structures and bioactivity data for compounds **24**, **27 - 28**, **30 - 32** and **35 - 36** have been reported recently by us.[42]

Figure 8: NPI Compounds Having Modification at the P2 Site.

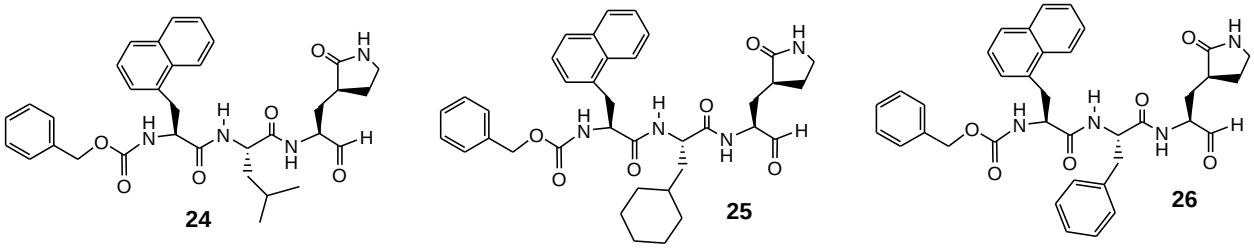

With this result, the P2 site was fixed to leucine and a series of compounds was synthesized with modification of P3 as shown in Figure 9. The P3 side chain was kept hydrophobic as this was shown necessary for better activity and cell permeability (*vide supra*).

Figure 9: Synthesized P2 Leucine NPI Candidates Having Modification at P3 Site.

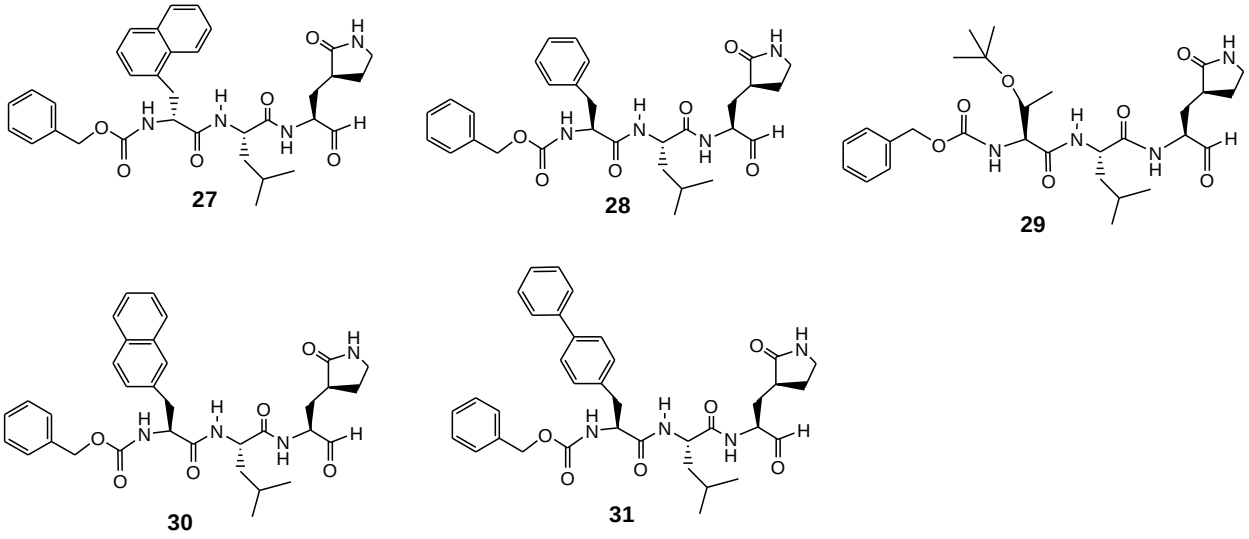

Table 2: Activity Data for Compounds 24 - 31 in NV3Cpro (enzyme) and NV (cell) Assays.

Compound	IC_{50} (Enzyme), µM	EC_{50} (Cell), µM
24	0.14 ± 0.2	0.04 ± 0.02
25	0.15	0.05
26	0.30	0.25
27	0.70 ± 0.3	0.45 ± 0.4
28	0.21 ± 0.1	0.06 ± 0.03
29	0.20	0.04
30	0.15 ± 0.1	0.08 ± 0.03
31	0.18 ± 0.06	0.05 ± 0.05

Compounds **27** - **31** all displayed very good inhibition profiles in both NV enzyme and NV cell based assays (Table 2). Compound **27** however, having a D-1-napthylalanine, was 5 fold less active than its L-1-napthylalanine isomer (compound **24**) which demonstrated that spacial recognition between substrate and enzyme is important and the natural configuration (L-configuration) gives superior binding despite the presence of unnatural (1-napthylalanine) side chain. This is not surprising since protease enzymes are built by cells to cleave peptides

containing almost entirely L-configurated amino acids. Compound **24** showed the best *in vitro* inhibition of NV3CL^{pro} and thus the best P3 group (L-1-napthylalanine) was kept fixed along with the best P2 group (alanine) and a study was performed to investigate the SAR effects with changing to different warhead functionalities. Figure 10 shows a series of compounds that were synthesized with modification about the *C*-terminal warhead region while keeping P2 and P3 structure constant, with few exceptions in which cyclohexylmethylglycine presented at P2. The bioactivity data for this series of compounds are shown in Table 3.

Figure 10: Modification of C-terminal Warhead.

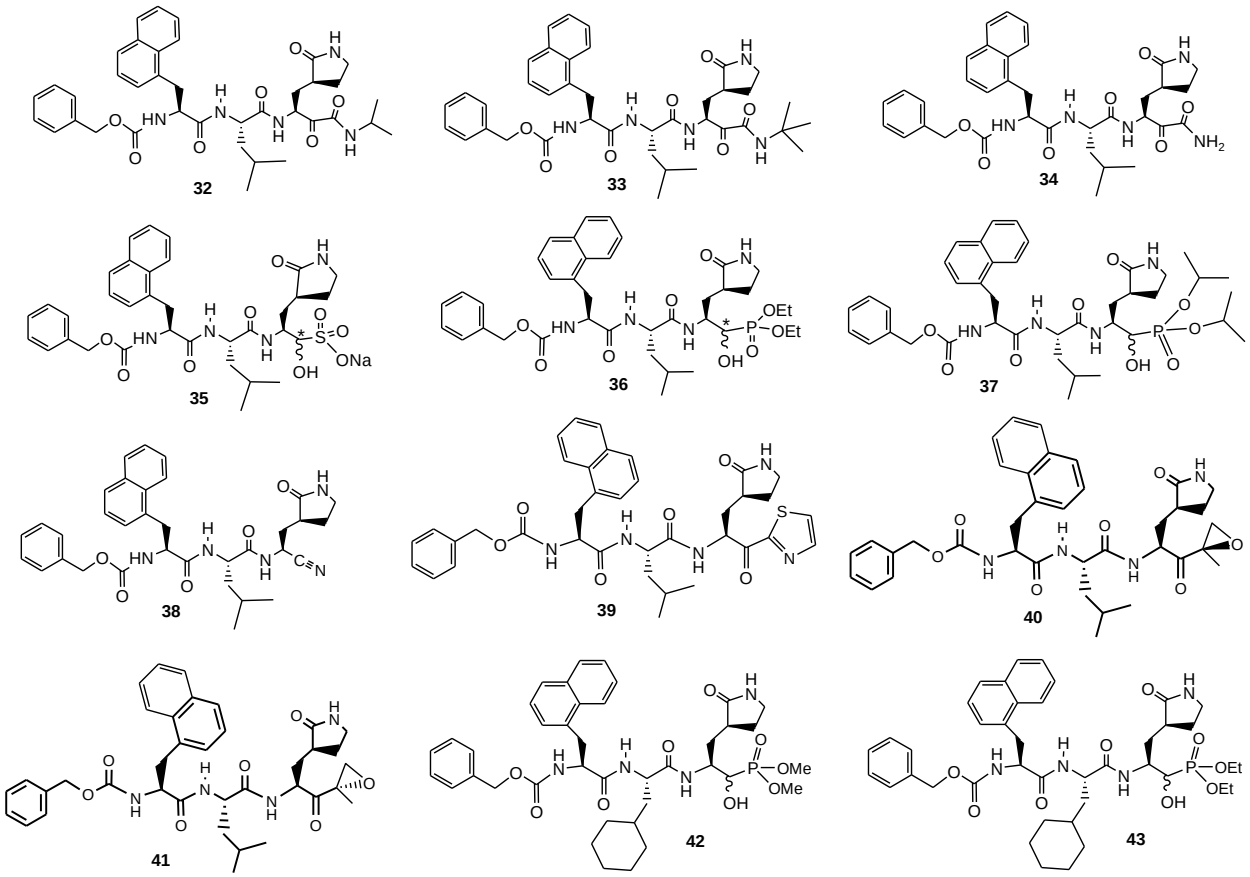

Table 3: Activity Data for Compounds 32 - 43 in NV3CLpro (enzyme) and NV (cell) Assays.

Compound	IC_{50} (Enzyme), µM	EC_{50} (Cell), µM
32	2.6 ± 1.5	4.2 ± 2.4
33	0.51	2
34	0.60	4.5
35	0.24 ± 0.1	0.04 ± 0.03
36	35.5 ± 5.7	0.1 ± 0.3
37	>50	2
38	>50	>10
39	>50	>10
40	>50	>10
41	>50	>10
42	>50	2.5
43	>50	0.8

Aldehyde functionalities are known to have poor stability in the body due to ease of oxidation and are thus not considered optimal for drug development purposes. For this reason, the ketoamide warheads **32 - 34** were incorporated onto the *C*-terminal end of the most active compounds (Figure 10). The activity data show that these ketoamide derivatives still show good activity, however, they range from having 3 to 18 times lower activity in enzyme assay and 50 to 100 times lower activity in cell assay (Table 3) compared to their aldehyde precursors. The best ketoamide during the initial screening was *t*-butyl ketoamide **33**, as this revealed an IC_{50} value of 0.51 µM and EC_{50} value of 2 µM. The sodium bisulfite adduct **35** showed good enzyme inhibition (IC_{50} 0.24 µM) and excellent activity in NV cell assay (EC_{50} 0.04 µM). Interestingly, the bisulfite adduct **35** displayed exactly the same cell based activity as its aldehyde precursor **24**, suggesting that the sodium bisulfite may act as a pro-drug, converting the hydroxy bisulfite group back to the aldehyde inside the cell. A similar phenomenon was observed within the series of dialkylphosphite adducts **37** and **42 - 43**, which showed no enzyme inhibition up to the highest

concentration tested (50 µM) in FRET assay, however all showed very good inhibition in cell based assay ranging from 0.1 to 2.5 µM. The dialkylphosphite adduct may therefore be acting as a pro-drug, which can be converted back to aldehyde in the cell, or a transition-state mimic. Compounds **38 - 41** were not found active in enzyme or cell based assays.

In order to assess the possibility of conversion of pro-drug **35** to aldehyde **24**, an HPLC study was performed as shown in Figure 11.

Figure 11: HPLC Data of Compounds 24 and 35 to Show Stability of Bisulfite Adduct 35 in PBS Buffer, pH 7.4.

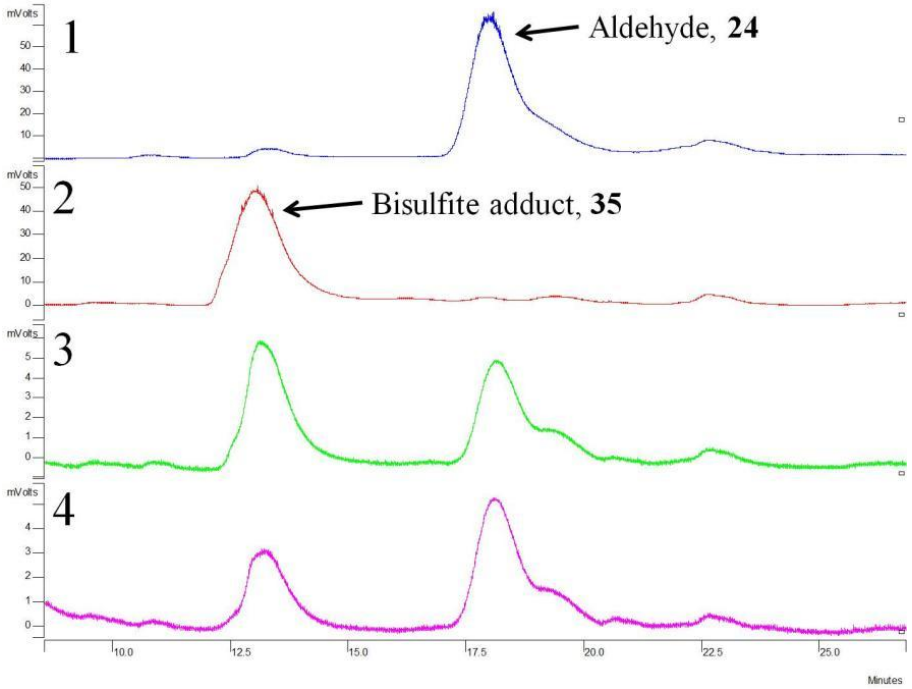

1) Aldehyde **24**; 2) Bisulfite adduct **35**; 3) Bisulfite adduct **35** after dissolved in phosphate buffer (25^{o}C, pH = 7.4) for 20 minutes; 4) Bisulfite adduct **35** after dissolved in phosphate buffer (25^{o}C, pH = 7.4) for 60 minutes.

Chromatogram 1 shows the retention time of aldehyde **24** after injecting 50 µL of a 10 mM solution of **24** in DMSO. Mass spectrometry of the peak collected at 18 minutes confirms the presence of aldehyde **24**. Chromatogram 2 shows the retention time of the sodium bisulfite adduct **35** after similarly injecting 50 µL of a 10 mM solution of bisulfite adduct **35** in DMSO. The peak at 13 minutes was confirmed to be bisulfite adduct **35** by mass spectrometry analysis.

Chromatogram 3 and 4 show the result after the bisulfite adduct **35** (1.3 mM) was allowed to sit at room temperature in PBS buffer (pH = 7.4) for 20 minutes (chromatogram 3) and 1 hour (chromatogram 4). Mass spectrometry analysis of the peaks at 13 and 18 minutes in chromatogram 3 was performed which confirmed the presence of bisulfite adduct **35** and aldehyde **24** respectively. The result was promising and supported the hypotheses of pro-drug **35** converting back to aldehyde *in vivo* at pH 7.4.

Some work was done to evaluate the *N*-terminal caps involvement in activity, but so far only three compounds have been synthesized (Figure 12) and tested (Table 4). Compound **44** was designed to present an amino-4-methylcoumarin (AMC) fluorophore onto the *N*-terminal end of the peptide to act has a fluorescence probe. The AMC is bulkier than the Cbz, which may not be ideal, since the enzyme and cell based inhibitory activity was lower, compared to compound **24**. The smaller thiazole cap in compound **45** proved to be better than the AMC, however, it was still inferior to the Cbz cap (compound **24**). The 3-hydroxyl-Cbz cap (compound **46**) was the most active of these three, but exhibited slightly lower activity than the Cbz cap (compound **24**). However, the presence of a hydroxyl function in the cap lowers cLog P value and thereby would increase bioavailability.

Figure 12: Modification of *N*-Terminal Cap.

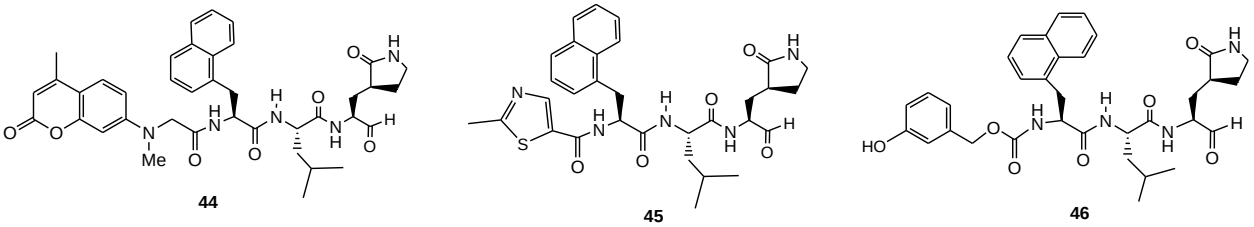

Table 4: Activity Data for Compounds 44-46 in NV3CLpro (enzyme) and NV (cell) Assays.

Compound	IC_{50} (Enzyme), µM	EC_{50} (Cell), µM
44	1.5	2.5
45	0.5	0.08
46	0.35	0.07

It is known that macrocyclic peptides may offer advantages over linear peptides when considering drug like characteristics and therefore a macrocyclic skeleton was constructed as shown in Figure 13. By closing up the ring using the P1 and P3 side chains, it locks the peptide into a β-strand conformation (alternating side chains) which is the conformation recognized by protease enzymes.[43, 44] The macrocyclization employing P1 and P3 side chains is therefore causing "pre-organization" of the peptide into a β-strand conformation, and this "transition state mimic" should provide a stronger binding to the active site of the protease.[45, 46] The stronger binding should arise because pre-organization can reduce the loss of entropy upon inhibitor binding. Other advantages to macrocyclization include better cell permeability and proteolytic stability[47] and improved drug-like characteristics.[48] Macrocyclic peptides **47** and **48** were synthesized and their anti-NV activities were assessed in enzyme and cell based assays (Table 5). The activity for aldehyde **48** was not as good as expected and only showed inhibition in enzyme assay (IC_{50} 8.5 µM). The ester **47** could not cause inhibition in both enzyme and cell based assays which was less surprising since an ester functional group was shown earlier not to be a good *C*-terminal warhead *vide supra*.

Figure 13: Macrocyclic anti-NV Candidates.

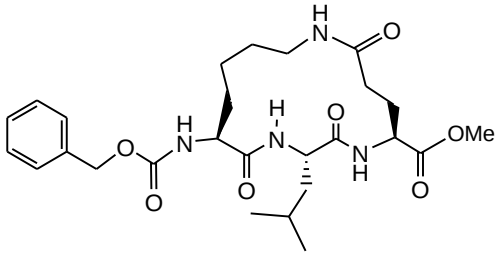

47

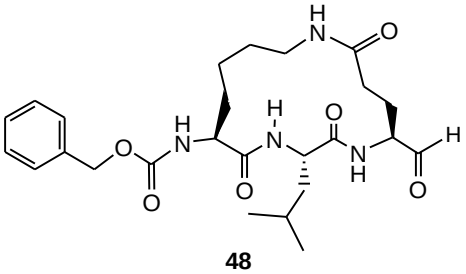

48

Table 5: Activity Data for Compounds 47-48 in NV3CL^{pro} (enzyme) and NV (cell) Assays.

Compound	IC_{50} (Enzyme), µM	EC_{50} (Cell), µM
47	>50	>10
48	8.5	>10

To date, the strongest inhibitor of NV3CL^{pro} in enzyme and cell based assays remains compound **24** (IC_{50} 0.14 µM; EC_{50} 0.04 µM) although compounds **25**, **28**, **29**, **30**, **31**, **35** and **46** also show comparable EC_{50} values. Compound **24** and its ketoamide derivative, **32**, were screened against other viral strains in the caliciviridae, picornaviridae and coronaviridae families using enzyme and cell based assays. The results were encouraging as both compounds were found to be strongly active in all of these viral strains with minimal cell cytotoxicity (Tables 6 and 7). The activity data of compounds **24** and **32** (Tables 6 and 7) have recently been reported by us.[42]

Table 6: IC_{50} Values of Compounds 24 and 32 against Other Viral 3C^{pro} and 3CL^{pro} in Enzyme Assay.

Compound	NV[a] (µM)	MD145[b] (µM)	HRV[c] (µM)	SARS-CoV[d] (µM)
24	0.14 ± 0.1	0.51 ± 0.2	0.15 ± 0.05	0.23 ± 0.1
32	2.6 ± 2.5	3.1 ± 1.6	0.12 ± 0.2	0.61 ± 0.2

a) Norovirus enzyme assay (caliciviridae family)
b) MD145-12 norovirus strain (GII/4) (caliciviridae family)
c) Human rhino virus (picornaviridae family)
d) Severe acute respiratory syndrome-coronavirus (coronaviridae family)

Table 7: EC_{50} Values of Compounds 24 and 32 against Other Viral Cell Lines and CC_{50} Values.

Compound	NV[a] (µM)	MNV-1[b] (µM)	HRV18[c] (µM)	EV-229E[d] (µM)	CC_{50}[e] (µM)
24	0.04 ± 0.02	0.6 ± 0.2	0.015 ± 0.03	0.2 ± 0.1	87 ± 6.3
32	4.2 ± 1.3	4.2 ± 2.1	0.03 ± 0.04	0.5 ± 0.2	> 100

a) Norovirus cell assay (caliciviridae family)
b) Murine norovirus (caliciviridae family)
c) Human rhino virus (picornaviridae family)
d) Enterovirus (picornaviridae family)
e) Cell cytotoxicity

A crystal structure of compound **24** with SARS protease enzyme was obtained, which demonstrates that the NPI compounds can target the protease active site (Figure 14). Moreover,

structural insight obtained from this data could better help tailor a more suitable compound in the future to have stronger inhibition of SARS-CoV protease enzymes. The study of crystal structure was carried out by Dr. Scott Lovell at the University of Kansas, Lawrence, KS.

Figure 14: X-Ray Crystal structure of Compound 24 in Complex with SARS 3CLpro.

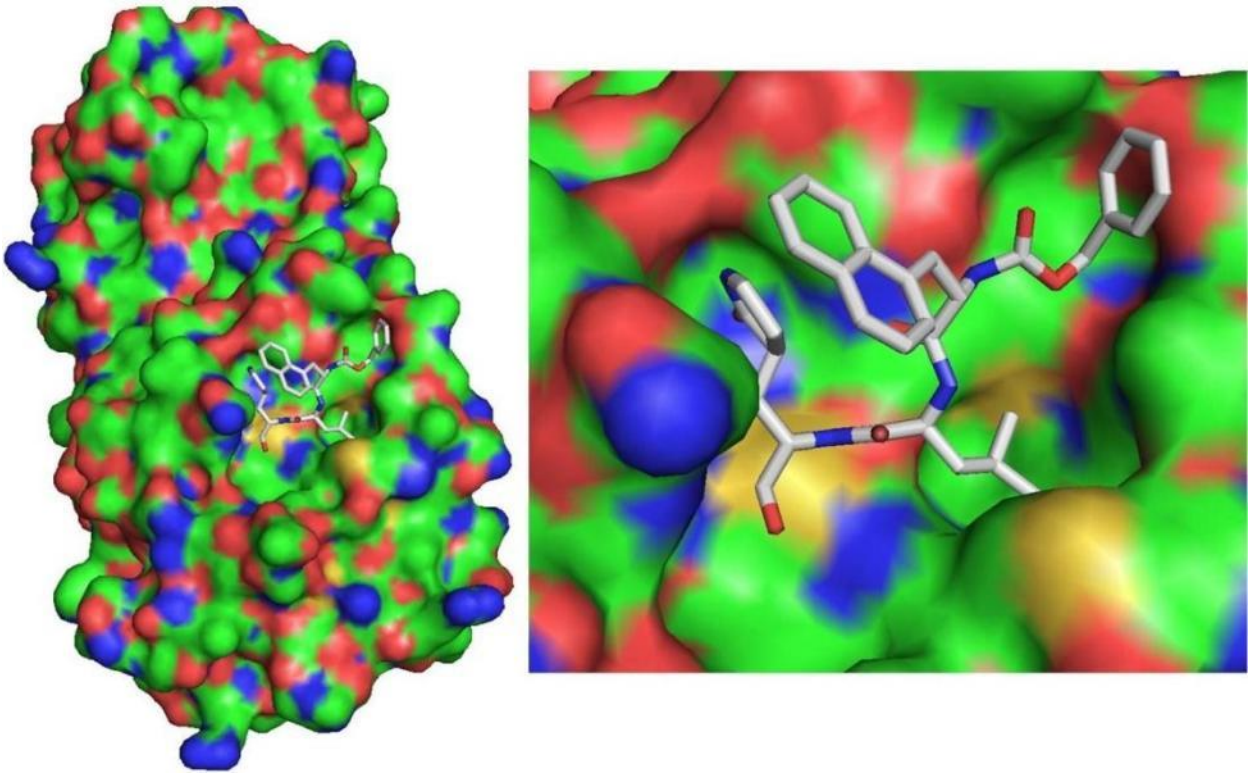

The results shown in Tables 6 and 7 demonstrated that this class of NPIs could act as broad spectrum anti-viral compounds with excellent inhibitory activity against protease enzymes belonging to noroviruses, picornaviruses and coronaviruses. The initial design was that of transition state inhibitors and transition state mimics that should bind to the active site of viral $3C^{pro}$ or $3CL^{pro}$. The presence of a leucine at P2 site, a 1-naphthylalanine residue at P3 site, a Cbz cap at the *N*-terminus and a *C*-terminal aldehyde warhead was found to be the best in terms of activity among all synthesized compounds. Animal studies are currently being pursued with compound **24** and SAR studies are ongoing in our lab to try and improve upon broad spectrum anti-viral activity.

I.III. Synthesis of NPI compounds 1 - 48

The glutamine surrogate methyl ester **53** and glutamine surrogate aldehyde **53a** were prepared according to a recent literature procedure.[49] In brief, *N*-boc glutamic acid **49** was treated with sodium iodide and sodium bicarbonate in DMF for 5 days to give *N*-Boc-glutamic dimethyl ester **50** (Scheme 1).

Scheme 1: Synthesis of Glutamine Surrogate Methyl Ester 53 and Glutamine Surrogate Aldehyde (53a).

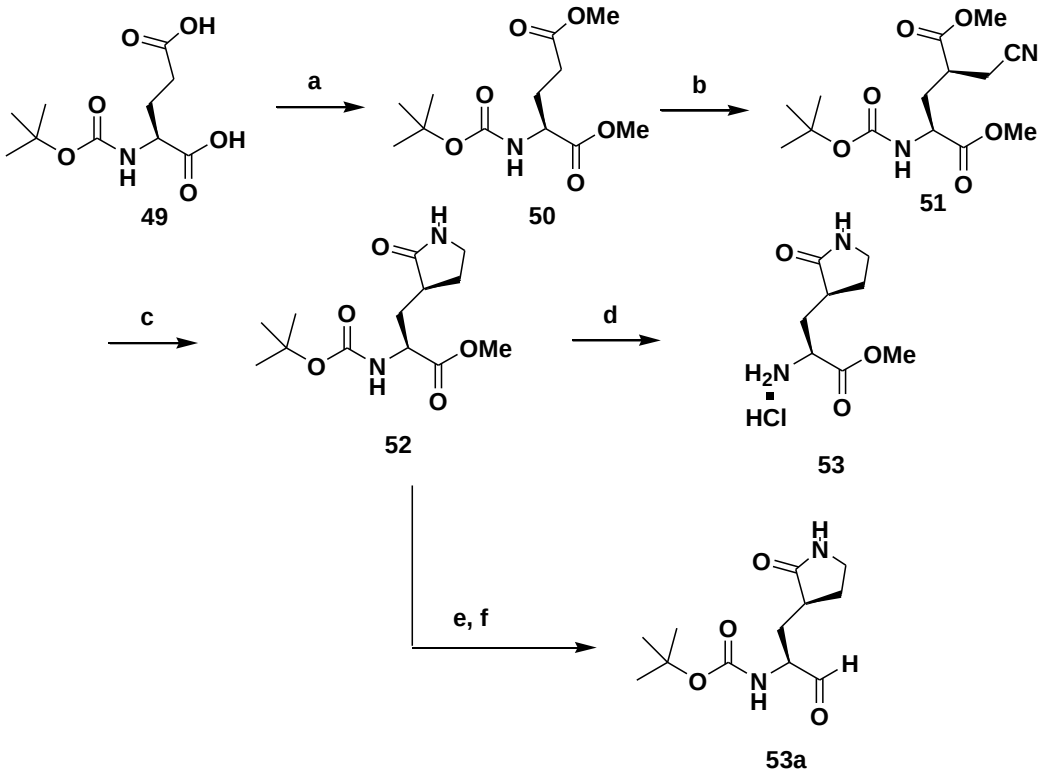

Reagents and Conditions: (a) MeI, $NaHCO_3$, DMF, 5 days, 80%; (b) 1. LiHMDS, THF, -78^oC, 1h; 2. Bromoacetonitrile, -78^oC, 3 h, 91%; (c) $NaBH_4$, $CoCl_2$, MeOH, 25^oC, 18 h, 63%; (d) 4M HCl/Dioxane, 25^oC, 2h, 100%; (e) $NaBH_4$, CH_2Cl_2/EtOH/MEOH (5:3:2), 0 ^oC, 4 h, 100%; (f) DMP, CH_2Cl_2, 25 ^oC, 2 h, 94%.

Double deprotonation of **50** using 2 equivalents of lithiumhexamethyldisilazane (liHMDS) followed by 1 equivalent of bromoacetonitrile at -78^oC for 3 hours followed by quenching with acetic acid furnished the alkylated nitrile compound **51** with excellent diastereoselectivity, as only one diastereomer (1,3-*anti*) of **51** was observed from the reaction. The nitrile **51** was

reduced with sodium borohydride and cobalt(II) chloride in methanol to give an amine intermediate which undergoes ring closure by an acyl substitution reaction with the side chain ester group to produce the lactam ring as seen in compound **52**. The boc protecting group of **52** can be removed by treatment with 4M HCl in dioxane to form **53**, or the ester group of **52** can be converted to aldehyde **53a** by reduction of **52** with sodium borohydride followed by oxidation of the alcohol intermediate by Dess-Martin periodinane (DMP). The surrogate molecules **53** and **53a** are key starting materials for the synthesis of all NPI compounds.

The high level of 1,3-asymmetric induction obtained in the synthesis of compound **51** (Scheme 1) has been also been described by Hanessian and Schaum.[50] It has been speculated that the reaction proceeds *via* the alkylation of a lithium coordinated transition state **B** as shown in Figure 15 from the less hindered face to generate a 1,3-*anti* product.[50] Narasaka and coworkers[51, 52] observed similar asymmetric induction during the alkylation of lithium enolates, generated from *t*-butyl esters of 4-alkyl-substituted 5-hydroxypentanoic acids. A lithium coordinated transition state was also proposed in these reactions.

Figure 15: Lithium Coordinated Transition State Proposed by Hanessian and Schaum[50] that Accounts for the High Asymmetric Induction Observed in the Synthesis of Compound 51.

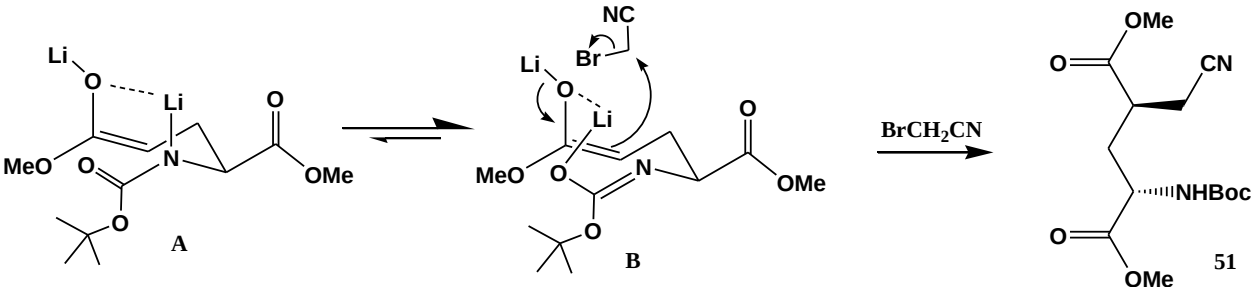

The dipeptidyl aldehyde **1** was synthesized by firstly coupling the glutamine surrogate-amine **53** with Cbz-alanine in the presence of EDCI and DMAP in methylene chloride and DMF (Scheme 2). The resulting ester **54** was reduced to an alcohol intermediate using sodium borohydride followed by DMP oxidation to provide aldehyde **1**. The aldehyde **2** was constructed in a similar fashion as described for compound **1**, but, a mixture of two diastereomers of **2** were obtained.

Scheme 2: Synthesis of Dipeptidyl Aldehydes 1 and 2.

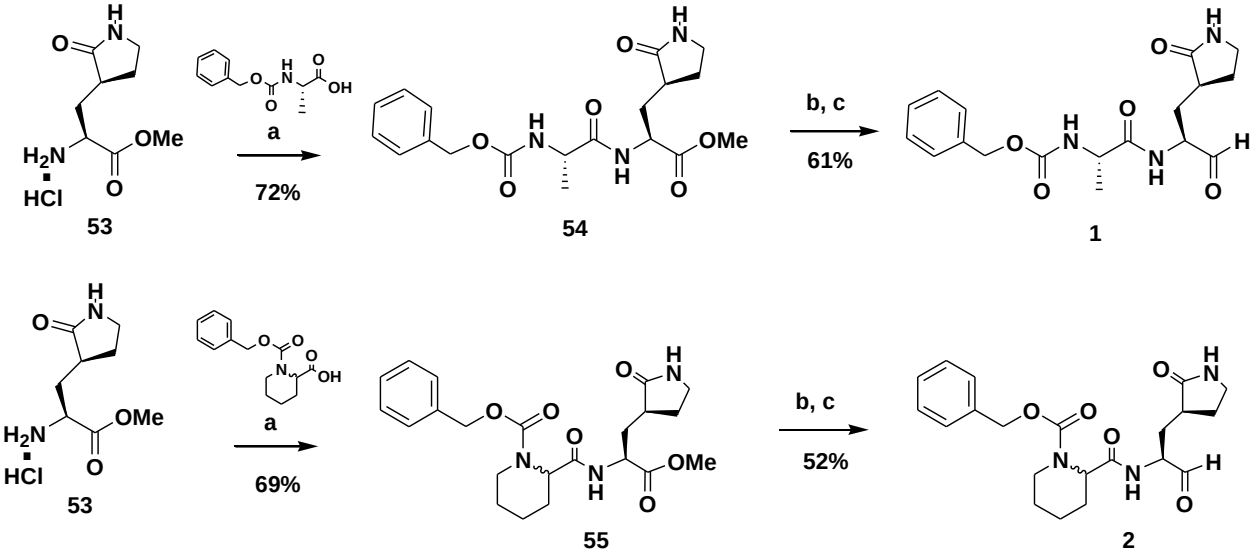

Reagents and Conditions: (a) EDCI, DMAP, DMF/CH_2Cl_2, 25 ^oC, 18h; (b) $NaBH_4$, CH_2Cl_2/EtOH/MEOH (5:3:2), 0 ^oC, 4 h; (c) DMP, CH_2Cl_2, 25 ^oC, 2 h.

The piperidine-1,2-dicarboxylic acid 1-benzyl ester (**a**) was synthesized in house according to Scheme 3. D,L-2-Piperidinecarboxylic acid was dissolved in water and treated with sodium hydroxide and benzylchloroformate at 25^oC for 18 hours. Pure compound **a** was obtained after purification from silica gel column chromatography, in a 69% yield.

Scheme 3: Synthesis of Piperidine-1,2-dicarboxylic acid 1-benzyl ester (Compound a).

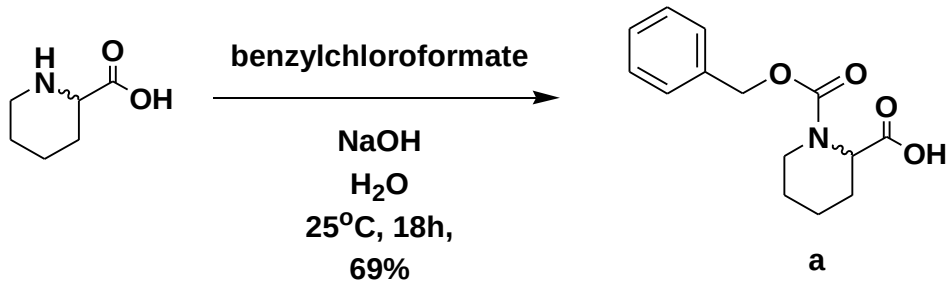

Aldehydes **3**, **5** and **7** were synthesized as depicted in Scheme 4. The 2-chlorotrityl-L-alanine resin (200 mesh) was coupled with the P3 amino acid residue containing an R side chain using solid phase peptide synthesis to form resin-bound intermediates **57** - **59**. After separately cleaving resin-bound peptides **57** - **59** from resin using TFA, the dipeptidyl carboxylic acids **60** - **62** could be obtained. Each of these carboxylic acids could be coupled separately with the P1

glutamine surrogate-amine **53** to form their corresponding tripeptidyl esters **63** - **64** and **23**. Each of these esters was reduced and re-oxidized using sodium borohydride and DMP respectively to yield aldehydes **3**, **5** and **7**.

Scheme 4: Synthesis of Tripeptidyl Aldehydes 3, 5 and 7.

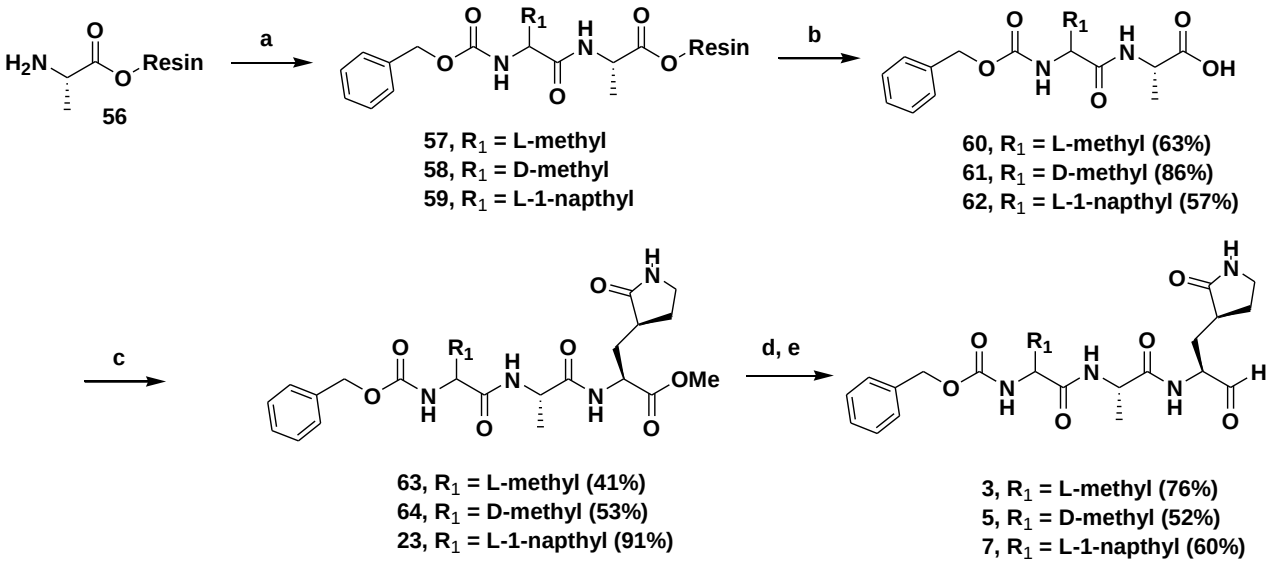

Reagents and Conditions: (a) Cbz-NH-CHR_1-CO_2H, HBTU, 4.2% DIPEA/DMF, microwave (25 W, 75^oC, 5 min); (b) 95% TFA, 2.5% TIPS, 2.5% water, microwave (20 W, 38^oC, 18 min); (c) EDCI, DMAP, DMF/CH_2Cl_2, 25 ^oC, 18h; (d) $NaBH_4$, CH_2Cl_2/EtOH/MEOH (5:3:2), 0 ^oC, 4 h; (e) DMP, CH_2Cl_2, 25 ^oC, 2 h.

The tripeptidyl formamide aldehyde **4** and its ketoamide derivative **15** were synthesized according to the procedure outlined in Scheme 5. The Cbz-alanine **65** was converted into ester **66** using Fischer esterification conditions. The ester **66** was converted to aldehyde **67** *via* reduction and re-oxidation using sodium borohydride and DMP respectively.

Scheme 5: Synthesis of Tripeptidyl Formamidyl Aldehyde 4 and Corresponding Ketoamide 15.

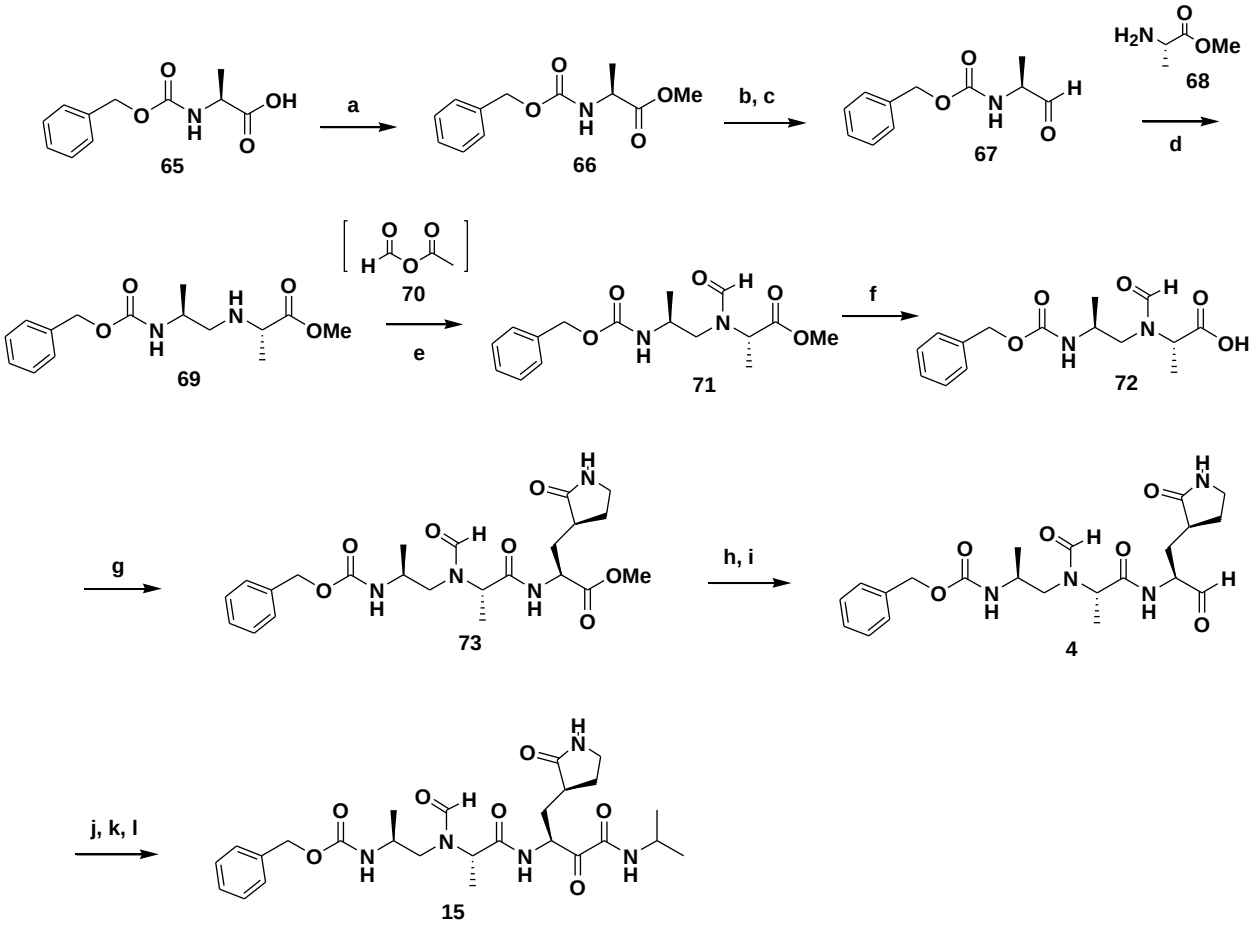

Reagents and Conditions: (a) MeOH, H_2SO_4 (cat.), 100%; (b) $NaBH_4$, CH_2Cl_2/EtOH/MEOH (5:3:2), 0 ^oC, 4 h; 100% (c) DMP, CH_2Cl_2, 25 ^oC, 2 h, 70%; (d) $NaCNBH_4$, MeOH, 40%; (e) HCO_2H/AcO_2O, 93%; (f) NaOH, 1:1 dioxane/water, 96%; (g) glutamine surrogate-amine **53**, EDCI, DMAP, DMF/CH_2Cl_2, 25 ^oC, 18h; 55%; (h) $NaBH_4$, CH_2Cl_2/EtOH/MEOH (5:3:2), 0 ^oC, 4 h; 100%; (i) DMP, CH_2Cl_2, 25 ^oC, 2 h, 65%; (j) isopropylisocyanide, AcOH, EtOAc, 25 ^oC, 18 h; (k) K_2CO_3, MeOH/H_2O (1:1), 25 ^oC, 3 h; (l) DMP, CH_2Cl_2, 25 ^oC, 2 h, yield 79% over three steps.

Aldehyde **67** was condensed with alanine methylester **68** in the presence of sodium cyanoborohydride (reductive amination) to afford the coupled product **69**. The secondary amine of **69** was formylated using a mixed anhydride **70** *via* premixing a solution of formic acid and

acetic anhydride and adding compound **69** to give compound **71**. Basic hydrolysis of ester **71** gave the acid **72** which was coupled to glutamine surrogate-amine **53** using EDCI and DMAP to furnish the ester **73**. Reduction of the ester **73** gave an alcohol intermediate that was re-oxidized to the aldehyde **4** using DMP. The aldehyde **4** was converted into the ketoamide derivative **15** using a 3 step procedure. Firstly, the aldehyde is treated with isopropylisocyanide to give an isopropylisocyanide adduct. Secondly, the isopropylisocyanide adduct was converted into a hydroxyamide form employing basic and aqueous reaction conditions. The hydroxyamide functionality was lastly oxidized to give the ketoamide **15** using DMP.

The tripeptidyl aldehydes **7 - 11** and **24 - 31** were synthesized starting from the glutamine surrogate-amine **53** in a 5 step manor (Scheme 6). The glutamine surrogate-amine **53** is coupled with the **P2** amino acid using EDCI and DMAP to form *N*-boc-dipeptides **74 - 78** in excellent yields. The boc protecting group was removed using 10% TFA in methylene chloride to give an amine intermediate which was immediately coupled with a Cbz protected P3 amino acid using EDCI and DMAP in methylene chloride to give tripeptidyl esters **23** and **80 - 91** in good to excellent yields. The esters were reduced and re-oxidized to their corresponding aldehydes using sodium borohydride and DMP respectively to give compounds **7 - 11** and **24 - 31** in good to excellent yields. The synthesis of compounds **24, 27 - 28, 30 - 32 and 25 - 36** that are captured in Schemes 5, 6, 7 and 10 have recently been reported.[42]

The *N*-Cbz protected amino acids **86a - 91a** were synthesized from commercially available amino acids as highlighted in Scheme 7. The amino acids have side chain (R_2) was dissolved in 1:1 dioxane/water and treated with 3 molar equivalents of sodium bicarbonate, followed by 1.2 molar equivalents of benzylchloroformate. After 3 hours the reactions were worked up and the obtained solids were recrystallized from ether/hexane to yield the *N*-Cbz protected amino acids **86a - 91a** in 72 - 95 % yields.

Scheme 6: Synthesis of Tripeptidyl Aldehydes 7 - 11 and 24 - 31.

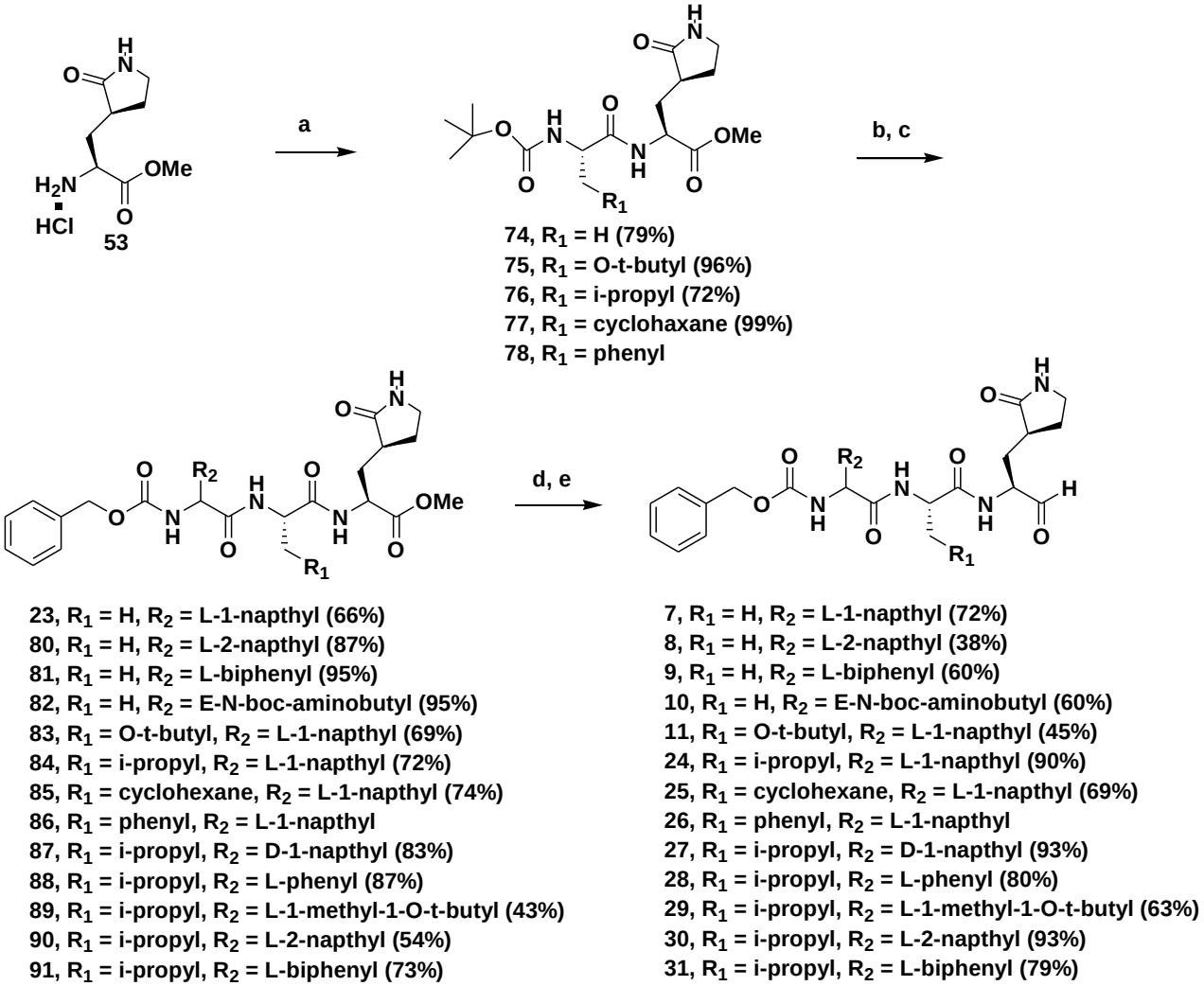

Reagents and Conditions: (a) Boc-NH-CHCH$_2$R$_1$-CO$_2$H, EDCI, DMAP, DMF/CH$_2$Cl$_2$, 25 ^{o}C, 18h; (b) 10% TFA/CH$_2$Cl$_2$, 25 ^{o}C, 4 h, yield 100%; (c) Cbz-NH-CHR$_2$-CO$_2$H, EDCI, DMAP, CH$_2$Cl$_2$, 25 ^{o}C, 18 h; (d) NaBH$_4$, CH$_2$Cl$_2$/EtOH/MEOH (5:3:2), 0 ^{o}C, 4 h, 100%; (e) DMP, CH$_2$Cl$_2$, 25 ^{o}C, 2 h.

Scheme 7: Synthesis of Cbz Protected Amino Acids 86a - 91a.

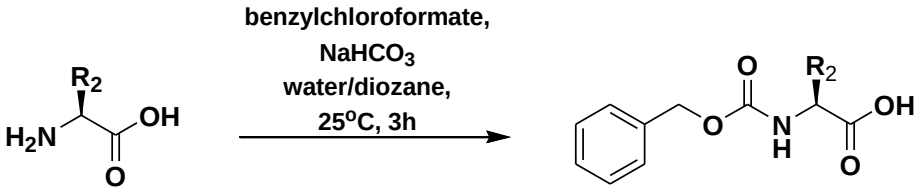

86a: R_2 = L-1-napthyl (95%)
87a: R_2 = D-1-napthyl (86%)
88a: R_2 = L-phenyl (94%)
89a: R_2 = L-1-methyl-1-O-t-butyl (91%)
90a: R_2 = L-2-napthyl (72%)
91a: R_2 = L-biphenyl (90%)

The biphenylalanine **91d** was synthesized starting from commercially available *N*-Boc-4-bromo-phenyl alanine **91b** as shown in Scheme 8. The key step involved a Suzuki-Miyaura[53] cross-coupling reaction between *N*-Boc-4-bromo-phenylalanine **91b** and phenylboronic acid to furnish *N*-Boc-biphenylalanine **91c** (Scheme 8). The NMR spectral data for **91c** compared favorably to literature values.[53] Subsequent removal of the *N*-Boc protecting group provided biphenylalanine **91d** in an 86% overall yield from **91b**.

Scheme 8: Synthesis of Biphenylalanine 91d.

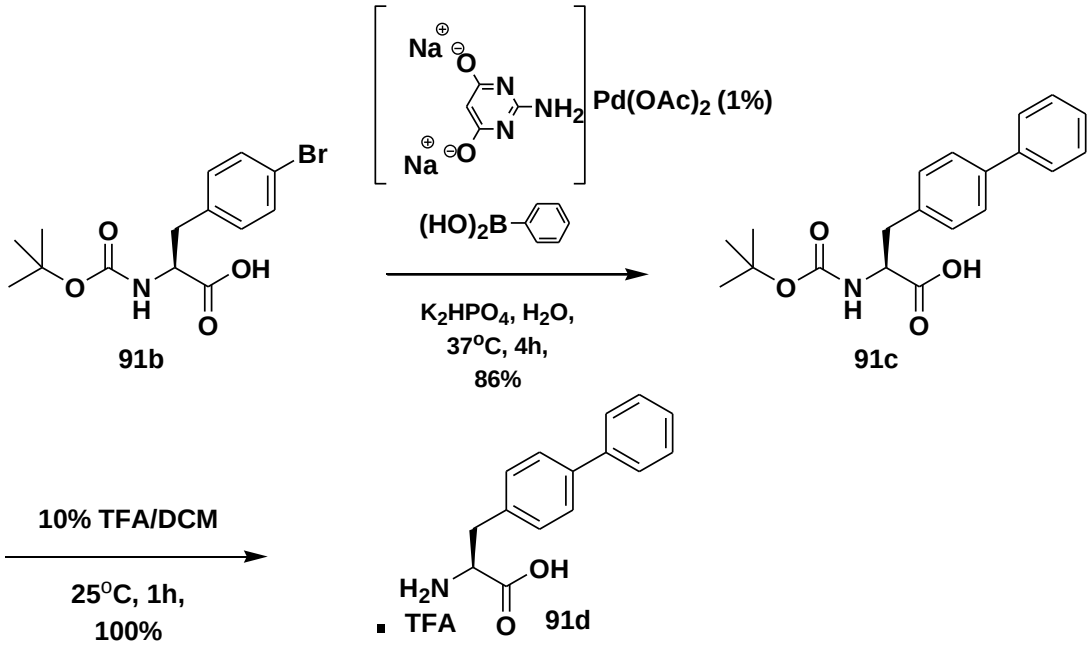

The ketoamides **13 - 14**, **16 - 20** and **32 - 33** were synthesized using a three step procedure (Schemes 9 and 10). The aldehyde precursors are treated with isopropylisocyanide which gave an isopropylisocyanide adduct. This isopropylisocyanide adduct was converted into a hydroxyamide by employing basic, aqueous reaction conditions. The hydroxyamide functionality was then oxidized by DMP to give the ketoamides **13 - 14**, **16 - 20** and **32 - 33** in good to excellent yields.

Scheme 9: Synthesis of Ketoamide 13.

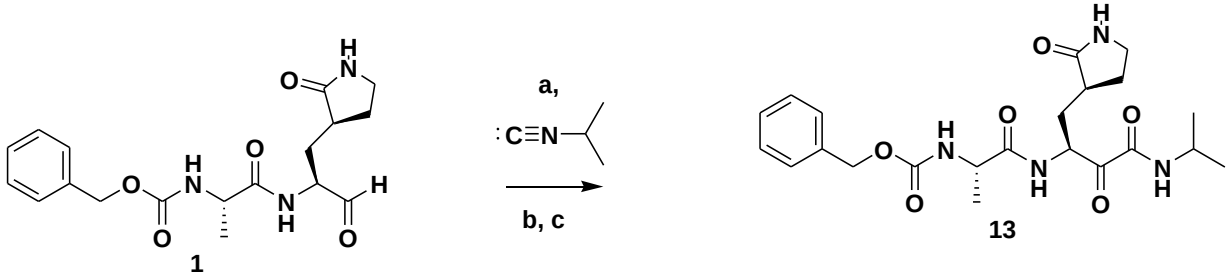

Reagents and Conditions: (a) AcOH, EtOAc, 25 ^{o}C, 18 h; (b) K_2CO_3, MeOH/H_2O (1:1), 25 ^{o}C, 3 h; (c) DMP, CH_2Cl_2, 25 ^{o}C, 2 h, yield 46% over three steps.

Scheme 10: Synthesis of Ketoamides 14, 16-20 and 32-33.

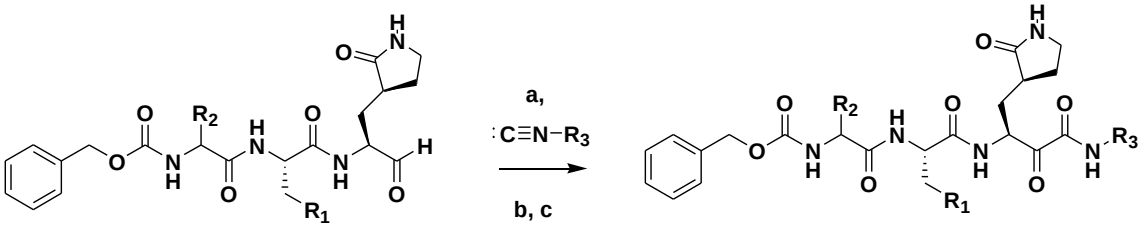

14, R_1 = H, R_2 = L-methyl, R_3 = i-propyl (64%)
16, R_1 = H, R_2 = D-methyl, R_3 = i-propyl (47%)
17, R_1 = H, R_2 = L-1-napthyl, R_3 = i-propyl (81%)
18, R_1 = H, R_2 = L-2-napthyl, R_3 = i-propyl (94%)
19, R_1 = H, R_2 = E-N-boc-aminobutyl, R_3 = i-propyl (94%)
20, R_1 = O-t-butyl, R_2 = L-1-napthyl, R_3 = i-propyl (53%)
32, R_1 = i-propyl, R_2 = L-1-napthyl, R_3 = i-propyl (79%)
33, R_1 = i-propyl, R_2 = L-1-napthyl, R_3 = t-butyl (54%)

Reagents and Conditions: (a) AcOH, EtOAc, 25 ^{o}C, 18 h; (b) K_2CO_3, MeOH/H_2O (1:1), 25 ^{o}C, 3 h; (c) DMP, CH_2Cl_2, 25 ^{o}C, 2 h.

The ketoamide **34** is prepared by treating aldehyde **24** with acetone cyanohydrin and triethylamine in methylene chloride followed by oxidation of the cyano adduct to form a hydroxyl amide intermediate, which was immediately oxidized by DMP to form the ketoamide **34** in a 34% overall yield (Scheme 11).

Scheme 11: Synthesis of Ketoamide 34.

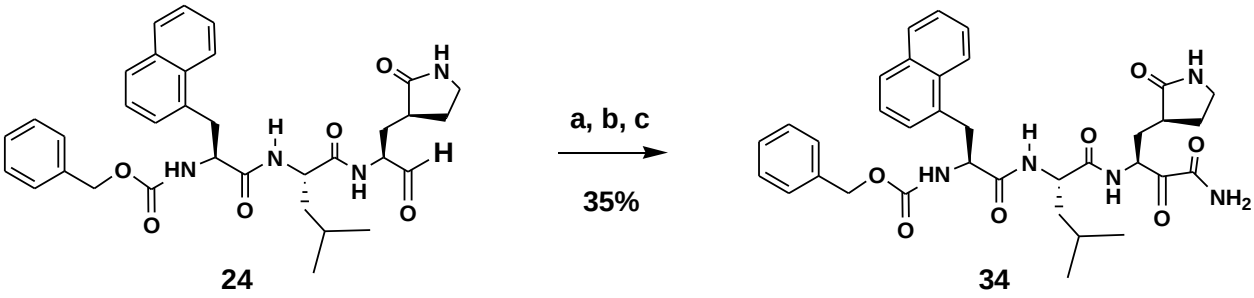

Reagents and Conditions: (a) Acetone cyanohydrin, NEt_3, CH_2Cl_2, 25^oC, 15 h; (b) 30% H_2O_2, LiOH,0^oC, 3 h; (c) DMP, CH_2Cl_2, 25^oC, 2 h.

The tripeptidyl amides **21** and **22** were synthesized using an acyl substitution reaction whereby ester **23** was treated with isopropyl amine or cyclopropyl amine in 50^oC methanol respectively (Scheme 12).

Scheme 12: Synthesis of Tripeptidyl Amides 21-22.

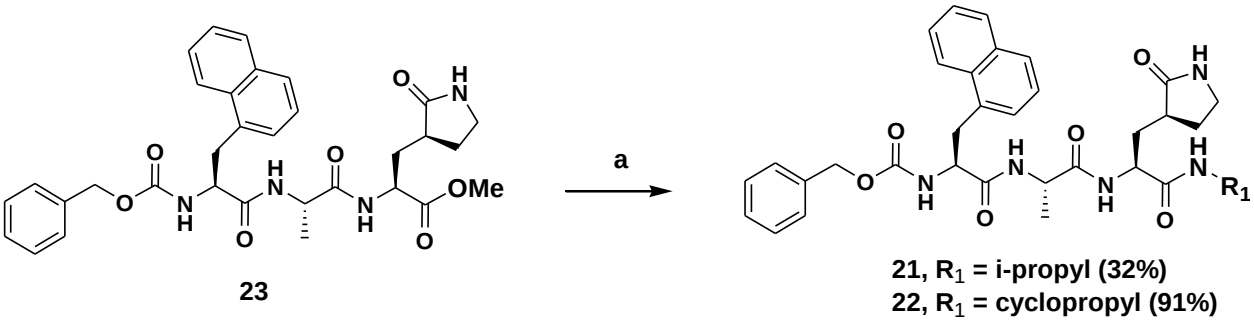

Reagents and Conditions: (a) H_2N-R_1, MeOH, 50^oC, 48h.

The sodiumbisulfite adduct **35** was prepared by treating the aldehyde **24** with sodium bisulfite in a mixture of ethyl acetate, ethanol and water at 40^{o}C with a 100% yield (Scheme 13).

Scheme 13: Synthesis of Sodiumbisulfite Adduct 35.

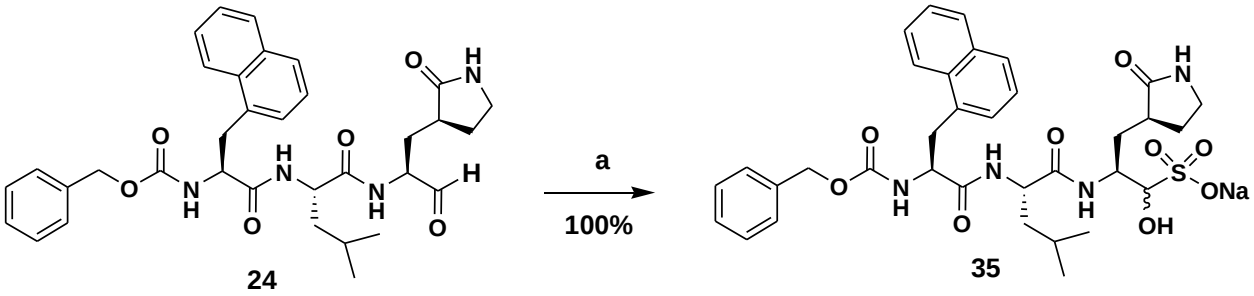

Reagents and Conditions: (a) sodium bisulfite, EtOAc/EtOH/H_2O (4:2:1), 40^{o}C, 2 h.

The dialkylphosphonates **36 - 37** and **42 - 43** were made by treating the aldehyde precursor with a dialkyl phosphite and diisopropylethylamine in methylene chloride (Scheme 14). The dialkyl phosphite adds to either face of the aldehyde and therefore two diastereomers of **36 - 37** and **42 - 43** are obtained.

Scheme 14: Synthesis of Dialkylphosphonates 36 - 37 and 42 - 43.

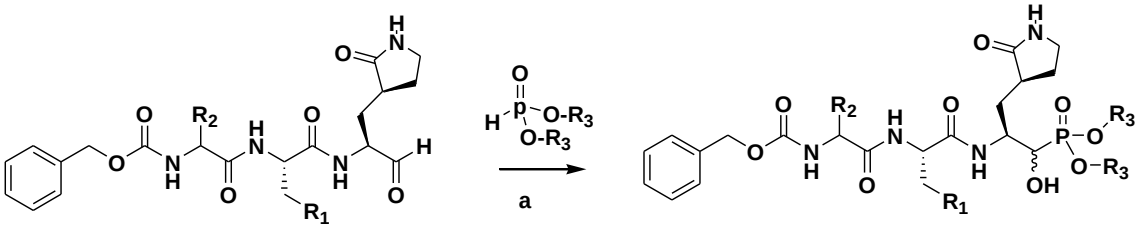

36, R_1 = i-propyl, R_2 = L-1-napthyl, R_3 = ethyl (54%)
37, R_1 = i-propyl, R_2 = L-1-napthyl, R_3 = i-propyl (73%)
42, R_1 = cyclohexane, R_2 = L-1-napthyl, R_3 = methyl (64%)
43, R_1 = cyclohexane, R_2 = L-1-napthyl, R_3 = ethyl (90%)

Reagents and Conditions: (a) Diisopropylethylamine, CH_2Cl_2, 25 ^{o}C, 18 h.

The nitrile **38** was made by treating the aldehyde **24** to a mixture (diacetoxyiodo)benzene, sodium dodecylsulfate and ammonium acetate in water at 70^{o}C (Scheme 15). After workup and column chromatography over silica gel, the nitrile **38** was obtained in 61% yield.

Scheme 15: Synthesis of Tripeptidyl-nitrile 38.

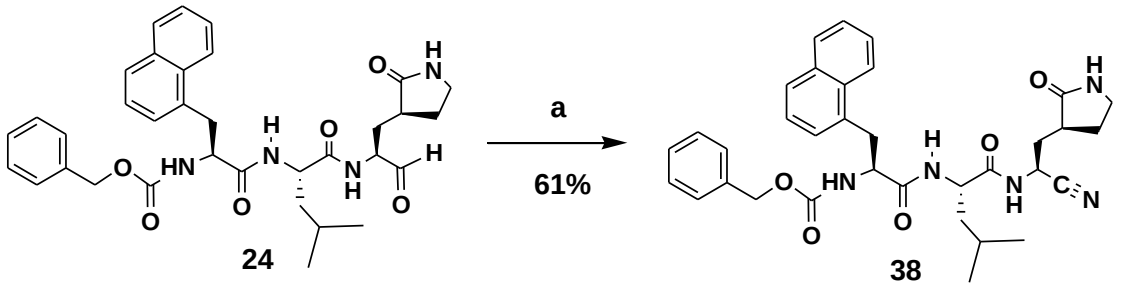

Reagents and Conditions: (a) $PhI(OAc)_2$, SDS, NH_4OAc, water, 70^{o}C, 9 h.

In order to synthesize thiazole warhead **39**, a series of reactions were carried out as shown in Scheme 16.

Scheme 16: Synthesis of Tripeptidyl-thiozole 39.

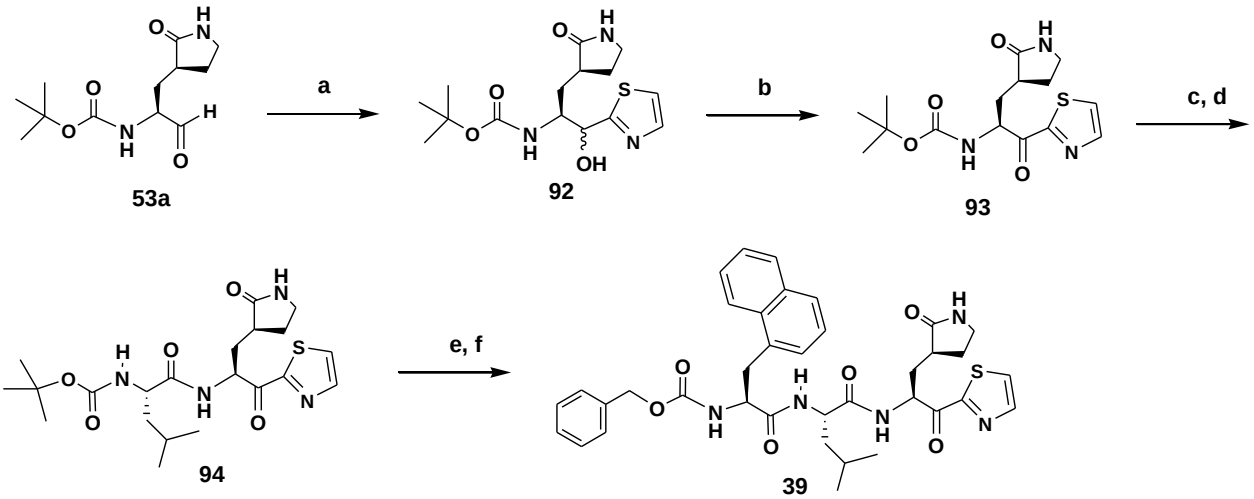

Reagents and Conditions: (a) *n*-Buli, thiazole, THF, -78^{o}C, 3h, 36%; (b) DMP, CH_2Cl_2, 25^{o}C, 2 h, 80%; (c) 10% TFA/CH_2Cl_2, 25 ^{o}C, 4 h, yield 100%; (d) Boc-NH-Leu-CO_2H, EDCI, DMAP, CH_2Cl_2, 25 ^{o}C, 18 h, 55%; (e) 10% TFA/CH_2Cl_2, 25 ^{o}C, 4 h, yield 100%; (f) Cbz-NH-1-napthylalanine-CO_2H, EDCI, DMAP, CH_2Cl_2, 25 ^{o}C, 18 h, 37%.

The thiazole methine proton was removed with *n*-butyllithium and the thiazole anion was treated with aldehyde **53a** to afford the alcohol **92** as a mixture of two diastereomers. Oxidation of the alcohol **92** with DMP provided ketone **93** in excellent yield. The *N*-boc protecting group of **93** was quantitatively removed using 10% TFA in methylene chloride and the resulting amine was coupled with the P2 leucine to give compound **94** in a 55% yield. The *N*-boc protecting group of **94** was similarly removed using 10% TFA in methylene chloride and the resulting amine was coupled with the P3 Cbz-*N*-1-napthylalanine to provide the tripeptidyl thiazole **39** in 37% yield.

The epoxyketone **40** and **41** were synthesized according to Scheme 17. An organometallic intermediated, formed from the combination of 2-bromopropene and nickel dichloride, was added to the aldehyde functionality of **53a** to form alcohol **95** as a mixture of two diastereomers. The alkene of **95** was converted to epoxide functionality using *m*-CPBA after which the alcohol was oxidized to ketone to furnish two stereoisomers of epoxyketone **96** which were separable by silica gel column chromatography. The more polar isomer is denoted **96-mp** and the less polar isomer is denoted **96-lp** and the absolute stereo configuration of each was not determined. The two isomers of **96** were treated separately with 10% TFA in methylene chloride to remove the boc protecting group followed by EDCI mediated coupling with *N*-Boc-leucine to afford the dipeptides **97-lp** and **97-mp**. These dipeptides were again separately treated with 10% TFA in methylene chloride to remove the boc protecting group followed by EDCI mediated coupling with *N*-Cbz-1-napthylalanine to afford the tripeptides **40** and **41**.

In order to replace the *N*-terminal cap with other groups the ester **84** is a convenient starting point since the *N*-terminal Cbz cap can easily be removed by palladium (carbon) and hydrogen gas (Scheme 18). This provided the amine **98** in quantitative yield after 3 hours. The alternative *N*-terminal caps were installed by an EDCI mediated coupling of the appropriate carboxylic acid to form the amide bond in compounds **99** and **100**. The ester groups of **99** and **100** were separately converted smoothly into their corresponding aldehydes **44** and **45** by a reduction/reoxidation technique using sodium borohydride and DMP respectively.

Scheme 17: Synthesis of Tripeptidyl-Epoxyketones 40 and 41.

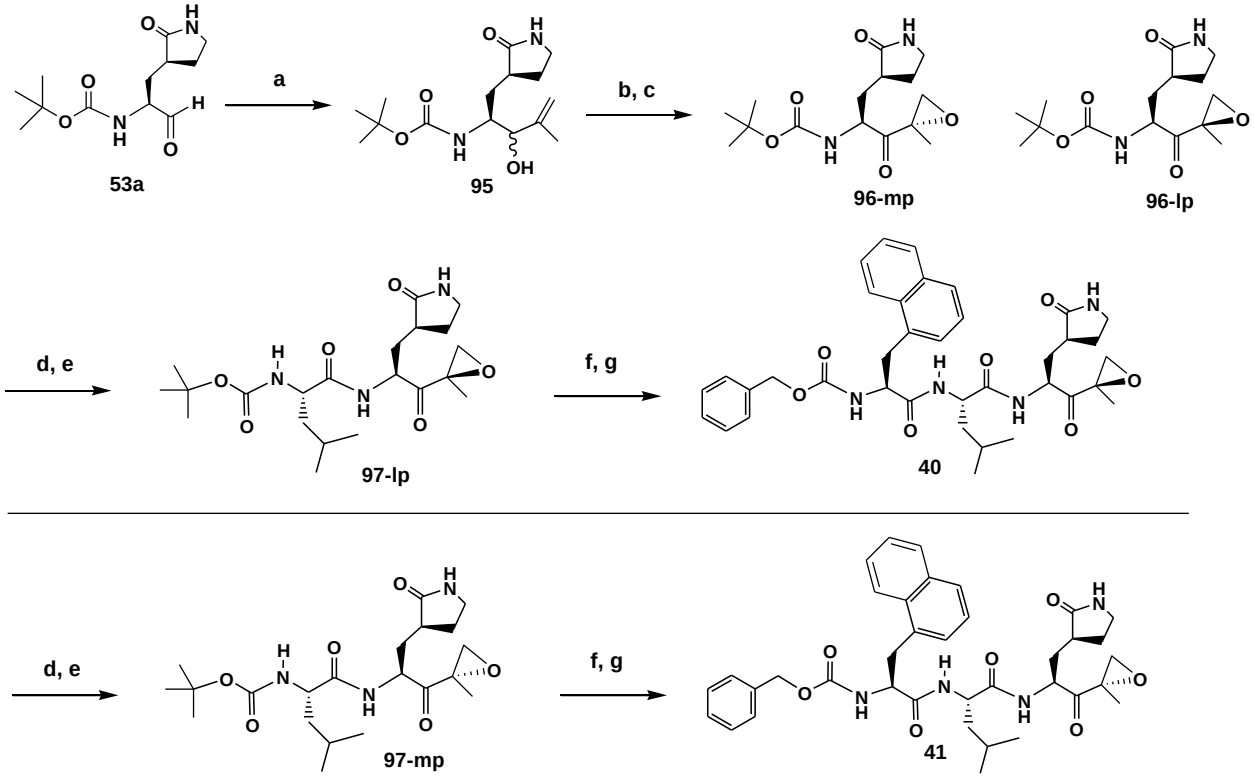

Reagents and Conditions: (a) 2-bromopropene, $NiCl_2$, DMF, 25^oC, 1 h; (b) *m*-CPBA, $NaHCO_3$, CH_2Cl_2, 0^oC, 2h; (c) DMP, CH_2Cl_2, 25^oC, 2 h, 55% (2 steps); (d) 10% TFA/CH_2Cl_2, 25^oC, 4 h, yield 100%; (e) Boc-NH-Leu-CO_2H, EDCI, DMAP, CH_2Cl_2, 25^oC, 18 h, 51%; (f) 10% TFA/CH_2Cl_2, 25^oC, 4 h, yield 100%; (g) Cbz-NH-1-napthylalanine-CO_2H, EDCI, DMAP, CH_2Cl_2, 25^oC, 18 h, 72%.

Scheme 18: Synthesis of Tripeptides 44 and 45 with Different N-Terminal Caps.

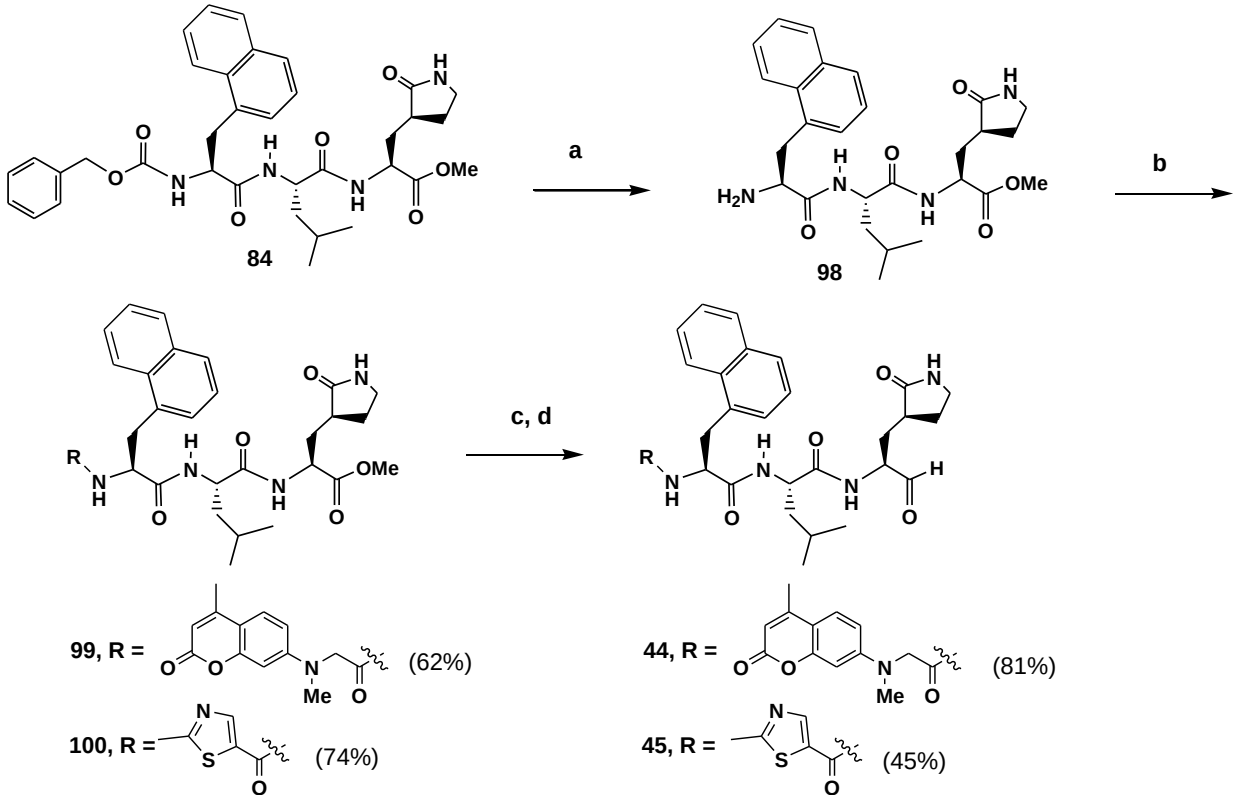

Reagents and Conditions: (a) Pd(C), H_2(g), MeOH, 25^{o}C, 3 h, 100%; (b) R-CO_2H, EDCI, DMAP, CH_2Cl_2, 25^{o}C, 18 h; (c) $NaBH_4$, CH_2Cl_2/EtOH/MEOH (5:3:2), 0^{o}C, 4 h, 100%; (e) DMP, CH_2Cl_2, 25^{o}C, 2 h.

In order to synthesize compound **44** the acid precursor **104** was required to be synthesized as shown in Scheme 19. Commercially obtained AMC (**101**) was alkylated using methylbromoacetate in refluxing acetonitrile followed by methylation of the amine with methyl iodide and potassium carbonate in refluxing acetonitrile. Lastly, the ester was hydrolyzed using sodium hydroxide in dioxane/water to provide the acid **104**.

Scheme 19: Synthesis of AMC Cap 104.

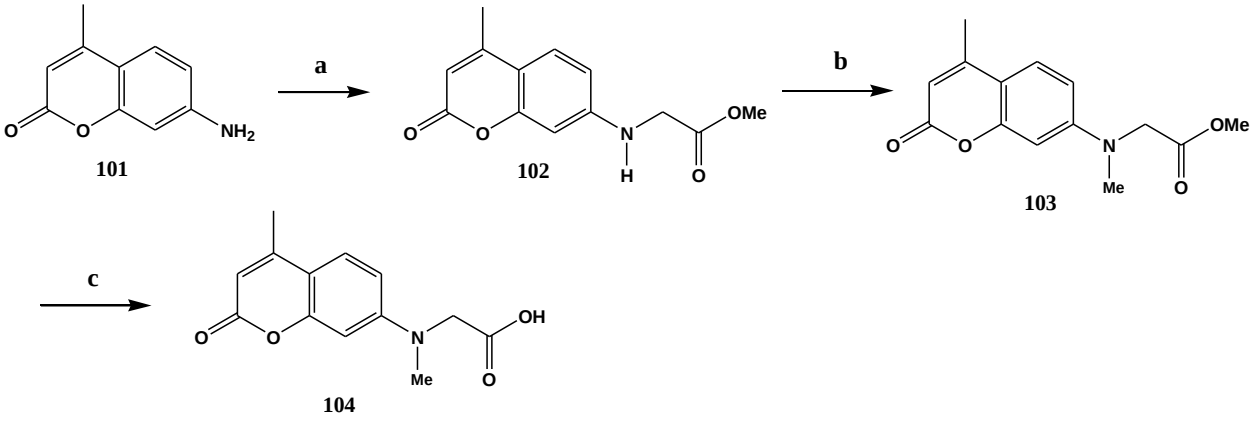

Reagents and Conditions: (a) methylbromoacetate, NaI, DIPEA, CH_3CN, 82^oC, 18 h, 85%; (b) MeI, K_2CO_3, 82^oC, 18 h, 24%; (c) NaOH, dioxane/water, 25^oC, 1 h, 100%.

The synthesis of the macrocyclic NPI candidates **47** and **48** was carried out according to Scheme 20. The crude diene **105** was obtained from Groutas group and was purified by silica gel column chromatography before treatment with Grubbs second generation catalyst, to form ring-closing metathesis product **106** in good yield. The double bond that resulted was reduced with hydrogen and palladium (carbon) to form compound **107** in quantitative yield. Compound **47** was obtained by removing the *N*-boc protecting group of **107** with 10% TFA in methylene chloride and replacing it with Cbz using benzylchloroformate in methylene chloride and dioxane. The aldehyde **48** was smoothly obtained from **47** using the standard reduction/re-oxidation technique with sodium borohydride and DMP respectively.

Scheme 20: Synthesis of Macrocyclic Tripeptidyl Ester 47 and Aldehyde 48.

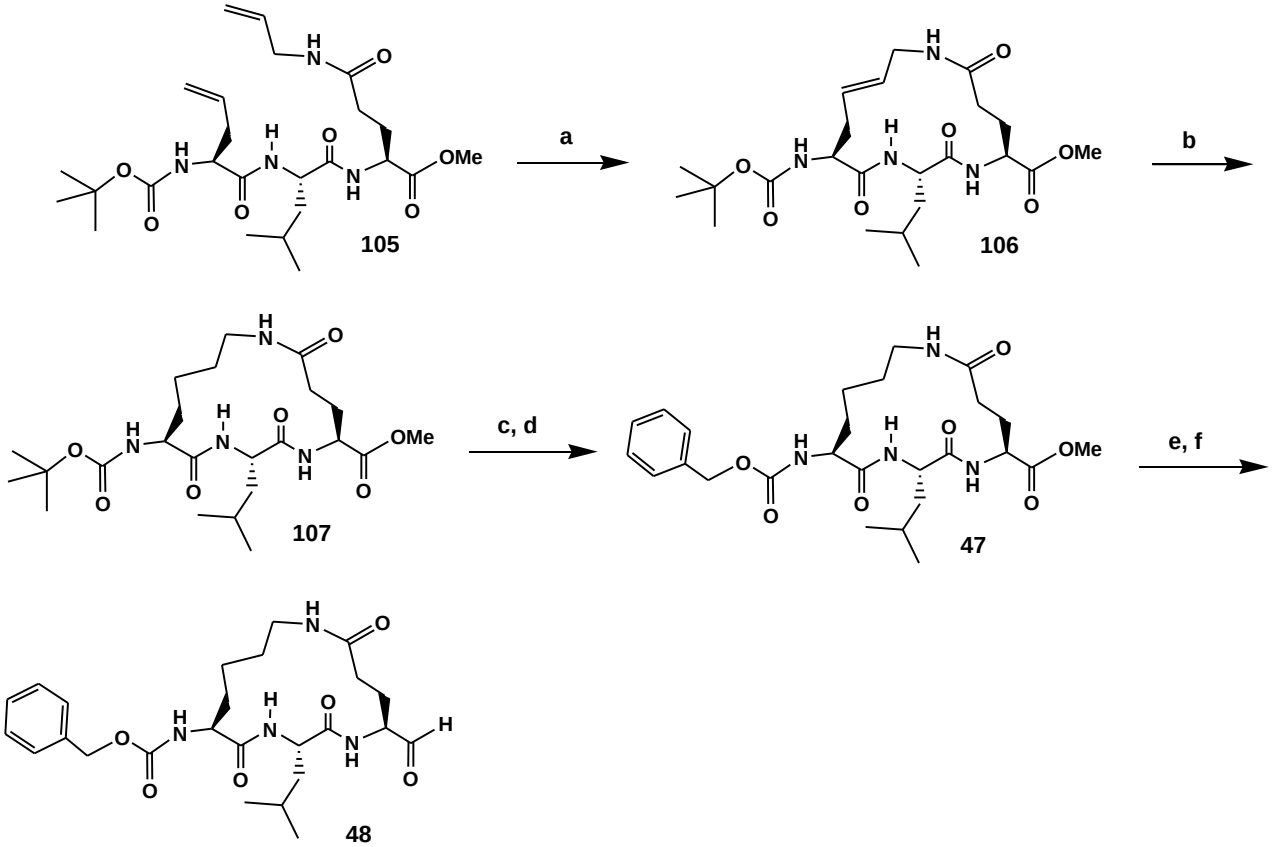

Reagents and Conditions: (a) Grubbs catalyst (2nd gen), CH_2Cl_2, 40°C, 48 h, 57%; (b) Pd(C), H_2(g), MeOH, 25°C, 20 h, 100%; (c) 10% TFA/CH_2Cl_2, 25 °C, 4 h, yield 100%; (d) Cbz-Cl, DMAP, CH_2Cl_2/dioxane (4:1), 25°C, 2 h, 72%; (e) $NaBH_4$, CH_2Cl_2/EtOH/MEOH (5:3:2), 0°C, 4 h, 100%; (f) DMP, CH_2Cl_2, 25°C, 2 h, 92%.

I.IV. Conclusion

Noroviruses fall into the family of Caliciviridae viruses and are non-enveloped, single stranded RNA viruses that are the leading cause of severe gastroenteritis worldwide. Currently no drug or vaccine is available for norovirus treatment or prophylaxis. We describe herein a novel class of tripeptidyl anti-noroviral compounds which strongly inhibit NV3CL^{pro} in enzyme and cell based assays. The most active compound in enzyme and cell based assays was compound **24** (IC_{50} 0.14 µM; EC_{50} 0.04 µM). This compound has an aldehyde warhead, a P1 glutamine surrogate, a P2 leucine, a P3 L-1-napthylalanine and an *N*-terminal Cbz cap. The corresponding bisulfite adduct, compound **35** showed comparable activity to **24** in enzyme and cell based assay (IC_{50} 0.24 µM; EC_{50} 0.04 µM). The corresponding ketoamide warhead derivative also showed good activity with an IC_{50} of 2.6 µM and EC_{50} of 4.2 µM. Compounds **25**, **28**, **29**, **30**, **31** and **46** also showed excellent and very similar EC_{50} values with **24**. Compound **24** and its ketoamide derivative **32** were screened against other viral strains in the CV, PV and coronaviridae (CoV) viral families using enzyme and cell based assays. The results were encouraging as both **24** and **32** were found to be strongly active in human rhino virus (HRV) and SARS viral assays. This suggests advantageous broad spectrum anti-viral activity for these compounds. The compounds showed minimal cell cytotoxicity. An x-ray crystal structure was obtained for compound **24** with SARS protease enzyme and proves that **24** binds with and targets the active site. Further SAR studies are ongoing to improve activity and bioavailability for the lead compounds.

II. Facial Surface Modification of Graphene Oxides with *tert*-Butyl Ester and Carboxylic Acid Functionality and Its Study in a Bioelectronic Sensor Device to Detect Noroviral RNA.

II.I. Introduction

Graphene oxide (GO) is a newly discovered material that has a similar two dimensional atomic structure to graphene, except, GO has randomly distributed aromatic regions and is highly decorated with oxygen containing groups such as hydroxyl, epoxide and carboxylic acid (Figure 16).[54]

Figure 16: Structures of Graphene and Graphene Oxide

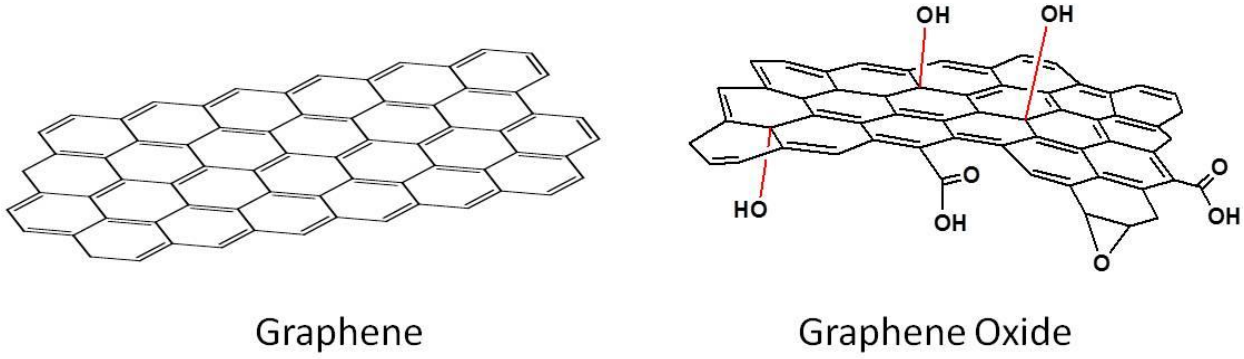

GO is prepared using strong oxidizing agents in acidic media[55] (e.g. Hummers method),[56] treatment with ozone[57] or chemical/thermal exfoliation of graphite oxide.[58] The oxidation process removes many of the sp^2 hybridized carbons and replaces them with sp^3 hybridized carbons with bonds to oxygen. The result is that GO exhibits lower electrical conductivities than its graphene precursor. A study by Jeong *et al.* showed that the band gap of GO is dependent on the degree of oxidation (oxygen-to-carbon ratio) and had values ranging from 1.7 to 2.4 eV.[59] The band gap values reported by Jeong *et al.* were extracted from the UV–visible diffuse reflection spectroscopy data recorded at room temperate. A study by Huang *et al.* showed that the band gap of GO increases with increasing oxygen-to-carbon ratios.[60] The band gap is the energy difference (in eV) between an outer shell ground state valence electron and the bottom of the conduction band. Electrons in the valence shell are immobile whereas electrons excited to a

conduction band are free to move around the solid and be mobile charge carriers. The size of the band gap is important because it may determine whether the solid material will behave as a conductor, semiconductor or insulator. Usually when the band gap energy is greater than 3 eV an insulator exists. Since GO has been found to have band gap energies from around 1.7 to 2.4 eV *vide supra*, they display semiconducting electrical properties.

GO has attracted a lot of interest due to its semiconductor properties, high intrinsic mobility,[61] good water dispersibility, high mechanical strength, large theoretical specific surface area,[61] high Young's modulus,[61] low cell toxicity,[62] fluorescence quenching ability[63] and facile surface modification.[64] Reports of GO functionalization using the carboxyl groups of GO with PEG,[65] chitosan[66, 67] ferrocene,[68] imidazolium fragments,[69] peptides,[70] triphenylamine-based polymers[71] and folic acid[72] have demonstrated that chemical modification of GO is possible. Reports have suggested that the PEG and chitosan modified GO could have use in drug delivery applications as they can be internalized by cells and with low cellular toxicities.[62] Functionalization of GO at the sp^2 hybridized surface has also been demonstrated using carbethoxycarbene under microwave irradiation,[73] photo-initiated radical polymerization with 2-chloro-2-methyl-1-phenyl-1-propanone[54] and reactions of diazo-benzoic acid with reduced GOs.[74] Due to their extraordinary chemical and physical properties, GO and its graphene precursor are finding their full potentials in important fields such as biomedical, bioanalytical, nanoelectronics, materials science, energy technology and catalysis.[64, 75-77]

Most of the GO modifications have made use of the epoxy[73] and carboxylic groups[73] and thus little work describing functionalization of GO using the surface hydroxyl groups has been done. Our brief work in this area has involved the synthesis and characterization of a *t*-butyl ester and carboxylic acid functionalized GO and probed its potential for application in a biosensor devise. Some ground work was also done in synthesizing one sided DNA functionalized GO using a solid phase synthesis.

II.II. Synthesis and Characterization of *t*-Butylester and Carboxylic acid Functionalized Graphene Oxide

The first requirement for such a project was a synthetic route to access good quality, large, single layered GO sheets. The synthetic method that was followed was similar to modified Hummers method[56] except the graphite was pre-expanded using a microwave reactor before any oxidative treatments (Scheme 21). The pre-expansion step proved to be necessary to increase the overall yield of GO (~60%) probably because it helps separate the graphite layers allowing for easier access of oxidizers and therefore more effective oxidation. The expanded graphite is subsequently treated with P_2O_5 and $K_2S_2O_8$ in HCl at 85°C for 4 hours which causes pre-oxidation of the graphite to graphitic oxide. The graphitic oxide is then oxidized to graphene oxide using $KMnO_4$ in H_2SO_4 at 40°C for 2 hours which oxidizes and exfoliates the graphitic oxide into thin sheets of GO. A mixture of suspended GO sheets and insoluble inorganic metal compounds is then treated with H_2O_2 which helps solubilize any metal precipitates. After standing at room temperature for 2 days the GO settles to the bottom and can be recovered by carefully decanting the supernatant. The GO residue is washed with dilute HCl, dialyzed and lyophilized to provide GO **108** as a light brown fluffy solid.

Scheme 21: Synthesis of Graphene Oxide using a Modified Hummers Method.

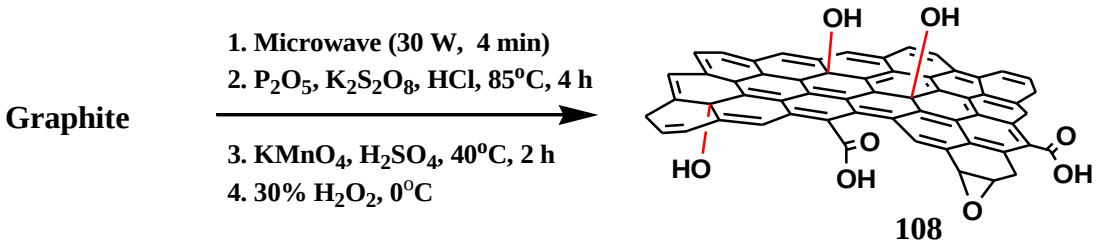

108

The FTIR and Raman spectra obtained for the GO compares favorably to literature values. The FTIR spectrum of GO has a broad and strong absorption in the region of 3340 cm^{-1} which corresponds to O-H stretching vibrations of hydroxyl and carboxyl functionalities. There are also prominent absorption bands at 1737 cm^{-1} and 1631 cm^{-1} that result from C=C stretching vibrations of the carbon framework that likely contains isolated, conjugated and aromatic C=C

functionalities. A strong absorption at 1076 cm^{-1} could be due to C-O stretch vibrations as the surface of GO is decorated with many hydroxyl and epoxy groups.

The Raman spectrum obtained for GO **108** did contain the expected D, G and 2D (also called G') bands that are characteristic for GO (Figure 17). The 2D band is designated "2D" since its wavenumber value is approximately double to that of the D band value.[78] Some prefer to call the 2D band the G' band to avoid confusion with the term "two dimensional" (also called 2D).[78]

Figure 17: Raman Spectrum of Synthesized GO 108.

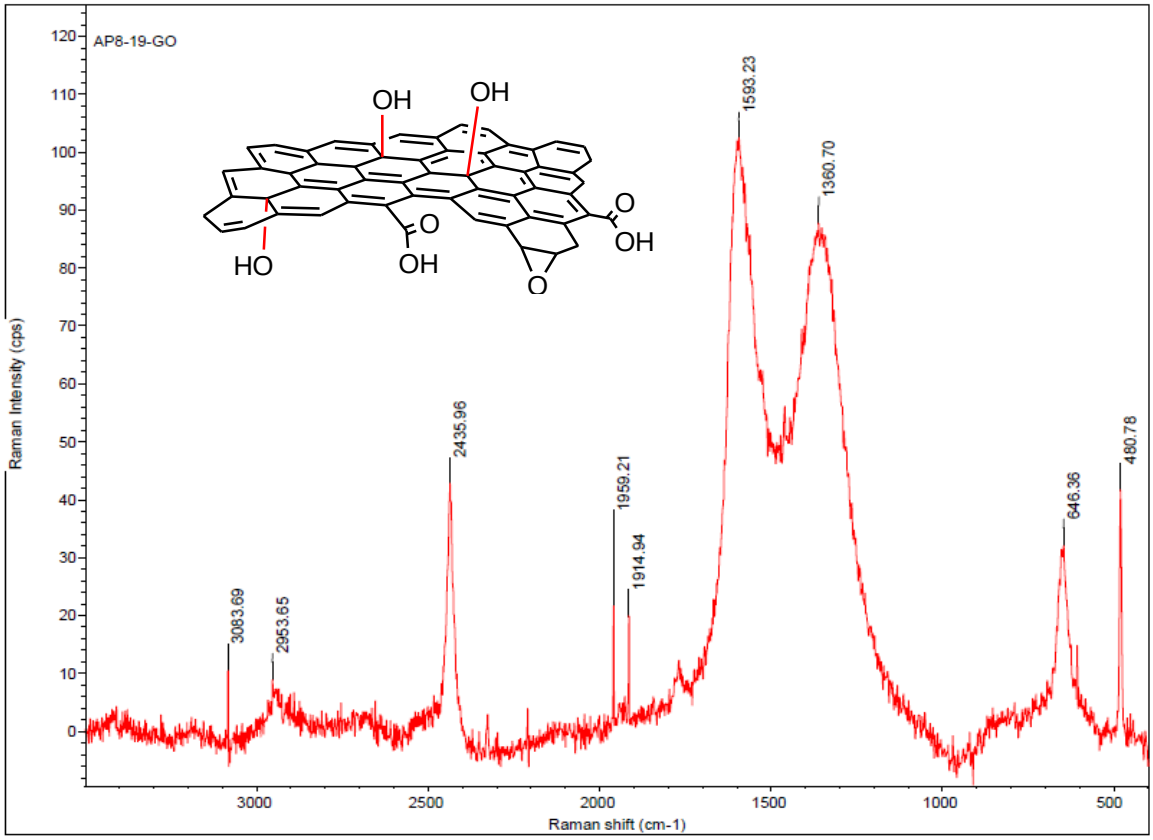

The G band resonance corresponds to the first-order scattering of the E_{2g} phonons[79] and is showing the in-plane vibrations of the carbon lattice.[80] The presence of a D-band is due to defects in the GO sheets and higher amount of "edges" as the sheets get smaller.[80] The D-band does not appear in pristine graphene.[81] The 2D band is due to second-order zone boundary phonons.[81] The G band in our synthesized GO resonates at 1593 cm^{-1} which is slightly blue field shifted when compared to the G band of the graphite starting material (1581 cm^{-1}). These values were exactly comparable to a literature report that showed the G band to shift from 1581 cm^{-1} in

graphite to 1593 cm^{-1} in GO.[80] The reason for this blue field shift has been attributed to the presence of more isolated C=C double bonds in GO which have resonance at slightly higher frequencies.[80] Other observations that were consistent with the literature was the presence of a broader G band and a more prominent D band in the Raman spectrum for GO when compared with the Raman spectrum of the graphite starting material.[80] This is attributed to the fact that GO has a higher degree of structural defects when compared with graphite or pristine graphene. The D-band/G-band intensity ratio, I(D)/I(G), was found to be 0.85.

The GO **108** was found to exist as mostly single layered sheets as seen by the AFM image (Figure 18) which shows the GO thickness to be 1.57 nm.

Figure 18: AFM image of GO 108 Showing Cross Sectional Height.

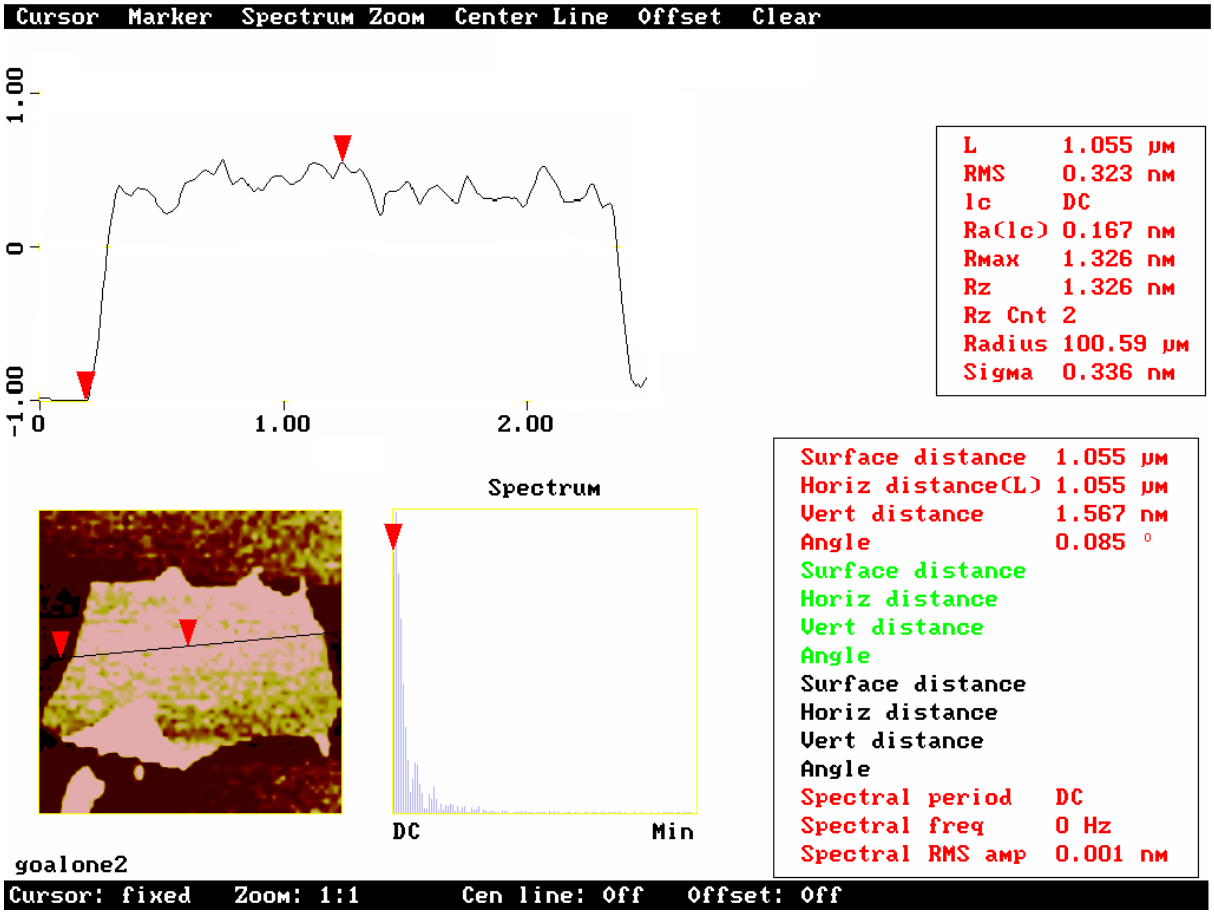

The synthesis of a *t*-butyl ester functionalized GO **109** was carried out according to Scheme 22. The GO **108** was suspended in distilled DMF and treated with NaH followed by *t*-butyl-bromoacetate. The NaH deprotonated the hydroxyl group protons and the resulting alkoxide ions underwent S_N2 substitution reaction with *t*-butyl-bromoacetate to form **109**.

Scheme 22: Synthesis of t-Butyl Ester Functionalized Graphene Oxide 109.

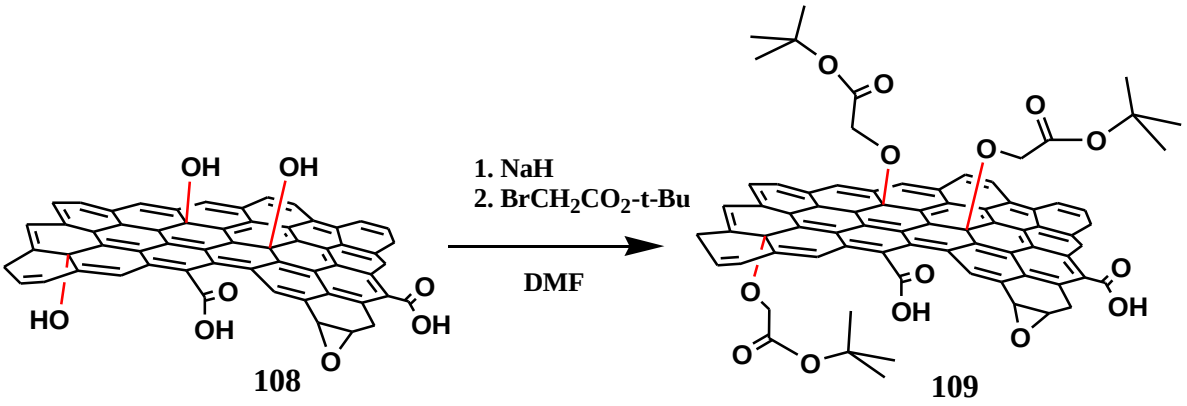

The reaction was monitored by NMR and FTIR to probe for reaction completeness. The reaction was sampled for any un-reacted *t*-butyl-bromoacetate after 19 and 48 hours by removing 108 µL of the reaction solution, spiking it with 10 µmol of an internal standard (phenyl acetic acid) and recording a proton NMR spectrum in deuterated chloroform. The theoretical concentration of *t*-butyl-bromoacetate inside the solvent before any chemical reaction was calculated to be 94 mM and so in the event that no reaction takes place, 10 µmol of *t*-butyl-bromoacetate should be present inside the 108 µL sampled aliquot. When integrating the methylene proton signals at 3.77 ppm and 3.64 ppm, which correspond to *t*-butyl-bromoacetate and phenyl acetic acid standard respectively, a ratio of 1:6 was found after 19 hours. This showed that after 19 hours only 17% of the *t*-butyl-bromoacetate remained and hence 83% has undergone chemical reaction. Since the proton NMR spectrum of the crude reaction did not show signs of significant decomposition of *t*-butyl-bromoacetate it was assumed that the *t*-butyl-bromoacetate had coupled with the GO. The reaction was again sampled after 48 hours and the ratio of the methylene proton signals at 3.77 ppm and 3.64 ppm changed to 1:7 respectively suggesting that after 48 hours only 14% of the original *t*-butyl-bromoacetate remained and hence 87% reaction completion. The additional 29 hours of reaction time only depreciated the amount of remaining *t*-

butyl-bromoacetate from 17% to 14% and so it was concluded that the reaction had reached near completion. Moreover, a small portion of the reaction mixture was centrifuged at 30000 rpm for 5 min to isolate GO material from the reaction. After washing the GO sediment with ether (x1) and water (x3) the sample was lyophilized and its Raman and FTIR spectrum were recorded (Figure 19 and 20). The Raman spectrum for GO-ester **109** (Figure 19) showed a prominent D-band and G-band at 1345 cm^{-1} and 1589 cm^{-1} respectively with a I(D)/I(G) ratio of 0.96. The higher I(D)/I(G) ratio in GO-ester **109** results from a more intense D-band and suggests a higher level of disorder in the GO lattice due to chemical functionalization. A small 2D band at 2435 cm^{-1} in the Raman spectrum was also observed.

Figure 19: Raman Spectrum of t-Butylester Functionalized Graphene Oxide 109

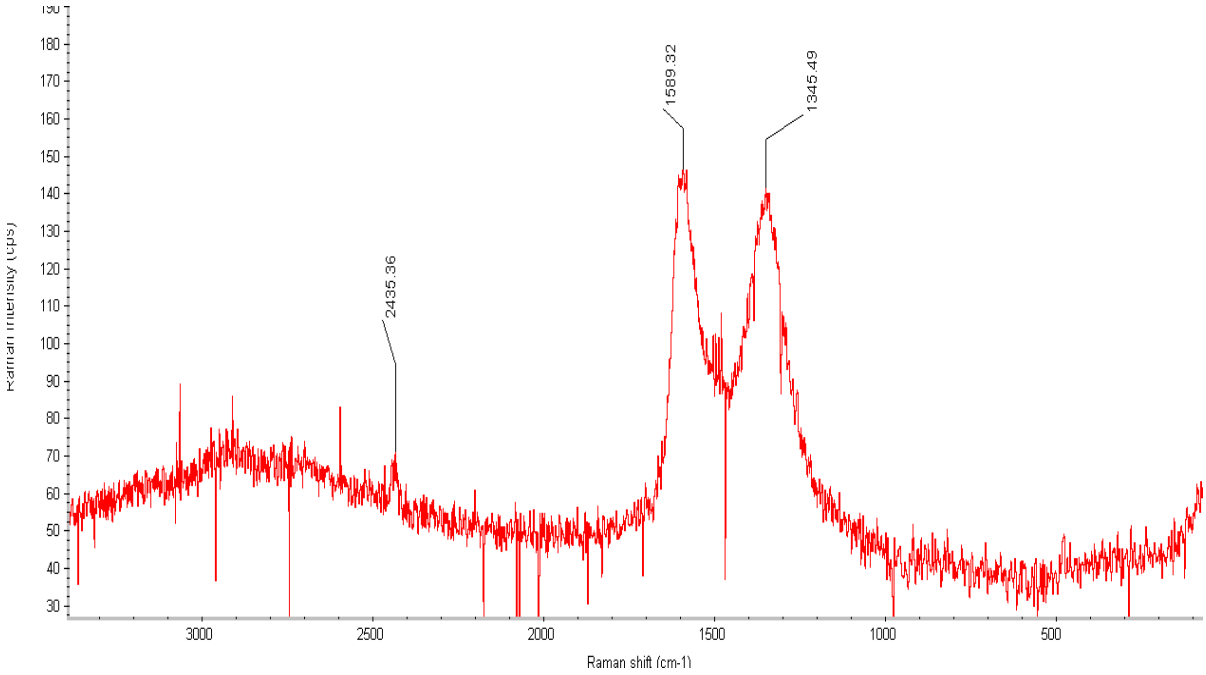

The FTIR spectrum is overlaid with the original GO spectrum for comparison (Figure 20). It is evident that many structural features have changed suggesting successful functionalization of the surface of GO with *t*-butylester. Firstly, the strong O-H stretching signal at 3359 cm^{-1} in the GO spectrum (top) has reduced in intensity (bottom) showing loss of hydroxyl functionality. The bottom spectrum shows the presence of sp^3 C-H stretching vibrations at 2977 and 2931 cm^{-1} which should be coming from methylene and methyl C-H bonds contained in the *t*-butylacetate

moiety. The bottom spectrum shows a strong absorption at 1722 cm^{-1} which corresponds to a carbonyl (C=O) stretch suggesting the *t*-butylester group is attached and a strong absorption at 1141 cm^{-1} which corresponds to a C-O (*O*-*t*-butyl) stretching vibration.

Figure 20: Overlaid FTIR Spectra of GO 108 and t-Butyl Ester Functionalized GO 109.

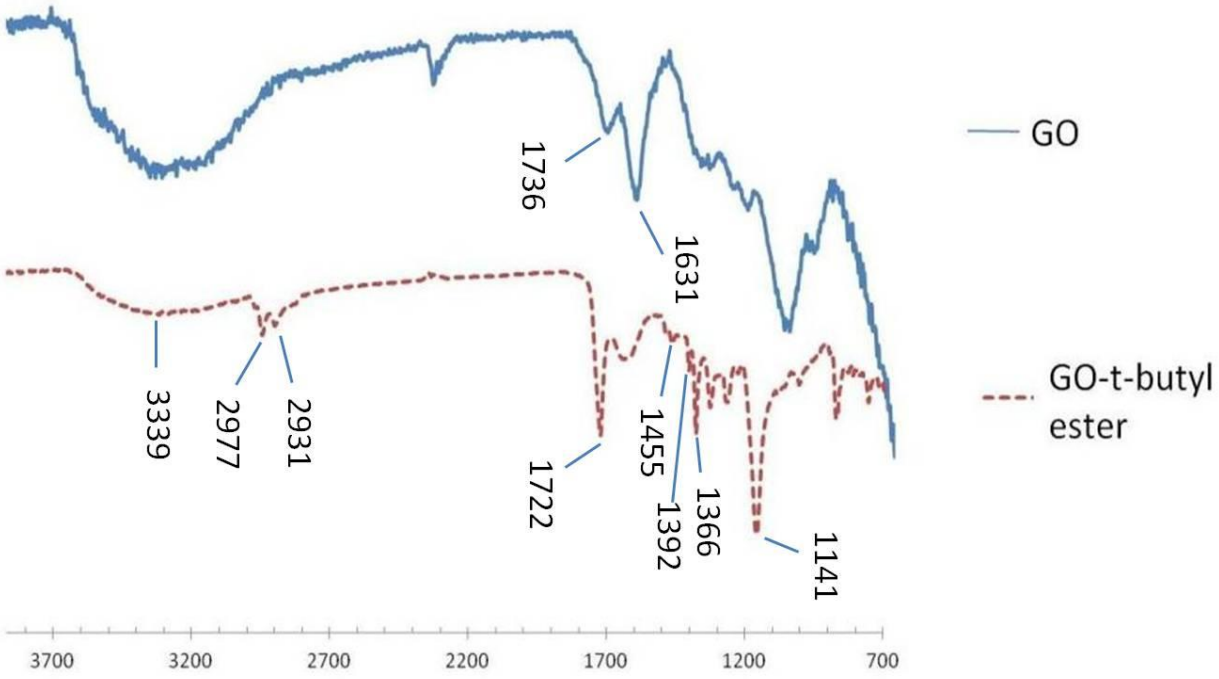

To further validate that these reaction conditions will attach a *t*-butylacetate functionality to the GO surface, a ^{13}C labeled *t*-butylbromoacetate **112** was synthesized and used in the coupling reaction with GO. The synthesis of **112** is shown in Scheme 23, and started from commercially available ^{13}C-acetic acid **110**. Compound **110** was first converted into a mixed anhydride intermediate using TFA anhydride followed by α-bromination using one equivalent of bromine liquid to yield ^{13}C labeled bromoacetic acid **111** in quantitative yield. The carboxylic acid moiety of **111** was alkylated using isobutylene in dichloromethane to yield the *t*-butyl ester **112** in 63% yield.

Scheme 23: Synthesis of ^{13}C labeled t-Butyl-bromoacetate 112.

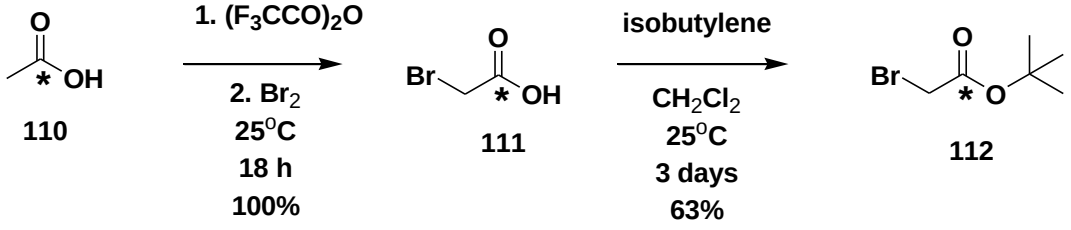

With the ^{13}C labeled *t*-butylbromoacetate **112** in hand, the GO alkylation reaction was repeated as shown is Scheme 24, employing the same reaction conditions used to previously make compound **109**. The NaH deprotonated the hydroxyl group protons of GO and the resulting alkoxide ions underwent S_N2 substitution reaction with ^{13}C-labeled *t*-butyl-bromoacetate to form **113**.

Scheme 24: Synthesis of ^{13}C-labeled t-Butyl Ester Functionalized Graphene Oxide 113.

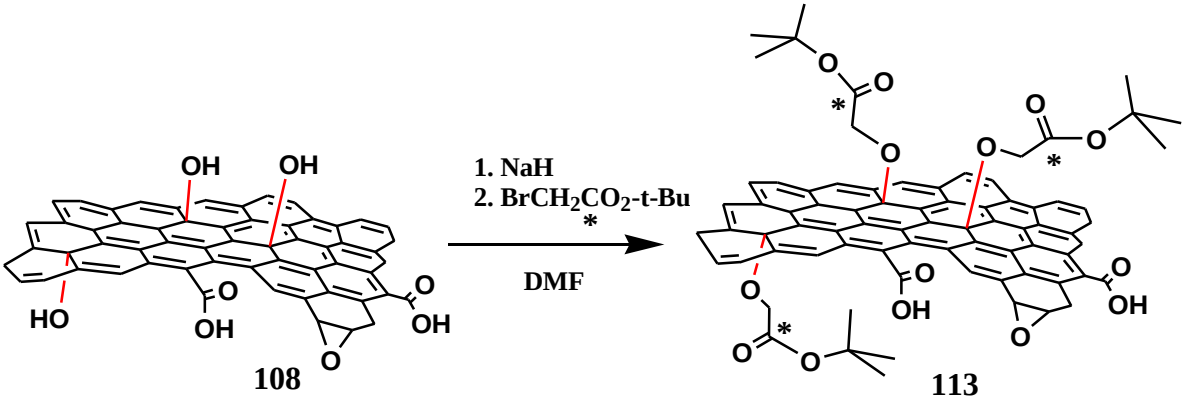

The reaction was similarly monitored by proton NMR using an internal standard *vide supra* and the reaction was deemed complete after 6 days. The reaction was worked up by high speed centrifugation to remove un-reacted organic material contained in the supernatant. The functionalized GO sediment was washed vigorously with ether (x1) and deionized water (x3) using centrifugation and careful removal of the supernatant layer after each wash cycle. The washed compound **113** was suspended in deionized water and lyophilized to give **113** as a light brown fluffy solid. FTIR analysis of compound **113** showed a reduction in the O-H stretching absorbance and the appearance of a strong carbonyl C=O stretching absorbance at 1647 cm^{-1} suggesting successful alkylation of GO. Most interesting was the solid state carbon NMR spectra for GO **108** and the ^{13}C labeled GO **113** which are overlaid in Figure 21.

Figure 21: Solid State NMR Spectra for GO 108 and ^{13}C-t-Butyl ester Functionalized GO 113.

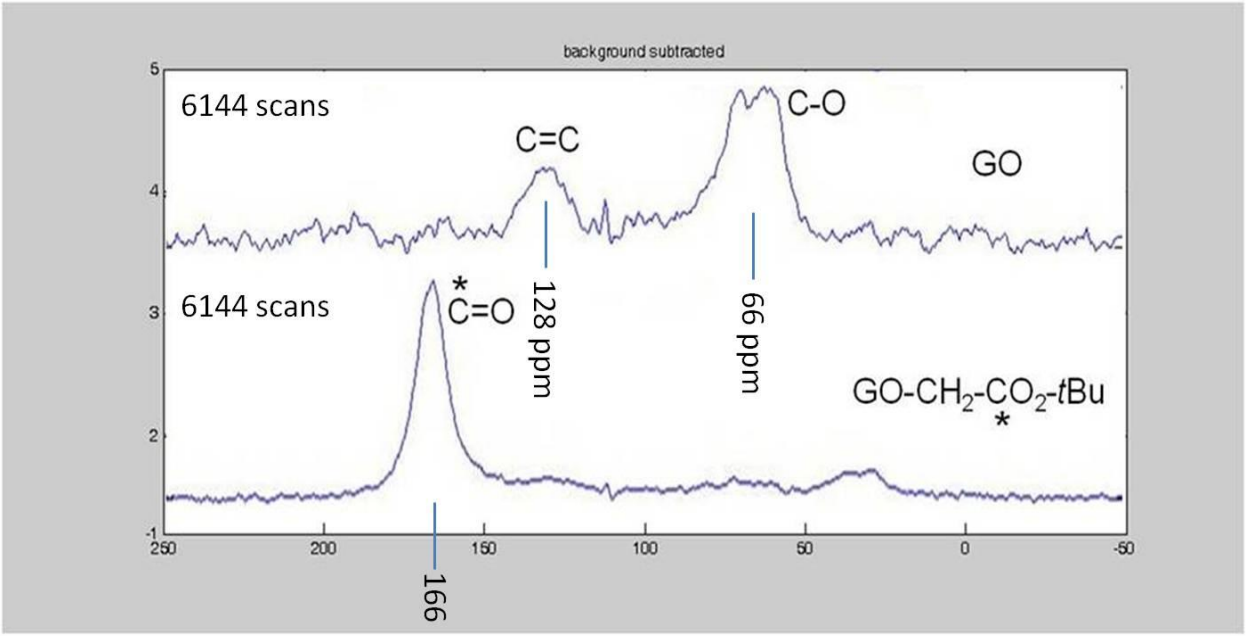

The top carbon NMR spectrum in Figure 21 shows the GO starting material, and was recorded with 6144 scans. The broad peaks at 128 ppm and 66 ppm arise due to the presence of C=C and C-O carbons respectively. The bottom carbon NMR spectrum was obtained for compound **113** after 6144 scans, and clearly shows the presence of a dominant peak at 166 ppm. This was assigned as the ^{13}C-labeled carbonyl (*C=O) carbon, and helps to support a successful alkylation reaction with *t*-butyl-bromoacetate. To our knowledge this is the first report of a ^{13}C-labeled GO where the ^{13}C label is grafted onto the GO surface through chemical functionalization. Previously, in 2008, a ^{13}C-labeled GO with carbon backbone labeling was reported by Cai *et al.*.[82] Their ^{13}C-labeled GO was synthesized from ^{13}C-graphene. The ^{13}C-labeled graphene was synthesized by a thermal chemical vapor deposition (CVD) method incorporating ^{13}C-methane gas.[82] Cai *et al*. analyzed their ^{13}C-labeled GO with solid state NMR spectroscopy which clearly showed strong resonance belonging to the sp^2 hybridized carbon lattice (C=C) as well as sp^3 hybridized C-O functionalities.[82]

The *t*-butyl group of **109** was hydrolyzed to carboxylic acid **114** by employing 10% TFA in water (Scheme 25). The reaction was monitored by mass spectrometry and FTIR.

Scheme 25: Synthesis of Carboxylic Acid Functionalized Graphene Oxide 114.

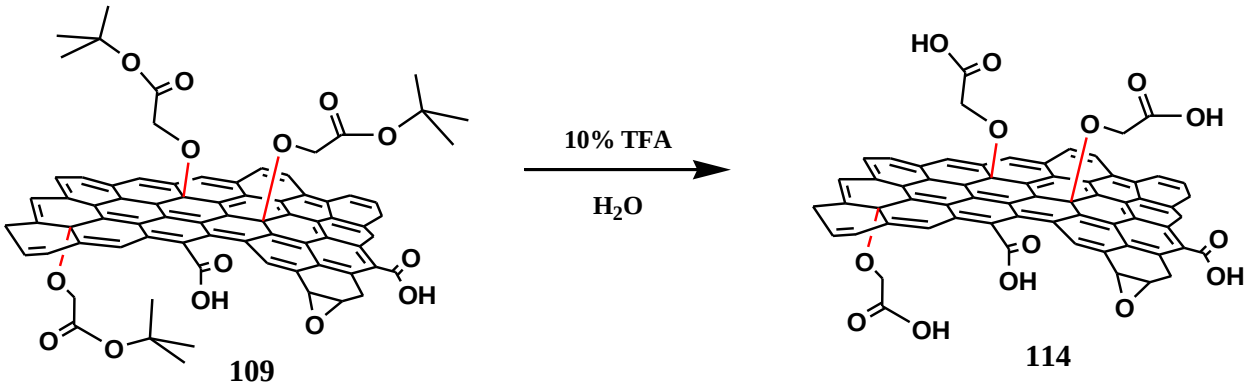

During exposure of the *t*-butyl ester **109** with TFA, it is expected that the carbonyl oxygen will become protonated which catalyses the cleavage of the ester C-O bond giving rise to the carboxylic acid and a tertiary carbocation (*t*-butyl). Since the reaction is carried out under aqueous conditions, the tertiary carbocation should be scavenged rapidly by a water molecule to form *t*-butanol. The production of *t*-butanol coming from the TFA hydrolysis reaction was therefore monitored by mass spectrometery equipped with electrospray ionization (ESI), and the results are shown in Figure 22.

Firstly, a dilute solution (~50 µM) of authentic *t*-butanol was prepared and analyzed by mass spectrometry using ESI in the positive mode with a declustering potential of 130 mV. This showed that *t*-butanol can be detected under these mass spec conditions because a prominent peak for *t*-butanol at m/z = 97.2 $(M+Na)^+$ was observed. A background mass spectrum was also taken by infusing 100% methanol into the mass spectrometer which proved that no peaks in the vicinity of 97.2 are coming from the background.

Figure 22: Monitoring of the Intensity of t-Butanol $(M+Na)^+$ Peak in Mass Spectrum over Time During TFA Hydrolysis of 109 to form compound 114.

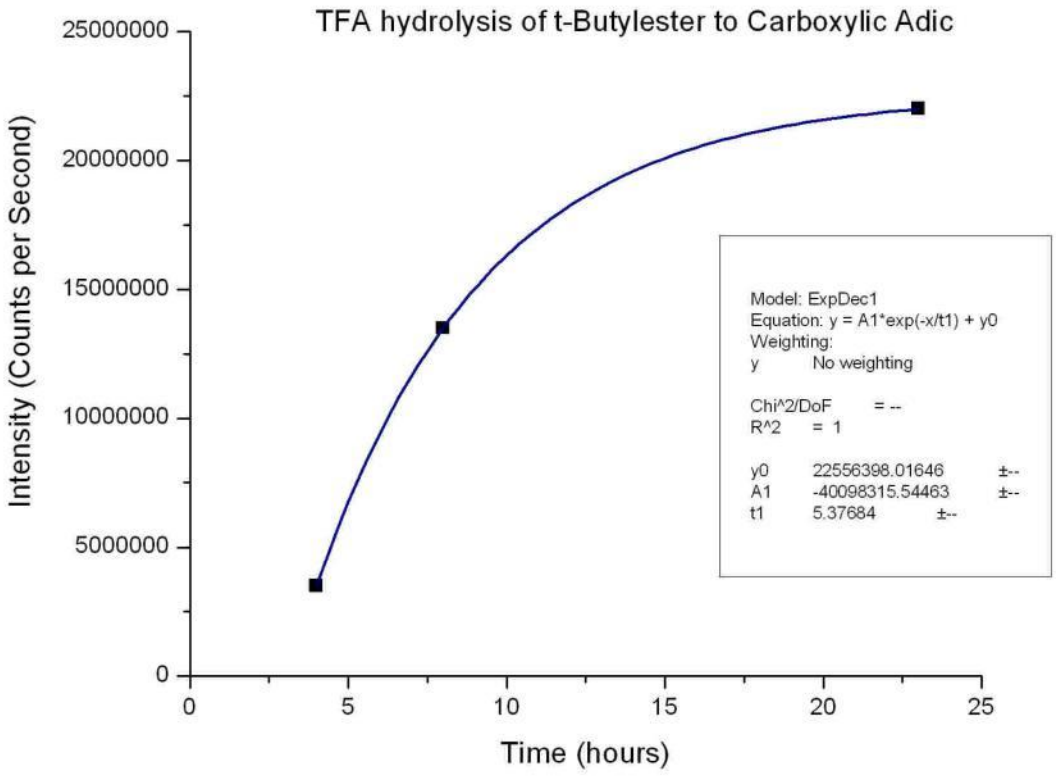

The TFA hydrolysis reaction was sampled for the presence of *t*-butanol after 4, 8 and 23 hours by infusing exactly 50 µL of the reaction solution into the mass spectrometer after applying a 1000 fold dilution in clean methanol and filtration through a 0.2 micron syringe tip filter. In each case, data was obtained by averaging 54 scans and the intensity (counts per second) for the $(M+Na)^+$ at m/z 97.2 was recorded and plotted against time. Figure 20 shows a plot of $(M+Na)^+$ peak intensity versus time and shows that the concentration of *t*-butanol increased during the course of the reaction and followed a negative exponential increase (R^2=1) reaching a maximum after 23 hours. This result confirmed that *t*-butanol is generated from the TFA hydrolysis reaction and that the GO-ester **109** is successfully converted into GO-carboxylic acid **114**.

The black suspended GO material was monitored by FTIR during the course of the TFA hydrolysis reaction over 24 hours, and the results are shown in Figure 23 as stacked FTIR spectra.

Figure 23: TFA hydrolysis of t-Butylester 109 to Carboxylic acid 114.

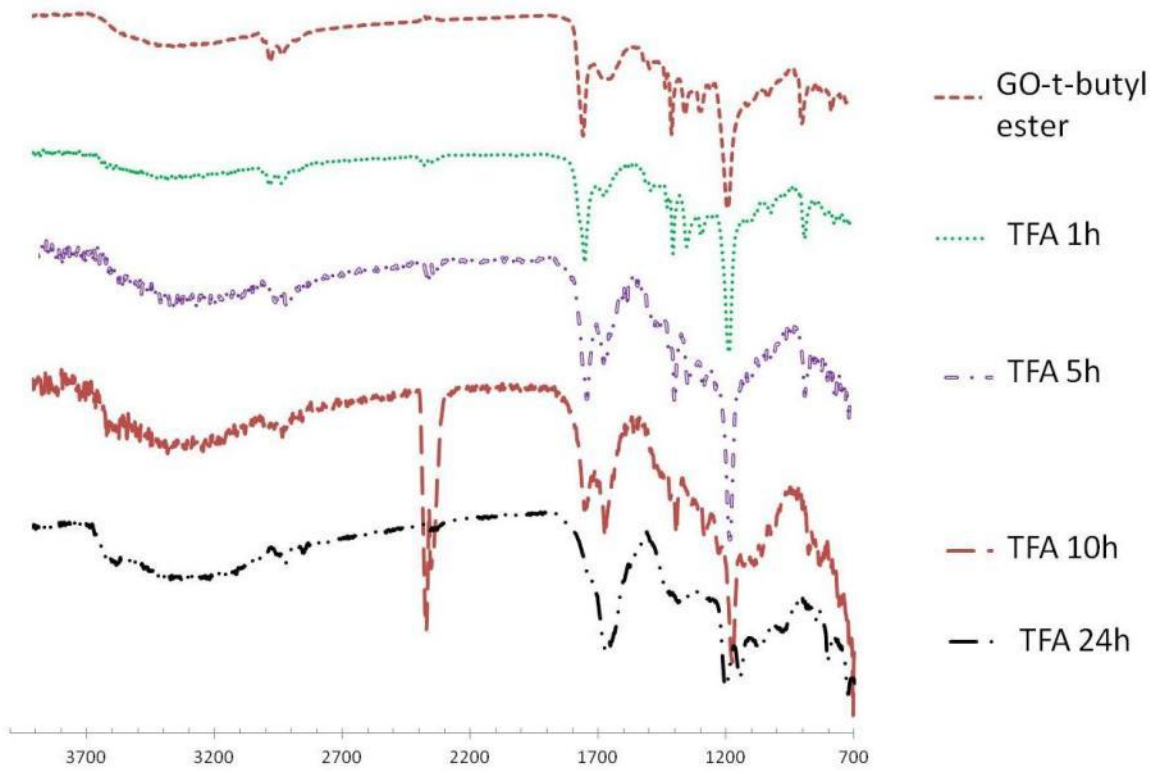

Over the course of 24 hours the O-H stretching absorption at 3359 cm^{-1} increased in intensity and took on a broader shape, suggesting the formation of carboxylic acid. The sp^3 C-H stretching vibrations at 2977 and 2931 cm^{-1} diminished in intensity and shifted slightly to 2923 and 2851 cm^{-1}. The strong carbonyl C=O stretch absorption at 1722 cm^{-1} gradually disappeared and a new strong absorption at 1674 cm^{-1} appeared, which may be the result of overlapping C=O (carboxylic acid) and C=C functional group absorptions. The strong absorption at 1142 cm^{-1} due to the C-O (*O*-*t*-butyl) stretching vibration in **109** diminished and new peaks at 1200 and 1145 cm^{-1} were recorded. The strong absorption at ~2400 cm^{-1} seen in the spectrum of TFA 10 hour is due to carbon dioxide that was not perfectly subtracted from the recorded background. The results from the mass spec and FTIR analysis concludes that the TFA hydrolysis reaction was successful at converting the *t*-butylester functionalized GO **109** into the carboxylic acid functionalized GO **114**. Figure 24 shows the overlay FTIR spectra of only *t*-butylester **109** and carboxylic acid functionalized GO **114** which more clearly shows the spectral differences.

Figure 24: Overlaid FTIR Spectra of t-Butylester 109 (Top) and carboxylic acid 114 (Bottom) Functionalized GO.

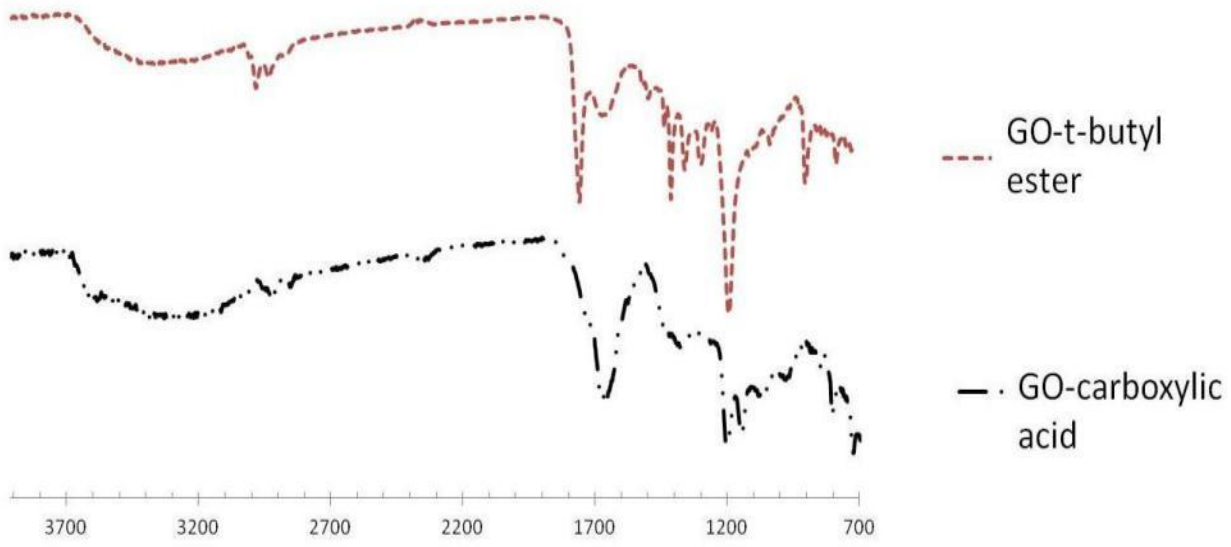

The Raman spectrum for GO-carboxylic acid **114** (Figure 25) was obtained and showed a D band at 1350 cm^{-1}, a G band at 1591 cm^{-1} and a 2D band at 2436 cm^{-1}. The ratio of the I(D)/I(G) was calculated to be 0.78 which is lower than the value observed for GO-ester **109**. The lower I(D)/I(G) ratio was due to a decrease in intensity for the disorder band (D-band) suggesting that the GO showed "self-healing" properties (gain in order), a phenomenon that has been reported to occur in GO.[80] The I(D)/I(G) ratio for GO-acid **114** was similar to the value seen for GO **108**. The GO-carboxylic acid **114** was analyzed by AFM which proved that the material consisted mostly of single layer sheets of ~1.5 nm thick.

To further prove that the TFA hydrolysis reaction removes the t-butylester groups to afford carboxylic acid functionalized GO, the ^{13}C-labeled *t*-butylester functionalized GO **113** was subjected to analogous hydrolysis reaction conditions employing 10% TFA in water for 48 hours (Scheme 26). After the reaction was complete (seen by FTIR analysis) the reaction was worked up and the ^{13}C-labeled carboxylic acid GO **115** was analyzed by solid state carbon NMR spectroscopy (Figure 27).

Figure 25: Raman Spectrum of Carboxylic Acid Functionalized Graphene Oxide 114

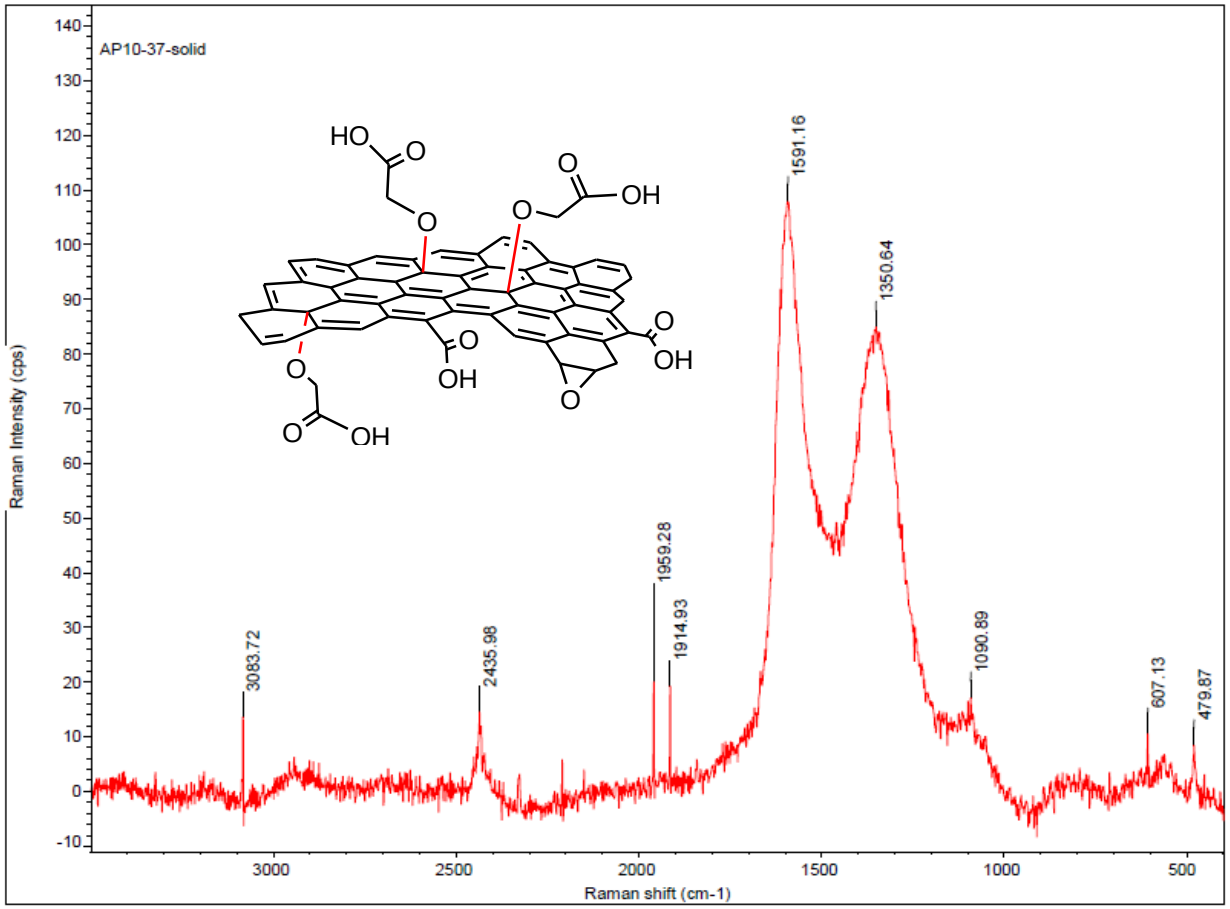

Scheme 26: Synthesis of ^{13}C labeled Carboxylic Acid Functionalized Graphene Oxide 115.

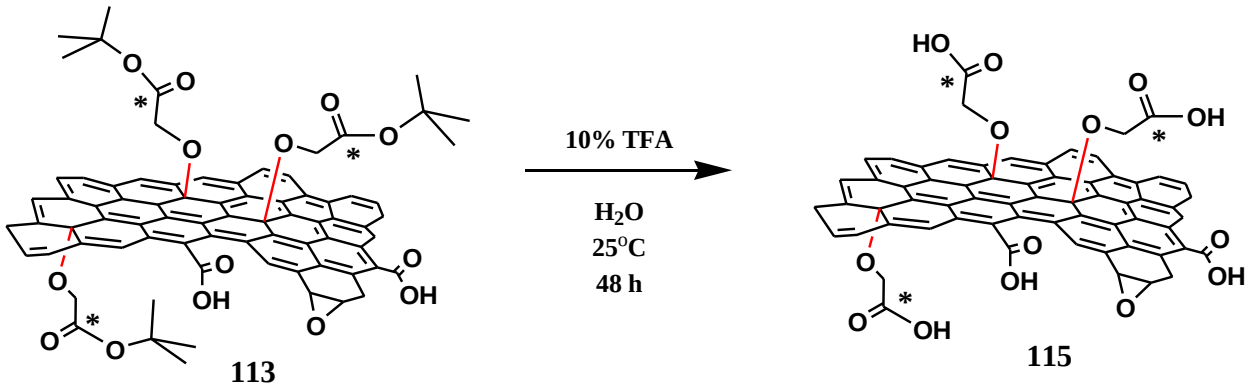

113 **115**

The solid state carbon NMR spectrum of the ^{13}C-labeled carboxylic acid functionalized GO **115** after 4096 scans is shown in Figure 26 (bottom spectrum). The presence of a dominant peak at 171 ppm was clearly observed, and corresponds to the ^{13}C-labeled carbonyl carbon. This peak was downfield shifted from 166 ppm (ester) to 171 ppm (acid) which is expected since the acid is now lacking the electron donating *t*-butyl group, and therefore experiences less shielding *via* inductive effects.

Figure 26: Overlay of Solid State NMR Spectra of GO (top), ^{13}C-t-Butylester (middle) and ^{13}C-Carboxylic Acid (bottom) Functionalized Graphene Oxides.

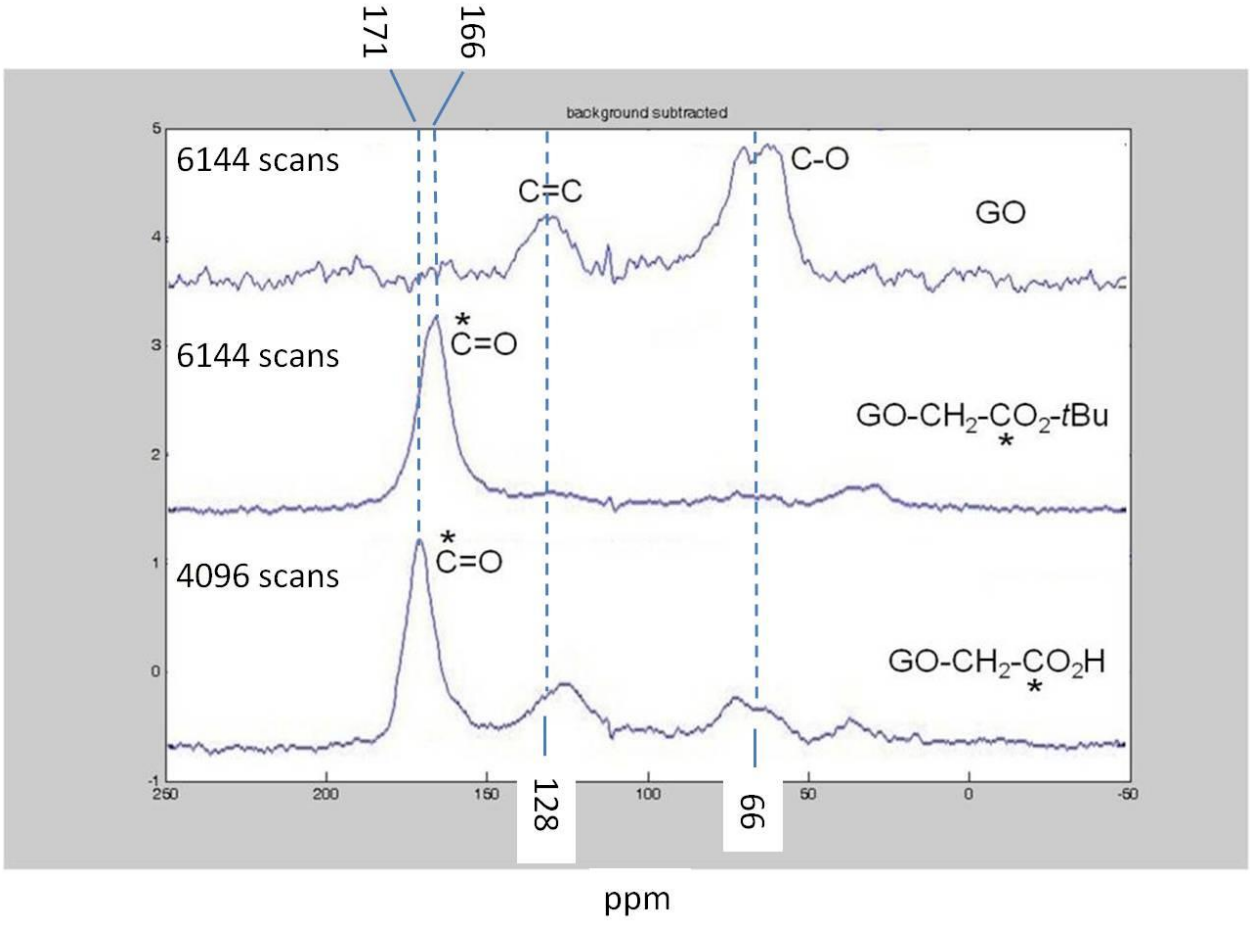

The bottom spectrum still contains peaks at 128 ppm and 66 ppm and confirms that the C=C and C-O functionality of the GO framework remained intact during exposure to TFA and long reaction time.

Figure 27 shows microscope images of representative samples of GO, *t*-butylester functionalized GO **109** and carboxylic acid functionalized GO **114**.

Figure 27: Stage Microscope Images of GOs. A) GO 108, scale bar = 10 µm; B) GO, scale bar = 100 µm ; C) t-Butylester functionalized GO 109, scale bar = 10 µm; D) t-Butylester functionalized GO 109, scale bar = 50 µm ; E) Carboxylic Acid functionalized GO 114, scale bar = 10 µm ; F) Carboxylic Acid functionalized GO 114, scale bar = 100 µm.

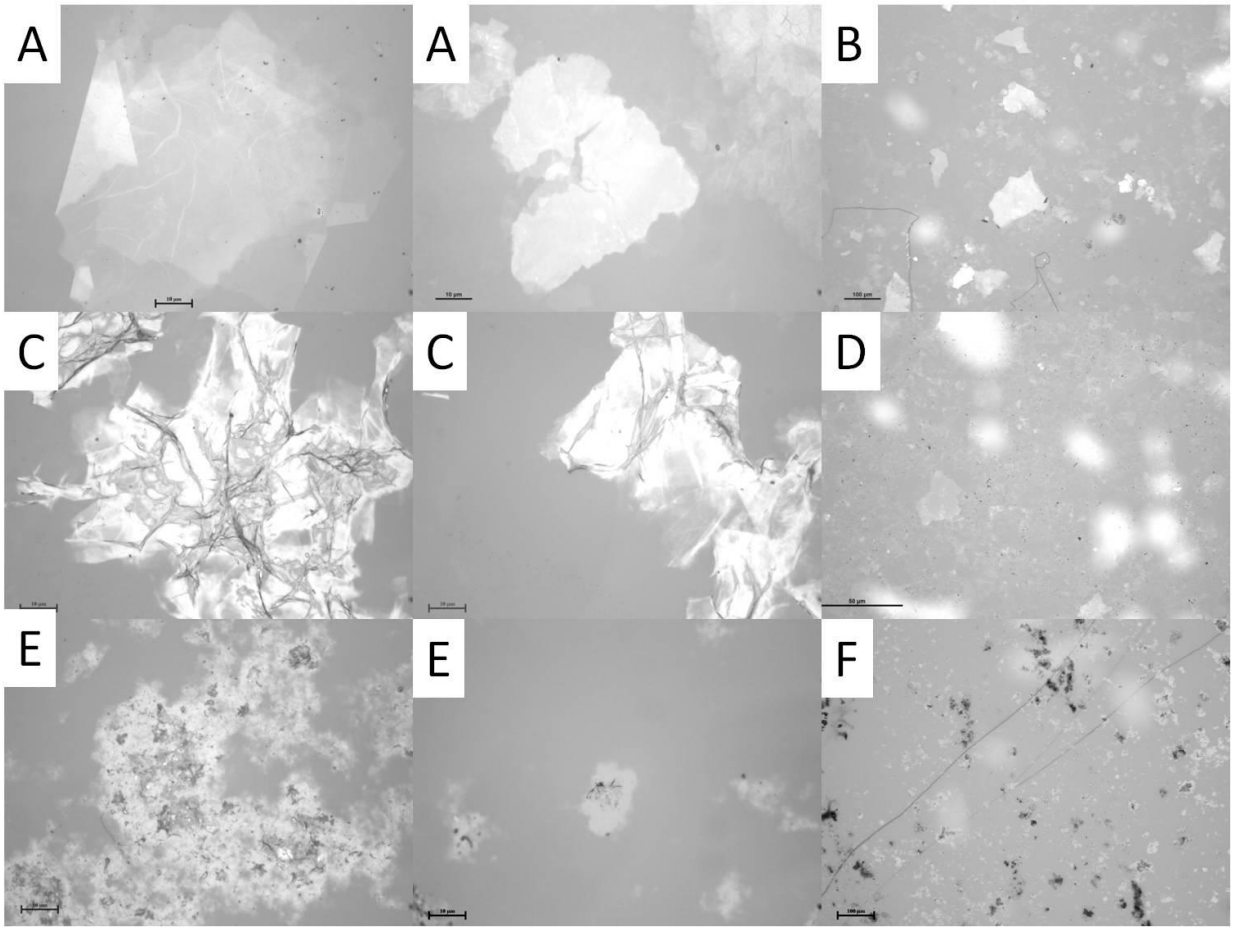

The images labeled **A** show the GO at 1000x magnification and the scale bar is 10 µm. The image **B** shows the GO at 100x magnification and the scale bar is 100 µm. It can be seen that large, flat and thin GO sheets were obtained (~ 5 - 200 µm in diameter) and mostly are one or two layers thick. Images **C** and **D** show the *t*-Butylester functionalized GO **109** at 1000x and 100x magnification respectively. It was noticed that after the introduction of the *t*-butyl ester function the GO sheets on average had reduced in size to about 1 - 80 µm in diameter and contained more wrinkles and creases. This trend continued with the synthesis of carboxylic acid functionalized GO **114** which showed further decreases in GO sheet sizes (~1 - 60 µm) and

reduction in the surface quality of GO (Images **E** and **F**). The decrease in GO sheet size and reduced GO surface quality is probably attributed to factors such as chemical modification of GO surface, prolonged reaction times spent in solution and lyophilization during workup. Nevertheless, FTIR, solid state carbon NMR and Raman spectroscopy show that the GO framework is still intact and that GO has be functionalized with additional surface carboxyl groups.

II.III. Solid State Synthesis of DNA Functionalized Graphene Oxide

With the GO-carboxylic acid **114** in hand we attempted a novel solid state synthesis with the intention of selectively functionalizing only one side of GO sheet with an oligonucleotide (19 mer; 5'-AmMC12-AGC CAG ATT GCG ATC GCC C). The outline for this endeavor is shown below in Scheme 27. The reason for synthesizing an oligonucleotide functionalized GO is because it may find use in a biosensor electronic devise. GO has semi-conductive properties and a grafted oligonucleotide could serve as a probe sequence to detect complementary target DNA/RNA sequences through hybridization processes that may be detected electronically through changes in current. Stemming from our experience using 2-chlorotrityl polymer resins, we decided to use this resin in the solid state synthesis of one sided oligonucleotide functionalized GO **118**. The first step involved attachment of GO-carboxylic acid **114** to the 2-chlorotrityl resin (Scheme 27). The glassware used for the reaction was firstly deactivated using 20% trimethylsilyl chloride in chloroform to block any free hydroxyl groups on the surface of the glass. After washing with distilled chloroform and drying, the argon flushed reaction vessel was charged with 1 g of 2-chlorotrityl resin and distilled dichloromethane. After resin swell (~30 min) the 10 mg GO-carboxylic acid **114** was added followed by diisopropylethylamine. The mixture was shaken in a shaker for 2 days during which time the GO-carboxylic acid **114** became attached to the resin to form **116**. The resin was washed with dichloromethane to remove any excess suspended GO-carboxylic acid and the GO coated resin **116** was functionalized with oligonucleotide using HATU in DMF to form **117**. Cleavage of the oligonucleotide functionalized GO from the resin was slow and required multiple sonication cycles probably because the GO sheet is a good chemical barrier and prevents TFA from efficiently cleaving the C-O trityl bond. Nevertheless, 5 mg of oligonucleotide functionalized GO **118** was obtained which was analyzed by brightfield microscopy, FTIR, Raman and solid state carbon NMR spectroscopy.

Scheme 27: Solid State Synthesis of oligonucleotide functionalized GO 118.

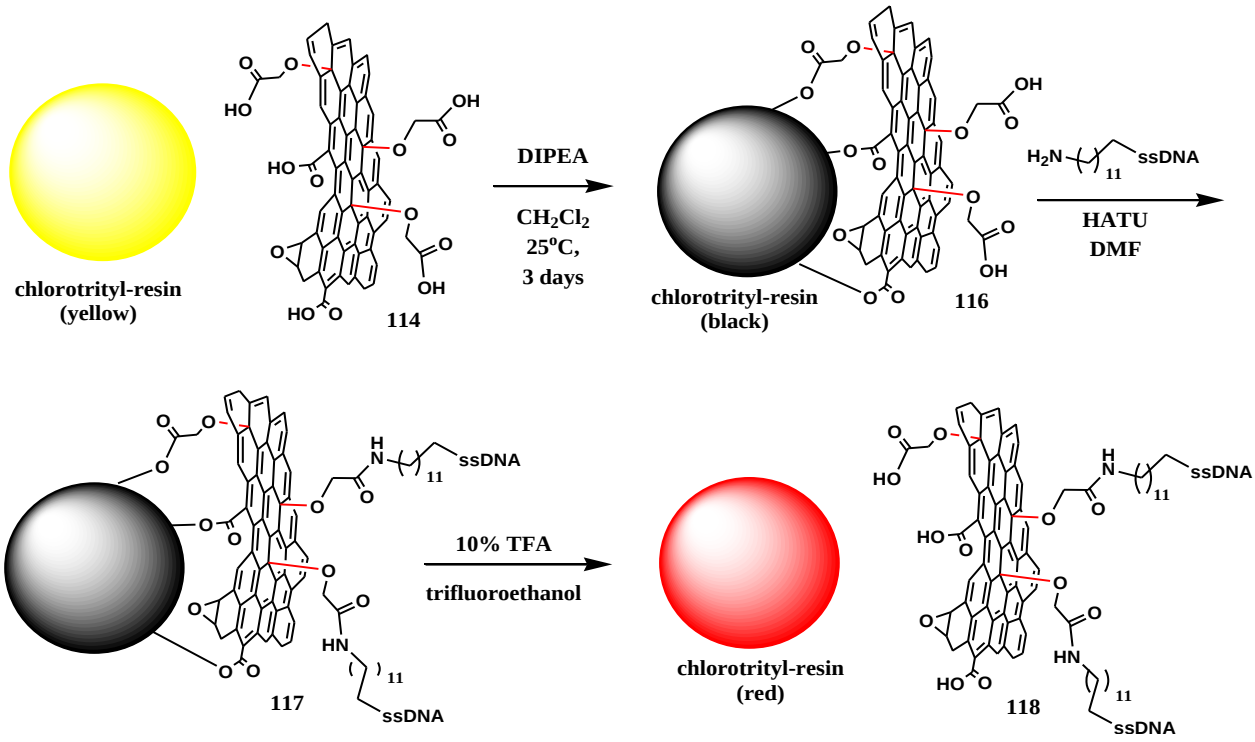

The brightfield microscope images, taken at difference stages of the solid state synthesis, are shown in Figure 28. Figure **A** shows the 2-chlorotrityl resin starting material comprising of white or light colored beads of approximately 100 µm in diameter. After treating the resin with GO-carboxylic acid **114** it gets coated with layers of GO and takes on a black appearance as seen in image **B**. Some of the beads were only partially coated with GO acid **114**, and these took on a light brown appearance as shown in picture **C**. When oligo-GO coated resin **117** was cleaved with 10% TFA in trifluoroethanol, some of the crude mixture was visualized under a stage microscope as shown in image **D**. The resin had taken on a red appearance, and small pieces of GO material could be seen suspended in the solvent, which showed that the GO was cleaved from the resin. Image **E** shows the recovered resin after workup, which was red in color. Since no GO material remained bound to the resin, it was concluded that successful cleavage fully took place. The final oligo-GO **118** is shown in images **F**, and was found to range from 5-50 µm in diameter, and had a rougher surface appearance as compared to GO-carboxylic acid **114**.

Figure 28: Microscope Images Taken at Different Stages of the Solid State Synthesis of Oligonucleotide Functionalized GO 118. A) 2-Chlorotrityl resin at 100x magnification (scale bar = 100 µm); B) GO coated resin 116 at 100x magnification (scale bar = 100 µm); C) GO coated resin 116 at 300x magnification (scale bar = 100 µm); D) Crude mixture of Resin and Oligo-GO 118 in trifluoroethanol at 100x magnification; E) Resin remains after cleavage at 100x magnification; F) Oligo-GO 118 after cleavage from resin at 1000x magnification (scale bar = 10 µm).

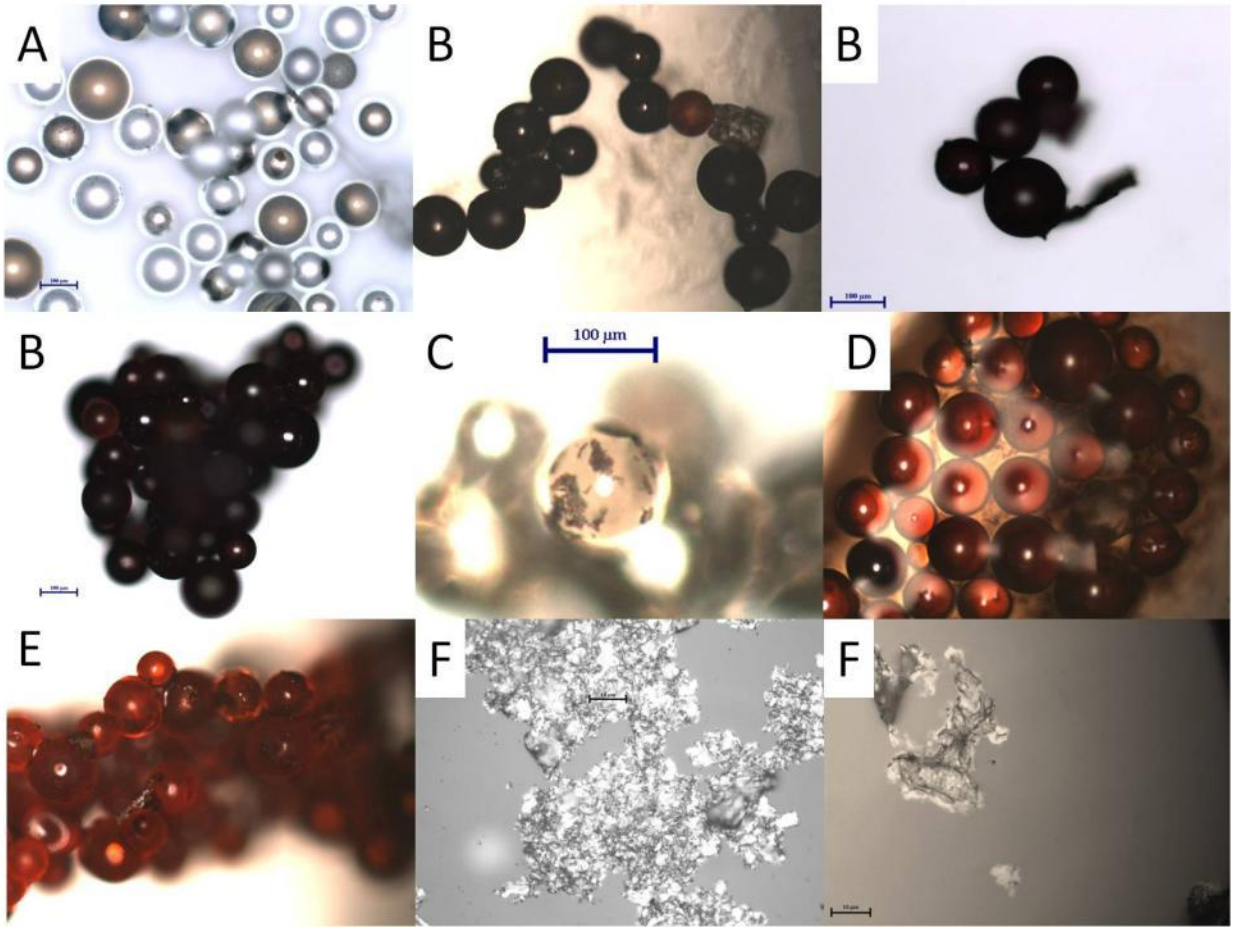

The DNA functionalized GO **118** was analyzed by FTIR, Raman and solid state carbon NMR spectroscopy. FTIR is a well established and useful technique to analyze DNA material because it can be performed on crystalline, amorphous or solution state DNA samples.[83] Another advantage of FTIR is that there is no limit to the size and one can analyze high molecular weight ds- or ss-DNA or RNA, medium length DNA fragments obtained from enzymatic or chemical

cleavage or short synthetic oligonucleotides.[83] The FTIR spectra for GO-carboxylic acid **114** and GO-DNA **118** are overlaid in Figure 29.

Figure 29: Overlay of FTIR Spectra of GO-acid 114 and GO-DNA 118 (Scale units in cm^{-1}).

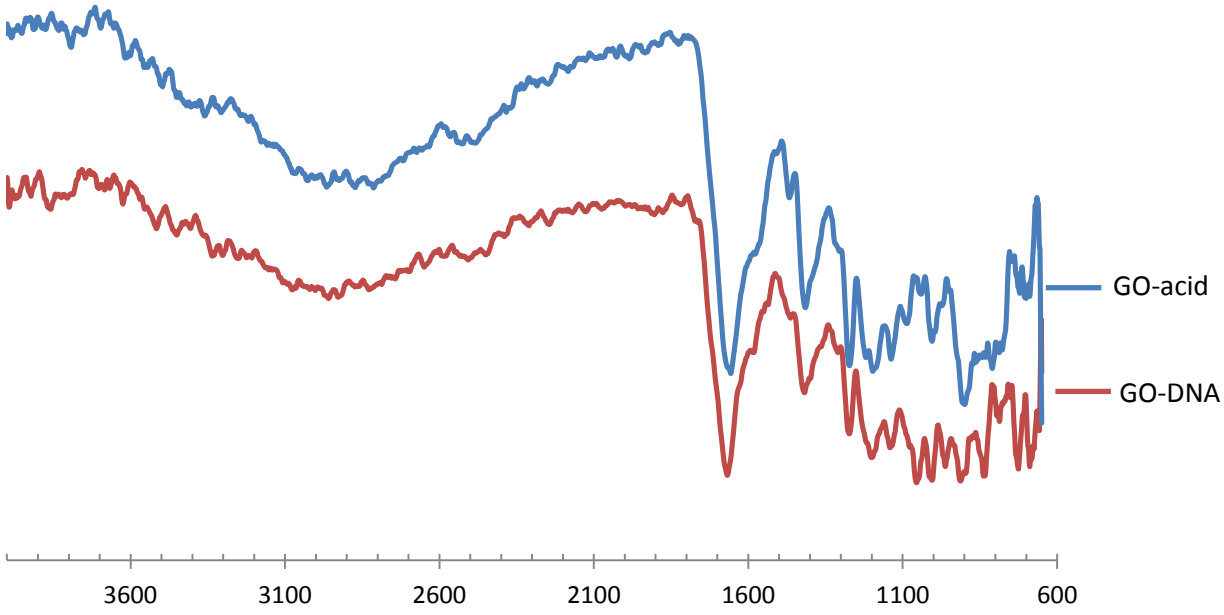

The two spectra look mostly similar except for subtle differences to the fingerprint region. The fingerprint region is shown below is Figure 30. A new absorption in the GO-DNA **118** spectrum can be seen at 1058 cm^{-1} and may correspond to phosphate group vibration.[83] New absorption peaks can be seen at 960, 833, 728 and 673 cm^{-1} and these vibrations should result from vibrations to the phosphate-sugar backbone.[83] These resonances are sensitive to molecular conformation such as sugar pucker. In-plane C=C stretching from the DNA base pairs (1550-1720 cm^{-1})[83] and base-sugar bending motions (1300-1500 cm^{-1})[83] from the DNA could not be observed however, probably due to having weak and overlapping absorptions with the GO framework.

Figure 30: FTIR Overlay Spectra of Fingerprint Regions of GO-acid 114 and GO-DNA 118

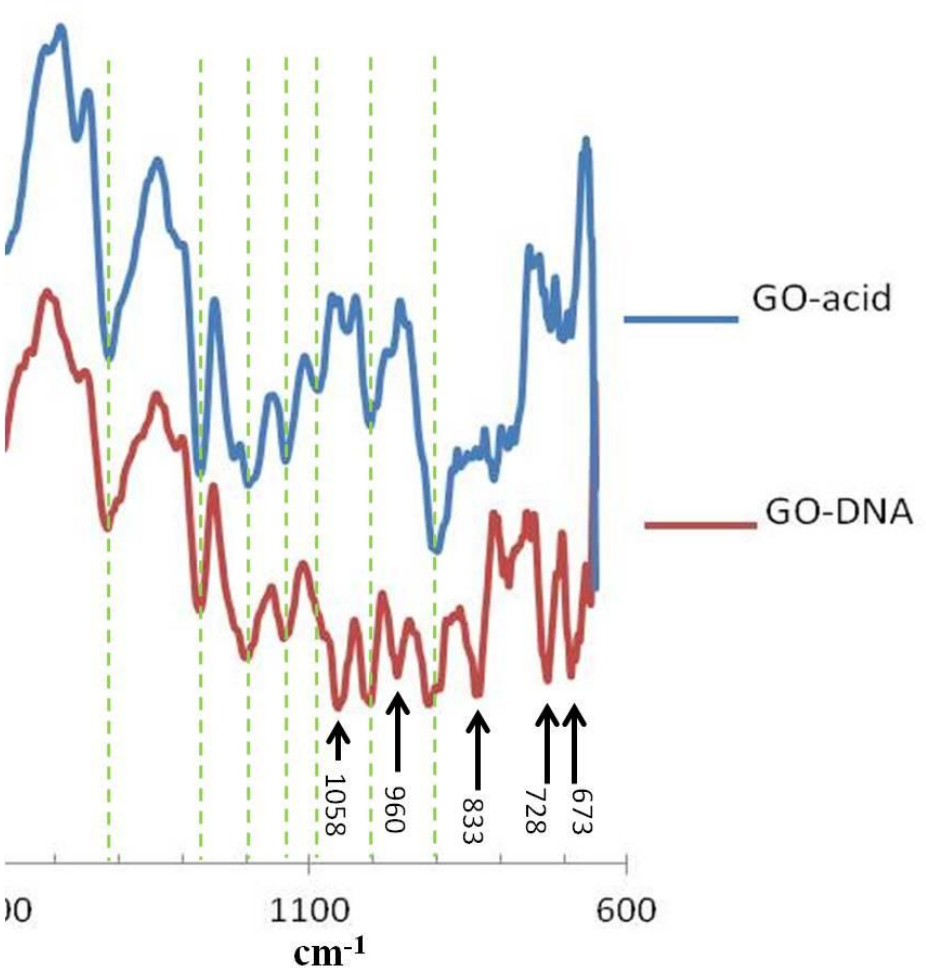

The Raman spectrum (Figure 31) contained a D-band and a G-band, as expected for bulk GO, at 1589 cm^{-1} and 1343 cm^{-1} respectively, with a I(D)/I(G) ratio of 0.95. The increased I(D)/I(G) ratio in **118** compared with GO-acid **114** suggests a higher disorder in the GO structure of **118**, and this may arise from a decreased sheet size, or because the ssDNA is randomly attached to the GO surface undergoing π-π stacking between DNA bases and hexagonal rings of GO.

Figure 31: Raman Spectrum of Carboxylic Acid Functionalized Graphene Oxide 114

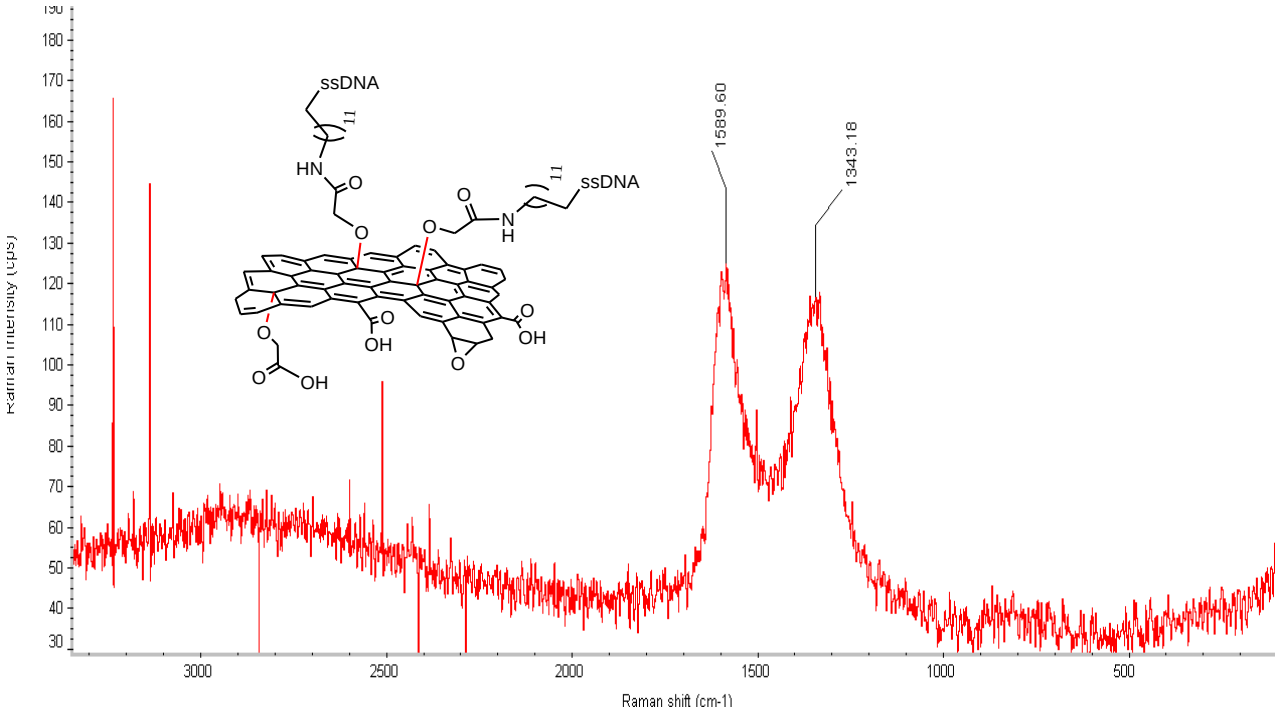

The carboxylic acid functionalized GO **114** was subsequently used in a noroviral electronic biosensor device as described in the next section.

II.IV. Studies Towards the Development of a Novel Noroviral Bioelectronic Sensor Device using Carboxylic acid Functionalized Graphene Oxide 114.

The carboxylic acid functionalized GO **114** was utilized in a novel electrochemical "sensor" device with the hope of detecting noroviral RNA by taking advantage of the excellent semiconductive property of GO. Since norovirus has been an attractive target for drug development in our lab we embarked on a translational research project which involved using our chemically modified GO in an electrical sensor device with the goal of detecting noroviral ssRNA. The design of the electronic sensor device is shown in Figure 32. A Kiethley source meter, capable of measuring small currents/voltages, was connected across gold electrodes on a silicon dioxide coated silicon wafer. The newly synthesized GO-acid **114** semi-conductive material was deposited on the gold electrodes and chemical/physical changes that occurred on its surface was detected electronically, due to changes in current.

Figure 32: Design of the Electronic Sensor Device.

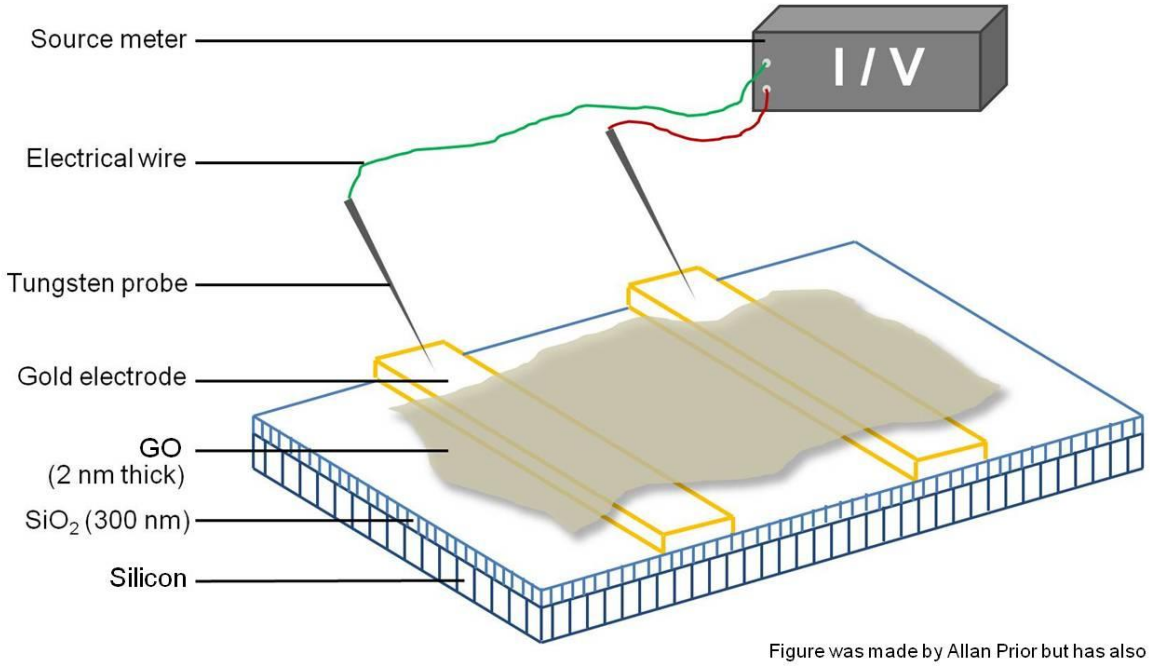

Figure 33 shows a microscope image of the chip at 100x magnification and the distance between gold electrodes is 5 or 10 µm. The entire chip has a dimension of 1 cm x 1 cm. The outline of this venture is highlighted in Scheme 28 and involved initial deposition of GO-carboxylic acid

114 onto the surface of the chip, to bridge between gold electrodes. The full experimental details for these procedures have been recently reported by Duy Le and therefore will not be discussed in great detail. In brief, the best method for deposition of GO-carboxylic acid **114** onto the chip was found to be a direct deposition method. This involved slow evaporation of a dilute aqueous suspension of GO-carboxylic acid **114** (50 µL), placed strategically over the gold electrode lanes. Once bound to the chip, the GO sheets remained secure in position (Figure 34), and could not be washed away, despite vigorous washing stages, probably due to the presence of strong ionic bonds formed between the carboxylate ions (from GO) and ammonium ions (from chip surface). The next step was the attachment of small probe oligonucleotides to the surface of the GO by making use of the newly installed carboxylic acid groups. These is a terminal amine situated on the 5' end of each oligonucleotide (19 mer). These functional groups are coupled to form an amide bond in the presence of HATU coupling reagent. We envisioned that hybridization of surface bound oligonucleotide with complementary noroviral ssRNA could be detected by carefully monitoring the electrical conductivity of GO before and after the reaction. This forms the basis of the electrochemical sensor to detect noroviruses, since noroviruses contains a ssRNA genome. Dehydridization of the DNA/RNA duplex with 10M urea should remove the ssRNA from the GO surface.

Figure 33: Microscope Image of Electronic Chip at 100x magnification (Image made by Allan Prior but has been included in the MSc thesis of Duy Le).

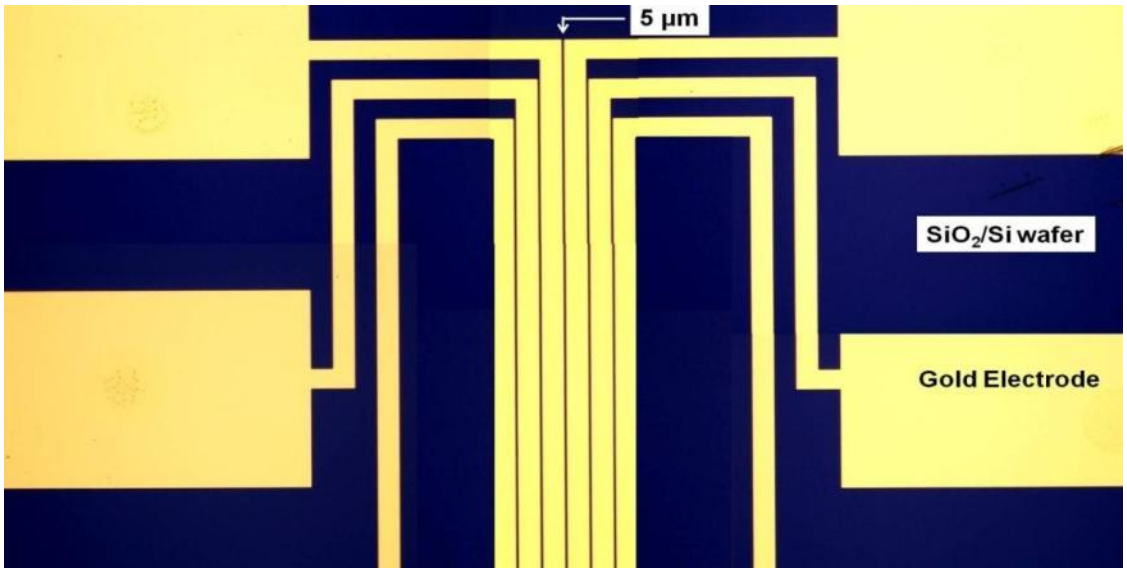

Scheme 28: Experimental Design to Detect Noroviral ssRNA.

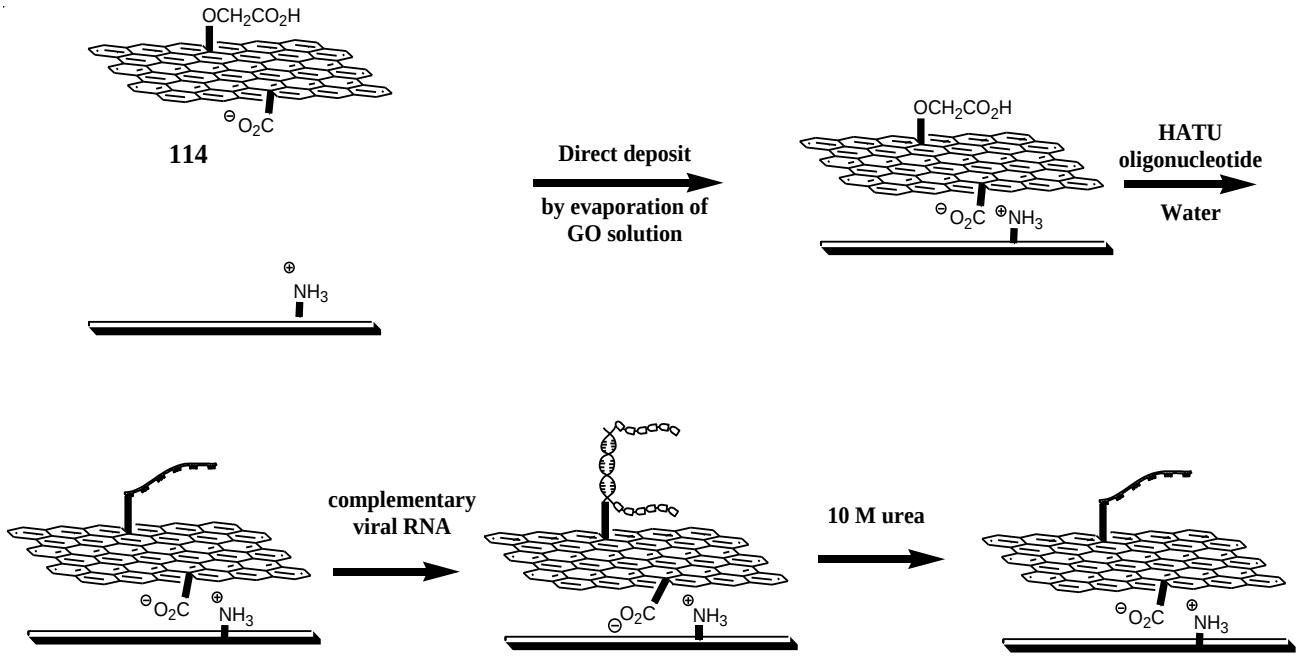

Figure 34: Microscope Image at 1000x Magnification Showing a Sheet of GO-Carboxylic acid 114 Bridging Two Gold electrodes (scale bar = 10 µm).

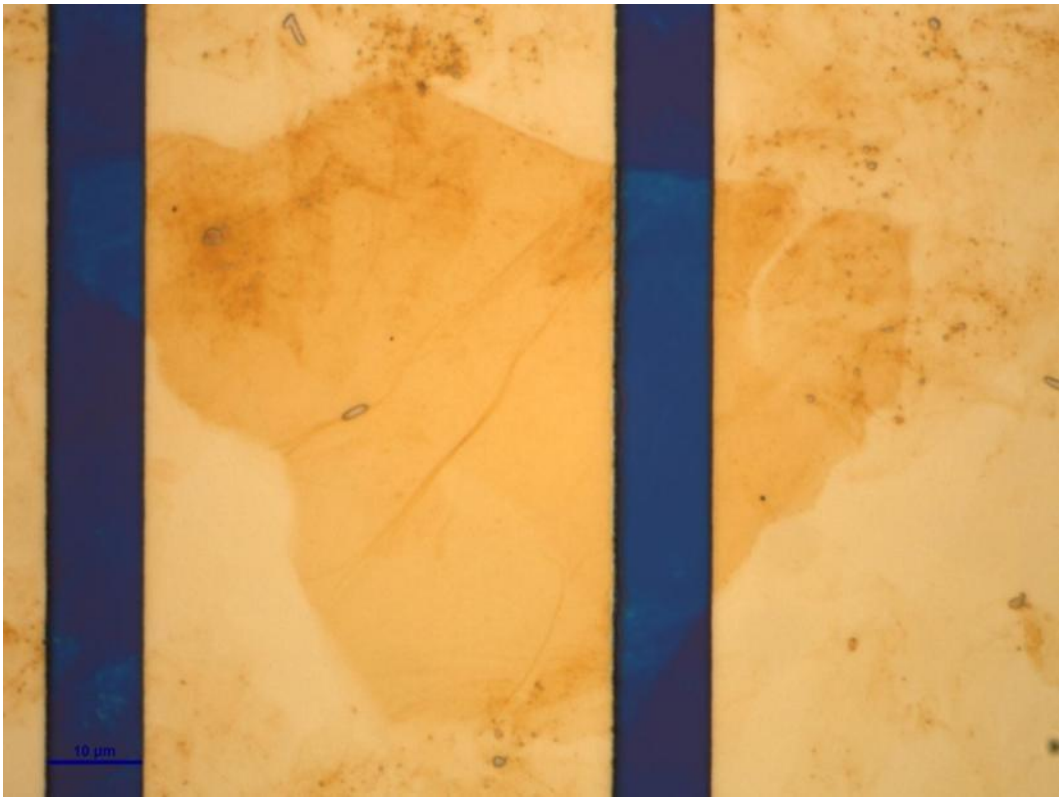

Figure 35 shows a bar chart of current values obtained at 4V during the course of RNA hybridization and dehybridization treatments. The first column (purple) shows the chip current containing immobilized GO-carboxylic acid **114** only. The second column (blue) shows that attachment of probe oligonucleotide (oligo-II) caused a 100% increase in chip current from 0.48 µA to 0.96 µA. Hybridization with target ssRNA caused a 17% increase in current from 0.96 µA to 1.12 µA (green column). Dehybridization with 10M urea caused the current to return to pre-hybridization values (red column). A drying period of 18-48 hours was required after each event to remove excess moisture from affecting current readings.

Figure 35: Hybridization and Dehybridization of Oligonucleotide Probe with ssRNA Target (Current values recorded at +4V).

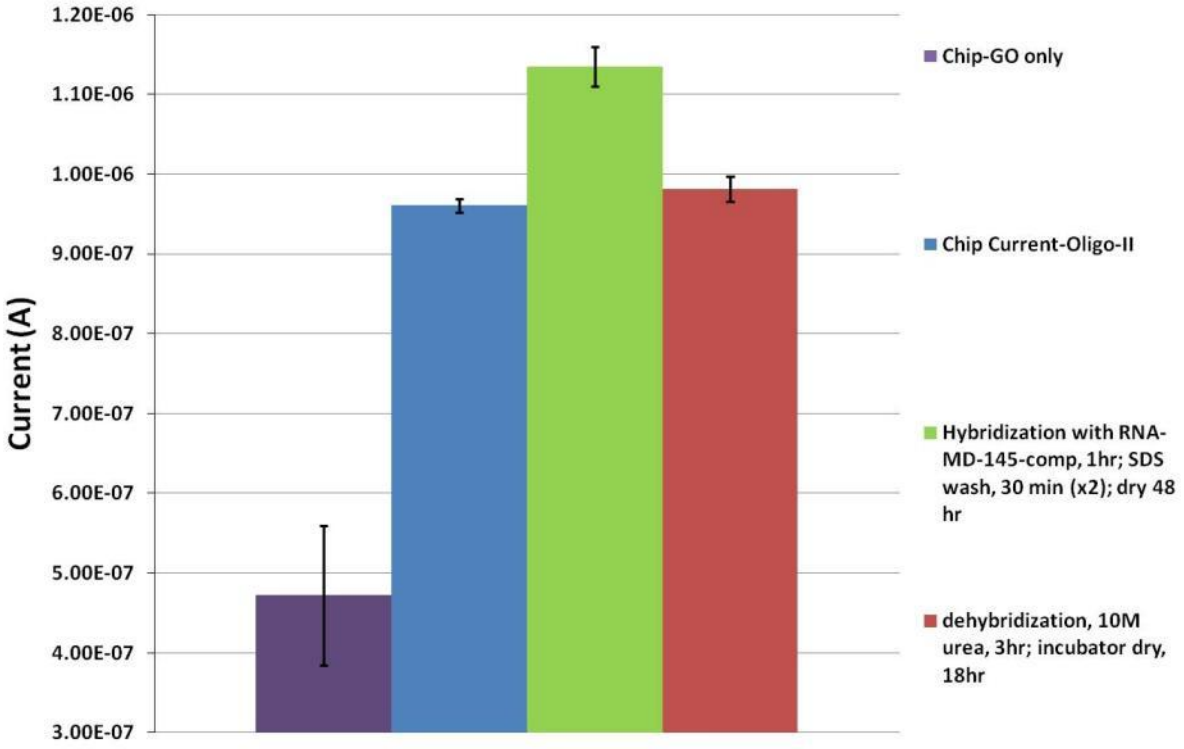

The current was swept from -4V to +4V and the I/V data is shown in Figure 36. The S-shape I/V profile is indicative that the GO is behaving as a semiconductor, and not a conductor. The blue curve labeled 1 shows the I/V data for oligonucleotide bound GO. The green curve labeled 2 shows the I/V data after hybridization with complementary target ssRNA, and shows an increase

in current. After treating with 10 M urea, the current returned to pre-hybridization levels as shown by curve 3 (orange), suggesting successful dehydridization of RNA from the DNA probe.

Figure 36: Hybridization and Dehybridization of Oligonucleotide Probe with ssRNA Target (I/V data was recorded by sweeping the voltage from -4 to +4V).

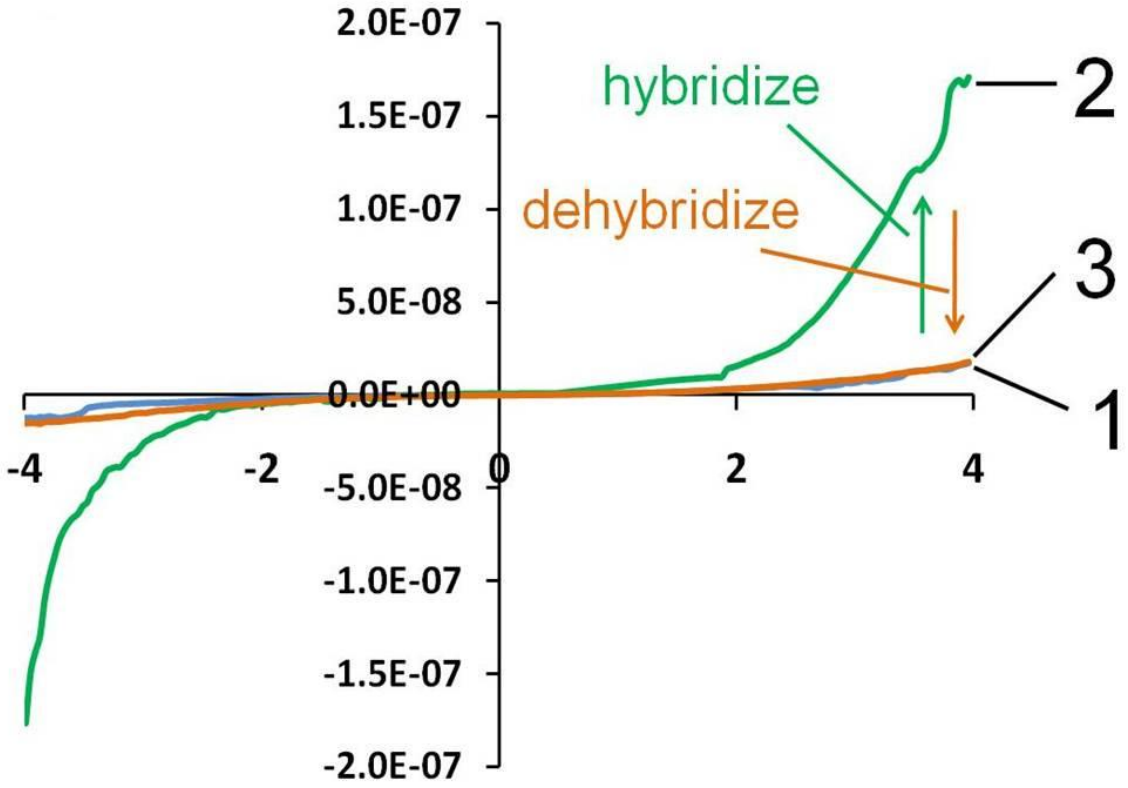

To confirm that the increase in current was a result of successful hybridization of probe DNA with the target RNA, the experiment was repeated using a non-complementary sequence of target RNA (Figure 37). The result was interesting because even the non-complementary RNA caused a similar increase in current (26%, purple column), as observed for complementary RNA *vide supra*. When the chip current was re-measured after sitting for 5 days at room temperature the current remained unchanged (red column), but when treated with a complementary sequence of target DNA-FAM a further current increase was observed (blue column), which is a 48% current increase from the baseline (Oligo-II only).

Figure 37: Treatment of Oligonucleotide Probe with Non-Complementary ssRNA (Current values recorded at +4V).

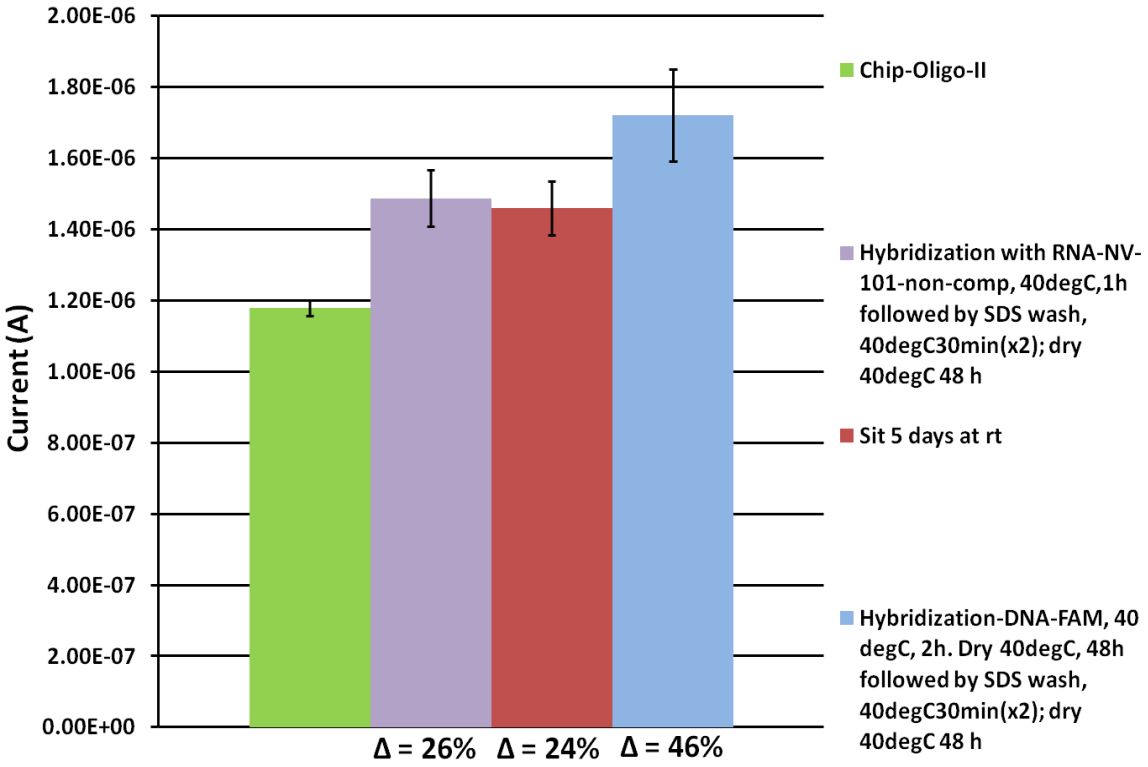

The overall result was suspicious, and indicative that the increase in current was due to non-specific binding of RNA and DNA to the GO surface, and not due to hybridization effect. This conclusion was confirmed by taking fluorescence images of the chips after treatment of DNA-FAM and SDS washing (Figure 38). The fluorescence image (**B**, Figure 38) showed intense fluorescence on the surface of GO confirming the aggregation of many FAM fluorophores. The fluorescence intensity was partially reduced after a treatment with 10 M urea but some fluorescence still remained, suggesting a strong affinity of DNA to the GO surface through non-specific binding. This was further confirmed by treating a fresh GO-carboxylic acid immobilized chip with DNA-FAM which proved to similarly develop intense fluorescence from the attached FAM fluorophores, due to non-specific binding of DNA to the GO surface (data not shown). This conclusion is supported by literature evidence that demonstrates that ssDNA has a strong affinity for the surface of GO, due to the flat, conjugated nature of nucleobases that can undergo π-π stacking with the randomly distributed flat, aromatic regions of GO.[64, 84, 85] Interestingly, the literature shows that dsDNA has a much lower affinity for GO surface, due to the effective

shielding of the nucleobases deep within the centre of the DNA duplex rendering then inaccessible to bind with the GO surface.[64] Moreover, the highly negative charge of the phosphate backbone of the DNA duplex is not attracted onto the GO surface.[64] In order to thwart non-specific binding issues of DNA/RNA to GO surface, a passivation layer such as polyethylene glycols (PEGs) must be used in future studies. Another inherent problem that exists with using this technique is the suspected adsorption of moisture onto the GO surface, causing large changes in the measured current. Prolonged drying periods 48 - 64 hours in a desiccator or vacuum tube resulted in loss in current, presumably due to loss of GO surface adsorbed moisture. The experiment was repeated many times, but the data shown in Figure 35 and 36 could never be reproduced. Instead, it was found that the current varies greatly between experiments, and no trend in current could be observed between repeated experiments. It is proposed that nonspecific binding of ssRNA to the GO surface, and, adsorbed moisture on the GO surface, are two limiting factors that hinder rapid progress in this area.

Figure 38: Images of Chip After Treatment with Non-Complementary ssRNA and Complementary DNA-FAM. A) Bright field Image; B) Fluorescence Image (exposure time = 100 ms).

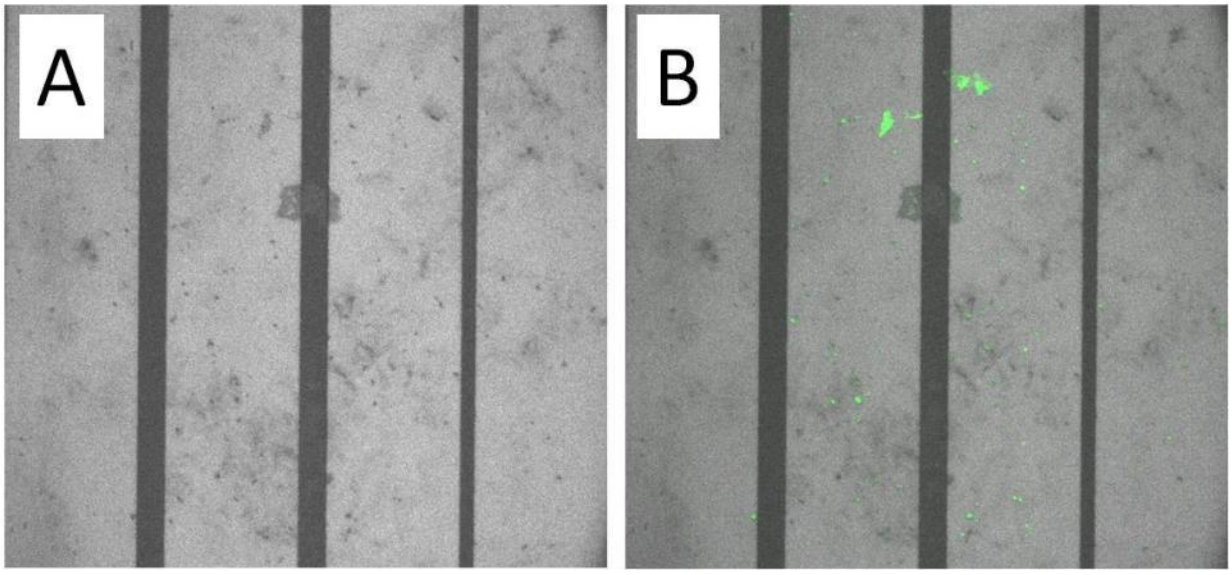

II.V. Conclusion

In conclusion, this data shows that the surface of GO can be chemically modified with *t*-butylester and carboxylic acid functionalities. FTIR, Raman and solid state NMR spectroscopy confirmed the presence of with *t*-butylester and carboxylic acid functionalized GO. The final carboxylic acid functionalized GO **114** was showed by AFM to exist mostly as mono layered sheets and ~1 - 60 µm in diameter. One sided oligonucleotide functionalized GO **118** was also synthesized using a solid state technique and was characterized by FTIR, Raman and solid state NMR spectroscopy. The FTIR data suggests that the oligonucleotide has been attached due to new absorption peaks in the fingerprint region that are expected for phosphate and phosphate-sugar backbone vibrations of DNA. Microscope pictures and Raman spectroscopy showed that the GO-acid **114** to had higher quality and less disorder compared to GO-DNA **118** and was subsequently used in the development of a noroviral electronic biosensor device. The GO-acid **114** was successfully deposited onto the surface of an electronic chip bridging two gold electrodes using a direct deposition technique. The GO-acid **114** displayed semi-conductive properties with currents in the low µA range when applying a voltage of 4V. Attachment of oligonucleotide to the surface of the chip caused a 100% increase in conductivity. Although hybridization with complementary RNA caused an initial increase in conductivity, a separate experiment employing hybridization with a non-complementary RNA caused a similar increase in current, and therefore the current increase could not be attributed to a successful hybridization. Hybridization with complementary DNA-FAM also showed an increase in conductivity but fluorescence images showed intense fluorescence due to non-specific binding and aggregation of DNA-FAM on GO surface. In order to circumvent issues with the apparent non-specific binding of DNA/RNA to GO surface, incorporation of a passivation layer containing PEG should be investigated. Another inherent problem that exists with using this technique is the suspected adsorption of moisture onto the GO surface, causing large changes in the measured current. The experiment was repeated many times, but no trend in current could be observed between repeated experiments. It was proposed that apart from nonspecific binding of ssRNA to the GO surface, adsorbed moisture on the GO surface is another limiting factor that currently prevents progress with this project.

III. Electrochemical Detection of the Breast Cancer Related Protease Enzymes Legumain and Cathepsin B using Redox Active Peptide Substrates Attached to Carbon Nanofibre Nanoelectrode Arrays

III.I. Introduction

Cancer occurs when cells divide uncontrollably and form malignant tumors.[86] The past 30 years or so have generated a vast and complex body of knowledge regarding various types of cancers.[87] The causes can be hereditary or as a result of external factors such as tobacco, radiation, chemical pollutants or poor diet and exercise. These factors can damage the genes found in DNA leading to compromised cell regulatory function. A recent report by Hanahan and Weinberg has suggested the six hallmarks of cancer.[87] "Self-sufficiency in growth signals, insensitivity to growth-inhibitory (antigrowth) signals, evasion of programmed cell death (apoptosis), limitless replicative potential, sustained angiogenesis/tissue invasion and metastasis". Uncontrolled cell growth can invaded nearby organs compromising their proper function or can travel to other parts of the body through the lymphatic system or bloodstream (metastases). According to a recent report 12.7 million cancers were diagnosed worldwide in 2008 and 7.6 million deaths were reported in just one year.[86] This accounts for 13% of all deaths each year.

Breast cancer is one of the most common and most challenging diseases that affects woman worldwide.[88] Breast cancer is the leading cause of mortality in females aged 40-59 with more than one million new cases each year and a lifetime risk estimate of 1 out of every 9 woman.[88, 89] It has been said that the identification of reliable biomarkers in early stage breast cancer for early detection is a major challenge.[88] Early stage detection of breast cancer is recognized as the most important criteria to improve prognosis and treatment.[89] Mammography is the most utilized technique to screen for breast cancers and has been proven to successfully reduce breast cancer mortalities *via* population based screening programs.[90] Mammography however comes with certain limitations such as false positive results causing high call back rates, unnecessary exposure to radiation from additional mammograms, unnecessary and expensive biopsies and

patient anxiety.[90] False negative results can also occur, especially in woman with dense breast tissue, having only 36% sensitivity.[90] Other breast cancer imaging techniques such as magnetic resonance imaging (MRI), computed tomography (CT), mammoscintigraphy and positron emission tomography (PET) are used to detect and monitor breast cancers but these are expensive and inconvenient for routine screening.

III.II. Results and Discussion

The aim of this research was to develop an electrochemical biosensor devise capable of detecting important breast cancer relater biomarkers at an early stage. The biomarkers that were investigated in these studies were legumain and cathepsin B which are important protease enzymes implicated in breast cancers by over activation or over expression.[91-94] Legumain is a cysteine protease found in metastatic and invasive tumors and is expressed on the cell surface, in the macrophage and other membranous vesicles.[91] The higher activity of legumain in breast cancer results in activation of other proteases especially cathepsin B which has the ability to degrade connective tissues such as elastin and collagen, assisting in tumor growth.[91] Cysteine protease activity has been shown to be linked to tumor growth because the presence of cysteine protease inhibitors attenuated tumor growth and metastasis.[91] Development of an electrochemical device capable of detecting legumain and cathepsin B is highly relevant as this would allow for rapid and convenient screening of patients for breast cancers. A device of this nature could also be portable allowing for convenient point-of-care screening and treatment monitoring.[91]

In our recent paper by Syed *et al*.[95] we demonstrated that redox active ferrocene (Fc) molecules could be electrochemically detected *via* alternating current voltammetry (ACV) when covalently attached to the end of vertically aligned carbon nanofibers (VACNFs) in an embedded nanoelectrode array (NEA). The nanofibers are embedded in a layer of silicon dioxide but have their tips exposed on the surface as shown in the SEM image below (Figure 39). The VACNFs were grown in the lab of Dr. Jun Li using a DC-biased plasma enhanced chemical vapor deposition (PECVD) method starting from a Cr-coated silicon wafer.[95] The VACNFs were then coated with a SiO_2 encapsulation layer using a process of tetraethyl-*ortho*-silicate chemical vapor deposition. The CNF tips are exposed *via* mechanical polishing and reactive ion etching.[95] The

CNF tip are lastly electrochemically activated (generate carboxyl groups) by applying four cycles of CV -0.10 to 1.20 V in a solution of 1.0 M NaOH.[95]

Figure 39: Field-emission scanning electron microscopy image of VACNFs coated with a SiO_2 matrix. Reprinted with permission from (Swisher et al., J. Phys. Chem. C: 2013, 117, 4268-4277). Copyright (2013) American Chemical Society.

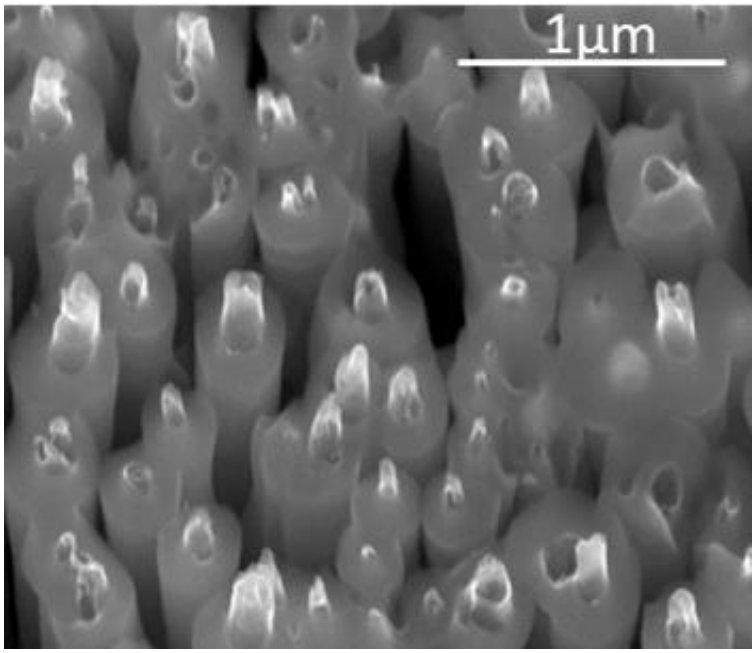

The NEA showed better detection sensitivity and temporal resolution compared to conventional electrodes because of its extremely small electrode size (nanometers).[95] This phenomenon allows the NEA to be utilized in biosensing applications requiring rapid and highly sensitive electroanalysis.[95]

This ACV technique was therefore expanded upon in order to develop an electrochemical biosensor device to detect the breast cancer related protease enzymes legumain and cathepsin B. This was achieved by covalently attaching Fc labeled peptide substrates to the end of the CNFs. The underlying idea for this electrochemical biosensor technique was that when protease enzymes cleave the Fc labeled peptide substrates, a decrease in current should result when monitored by ACV, due to loss of redox active Fc moieties from the surface of the CNF nanoelectrode.

The amino acid sequences for the Fc labeled peptide substrates were carefully designed by consulting substrate specificity profiles for legumain and cathepsin B found in literature studies. The structures of these peptides are shown below in Figure 40. Compound **119** for legumain contained a primary sequence of Ala-Ala-Asn-Leu while compound **120** for cathepsin B contained a primary sequence of Leu-Arg-Phe-Gly. In both tetrapeptides a Fc moiety was covalently attached to the *C*-terminal end of the peptide *via* coupling with an aminomethylferrocene group. Both peptides have a 5 carbon linker/spacer attached to the *N*-terminal end, the purpose of which was to extend the peptide away from the CNF surface reducing the occurrence of any steric interaction that may happen between protease enzymes and CNF surface.

Figure 40: Ferrocene labeled peptide substrates for legumain (left, compound 119) and cathepsin B (right, compound 120).

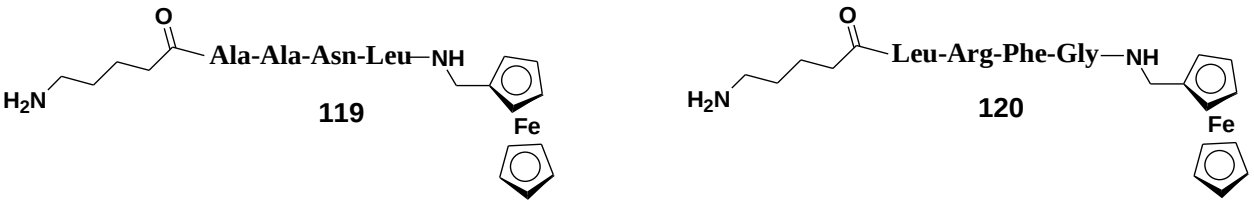

Figure 41 shows the expected cleavage sites for peptide **119** (legumain) and peptide **120** (cathepsin B). Legumain is an asparaginyl endopeptidase that specifically cleaves peptide bonds with P1 asparagine i.e. at the *C*-terminal side of an asparagine residue.[96] The literature evidence shows that when the P2 and P3 residues are alanine successful peptide cleavage Asn can take place.[97, 98] This prompted us to incorporate this verified Ala-Ala-Asn sequence into our biosensor device. The P1' position is not as important when it comes to substrate specificity and thus the Leu at position P1' was arbitrarily chosen.[97] The peptide substrate specificity profile for cathepsin B recognition and cleavage was recently uncovered by Choe *et al.* and was reported in 2006.[99]

Figure 41: Expected cleavage sites for peptide 119 (legumain) and peptide 120 (cathepsin B).

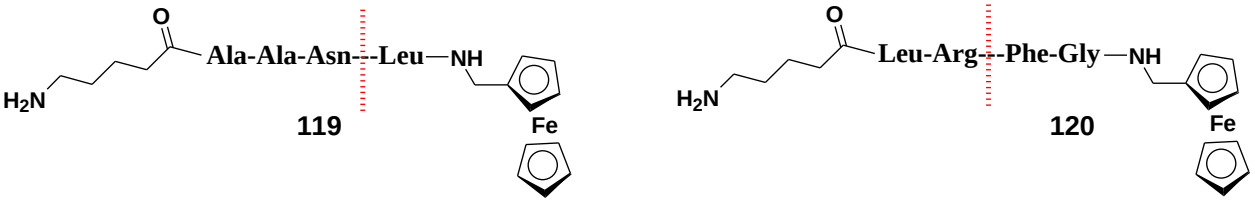

In order to confirm that the designed peptide sequences could be cleaved by legumain and cathepsin B enzymes, a HPLC study was performed in conjunction with mass spectrometry. The results from this study have been captured in our recent paper by Swisher *et al.*[91] Figure 42 shows the data for the cleavage of peptide **119** by legumain. Chromatogram **A** shows peptide **119** in MES buffer (no legumain). The tetrapeptide **119** appeared at 9.7 min in the HPLC chart and was confirmed by mass spectrometry analysis. Chromatogram **B** is a positive control and shows the expected cleaved fragment Leu-$NHCH_2Fc$ (compound **119**) after injection into HPLC as a solution in MES buffer. The presence of Leu-$NHCH_2Fc$ at 12.2 min was confirmed by mass spectrometry analysis. Chromatogram **C** shows the result after peptide **119** was incubated with 98.7 ng/µL (2.01 µM) of legumain for 2 hours. The peak at 12.2 min was collected and lyophilized and subjected to mass spectrometry analysis which proved it to be Leu-$NHCH_2Fc$ demonstrating that peptide **119** can be recognized and cleaved by legumain.

Figure 43 shows the data for the cleavage of peptide **120** by cathepsin B. Chromatogram **A** shows peptide **120** in MES buffer (no cathepsin B). The tetrapeptide **120** appeared at 9.4 min in the HPLC chart and was confirmed by mass spectrometry analysis. Chromatogram **B** is a positive control and shows the expected cleaved fragment Phe-Gly-$NHCH_2Fc$ (compound **136**) after injection into HPLC as a solution in MES buffer. The presence of Phe-Gly-$NHCH_2Fc$ at 6.7 min was confirmed by mass spectrometry analysis. Chromatogram **C** shows the result after peptide **120** was incubated with (56 µl, 4.95 ng/µl) of cathepsin B for 2 hours. The peak at 6.7 min was collected and lyophilized and subjected to mass spectrometry analysis which proved it to be Phe-Gly-$NHCH_2Fc$ demonstrating that peptide **120** can be recognized and cleaved by cathepsin B.

Figure 42: HPLC data showing proteolytic activity of legumain. A: Compound 119 only in 50 mM MES buffer (pH 5.0) and 250 mM NaCl (no legumain). B: Compound 133 only (cleavage fragment) in 50 mM MES buffer (pH 5.0) and 250 mM NaCl. C: Compound 119 in 50 mM MES buffer (pH 5.0) and 250 mM NaCl incubated with 98.7 ng/µL (2.01 µM) legumain for 2 hours. Modified with permission from (Swisher *et al., J. Phys. Chem. C:* 2013*, 117,* 4268-4277). Copyright (2013) American Chemical Society.

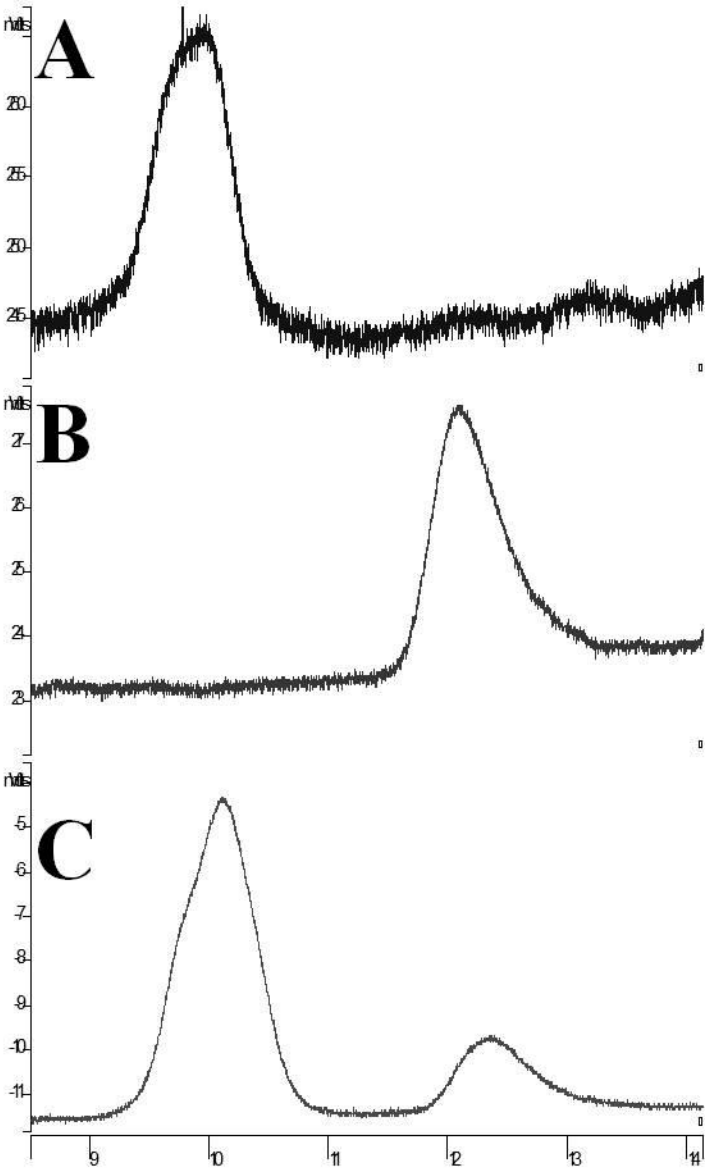

Figure 43: HPLC data showing proteolytic activity of cathepsin B. A: Compound 120 only in 25 mM MES buffer (pH 5.0) (no cathepsin B). B: Compound 136 only in 25 mM MES buffer (pH 5.0). C: Compound 120 in 25 mM MES buffer (pH 5.0) incubated with 4.95 ng μl^{-1} (0.17 µM) cathepsin B for 2 hours. Modified with permission from (Swisher *et al.*, *J. Phys. Chem. C:* 2013, *117*, 4268-4277). Copyright (2013) American Chemical Society.

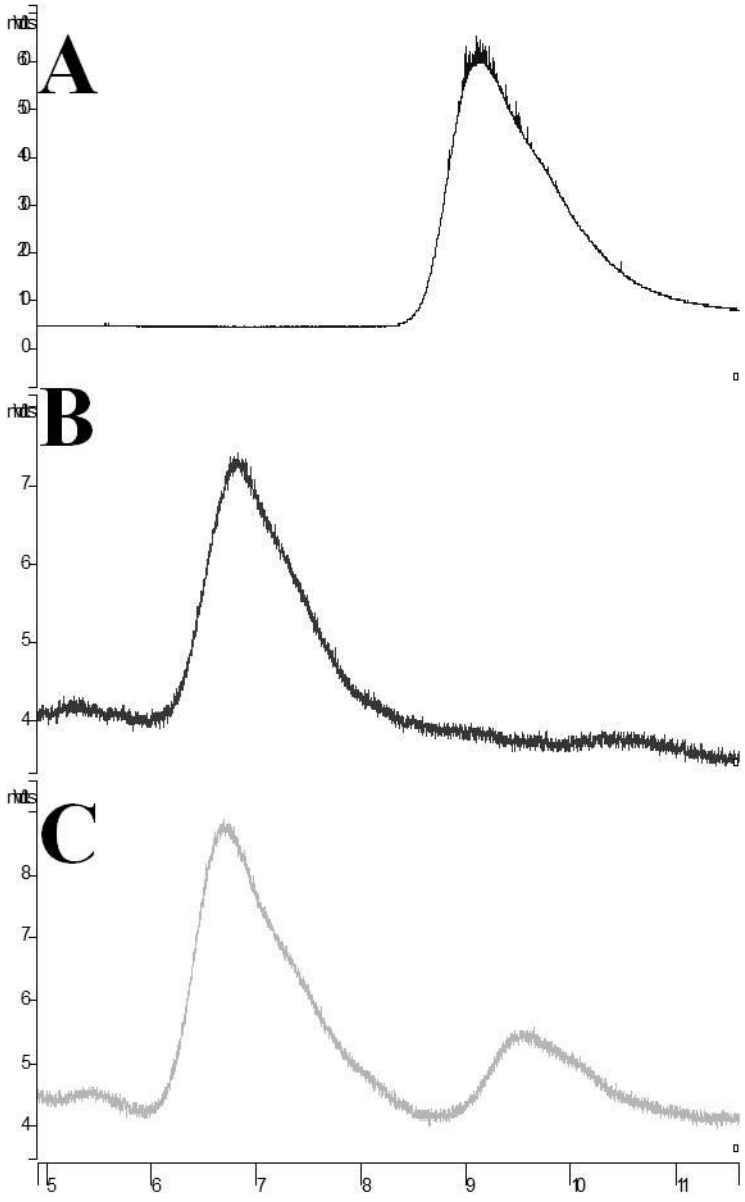

The tetrapeptides **119** and **120** were then utilized in an electrochemical biosensor device developed in the lab of Dr. Jun Li. The electrochemical data were recorded and processed by

Luxi Swisher and results from these studies have been captured in our recent paper by Swisher *et al*.[91] The design of the three electrode ACV electrochemical cell incorporating a covalently attached Fc-labeled tetrapeptide is shown below in Figure 44. The working electrode consists of Fc-tetrapeptide functionalized VACNFs embedded in a SiO_2 matrix. The reference electrode is Ag/AgCl and the auxiliary electrode is platinum. The three electrodes are connected to a potentiostat which allows the current to be monitored while the AC potential ramp is applied during ACV measurements. When the oxidation potential of the Fc is reached, a current is recorded in the potentiostat due to the oxidation of ferrocene (Fc) to ferricinium (Fc^+). When the applied potential is turned off an open cell results and the Fc^+ spontaneously and rapidly reduces back to Fc.

Figure 44: Three electrode ACV electrochemical cell containing covalently attached Fc-labeled tetrapeptide for legumain and cathepsin B detection.

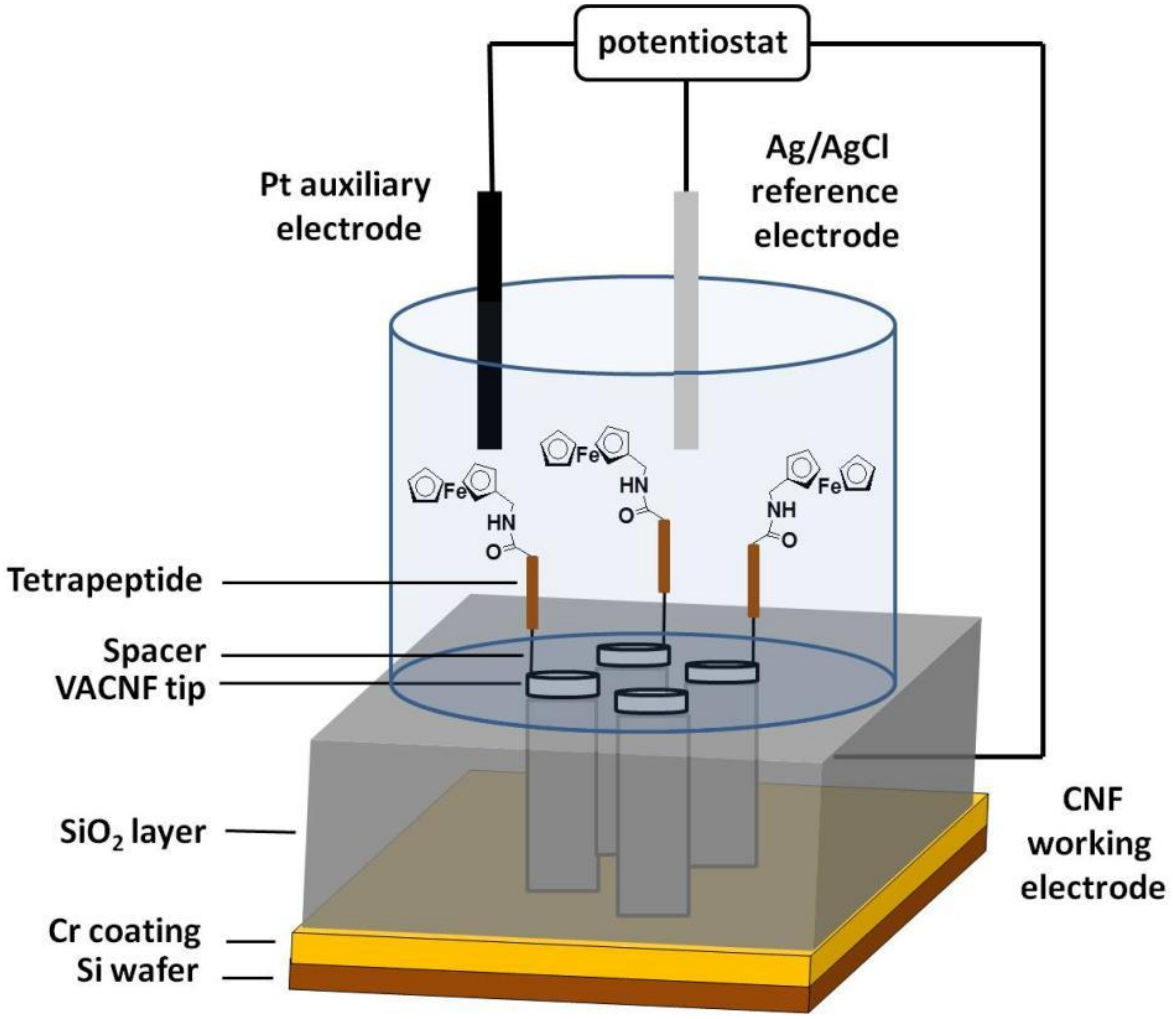

To start, the Fc-peptide **119** was coupled to the surface of both glassy carbon electrode and CNF electrode using a conventional EDC coupling technique. The presence of attached Fc-peptide **119** could be detected on glassy carbon electrode by cyclic voltammetry (CV) as can be seen by the peaks at 0.33V (oxidation) and 0.24V (reduction) in Figure 45 (a), which correspond to Faradic current due to the oxidation and reduction of Fc and Fc^+ respectively. The measurements were carried out by Luxi Swisher, using a scan rate of 50 mV s^{-1} in 1 mL of 1.0 M KCl.[91] The oxidation and reduction of ferrocene on a VACNF electrode could not be observed by CV as shown in Figure 45 (b). The absence of Faradic current signals showed that DC CV technique is not adequately sensitive for use with VACNF electrodes. The reason for this is due to the higher intrinsic resistance of the VACNF due to their stacked cone structures. This results in a slower electron transfer rate (ETR). To solve this problem, ACV was used in place of CV which proved to increased ETR for Fc-peptide functionalized VACNFs by a factor of ~100.[91] The reason for the significant increase in current seen in ACV measurements was attributed to the opening up of capacitive pathways in the stacked cone structures of VACNFs (due to the alternating current) causing a significant decrease in resistance and an increase in ETR.[91, 95]

Figure 45: Cyclic voltammograms of compound 119 immobilized on (a) GCE and (b) VACNF electrode. Reprinted with permission from (Swisher *et al., J. Phys. Chem. C:* 2013, *117*, 4268-4277). Copyright (2013) American Chemical Society.

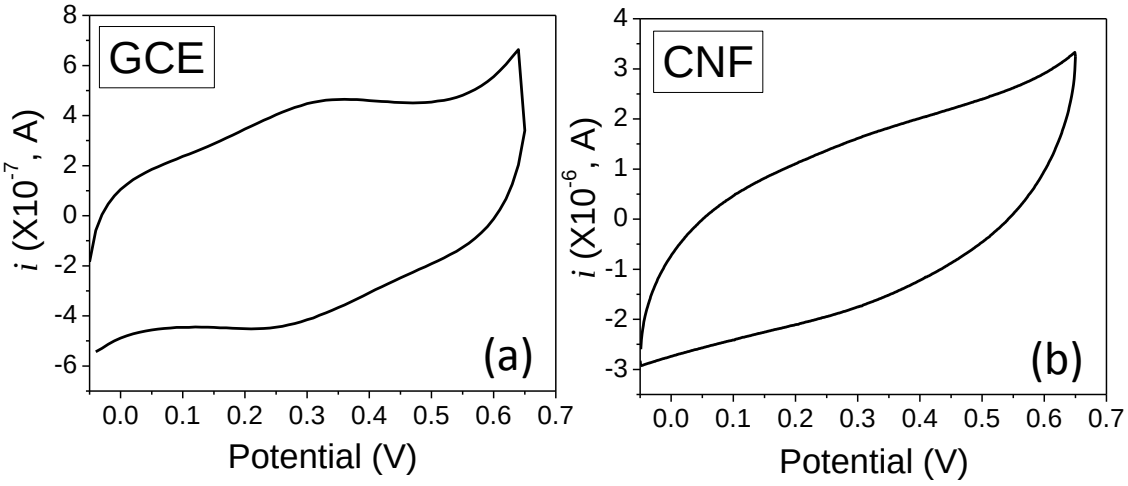

When using ACV to record Faradic current, two important factors to consider are the frequency of the applied AC potential and the amplitude of the applied AC potential. The frequency of the applied AC potential was varied from 0 to 8 KHz for compound **119** attached to GCE and CNF

electrode. These results have been captured in our recent publication by Swisher *et al*.[91] For GCE a maximum current density was obtained at 40 Hz but for CNF electrode the maximum current density was observed at 1.75 KHz. The higher current density at higher AC frequency exhibited for CNF NEA is advantages since it allows for a faster scan rate giving better temporal resolution.[91] The amplitude of the AC potential was also investigated and was varied from 0.01V to 0.5V for compound **119** on GCE and CNF electrode and its effect on current density monitored. It was determined that the current density reached a maximum at 0.35V for GCE but continued to increase non-linearly in CNF electrode up to 0.5V. Despite the fact the CNF electrode produced a higher current density at higher amplitudes, the optimal amplitude value that was used for subsequent study was 0.15 V as this provided the best balance between current peak resolution and satisfactory current density.[91] The following ACV measurements for compound **119** and legumain studies were therefore recorded using these optimized ACV frequency and amplitude values of 1.75 KHz and 0.15V respectively.

In order to monitor the cleavage of peptide **119** with legumain in real time, the current was monitored by continuously repeating ACV measurements. These data were recorded by Luxi Swisher and have been captured in our recent publication by Swisher *et al*.[91] The ACV potential was swept from -0.05 V to +0.65V using a scan rate of 10 mV/s. At a time of 22 minutes 11 µL of a 90.9 ng/µL [1.9 µM] solution of activated legumain solution was added into the electrochemical cell containing 50 mM MES (pH 5.0) and 250 mM NaCl. Final enzyme concentration was 80.1 nM in legumain. Figure 46 shows a plot of peak current vs time for the legumain cleavage experiment. Legumain was added at 22 min and the disturbance to the electrolyte caused an abrupt spike in the observed current. Thereafter, legumain action on the attached peptide **119** was observed by the occurrence of an exponential decay of the ACV current. The specificity constant (k_{cat}/K_m) for legumain and peptide **119** was calculated to be 11.3 x 10^3 $M^{-1}s^{-1}$ (Table 8) which compared favorably to a value obtained by fluorescence measurements when legumain acted on a commercial substrate (Ala-Ala-Asn-AMC; k_{cat}/K_m = 4.3 x 10^3 $M^{-1}s^{-1}$). Two separate control experiments were performed which involved treating the peptide **119** functionalized CNF with either buffer only or, buffer plus deactivated legumain, none of which displayed exponential signal decay in ACV measurements.[91]

Figure 46: Plot of peak current ($i_{p,acv}$) vs time for compound 119 on a VACNF electrode showing cleavage of peptide 119 by legumain starting at ~20 minutes with [E_o] of 80.1 nM. Adapted with permission from (Swisher *et al., J. Phys. Chem. C:* 2013, *117*, 4268-4277). Copyright (2013) American Chemical Society.

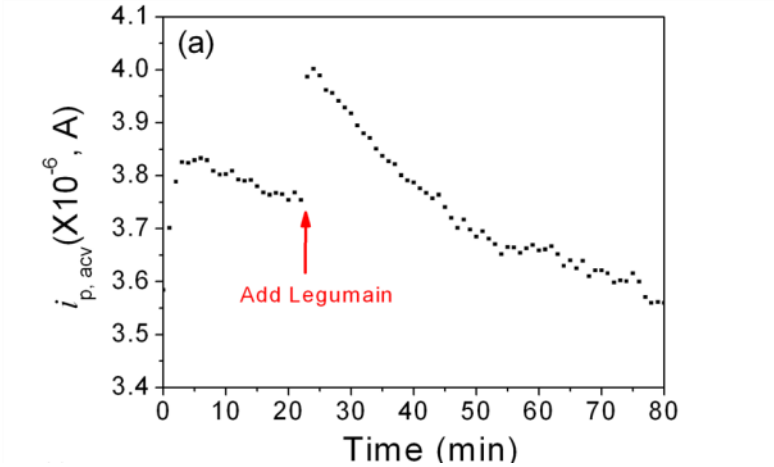

Table 8: Calculated kcat/Km values for the commercial legumain substrate (Ala-Ala-Asn-AMC) and compound 119 from fluorescence and electrochemical data respectively.

Peptide Sequence	k_{cat}/K_m ($M^{-1}s^{-1}$)	Method
Ala-Ala-Asn-AMC	$(4.3 \pm 0.6) \times 10^3$	fluorescence data
Ala-Ala-Asn-Leu-NH-CH_2-Fc	$(11.3 \pm 3.8) \times 10^3$	electrochemistry data.

The electrochemical ACV experiments were repeated by Luxi Swisher using peptide **120** on VACNF employing cathepsin B for cleavage studies. These results have been captured in our recent publication by Swisher *et al.*[91] The ACV frequency and amplitude were again optimized for the new peptide **120**, as mentioned previously. The highest current density was observed at a frequency of 800 Hz and was therefore used for subsequent ACV measurements. The current density increased linearly with increasing ACV amplitude up to 0.5V but as before, an ACV

amplitude of 0.15V was used for all measurements in order to prevent the ACV current peak from becoming broad and unstable.[91]

Luxi tracked the cleavage of peptide **120** attached to VACNF by cathepsin B in real time using ACV (Figure 47). These results have been captured in our recent publication by Swisher *et al*.[91] The ACV potential was swept from -0.05 V to +0.75V using a scan rate of 10 mV/s. At time 20 minutes 25 µL of a 9.8 ng/µL [338 nM] solution of cathepsin B in activation buffer (25 mM DTT and 25 mM MES @ pH 5.0) was added to the electrochemical cell containing 25 mM MES (pH 5.0). Final enzyme concentration was 30.7 nM in cathepsin B. A small spike in current at 20 minutes was observed because of disturbance to the electrolyte solution after which exponential decay of current signal occurred. Two separate control experiments were again performed and involved treating the peptide **120** functionalized CNF with either buffer only or, buffer plus deactivated cathepsin B, none of which displayed exponential signal decay in ACV measurements.[91]

Figure 47: Plot of peak Current ($i_{p,acv}$) for compound 120 on CNF electrode vs time. Cathepsin B was added at time 20 Minutes with [E_o] of 30.7 nM. Adapted with permission from (Swisher *et al., J. Phys. Chem. C:* 2013, *117,* 4268-4277). Copyright (2013) American Chemical Society.

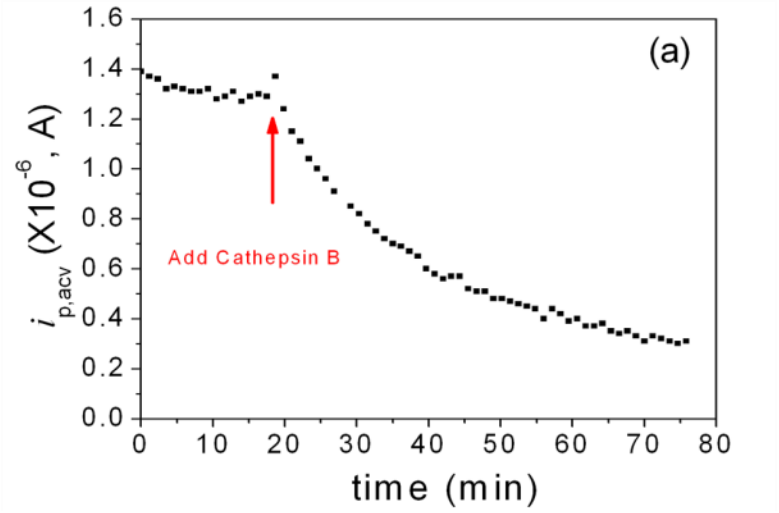

The specificity constant (k_{cat}/K_m) for cathepsin B and peptide **120** was calculated to be 4.3 x 10^4 $M^{-1}s^{-1}$ (Table 9) which compared favorably to a value obtained by fluorescence measurements when cathepsin B acted on a commercial substrate (Leu-Arg-AMC; k_{cat}/K_m = 2.3 x 10^4 $M^{-1}s^{-1}$). It

can be seen that the enzyme activity for cathepsin B is about 4 times higher than for legumain (higher specificity constant) and agrees with literature findings.[91, 100-102]

Table 9: Calculated kcat/Km Values for the Commercial Cathepsin B Substrate (Leu-Arg-AMC) and Compound 120 from Fluorescence and Electrochemical Data Respectively.

Peptide Sequence	k_{cat}/K_m ($M^{-1}s^{-1}$)	Method
Leu-Arg-AMC	$(2.3 \pm 1.7) \times 10^4$	fluorescence data
Leu-Arg-Phe-Gly-NH-CH_2-Fc	$(4.3 \pm 0.8) \times 10^4$	electrochemistry data.

III.III. Synthesis of Peptide Substrates 119 and 120.

The peptide substrate **119** was synthesized using solid phase peptide synthesis followed by post cleavage synthetic modification as shown in Scheme 29. The resin bound tetrapeptide **121** was constructed using conventional solid phase peptide synthesis starting from commercially available Leu-2-chlorotrityl resin. The coupling steps envolved microwave assisted HBTU mediated coupling of Fmoc-*N*-protected amino acids to the amino function of the resin bound peptide in DMF containing 4.2% diisopropylethylamine. Deprotection steps involved microwave assisted removal of the Fmoc protecting group using 20% piperidine in DMF. The resin bound peptide **121** was cleaved from the resin to form compound **122** in 45% overall yield. The N-terminal amine of **122** was protected with a Boc group using Boc anhydride in dioxane/water to furnish an *N*-Boc intermediate in 96% yield. The carboxyl group of the *N*-Boc intermediate was coupled with aminomethyl ferrocene using HATU in DMF to form **123** in 48% yield after purification using preparative HPLC. The aminomethyl ferrocene was made in house according to the reported procedure.[103] The Boc protecting group of **123** was removed using 10% TFA in dichloromethane to quantitatively form an amine intermediate which was coupled with *N*-Boc-5-aminovaleric acid using HATU to form compound **124** in 45% yield after purification using preparative HPLC. The *N*-Boc protection group of **124** was removed using 10% TFA in

dichloromethane in 98% yield to furnish compound **119** in a 9% overall yield as a fluffy green solid. The structure of compound **119** was confirmed by mass spectrometry analysis.

Scheme 29: Synthesis of Legumain Substrate 119.

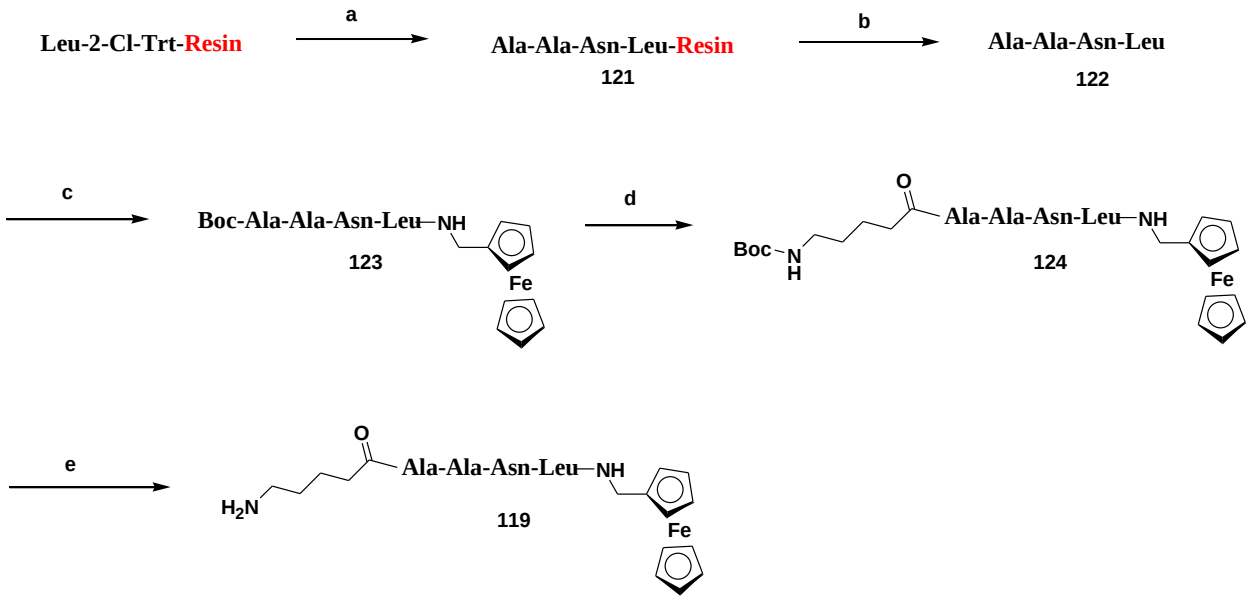

Reagents and conditions: (a) 1. Fmoc-Asn, HBTU, 4.2 % DIPEA/DMF, microwave; 2. 20% piperidine/DMF, microwave; 3. Fmoc-Ala, HBTU, 4.2 % DIPEA/DMF, microwave; 4. 20% piperidine/DMF, microwave; 5. Fmoc-Ala, HBTU, 4.2 % DIPEA/DMF, microwave; 6. 20% piperidine/DMF, microwave; (b) 95% TFA, 2.5% TIPS, 2.5% water, microwave, 45% overall yield; (c) 1. Boc_2O, NEt_3, dioxane/water (1:1), 25^{o}C, 12 h, 96%; 2. HATU, H_2NCH_2Fc, DMF, 25^{o}C, 2 h, 48%; (d) 1. 10% TFA/CH_2Cl_2, 25^{o}C, 30 min, 100%; 2. HATU, *N*-Boc-5-aminovaleric acid, DMF, 25^{o}C, 2 h, 45%; (e) 10% TFA/CH_2Cl_2, 25^{o}C, 30 min, 98%.

The peptide substrate **120** for cathepsin B studies was synthesized using solid phase peptide synthesis followed by post cleavage synthetic modification as shown in Scheme 30. The resin bound tetrapeptide **125** was constructed using conventional solid phase peptide synthesis starting from commercially available Gly-2-chlorotrityl resin. The coupling steps evolved microwave assisted HBTU mediated coupling of Fmoc-*N*-protected amino acids to the amino function of the resin bound peptide in DMF containing 4.2% diisopropylethylamine. Deprotection steps involved microwave assisted removal of the Fmoc protecting group using 20% piperidine in

DMF. The resin bound peptide **125** was cleaved from the resin to form compound **126** in 94% overall yield. The *N*-terminal amine of **126** was protected with a Boc group using Boc anhydride in dioxane/water to furnish an *N*-Boc intermediate in 99% yield. The carboxyl group of the *N*-Boc intermediate was coupled with aminomethyl ferrocene using HATU in DMF to form **127** in 50% yield after purification using preparative HPLC. The *N*-Boc protection group from **127** was removed using 10% TFA in dichloromethane in 98% yield to furnish compound **120** in a 46% overall yield as a fluffy green solid. The structure of compound **120** was confirmed by NMR spectroscopy and mass spectrometry analysis.

Scheme 30: Synthesis of Cathepsin B substrate 120.

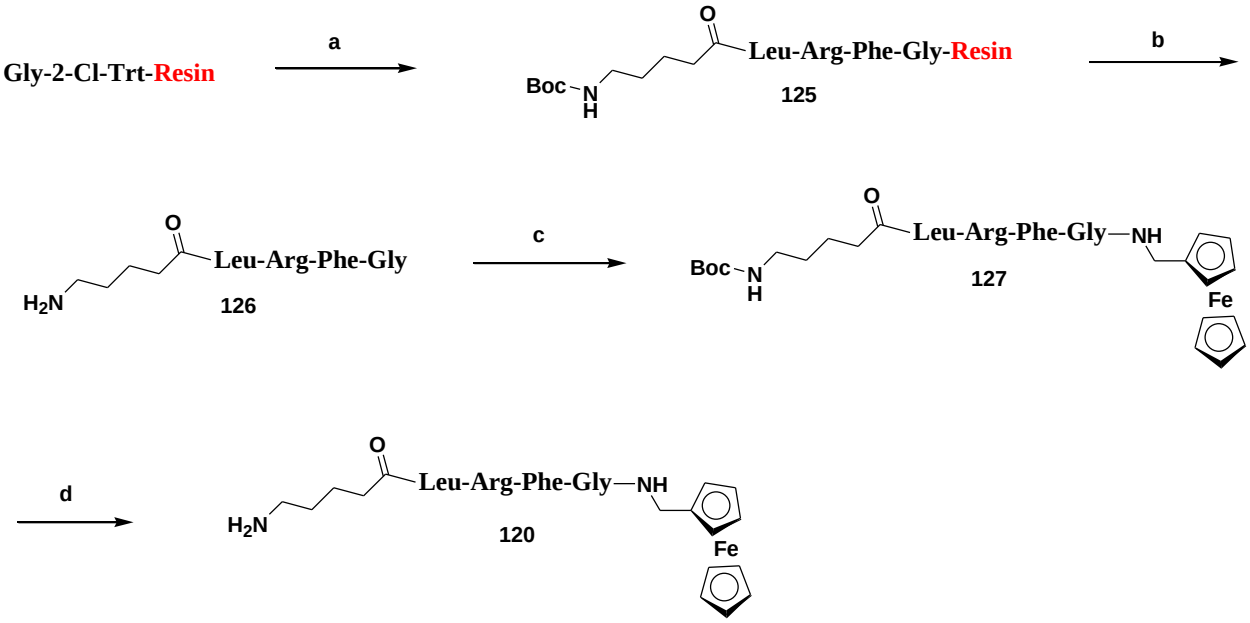

Reagents and conditions: (a) 1. Fmoc-Phe, HBTU, 4.2 % DIPEA/DMF, Microwave; 2. 20% piperidine/DMF, microwave; 3. Fmoc-Arg, HBTU, 4.2 % DIPEA/DMF, Microwave; 4. 20% piperidine/DMF, microwave; 5. Fmoc-Leu, HBTU, 4.2 % DIPEA/DMF, Microwave; 6. 20% piperidine/DMF, microwave; 7. *N*-Boc-5-aminovaleric acid, HBTU, 4.2 % DIPEA/DMF; microwave; 8. 20% piperidine/DMF, microwave; (b) 95% TFA, 2.5% TIPS, 2.5% water, microwave, 94% overall yield; (c) 1. Boc_2O, $NaHCO_3$, dioxane/water (1:1), 25^oC, 12 h, 99%; 2. HATU, H_2NCH_2Fc, DMF, 25^oC, 2 h, 50%; (d) 10% TFA/CH_2Cl_2, 25^oC, 30 min, 98%.

The non-substrate peptide **130** for cathepsin B studies was synthesized using solid phase peptide synthesis followed by post cleavage synthetic modification as shown in Scheme 31. The resin

bound tetrapeptide **128** was constructed using conventional solid phase peptide synthesis starting from commercially available Gly-2-chlorotrityl resin.

Scheme 31: Synthesis of Cathepsin B Non-Substrate 131.

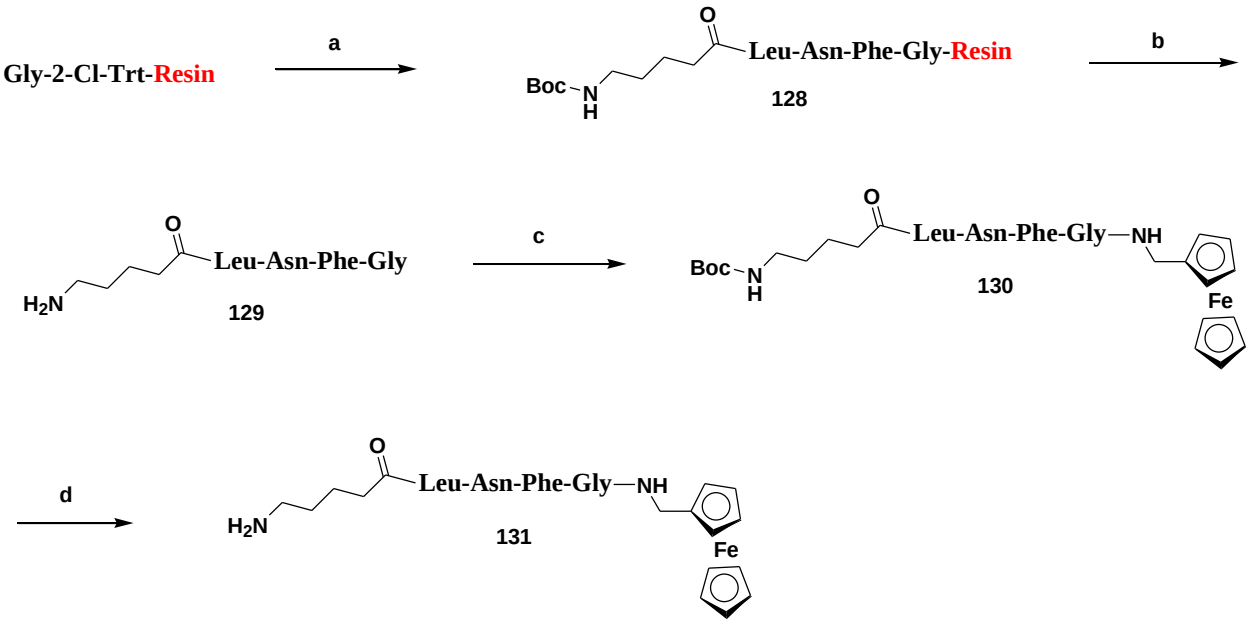

Reagents and conditions: (a) 1. Fmoc-Phe, HBTU, 4.2 % DIPEA/DMF, Microwave; 2. 20% piperidine/DMF, microwave; 3. Fmoc-Asn, HBTU, 4.2 % DIPEA/DMF, Microwave; 4. 20% piperidine/DMF, microwave; 5. Fmoc-Leu, HBTU, 4.2 % DIPEA/DMF, Microwave; 6. 20% piperidine/DMF, microwave; 7. *N*-Boc-5-aminovaleric acid, HBTU, 4.2 % DIPEA/DMF, Microwave; 8. 20% piperidine/DMF, microwave; (b) 95% TFA, 2.5% TIPS, 2.5% water, microwave, 83% overall yield; (c) 1. Boc_2O, $NaHCO_3$, dioxane/water (1:1), 25^{o}C, 12 h, 100%; 2. HATU, H_2NCH_2Fc, DMF, 25^{o}C, 2 h, 65%; (d) 10% TFA/CH_2Cl_2, 25^{o}C, 30 min, 100%.

The coupling steps evolved microwave assisted HBTU mediated coupling of Fmoc-*N*-protected amino acids to the amino function of the resin bound peptide in DMF containing 4.2% diisopropylethylamine. Deprotection steps involved microwave assisted removal of the Fmoc protecting group using 20% piperidine in DMF. Since this was designed to be a non-substrate for cathepsin B the P3 arginine was replaced with a P3 asparagine because this sequence was shown in literature to not be cleaved by cathepsin B. The resin bound peptide **128** was cleaved from the resin to form compound **129** in 83% overall yield. The *N*-terminal amine of **129** was protected

with a Boc group using Boc anhydride in dioxane/water to quantitatively furnish an *N*-Boc intermediate. The carboxyl group of an *N*-Boc intermediate was coupled with aminomethyl ferrocene using HATU in DMF to form **130** in 65% yield after purification using preparative HPLC. The *N*-Boc protection group from **130** was quantitatively removed using 10% TFA in dichloromethane to furnish compound **131** in a 54% overall yield as a fluffy green solid. The structure of compound **131** was confirmed by NMR spectroscopy and mass spectrometry analysis.

The authentic legumain cleaved fragment **133** was synthesized for HPLC study according to Scheme 32. Fmoc-Leu was coupled with aminomethyl ferrocene to form **132** in 54% yield after purification by column chromatography. The Fmoc protecting group was removed using 20% piperidine in DMF for form compound **133** in 67% yield. HPLC and mass spectrometry analysis confirmed that legumain does cleave peptide **119** to generate compound **133** as a fragment.

Scheme 32: Synthesis of Legumain Substrate Fragment 133 for HPLC Study.

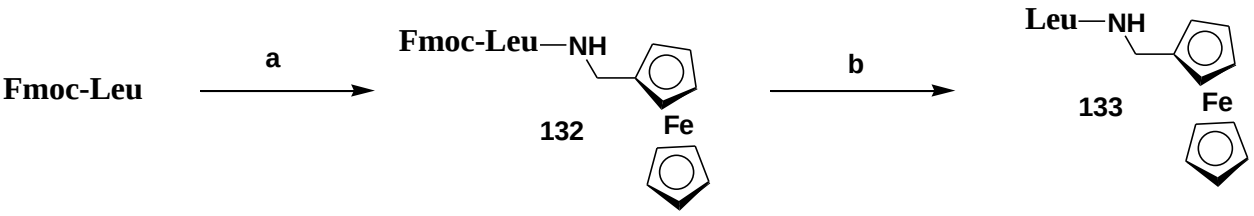

Reagents and conditions: (a) *N*-Boc-5-aminovaleric acid, HATU, DMF, 25^{o}C, 30 min, 54%; (b) 20% piperidine/DMF, 25^{o}C, 30 min, 67%.

The authentic cathepsin B cleaved fragment **136** was synthesized for HPLC study according to Scheme 33. The carboxyl group of boc-glycine was coupled with aminomethyl ferrocene using HATU to form compound **134** in 36% yield after column chromatography. Removal of Boc protecting group by 10% TFA in dichloromethane followed by HATU coupling with *N*-Boc phenylalanine provided compound **135** in 48% yield after purification by column chromatography. Removal of the Boc protecting group by 10% TFA in dichloromethane gave dipeptide **136** in 98% yield. HPLC and mass spectrometry analysis confirmed that cathepsin B does cleave peptide **120** to generate compound **136** as a fragment.

Scheme 33: Synthesis of Cathepsin B Substrate Fragment 136 for HPLC Study.

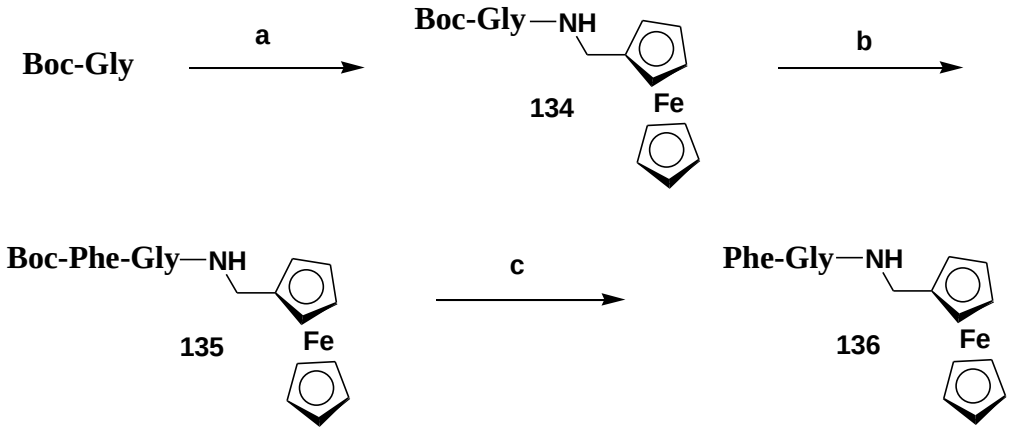

Reagents and conditions: (a) HATU, H_2NCH_2Fc, DMF, 25°C, 2 h, 36%; (b) 10% TFA/CH_2Cl_2, 25°C, 30 min, 100%; 2. HATU, *N*-Boc-Phe, DMF, 25°C, 2 h, 48%; (c) 10% TFA/CH_2Cl_2, 25°C, 30 min, 98%.

III.IV. Conclusion

The tetrapeptide protease substrates **119** and **120** were successfully synthesized and used in a bioelectronic cancer protease detection device. When attached to the tips of CNF NEAs, substrates **119** and **120** could successfully detect breast cancer related protease enzymes legumain and cathepsin B respectively by employing an ACV technique. In both cases an exponential decrease in ACV current could be detected at initial enzyme concentrations of 80.1 nM (legumain) and 30.7 nM (cathepsin B) showing excellent sensitivity for this technique. HPLC peptide cleavage studies confirmed activity and specificity for legumain and cathepsin B proteases. Legumain was found to have a specificity constant (k_{cat}/K_m) value of 11.3 x 10^3 $M^{-1}S^{-1}$ while cathepsin B was found to have higher value of k_{cat}/K_m (4.3 x 10^4 $M^{-1}S^{-1}$) which agreed with literature findings. Legumain was shown to cleave peptide **119** at the *C*-terminal side of asparagine residue while cathepsin B cleaved peptide **120** at the *C*-terminal side of arginine residue. Further studies are ongoing and will involve using this technique to detect legumain and cathepsin B enzymes in real cancer cell samples as well as investigate the use of alternative peptide probes for the detection of other cancer related proteases for example MMP-7.

IV. Experimental Section

IV.I. General Experimental Procedures

Nuclear magnetic resonance spectra were obtained from a Varian 400-MHz spectrometer using $CDCl_3$ as the solvent unless otherwise stated and all chemical shifts reported in ppm. Low resolution mass spectra were obtained using an API-2000-triple quadrupole electrospray ionization (ESI) MS/MS mass spectrometer (Applied Biosystems). High resolution mass spectra were obtained using LCT Premier (Waters Corp., Milford MA) time of flight mass spectrometer based at the University of Kansas Mass Spectrometry Laboratory. Infrared spectra were taken from a ThermoScientific Nicolet 380 FT-IR instrument. A Hewlett-Packard diode array UV/VIS spectrophotometer was used in the survey of proteases assays. Compound **91a** is available commercially, however, this compound was prepared as described in the manuscript. The enzyme assays for 3Cpro and 3CLpro with FRET-based assays have been previously reported.[39, 40] Cell based assays for virus replication for noroviruses, picornaviruses and coronaviruses have been previously reported.[40, 41] FT-Raman spectra were taken using a ThermoScientific DXR microRaman Microscope at a laser wavelength of 532 nm; laser power of 5 mW; confocal hole diameter of 3.1 μm; entrance slit width of 50 μm; grading of 900 lines/mm and an Olympus 10x objective lens. Solid state NMR spectra we obtained using a 3-channel solid-state NMR spectrometer with a Tecmag Apollo console attached to a 8.4 T (357 MHz) wide bore magnet. Peptides were synthesized using a CEM microwave peptide synthesizer. The 2-chlorotrityl resins (0.54 mmol/g; 200 mesh) were purchased from Peptide International. The experimental procedures for chapter 2.2 including ACV data have been reported in the supporting information of our recent journal article, Swisher *et al.* titled "Electrochemical Protease Biosensor Based on Enhanced AC Voltammetry Using Carbon Nanofiber Nanoelectrode Arrays."[91] Chemicals were purchased from Fisher Scientific, Aldrich Chemical Co., Chem-Impex International, and VWR.

General Procedure A: The *N*-Boc-dipeptide **76** (1 mmol) was dissolved in 10% TFA/CH_2Cl_2 (5 mL) and stirred at 25^{o}C for 4 h. The solvent was removed on a rotary evaporator to yield a sticky oil that was re-dissolved in chloroform followed by removal of the solvent once again on the

rotary evaporator to yield a semi-solid material. After sitting under high vacuum for 0.5 h, a white solid (amine intermediate) was obtained in quantitative yield. To this amine intermediate (1 mmol) was added (*S*)-*N*-Cbz-1-naphthylalanine (1 mmol), EDCI (2 mmol) and DMAP (2 mmol) followed by dry CH_2Cl_2 (15 mL) and the resulting solution was stirred at 25^oC for 18 h under argon atmosphere. The reaction mixture was partitioned between water (150 mL) and CH_2Cl_2 (150 mL), the aqueous layer was acidified to pH = 2 using 2 N HCl, and extracted three times with CH_2Cl_2 (150 mL each). The combined organic layers were dried (anhydrous $MgSO_4$), filtered, and concentrated to yield a solid which was purified by silica gel chromatography (30:1 CH_2Cl_2:MeOH) to yield compound **84**, 0.5 g (72% yield) as a white solid.

General Procedure B: To a solution of ester **84** (0.63 mmol) in CH_2Cl_2/MeOH (1:1) (8 mL) at 0^oC was added $NaBH_4$ (5.6 mmol) in small portions over a period of 4 h. The reaction was quenched with water (0.5 mL) and diluted with 100 mL of CH_2Cl_2. The solution was passed through a short plug of silica gel and the organic material washed thoroughly with 30:1 CH_2Cl_2/MeOH (100 mL). The filtrate was concentrated to yield a solid which was dissolved in distilled CH_2Cl_2 (15 mL) and treated with Dess-Martin periodinane (DMP) for 2 h at 25^oC. The reaction mixture was filtered and the filtrate was concentrated and purified by silica gel chromatography using a gradient solvent elution of 25% acetone/CH_2Cl_2 to 100% acetone. The fractions containing the product were combined and concentrated to give a white solid to which was added $CHCl_3$ (20 mL). After sitting for 10 min the mixture was filtered through a glass frit funnel (fine) and the filtrate was concentrated to provide aldehyde **24** (90% yield) as a white solid.

General procedure C: Isopropylisocyanide (0.067 mmol) was added to a solution of aldehyde **24** (0.067 mmol) in distilled EtOAc (2 mL) and AcOH (1 drop) and the resulting solution stirred at 25^oC for 18 h. The solvent was removed *in vacuo* and the residue was dissolved in a 1:1 solution of MeOH/H_2O (5 mL) and K_2CO_3 (0.16 mmol). After stirring for 3 h at 25^oC, the reaction was diluted with water and extracted with EtOAc (4 times). The combined organic layers were dried (anhydrous $MgSO_4$), filtered, and concentrated to yield a residue. To it, CH_2Cl_2 (2 mL) was added followed by DMP (0.13 mmol) and the reaction was stirred at 25^oC for 2 h. The solvent was removed *in vacuo* and the residue was purified by silica gel chromatography using a gradient solvent elution of 25% acetone/CH_2Cl_2 to 100% acetone. The fractions containing the

product were combined and concentrated to give a white solid to which was added $CHCl_3$ (10 mL). After sitting for 10 min the mixture was filtered through a glass frit funnel (fine) and the filtrate was concentrated to provide ketoamide **32** (36 mg, 79% yield) as a white solid.

General Procedure D: Diisopropylethylamine (0.25 mmol) was added to a solution of aldehyde **24** (0.25 mmol) and diethylphosphite (0.25 mmol) in distilled CH_2Cl_2. After stirring at 25^oC for 18 h, the reaction was diluted with ethyl acetate and washed with dilute HCl followed by brine. The organic layer was dried (anhydrous $MgSO_4$), filtered, and concentrated to yield an oil which was purified by silica gel column chromatography (9:1 CH_2Cl_2/MeOH) to afford two diastereomers (a mixture of *R* and *S* at carbon adjacent to phosphorus) of compound **36** (10 mg, 54% yield) as white solids.

General Procedure E: To a mixture of glutamine surrogate HCl salt (**53**, 5.59 mmol), *N*-Boc-leucine (5.59 mmol), 1-ethyl-3-(3-dimethylaminopropyl)carbodiimide (EDCI) (10.2 mmol), and 4-(dimethylamino)pyridine (DMAP) (10.2 mmol) under argon was added dry DMF (10 mL). The solution was stirred at 25^oC and dry CH_2Cl_2 (25 mL) was added, and the resulting solution was stirred for 18 h. The reaction was partitioned between water (150 mL) and CH_2Cl_2 (150 mL). The pH of the aqueous layer was adjusted to 3 using 2N HCl. The organic layer was removed, and the aqueous layer was extracted twice with CH_2Cl_2 (150 mL each). The combined organic layers were dried (anhydrous $MgSO_4$), filtered and concentrated to yield a sticky solid which was purified by silica gel chromatography (30:1 CH_2Cl_2:MeOH) to yield compound **76**, 1.6 g (72% yield) as a white solid.

General Procedure F (Coupling):

To the 2-chlorotrityl resin attached peptide (0.54 mmol) with free *N*-terminal amine was added a solution of Fmoc-amino acid (1.62 mmol, 3 equiv.) and HBTU (1.46 mmol, 2.7 equiv.) in dry DMF (13 mL) containing 4.2 % diisopropylethyl amine. The mixture was subjected to microwave irradiation (25 W, 5 min, 75 ^oC) with stirring. The reaction mixture was filtered and washed with DMF (20 mL each, 5 times).

General Procedure G (Fmoc deprotection):

A solution of 20% piperidine in DMF (20 mL) was added to the 2-chlorotrityl resin attached peptide (0.54 mmol) having an Fmoc protected *N*-terminal amine and subjected to microwave irradiation (50 W, 3 min, 75 ^{o}C). The reaction mixture was filtered and washed with DMF (20 ml each, 5 times).

General Procedure H (Cleavage):

The 2-chlorotrityl resin attached peptide (0.54 mmol) was washed with dichloromethane (20 mL) and mixed with 20 mL of a cleavage cocktail solution consisting of 95% trifluoroacetic acid (TFA), 2.5% triisopropylsilane (TIPS), and 2.5% water. The mixture was irradiated in a microwave reactor (20 W, 38 ^{o}C) for 18 min. The reaction mixture was filtered into a 100 mL flask and diluted with 100 mL of cold hexane:ether (1:1) to precipitate out the desired peptide as a white solid. The solid peptide was collected by centrifugation (2500 rpm) and washed three times with cold hexane:ether (1:1) to give the product peptide as a white solid (yields 45-94%).

IV.II. Experimental Procedures

{1-[1-Formyl-2-(2-oxo-pyrrolidin-3-yl)-ethylcarbamoyl]-ethyl}-carbamic acid benzyl ester (1).

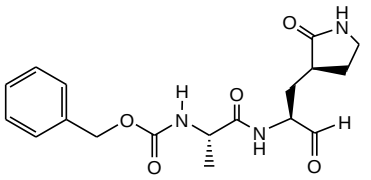

Followed General Procedure B: Started with ester **54** yielding compound **1** (61%) as a white solid. ^{1}H NMR δ 9.48 (br. s., 1H), 8.32 (br. s., 1H), 7.28 - 7.39 (m, 5H), 6.02 (br. s., 1H), 5.57 (d, *J* = 6.64 Hz, 1H), 5.11 (s, 2H), 4.28 - 4.41 (m, 2H), 3.27 - 3.39 (m, 2H), 2.33 - 2.50 (m, 2H), 1.95 (d, *J* = 5.47 Hz, 1H), 1.78 - 1.90 (m, 1H), 1.70 (br. s., 1H), 1.44 (d, *J* = 7.03 Hz, 3H); ^{13}C NMR δ 199.6, 180.0, 173.6, 155.8, 136.3, 128.5, 128.1, 128.0, 66.9, 58.0, 50.5, 40.6, 38.3, 29.6, 28.8, 19.2; MS, m/z 384.1 $(M+Na)^{+}$.

2-[1-Formyl-2-(2-oxo-pyrrolidin-3-yl)-ethylcarbamoyl]-piperidine-1-carboxylic acid benzyl ester (2).

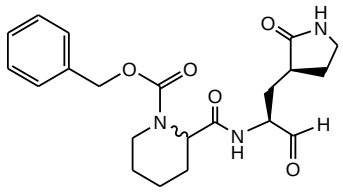

Followed General Procedure B. Started with ester **55** yielding compound **2** (52%) as a white solid. ^{1}H NMR δ 9.44 (s, 1H), 8.25 (s, 1H), 7.28 - 7.39 (m, 5H), 5.69 - 5.99 (m, 1H), 5.11 (s, 2H), 4.80 - 4.98 (m, 1H), 4.02 - 4.40 (m, 1H), 3.20 - 3.39 (m, 2H), 3.80 - 3.11 (m, 2H), 2.21 - 2.44 (m, 3H), 1.78 - 1.99 (m, 3H), 1.58 - 1.72 (m, 3H), 1.39 - 1.50 (m, 2H); MS, m/z 424.5 $(M+Na)^{+}$.

(1-{1-[1-Formyl-2-(2-oxo-pyrrolidin-3-yl)-ethylcarbamoyl]-ethylcarbamoyl}-ethyl)-carbamic acid benzyl ester (3).

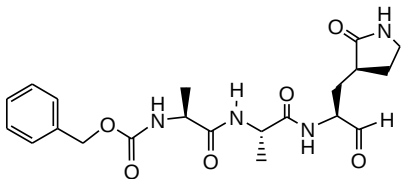

Followed General Procedure B: Started with ester **63** yielding compound **3** (76%) as a white solid. ^{1}H NMR δ 9.48 (s, 1H), 8.39 (br. s., 1H), 7.29 - 7.38 (m, 5H), 7.00 (br. s., 1H), 6.18 (br. s., 1H), 5.64 (br. s., 1H), 5.04 - 5.14 (m, 2H), 4.53 - 4.60 (m, 1H), 4.20 - 4.34 (m, 2H), 3.26 - 3.37 (m, 2H), 2.34 - 2.51 (m, 2H), 1.90 - 1.97 (m, 2H), 1.77 - 1.88 (m, 1H), 1.42 (d, *J* = 7.03 Hz, 3H), 1.38 (d, *J* = 7.03 Hz, 3H); ^{13}C NMR δ 199.7, 179.9, 173.4, 172.5, 156.0, 136.2, 128.3, 128.0, 127.9, 66.7, 57.4, 50.7, 48.9, 40.4, 38.0, 29.7, 28.2, 18.4, 18.3; MS, m/z 455.6 $(M+Na)^{+}$.

[2-(Formyl-{1-[1-formyl-2-(2-oxo-pyrrolidin-3-yl)-ethylcarbamoyl]-ethyl}-amino)-1-methyl-ethyl]-carbamic acid benzyl ester (4).

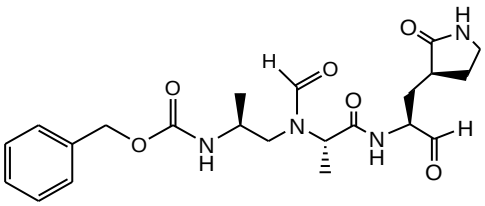

Followed General Procedure B: Started with ester **73** yielding compound **4** (65%) as a white solid. ^{1}H NMR δ 9.41 - 9.49 (m, 1H), 9.03 (br. s., 1H), 8.81 - 8.87 (m, 1H), 8.55 - 8.60 (m, 1H), 8.39 (d, *J* = 5.86 Hz, 1H), 8.27 (br. s., 1H), 7.94 - 8.09 (m, 1H), 7.23 - 7.38 (m, 5H), 6.11 - 6.29 (m, 1H), 5.53 - 5.78 (m, 1H), 4.95 - 5.14 (m, 2H), 4.08 - 4.42 (m, 2H), 3.78 - 4.01 (m, 2H), 3.59 - 3.73 (m, 2H), 3.03 - 3.48 (m, 3H), 2.25 - 2.54 (m, 2H), 2.01 - 2.23 (m, 2H), 1.70 - 1.95 (m, 2H), 1.37 - 1.60 (m, 2H), 1.07 - 1.29 (m, 6H); MS, m/z 469.3 $(M+Na)^{+}$.

(1-{1-[1-Formyl-2-(2-oxo-pyrrolidin-3-yl)-ethylcarbamoyl]-ethylcarbamoyl}-ethyl)-carbamic acid benzyl ester (5).

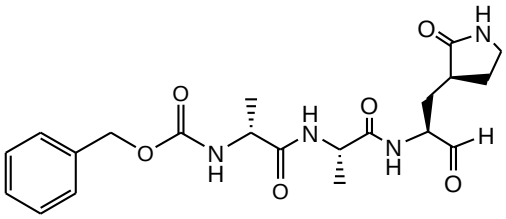

Followed General Procedure B: Started with ester **64** yielding compound **5** (52%) as a white solid. ^{1}H NMR δ 9.44 (s, 1H), 8.63 (d, *J* = 5.08 Hz, 1H), 7.30 - 7.39 (m, 5H), 6.96 (d, *J* = 7.81 Hz, 1H), 6.18 (d, *J* = 7.81 Hz, 1H), 6.00 (br. s., 1H), 5.02 - 5.12 (m, 2H), 4.66 (quin, *J* = 7.32 Hz, 1H), 4.32 (quin, *J* = 7.22 Hz, 1H), 4.20 - 4.27 (m, 1H), 3.18 - 3.28 (m, 2H), 2.29 - 2.48 (m, 2H), 1.86 - 1.92 (m, 2H), 1.74 - 1.85 (m, 1H), 1.37 - 1.45 (m, 6H); ^{13}C NMR δ 200.1, 180.2, 173.4, 172.2, 156.2, 136.1, 128.6, 128.3, 128.2, 67.1, 58.2, 50.7, 48.8, 40.7, 38.7, 29.4, 28.8, 18.5, 18.3; MS, m/z 455.2 $(M+Na)^{+}$.

(1-{1-[1-Formyl-2-(2-oxo-pyrrolidin-3-yl)-ethylcarbamoyl]-ethylcarbamoyl}-2-naphthalen-1-yl-ethyl)-carbamic acid benzyl ester (7).

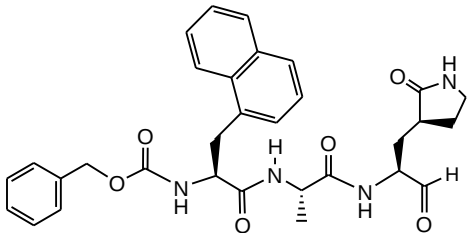

Followed General Procedure B: Started with ester **23** yielding compound **7** (72%) as a white solid. ^{1}H NMR δ 9.40 (s, 1H), 8.16 (d, *J* = 8.20 Hz, 1H), 8.08 (d, *J* = 5.86 Hz, 1H), 7.83 (d, *J* = 8.98 Hz, 1H), 7.70 - 7.76 (m, 1H), 7.44 - 7.54 (m, 2H), 7.23 - 7.35 (m, 7H), 7.01 (d, *J* = 7.42 Hz, 1H), 6.19 (s, 1H), 5.69 (d, *J* = 7.03 Hz, 1H), 5.02 (s, 2H), 4.56 - 4.66 (m, 1H), 4.45 - 4.53 (m, 1H), 4.21 (d, *J* = 4.69 Hz, 1H), 3.60 (dd, *J* = 6.64, 14.06 Hz, 1H), 3.45 (dd, *J* = 6.64, 13.86 Hz, 1H), 3.21 - 3.28 (m, 2H), 2.26 - 2.39 (m, 2H), 1.70 - 1.87 (m, 3H), 1.35 (d, *J* = 7.07 Hz, 3H); ^{13}C NMR δ 199.9, 179.9, 173.0, 170.9, 156.1, 136.0, 133.8, 132.5, 132.0, 128.8, 128.5, 128.2, 128.0, 127.9, 127.7, 126.4, 125.8, 125.3, 123.6, 67.0, 57.7, 55.8, 49.0, 40.5, 38.2, 35.4, 29.7, 29.2, 28.6, 18.4; MS, m/z 581.4 $(M+Na)^{+}$.

(1-{1-[1-Formyl-2-(2-oxo-pyrrolidin-3-yl)-ethylcarbamoyl]-ethylcarbamoyl}-2-naphthalen-2-yl-ethyl)-carbamic acid benzyl ester (8).

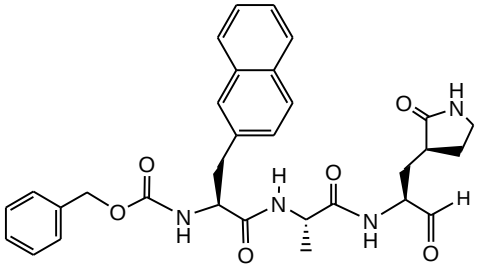

Followed General Procedure B: Started with ester **80** yielding compound **8** (38%) as a white solid. ^{1}H NMR δ 9.36 (s, 1H), 8.26 (d, *J* = 5.08 Hz, 1H), 7.75 - 7.80 (m, 2H), 7.71 - 7.75 (m, 2H), 7.62 (s, 1H), 7.42 - 7.46 (m, 2H), 7.21 - 7.34 (m, 7H), 7.12 (d, *J* = 7.42 Hz, 1H), 6.22 (br. s., 1H), 5.61 (d, *J* = 7.42 Hz, 1H), 4.97 - 5.07 (m, 2H), 4.49 - 4.64 (m, 2H), 4.15 - 4.22 (m, 2H), 3.13 - 3.33 (m, 4H), 2.22 - 2.42 (m, 2H), 1.65 - 1.84 (m, 3H), 1.32 - 1.38 (m, 3H); ^{13}C NMR δ 199.9, 180.0, 173.2, 170.9, 156.2, 136.0, 133.8, 133.3, 132.3, 128.5, 128.3, 128.2, 128.1, 127.9, 127.6, 127.6, 127.4, 126.1, 125.8, 67.1, 57.9, 56.0, 49.0, 40.5, 38.3, 29.5, 29.2, 28.6, 18.5; MS, m/z 581.5 $(M+Na)^{+}$.

(2-Biphenyl-4-yl-1-{1-[1-formyl-2-(2-oxo-pyrrolidin-3-yl)-ethylcarbamoyl]-ethylcarbamoyl}-ethyl)-carbamic acid benzyl ester (9).

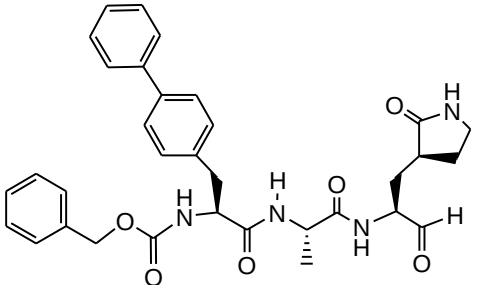

Followed General Procedure B: Started with ester **81** to give compound **9** (60% yield) as a white solid. ^{1}H NMR δ 9.44 (s, 1H), 8.39 (br. s., 1H), 7.18 - 7.58 (m, 15H), 6.53 (br. s., 1H), 5.74 (d, *J* = 7.03 Hz, 1H), 4.97 - 5.10 (m, 2H), 4.51 - 4.63 (m, 2H), 4.22 - 4.30 (m, 1H), 3.00 - 3.28 (m, 4H), 2.34 - 2.43 (m, 1H), 2.21-2.32 (m, 1H), 1.88 - 1.98 (m, 1H), 1.79 - 1.88 (m, 1H), 1.67 - 1.78 (m, 1H), 1.32 - 1.43 (m, 3H); ^{13}C NMR δ 200.0, 180.3, 173.6, 171.2, 156.4, 140.8, 140.0, 136.3, 135.5, 130.0, 129.0, 128.8, 128.5, 128.3, 127.5, 127.2, 67.4, 58.2, 56.3, 49.3, 40.8, 38.5, 38.0, 29.9, 28.8, 19.0; MS, m/z 607.1 $(M+Na)^{+}$.

(1-{2-tert-Butoxy-1-[1-formyl-2-(2-oxo-pyrrolidin-3-yl)-ethylcarbamoyl]-ethylcarbamoyl}-2-naphthalen-1-yl-ethyl)-carbamic acid benzyl ester (11).

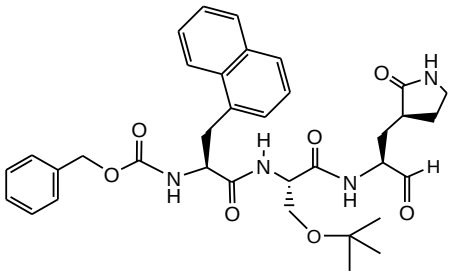

Followed General Procedure B: Started with ester **83** yielding compound **11** (45%) as a white solid. ^{1}H NMR δ 9.46 (s, 1H), 8.20 (d, *J* = 8.20 Hz, 1H), 7.88 (d, *J* = 7.03 Hz, 1H), 7.84 (d, *J* = 8.59 Hz, 1H), 7.74 (d, *J* = 7.42 Hz, 1H), 7.46 - 7.57 (m, 2H), 7.27 - 7.38 (m, 7H), 6.91 (d, *J* = 7.42 Hz, 1H), 5.63 (br. s., 1H), 5.45 (d, *J* = 6.64 Hz, 1H), 5.06 (s, 2H), 4.59 - 4.68 (m, 1H), 4.48 - 4.53 (m, 1H), 4.26 - 4.34 (m, 1H), 3.81 (d, *J* = 6.64 Hz, 1H), 3.67 (dd, *J* = 7.03, 14.25 Hz, 1H), 3.51 (dd, *J* = 7.03, 14.06 Hz, 1H), 3.19 - 3.32 (m, 2H), 2.25 - 2.36 (m, 2H), 1.72 - 1.85 (m, 3H), 1.06 (s, 9H); ^{13}C NMR δ 200.0, 184.7, 179.4, 170.8, 156.3, 135.9, 134.9, 133.9, 132.4, 132.0, 128.8, 128.5, 128.2, 128.1, 127.7, 126.5, 125.9, 125.4, 123.7, 73.5, 67.3, 61.4, 57.5, 56.0, 53.3, 40.3, 37.7, 35.4, 29.8, 28.5, 27.3; MS, m/z 653.3 $(M+Na)^{+}$.

(1-{1-[1-Formyl-2-(2-oxo-pyrrolidin-3-yl)-ethylcarbamoyl]-2-hydroxy-ethylcarbamoyl}-2-naphthalen-1-yl-ethyl)-carbamic acid benzyl ester (12).

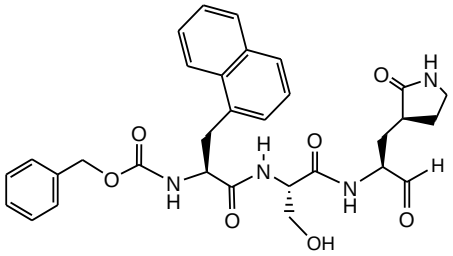

The aldehyde **11** (0.0095 mmol) was dissolved in 1:1 TFA:CH_2Cl_2 (0.5 mL) and stirred at 25^{o}C for 1 h. The solvents were removed on a rotary evaporator and the remaining residue was purified by silica gel column chromatography (1:1 CH_2Cl_2:2-propanol) to yield compound **12** (4 mg, 73%) as a white solid. ^{1}H NMR δ 9.44 (s, 1H), 8.11 - 8.21 (m, 1H), 7.84 (d, *J* = 8.20 Hz, 1H), 7.74 (d, *J* = 8.20 Hz, 1H), 7.43 - 7.58 (m, 2H), 7.22 - 7.39 (m, 7H), 5.84 - 5.90 (m, 1H), 5.55 - 5.62 (m, 1H), 5.02 (br. s., 2H), 4.50 - 4.68 (m, 2H), 4.32 - 4.48 (m, 1H), 3.83 - 3.99 (m,

2H), 3.57 - 3.70 (m, 2H), 3.40 - 3.50 (m, 1H), 3.20 - 3.21 (m, 1H), 2.36 (br. s., 1H), 1.95 - 2.08 (m, 1H), 1.13-1.22 (m, 2H); MS, m/z 597.5 $(M+Na)^+$.

{1-[2-Isopropylcarbamoyl-2-oxo-1-(2-oxo-pyrrolidin-3-ylmethyl)-ethylcarbamoyl]-ethyl}-carbamic acid benzyl ester (13).

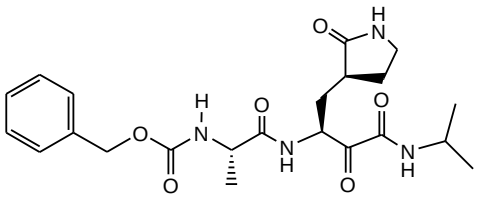

Followed General Procedure C: Started with aldehyde **1** yielding compound **13** (46%) as a white solid. ^{1}H NMR δ 8.30 (s, 1H), 7.28 - 7.39 (m, 5H), 6.73 (s, 1H), 5.81 (s, 1H), 5.42 (d, *J* = 7.22 Hz, 1H), 5.19 - 5.29 (m, 1H), 5.11 (s, 2H), 4.28 - 4.39 (m, 1H), 3.95 - 4.09 (m, 1H), 3.23 - 3.40 (m, 2H), 2.41 - 2.59 (m, 2H), 2.05 - 2.15 (m, 1H), 1.85 - 2.01 (m, 2H), 1.39 (d, *J* = 7.03 Hz, 3H), 1.13 - 1.21 (m, 6H); ^{13}C NMR δ 195.5, 180.1, 171.1, 165.9, 158.7, 136.6, 128.7, 128.3, 128.2, 67.1, 54.1, 50.5, 42.0, 40.8, 39.3, 32.1, 29.5, 28.9, 22.6, 22.5; MS, m/z 469.1 $(M+Na)^+$.

(1-{1-[2-Isopropylcarbamoyl-2-oxo-1-(2-oxo-pyrrolidin-3-ylmethyl)-ethylcarbamoyl]-ethylcarbamoyl}-ethyl)-carbamic acid benzyl ester (14).

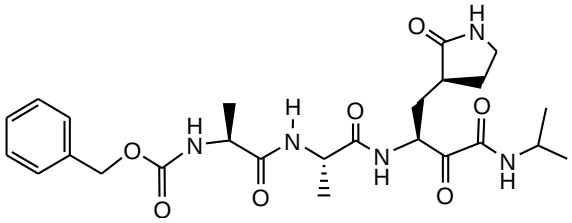

Followed General Procedure C: Started with aldehyde **3** yielding compound **14** (64%) as a white solid. ^{1}H NMR δ 8.37 (br. s., 1H), 7.29 - 7.38 (m, 5H), 6.90 (br. s., 1H), 6.80 (d, *J* = 8.20 Hz, 1H), 6.17 (br. s., 1H), 5.60 (d, *J* = 6.25 Hz, 1H), 5.20 - 5.27 (m, 1H), 5.05 - 5.15 (m, 2H), 4.52 - 4.60 (m, 1H), 4.20 - 4.29 (m, 1H), 3.99 - 4.08 (m, 1H), 3.34 (dd, *J* = 4.30, 8.98 Hz, 2H), 2.50 - 2.60 (m, 1H), 2.45 (td, *J* = 4.10, 8.20 Hz, 1H), 2.04 - 2.11 (m, 1H), 1.88 - 2.01 (m, 2H), 1.34 - 1.43 (m, 6H), 1.21 (d, *J* = 6.53 Hz, 3H), 1.20 (d, *J* = 6.54 Hz, 3H); ^{13}C NMR δ 195.2, 180.0,

172.4, 171.9, 158.5, 155.9, 136.2, 128.5, 128.2, 128.0, 67.0, 53.7, 50.7, 48.8, 41.8, 40.6, 39.0, 31.9, 29.3, 28.4, 22.3, 22.3, 18.7; MS, m/z 540.4 $(M+Na)^+$.

[2-(Formyl-{1-[2-isopropylcarbamoyl-2-oxo-1-(2-oxo-pyrrolidin-3-ylmethyl)-ethylcarbamoyl]-ethyl}-amino)-1-methyl-ethyl]-carbamic acid benzyl ester (15).

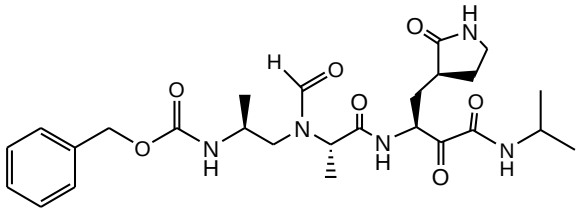

Followed General Procedure C: Started with aldehyde **4** yielding compound **15** (79%) as a white solid. ^{1}H NMR δ 9.21 - 9.29 (m, 2H), 8.59 - 8.65 (m, 1H), 8.33 - 8.41 (m, 1H), 8.20 - 8.29 (m, 1H), 7.24 - 7.38 (m, 5H), 6.71 - 6.82 (m, 2H), 6.14 - 6.24 (m, 1H), 5.66 (d, *J* = 7.03 Hz, 1H), 4.96 - 5.20 (m, 3H), 4.08 - 4.19 (m, 1H), 3.79 - 4.05 (m, 3H), 3.59 - 3.76 (m, 1H), 3.18 - 3.43 (m, 4H), 2.48 - 2.62 (m, 1H), 2.41 (d, *J* = 3.91 Hz, 1H), 1.98 - 2.13 (m, 1H), 1.78 - 1.95 (m, 2H), 1.38 - 1.55 (m, 3H), 1.10 - 1.29 (m, 9H); MS, m/z 554.6 $(M+Na)^+$.

(1-{1-[2-Isopropylcarbamoyl-2-oxo-1-(2-oxo-pyrrolidin-3-ylmethyl)-ethylcarbamoyl]-ethylcarbamoyl}-ethyl)-carbamic acid benzyl ester (16).

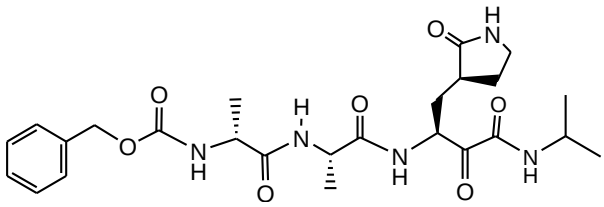

Followed General Procedure C: Started with aldehyde **5** yielding compound **16** (47%) as a white solid. ^{1}H NMR δ 8.67 (d, *J* = 4.30 Hz, 1H), 7.31 - 7.40 (m, 5H), 6.73 - 6.82 (m, 2H), 6.21 (d, *J* = 8.20 Hz, 1H), 5.86 (d, *J* = 13.28 Hz, 1H), 5.15 - 5.22 (m, 1H), 5.04 - 5.13 (m, 2H), 4.59 - 4.67 (m, 1H), 4.29 - 4.38 (m, 1H), 3.96 - 4.08 (m, 1H), 3.16 - 3.26 (m, 2H), 2.48 - 2.59 (m, 1H), 2.34 - 2.46 (m, 1H), 2.02 - 2.10 (m, 1H), 1.79 - 1.96 (m, 2H), 1.41 (d, *J* = 7.42 Hz, 3H), 1.38 (d, *J* = 6.64 Hz, 3H), 1.20 (d, *J* = 6.45 Hz, 3H), 1.19 (d, *J* = 6.57 Hz, 3H); ^{13}C NMR δ 195.0, 180.1, 172.4, 171.9, 158.5, 156.1, 136.1, 128.6, 128.3, 128.3, 67.1, 54.0, 50.7, 48.5, 41.7, 40.7, 39.6, 31.2, 28.8, 22.3, 22.2, 18.6, 18.4; MS, m/z 540.2 $(M+Na)^+$.

(1-{1-[2-Isopropylcarbamoyl-2-oxo-1-(2-oxo-pyrrolidin-3-ylmethyl)-ethylcarbamoyl]-ethylcarbamoyl}-2-naphthalen-1-yl-ethyl)-carbamic acid benzyl ester (17).

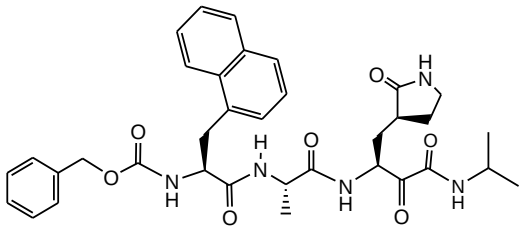

Followed General Procedure C: Started with aldehyde **7** yielding compound **17** (81%) as a white solid. ^{1}H NMR δ 8.30 (d, *J* = 5.47 Hz, 1H), 8.16 (d, *J* = 7.81 Hz, 1H), 7.84 (d, *J* = 8.59 Hz, 2H), 7.74 (d, *J* = 7.42 Hz, 2H), 7.44 - 7.55 (m, 2H), 7.22 - 7.38 (m, 7H), 6.81 (d, *J* = 7.81 Hz, 1H), 6.16 (br. s., 1H), 5.58 (d, *J* = 7.42 Hz, 1H), 5.15 - 5.22 (m, 1H), 5.02 (s, 2H), 4.55 - 4.64 (m, 1H), 4.42 - 4.50 (m, 1H), 3.97 - 4.07 (m, 1H), 3.61 (dd, *J* = 6.44, 14.25 Hz, 1H), 3.46 (dd, *J* = 6.44, 14.06 Hz, 1H), 3.26 - 3.35 (m, 1H), 2.37 - 2.56 (m, 2H), 2.00 - 2.08 (m, 1H), 1.86 - 1.97 (m, 2H), 1.30 (d, *J* = 7.03 Hz, 3H), 1.15 - 1.22 (m, 6H); ^{13}C NMR δ 195.5, 180.2, 172.3, 170.9, 158.7, 156.3, 136.3, 134.1, 132.8, 132.3, 129.1, 128.7, 128.4, 128.2, 128.1, 128.0, 126.7, 126.0, 125.6, 123.9, 67.2, 56.0, 53.9, 49.1, 42.0, 40.9, 39.3, 35.7, 32.1, 28.7, 22.6, 22.5, 18.9; MS, m/z 666.5 $(M+Na)^{+}$.

(1-{1-[2-Isopropylcarbamoyl-2-oxo-1-(2-oxo-pyrrolidin-3-ylmethyl)-ethylcarbamoyl]-ethylcarbamoyl}-2-naphthalen-2-yl-ethyl)-carbamic acid benzyl ester (18).

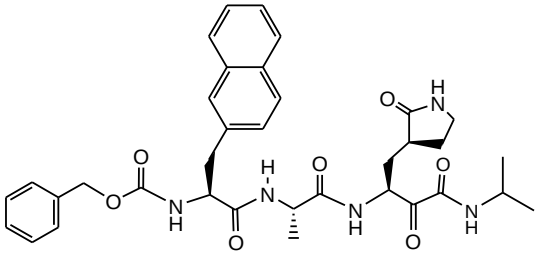

Followed General Procedure C: Started with aldehyde **9** yielding compound **18** (94%) as a white solid. ^{1}H NMR δ 8.40 (d, *J* = 5.47 Hz, 1H), 7.77 - 7.81 (m, 1H), 7.71 - 7.76 (m, 2H), 7.61 (s, 1H), 7.42 - 7.46 (m, 2H), 7.20 - 7.36 (m, 9H), 6.96 - 7.04 (m, 1H), 6.81 (d, *J* = 7.81 Hz, 1H), 6.16 - 6.23 (m, 1H), 5.51 (br. s., 1H), 5.15 - 5.22 (m, 1H), 4.98 - 5.07 (m, 2H), 4.51 - 4.62 (m, 2H), 3.98 - 4.07 (m, 1H), 3.18 - 3.32 (m, 4H), 2.44 - 2.54 (m, 1H), 2.34 - 2.43 (m, 1H), 2.00 - 2.08 (m, 1H), 1.80 - 1.96 (m, 3H), 1.35 (d, *J* = 7.03 Hz, 3H), 1.20 (d, *J* = 6.46 Hz, 3H), 6.62 (d, *J* = 3.12 Hz, 3H); ^{13}C NMR δ 195.2, 179.9, 172.2, 170.6, 158.4, 156.0, 136.0, 133.8, 133.3, 132.4,

128.5, 128.3, 128.1, 127.9, 127.6, 127.4, 126.1, 125.7, 67.0, 55.9, 53.7, 48.8, 41.7, 40.6, 39.0, 38.3, 31.7, 28.4, 22.3, 22.2, 18.7; MS, m/z 682.6 $(M+K)^+$.

(1-{2-tert-Butoxy-1-[2-isopropylcarbamoyl-2-oxo-1-(2-oxo-pyrrolidin-3-ylmethyl)-ethylcarbamoyl]-ethylcarbamoyl}-2-naphthalen-1-yl-ethyl)-carbamic acid benzyl ester (20).

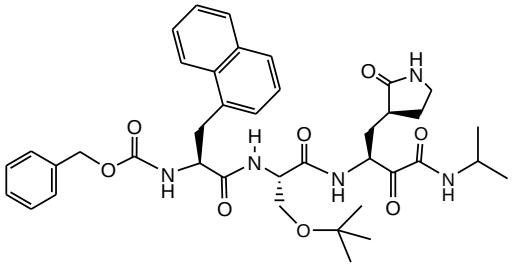

Followed General Procedure C: Started with aldehyde **11** yielding compound **20** (53%) as a white solid. ^{1}H NMR δ 8.20 (br. s., 1H), 7.81 - 7.89 (m, 1H), 7.71 - 7.79 (m, 1H), 7.45 - 7.59 (m, 2H), 7.23 - 7.41 (m, 7H), 6.75 - 6.80 (m, 1H), 6.65 - 6.71 (m, 1H), 6.00 (s, 1H), 5.42 - 5.49 (m, 1H), 5.35 (d, *J* = 5.08 Hz, 1H), 4.98 - 5.18 (m, 2H), 4.61 - 4.69 (m, 1H), 4.35 - 4.41 (m, 1H), 4.01 - 4.09 (m, 1H), 3.96 - 4.01 (m, 1H), 3.75 - 3.82 (m, 1H), 3.62 - 3.74 (m, 1H), 3.47 - 3.57 (m, 1H), 3.27 - 3.38 (m, 2H), 3.15-3.21 (m, 1H), 2.45 (br. s., 1H), 2.26 - 2.36 (m, 1H), 2.01 (d, *J* = 4.69 Hz, 2H), 1.54 - 1.70 (m, 2H), 1.16 - 1.38 (m, 15H); MS, m/z 738.3 $(M+Na)^+$.

(1-{1-[1-Isopropylcarbamoyl-2-(2-oxo-pyrrolidin-3-yl)-ethylcarbamoyl]-ethylcarbamoyl}-2-naphthalen-1-yl-ethyl)-carbamic acid benzyl ester (21).

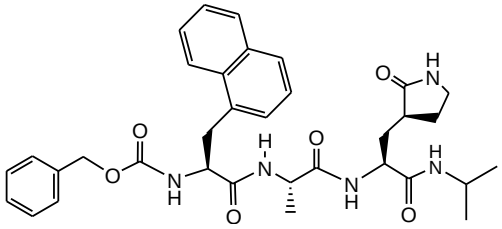

To a solution of ester **23** (0.03 mmol) in MeOH (0.5 mL) was added isopropylamine (0.03 mmol) and the solution was heated at 50^{o}C for 48 h. The solvent was removed to give a crude solid that was purified by silica gel column chromatography (15:1 CH_2Cl_2:MeOH) to yield compound **21** (5 mg, 32%) as a white solid. ^{1}H NMR δ 8.51 (d, *J* = 7.35 Hz, 1H), 8.17 (d, *J* = 7.81 Hz, 1H), 8.02 - 8.07 (m, 1H), 7.83 - 7.94 (m, 2H), 7.74 - 7.82 (m, 1H), 7.46 - 7.58 (m, 2H), 7.28 - 7.43 (m, 5H), 6.81 - 6.94 (m, 2H), 5.99 (br. s., 1H), 5.47 (d, *J* = 5.86 Hz, 1H), 5.01 (s, 2H),

4.51 - 4.66 (m, 1H), 4.26 - 4.40 (m, 1H), 3.98 - 4.07 (m, 1H), 3.63 - 3.73 (m, 1H), 3.32 - 3.44 (m, 1H), 3.23 - 3.30 (m, 2H), 2.26 - 2.35 (m, 2H), 1.75 - 2.08 (m, 3H), 1.54 - 1.64 (m, 1H), 1.12 - 1.20 (m, 9H); MS, m/z 638.1 $(M+Na)^+$.

(1-{1-[1-Cyclopropylcarbamoyl-2-(2-oxo-pyrrolidin-3-yl)-ethylcarbamoyl]-ethylcarbamoyl}-2-naphthalen-1-yl-ethyl)-carbamic acid benzyl ester (22).

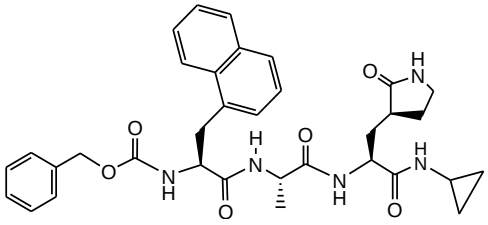

To a solution of ester **23** (0.03 mmol) in MeOH (0.5 mL) was added cyclopropylamine (0.5 mL) and the solution was heated at 50^{o}C for 48 h. The solvent was removed to give a crude solid that was purified by silica gel column chromatography (15:1 CH_2Cl_2:MeOH) to yield compound **22** (14 mg, 91%) as a white solid. ^{1}H NMR δ 8.15 (d, *J* = 8.20 Hz, 1H), 7.91 (d, *J* = 6.64 Hz, 1H), 7.85 (d, *J* = 8.20 Hz, 1H), 7.76 (d, *J* = 7.81 Hz, 1H), 7.46 - 7.57 (m, 2H), 7.27 - 7.38 (m, 7H), 7.07 (br. s., 1H), 6.94 (br. s., 1H), 6.00 (br. s., 1H), 5.46 (d, *J* = 5.86 Hz, 1H), 5.01 (s, 2H), 4.56 - 4.64 (m, 1H), 4.29 - 4.37 (m, 1H), 4.22 - 4.28 (m, 1H), 3.84 - 3.89 (m, 1H), 3.63 - 3.73 (m, 1H), 3.34 - 3.43 (m, 1H), 3.23 - 3.29 (m, 2H), 2.67 - 2.78 (m, 1H), 2.35 - 2.40 (m, 1H), 2.24 - 2.33 (m, 1H), 1.96 - 2.06 (m, 1H), 1.72 - 1.90 (m, 1H), 1.55 - 1.64 (m, 1H), 0.84 - 0.90 (m, 4H), 0.71 - 0.79 (m, 3H); MS, m/z 636.3 $(M+Na)^+$.

2-[2-(2-Benzyloxycarbonylamino-3-naphthalen-1-yl-propionylamino)-propionylamino]-3-(2-oxo-pyrrolidin-3-yl)-propionic acid methyl ester (23).

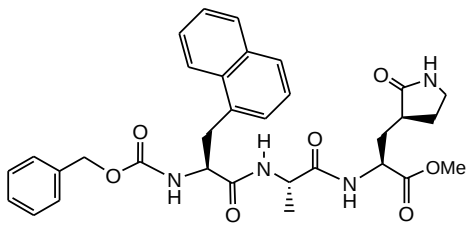

Followed General Procedure A: The *N*-Boc-dipeptide **74** was used in place of **76** to give compound **23** (91% yield) as a white solid. ^{1}H NMR δ 8.16 (d, *J* = 8.20 Hz, 1H), 7.83 (d, *J* = 8.20 Hz, 2H), 7.73 (d, *J* = 7.03 Hz, 1H), 7.43 - 7.53 (m, 2H), 7.22 - 7.36 (m, 7H), 6.98 (d, *J* = 4.30 Hz, 1H), 6.40 (br. s., 1H), 5.65 (d, *J* = 6.64 Hz, 1H), 5.02 (s, 2H), 4.57 - 4.65 (m, 1H), 4.40

- 4.53 (m, 2H), 3.71 (s, 3H), 3.60 (dd, *J* = 6.25, 14.06 Hz, 1H), 3.45 (dd, *J* = 6.25, 13.99 Hz, 1H), 3.23 - 3.32 (m, 2H), 2.30 - 2.43 (m, 2H), 2.07 - 2.16 (m, 1H), 1.75 - 1.90 (m, 2H), 1.31 (d, *J* = 7.03 Hz, 3H); ^{13}C NMR δ 179.8, 172.3, 172.0, 170.8, 156.0, 136.1, 133.8, 132.5, 132.0, 128.8, 128.5, 128.1, 127.9, 127.8, 127.7, 126.4, 125.7, 125.3, 123.6, 66.9, 55.7, 52.4, 51.5, 49.0, 40.5, 38.4, 35.5, 32.9, 28.3, 18.5; MS, m/z 611.5 $(M+Na)^+$.

(1-{1-[1-Hydroxymethyl-2-(2-oxo-pyrrolidin-3-yl)-ethylcarbamoyl]-ethylcarbamoyl}-2-naphthalen-1-yl-ethyl)-carbamic acid benzyl ester (23a).

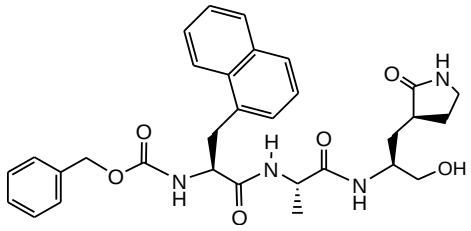

To a solution of ester **23** (0.31 mmol) in CH_2Cl_2/THF (1:1) (5 mL) at 0^{o}C was added $LiBH_4$ (0.46 mmol) in small portions over a period of 1 h. The reaction was quenched with NH_4Cl (0.5 mL) and diluted with CH_2Cl_2 (50 mL) and water (50 mL). The organic layer was removed and aqueous layer extracted with CH_2Cl_2 (50 mL x 4). The combined organic layers were dried ($MgSO_4$), filtered and concentrated to yield compound **23a** (143 mg, 84%) as a white solid. ^{1}H NMR δ 8.15 (d, *J* = 8.20 Hz, 1H), 7.84 (d, *J* = 7.81 Hz, 1H), 7.75 (d, *J* = 8.20 Hz, 1H), 7.57 (d, *J* = 7.03 Hz, 1H), 7.45 - 7.54 (m, 2H), 7.23 - 7.39 (m, 7H), 6.99 (d, *J* = 6.64 Hz, 1H), 6.00 (br. s., 1H), 5.60 (d, *J* = 6.64 Hz, 1H), 5.02 (s, 2H), 4.58 (d, *J* = 6.64 Hz, 1H), 4.35 - 4.44 (m, 1H), 3.87 - 3.96 (m, 1H), 3.49 - 3.67 (m, 3H), 3.41 (dd, *J* = 7.81, 14.06 Hz, 1H), 3.20 - 3.27 (m, 2H), 2.27 - 2.38 (m, 2H), 1.66 - 1.94 (m, 3H), 1.27 (d, *J* = 7.42 Hz, 3H); MS, m/z 583.3 $(M+Na)^+$.

(1-{3-Methyl-1-[2-oxo-1-(2-oxo-pyrrolidin-3-ylmethyl)-ethylcarbamoyl]-butylcarbamoyl}-2-naphthalen-1-yl-ethyl)-carbamic acid benzyl ester (24).

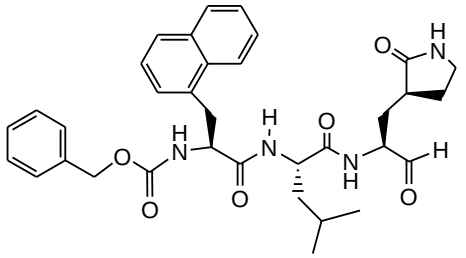

Followed General Procedure B: To a solution of ester **84** (0.63 mmol) in CH_2Cl_2/MeOH (1:1) (8 mL) at 0°C was added $NaBH_4$ (5.6 mmol) in small portions over a period of 4 h. The reaction was quenched with water (0.5 mL) and diluted with 100 mL of CH_2Cl_2. The solution was passed through a short plug of silica gel and the organic material washed thoroughly with 30:1 CH_2Cl_2/MeOH (100 mL). The filtrate was concentrated to yield a solid which was dissolved in distilled CH_2Cl_2 (15 mL) and treated with Dess-Martin periodinane (DMP) for 2 h at 25°C. The reaction mixture was filtered and the filtrate was concentrated and purified by silica gel chromatography using a gradient solvent elution of 25% acetone/CH_2Cl_2 to 100% acetone. The fractions containing the product were combined and concentrated to give a white solid to which was added $CHCl_3$ (20 mL). After sitting for 10 min the mixture was filtered through a glass frit funnel (fine) and the filtrate was concentrated to provide aldehyde **24** (90% yield) as a white solid, mp 85 – 88°C. ^{1}H NMR δ 9.39 (s, 1H), 8.15 (s, 1H), 8.14 (s, 1H), 7.81 - 7.86 (m, 1H), 7.70 - 7.75 (m, 1H), 7.44 - 7.53 (m, 2H), 7.28 - 7.36 (m, 5H), 7.25 (br. s., 1H), 7.03 - 7.10 (m, 1H), 6.50 (s, 1H), 5.60 (d, *J* = 7.8 Hz, 2H), 5.01 (s, 2H), 4.57 - 4.68 (m, 2H), 4.20 - 4.26 (m, 1H), 3.64 (dd, *J* = 6.6, 14.1 Hz, 1H), 3.42 (dd, *J* = 6.6, 14.1 Hz, 1H), 3.25 (d, *J* = 7.8 Hz, 2H), 2.22 - 2.38 (m, 2H), 1.95 - 2.08 (m, 2H), 1.39 - 1.84 (m, 6H), 0.89 (d, *J* = 6.7 Hz, 3H, CH_3), 0.88 (d, *J* = 6.7 Hz, 3H, CH_3); ^{13}C NMR δ 199.9, 179.8, 173.0, 171.1, 156.2, 135.9, 133.8, 132.5, 132.0, 128.8, 128.5, 128.2, 127.9, 127.9, 127.7, 126.4, 125.8, 125.3, 123.6, 67.1, 57.5, 55.8, 51.8, 41.6, 40.5, 38.1, 35.1, 29.7, 28.4, 24.7, 22.8, 21.8; MS, m/z 623.3 $(M+Na)^+$; HRMS calcd for $C_{34}H_{40}N_4O_6Na$ $(M+Na)^+$ 623.2846, found 623.2860.

(1-{2-Cyclohexyl-1-[1-formyl-2-(2-oxo-pyrrolidin-3-yl)-ethylcarbamoyl]-ethylcarbamoyl}-2-naphthalen-1-yl-ethyl)-carbamic acid benzyl ester (25).

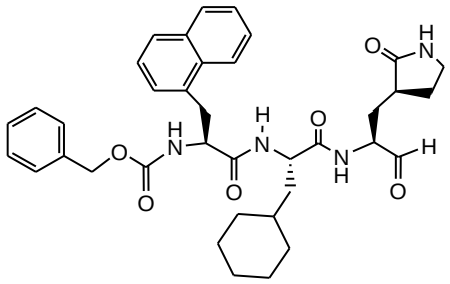

Followed General Procedure B: Started with ester **85** yielding compound **25** (69%) as a white solid. ^{1}H NMR δ 9.39 (s, 1H), 8.14 (d, *J* = 7.81 Hz, 1H), 8.03 (d, *J* = 5.47 Hz, 1H), 7.82 (d, *J* =

9.37 Hz, 1H), 7.72 (dd, *J* = 3.51, 5.86 Hz, 1H), 7.43 - 7.52 (m, 2H), 7.20 - 7.35 (m, 7H), 7.08 (d, *J* = 7.81 Hz, 1H), 6.46 (s, 1H), 5.63 (d, *J* = 7.03 Hz, 1H), 5.01 (br. s., 2H), 4.56 - 4.66 (m, 2H), 4.19 - 4.28 (m, 1H), 3.63 (dd, *J* = 6.64, 13.67 Hz, 1H), 3.42 (dd, *J* = 6.64, 13.50 Hz, 1H), 3.16 - 3.28 (m, 2H), 2.21 - 2.37 (m, 2H), 2.07 - 2.20 (m, 1H), 1.55 - 1.83 (m, 9H), 1.37 - 1.47 (m, 1H), 1.20 - 1.29 (m, 1H), 1.07 - 1.17 (m, 2H), 0.79 - 0.95 (m, 2H); ^{13}C NMR δ 200.1, 180.1, 173.3, 171.3, 156.4, 136.2, 134.1, 132.8, 132.2, 129.0, 128.7, 128.4, 128.1, 128.1, 127.9, 126.6, 126.0, 125.6, 123.8, 67.3, 57.7, 56.0, 51.5, 40.7, 40.3, 38.3, 35.4, 34.3, 33.7, 32.7, 30.0, 28.6, 26.5, 26.4, 26.2; MS, m/z 663.3 $(M+Na)^+$.

(1-{3-Methyl-1-[2-oxo-1-(2-oxo-pyrrolidin-3-ylmethyl)-ethylcarbamoyl]-butylcarbamoyl}-2-naphthalen-1-yl-ethyl)-carbamic acid benzyl ester (27).

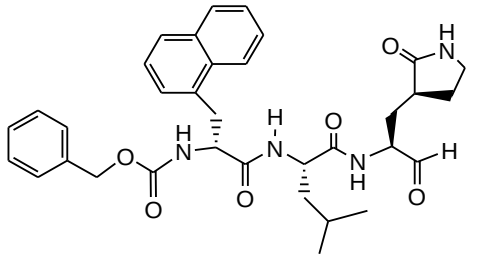

Followed General Procedure B: Started with ester **87** giving compound **27** (93% yield) as a white solid, mp 95 – 97^{o}C. ^{1}H NMR δ 9.38 (s, 1H), 8.40 (d, *J* = 5.1 Hz, 1H), 8.15 (d, *J* = 8.2 Hz, 1H), 7.82 (d, *J* = 8.6 Hz, 1H), 7.69 - 7.75 (m, 1H), 7.43 - 7.53 (m, 3H), 7.20 - 7.36 (m, 6H), 6.33 (d, *J* = 6.6 Hz, 1H), 6.21 (d, *J* = 7.4 Hz, 1H), 5.69 (br. s., 1H), 4.94 - 5.04 (m, 2H), 4.60 - 4.69 (m, 1H), 4.48 - 4.55 (m, 1H), 4.08 - 4.16 (m, 1H), 3.57 (d, *J* = 6.6 Hz, 2H), 3.09 - 3.18 (m, 2H), 2.26 (br. s., 2H), 2.07 (br. s., 1H), 1.69 - 1.79 (m, 2H), 1.55 (br. s., 1H), 1.14 (br. s., 2H), 0.70 - 0.83 (m, 6H, 2 x CH_3); ^{13}C NMR δ 200.4, 180.0, 173.3, 171.2, 156.4, 136.4, 134.1, 133.0, 132.4, 129.0, 128.8, 128.5, 128.4, 128.3, 128.0, 126.6, 126.0, 125.7, 124.0, 67.2, 58.3, 56.5, 51.8, 41.2, 40.8, 38.7, 35.6, 29.8, 28.9, 24.7, 23.1, 21.8. MS, m/z 623.1 $(M+Na)^+$; HRMS calcd for $C_{34}H_{40}N_4O_6Na$ $(M+Na)^+$ 623.2846, found 623.2829.

(1-{3-Methyl-1-[2-oxo-1-(2-oxo-pyrrolidin-3-ylmethyl)-ethylcarbamoyl]-butylcarbamoyl}-2-phenyl-ethyl)-carbamic acid benzyl ester (28).

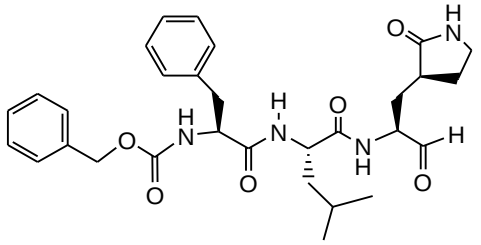

Followed General Procedure B: Started with ester **88** giving compound **28** (80% yield) as a white solid, mp 91 – 93°C. ^{1}H NMR δ 9.44 (s, 1H), 8.13 (br. s., 1H), 7.08 - 7.37 (m, 10H), 6.68 (d, *J* = 5.1 Hz, 1H), 5.49 (br. s., 1H), 5.00 - 5.08 (m, 2H), 4.60 - 4.68 (m, 1H), 4.46 - 4.53 (m, 1H), 4.27 - 4.35 (m, 1H), 3.21 - 3.34 (m, 2H), 2.99 - 3.14 (m, 2H), 2.27 - 2.42 (m, 2H), 1.44 - 2.10 (m, 6H), 0.90 (d, *J* = 6.3 Hz, 6H, 2 x CH_3); ^{13}C NMR δ 200.1, 180.2, 173.3, 171.3, 156.4, 136.5, 136.3, 129.6, 128.8, 128.7, 128.5, 128.2, 127.3, 67.4, 57.6, 56.3, 52.0, 42.0, 40.8, 38.3, 38.2, 30.0, 28.5, 25.0, 23.1, 22.1. MS, m/z 573.2 $(M+Na)^+$; HRMS calcd for $C_{30}H_{39}N_4O_6$ $(M+H)^+$ 551.2870, found 551.2882.

(2-tert-Butoxy-1-{1-[1-formyl-2-(2-oxo-pyrrolidin-3-yl)-ethylcarbamoyl]-3-methyl-butylcarbamoyl}-propyl)-carbamic acid benzyl ester (29).

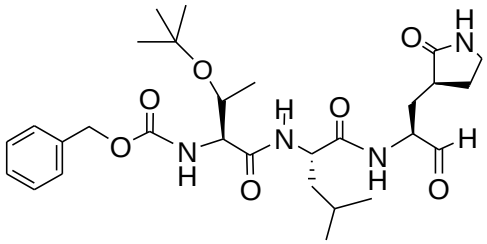

Followed General Procedure B: Started with ester **89** yielding compound **29** (63%) as a white solid. ^{1}H NMR δ 9.49 (s, 1H), 8.12 (d, *J* = 5.86 Hz, 1H), 7.48 (d, *J* = 7.81 Hz, 1H), 7.30 - 7.38 (m, 5H), 6.40 (br. s., 1H), 5.91 (d, *J* = 4.69 Hz, 1H), 5.04 - 5.16 (m, 2H), 4.45 - 4.55 (m, 1H), 4.31 - 4.40 (m, 1H), 4.14 - 4.21 (m, 2H), 3.23 - 3.36 (m, 2H), 2.27 - 2.47 (m, 2H), 1.95 - 2.06 (m, 2H), 1.84 - 1.93 (m, 1H), 1.74 - 1.83 (m, 1H), 1.64 - 1.74 (m, 1H), 1.53 - 1.62 (m, 1H), 1.25 (s, 9H), 1.06 (d, *J* = 5.86 Hz, 3H), 0.89 - 0.98 (m, 6H); ^{13}C NMR δ 199.8, 180.1, 173.0, 169.9, 156.4, 136.4, 128.8, 128.5, 128.3, 75.6, 67.2, 67.0, 59.2, 57.7, 52.2, 41.9, 40.7, 38.1, 30.0, 28.7, 28.4, 25.1, 23.1, 22.3, 17.5; MS, m/z 583.3 $(M+Na)^+$.

(1-{3-Methyl-1-[2-oxo-1-(2-oxo-pyrrolidin-3-ylmethyl)-ethylcarbamoyl]-butylcarbamoyl}-2-naphthalen-2-yl-ethyl)-carbamic acid benzyl ester (30).

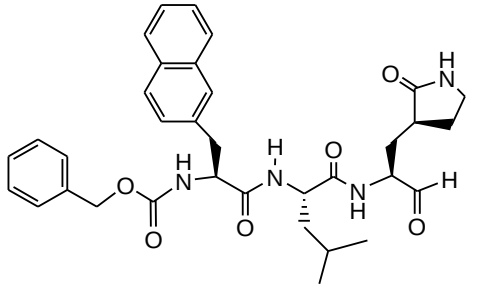

Followed General Procedure B: Started with ester **90** yielding compound **30** (93% yield) as a white solid, mp 146 – 148°C. ^{1}H NMR δ 9.36 (s, 1H), 8.24 (br. s., 1H), 7.75 - 7.80 (m, 1H), 7.70 - 7.73 (m, 2H), 7.62 (s, 1H), 7.40 - 7.46 (m, 3H), 7.20 - 7.32 (m, 5H), 6.98 (d, *J* = 7.8 Hz, 1H), 6.35 (br. s., 1H), 5.51 (d, *J* = 7.0 Hz, 1H), 4.98 - 5.07 (m, 2H), 4.56 - 4.65 (m, 2H), 4.20 (q, *J* = 7.0 Hz, 1H), 3.13 - 3.32 (m, 4H), 2.20 - 2.39 (m, 2H), 1.75 - 1.82 (m, 2H), 1.61 - 1.74 (m, 2H), 1.42 - 1.58 (m, 2H), 0.88 (d, *J* = 6.5 Hz, 3H, CH_3), 0.86 (d, *J* = 6.5 Hz, 3H, CH_3); ^{13}C NMR δ 200.1, 180.1, 173.3, 171.2, 156.4, 136.2, 134.0, 133.6, 132.6, 128.8, 128.5, 128.45, 128.4, 128.2, 127.9, 127.6, 126.4, 126.0, 67.4, 58.0, 56.4, 52.1, 41.9, 40.8, 38.5, 38.4, 29.8, 28.8, 25.0, 23.1, 22.1. MS, m/z 623.2 $(M+Na)^+$; HRMS calcd for $C_{34}H_{41}N_4O_6$ $(M+H)^+$ 601.3026, found 601.3029.

(2-Biphenyl-4-yl-1-{3-methyl-1-[2-oxo-1-(2-oxo-pyrrolidin-3-ylmethyl)-ethylcarbamoyl]-butylcarbamoyl}-ethyl)-carbamic acid benzyl ester (31).

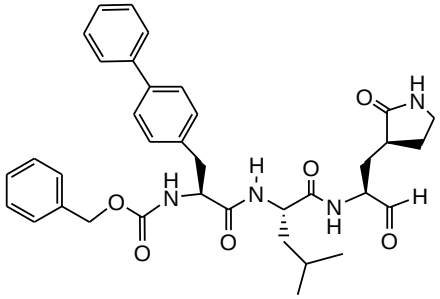

Followed General Procedure B: Started with ester **91** to give compound **31** (79% yield) as a white solid, mp 127 – 130°C. ^{1}H NMR δ 9.45 (s, 1H), 8.34 (br. s., 1H), 7.20 - 7.56 (m, 14H),

6.99 (br. s., 1H), 6.45 (br. s., 1H), 5.51 (br. s., 1H), 5.01 - 5.10 (m, 2H), 4.58 - 4.66 (m, 1H), 4.50 - 4.57 (m, 1H), 4.23 - 4.30 (m, 1H), 3.19 - 3.32 (m, 2H), 3.05 - 3.19 (m, 2H), 2.33 - 2.44 (m, 1H), 2.21 - 2.32 (m, 1H), 1.89 - 2.01 (m, 1H), 1.79 - 1.88 (m, 1H), 1.63 - 1.77 (m, 2H), 1.47 - 1.62 (m, 2H), 0.91 (d, *J* = 6.2 Hz, 3H, CH_3), 0.90 (d, *J* = 6.2 Hz, 3H, CH_3); ^{13}C NMR δ 199.9, 180.2, 173.3, 171.2, 156.4, 140.8, 140.1, 136.2, 135.5, 130.0, 129.0, 128.8, 128.5, 128.3, 127.6, 127.5, 127.1, 67.4, 58.0, 56.3, 52.1, 41.9, 40.8, 38.5, 37.8, 29.9, 28.8, 25.0, 23.1, 22.1. MS, m/z 649.6 $(M+Na)^+$; HRMS calcd for $C_{36}H_{42}N_4O_6Na$ $(M+Na)^+$ 649.3002, found 649.2995.

(1-{1-[2-Isopropylcarbamoyl-2-oxo-1-(2-oxo-pyrrolidin-3-ylmethyl)-ethylcarbamoyl]-3-methyl-butylcarbamoyl}-2-naphthalen-1-yl-ethyl)-carbamic acid benzyl ester (32).

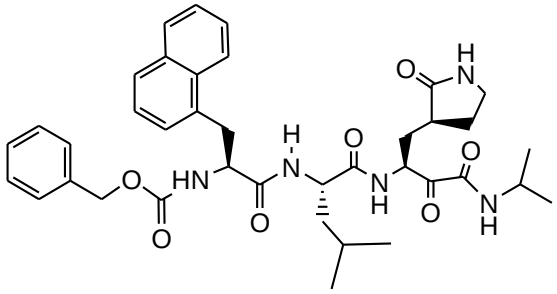

Followed General procedure C: Isopropylisocyanide (0.067 mmol) was added to a solution of aldehyde **24** (0.067 mmol) in distilled EtOAc (2 mL) and AcOH (1 drop) and the resulting solution stirred at 25^{o}C for 18 h. The solvent was removed *in vacuo* and the residue was dissolved in a 1:1 solution of MeOH/H_2O (5 mL) and K_2CO_3 (0.16 mmol). After stirring for 3 h at 25^{o}C, the reaction was diluted with water and extracted with EtOAc (4 times). The combined organic layers were dried (anhydrous $MgSO_4$), filtered, and concentrated to yield a residue. To it, CH_2Cl_2 (2 mL) was added followed by DMP (0.13 mmol) and the reaction was stirred at 25^{o}C for 2 h. The solvent was removed *in vacuo* and the residue was purified by silica gel chromatography using a gradient solvent elution of 25% acetone/CH_2Cl_2 to 100% acetone. The fractions containing the product were combined and concentrated to give a white solid to which was added $CHCl_3$ (10 mL). After sitting for 10 min the mixture was filtered through a glass frit funnel (fine) and the filtrate was concentrated to provide ketoamide **32** (36 mg, 79% yield) as a white solid, mp 119 – 121^{o}C. ^{1}H NMR δ 8.37 (d, *J* = 5.9 Hz, 1H), 8.16 (d, *J* = 8.2 Hz, 1H), 7.82 - 7.86 (m, 2H), 7.74 (d, *J* = 7.8 Hz, 2H), 7.44 - 7.53 (m, 3H), 7.21 - 7.36 (m, 4H), 6.83 (d, *J* = 8.6

Hz, 1H), 6.80 (d, *J* = 8.2 Hz, 2H), 6.53 (s, 1H), 5.48 (d, *J* = 7.4 Hz, 1H), 5.17 - 5.24 (m, 1H), 5.01 (s, 2H), 4.57 - 4.66 (m, 2H), 3.98 - 4.08 (m, 1H), 3.65 (dd, *J* = 6.1, 13.9 Hz, 1H), 3.44 (dd, *J* = 6.1, 14.0 Hz, 1H), 3.31 (d, *J* = 7.8 Hz, 2H), 2.38 - 2.55 (m, 2H), 1.88 - 2.06 (m, 2H), 1.50 - 1.66 (m, 3H), 1.38 - 1.46 (m, 1H), 1.20 (d, *J* = 6.6 Hz, 3H, CH_3), 1.19 (d, *J* = 6.5 Hz, 3H, CH_3), 0.89 (d, *J* = 6.2 Hz, 6H, 2xCH_3); ^{13}C NMR δ 195.4, 180.0, 172.2, 171.1, 158.6, 156.3, 136.2, 134.1, 132.7, 132.2, 129.0, 128.7, 128.4, 128.2, 128.1, 127.9, 126.6, 126.0, 125.6, 123.8, 67.3, 55.9, 53.6, 51.7, 42.1, 41.9, 40.8, 39.2, 35.3, 32.1, 28.4, 24.8, 23.0, 22.6, 22.5, 22.2. MS, m/z 724.3 $(M+K)^+$; HRMS calcd for $C_{38}H_{47}N_5O_7Na$ $(M+Na)^+$ 708.3373, found 708.3378.

(1-{1-[2-tert-Butylcarbamoyl-2-oxo-1-(2-oxo-pyrrolidin-3-ylmethyl)-ethylcarbamoyl]-3-methyl-butylcarbamoyl}-2-naphthalen-1-yl-ethyl)-carbamic acid benzyl ester (33).

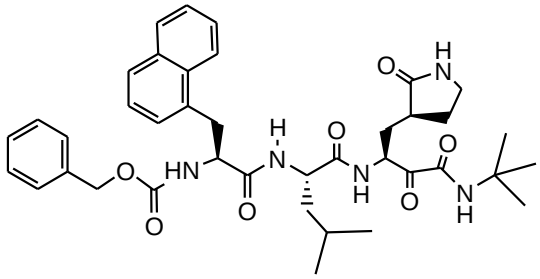

Followed General Procedure C: Started with aldehyde **24** and used tert-butylisocyanide in place of isopropylisocyanide yielding compound **33** (54%) as a white solid.^{1}H NMR δ 8.28 (br. s., 1H), 8.17 (d, *J* = 7.42 Hz, 1H), 7.84 (d, *J* = 8.20 Hz, 1H), 7.74 (d, *J* = 7.81 Hz, 1H), 7.43 - 7.54 (m, 2H), 7.21 - 7.36 (m, 7H), 6.76 (br. s., 1H), 6.44 (br. s., 1H), 5.44 - 5.49 (m, 1H), 5.16 - 5.23 (m, 1H), 5.01 (br. s., 2H), 4.51 - 4.64 (m, 2H), 3.61 - 3.68 (m, 1H), 3.41 - 3.50 (m, 1H), 3.21 - 3.35 (m, 2H), 2.38 - 2.55 (m, 2H), 1.99 - 2.03 (m, 1H), 1.89 - 1.98 (m, 2H), 1.52 - 1.66 (m, 2H), 1.38 (s, 9H), 0.89 (d, *J* = 5.86 Hz, 6H); ^{13}C NMR δ 196.0, 180.2, 172.2, 171.1, 158.8, 156.3, 136.3, 134.1, 132.8, 132.2, 129.1, 128.7, 128.4, 128.2, 128.1, 127.9, 126.6, 126.0, 125.6, 123.8, 67.3, 56.0, 53.5, 51.8, 42.0, 40.9, 39.3, 35.4, 32.3, 28.5, 24.8, 23.0, 22.2; MS, m/z 722.3 $(M+Na)^+$.

(1-{1-[2-Carbamoyl-2-oxo-1-(2-oxo-pyrrolidin-3-ylmethyl)-ethylcarbamoyl]-3-methyl-butylcarbamoyl}-2-naphthalen-1-yl-ethyl)-carbamic acid benzyl ester (34).

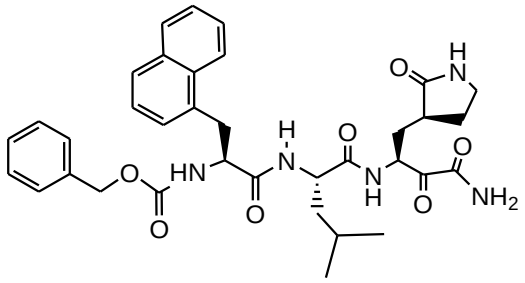

Acetone cyanohydrin (0.084 mmol) was added to a solution of aldehyde **24** (0.042 mmol) and NEt_3 (0.05 mmol) in CH_2Cl_2 (0.5 mL) and stirred at 25^oC for 15 h. The reaction diluted with CH_2Cl_2 (5 mL) and 1M HCl (1 mL). The organic layer was removed and the aqueous layer was extracted with CH_2Cl_2 (5 mL x 4), combined organic layers were dried (Na_2SO_4), filtered and concentrated to yield the cyanohydrin intermediate as clear residue. The cyanohydrin intermediate (0.042 mmol) was dissolved in MeOH (1 mL) and cooled to 0^oC followed by the addition of 30% H_2O_2 (0.29 mmol) and LiOH (0.063 mmol). After stirring at 0^oC for 3 h the reaction was combined with saturated aq. $NaHSO_3$ (1 mL) and water (10 mL). The reaction was extracted with CH_2Cl_2 (4 x 15 mL) and the combined organic extracts were dried (Na_2SO_4), filtered and concentrated to yield a hydroxyamide intermediate as a white solid. The hydroxyamide (0.042 mmol) was dissolved in dry CH_2Cl_2 (2 mL) and DMP (0.09 mmol) was added. After stirring at 25^oC for 2 h the reaction was concentrated to yield a residue that was purified by silica gel column chromatography (1:1 CH_2Cl_2:Acetone) to give compound **34** (10 mg, 35%) as a white solid. ^1H NMR δ 8.63 (br. s., 1H), 8.18 (d, *J* = 7.81 Hz, 1H), 7.85 (d, *J* = 8.59 Hz, 1H), 7.75 (d, *J* = 7.81 Hz, 1H), 7.45 - 7.55 (m, 2H), 7.28 - 7.39 (m, 7H), 6.84 (br. s., 1H), 6.60 (br. s., 1H), 5.93 (br. s., 1H), 5.65 (br. s., 1H), 5.46 (d, *J* = 7.42 Hz, 1H), 5.12 (br. s., 1H), 5.02 (br. s., 2H), 4.58 - 4.66 (m, 1H), 4.45 - 4.52 (m, 1H), 3.61 - 3.69 (m, 1H), 3.41 - 3.51 (m, 1H), 3.20 - 3.36 (m, 3H), 2.47 - 2.55 (m, 1H), 2.27 - 2.46 (m, 1H), 1.98 - 2.06 (m, 1H), 1.80 - 1.96 (m, 3H), 1.37 - 1.46 (m, 1H), 0.89 (d, *J* = 6.25 Hz, 6H); MS, m/z 666.4 $(M+Na)^+$

2-[2-(2-Benzyloxycarbonylamino-3-naphthalen-1-yl-propionylamino)-4-methyl-pentanoylamino]-1-hydroxy-3-(2-oxo-pyrrolidin-3-yl)-propane-1-sulfonic acid monosodium salt (35).

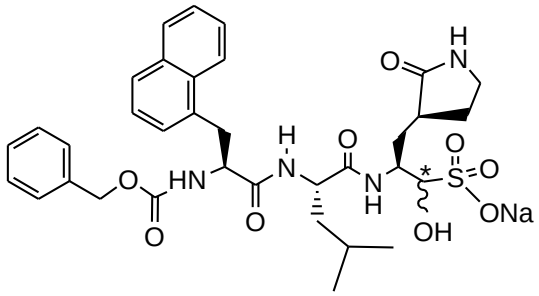

A mixture of aldehyde **24** (0.05 mmol) and sodium bisulfite (0.05 mmol) was dissolved in 4:2:1 EtOAc/EtOH/H_2O (0.7 mL) and stirred at 40^oC for 2 h. The solution was cooled and filtered, and the filtrate was concentrated to yield two diastereomers (a mixture of *R* and *S* at carbon adjacent to sulfur) of compound **35** as white solids (35 mg, 100% yield), mp 109 – 111^oC. ^1H NMR δ 8.50 (d, *J* = 7.0 Hz, 1H), 8.28 (d, *J* = 8.6 Hz, 1H), 8.22 (d, *J* = 8.2, 1H), 8.18 (d, *J* = 8.2, 1H), 8.11 (d, *J* = 7.8 Hz, 1H), 7.89 (d, *J* = 3.9 Hz, 2H), 7.74 - 7.81 (m, 2H), 7.66 (d, *J* = 9.4 Hz, 1H), 7.61 (d, *J* = 7.8 Hz, 1H), 7.53 - 7.59 (m, 3H), 7.48 - 7.53 (m, 2H), 7.44 (t, *J* = 4.7 Hz, 3H), 7.34 - 7.40 (m, 2H), 7.23 - 7.32 (m, 4H), 7.15 (d, *J* = 6.6 Hz, 3H), 6.90 (br. s., 1H), 5.50 (d, *J* = 6.3 Hz, 1H), 5.35 (d, *J* = 5.9 Hz, 1H), 4.81 - 4.90 (m, 4H), 4.43 (br. s., 2H), 4.30 - 4.37 (m, 1H), 4.26 (br. s., 1H), 3.96 - 4.00 (m, 1H), 3.88 (t, *J* = 5.5 Hz, 1H), 3.64 (br. s., 1H), 3.57 - 3.62 (m, 1H), 3.54 (d, *J* = 9.4 Hz, 1H), 2.97 - 3.19 (m, 6H), 1.91 - 2.35 (m, 6H), 1.71 - 1.80 (m, 1H), 1.44 - 1.68 (m, 8H), 1.18 - 1.25 (m, 1H), 0.77 - 0.93 (m, 12H); ^{13}C NMR δ 179.9, 179.7, 179.4, 178.9, 173.3, 172.2, 172.1, 172.0, 156.4, 137.7, 134.8, 134.7, 134.4, 134.0, 132.3, 129.2, 128.9, 128.3, 128.1, 127.9, 127.6, 127.3, 126.7, 126.2, 126.0, 124.9, 124.6, 124.4, 85.2, 84.5, 65.8, 57.0, 55.9, 52.5, 52.2, 51.9, 49.8, 49.3, 41.6, 41.2, 38.5, 35.2, 35.0, 34.9, 32.8, 30.6, 29.9, 28.7, 28.3, 28.1, 27.9, 24.9, 24.8, 23.8, 23.6, 22.5, 22.3. MS (negative mode, m/z 681.6 $(M-Na)^-$; HRMS (negative mode) calcd for $C_{34}H_{41}N_4O_9S$ $(M-Na)^-$ 681.2594, found 681.2713.

[2-[2-(2-Benzyloxycarbonylamino-3-naphthalen-1-yl-propionylamino)-4-methyl-pentanoylamino]-1-hydroxy-3-(2-oxo-pyrrolidin-3-yl)-propyl]-phosphonic acid diethyl ester (36).

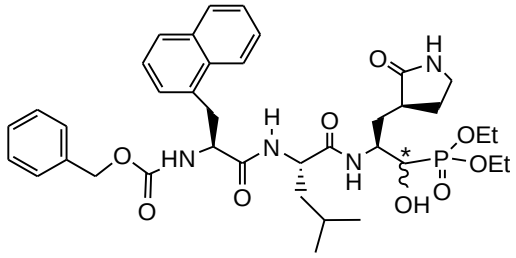

Followed General Procedure D: Diisopropylethylamine (0.25 mmol) was added to a solution of aldehyde **24** (0.25 mmol) and diethylphosphite (0.25 mmol) in distilled CH_2Cl_2. After stirring at 25^{o}C for 18 h, the reaction was diluted with ethyl acetate and washed with dilute HCl followed by brine. The organic layer was dried (anhydrous $MgSO_4$), filtered, and concentrated to yield an oil which was purified by silica gel column chromatography (9:1 CH_2Cl_2/MeOH) to afford two diastereomers (a mixture of *R* and *S* at carbon adjacent to phosphorus) of compound **36** (10 mg, 54% yield) as white solids, mp 85 – 88^{o}C. ^{1}H NMR δ 8.17 (br. s., 1H), 8.12 (d, *J* = 7.8 Hz, 1H), 7.82 (d, *J* = 6.3 Hz, 2H), 7.72 (t, *J* = 7.4 Hz, 2H), 7.41 - 7.54 (m, 4H), 7.24 - 7.37 (m, 10H), 7.21 (br. s., 2H), 6.58 (br. s., 1H), 6.47 (br. s., 1H), 6.38 (br. s., 1H), 6.19 - 6.24 (m, 1H), 5.68 (d, *J* = 7.4 Hz, 1H), 5.50 - 5.56 (m, 1H), 5.19 - 5.31 (m, 1H), 5.01 (br. s., 1H), 4.97 (br. s., 4H), 4.66 - 4.75 (m, 1H), 4.60 (br. s., 2H), 4.50 (br. s., 1H), 4.42 (br. s., 1H), 4.31 (br. s., 1H), 4.02 - 4.21 (m, 8H), 3.88 (br. s., 1H), 3.62 - 3.76 (m, 1H), 3.29 - 3.42 (m, 1H), 3.14 - 3.24 (m, 3H), 2.29 - 2.40 (m, 2H), 2.18 (br. s., 4H), 1.72 - 1.85 (m, 2H), 1.61 - 1.70 (m, 2H), 1.43 - 1.55 (m, 4H), 1.19 - 1.37 (m, 12H), 0.80 - 0.92 (m, 12H); ^{13}C NMR δ 181.1, 181.1, 172.9, 172.7, 172.3, 172.0, 171.6, 156.6, 136.2, 136.1, 134.1, 133.1, 133.0, 132.2, 129.0, 128.7, 128.3, 128.2, 128.0, 127.7, 126.6, 126.0, 125.9, 125.6, 123.9, 123.8, 71.5, 71.3, 69.9, 69.7, 67.3, 63.6, 63.5, 63.1, 62.9, 62.8, 62.7, 56.0, 53.0, 52.7, 50.6, 50.5, 50.2, 48.9, 41.7, 41.5, 40.8, 38.6, 38.1, 35.1, 34.9, 33.7, 33.6, 32.8, 32.7, 31.4, 31.2, 29.9, 28.7, 28.5, 28.4, 28.0, 25.0, 23.4, 23.3, 21.9, 21.7, 16.7; MS, m/z 761.1 $(M+Na)^+$; HRMS calcd for $C_{38}H_{51}N_4O_9PNa$ $(M+Na)^+$ 761.3291, found 761.3271.

[2-[2-(2-Benzyloxycarbonylamino-3-naphthalen-1-yl-propionylamino)-4-methyl-pentanoylamino]-1-hydroxy-3-(2-oxo-pyrrolidin-3-yl)-propyl]-phosphonic acid diisopropyl ester (37).

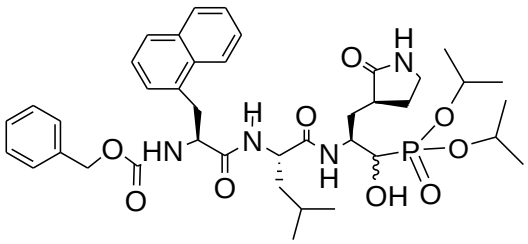

Followed General Procedure D: Started with aldehyde **24** and used diisopropylphosphite in place of diethylphosphite, yielding compound **37** (73%) as a white solid. ^{1}H NMR δ 8.15 (d, *J* = 7.42 Hz, 1H), 7.83 (d, *J* = 7.03 Hz, 1H), 7.73 (d, *J* = 7.03 Hz, 1H), 7.38 - 7.53 (m, 3H), 7.12 - 7.36 (m, 7H), 6.29 (br. s., 1H), 5.58 (br. s., 1H), 4.98 (br. s., 2H), 4.65 - 4.85 (m, 2H), 4.56 - 4.65 (m, 1H), 4.41 - 4.50 (m, 1H), 4.26 - 4.35 (m, 1H), 3.76 - 3.84 (m, 1H), 3.65 - 3.73 (m, 1H), 3.34 - 3.43 (m, 1H), 3.17 - 3.24 (m, 2H), 2.28 - 2.43 (m, 1H), 2.05 - 2.17 (m, 1H), 1.85 (br. s., 1H), 1.61 - 1.76 (m, 1H), 1.42 - 1.56 (m, 1H), 1.26 - 1.38 (m, 12H), 0.83 - 0.93 (m, 6H); MS, m/z 789.4 $(M+Na)^+$.

(1-{1-[1-Cyano-2-(2-oxo-pyrrolidin-3-yl)-ethylcarbamoyl]-3-methyl-butylcarbamoyl}-2-naphthalen-1-yl-ethyl)-carbamic acid benzyl ester (38).

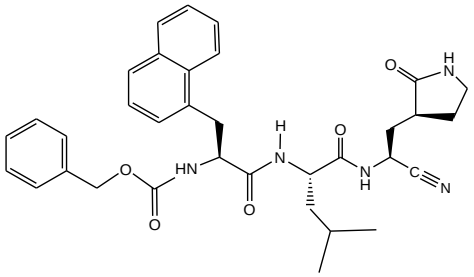

Iodobenzenediacetate (0.06 mmol) was added to a solution of aldehyde **24** (0.03 mmol), sodium dodecyl sulfate (0.006 mmol) and NH_4OAc in water (2 mL) and heated to 70^{o}C for 9 h. Aqueous sodium thiosulfate (20 mL) and CH_2Cl_2 (20 mL) were added and the organic layer removed. The aqueous layer was extracted with CH_2Cl_2 (10 mL x 3), the combined organic layers were dried (Na_2SO_4), filtered and concentrated to yield an oil that was purified by silica gel column chromatography (9:1 CH_2Cl_2:MeOH) to give compound **38** (11 mg, 61%) as a white solid. ^{1}H NMR δ 8.13 (d, *J* = 7.42 Hz, 1H), 7.99 (br. s., 1H), 7.85 (d, *J* = 8.59 Hz, 1H), 7.77 (d, *J* = 7.81 Hz, 1H), 7.45 - 7.55 (m, 2H), 7.20 - 7.41 (m, 7H), 6.85 (d, *J* = 7.03 Hz, 1H), 6.30 (s, 1H), 5.54 (br. s., 1H), 5.03 (br. s., 2H), 4.71 - 4.78 (m, 1H), 4.55 - 4.63 (m, 1H), 4.45 - 4.55 (m, 1H), 3.62 (dd, *J* = 6.44, 13.86 Hz, 1H), 3.43 (dd, *J* = 6.44, 13.24 Hz, 1H), 3.19 - 3.30 (m, 2H), 2.25 - 2.36

(m, 2H), 2.11 - 2.23 (m, 1H), 1.70 - 1.87 (m, 2H), 1.58 - 1.68 (m, 1H), 1.44 - 1.54 (m, 1H), 1.35 - 1.43 (m, 1H), 0.87 (d, *J* = 6.25 Hz, 6H); ^{13}C NMR δ 179.1, 172.3, 171.4, 156.5, 136.1, 134.1, 132.6, 132.2, 129.1, 128.8, 128.5, 128.3, 128.2, 127.9, 126.7, 126.1, 125.7, 123.7, 118.4, 67.4, 56.1, 51.9, 41.4, 40.7, 39.5, 38.1, 35.4, 34.0, 29.9, 28.4, 24.9, 23.1, 22.1; MS, m/z 620.4 $(M+Na)^+$.

(1-{3-Methyl-1-[2-oxo-1-(2-oxo-pyrrolidin-3-ylmethyl)-2-thiazol-2-yl-ethylcarbamoyl]-butylcarbamoyl}-2-naphthalen-1-yl-ethyl)-carbamic acid benzyl ester (39).

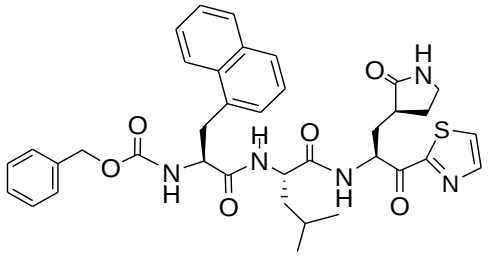

Followed General Procedure A: The *N*-Boc-dipeptide **94** was used in place of **76,** to give compound **39** (15 mg, 37% yield) as a white solid. ^{1}H NMR δ 8.17 (br. s., 1H), 8.02 (d, *J* = 3.12 Hz, 1H), 7.83 (d, *J* = 8.59 Hz, 1H), 7.73 (d, *J* = 7.81 Hz, 1H), 7.69 (d, *J* = 2.73 Hz, 1H), 7.42 - 7.55 (m, 2H), 7.21 - 7.38 (m, 6H), 6.55 (br. s., 1H), 5.84 (s, 1H), 5.51 - 5.59 (m, 1H), 5.37 (d, *J* = 7.81 Hz, 1H), 5.11 (s, 1H), 5.02 (br. s., 2H), 4.56 - 4.64 (m, 1H), 4.48 - 4.55 (m, 1H), 3.61 - 3.70 (m, 1H), 3.43 - 3.51 (m, 1H), 3.29 - 3.35 (m, 2H), 2.44 - 2.60 (m, 2H), 2.07 - 2.13 (m, 1H), 1.92 - 2.02 (m, 1H), 1.51 - 1.69 (m, 2H), 1.38 - 1.46 (m, 1H), 0.89 (d, *J* = 6.25 Hz, 6H); ^{13}C NMR δ 190.6, 179.9, 172.0, 170.9, 156.6, 145.1, 134.1, 132.8, 132.2, 131.1, 129.1, 128.7, 128.4, 128.2, 128.1, 128.0, 127.0, 126.7, 126.0, 125.6, 123.9, 67.3, 56.0, 55.1, 52.1, 42.1, 40.8, 39.2, 35.4, 33.4, 28.9, 24.9, 23.1, 22.3; MS, m/z 706.1 $(M+Na)^+$.

(1-{3-Methyl-1-[2-(2-methyl-oxiranyl)-2-oxo-1-(2-oxo-pyrrolidin-3-ylmethyl)-ethylcarbamoyl]-butylcarbamoyl}-2-naphthalen-1-yl-ethyl)-carbamic acid benzyl ester (40).

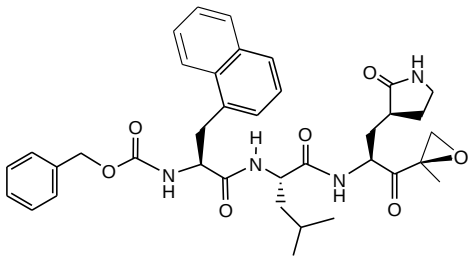

Followed General Procedure A: The *N*-Boc-dipeptide **97-lp** was used in place of **76**, to give compound **40** (19 mg, 72% yield) as a white solid. ^{1}H NMR δ 8.12 - 8.24 (m, 1H), 7.84 (d, *J* = 8.98 Hz, 1H), 7.74 (d, *J* = 7.81 Hz, 1H), 7.44 - 7.55 (m, 2H), 7.22 - 7.38 (m, 8H), 6.55 (d, *J* = 7.42 Hz, 1H), 6.16 (br. s., 1H), 5.41 (d, *J* = 7.81 Hz, 1H), 5.02 (br. s., 2H), 4.54 - 4.62 (m, 1H), 4.42 - 4.52 (m, 1H), 4.29 - 4.36 (m, 1H), 3.62 (dd, *J* = 6.05, 13.86 Hz, 1H), 3.39 - 3.51 (m, 1H), 3.21 - 3.38 (m, 3H), 2.90 (d, *J* = 5.08 Hz, 1H), 2.35 - 2.46 (m, 2H), 1.75 - 1.94 (m, 2H), 1.54 - 1.62 (m, 2H), 1.50 (s, 3H), 1.31 - 1.45 (m, 2H), 0.84 - 0.92 (m, 6H); ^{13}C NMR δ 206.7, 179.9, 172.3, 170.9, 156.3, 134.1, 132.9, 132.3, 129.0, 128.7, 128.4, 128.2, 128.0, 127.9, 126.6, 126.0, 125.6, 123.8, 67.2, 59.6, 56.0, 52.9, 51.8, 42.2, 40.8, 39.3, 31.9, 29.9, 28.7, 28.5, 24.8, 23.0, 22.3, 17.0; MS, m/z 679.3 $(M+Na)^{+}$.

(1-{3-Methyl-1-[2-(2-methyl-oxiranyl)-2-oxo-1-(2-oxo-pyrrolidin-3-ylmethyl)-ethylcarbamoyl]-butylcarbamoyl}-2-naphthalen-1-yl-ethyl)-carbamic acid benzyl ester (41).

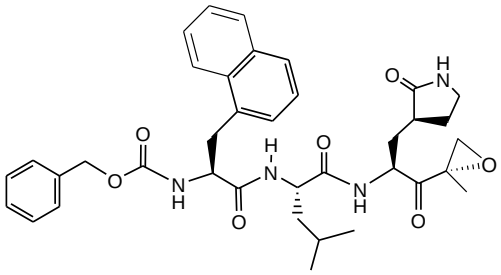

Followed General Procedure A: The *N*-Boc-dipeptide **97-mp** was used in place of **76**, to give compound **41** (16 mg, 61% yield) as a white solid. ^{1}H NMR δ 8.16 - 8.21 (m, 1H), 7.98 - 8.04 (m, 1H), 7.86 (d, *J* = 7.81 Hz, 1H), 7.77 (d, *J* = 7.81 Hz, 1H), 7.45 - 7.59 (m, 2H), 7.21 - 7.41 (m, 7H), 6.44 - 6.50 (m, 1H), 5.58 - 5.63 (m, 1H), 5.32 (d, *J* = 7.03 Hz, 1H), 4.97 - 5.06 (m, 2H), 4.67 - 4.76 (m, 1H), 4.53 - 4.59 (m, 1H), 4.43 - 4.51 (m, 1H), 3.64 - 3.75 (m, 1H), 3.36 - 3.48 (m, 1H), 3.25 - 3.32 (m, 1H), 2.98 (d, *J* = 5.08 Hz, 1H), 2.84 (d, *J* = 5.08 Hz, 1H), 2.33 - 2.44 (m,

2H), 1.98 - 2.08 (m, 1H), 1.87 - 1.97 (m, 1H), 1.75 - 1.84 (m, 1H), 1.64 - 1.74 (m, 1H), 1.48 - 1.55 (m, 1H), 1.38 - 1.46 (m, 2H), 1.25 (s, 3H), 0.83 - 0.92 (m, 6H); MS, m/z 679.4 $(M+Na)^+$.

[2-[2-(2-Benzyloxycarbonylamino-3-naphthalen-1-yl-propionylamino)-3-cyclohexyl-propionylamino]-1-hydroxy-3-(2-oxo-pyrrolidin-3-yl)-propyl]-phosphonic acid dimethyl ester (42).

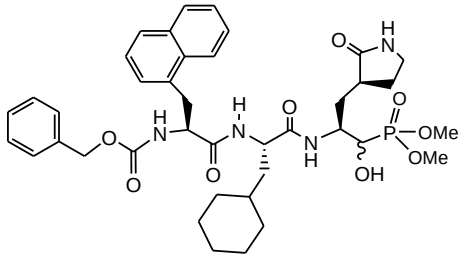

Followed General Procedure D: Started with aldehyde **25** and dimethylphosphite was used in place of diethylphosphite, yielding compound **42** (64%) as a white solid. ^{1}H NMR δ 8.12 (d, *J* = 8.20 Hz, 1H), 7.84 (d, *J* = 9.37 Hz, 1H), 7.73 (d, *J* = 7.81 Hz, 1H), 7.43 - 7.53 (m, 2H), 7.19 - 7.40 (m, 8H), 6.38 (br. s., 1H), 5.47 (d, *J* = 6.64 Hz, 1H), 5.25 (br. s., 1H), 5.01 (br. s., 2H), 4.50 - 4.64 (m, 2H), 4.25 - 4.31 (m, 1H), 3.87 - 3.93 (m, 1H), 3.78 - 3.83 (m, 3H), 3.71 - 3.77 (m, 3H), 3.64 - 3.70 (m, 1H), 3.30 - 3.39 (m, 1H), 3.17 - 3.28 (m, 2H), 2.29 - 2.40 (m, 1H), 2.10 - 2.20 (m, 1H), 1.55 - 1.79 (m, 10H), 1.39 - 1.48 (m, 1H), 1.05 - 1.26 (m, 3H), 0.79 - 0.96 (m, 2H); MS, m/z 773.5 $(M+Na)^+$.

[2-[2-(2-Benzyloxycarbonylamino-3-naphthalen-1-yl-propionylamino)-3-cyclohexyl-propionylamino]-1-hydroxy-3-(2-oxo-pyrrolidin-3-yl)-propyl]-phosphonic acid diethyl ester (43).

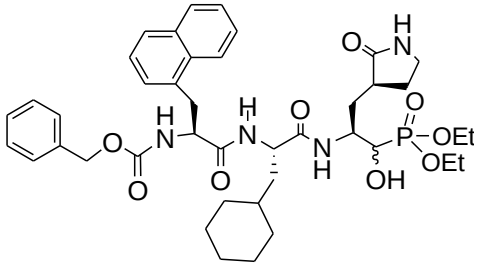

Followed General Procedure D: Started with aldehyde **25**, yielding compound **43** (90%) as a white solid. ^{1}H NMR δ 8.19 (d, *J* = 7.81 Hz, 1H), 8.11 (d, *J* = 7.42 Hz, 1H), 7.79 - 7.86 (m, 2H), 7.68 - 7.77 (m, 2H), 7.41 - 7.55 (m, 4H), 7.17 - 7.38 (m, 7H), 5.50 - 5.66 (m, 1H), 5.19 - 5.34 (m,

1H), 4.95 - 5.04 (m, 2H), 4.50 - 4.64 (m, 3H), 4.37 - 4.47 (m, 1H), 4.26 - 4.34 (m, 1H), 3.94 - 4.21 (m, 4H), 3.76 - 3.88 (m, 1H), 3.60 - 3.73 (m, 1H), 3.29 - 3.40 (m, 1H), 3.13 - 3.27 (m, 2H), 2.25 - 2.41 (m, 1H), 2.11 - 2.23 (m, 1H), 1.71 - 1.87 (m, 1H), 1.53 - 1.69 (m, 2H), 1.39 - 1.49 (m, 1H), 1.19 - 1.37 (m, 8H), 1.05 - 1.17 (m, 2H), 0.77 - 0.97 (m, 4H); ^{13}C NMR δ 181.1, 180.8, 173.0, 127.7, 127.4, 171.8, 171.5, 157.0, 156.6, 156.5, 136.2, 136.0, 134.2, 134.1, 133.1, 133.0, 132.2, 129.0, 128.7, 128.4, 128.1, 127.9, 127.6, 126.7, 126.5, 126.0, 125.9, 125.7, 125.6, 123.9, 123.8, 67.5, 67.3, 63.5, 63.3, 62.8, 56.4, 55.9, 52.4, 52.0, 51.4, 50.2, 48.6, 40.8, 40.3, 39.5, 38.5, 38.0, 35.1, 34.4, 34.0, 33.8, 32.6, 32.4, 29.9, 28.7, 28.4, 26.6, 26.6, 26.5, 26.4, 26.3, 26.2, 16.7; MS, m/z 801.2 $(M+Na)^+$.

4-Methyl-2-(2-{2-[methyl-(4-methyl-2-oxo-2H-chromen-7-yl)-amino]-acetylamino}-3-naphthalen-1-yl-propionylamino)-pentanoic acid [1-formyl-2-(2-oxo-pyrrolidin-3-yl)-ethyl]-amide (44).

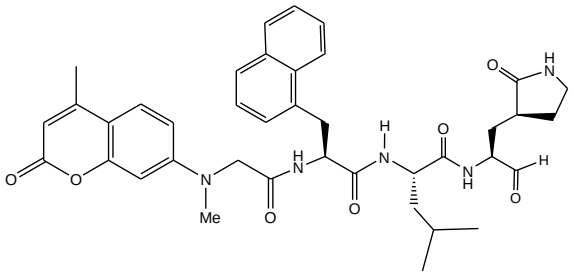

Followed General Procedure B: Started with ester **99**, yielding compound **44** (81%) as a white solid. ^{1}H NMR δ (major isomer) 9.48 (s, 1H), 8.30 - 8.38 (m, 1H), 8.10 (d, *J* = 8.98 Hz, 1H), 7.83 - 7.93 (m, 1H), 7.76 (d, *J* = 8.59 Hz, 1H), 7.62 (d, *J* = 8.98 Hz, 1H), 7.42 - 7.51 (m, 2H), 7.18 - 7.29 (m, 4H), 6.81 (d, *J* = 8.59 Hz, 1H), 6.70 (d, *J* = 6.25 Hz, 1H), 6.42 (s, 1H), 6.33 (br. s., 1H), 6.07 (s, 1H), 5.80 - 5.86 (m, 1H), 4.75 - 4.83 (m, 1H), 4.54 - 4.62 (m, 1H), 4.45 - 4.53 (m, 1H), 4.26 - 4.35 (m, 1H), 3.85 - 3.89 (m, 2H), 3.65 - 3.75 (m, 2H), 3.29 - 3.38 (m, 2H), 2.72 (s, 3H), 2.36 (s, 3H), 1.37 - 1.93 (m, 6H), 0.88 - 0.93 (m, 6H); MS, m/z 718.3 $(M+Na)^+$.

2-Methyl-thiazole-5-carboxylic acid (1-{1-[1-formyl-2-(2-oxo-pyrrolidin-3-yl)-ethylcarbamoyl]-3-methyl-butylcarbamoyl}-2-naphthalen-1-yl-ethyl)-amide (45).

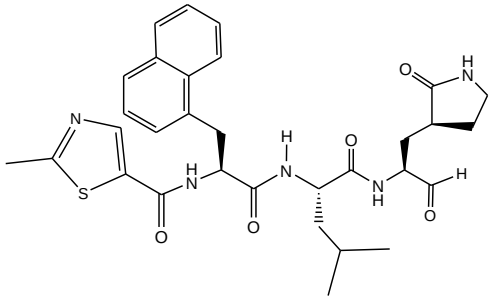

Followed General Procedure B: Started with ester **100**, yielding compound **45** (45%) as a white solid. ^{1}H NMR δ 9.42 (s, 1H), 8.25 (d, *J* = 8.59 Hz, 1H), 8.17 (d, *J* = 5.86 Hz, 1H), 7.80 - 7.85 (m, 1H), 7.73 (d, *J* = 8.20 Hz, 1H), 7.51 - 7.57 (m, 1H), 7.45 - 7.51 (m, 1H), 7.32 - 7.43 (m, 3H), 6.96 (d, *J* = 7.03 Hz, 1H), 6.84 (d, *J* = 7.81 Hz, 1H), 5.89 (br. s., 1H), 4.97 - 5.05 (m, 1H), 4.46 - 4.54 (m, 1H), 4.20 - 4.27 (m, 1H), 3.62 - 3.67 (m, 2H), 3.25 - 3.40 (m, 2H), 2.66 (s, 3H), 2.32 - 2.41 (m, 1H), 1.60 - 1.94 (m, 5H), 1.39 - 1.56 (m, 2H), 0.81 - 0.90 (m, 6H); ^{13}C NMR δ 200.1, 180.1, 173.0, 170.9, 161.0, 143.7, 135.9, 134.2, 133.5, 132.7, 132.3, 129.2, 128.3, 128.1, 126.8, 126.1, 125.7, 123.9, 58.3, 54.9, 52.5, 41.5, 40.8, 38.7, 35.1, 30.0, 29.2, 25.0, 23.1, 22.0, 19.8; MS, m/z 614.4 $(M+Na)^{+}$.

14-Benzyloxycarbonylamino-2-isobutyl-3,8,15-trioxo-1,4,9triaza-cyclopentadecane-5-carboxylic acid methyl ester (47).

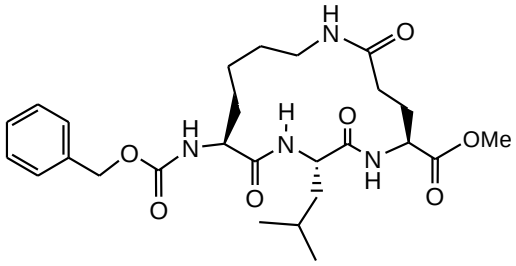

Compound **107** (0.11 mmol) was dissolved in 10% TFA/CH_2Cl_2 (2 mL) and stirred at 25^{o}C for 1 h. The solvent was removed and remaining residue was placed under high vacuum to yield the amine intermediate as a sticky solid. The de-Boc intermediate was immediately dissolved in (4:1) CH_2Cl_2/dioxane (4 mL) and treated with DMAP (0.34 mmol) and benzylchloroformate (0.14 mmol) followed by stirring at 25^{o}C for 2 h. The reaction was combined with water (50 mL) and CH_2Cl_2 (50 mL) and the aqueous layer was acidified to pH 2 using aq. HCl. The organic layer was removed and the aqueous layer was extracted with CH_2Cl_2 (40 mL x 3). The combined CH_2Cl_2 layers were dried ($MgSO_4$), filtered and concentrated using a rotary evaporator to yield a

solid which was purified by silica gel column chromatography (15:1 CH_2:Cl_2: MeOH) to give compound **47** (42 mg, 72%) as a white solid. ^{1}H NMR δ 7.87 (d, *J* = 5.43 Hz, 1H), 7.77(d, *J* = 5.23 Hz, 1H), 7.30 - 7.42 (m, 5H), 6.81 - 6.88 (m, 1H), 5.99 (d, *J* = 6.01 Hz, 1H), 5.09 (s, 2H), 4.49 - 4.56 (m, 1H), 4.39 - 4.46 (m, 1H), 4.19 - 4.28 (m, 1H), 3.59 (s, 3H), 2.89 - 2.97 (m, 1H), 2.27 - 2.39 (m, 2H), 1.87 - 1.98 (m, 1H), 1.51 - 1.84 (m, 6H), 1.36 - 1.46 (m, 2H), 1.15 - 1.31 (m, 2H), 0.87 - 1.00 (m, 6H); ^{13}C NMR δ 173.1, 173.0, 172.6, 156.0, 136.3, 128.6, 128.3, 128.0, 67.0, 54.2, 52.4, 52.1, 51.5, 40.8, 37.7, 31.4, 31.2, 28.1, 25.5, 24.6, 22.7, 22.0, 20.4; MS, m/z 541.0 $(M+Na)^+$.

(5-Formyl-2-isobutyl-3,8,15-trioxo-1,4,9triaza-cyclopentadec-14-yl)-carbamic acid benzyl ester (48).

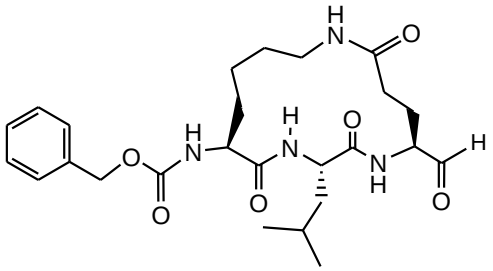

Followed General Procedure B: Started with ester **107**, yielding compound **48** (92%) as a white solid. ^{1}H NMR (DMSO-d6) δ 9.37 (s, 1H), 8.16 (d, *J* = 5.64 Hz, 1H), 7.42 - 7.47 (m, 1H), 7.27 - 7.38 (m, 6H), 7.16 (d, *J* = 5.54 Hz, 1H), 4.97 - 5.04 (m, 2H), 4.35 - 4.43 (m, 1H), 4.29 - 4.34 (m, 1H), 4.07 - 4.14 (m, 1H), 2.75 - 2.83 (m, 1H), 2.17 - 2.33 (m, 2H), 2.03 - 2.16 (m, 2H), 1.51 - 1.61 (m, 6H), 1.44 - 1.50 (m, 1H), 1.25 - 1.32 (m, 2H), 0.82 - 0.93 (m, 6H); MS, m/z 511.3 $(M+Na)^+$.

[1-Formyl-2-(2-oxo-pyrrolidin-3-yl)-ethyl]-carbamic acid tert-butyl ester (53a).

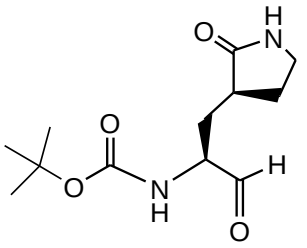

Followed General Procedure B: Started with ester **52**, yielding compound **53a** (94%) as a white solid. ^{1}H NMR δ 9.57 (s, 1H), 6.10 - 6.22 (m, 1H), 4.14 - 4.23 (m, 1H), 3.29 - 3.43 (m, 2H), 2.39

- 2.53 (m, 2H), 1.77 - 2.07 (m, 3H), 1.46 (s, 9H); ^{13}C NMR δ 200.5, 180.0, 156.3, 80.3, 58.9, 40.6, 38.0, 30.6, 28.8, 28.5.

2-(2-Benzyloxycarbonylamino-propionylamino)-3-(2-oxo-pyrrolidin-3-yl)-propionic acid methyl ester (54).

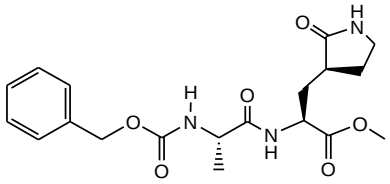

A solution of Cbz-Ala-OH (0.84 mmol) and CDI (0.94 mmol) in dry THF (4 mL) was added to a solution of **53** (0.70 mmol) and NEt_3 (1.4 mmol) in DMF (4 mL). The resulting solution was stirred at 25^{o}C for 18 h. The Reaction was partitioned between water (30 mL) and EtOAc (30 mL). The organic layer was removed and the aqueous layer was extracted with EtOAc (3 x 20 mL). The combined organic layers were dried ($MgSO_4$), filtered and concentrated to give an oil that was purified by silica gel column chromatography (20:1 CH_2Cl_2:MeOH) to afford **54** (198 mg, 72%) as a white solid. ^{1}H NMR δ 7.94 (s, 1H), 7.40 - 7.25 (m, 5H), 6.75 (s, 1H), 5.86 (s, 1H), 5.09 (s, 2H), 4.42 - 4.51 (m, 1H), 4.38 - 4.42 (m, 1H), 3.71 (s, 3H), 3.24 - 3.39 (m, 2H), 2.33 - 2.50 (m, 2H), 2.11 - 2.23 (m, 1H), 1.71 - 1.91 (m, 2H), 1.40 (d, *J* = 6.83 Hz, 3H); ^{13}C NMR δ 180.1, 173.3, 172.4, 156.0, 136.6, 128.7, 128.3, 128.2, 67.0, 52.6, 51.5, 50.6, 40.7, 38.6, 33.3, 28.3, 19.4; MS, m/z 414.1 $(M+Na)^+$.

2-(2-Benzyloxycarbonylamino-propionylamino)-propionic acid (60).

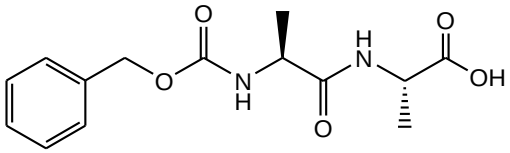

(S)-Alanine-2-chlorotritylresin (0.6 mmol) was swelled in DMF (2 mL) for 30 min and then filtered. To the alanine resin was added a solution of (S)-N-cbz-alanine (1.8 mmol) and HBTU (1.6 mmol) in 4.2% DIPEA in DMF (14 mL). Subjected to microwave irradiation (25 W, 75^{o}C, 5

min) and then filtered and washed with DMF (15 mL x3) and CH_2Cl_2 (15 mL x 2). The resin was then treated with cleavage cocktail (95% TFA, 2.5% TIPS, 2.5% water; 20 mL) and heated in the microwave reactor (20 W, 38°C, 18 min). The reaction was filtered and the filtrate was concentrate on a rotary evaporator to yield an oil that was purified by silica gel chromatography (15:1 CH_2Cl_2:MeOH) to give the product **60** (63%) as a white solid. ^{1}H NMR δ 9.53 (br. s., 1H), 7.25 - 7.39 (m, 5H), 7.12 (br. s., 1H), 5.82 (br. s., 1H), 5.02 - 5.18 (m, 2H), 4.46 - 4.60 (m, 1H), 4.28 - 4.39 (m, 1H), 1.28 - 1.52 (m, 6H).

2-(2-Benzyloxycarbonylamino-propionylamino)-propionic acid (61).

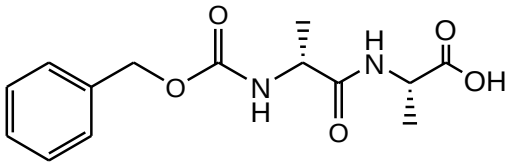

(S)-Alanine-2-chlorotritylresin (0.59 mmol) was swelled in DMF (2 mL) for 30 min and then filtered. To the alanine resin was added a solution of (R)-N-cbz-alanine (0.94 mmol) and HBTU (0.88 mmol) in 4.2% DIPEA in DMF (13 mL). Subjected to microwave irradiation (25 W, 75°C, 5 min) and then filtered and washed with DMF (15 mL x3) and CH_2Cl_2 (15 mL x 2). The resin was then treated with cleavage cocktail (95% TFA, 2.5% TIPS, 2.5% water; 10 mL) and heated in the microwave reactor (20 W, 38°C, 18 min). The reaction was filtered and the filtrate was concentrate on a rotary evaporator to yield an oil that was purified by silica gel chromatography (15:1 CH_2Cl_2:MeOH) to give the product **61** (150 mg, 86%) as a white solid. ^{1}H NMR δ 7.30 - 7.38 (m, 5H), 5.95 (d, *J* = 6.45 Hz, 1H), 5.01 - 5.13 (m, 2H), 4.51 - 4.59 (m, 1H), 4.41 - 4.51 (m, 1H), 1.39 (d, *J* = 7.42 Hz, 3H), 1.42 (d, *J* = 7.42 Hz, 3H); MS, m/z 317.0 $(M+Na)^+$.

2-(2-Benzyloxycarbonylamino-3-naphthalen-1-yl-propionylamino)-propionic acid (62).

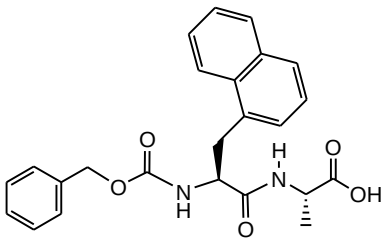

(S)-Alanine-2-chlorotritylresin (0.6 mmol) was swelled in DMF (2 mL) for 30 min and then filtered. To the alanine resin was added a solution of (S)-N-cbz-1-napthylalanine (1.8 mmol) and HBTU (1.6 mmol) in 4.2% DIPEA in DMF (14 mL). Subjected to microwave irradiation (25 W, 75^{o}C, 5 min) and then filtered and washed with DMF (15 mL x3) and CH_2Cl_2 (15 mL x 2). The resin was then treated with cleavage cocktail (95% TFA, 2.5% TIPS, 2.5% water; 20 mL) and heated in the microwave reactor (20 W, 38^{o}C, 18 min). The reaction was filtered and the filtrate was concentrate on a rotary evaporator to yield an oil that was purified by silica gel chromatography (15:1 CH_2Cl_2:MeOH) to give the product **62** (135 mg, 57%) as a white solid. ^{1}H NMR δ 8.10 (d, *J* = 7.42 Hz, 1H), 7.79 (d, *J* = 7.42 Hz, 1H), 7.69 (d, *J* = 5.08 Hz, 1H), 7.39 - 7.52 (m, 2H), 7.21 - 7.38 (m, 7H), 6.47 (d, *J* = 6.25 Hz, 1H), 5.80 (d, *J* = 7.81 Hz, 1H), 5.03 (br. s., 2H), 4.61 - 4.70 (m, 1H), 4.31 - 4.41 (m, 1H), 3.39 - 3.57 (m, 2H), 1.28 (d, *J* = 7.03 Hz, 3H); ^{13}C NMR δ 175.4, 171.1, 156.1, 135.9, 133.8, 132.1, 131.8, 128.9, 128.5, 128.2, 128.0, 126.5, 125.8, 125.3, 123.4, 67.2, 55.5, 48.3, 36.0, 17.8; MS, m/z 443.1 $(M+Na)^{+}$.

2-[2-(2-Benzyloxycarbonylamino-propionylamino)-propionylamino]-3-(2-oxo-pyrrolidin-3-yl)-propionic acid methyl ester (63).

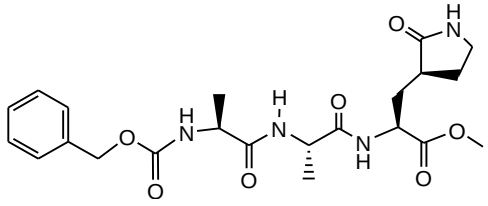

Followed General Procedure E: The *N*-Cbz-dipeptide **60** was used in place of *N*-Boc-leucine, to give compound **63** (41% yield) as a white solid. ^{1}H NMR δ 8.00 (d, *J* = 5.47 Hz, 1H), 7.29 - 7.38 (m, 5H), 6.95 (d, *J* = 5.86 Hz, 1H), 6.11 (s, 1H), 5.60 (d, *J* = 7.42 Hz, 1H), 5.05 - 5.15 (m, 2H), 4.51 - 4.60 (m, 1H), 4.44 - 4.51 (m, 1H), 4.21 - 4.30 (m, 1H), 3.72 (s, 3H), 3.30 - 3.36 (m, 2H), 2.35 - 2.48 (m, 2H), 2.11 - 2.20 (m, 1H), 1.87 - 1.95 (m, 1H), 1.80 - 1.87 (m, 1H), 1.35 - 1.43 (m, 6H); ^{13}C NMR δ 179.8, 172.6, 172.1, 172.0, 155.9, 136.2, 128.5, 128.1, 128.0, 66.9, 52.4, 51.6, 50.6, 48.8, 40.5, 38.4, 33.0, 28.4, 18.7, 18.7; MS, m/z 485.3 $(M+Na)^{+}$.

2-[2-(2-Benzyloxycarbonylamino-propionylamino)-propionylamino]-3-(2-oxo-pyrrolidin-3-yl)-propionic acid methyl ester (64).

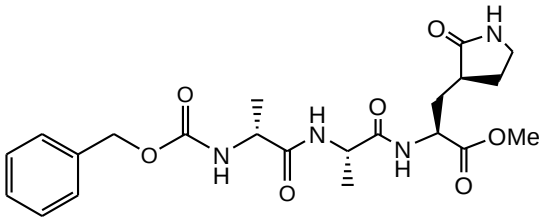

Followed General Procedure E: The *N*-Cbz-dipeptide **61** was used in place of *N*-Boc-leucine, to give compound **64** (54% yield) as a white solid. ^{1}H NMR δ 8.19 (d, *J* = 7.03 Hz, 1H), 7.29 - 7.38 (m, 5H), 7.21 (d, *J* = 8.20 Hz, 1H), 6.52 - 6.61 (m, 1H), 6.12 (d, *J* = 7.42 Hz, 1H), 5.01 - 5.13 (m, 2H), 4.58 - 4.67 (m, 1H), 4.41 - 4.49 (m, 1H), 4.26 - 4.35 (m, 1H), 3.69 (s, 3H), 3.16 - 3.31 (m, 2H), 2.37 - 2.47 (m, 1H), 2.28 - 2.36 (m, 1H), 2.08 - 2.19 (m, 1H), 1.81 - 1.90 (m, 1H), 1.73 - 1.81 (m, 1H), 1.33 - 1.42 (m, 6H); ^{13}C NMR δ 180.0, 172.8, 172.2, 156.0, 136.1, 128.5, 128.1, 128.1, 66.9, 52.4, 51.6, 50.5, 48.7, 40.5, 38.5, 32.6, 28.2, 18.7, 18.3; MS, m/z 485.3 $(M+Na)^{+}$.

2-Benzyloxycarbonylamino-propionic acid methyl ester (66).

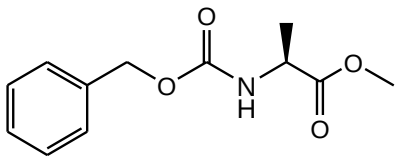

N-Cbz-alanine (1.0 mmol) was dissolved in dry MeOH (3 mL) and 1 drop conc. HCl was added. The solution was stirred at 25^{o}C for 18 h after which it was concentrate to yield **66** (240 mg, 100%) as an oil that was used without further purification. ^{1}H NMR δ 7.25 - 7.39 (m, 5H), 5.32 (br. s., 1H), 5.11 (s, 2H), 4.35 - 4.42 (m, 1H), 3.72 (s, 3H), 1.40 (d, *J* = 7.42 Hz, 3H); ^{13}C NMR δ 173.8, 156.0, 136.6, 128.7, 128.3, 128.3, 67.1, 52.6, 49.8, 18.6; MS, m/z 260.1 $(M+Na)^{+}$.

(1-Methyl-2-oxo-ethyl)-carbamic acid benzyl ester (67).

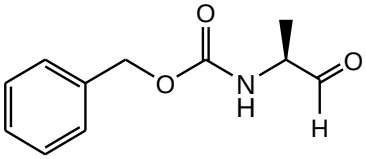

Followed General Procedure B: Started with ester **66**, yielding compound **67** (70%) as a white solid. ^{1}H NMR δ 9.55 (s, 1H), 7.29 - 7.39 (m, 5H), 5.46 (br. s., 1H), 5.12 (s, 2H), 4.26 - 4.35 (m,

1H), 1.36 (d, *J* = 7.42 Hz, 3H); ^{13}C NMR δ 199.0, 155.8, 136.1, 128.5, 128.2, 128.1, 67.0, 55.9, 14.7; MS, m/z 230.1 $(M+Na)^+$.

2-(2-Benzyloxycarbonylamino-propylamino)-propionic acid methyl ester (69).

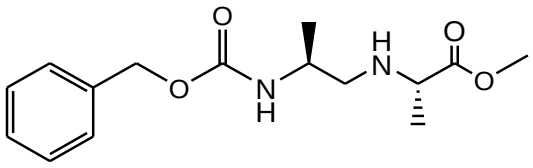

(1-Methyl-2-oxo-ethyl)-carbamic acid benzyl ester **67** (0.60 mmol) was added to a solution of alanine-methylester **68** (0.60 mmol) and NEt_3 (0.60 mmol) in MeOH (2mL) and the reaction allowed to stir overnight. $NaCNBH_3$ (0.90 mmol) was added and the reaction stirred for 3 h. The reaction was quenched with sat. aq. NH_4Cl (5 mL) and the reaction partitioned between water (20 mL) and EtOAc (25 mL). The organic layer was removed and the aqueous layer was extracted with EtOAc (3 x 25 mL), the combined organinc layers were dried ($MgSO_4$), filtered and concentrated to yield an oil that was purified by silica gel column chromatography (1:1 EtOAc:Hexane) to yield **69** (70 mg, 40%) as a white solid. ^{1}H NMR δ 7.29 - 7.39 (m, 5H), 5.10 (s, 2H), 3.73 - 3.78 (m, 1H), 3.71(s, 3H), 3.28 - 3.38 (m, 1H), 2.68 (dd, *J* = 5.10, 11.60 Hz, 1H), 2.49 (dd, *J* = 5.10, 11.83 Hz, 1H), 1.27 (d, *J* = 7.09 Hz, 3H), 1.17 (d, *J* = 7.08 Hz, 3H); ^{13}C NMR δ 176.2, 156.3, 136.9, 128.7, 128.3, 128.3, 66.7, 57.0, 52.8, 52.0, 47.4, 19.1; MS, m/z 317.0 $(M+Na)^+$.

2-[(2-Benzyloxycarbonylamino-propyl)-formyl-amino]-propionic acid methyl ester (71).

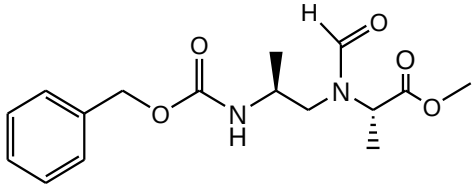

Formic acid (1.84 mmol) was dissolved in dry CH_2Cl_2 (2 mL) and cooled to 0^{o}C. Acetic anhydride (0.31 mmol) was added and stirred for 2 h at 25^{o}C to form a mixed anhydride **70**. The solution was cooled to 0^{o}C and the amine **69** (0.15 mmol) was added followed by stirring for 8 h at 25^{o}C. The solvent was removed on a rotary evaporator and the residue was purified by silica gel column chromatography (15:1 CH_2Cl_2:MeOH) to give compound **71** (46 mg, 93%) and a white solid. ^{1}H NMR (two diastereomers) δ 7.99 - 8.22 (m, 2H), 7.25 - 7.29 (m, 10H), 5.02 -

5.12 (m, 4H), 4.41 - 4.48 (m, 1H), 4.12 - 4.21 (m, 1H), 3.81 - 3.91 (m, 1H), 3.71 (s, 6H), 3.61 - 3.73 (m, 1H), 3.40 - 3.45 (m, 1H), 3.20 - 3.29 (m, 1H), 3.01 - 3.09 (m, 1H), 1.47 - 1.60 (m, 6H), 1.12 - 1.26 (m, 6H); ^{13}C NMR δ 172.1, 172.0, 164.9, 164.3, 163.6, 163.5, 156.3, 155.9, 136.9, 136.5, 128.8, 128.6, 128.5, 128.3, 128.2, 67.0, 66.6, 56.8, 56.3, 53.2, 53.0, 52.7, 51.8, 48.2, 47.7, 47.4, 46.9, 46.7, 19.4, 19.1, 18.3, 18.1, 17.2, 17.0, 14.7, 14.6; MS, m/z 345.1 $(M+Na)^+$.

2-[(2-Benzyloxycarbonylamino-propyl)-formyl-amino]-propionic acid (72).

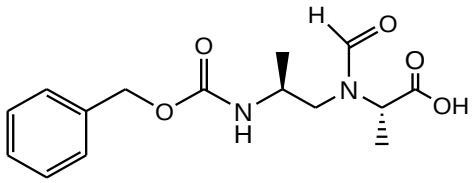

The ester **71** (1.24 mmol) was dissolved in 1:1 dioxane:water (6 mL) and treated with 6N NaOH (1 mL). After stirring at 25^{o}C for 1 h the reaction was partitioned between water and ether, the ether layer was removed and the aqueous layer was acidified to pH 2 using aq. HCl. The aqueous layer was extracted with CH_2Cl_2 (30 mL x 5), the combined CH_2Cl_2 layers were dried (Na_2SO_4), filtered and concentrated to yield compound **72** (366 mg, 96%) as a clear oil. ^{1}H NMR (two diastereomers) δ 7.97 - 8.24 (m, 2H), 7.24 - 7.29 (m, 10H), 5.45 - 5.52 (m, 1H), 4.99 - 5.18 (m, 4H), 4.31 - 4.43 (m, 1H), 4.13 - 4.20 (m, 1H), 3.84 - 3.94 (m, 1H), 3.36 - 3.48 (m, 1H), 3.20 - 3.30 (m, 1H), 3.02 - 3.13 (m, 1H), 1.47 - 1.60 (m, 6H), 1.12 - 1.24 (m, 6H); MS, m/z 331.1 $(M+Na)^+$.

2-{2-[(2-Benzyloxycarbonylamino-propyl)-formyl-amino]-propionylamino}-3-(2-oxo-pyrrolidin-3-yl)-propionic acid methyl ester (73).

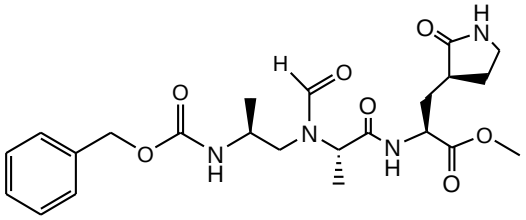

The acid **72** (0.11 mmol) and CDI (0.14 mmol) were dissolved in dry DMF (1 mL) and stirred for 20 min. Concurrently and separately, the amine **53** was dissolved in dry DMF and treated with NEt_3 (0.11 mmol) and stirred for 20 min. The amine solution was added to the CDI solution and the resulting solution was stirred for 18 h at 25^{o}C. The reaction was dissolved in EtOAc (20

mL) and water (20 mL) was added. The organic layer was removed and the aqueous layer was extracted with EtOAc (3 x 15 mL), the combined organic layers were dried ($MgSO_4$), filtered and concentrated to give an oil that was purified by silica gel chromatography (5:1 CH_2Cl_2:MeOH) to provide compound **73** (29 mg, 55%) as a sticky oil and as two diastereomers. ^{1}H NMR δ 9.60 (s, 1H), 8.89 - 8.89 (m, 1H), 8.21 - 8.29 (m, 1H), 7.95 - 8.06 (m, 1H), 7.59 (s, 1H), 7.22 - 7.39 (m, 10H), 7.08 (s, 1H), 5.58 - 5.65 (m, 1H), 4.99 - 5.12 (m, 4H), 4.25 - 4.51 (m, 3H), 4.05 - 4.18 (m, 1H), 3.72 (s, 3H), 3.70 (s, 3H), 3.20 - 3.39 (m, 4H), 3.05 - 3.18 (m, 1H), 2.30 - 2.50 (m, 4H), 2.01 - 2.20 (m, 2H), 1.62 - 1.95 (m, 4H), 1.21 (d, *J* = 6.53 Hz, 6H), 1.20 (d, *J* = 6.54 Hz, 6H); MS, m/z 499.3 $(M+Na)^+$.

2-(2-tert-Butoxycarbonylamino-propionylamino)-3-(2-oxo-pyrrolidin-3-yl)-propionic acid methyl ester (74).

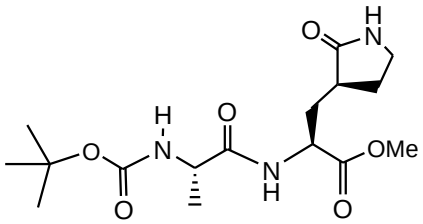

Followed General Procedure E: N-Boc-alanine was used in place of *N*-Boc-leucine to give compound **74** (79% yield) as a white solid. ^{1}H NMR δ 7.81 (d, *J* = 7.42 Hz, 1H), 7.03 (br. s., 1H), 5.43 (d, *J* = 7.42 Hz, 1H), 4.44 - 4.52 (m, 1H), 4.20 - 4.29 (m, 1H), 3.66 (s, 3H), 3.22 - 3.33 (m, 2H), 2.28 - 2.46 (m, 2H), 2.10 - 2.20 (m, 1H), 1.72 - 1.84 (m, 2H), 1.36 (s, 9H), 1.32 (d, *J* = 7.03 Hz, 3H); ^{13}C NMR δ 179.8, 173.4, 172.2, 155.2, 79.5, 52.3, 50.8, 49.8, 40.4, 38.1, 33.1, 28.2, 27.9, 18.9; MS, m/z 380.1 $(M+Na)^+$.

2-(3-tert-Butoxy-2-tert-butoxycarbonylamino-propionylamino)-3-(2-oxo-pyrrolidin-3-yl)-propionic acid methyl ester (75).

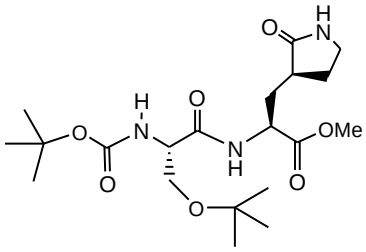

Followed General Procedure E: N-Boc-*O*-t-butyl-serine was used in place of *N*-Boc-leucine to give compound **75** (96% yield) as a white solid. ^{1}H NMR δ 7.42 - 7.50 (m, 1H), 6.11 - 6.24 (m, 1H), 5.41 - 5.50 (m, 1H), 4.63 - 4.72 (m, 1H), 4.20 - 4.27 (m, 1H), 3.79 - 3.86 (m, 1H), 3.73 (s, 3H), 3.38 - 3.45 (m, 1H), 3.26 - 3.38 (m, 3H), 2.36 - 2.50 (m, 2H), 2.17 - 2.27 (m, 1H), 1.80 - 1.91 (m, 2H), 1.47 (s, 9H), 1.18 (s, 9H); ^{13}C NMR δ 179.5, 172.0, 170.8, 155.4, 80.1, 73.8, 61.8, 54.3, 52.4, 50.6, 40.3, 37.8, 34.2, 28.3, 28.1, 27.3; MS, m/z 452.6 $(M+Na)^{+}$.

2-(2-tert-Butoxycarbonylamino-4-methyl-pentanoylamino)-3-(2-oxo-pyrrolidin-3-yl)-propionic acid methyl ester (76).

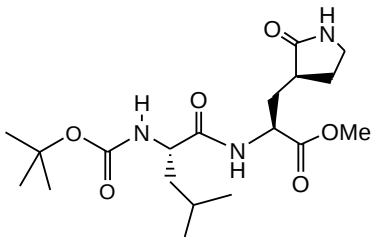

Followed General Procedure E: To a mixture of glutamine surrogate HCl salt **53** (5.59 mmol), *N*-Boc-leucine (5.59 mmol), 1-ethyl-3-(3-dimethylaminopropyl)carbodiimide (EDCI) (10.2 mmol), and 4-(dimethylamino)pyridine (DMAP) (10.2 mmol) under argon was added dry DMF (10 mL). The solution was stirred at 25^{o}C and dry CH_2Cl_2 (25 mL) was added, and the resulting solution was stirred for 18 h. The reaction was partitioned between water (150 mL) and CH_2Cl_2 (150 mL). The pH of the aqueous layer was adjusted to 3 using 2 N HCl. The organic layer was removed, and the aqueous layer was extracted twice with CH_2Cl_2 (150 mL each). The combined organic layers were dried (anhydrous $MgSO_4$), filtered and concentrated to yield a sticky solid which was purified by silica gel chromatography (30:1 CH_2Cl_2:MeOH) to yield compound **76**, 1.6 g (72% yield) as a white solid, mp 70 – 73^{o}C. ^{1}H NMR δ 7.84 (d, *J* = 7.03 Hz, 1H), 6.96 (br. s., 1H), 5.18 (d, *J* = 8.59 Hz, 1H), 4.43 - 4.50 (m, 1H), 4.25 - 4.33 (m, 1H), 3.70 (s, 3H), 3.24 - 3.38 (m, 2H), 2.30 - 2.46 (m, 2H), 2.18 - 2.27 (m, 1H), 1.76 - 1.88 (m, 2H), 1.57 - 1.75 (m, 2H), 1.43 - 1.50 (m, 1H), 1.40 (s, 9H), 0.94 (d, *J* = 6.06 Hz, 3H, CH_3), 0.93 (d, *J* = 6.12 Hz, 3H, CH_3); ^{13}C NMR δ 180.0, 173.6, 172.5, 155.9, 80.0, 53.0, 52.6, 51.3, 42.5, 40.7, 38.5, 33.3, 28.5, 28.3, 24.8, 23.1, 22.4; MS, m/z 422.3 $(M+Na)^{+}$.

2-(2-tert-Butoxycarbonylamino-3-cyclohexyl-propionylamino)-3-(2-oxo-pyrrolidin-3-yl)-propionic acid methyl ester (77).

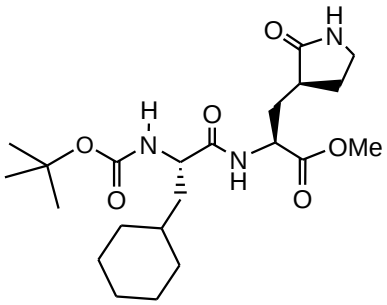

Followed General Procedure E: N-Boc-cyclohexylalanine was used in place of *N*-Boc-leucine to give compound **77** (99% yield) as a white solid. ^{1}H NMR δ 7.71 (br. s., 1H), 6.83 (br. s., 1H), 5.18 (br. s., 1H), 4.49 - 4.57 (m, 1H), 4.25 - 4.34 (m, 1H), 3.72 (s, 3H), 3.26 - 3.40 (m, 2H), 2.33 - 2.50 (m, 3H), 2.17 - 2.27 (m, 1H), 1.77 - 1.91 (m, 4H), 1.60 - 1.74 (m, 5H), 1.43 (s, 9H), 1.09 - 1.30 (m, 3H), 0.84 - 1.03 (m, 2H); ^{13}C NMR δ 179.9, 173.5, 172.4, 155.7, 79.9, 52.5, 52.4, 51.2, 40.8, 40.6, 38.4, 34.1, 33.7, 33.4, 32.8, 28.4, 28.2, 26.6, 26.4, 26.3; MS, m/z 462.2 $(M+Na)^{+}$.

2-[2-(2-Benzyloxycarbonylamino-3-naphthalen-2-yl-propionylamino)-propionylamino]-3-(2-oxo-pyrrolidin-3-yl)-propionic acid methyl ester (80).

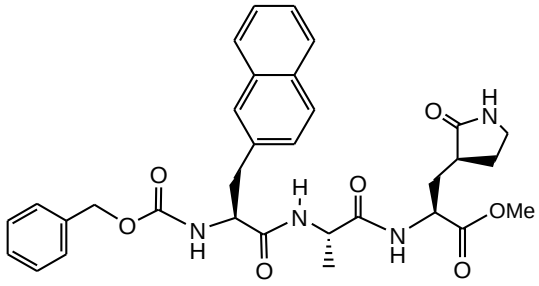

Followed General Procedure A: (*S*)-*N*-Cbz-2-napthylalanine was used in place of (*S*)-*N*-Cbz-1-napthylalanine and *N*-Boc-dipeptide **74** was used in place of *N*-Boc-dipeptide **76**, to give compound **80** (87% yield) as a white solid. ^{1}H NMR δ 8.03 (d, *J* = 7.03 Hz, 1H), 7.74 - 7.79 (m, 1H), 7.69 - 7.73 (m, 2H), 7.61 (s, 1H), 7.40 - 7.44 (m, 2H), 7.27 - 7.34 (m, 3H), 7.22 - 7.26 (m, 2H), 7.18 - 7.22 (m, 2H), 6.57 (s, 1H), 5.70 (d, *J* = 7.81 Hz, 1H), 5.07 (d, *J* = 4.30 Hz, 1H), 4.94 - 5.06 (m, 2H), 4.57 - 4.65 (m, 2H), 4.38 - 4.47 (m, 1H), 3.69 (s, 3H), 3.12 - 3.30 (m, 2H), 2.32 - 2.43 (m, 1H), 2.20 - 2.31 (m, 1H), 2.09 - 2.18 (m, 1H), 1.79 - 1.87 (m, 1H), 1.66 - 1.78 (m, 1H), 1.35 (d, *J* = 6.64 Hz, 3H); ^{13}C NMR δ 180.8, 172.8, 172.3, 171.1, 156.3, 136.3, 134.1, 133.5,

132.5, 128.6, 128.4, 128.3, 128.3, 128.2, 128.1, 127.8, 127.6, 126.2, 125.8, 67.1, 56.1, 52.6, 51.6, 49.1, 40.7, 38.6, 38.6, 33.1, 28.3, 18.9; MS, m/z 611.6 $(M+Na)^+$.

2-[2-(2-Benzyloxycarbonylamino-3-biphenyl-4-yl-propionylamino)-propionylamino]-3-(2-oxo-pyrrolidin-3-yl)-propionic acid methyl ester (81).

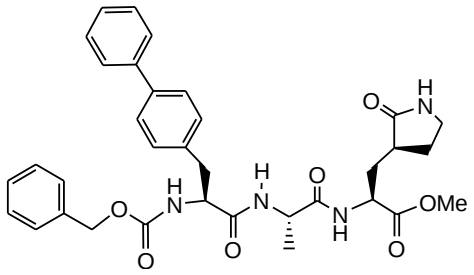

Followed General Procedure A: (*S*)-*N*-Cbz-biphenylalanine was used in place of (*S*)-*N*-Cbz-1-napthylalanine and *N*-Boc-dipeptide **74** was used in place of *N*-Boc-dipeptide **76**, to give compound **81** (95% yield) as a white solid. ^{1}H NMR δ 8.11 (d, *J* = 7.03 Hz, 1H), 7.52 (d, *J* = 7.81 Hz, 2H), 7.37 - 7.49 (m, 5H), 7.21 - 7.34 (m, 8H), 6.86 (s, 1H), 5.90 (d, *J* = 7.81 Hz, 1H), 4.96 - 5.10 (m, 2H), 4.61 - 4.69 (m, 1H), 4.53 - 4.61 (m, 1H), 4.41 - 4.49 (m, 1H), 3.67 (s, 3H), 3.00 - 3.25 (m, 4H), 2.35 - 2.44 (m, 1H), 2.14 - 2.27 (m, 2H), 1.78 - 1.87 (m, 1H), 1.65 - 1.77 (m, 1H), 1.37 (d, *J* = 6.64 Hz, 3H); ^{13}C NMR δ 180.1, 173.0, 172.4, 171.2, 156.4, 140.9, 139.8, 136.5, 135.8, 130.1, 129.0, 128.7, 128.3, 128.2, 127.5, 127.4, 127.2, 67.2, 56.2, 52.7, 51.6, 49.1, 40.8, 38.6, 38.3, 33.2, 28.2, 19.1; MS, m/z 637.1 $(M+Na)^+$.

2-[2-(2-Benzyloxycarbonylamino-3-naphthalen-1-yl-propionylamino)-3-tert-butoxy-propionylamino]-3-(2-oxo-pyrrolidin-3-yl)-propionic acid methyl ester (83).

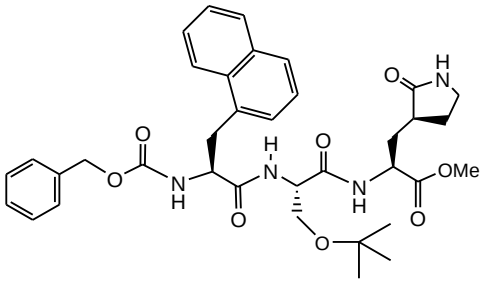

Followed General Procedure A: *N*-Boc-dipeptide **75** was used in place of *N*-Boc-dipeptide **76**, to give compound **83** (69% yield) as a white solid. ^{1}H NMR δ 8.20 (d, *J* = 8.59 Hz, 1H), 7.85 (d, *J* = 8.20 Hz, 1H), 7.76 (d, *J* = 7.81 Hz, 1H), 7.45 - 7.60 (m, 3H), 7.24 - 7.40 (m, 7H), 6.85 (d, *J* = 6.64 Hz, 1H), 6.09 (br. s., 1H), 5.49 (d, *J* = 7.03 Hz, 1H), 5.06 (s, 2H), 4.55 - 4.68 (m, 2H),

4.39 - 4.45 (m, 1H), 3.75 - 3.81 (m, 1H), 3.73 (s, 3H), 3.61 - 3.68 (m, 2H), 3.52 (dd, *J* = 7.42, 14.06 Hz, 1H), 3.17 - 3.31 (m, 2H), 2.29 - 2.41 (m, 2H), 2.12-2.22 (m, 1H), 1.74 - 1.86 (m, 2H), 1.09 (s, 9H); ^{13}C NMR δ 179.5, 171.9, 170.8, 169.9, 156.1, 135.9, 133.9, 132.4, 131.9, 128.8, 128.5, 128.1, 128.0, 127.6, 126.5, 125.8, 125.4, 123.6, 73.8, 67.2, 61.2, 55.8, 53.2, 52.5, 50.8, 40.3, 37.9, 35.5, 33.6, 28.1, 27.2; MS, m/z 683.5 $(M+Na)^+$.

2-[2-(2-Benzyloxycarbonylamino-3-naphthalen-1-yl-propionylamino)-4-methyl-pentanoylamino]-3-(2-oxo-pyrrolidin-3-yl)-propionic acid methyl ester (84).

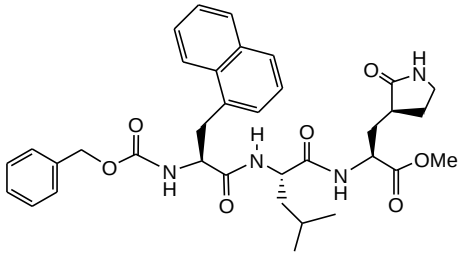

Followed General Procedure A: The *N*-Boc-dipeptide **76** (1 mmol) was dissolved in 10% TFA/CH_2Cl_2 (5 mL) and stirred at 25^{o}C for 4 h. The solvent was removed on a rotary evaporator to yield a sticky oil that was re-dissolved in chloroform followed by removal of the solvent once again on the rotary evaporator to yield a semi-solid material. After sitting under high vacuum for 0.5 h, a white solid (amine intermediate) was obtained in quantitative yield. To this amine intermediate (1 mmol) was added (*S*)-*N*-Cbz-1-naphthylalanine (1 mmol), EDCI (2 mmol) and DMAP (2 mmol) followed by dry CH_2Cl_2 (15 mL) and the resulting solution was stirred at 25^{o}C for 18 h under argon atmosphere. The reaction mixture was partitioned between water (150 mL) and CH_2Cl_2 (150 mL), the aqueous layer was acidified to pH = 2 using 2 N HCl, and extracted three times with CH_2Cl_2 (150 mL each). The combined organic layers were dried (anhydrous $MgSO_4$), filtered, and concentrated to yield a solid which was purified by silica gel chromatography (30:1 CH_2Cl_2:MeOH) to yield compound **84**, 0.5 g (72% yield) as a white solid, mp 119 – 121^{o}C. ^{1}H NMR δ 8.12 (d, *J* = 7.4 Hz, 1H), 8.05 (d, *J* = 5.9 Hz, 1H), 7.80 - 7.85 (m, 1H), 7.72 (d, *J* = 5.5 Hz, 1H), 7.42 - 7.51 (m, 2H), 7.19 - 7.33 (m, 8H), 6.95 (d, *J* = 9.8 Hz, 1H), 5.62 - 5.68 (m, 1H), 4.98 (s, 2H), 4.61 - 4.72 (m, 2H), 4.41 - 4.49 (m, 1H), 3.70 (s, 3H), 3.65 (dd, *J* = 5.5, 14.8 Hz, 1H), 3.39 (dd, *J* = 5.5, 14.5 Hz, 1H), 3.16 - 3.28 (m, 2H), 2.15 - 2.44 (m, 3H), 1.55 - 1.87 (m, 4H), 1.41 - 1.50 (m, 1H), 0.89 (d, *J* = 5.9 Hz, 6H); ^{13}C NMR δ 179.9, 172.7,

172.4, 171.4, 156.3, 136.3, 134.1, 132.9, 132.3, 129.1, 128.7, 128.4, 128.2, 128.0, 127.8, 126.6, 126.0, 125.5, 123.8, 67.2, 55.9, 52.6, 51.9, 51.4, 42.2, 40.8, 38.6, 35.5, 33.3, 28.2, 24.8, 23.1, 22.3; MS, m/z 653.2 $(M+Na)^+$.

2-[2-(2-Benzyloxycarbonylamino-3-naphthalen-1-yl-propionylamino)-3-cyclohexyl-propionylamino]-3-(2-oxo-pyrrolidin-3-yl)-propionic acid methyl ester (85).

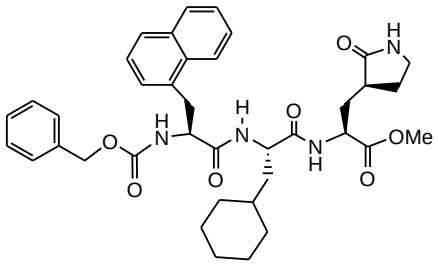

Followed General Procedure A: N-Boc-dipeptide **77** was used in place of *N*-Boc-dipeptide **76**, to give compound **85** (74% yield) as a white solid. ^{1}H NMR δ 8.15 (d, *J* = 7.81 Hz, 1H), 7.83 (d, *J* = 9.37 Hz, 1H), 7.74 (d, *J* = 7.42 Hz, 1H), 7.44 - 7.53 (m, 2H), 7.28 - 7.36 (m, 6H), 7.21 - 7.26 (m, 2H), 6.94 (d, *J* = 6.64 Hz, 1H), 6.44 (br. s., 1H), 5.52 (d, *J* = 7.03 Hz, 1H), 5.01 (br. s., 2H), 4.56 - 4.65 (m, 2H), 4.43 - 4.50 (m, 1H), 3.71 (s, 3H), 3.64 (dd, *J* = 5.66, 14.25 Hz, 1H), 3.39 - 3.47 (m, 1H), 3.22 - 3.29 (m, 2H), 2.30 - 2.42 (m, 2H), 2.11 - 2.20 (m, 1H), 1.97 (br. s., 2H), 1.71 - 1.89 (m, 4H), 1.56 - 1.70 (m, 4H), 1.37 - 1.47 (m, 1H), 1.08 - 1.21 (m, 2H), 0.80 - 0.95 (m, 2H); ^{13}C NMR δ 179.9, 172.7, 172.3, 171.3, 156.2, 136.3, 134.0, 132.9, 132.2, 128.9, 128.6, 128.2, 128.0, 127.9, 127.7, 126.5, 125.8, 125.4, 123.7, 67.0, 55.8, 52.5, 51.3, 51.2, 40.6, 40.5, 38.4, 35.4, 34.0, 33.6, 33.3, 32.8, 28.0, 26.5, 26.3, 26.2; MS, m/z 693.5 $(M+Na)^+$.

2-[2-(2-Benzyloxycarbonylamino-3-naphthalen-1-yl-propionylamino)-4-methyl-pentanoylamino]-3-(2-oxo-pyrrolidin-3-yl)-propionic acid methyl ester (87).

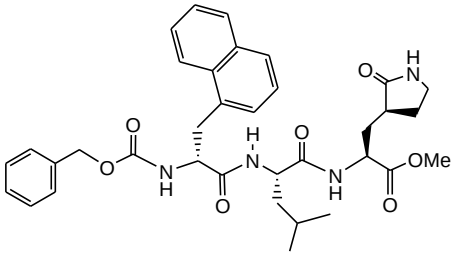

Followed General Procedure A: (*R*)-*N*-Cbz-1-naphthylalanine was used in place of (*S*)-*N*-Cbz-1-naphthylalanine, to give compound **87** (83% yield) as a white solid, mp 195 – 197^{o}C. ^{1}H NMR δ 8.18 (d, *J* = 7.8 Hz, 1H), 8.04 (d, *J* = 6.3 Hz, 1H), 7.82 (d, *J* = 9.0 Hz, 1H), 7.72 (d, *J* = 7.4 Hz, 1H), 7.43 - 7.54 (m, 3H), 7.27 - 7.36 (m, 6H), 6.34 (br. s., 1H), 6.17 (br. s., 1H), 6.03 (d, *J* = 7.8 Hz, 1H), 5.00 (s, 2H), 4.58 - 4.66 (m, 1H), 4.47 - 4.54 (m, 1H), 4.30 - 4.38 (m, 1H), 3.64 - 3.69 (s, 3H), 3.53 (d, *J* = 5.9 Hz, 2H), 3.09 - 3.21 (m, 2H), 2.28 (br. s., 2H), 2.04 - 2.14 (m, 1H), 1.66 - 1.84 (m, 2H), 1.41 - 1.51 (m, 1H), 1.17 - 1.28 (m, 1H), 1.05 - 1.15 (m, 1H), 0.79 (s, 6H); ^{13}C NMR δ 179.9, 172.6, 172.2, 171.0, 156.2, 136.5, 134.1, 133.0, 132.3, 129.0, 128.7, 128.4, 128.3, 128.1, 128.0, 126.7, 126.0, 125.7, 123.9, 67.15, 56.4, 52.5, 51.9, 51.7, 41.5, 40.7, 38.8, 36.2, 32.9, 28.5, 24.5, 23.0, 22.1; MS, m/z 653.1 $(M+Na)^{+}$.

2-[2-(2-Benzyloxycarbonylamino-3-phenyl-propionylamino)-4-methyl-pentanoylamino]-3-(2-oxo-pyrrolidin-3-yl)-propionic acid methyl ester (88).

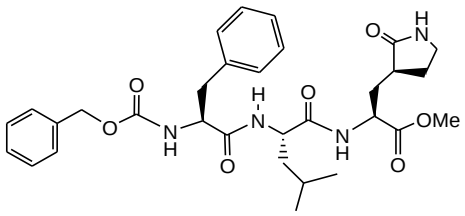

Followed General Procedure A: (*S*)-*N*-Cbz-phenylalanine was used in place of (*S*)-*N*-Cbz-1-naphthylalanine, and furnished compound **8** (87% yield) as a white solid, mp 71 – 73^{o}C. ^{1}H NMR δ 7.96 (d, *J* = 5.9 Hz, 1H), 7.05 - 7.36 (m, 11H), 6.81 (br. s., 1H), 5.47 (d, *J* = 7.8 Hz, 1H), 4.99 - 5.08 (m, 2H), 4.63 - 4.71 (m, 1H), 4.42 - 4.53 (m, 2H), 3.70 (s, 3H), 3.17 - 3.33 (m, 2H), 2.97 - 3.14 (m, 2H), 2.17 - 2.42 (m, 3H), 1.73 - 1.89 (m, 2H), 1.55 - 1.70 (m, 2H), 1.43 - 1.51 (m, 1H), 0.90 (d, *J* = 5.9 Hz, 6H, 2 x CH_3); ^{13}C NMR δ 179.9, 172.7, 172.3, 171.1, 156.2, 136.6,

136.4, 129.6, 128.8, 128.4, 128.2, 127.1, 67.3, 56.2, 52.6, 51.8, 51.4, 42.2, 40.7, 38.6, 38.4, 33.2, 28.2, 24.8, 23.1, 22.3; MS, m/z 603.2 $(M+Na)^+$.

2-[2-(2-Benzyloxycarbonylamino-3-tert-butoxy-butyrylamino)-4-methyl-pentanoylamino]-3-(2-oxo-pyrrolidin-3-yl)-propionic acid methyl ester (89).

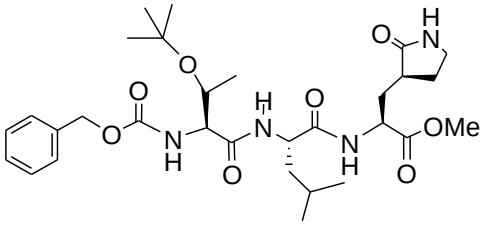

Followed General Procedure A: (*S*)-*N*-Cbz-*O*-t-butyl-threonine was used in place of (*S*)-*N*-Cbz-1-napthylalanine, to give compound **89** (43% yield) as a white solid. ^{1}H NMR δ 7.76 (d, *J* = 5.86 Hz, 1H), 7.48 (d, *J* = 7.81 Hz, 1H), 7.29 - 7.37 (m, 5H), 6.42 (br. s., 1H), 5.90 (d, *J* = 4.69 Hz, 1H), 5.03 - 5.16 (m, 2H), 4.45 - 4.55 (m, 2H), 4.14 - 4.19 (m, 1H), 3.70 (s, 3H), 3.22 - 3.33 (m, 3H), 2.30 - 2.42 (m, 3H), 2.14 - 2.24 (m, 1H), 1.97 - 2.02 (m, 1H), 1.75 - 1.89 (m, 2H), 1.64 - 1.73 (m, 3H), 1.48 - 1.58 (m, 1H), 1.25 (s, 9H), 1.05 (d, *J* = 5.86 Hz, 3H), 0.89 - 0.97 (m, 6H); ^{13}C NMR δ 179.8, 172.4, 172.4, 169.7, 156.4, 136.4, 128.8, 128.4, 128.3, 75.6, 67.2, 67.0, 59.1, 52.6, 52.1, 51.3, 42.0, 40.7, 38.4, 33.2, 28.4, 25.0, 23.1, 22.4, 17.4; MS, m/z 613.2 $(M+Na)^+$.

2-[2-(2-Benzyloxycarbonylamino-3-naphthalen-2-yl-propionylamino)-4-methyl-pentanoylamino]-3-(2-oxo-pyrrolidin-3-yl)-propionic acid methyl ester (90).

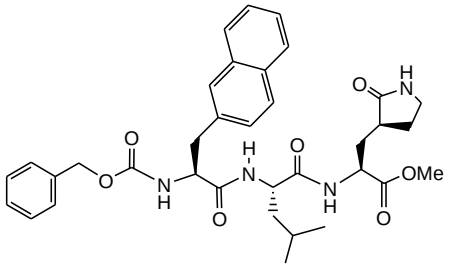

Followed General Procedure A: (*S*)-*N*-Cbz-2-naphthylalanine was used in place of (*S*)-*N*-Cbz-1-naphthylalanine, to give compound **90** (54% yield) as a white solid, mp 98 – 101^{o}C. ^{1}H NMR δ 8.10 (br. s., 1H), 7.73 - 7.78 (m, 1H), 7.66 - 7.72 (m, 2H), 7.59 (s, 2H), 7.39 - 7.44 (m, 3H), 7.17

- 7.30 (m, 5H), 6.85 (br. s., 1H), 5.61 (br. s., 1H), 4.95 - 5.07 (m, 2H), 4.68 - 4.75 (m, 1H), 4.61 - 4.67 (m, 1H), 4.41 - 4.48 (m, 1H), 3.69 (s, 3H), 3.25 - 3.31 (m, 1H), 3.18 (t, *J* = 8.0 Hz, 2H), 3.01 - 3.10 (m, 1H), 2.30 - 2.41 (m, 1H), 2.16 - 2.26 (m, 2H), 1.78 - 1.86 (m, 1H), 1.55 - 1.75 (m, 3H), 1.44 - 1.53 (m, 1H), 0.89 (d, *J* = 6.3 Hz, 3H, CH_3), 0.87 (d, *J* = 6.3 Hz, 3H, CH_3); ^{13}C NMR δ 179.9, 172.9, 172.3, 171.2, 156.3, 136.4, 134.2, 133.6, 132.6, 128.7, 128.4, 128.3, 128.1, 127.9, 127.7, 126.3, 125.9, 67.2, 56.1, 52.6, 51.9, 51.5, 42.2, 40.7, 38.6, 33.1, 28.2, 24.8, 23.0, 22.3; MS, m/z 653.3 $(M+Na)^+$.

2-[2-(2-Benzyloxycarbonylamino-3-biphenyl-4-yl-propionylamino)-4-methyl-pentanoylamino]-3-(2-oxo-pyrrolidin-3-yl)-propionic acid methyl ester (91).

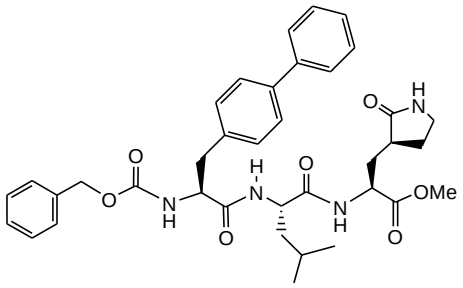

Followed General Procedure A: (*S*)-*N*-Cbz-biphenylalanine was used in place of (*S*)-*N*-Cbz-1-napthylalanine, to give compound **91** (73% yield) as a white solid, mp 95 – 98°C. ^{1}H NMR δ 8.03 (d, *J* = 5.5 Hz, 1H), 7.53 (d, *J* = 7.4 Hz, 2H), 7.39 - 7.48 (m, 4H), 7.25 - 7.35 (m, 6H), 7.19 - 7.24 (d, *J* = 8.1 Hz, 2H), 6.96 (br. s., 1H), 6.56 (br. s., 1H), 5.46 (d, *J* = 7.4 Hz, 1H), 5.01 - 5.11 (m, 2H), 4.60 - 4.68 (m, 1H), 4.48 - 4.56 (m, 1H), 4.39 - 4.47 (m, 1H), 3.69 (s, 3H), 3.05 - 3.29 (m, 4H), 2.33 - 2.40 (m, 1H), 2.14 - 2.31 (m, 2H), 1.98 (br. s., 1H), 1.79 - 1.89 (m, 1H), 1.71 - 1.78 (m, 1H), 1.55 - 1.70 (m, 2H), 1.45 - 1.54 (m, 1H), 0.91 (d, *J* = 6.2 Hz, 3H, CH_3), 0.90 (d, *J* = 6.2 Hz, 3H, CH_3); ^{13}C NMR δ 179.9, 172.7, 172.3, 171.0, 156.3, 140.8, 140.0, 136.3, 135.6, 130.0, 129.0, 128.8, 128.4, 128.2, 127.5, 127.4, 127.1, 67.3, 56.2, 52.6, 51.9, 51.7, 42.2, 40.7, 38.7, 37.9, 33.1, 28.4, 24.8, 23.1, 22.3; MS, m/z 679.4 $(M+Na)^+$.

2-Benzyloxycarbonylamino-3-biphenyl-4-yl-propionic acid (91a).

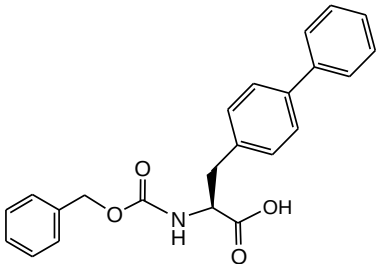

N-Boc-biphenylalanine (1.17 mmol) was dissolved in 20% TFA/CH_2Cl_2 (10 mL) and stirred at 25^oC for 2 h. The solvent was removed and remaining residue was placed under high vacuum to yield the amine intermediate as a sticky solid. The amine was immediately dissolved in (1:1) water/dioxane (20 mL) and treated with $NaHCO_3$ (3.51 mmol) and benzylchloroformate (1.4 mmol) followed by stirring at 25^oC for 3 h. The reaction was combined with water (200 mL) and basified to pH 10 using aq. NaOH followed by extraction with ether (100 mL). The aqueous layer was acidified to pH 2 using aq. HCl and then extracted three times with CH_2Cl_2 (100 mL each). The combined CH_2Cl_2 layers were dried (anhydrous Na_2SO_4), filtered, and concentrated using a rotary evaporator to yield a solid which was recrystallized from ether/hexane (two crops) to give compound **91a**,[9] 395 mg (90% yield) as a white solid. ^1H NMR δ 7.52 - 7.55 (m, 2H), 7.49 (d, *J* = 7.8 Hz, 2H), 7.40 - 7.45 (m, 2H), 7.36 (br. s., 1H), 7.31 - 7.35 (m, 5H), 7.19 (d, *J* = 8.2 Hz, 2H), 5.15 (d, *J* = 8.2 Hz, 1H), 5.10 (d, *J* = 2.3 Hz, 2H), 4.65 - 4.71 (m, 1H), 3.06 - 3.18 (m, 2H); ^{13}C NMR δ 176.3, 156.2, 140.8, 140.2, 136.2, 134.8, 131.2, 129.9, 128.9, 128.7, 128.4, 128.3, 127.5, 127.2, 67.4, 54.9, 37.5; MS, m/z 398.0 $(M+Na)^+$.

[2-Hydroxy-1-(2-oxo-pyrrolidin-3-ylmethyl)-2-thiazol-2-yl-ethyl]-carbamic acid tert-butyl ester (92).

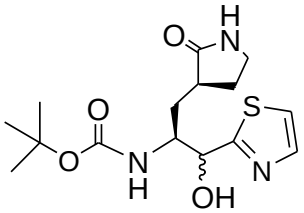

n-BuLi (4.68 mmol) was added drop wise to a solution of thiazole (4.68 mmol) in dry THF (15 mL) at -78^oC and stirred for 2 h. A solution of aldehyde **53a** (1.17 mmol) in dry THF (15 mL) was then added drop wise over 30 min and the resulting mixture was stirred at -78^oC for 3 h. The reaction was quenched with aq. NH_4Cl (15 mL) and slowly warmed to 0^oC. Brine water (30 mL)

and CH_2Cl_2 (20 mL) were added and the organic layer was removed. The aqueous layer was extracted with CH_2Cl_2 (20 mL x 5) and the combined organic layers were dried ($MgSO_4$), filtered and concentrated to give a yellow solid which was purified by silica gel column chromatography (9:1 CH_2Cl_2:MeOH) to separate two diastereomers of compound **92** (combined total = 142 mg, 36%) as yellow solids. (less polar isomer) ^{1}H NMR δ 7.75 (d, *J* = 3.51 Hz, 1H), 7.31 (d, *J* = 3.51 Hz, 1H), 6.12 (br. s., 1H), 5.97 (d, *J* = 7.42 Hz, 1H), 5.32 - 5.37 (m, 1H), 5.06 - 5.10 (m, 1H), 4.10 - 4.18 (m, 1H), 3.29 - 3.35 (m, 2H), 2.37 - 2.53 (m, 2H), 2.10 - 2.19 (m, 1H), 1.92 - 1.96 (m, 1H), 1.73 - 1.84 (m, 1H), 1.44 (s, 9H); MS, m/z 363.7 $(M+Na)^+$; (more polar isomer) ^{1}H NMR δ 7.75 (d, *J* = 3.12 Hz, 1H), 7.30 (d, *J* = 3.12 Hz, 1H), 6.16 (br. s., 1H), 5.60 (d, *J* = 8.98 Hz, 1H), 5.40 (br. s., 1H), 5.08 (br. s., 1H), 4.12 - 4.21 (m, 1H), 3.30 - 3.41 (m, 2H), 2.50 - 2.62 (m, 1H), 2.37 - 2.49 (m, 1H), 1.99 - 2.11 (m, 1H), 1.81 - 1.97 (m, 1H), 1.67 - 1.77 (m, 1H), 1.37 (s, 9H); MS, m/z 363.9 $(M+Na)^+$.

[2-Oxo-1-(2-oxo-pyrrolidin-3-ylmethyl)-2-thiazol-2-yl-ethyl]-carbamic acid tert-butyl ester (93).

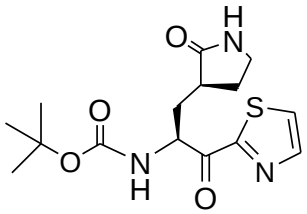

To a solution of **92** (0.19 mmol) in CH_2Cl_2 (2 mL) was added DMP (0.38 mmol). The reaction was stirred at 25^{o}C for 2 h after which the reaction was diluted with CH_2Cl_2 (15 mL) and water (15 mL). The organic layer was removed and the aqueous layer was extracted with CH_2Cl_2 (15 mL x 4), combined organic layers were dried ($MgSO_4$), filtered and concentrated to give a solid that was purified by silica gel column chromatography (30:1 EtOAc:MeOH) to give compound **93** (52 mg, 80%) as a white solid. ^{1}H NMR δ 8.03 (d, *J* = 3.12 Hz, 1H), 7.71 (d, *J* = 3.12 Hz, 1H), 6.07 (br. s., 1H), 5.79 (d, *J* = 8.59 Hz, 1H), 5.41 - 5.49 (m, 1H), 3.34 - 3.40 (m, 2H), 2.55 - 2.67 (m, 2H), 1.99 - 2.14 (m, 3H), 1.44 (s, 9H); ^{13}C NMR δ 191.8, 179.9, 164.7, 156.0, 145.3, 127.0, 80.1, 55.5, 40.6, 38.6, 34.9, 28.5, 28.2; MS, m/z 362.2 $(M+Na)^+$.

{3-Methyl-1-[2-oxo-1-(2-oxo-pyrrolidin-3-ylmethyl)-2-thiazol-2-yl-ethylcarbamoyl]-butyl}-carbamic acid tert-butyl ester (94).

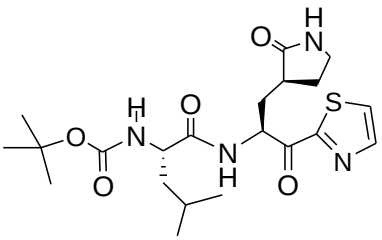

Followed General Procedure A: Compound **93** was used in place of *N*-Boc-dipeptide **76**, to give compound **94** (31 mg, 55% yield) as a white solid. ^{1}H NMR δ 8.03 (d, *J* = 3.12 Hz, 1H), 7.87 - 7.91 (m, 1H), 7.71 (d, *J* = 3.12 Hz, 1H), 6.03 - 6.08 (m, 1H), 5.59 - 5.67 (m, 1H), 4.98 - 5.04 (m, 1H), 4.20 - 4.28 (m, 1H), 3.29 - 3.41 (m, 2H), 2.50 - 2.64 (m, 2H), 1.97 - 2.21 (m, 3H), 1.63 - 1.70 (m, 3H), 1.44 (s, 9H), 0.93 - 0.99 (m, 6H); ^{13}C NMR δ 190.8, 179.9, 173.2, 164.8, 155.7, 145.1, 127.0, 80.0, 54.7, 53.2, 42.4, 40.7, 38.9, 34.0, 28.6, 28.5, 24.9, 23.2, 22.3; MS, m/z 475.2 $(M+Na)^{+}$.

[2-Hydroxy-3-methyl-1-(2-oxo-pyrrolidin-3-ylmethyl)-but-3-enyl]-carbamic acid tert-butyl ester (95).

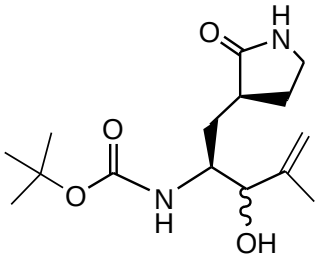

$CrCl_3$ was suspended in dry THF (4 mL) under argon and cooled to 0^{o}C. $LiEt_3BH$ was added drop wise and after stirring at 0^{o}C for 45 min the stirring was stopped and the solid contents was allowed to settle to the bottom. The supernatant was carefully syringed out and the remaining solid was suspended in dry DMF (2 mL). To the suspension was added drop wise a solution of aldehyde **53a** (0.16 mmol), 2-bromopropene (0.31 mmol) and $NiCl_2$ (0.008 mmol) followed by stirring at 25^{o}C for 1 h. The reaction was partitioned between brine (15 mL) and CH_2Cl_2 (15 mL), organic layer removed and aqueous layer was extracted with CH_2Cl_2 (15 mL x 6). The combined organic layers were dried (Na_2SO_4), filtered and concentrated to yield a green residue that was purified by silica gel column chromatography (5:1 EtOAc:MeOH) to yield compound **95** (18 mg, 39%) as a clear oil. ^{1}H NMR δ 5.04 - 6.08 (m, 2H), 5.27 - 5.34 (m, 1H), 5.00 - 5.12 (m, 3H), 4.90 - 4.97 (m, 2H), 4.12 - 4.16 (m, 1H), 3.92 - 3.99 (m, 1H), 3.75 - 3.84 (m, 2H), 3.28 -

3.37 (m, 4H), 3.21 (d, *J* = 3.12 Hz, 1H), 2.83 (br. s., 1H), 2.41 - 2.52 (m, 2H), 1.90 - 2.10 (m, 4H), 1.78 - 1.85 (m, 4H), 1.76 (s, 6H), 1.42 (s, 18H); MS, m/z 321.0 $(M+Na)^+$.

[2-(2-Methyl-oxiranyl)-2-oxo-1-(2-oxo-pyrrolidin-3-ylmethyl)-ethyl]-carbamic acid tert-butyl ester (96).

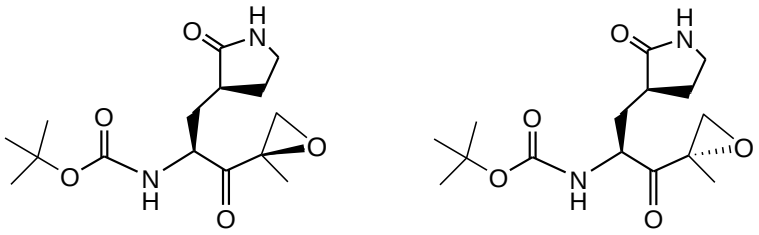

$NaHCO_3$ (3.6 mmol) and *m*-CPBA (1.2 mmol) were added to a solution of alkene **95** (0.6 mmol) in CH_2Cl_2 (10 mL) at 0^oC and stirred at 0^oC for 2 h. The reaction was partitioned between CH_2Cl_2 (20 mL) and 10% aq. Sodium thiosulfate (20 mL). The organic layer was removed and the aqueous layer was extracted with CH_2Cl_2 (20 mL x 6), the combined organic layers were dried (Na_2SO_4), filtered and concentrated to give a mixture of epoxy-alcohol intermediates. To a solution of epoxy-alcohols (0.61 mmol) in CH_2Cl_2 (5 mL) was added DMP (1.2 mmol). The reaction was stirred at 25^oC for 2 h after which the reaction was diluted with CH_2Cl_2 (15 mL) and filtered through a plug of celite. The filtrate was concentrated to give a solid that was purified by silica gel column chromatography (1:1 CH_2Cl_2:Acetone) to give compound two diastereomers (1:1) of **96** (104 mg, 55%) as white solids. (more polar isomer: **96-mp**) ^1H NMR δ 6.22 (br. s., 1H), 5.55 (d, *J* = 8.20 Hz, 1H), 4.21 - 4.29 (m, 1H), 3.29 - 3.41 (m, 2H), 3.24 (d, *J* = 5.08 Hz, 1H), 2.90 (d, *J* = 4.69 Hz, 1H), 2.40 - 2.54 (m, 2H), 1.88 - 1.99 (m, 1H), 1.73 - 1.81 (m, 2H), 1.52 (s, 3H), 1.40 (s, 9H); ^{13}C NMR δ 208.1, 179.9, 156.1, 80.0, 59.3, 52.7, 52.0, 40.5, 38.5, 33.2, 28.5, 28.0, 17.0; MS, m/z 335.0 $(M+Na)^+$. (less polar isomer: **96-lp**) ^1H NMR δ 6.07 (br. s., 1H), 5.52 (s, 1H), 4.56 - 4.65 (m, 1H), 3.28 - 3.39 (m, 2H), 3.09 (d, *J* = 5.08 Hz, 1H), 2.85 (d, *J* = 5.08 Hz, 1H), 2.37 - 2.52 (m, 2H), 1.94 - 2.02 (m, 1H), 1.79 - 1.87 (m, 1H), 1.62 - 1.69 (m, 1H), 1.55 (s, 3H), 1.43 (s, 9H); ^{13}C NMR δ 207.0, 179.7, 155.6, 80.2, 59.5, 53.4, 52.9, 40.5, 38.0, 33.3, 28.6, 28.5, 18.0; MS, m/z 335.1 $(M+Na)^+$.

{3-Methyl-1-[2-(2-methyl-oxiranyl)-2-oxo-1-(2-oxo-pyrrolidin-3-ylmethyl)-ethylcarbamoyl]-butyl}-carbamic acid tert-butyl ester (97-lp).

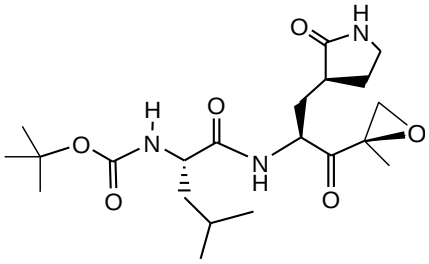

Followed General Procedure A: Compound **96-lp** was used in place of *N*-Boc-dipeptide **76**, to give compound **97-lp** (51% yield) as a white solid. ^{1}H NMR δ 7.91 (br. s., 1H), 6.24 (br. s., 1H), 4.95 (d, *J* = 7.81 Hz, 1H), 4.38 - 4.46 (m, 1H), 4.16 - 4.26 (m, 1H), 3.28 - 3.41 (m, 3H), 2.91 (d, *J* = 5.08 Hz, 1H), 2.36 - 2.51 (m, 1H), 1.76 - 1.97 (m, 3H), 1.71 (br. s., 2H), 1.57 - 1.66 (m, 2H), 1.51 (s, 3H), 1.43 (s, 9H), 0.91 - 0.98 (m, 6H); ^{13}C NMR δ 207.0, 179.9, 173.5, 155.7, 80.0, 59.6, 52.9, 52.8, 51.4, 42.6, 40.7, 39.0, 32.1, 28.5, 24.8, 23.1, 22.3, 17.0; MS, m/z 448.1 $(M+Na)^{+}$.

{3-Methyl-1-[2-(2-methyl-oxiranyl)-2-oxo-1-(2-oxo-pyrrolidin-3-ylmethyl)-ethylcarbamoyl]-butyl}-carbamic acid tert-butyl ester (97-mp).

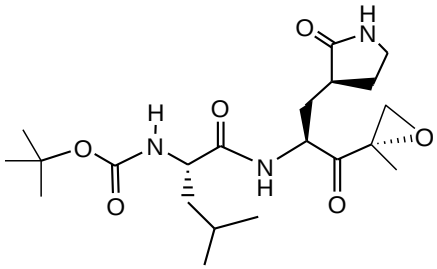

Followed General Procedure A: Compound **96-mp** was used in place of *N*-Boc-dipeptide **76**, to give compound **97-mp** (47% yield) as a white solid. ^{1}H NMR δ 7.78 (d, *J* = 5.86 Hz, 1H), 6.19 (br. s., 1H), 5.00 (d, *J* = 7.81 Hz, 1H), 4.75 - 4.82 (m, 1H), 4.13 - 4.21 (m, 1H), 3.26 - 3.38 (m, 2H), 3.02 (d, *J* = 4.69 Hz, 1H), 2.82 - 2.86 (m, 1H), 2.37 - 2.48 (m, 2H), 1.96 - 2.07 (m, 2H), 1.76 - 1.88 (m, 2H), 1.59 - 1.73 (m, 2H), 1.57 (s, 3H), 1.43 (s, 9H), 0.95 (d, *J* = 6.25 Hz, 6H); ^{13}C NMR δ 206.2, 180.0, 173.0, 155.7, 80.1, 59.9, 53.1, 53.0, 52.7, 42.0, 40.7, 38.4, 32.5, 28.9, 28.5, 24.9, 23.2, 22.2, 18.0; MS, m/z 448.0 $(M+Na)^{+}$.

2-[2-(2-Amino-3-naphthalen-1-yl-propionylamino)-4-methyl-pentanoylamino]-3-(2-oxo-pyrrolidin-3-yl)-propionic acid methyl ester (98).

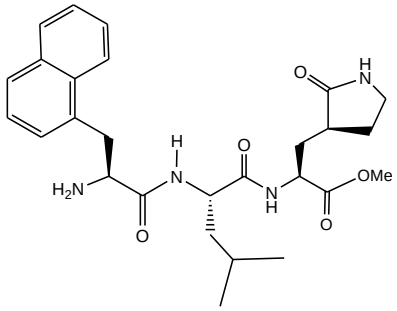

Palladium (on carbon) (10 mg) was added to a solution of **84** (0.16 mmol) in MeOH (2 mL) and the flask was flushed with hydrogen gas (1 atm). The reaction was stirred for 3 h at 25^{o}C. The reaction was filtered through a layer of celite and the filtrate was concentrated to yield compound **98** (80 mg, 100%) as a white solid. ^{1}H NMR δ 8.22 (d, *J* = 7.81 Hz, 1H), 8.17 (d, *J* = 5.86 Hz, 1H), 7.87 (d, *J* = 7.42 Hz, 1H), 7.78 (d, *J* = 8.20 Hz, 1H), 7.47 - 7.57 (m, 2H), 7.31 - 7.44 (m, 3H), 6.34 - 6.61 (m, 1H), 4.68 - 4.75 (m, 1H), 4.34 - 4.44 (m, 1H), 3.92 - 4.00 (dd, *J* = 2.73, 11.15 Hz, 1H), 3.82 (dd, *J* = 2.73, 10.15 Hz, 1H), 3.72 (s, 3H), 3.24 - 3.39 (m, 2H), 2.85 (dd, *J* = 10.35, 13.86 Hz, 1H), 2.30 - 2.44 (m, 2H), 2.14 - 2.26 (m, 1H), 1.68 - 1.92 (m, 4H), 1.54 - 1.63 (m, 1H), 0.91 - 1.03 (m, 6H); ^{13}C NMR δ 179.8, 174.8, 173.2, 134.2, 134.2, 132.0, 129.0, 127.9, 127.6, 126.4, 126.0, 125.5, 124.0, 55.9, 52.5, 51.8, 51.1, 42.2, 40.7, 38.7, 38.6, 32.9, 28.3, 24.9, 23.1, 22.3.

2-[4-Methyl-2-(2-{2-[methyl-(4-methyl-2-oxo-2H-chromen-7-yl)-amino]-acetylamino}-3-naphthalen-1-yl-propionylamino)-pentanoylamino]-3-(2-oxo-pyrrolidin-3-yl)-propionic acid methyl ester (99).

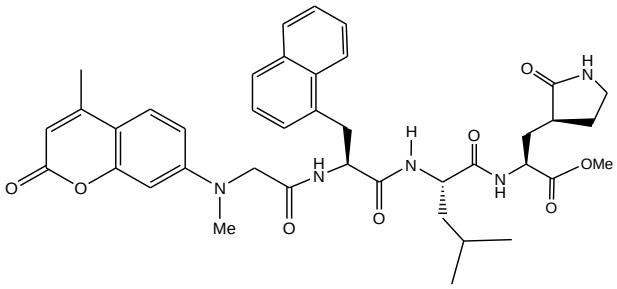

Followed General Procedure E: The amine **98** was used in place of **53** and the acid **104** was used in place of *N*-Boc-leucine, to give compound **99** (36 mg, 62% yield) as a yellow solid. ^{1}H NMR δ 8.06 (d, *J* = 7.01 Hz, 1H), 7.94 (d, *J* = 7.03 Hz, 1H), 7.76 (dd, *J* = 2.93, 6.44 Hz, 1H), 7.60 - 7.64 (m, 1H), 7.41 - 7.48 (m, 2H), 7.17 - 7.25 (m, 3H), 7.06 (d, *J* = 8.20 Hz, 1H), 6.78 (d, *J* = 7.03 Hz, 1H), 6.37 (d, *J* = 2.34 Hz, 1H), 6.30 (dd, *J* = 2.34, 8.98 Hz, 1H), 6.27 (s, 1H), 6.04

(s, 1H), 4.76 - 4.84 (m, 1H), 4.47 - 4.60 (m, 2H), 3.86 - 3.92 (m, 2H), 3.72 (s, 3H), 3.63 (dd, *J* = 5.86, 14.45 Hz, 1H), 3.38 (dd, *J* = 8.98, 14.45 Hz, 1H), 3.27 - 3.33 (m, 2H), 2.76 (s, 3H), 2.36 - 2.47 (m, 1H), 2.34 (s, 3H), 2.09 - 2.19 (m, 1H), 1.85 - 1.93 (m, 1H), 1.76 - 1.85 (m, 1H), 1.66 - 1.75 (m, 1H), 1.53 - 1.63 (m, 1H), 1.39 - 1.48 (m, 1H), 0.90 (d, *J* = 6.25 Hz, 6H); ^{13}C NMR δ 180.0, 172.4, 172.3, 170.8, 170.2, 161.8, 155.5, 152.8, 151.6, 134.0, 132.5, 132.2, 129.1, 128.1, 127.7, 126.7, 126.0, 125.8, 125.4, 123.5, 111.4, 110.8, 109.1, 99.5, 57.5, 54.4, 52.6, 52.2, 51.7, 41.8, 40.7, 39.6, 38.7, 34.2, 33.3, 28.7, 25.0, 23.2, 22.2, 18.7; MS, m/z 748.2 $(M+Na)^+$.

2-(4-Methyl-2-{2-[(2-methyl-thiazole-5-carbonyl)-amino]-3-naphthalen-1-yl-propionylamino}-pentanoylamino)-3-(2-oxo-pyrrolidin-3-yl)-propionic acid methyl ester (100).

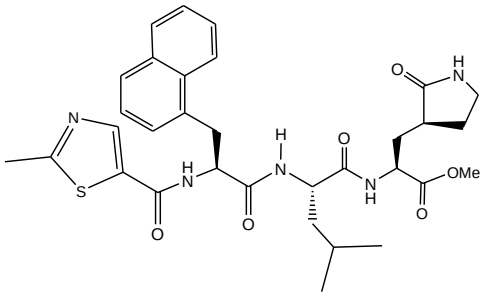

Followed General Procedure E: The amine **98** was used in place of **53** and 2-methyl-thiazole-5-carboxylic acid was used in place of *N*-Boc-leucine, to give compound **100** (37 mg, 74% yield) as a white solid. ^{1}H NMR δ 8.17 (d, *J* = 8.20 Hz, 1H), 7.92 (d, *J* = 7.42 Hz, 1H), 7.83 (s, 1H), 7.79 (d, *J* = 7.81 Hz, 1H), 7.70 (d, *J* = 7.81 Hz, 1H), 7.27 - 7.51 (m, 6H), 6.59 (br. s., 1H), 4.98 - 5.05 (m, 1H), 4.48 - 4.58 (m, 2H), 3.72 (s, 3H), 3.59 - 3.63 (m, 2H), 3.21 - 3.32 (m, 2H), 2.60 (s, 3H), 2.33 - 2.44 (m, 1H), 2.10 - 2.20 (m, 1H), 1.96 (br. s., 1H), 1.84 - 1.92 (m, 1H), 1.76 - 1.83 (m, 1H), 1.62 - 1.71 (m, 1H), 1.53 - 1.61 (m, 1H), 1.42 - 1.50 (m, 1H), 0.85 (d, *J* = 6.25 Hz, 6H); ^{13}C NMR δ 180.0, 172.5, 172.3, 171.3, 170.7, 160.9, 143.5, 134.1, 133.8, 132.8, 132.2, 129.1, 128.1, 127.8, 126.7, 126.0, 125.6, 123.7, 54.7, 52.6, 52.5, 51.5, 41.7, 40.8, 38.7, 35.0, 33.6, 29.9, 28.4, 24.9, 23.0, 22.2, 19.6; MS, m/z 644.2 $(M+Na)^+$.

(4-Methyl-2-oxo-2H-chromen-7-ylamino)-acetic acid methyl ester (102).

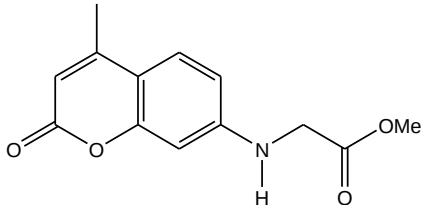

A solution containing 7-amino-4-methylcoumarin **101** (0.57 mmol), NaI (0.57 mmol), methylbromoacetate (0.63 mmol) and DIPEA (0.63 mmol) in dry acetonitrile (6 mL) was heated at 82^{o}C for 18 h. The reaction was filtered and the filtrate was concentrated to give an oil that was purified by silica gel column chromatography (15:1 CH_2Cl_2:MeOH) to afford compound **102** (120 mg, 85%) as a yellow solid. ^{1}H NMR δ 7.39 (d, *J* = 8.98 Hz, 1H), 6.56 (dd, *J* = 2.34, 8.98 Hz, 1H), 6.42 (d, *J* = 2.34 Hz, 1H), 6.02 (s, 1H), 4.78 - 4.84 (m, 1H), 3.97 (d, *J* = 5.08 Hz, 2H), 3.82 (s, 3H), 2.35 (s, 3H); ^{13}C NMR δ 170.8, 161.9, 156.0, 153.0, 150.3, 125.9, 111.6, 110.8, 110.4, 98.7, 52.8, 45.1, 18.8; MS, m/z 270.1 $(M+Na)^{+}$.

[Methyl-(4-methyl-2-oxo-2H-chromen-7-yl)-amino]-acetic acid methyl ester (103).

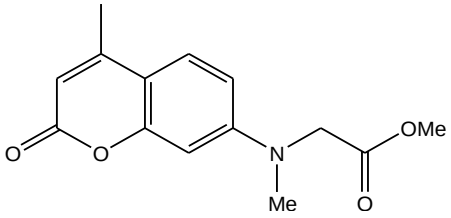

Methyl iodide (0.73 mmol) and K_2CO_3 (0.98 mmol) were added to a solution of **102** (0.49 mmol) in dry acetonitrile (5 mL) and refluxed at 82^{o}C for 18 h. The reaction was filtered and partitioned between CH_2Cl_2 (20 mL) and water (20 mL). The organic layer was removed and the aqueous layer was extracted with CH_2Cl_2 (20 mL x 3), the combined organic layers were dried ($MgSO_4$), filtered and concentrated to give a yellow oil that was purified by silica gel chromatography (15:1 CH_2Cl_2:MeOH) to yield compound **103** (31 mg, 24%) as a yellow solid. ^{1}H NMR δ 7.43 (d, *J* = 8.83 Hz, 1H), 6.61 (dd, *J* = 2.54, 8.83 Hz, 1H), 6.53 (d, *J* = 2.54 Hz, 1H), 6.02 (s, 1H), 4.15 (s, 2H), 3.76 (s, 3H), 3.15 (s, 3H); ^{13}C NMR δ 170.6, 162.0, 155.8, 152.9, 151.9, 125.7, 110.9, 110.3, 109.0, 99.1, 54.2, 52.5, 39.9, 18.7; MS, m/z 284.0 $(M+Na)^{+}$.

[Methyl-(4-methyl-2-oxo-2H-chromen-7-yl)-amino]-acetic acid (104).

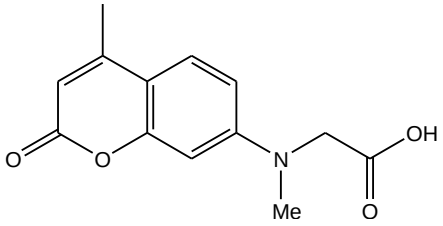

The ester **103** (0.08 mmol) was dissolved in 1:1 dioxane:water (1 mL) and treated with 2N NaOH (0.12 mL). After stirring at 25°C for 1 h the reaction was partitioned between water (20 mL) and CH_2Cl_2 (20 mL) then acidified to pH 2 using aq. HCl. The aqueous layer was extracted with CH_2Cl_2 (15 mL x 3), the combined CH_2Cl_2 layers were dried (Na_2SO_4), filtered and concentrated to yield compound **104** (20 mg, 100%) as a yellow solid. ^{1}H NMR δ 8.58 (br. s., 1H), 7.42 (d, *J* = 8.98 Hz, 1H), 6.62 (d, *J* = 8.98 Hz, 1H), 6.51 (s, 1H), 6.01 (s, 1H), 4.16 (s, 2H), 3.13 (s, 3H), 2.34 (s, 3H); ^{13}C NMR δ 174.4, 162.7, 155.6, 153.5, 151.9, 125.8, 110.9, 110.0, 109.2, 99.0, 61.4, 39.9, 18.7; MS, m/z 270.0 $(M+Na)^+$.

14-tert-Butoxycarbonylamino-2-isobutyl-3,8,15-trioxo-1,4,9triaza-cyclopentadec-11-ene-5-carboxylic acid methyl ester (106).

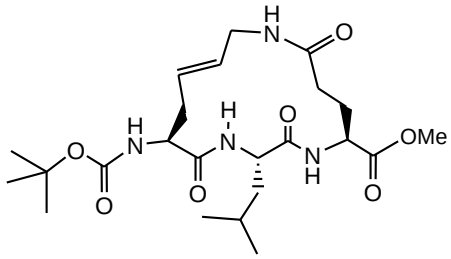

Grubbs second generation catalyst (0.098 mmol) was added to a degassed solution of diene **105** (0.98 mmol) in CH_2Cl_2. The resulting pink solution was heated at 40°C for 48 h. The reaction was filtered through a layer of celite and the filtrate was concentrated to give a solid that was purified by silica gel column chromatography (15:1 CH_2Cl_2:MeOH) to yield compound **106** (269 mg, 57%) as a white solid. ^{1}H NMR δ 7.16 (d, *J* = 8.20 Hz, 1H), 7.06 (d, *J* = 7.81 Hz, 1H), 6.55 (br. s., 1H), 5.43 - 5.59 (m, 3H), 4.58 - 4.66 (m, 1H), 4.51 - 4.57 (m, 1H), 4.37 - 4.44 (m, 1H), 3.84 - 3.92 (m, 1H), 3.73 (s, 3H), 3.49 - 3.57 (m, 1H), 2.44 - 2.52 (m, 2H), 2.33 - 2.42 (m, 2H), 1.80 - 2.05 (m, 2H), 1.53 - 1.75 (m, 2H), 1.43 (s, 9H), 1.23 - 1.28 (m, 1H), 0.87 - 0.97 (m, 6H); ^{13}C NMR δ 172.8, 172.6, 171.6, 171.2, 155.3, 131.1, 126.4, 80.1, 54.4, 52.6, 52.0, 51.8, 42.2, 41.0, 35.9, 32.3, 28.6, 26.1, 24.7, 23.0, 22.4; MS, m/z 505.3 $(M+Na)^+$.

14-tert-Butoxycarbonylamino-2-isobutyl-3,8,15-trioxo-1,4,9triaza-cyclopentadecane-5-carboxylic acid methyl ester (107).

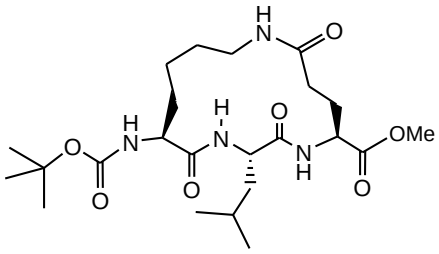

Palladium (carbon) (5 mg) was added to a solution of **106** (0.10 mmol) in MeOH (2 mL) and the flask was flushed with hydrogen gas (1 atm). After stirring at 25^{o}C for 20 h the reaction was filtered through a layer of celite and the filtrate was concentrated to yield **107** (50 mg, 100%) as a light brown solid. ^{1}H NMR δ 7.03 (br. s., 1H), 6.60 (br. s., 1H), 6.21 (br. s., 1H), 5.28 (br. s., 1H), 4.61 - 4.67 (m, 1H), 4.38 - 4.45 (m, 1H), 4.15 - 4.22 (m, 1H), 3.75 (br. s., 3H), 3.49 - 3.58 (m, 1H), 3.01 - 3.09 (m, 1H), 2.40 - 2.43 (m, 1H), 2.24 - 2.33 (m, 3H), 2.09 - 2.17 (m, 1H), 1.55 - 1.96 (m, 9H), 1.44 (m, 9H), 1.19 - 1.29 (m, 2H), 0.89 - 0.99 (m, 6H); ^{13}C NMR δ 184.1, 172.5, 172.2, 155.5, 80.2, 54.0, 52.9, 52.7, 52.2, 41.2, 37.4, 31.8, 30.5, 28.5, 28.1, 26.6, 24.8, 23.0, 22.2, 20.8; MS, m/z 507.5 $(M+Na)^{+}$.

Synthesis of Graphene Oxide (108). (AP8-19)

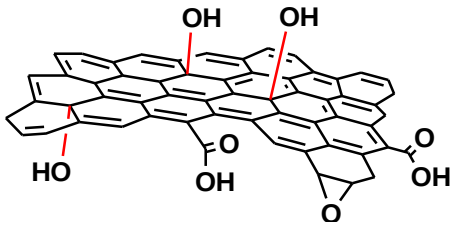

Portions of graphite flakes (3 x 330 mg) were separately heated in a microwave reactor (30 W, 4 min) under argon atmosphere. The expanded graphite flakes were added to a solution of P_2O_5 (30 g) and $K_2S_2O_8$ (30 g) in concentrated HCl at 90^{o}C with vigorous stirring. The mixture was stirred at 85^{o}C for 4 h. The mixture was allowed to cool to 10^{o}C after which it was added slowly to chilled deionized water (1.5 L). The mixture was passed through a glass frit funnel (medium gauge) and the black residue was washed with copious amount of deionized water (5 L). The black residue was dried in an incubator at 60^{o}C for 18 h to provide a fluffy black solid (1.12 g). The solid was added to H_2SO_4 (120 mL) at 0^{o}C followed by the addition of $KMnO_4$ (36 g) and the mixture was heated at 40^{o}C for 2 h with vigorous stirring. The mixture was allowed to cool to

25°C and diluted with cold deionized water (1 L) followed by stirring for 2 h. A solution of 30% H_2O_2 (40 mL) was added drop wise at 0°C using a dropping funnel. The yellow mixture that formed was allowed to stand of 25°C for 2 days. The supernatant layer was carefully decanted and the bottom layer containing the graphene oxide was transferred to many 15 mL centrifuge tubes. The tubes were centrifuged for 30 min at 2500 rpm. The supernatant layer from each tube was carefully decanted and the graphene oxide residue was suspended in 10% HCl (10 mL each). The tubes were centrifuged once again after which the supernatant layer was carefully decanted. The graphene oxide was washed three more times with deionized water (10 mL each) using the above mentioned centrifugation method. The graphene oxide was transferred into a dialysis bag (12000 Mw cut off) and dialyzed at 25°C with water changes twice daily for 1 week until the pH of the wash water remained constant between water changes (~ pH 5.3). The graphene oxide was suspended in deionized water, frozen and lyophilized to provide graphene oxide **108**, 600 mg (~ 60%) as light brown solid. FTIR (neat) υ 3339, 1736, 1631, 1373, 1279, 1224, 1076, 978 cm^{-1}; Raman υ 2436, 1593, 1361 cm^{-1}.

t-Butyl ester functionalized graphene oxide (109). (AP8-136)

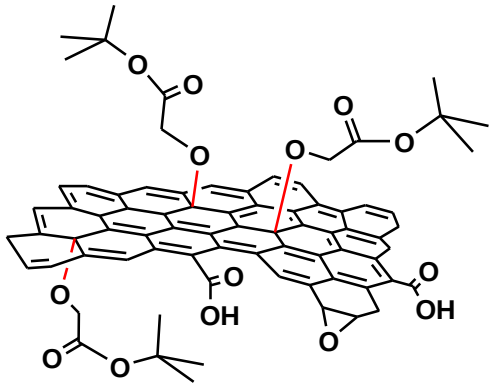

Sodium hydride (2.3 mmol) in a 25 mL round bottom flask was flame dried and purged with argon. Distilled ether (10 mL) was added and the mixture was shaken for 30 sec after which it was allowed to stand and the NaH was settled to the bottom. The ether was carefully syringed out and the remaining grey solid was dried under vacuum. Graphene oxide **108** (40 mg) was added followed by dry DMF (10 mL) and the mixture was shaken for 1 hr. *t*-Butylbromoacetate (2.23 mmol) was added and the mixture was allowed to stand for 2 days with intermittent

shaking. The reaction was transferred to two 15 mL centrifuge tubes. The tubes were centrifuged for 30 min at 2500 rpm. The supernatant layer from each tube was carefully decanted and the t-butyl ester functionalized-graphene oxide residue was re-suspended in deionized water (10 mL each). The tubes were centrifuged once again after which the supernatant layer was carefully decanted. The *t*-butyl ester functionalized-graphene oxide was washed three more times with deionized water (5 mL each) and once with diethyl ether (5 mL) using the above mentioned centrifugation method. The brown residue was suspended in deionized water (5 mL), frozen and lyophilized to give *t*-butyl ester functionalized-graphene oxide **109**, 29 mg (~ 72%) as a brown fluffy solid. IR (neat) υ 3359, 2977, 2930, 1721, 1632, 1455, 1366, 1313, 1250, 1142, 983, 844, 725 cm^{-1}; Raman υ 2435, 1589, 1345 cm^{-1}.

^{13}C-2-bromoacetic acid (111).

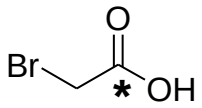

TFA anhydride (32.8 mmol) was added to ^{13}C-acetic acid (16.4 mmol) at 0^{o}C followed by stirring for 2 hr at 25^{o}C. The solution was cooled to 0^{o}C and Br_2 (16.4 mmol) was added followed by stirring overnight at 25^{o}C. Water (32.8 mmol) was added at 0^{o}C and the solution was stirred for 5 min. The volatiles were removed by distillation at atmospheric pressure (bath temp = 120^{o}C) until approximately 2 mL of liquid remained. The distillation apparatus was removed and the remaining liquid evaporated by purging with a stream of argon gas overnight to provide compound **111**, 2.3 g (100%) as a yellow solid. ^{1}H NMR δ 8.41 (br. s., 1H), 3.91 (d, *J* = 4.7 Hz, 2H).

^{13}C-*t*-Butylbromoacetate (112).

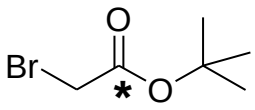

^{13}C-2-bromoacetic acid **111** (16.4 mmol) was dissolved in CH_2Cl_2 (15 mL) and chilled to – 78^{o}C. Chilled isobutylene liquid was obtained by flowing isobutylene gas into a chilled round bottom flask. The chilled isobutylene liquid (26.2 mmol) was added to the ^{13}C-2-bromoacetic acid solution and the temperature was allowed to stabilize at – 78^{o}C. H_2SO_4 (100 µL) was added and the reaction vessel was sealed tightly. The solution was allowed to warm to 25^{o}C and sit for 3 days. The cap was released and excess isobutylene gas was allowed to boil off. The reaction was poured into aqueous $NaHCO_3$ (50 mL) and the organic layer was removed followed by extraction of aqueous layer with ether (50 mL). The combined organic portions were dried ($MgSO_4$), filtered and concentrated to yield a colorless oil which was purified by column chromatography (3:1 hexane:ether) to yield pure compound **112**, 2 g (63%) as a clear oil. ^{1}H NMR δ 3.75 (d, *J* = 4.7 Hz, 2H), 1.49 (s, 9H); ^{13}C NMR δ 166.3, 82.9, 82.9, 28.1, 27.9, 27.9, 27.5.

^{13}C-*t*-Butyl ester functionalized graphene oxide (113). (AP9-125)

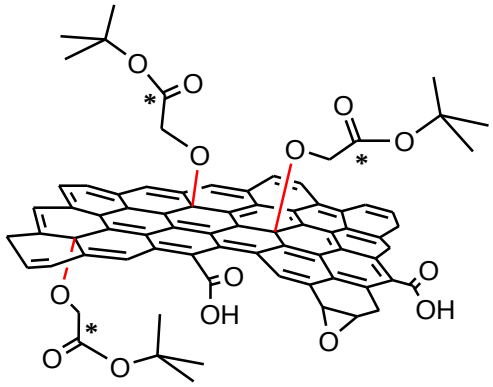

Sodium hydride (3.3 mmol) in a 25 mL round bottom flask was flame dried and purged with argon. Distilled ether (15 mL) was added and the mixture was shaken for 30 sec after which it was allowed to stand and the NaH was settled to the bottom. The ether was carefully syringed out and the remaining grey solid was dried under vacuum. Graphene oxide **108** (170 mg) was added followed by dry DMF (34 mL) and the mixture was shaken for 4 h. ^{13}C-*t*-butylbromoacetate (3.8 mmol) was added and the mixture was allowed to stand for 2 days with intermittent shaking. The reaction was transferred to four 15 mL centrifuge tubes. The tubes were centrifuged for 30 min at 2500 rpm. The supernatant layer from each tube was carefully

decanted and the ^{13}C-t-butyl ester functionalized-graphene oxide residue was re-suspended in deionized water (10 mL each). The tubes were centrifuged once again after which the supernatant layer was carefully decanted. The *t*-butyl ester functionalized-graphene oxide was washed three more times with deionized water (10 mL each) and once with diethyl ether (10 mL) using the above mentioned centrifugation method. The brown residue was suspended in deionized water (8 mL), frozen and lyophilized to give ^{13}C-*t*-butyl ester functionalized-graphene oxide **113**, 120 mg (~ 71%) as a brown fluffy solid. IR (neat) υ 3386, 2929, 1655, 1385, 1361, 1248, 1139, 1100, 1045, 963 cm^{-1}.

Carboxylic acid functionalized graphene oxide (114). (AP8-35)

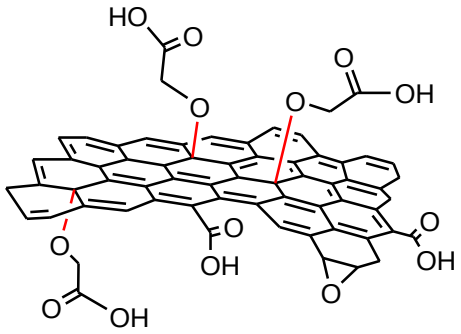

t-Butyl ester functionalized-graphene oxide **109** (40 mg) was suspended in 20% TFA/deionized water (12 mL) and allowed to stand at 25^{o}C for 3 days with intermittent shaking. The reaction was transferred to two 15 mL centrifuge tubes. The tubes were centrifuged for 30 min at 2500 rpm. The supernatant layer from each tube was carefully decanted and the carboxylic acid functionalized-graphene oxide was re-suspended in deionized water (10 mL each). The tubes were centrifuged once again after which the supernatant layer was carefully decanted. The carboxylic acid functionalized-graphene oxide was washed three more times with deionized water (5 mL each) using the above mentioned centrifugation method. The brown residue was suspended in deionized water (5 mL), frozen and lyophilized to give carboxylic acid functionalized-graphene oxide **114**, 31 mg (~ 78%) as a brown fluffy solid. FTIR (neat) υ 3195, 1725, 1631, 1369, 1186, 1135, 1057, 790 cm^{-1}; Raman υ 2436, 1591, 1351 cm^{-1}.

^{13}C-Carboxylic acid functionalized graphene oxide (115). (AP8-138)

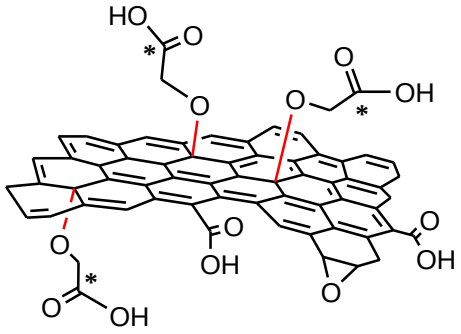

^{13}C-t-butyl ester functionalized-graphene oxide **113** (40 mg) was suspended in 20% TFA/deionized water (10 mL) and allowed to stand at 25^{o}C for 3 days with intermittent shaking. The reaction was transferred to two 15 mL centrifuge tubes. The tubes were centrifuged for 30 min at 2500 rpm. The supernatant layer from each tube was carefully decanted and the carboxylic acid functionalized-graphene oxide was re-suspended in deionized water (10 mL each). The tubes were centrifuged once again after which the supernatant layer was carefully decanted. The ^{13}C-carboxylic acid functionalized-graphene oxide was washed three more times with deionized water (5 mL each) using the above mentioned centrifugation method. The brown residue was suspended in deionized water (5 mL), frozen and lyophilized to give ^{13}C-carboxylic acid functionalized-graphene oxide **115**, 26 mg (~ 65%) as a brown fluffy solid. IR (neat) υ 3195, 1725, 1631, 1369, 1186, 1135, 1057, 790 cm^{-1}.

Solid State Synthesis-attachment of carboxylic acid functionalized graphene oxide to resin (116). (AP10-39) and (AP18-48)

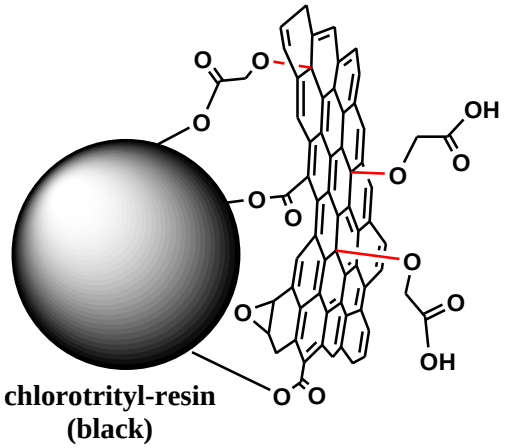

A 25 mL round bottom flask was silylated with 20% TMSCl in $CHCl_3$ (10 mL) for 1 hour. Solution was decanted and flask was washed with $CHCl_3$ (3 x 1 mL) and dried under vacuum. 2-Chlorotrityl resin (1 g) was added to the flask and purged with argon. Dry CH_2Cl_2 was added via syringe and resin was allowed to swell for 1 hr. Carboxylic acid functionalized-graphene oxide **114** (5 mg) was added followed by N,N-diisopropylethylamine (1.35 mL). The mixture was put in a shaker for 2 days. The reaction mixture was filtered and the black colored resin was washed with dry CH_2Cl_2 (20 mL). This whole process was repeated a second time and the black GO coated resin beads were combined. The GO-resin **116** was used immediately for of oligonucleotide attachment.

Solid State Synthesis-Attachment of oligonucleotide to graphene oxide coated resin (117). (AP10-41)

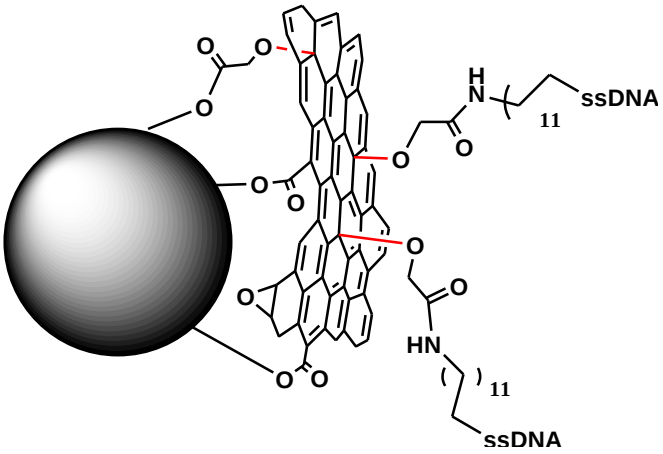

Dry DMF (5 mL) was added to the carboxylic acid functionalized graphene oxide coated-resin **116**. HATU (0.6 mg) was added and the mixture was shaken at 25^{o}C for 10 min. The oligonucleotide-GII, (sequence: 5'/5AmMC12/TGG GAG GGC GAT CGC AAT C), (0.074 μmol) was added and the mixture was reacted in microwave reactor (75 ^{o}C, 25 W, 5 min). The mixture was filtered and the black beads were washed with DMF (50 mL) to yield oligonucleotide-functionalized graphene oxide coated resin **117** as black beads.

Solid State Synthesis-Cleavage of oligonucleotide functionalized graphene oxide from resin (118). (AP10-43)

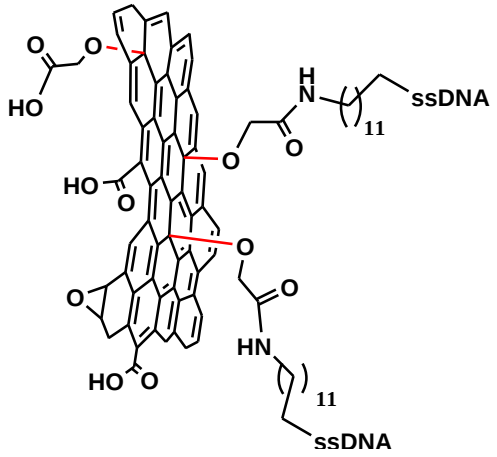

The solid black beads (oligonucleotide functionalized-GO coated resin) **117** was suspended in 10% TFA in trifluoroethanol (5 mL) and sonicated (1 h x 4) allowing the mixture to stand for 6 hours at room temperature in between each sonication period. The solution became red/brown in color and was centrifuged at 1500 rpm for 10 min. The oligonucleotide functionalized-GO sinks to the bottom while the resin resides on the top of the solvent. The top layer (resin and trifluoroethanol) was carefully decanted and the remaining solid (bottom) was washed with deionized water (x3) using the centrifugation method. The remaining solid was suspended in deionized water and lyophilized to give oligonucleotide functionalized graphene oxide **118**, 5 mg (~ 50%) as a brown solid. IR (neat) υ 2968, 2909, 1717.3, 1568.7, 1451.5, 1177.9 cm^{-1}; Raman υ 2436, 1592, 1350 cm^{-1}.

Experimental Details for the Synthesis of H_2N-$(CH_2)_4$CO-Ala-Ala-Asn-Leu-$NHCH_2$-Fc (119) for legumain detection.

Ala-Ala-Asn-Leu (122). AP8-93

Starting with Leucine 2-chlorotrityl resin, *N*-Fmoc protected amino acids were coupled using conventional solid state peptide synthesis by coupling (***General Procedure F***) and deprotection (***General Procedure G***) strategy in the order Asn, Ala and Ala. ***Standard procedure H*** was used to cleave and recover the peptide from the resin to give compound **122**, 95 mg (45%) as a white solid. MS calcd for $C_{16}H_{30}N_5O_6$ $(M+H)^+$ 388.2, found 388.4.

Boc-Ala-Ala-Asn-Leu-$NHCH_2$-Fc (123). **AP8-98**

To compound **122** (50 mg, 0.13 mmol) was added triethylamine (36 μL, 0.26 mmol) and dioxane:water (1:1) (10 mL), and the resulting solution was stirred for 10 min. Di-*t*-butyl dicarbonate (Boc_2O) (56 mg, 0.26 mmol) was added and the solution stirred at 25°C for 12 h. The reaction solution was concentrated to dryness yielding a *N*-Boc intermediate **122a**, 60 mg (96%) as a white solid which was directly used without further purification. MS calcd for $C_{21}H_{37}N_5NaO_8$ $(M+Na)^+$ 510.3, found 510.4. To a solution of **Boc-122** (60 mg, 0.12 mmol) in DMF (2 mL) under argon atmosphere was added HATU (47 mg, 0.12 mmol) and the solution was stirred at 25°C for 10 min. Aminomethylferrocene (26 mg, 0.12 mmol) was added and the solution was stirred at 25°C for 2 h followed by filtration (0.2 micron filter) and purification by HPLC using a preparative column (Phenomenex-Jupiter C18) and eluting with 40% acetonitrile/water to 80 % acetonitrile/water over 40 min with a 10 ml/min flow rate. The fractions containing the desired product were combined and lyophilized to yield compound **123**, 40 mg (48% yield) as a yellow solid. MS calcd for $C_{32}H_{48}FeN_6NaO_7$ $(M+Na)^+$ 707.3, found 707.5.

Boc-HN-$(CH_2)_4$CO-Ala-Ala-Asn-Leu-$NHCH_2$-Fc (124). **AP9-85**

Compound **123** (18 mg, 26 μmol) was dissolved in 10% TFA in dichloromethane (2 mL) and stirred at 25°C for 30 min, concentrated gently on a rotovap to give a residue. The residue was dissolved in deionized water (2 mL), frozen, and lyophilized to give a de-Boc intermediate **123a**, 15 mg (100%) as a green solid. MS calcd for $C_{27}H_{40}FeN_6NaO_5$ $(M+Na)^+$ 607.2, found 607.1. To a solution of *N*-Boc-5-aminovaleric acid (5.6 mg, 26 μmol) in DMF (2 mL) was added HATU (9 mg, 24 μmol), and the resulting solution was stirred at 25°C for 10 min. This solution was transferred *via* cannula to intermediate **123a** (10 mg, 17 μmol) and the resulting solution was stirred for 2 h at 25°C, filtered, and separated on a HPLC using a preparative column (Phenomenex-Jupiter C18) and eluting with 40% acetonitrile/water to 80 % acetonitrile/water over 40 min with a 10 ml/min flow rate and λ=254 nm. The fractions containing the desired product were combined and lyophilized to yield compound **124**, 6 mg (45% yield) as a yellow solid. MS calcd for $C_{37}H_{57}FeN_7NaO_8$ $(M+Na)^+$ 806.4, found 806.5.

H_2N-$(CH_2)_4$CO-Ala-Ala-Asn-Leu-NHCH$_2$-Fc (119). AP9-87

Compound **124** (6 mg, 8 μmol) was dissolved in 10% TFA in dichloromethane (1 mL) and stirred at 25°C for 30 min. The reaction solution was concentrated gently on a rotary evaporator to give a residue which was dissolved in deionized water (2 mL), frozen and lyophilized to give compound **119**, 4 mg (75% yield) as a green solid. MS calcd for $C_{32}H_{50}FeN_7O_6$ $(M+H)^+$ 684.3, found 684.4.

Experimental Details for the Synthesis of H_2N-$(CH_2)_4$CO-Leu-Arg-Phe-Gly-NHCH$_2$-Fc (120) for cathepsin B detection.

H_2N-$(CH_2)_4$CO-Leu-Arg-Phe-Gly (126). AP14-88

Starting with glycine 2-chlorotrityl resin, *N*-Fmoc protected amino acids were coupled using conventional solid state peptide synthesis by coupling (***General Procedure F***) and deprotection (***General Procedure G***) strategy in the order Phe, Arg, Leu and *N*-Boc-5-aminovaleric acid. ***Standard procedure H (cleavage)*** was used to cleave and recover the peptide from the resin to

give compound **126**, 0.32 g (94% yield) as a white solid. MS calcd for $C_{28}H_{47}N_8O_6$ $(M+H)^+$ 591.4, found 591.4.

Boc-HN-$(CH_2)_4$CO-Leu-Arg-Phe-Gly-NHCH$_2$-Fc (127). **AP14-97**

A solution of sodium bicarbonate (86 mg, 1.2 mmol) and compound **126** (0.300 g, 0.5 mmol) in 30 mL of dioxane:water (1:1) was stirred at 25^{o}C for 10 min. Di-*t*-butyl dicarbonate (Boc_2O) (0.22 g, 1.2 mmol) was added and the solution stirred at 25^{o}C for 12 h, concentrated to dryness yielding a *N*-Boc intermediate **126a** 0.35 g, (99% yield) as a white solid. MS calcd for $C_{33}H_{54}N_8O_8Na$ $(M+Na)^+$ 713.4, found 713.5. A solution of *N*-Boc intermediate **126a** (60 mg, 0.09 mmol) and HATU (47 mg, 0.12 mmol) in DMF (2 mL) was stirred at 25^{o}C for 10 min. Aminomethylferrocene (26 mg, 0.12 mmol) was added and the solution was stirred at 25^{o}C for 2 h followed by filtration (0.2 micron filter) and purification by HPLC using a preparative column (Phenomenex-Jupiter C18) and eluting with 40% acetonitrile/water to 80 % acetonitrile/water over 40 min with a 10 ml/min flow rate. The fractions containing the desired product were combined and lyophilized to yield compound **127**, 40 mg (50% yield) as a yellow solid. MS calcd for $C_{44}H_{66}FeN_9O_7$ $(M+H)^+$ 888.4, found 888.5.

H$_2$N-$(CH_2)_4$CO-Leu-Arg-Phe-Gly-NHCH$_2$-Fc (120). **AP14-103/AP17-64**

A solution of compound **127** (50 mg; 56 μmol) in 10% TFA in dichloromethane (2 mL) was stirred at 25^{o}C for 30 min, concentrated gently on a rotary evaporator, dissolved in deionized water (2 mL), frozen, and lyophilized to give compound **120**, 43 mg (98% yield) as a green solid. ^{1}H NMR (400 MHz, DMSO-d_6) δ 8.13 - 8.34 (m, 1H), 7.86 - 8.10 (m, 2H), 7.73 (br. s., 2H), 7.57 (br. s., 1H), 6.82 - 7.42 (m, 8H), 4.48 (br. s., 1H), 4.03 - 4.33 (m, 11H), 3.96 (br. s., 2H), 3.52 - 3.77 (m, 2H), 2.64 - 2.87 (m, 3H), 2.02 - 2.22 (m, 2H), 1.14 - 1.66 (m, 16H), 0.70 - 0.93 (m, 6H); ^{13}C NMR (100 MHz, DMSO-d_6) δ 173.1, 172.6, 172.0, 171.7, 168.7, 157.4, 138.2, 129.8, 128.7, 126.9, 86.5, 69.1, 68.5, 68.0, 54.6, 52.8, 51.6, 42.7, 39.3, 38.3, 38.0, 35.1, 29.7, 27.3, 25.6, 24.9, 23.8, 22.8, 22.1. MS calcd for $C_{39}H_{58}FeN_9O_5$ $(M+H)^+$ 788.4, found 788.3.

Reactivity Test of the Guanidine NH Function of Arginine Residue of Boc-HN-$(CH_2)_4$CO-Leu-Arg-Phe-Gly-$NHCH_2$-Fc (127). In order to test that the guanidine NH of arginine residue side chain in compound **127** does not couple with the carboxylic acid functionality on carbon nanofibers during peptide attachment, a model reaction was performed using the same coupling conditions used to coupling peptide to carbon nanofiber surface.

To a solution of compound **127** (3 mg, 3.4 μmol), benzoic acid (0.4 mg, 3.4 μmol) and *N*-hydroxysuccinimide (0.4 mg, 3.4 μmol) in deionized water (1 mL) was added 1-ethyl-3-(3-dimethylaminopropyl)carbodiimide hydrochloride (0.66 mg, 3.4 μmol) and the resulting solution was stirred at 25^{o}C for 2 h. Mass spectrometry analysis showed that no reaction took place between the NH group of arginine residue and the carboxylic acid moiety of benzoic acid. Since the *N*-terminal amine of compound **127** (Boc-HN-$(CH_2)_4$CO-Leu-Arg-Phe-Gly-$NHCH_2$-Fc) is protected with a Boc group, no reaction took place. This result suggests that the NH moiety of the guanidine side chain of arginine residue does not react with the carboxylic acid function of carbon nanofibers. The peptide attachment to the carbon nanofiber under normal reaction conditions must be made possible *via* the available primary *N*-terminal amine of the linker.

Synthesis of H_2N-$(CH_2)_4$CO-Leu-Asn-Phe-Gly-$NHCH_2$-Fc (131) non-substrate "negative control" tetrapeptide for cathepsin B enzymatic study.

H_2N-$(CH_2)_4$CO-Leu-Asn-Phe-Gly (129). AP17-46

Starting with glycine 2-chlorotrityl resin, *N*-Fmoc protected amino acids were coupled using conventional solid state peptide synthesis by coupling (***General Procedure F***) and deprotection (***General Procedure G***) strategy in the order Phe, Asn, Leu and *N*-Boc-5-aminovaleric acid. ***Standard procedure H (cleavage)*** was used to cleave and recover the peptide from the resin to give compound **129**, 260 mg (83%) as a white solid. ^{1}H NMR (400 MHz, DEUTERIUM OXIDE) δ 7.28 - 7.37 (m, 3H), 7.22 - 7.26 (m, 2H), 4.61 - 4.66 (m, 1H), 4.22 - 4.27 (m, 1H), 3.92 (d, *J* = 5.47 Hz, 1H), 3.15 - 3.21 (m, 1H), 2.93 - 3.01 (m, 4H), 2.61 - 2.76 (m, 2H), 2.28 -

2.34 (m, 2H), 1.60 - 1.66 (m, 4H), 1.49 - 1.58 (m, 2H), 1.37 - 1.45 (m, 2H), 0.90 (d, *J* = 6.25 Hz, 3H), 0.85 (d, *J* = 6.64 Hz, 3H); MS calcd for $C_{26}H_{41}N_6O_7$ $(M+H)^+$ 549.3, found 549.1.

Boc-HN-$(CH_2)_4$CO-Leu-Asn-Phe-Gly-NHCH$_2$-Fc (130). AP17-65

A solution containing sodium bicarbonate (46 mg, 0.55 mmol) and compound **129** (0.15 g, 0.27 mmol) in 20 mL of dioxane:water (1:1) was stirred at 25^{o}C for 10 min. Di-*t*-butyl dicarbonate (Boc_2O) (0.12 g, 0.55 mmol) was added, and the solution stirred for 24 h, concentrated to dryness to yield a *N*-Boc intermediate **129a**, (0.18 g; 100% yield) as a white solid. MS calcd for $C_{31}H_{48}N_6O_9Na$ $(M+Na)^+$ 671.3, found 671.3. A solution of *N*-Boc intermediate **129a** (177 mg, 0.27 mmol) and HATU (115 mg, 0.30 mmol) in distilled DMF (4 mL) was stirred at 25^{o}C for 5 min. Aminomethylferrocene (65 mg, 0.30 mmol) was added, and the solution was stirred for 18 h, filtered (0.2 micron paper) and purified by HPLC using a preparative column (Phenomenex-Jupiter C18) and eluting with 40% acetonitrile/water to 80 % acetonitrile/water over 40 min with a 10 ml/min flow rate. The fractions containing the desired product were combined and lyophilized to yield compound **130**, 150 mg (65% yield) as a yellow solid. MS calcd for $C_{42}H_{59}FeN_7O_8Na$ $(M+Na)^+$ 868.4, found 868.4.

H_2N-$(CH_2)_4$CO-Leu-Asn-Phe-Gly-NHCH$_2$-Fc (131). AP17-72

A solution of compound **130** (60 mg; 71 mmol) in 10% TFA in dichloromethane (3 mL) was stirred at 25^{o}C for 30 min, concentrated gently on a rotary evaporator, dissolved in deionized water (2 mL), frozen, and lyophilized to give compound **131**, 52 mg (100% yield) as a green solid. ^{1}H NMR (400 MHz, DMSO-d_6) δ 8.31 (t, *J* = 5.66 Hz, 1H), 8.17 (d, *J* = 7.81 Hz, 1H), 8.13 (d, *J* = 7.81 Hz, 1H), 7.99 (d, *J* = 7.81 Hz, 1H), 7.73 (br. s., 5H), 7.49 (br. s., 1H), 7.14 - 7.27 (m, 6H), 7.02 (br. s., 1H), 4.48 (q, *J* = 6.64 Hz, 1H), 4.36 - 4.42 (m, 1H), 4.15 - 4.31 (m, 9H), 4.11 (br. s., 2H), 3.97 (br. s., 2H), 3.59 - 3.75 (m, 2H), 3.11 (dd, *J* = 4.10, 13.86 Hz, 1H), 2.87 (d, *J* = 9.76 Hz, 1H), 2.84 (d, *J* = 9.76 Hz, 1H), 2.76 (d, *J* = 5.86 Hz, 2H), 2.56 (d, *J* = 6.64 Hz, 1H), 2.52 (d, *J* = 6.64 Hz, 1H), 2.44 (d, *J* = 6.25 Hz, 1H), 2.40 (d, *J* = 6.64 Hz, 1H), 2.10 - 2.18 (m, 2H), 1.45 - 1.59 (m, 4H), 1.28 - 1.44 (m, 2H), 0.86 (d, *J* = 6.64 Hz, 3H), 0.82 (d, *J* = 6.25 Hz,

3H); ^{13}C NMR (100 MHz, DMSO-d_6) δ 172.9, 172.7, 172.6, 171.8, 171.7, 168.7, 138.6, 129.7, 128.7, 126.9, 86.6, 69.1, 68.4, 68.0, 55.1, 51.5, 50.3, 42.9, 41.4, 39.3, 38.2, 37.4, 35.0, 27.3, 24.9, 23.8, 22.7, 22.1; MS calcd for $C_{37}H_{52}FeN_7O_6$ $(M+H)^+$ 746.3, found 746.2.

Synthesis of Leu-NHCH$_2$-Fc (133) fragment for HPLC analysis.

Fmoc-Leu-NHCH$_2$-Fc (132). AP9-115

To a solution of Fmoc-Leu-OH (126 mg, 0.36 mmol) and HATU (123 mg, 0.33 mmol) in DMF (1 mL) was added H_2NCH_2-Fc (70 mg, 0.33 mmol) and the resulting solution was stirred at 25^{o}C for 30 min. The reaction was diluted with ethyl acetate (100 mL) and the organic layer was washed with water (50 mL x 3) and brine (50 mL), dried ($MgSO_4$), filtered and concentrated to yield a brown oil which was purified by silica gel chromatography using (EtOAc/hexane 1:1) to give compound **132**, 98 mg (54% yield) as a yellow solid. MS calc'd for $C_{32}H_{34}FeN_2NaO_3$ 573.2 $(M+Na)^+$, found to be 573.3.

Leu-NHCH$_2$-Fc (133). AP9-117

Compound **132** (81 mg, 0.15 mmol) was dissolved in 20% piperidine/DMF (5 mL) and stirred at 25 ^{o}C for 30 min. The DMF was removed under reduced pressure and the resulting crude oil was purified by silica gel column chromatography (MeOH/EtOAc 5:95) to give compound **133**, 33 mg (67% yield) as a yellow solid. MS calc'd for $C_{17}H_{24}FeN_2NaO$ 351.1 $(M+Na)^+$, found to be 351.1.

Synthesis of Phe-Gly-NHCH$_2$-Fc (136) fragment for HPLC analysis.

Boc-Gly-NHCH$_2$-Fc (134). KC-1-67

To a solution of Boc-Gly-OH (32 mg, 0.19 mmol) in dry DMF under argon was added HATU (77 mg, 0.20 mmol), and the resulting solution was stirred for 5 minutes. To the above solution, H_2NCH_2-Fc (40 mg, 0.185 mmol) was added and the solution stirred at 25^oC for 12 h. The reaction solution was partitioned between deionized water (20 mL) and dichloromethane (20 mL). The organic layer was removed and the aqueous layer was extracted once with dichloromethane (20 mL). The organic layers were combined and dried ($MgSO_4$), filtered, concentrated and purified by silica gel column chromatography (CH_2Cl_2:MeOH 30:1) to give compound **134**, 25 mg (36% yield) as an orange oil. MS calc'd for $C_{18}H_{24}FeN_2NaO_3$ 395.1 $(M+Na)^+$, found to be 395.1.

Boc-Phe-Gly-NHCH$_2$-Fc (135). KC-1-70

To a solution of compound **134** (25 mg, 0.092 mmol) in dichloromethane (4 mL) under argon was added TFA (0.4 mL) and the solution was stirred at 25^oC for 1 h. The resulting solution was gently concentrated on a rotary evaporator and placed under high vacuum for 1 h to yield a de-Boc intermediate **134a**, 25mg (100%) as a green solid. MS calc'd for $C_{13}H_{17}FeN_2O$ 273.1 $(M+H)^+$, found to be 273.2. A solution of de-Boc intermediate **134a** (25 mg, 0.092 mmol), Boc-Phe-OH (24 mg, 0.092 mmol), 4-(dimethylamino)pyridine (23 mg, 0.184 mmol) and 1-ethyl-3-(3-dimethylaminopropyl) carbodiimide (EDC) (35 mg, 0.184 mmol) in dry DMF (1 mL) under argon atmosphere was stirred for 1 min at 25^oC followed by dilution with dry CH_2Cl_2 (2 mL) and additional stirring at 25^oC for 12 h. The reaction mixture was partitioned between CH_2Cl_2 (20 mL) and water (20 mL) and acidified to pH 2 using drop wise addition of 2N HCl. The combined organic layers were washed with brine, dried (anhydrous Na_2SO_4), filtered and concentrated to yield a crude oil that was purified by silica gel column chromatography (CH_2Cl_2:MeOH 40:1) to afford compound **135**, (23 mg, 48% yield) as a sticky yellow oil. MS calc'd for $C_{27}H_{33}FeN_3NaO_4$ 542.1 $(M+Na)^+$ and found to be 541.9.

Phe-Gly-NHCH$_2$-Fc (136). **KC-1-71**

A solution of compound **135** (23 mg, 0.044 mmol) in 10% TFA/CH_2Cl_2 (5 mL) was stirred at 25^oC for 1 h. The reaction solution was gently concentrated on a rotary evaporator to yield a

sticky oil. CH_2Cl_2 (20 mL) was added and concentrated again and the residue was placed under high vacuum to furnish compound **136**, 18 mg (98% yield) as a green solid. ^{1}H NMR ($CDCl_3$) δ 7.3 (s, 5 H), 7.12 (s, 2 H), 5.4 (s, 1 H), 4.4 - 4.0 (m, 9 H), 3.85 (m, 2 H), 3.5 (s, 2 H), 3.2 (s, 2 H), 2.85 (s, 2 H); MS calc'd for $C_{22}H_{25}FeN_3NaO_2$ 445.1 $(M+Na)^+$, found to be 445.1.

V. References

1. Chen, Z.; Sosnovtsev, S. V.; Bok, K.; Parra, G. I.; Makiya, M.; Agulto, L.; Green, K. Y.; Purcell, R. H., "Development of norwalk virus-specific monoclonal antibodies with therapeutic potential for the treatment of norwalk virus gastroenteritis." *J. Virol.* **2013,** 87, (17), 9547-57.
2. Hirneisen, K. A.; Kniel, K. E., "Norovirus surrogate survival on spinach during preharvest growth." *Phytopathology* **2013,** 103, (4), 389-94.
3. Rocha-Pereira, J.; Nascimento, M. S. J., *Targeting Norovirus: Strategies for the Discovery of New Antiviral Drugs*. InTech: Rijeka, 2012; p 121-150.
4. Hoelzer, K.; Fanaselle, W.; Pouillot, R.; Van Doren, J. M.; Dennis, S., "Virus inactivation on hard surfaces or in suspension by chemical disinfectants: systematic review and meta-analysis of norovirus surrogates." *J. Food Prot.* **2013,** 76, (6), 1006-16.
5. Said, M. A.; Perl, T. M.; Sears, C. L., "Healthcare epidemiology: gastrointestinal flu: norovirus in health care and long-term care facilities." *Clin. Infect. Dis.* **2008,** 47, (9), 1202-8.
6. Rocha-Pereira, J.; Jochmans, D.; Dallmeier, K.; Leyssen, P.; Cunha, R.; Costa, I.; Nascimento, M. S.; Neyts, J., "Inhibition of norovirus replication by the nucleoside analogue 2'-C-methylcytidine." *Biochem. Biophys. Res. Commun.* **2012,** 427, (4), 796-800.
7. Hutson, A. M.; Atmar, R. L.; Graham, D. Y.; Estes, M. K., "Norwalk virus infection and disease is associated with ABO histo-blood group type." *J. Infect. Dis.* **2002,** 9, 1335-1337.

8. Marionneau, S.; Ruvoen, N.; Le Moullac-Vaidye, B.; Clement, M.; Cailleau-Thomas, A.; Ruiz-Palacois, G.; Huang, P.; Jiang, X.; Le Pendu, J., "Norwalk virus binds to histo-blood group antigens present on gastroduodenal epithelial cells of secretor individuals." *Gastroenterology* **2002,** 7, 1967-1977.
9. Tan, M.; Jiang, X., "Norovirus and its histo-blood group antigen receptors: an answer to a historical puzzle. ." *Trends Microbiol.* **2005,** 6, 285-293.
10. Tan, M.; Jiang, X., "Norovirus gastroenteritis, increased understanding and future antiviral options." *Curr. Opin. Investig. Drugs* **2008,** 2, 146-151.
11. Rydell, G. E.; Nilsson, J.; Rodriguez-Diaz, J.; Ruvoen-Clouet, N.; Svensson, L.; Le Pendu, J.; Larson, G., "Human noroviruses recognize sialyl Lewis x neoglycoprotein." *Glycobiology* **2009,** 3, 309-320.
12. Tamura, M.; Natori, K.; Kobayashi, M.; Miyamura, T.; Takeda, N., "Genogroup II noroviruses efficiently bind to heparan sulfate proteoglycan associated with the cellular membrane." *J. Virol.* **2004,** 8, 3817-3826.
13. Sosnovtsev, S. V., *Proteolytic cleavage and viral proteins In: Caliciviruses: Molecular and Cellular Virology*. Caister Academic Press: 2010.
14. Bailey, D.; Kaiser, W. J.; Hollinshead, M.; Moffat, K.; Chaudhry, Y.; Wileman, T.; Sosnovtsev, S. V.; Goodfellow, I. G., "Feline calicivirus p32, p39 and p30 proteins localize to the endoplasmic reticulum to initiate replication complex formation." *J. Gen. Virol.* **2009,** 3, 739-749.
15. Hyde, J. L.; Mackenzie, J. M., "Subcellular localization of the MNV-1 ORF1 proteins and their potential roles in the formation of the MNV-1 replication complex. ." *Virology* **2010,** 1, 138-148.
16. Sharp, T. M.; Guix, S.; Katayama, K.; Crawford, S. E.; Estes, M. K., " Inhibition of Cellular Protein Secretion by Norwalk Virus Nonstructural Protein p22 Requires a Mimic of an Endoplasmic Reticulum Export Signal." *PLoS One* **2010,** 10, e13130.
17. Wessels, E.; Duijsings, D.; Lanke, K. H.; van Dooren, S. H.; Jackson, C. L.; Melchers, W. J.; vanKuppeveld, F. J., "Effects of picornavirus 3A proteins on protein transport and GBF1-dependent COP-I recruitment." *J. Virol.* **2006,** 23, 11852-11860.
18. Heinz, B. A.; Vance, L. M., "The antiviral compound enviroxime targets the 3A coding region of rhinovirus and poliovirus." *J. Virol.* **1995,** 7, 4189-4197.

19. De Palma, A. M.; Thibaut, H. J.; van der Linden, L.; Lanke, K.; Heggermont, W.; Ireland, S.; Andrews, R.; Arimilli, M.; Al-Tel, T. H.; De Clercq, E.; van Kuppeveld, F.; Neyts, J., "Mutations in the nonstructural protein 3A confer resistance to the novel enterovirus replication inhibitor TTP-8307." *Antimicrob. Agents Chemother.* **2009,** 5, 1850-1857.

20. Chaudhry, Y.; Nayak, A.; Bordeleau, M. E.; Tanaka, J.; Pelletier, J.; Belsham, G. J.; Roberts, L. O.; Goodfellow, I. G., "Caliciviruses differ in their functional requirements for eIF4F components." *J. Biol. Chem.* **2006,** 35, 25315-25325.

21. Bordeleau, M. E.; Cencic, R.; Lindqvist, L.; Oberer, M.; Northcote, P.; Wagner, G.; Pelletier, J., "RNA-mediated sequestration of the RNA helicase eIF4A by Pateamine A inhibits translation initiation." *Chem. Biol.* **2006,** 12, 1287-1295.

22. De Palma, A. M.; Heggermont, W.; Lanke, K.; Coutard, B.; Bergmann, M.; Monforte, A. M.; Canard, B.; De Clercq, E.; Chimirri, A.; Purstinger, G.; Rohayem, J.; van Kuppeveld, F.; Neyts, J., "The thiazolobenzimidazole TBZE-029 inhibits enterovirus replication by targeting a short region immediately downstream from motif C in the nonstructural protein 2C." *J. Virol.* **2008,** 10, 4720-4730.

23. De Palma, A. M.; Vliegen, I.; De Clercq, E.; Neyts, J., "Selective inhibitors of picornavirus replication." *Med. Res. Rev.* **2008,** 6, 823-884.

24. Norder, H.; De Palma, A. M.; Selisko, B.; Costenaro, L.; Papageorgiou, N.; Arnan, C.; Coutard, B.; Lantez, V.; De Lamballerie, X.; Baronti, C.; Sola, M.; Tan, J.; Neyts, J.; Canard, B.; Coll, M.; Gorbalenya, A. E.; Hilgenfeld, R., "Picornavirus non-structural proteins as targets for new anti-virals with broad activity." *Antiviral Res.* **2011,** 3, 204-218.

25. De Palma, A. M.; Purstinger, G.; Wimmer, E.; Patick, A. K.; Andries, K.; Rombaut, B.; De Clercq, E.; Neyts, J., "Potential Use of Antiviral Agents in Polio Eradication." *Emerg. Infect. Dis.* **2008,** 4, 545-551.

26. Goris, N.; De Palma, A.; Toussaint, J. F.; Musch, I.; Neyts, J.; De Clercq, K., "2'-C-Methylcytidine as a potent and selective inhibitor of the replication of foot-and-mouth disease virus." *Antiviral Res.* **2007,** 3, 161-168.

27. Klumpp, K.; Leveque, V.; Le Pogam, S.; Ma, H.; Jiang, W. R.; Kang, H.; Granycome, C.; Singer, M.; Laxton, C.; Hang, J. Q.; Sarma, K.; Smith, D. B.; Heindl, D.; Hobbs, C. J.;

Merrett, J. H.; Symons, J.; Cammack, N.; Martin, J. A.; Devos, R.; Najera, I., "The novel nucleoside analog R1479 (4'-azidocytidine) is a potent inhibitor of NS5B-dependent RNA synthesis and hepatitis C virus replication in cell culture." *J. Biol. Chem.* **2006,** 7, 3793-3799.

28. Rohayem, J.; Bergmann, M.; Gebhardt, J.; Gould, E.; Tucker, P.; Mattevi, A.; Unge, T.; Hilgenfeld, R.; Neyts, J., "Antiviral strategies to control calicivirus infections." *Antiviral Res.* **2010,** 2, 162-178.
29. Yang, Y.; Liang, Y. Q.; Qu, L.; Chen, Z. M.; Yi, M. K.; Li, K.; Lemon, S. M., "Disruption of innate immunity due to mitochondrial targeting of a picornaviral protease precursor. ." *PNAS* **2007,** 17, 7253-7258.
30. Binford, S. L.; Maldonado, F.; Brothers, M. A.; Weady, P. T.; Zalman, L. S.; Meador, J. W., 3rd,; Matthews, D. A.; Patick, A. K., "Conservation of amino acids in human rhinovirus 3C protease correlates with broad-spectrum antiviral activity of rupintrivir, a novel human rhinovirus 3C protease inhibitor." *Antimicrob. Agents Chemother.* **2005,** 2, 619-626.
31. Spurgers, K. B.; Sharkey, C. M.; Warfield, K. L.; Bavari, S., "Oligonucleotide antiviral therapeutics: antisense and RNA interference for highly pathogenic RNA viruses." *Antiviral Res.* **2008,** 1, 26-36.
32. Vinje, J., "A norovirus vaccine on the horizon?" *J. Infect. Dis.* **2010,** 202, (11), 1623-1625.
33. El-Kamary, S. S.; Pasetti, M. F.; Mendelman, P. M.; Frey, S. E.; Bernstein, D. I.; Treanor, J. J.; Ferreira, J.; Chen, W. H.; Sublett, R.; Richardson, C.; Bargatze, R. F.; Sztein, M. B.; Tacket, C. O., "Adjuvanted intranasal Norwalk virus-like particle vaccine elicits antibodies and antibody-secreting cells that express homing receptors for mucosal and peripheral lymphoid tissues." *J. Infect. Dis.* **2010,** 202, (11), 1649-58.
34. Tamminen, K.; Lappalainen, S.; Huhti, L.; Vesikari, T.; Blazevic, V., "Trivalent combination vaccine induces broad heterologous immune responses to norovirus and rotavirus in mice." *PLoS One* **2013,** 8, (7), e70409.
35. Nakamura, K.; Someya, Y.; Kumasaka, T.; Ueno, G.; Yamamoto, M.; Sato, T.; Takeda, N.; Miyamura, T.; Tanaka, N., "A norovirus protease structure provides insights into active and substrate binding site integrity. ." *J. Virol* **2005,** 79, 13685–13693.

36. Zeitler, C. E.; Estes, M. K.; Venkataram Prasad, B. V., "X-ray crystallographic structure of the Norwalk virus protease at 1.5-A resolution." *J. Virol.* **2006,** 80, (10), 5050-8.

37. Takahashi, D.; Hiromasa, Y.; Kim, Y.; Anbanandam, A.; Yao, X.; Chang, K.-O.; Prakash, O., "Structural and dynamics characterization of norovirus protease." *Protein Science* **2013,** 22, 347-357.

38. Tiew, K. C.; He, G.; Aravapalli, S.; Mandadapu, S. R.; Gunnam, M. R.; Alliston, K. R.; Lushington, G. H.; Kim, Y.; Chang, K. O.; Groutas, W. C., "Design, synthesis, and evaluation of inhibitors of Norwalk virus 3C protease." *Bioorg. & Med. Chem. Lett.* **2011,** 21, (18), 5315-9.

39. Chang, K. O.; Takahashi, D.; Prakash, O.; Kim, Y., "Characterization and inhibition of norovirus proteases of genogroups I and II using a fluorescence resonance energy transfer assay." *Virology* **2011,** 423, 125-133.

40. Kim, Y.; Lovell, S.; Tiew, K. C.; Mandadapu, S. R.; Alliston, K. R.; Battaile, K. P.; Groutas, W. C.; Chang, K. O., "Broad-spectrum antivirals against 3C or 3C-like proteases of picornaviruses, noroviruses, and coronaviruses." *J. Virol.* **2012,** 86, (21), 11754-11762.

41. Chang, K. O.; Sosnovtsev, S. V.; Belliot, G.; Green, K. Y., "Stable expression of a Norwalk virus RNA replicon in a human hepatoma cell line." *Virology* **2006,** 353, 463-473.

42. Prior, A. M.; Kim, Y.; Weerasekara, S.; Moroze, M.; Alliston, K. R.; Uy, R. A. Z.; Groutas, W. C.; Chang, K.-O.; Hua, D. H., "Design, synthesis, and bioevaluation of viral 3C and 3C-like protease inhibitors." *Bioorg. & Med. Chem. Lett.* **2013,** 23, 6317–6320.

43. Tyndall, J. D.; Nall, T.; Fairlie, D. P., "Proteases universally recognize beta strands in their active sites." *Chem. Rev.* **2005,** 105, 973.

44. Madala, P. K.; Tyndall, J. D.; Nall, T.; Fairlie, D. P., "Update 1 of: Proteases Universally Recognize Beta Strands in their active sites." *Chem. Rev.* **2010,** 110, 3299.

45. Tyndall, J. D.; Fairlie, D. P., "Macrocycles mimic the extended peptide conformation recognized by aspartic, serine, cysteine and metallo proteases." *Curr. Med. Chem.* **2001,** 8, 893.

46. Glenn, M. P.; Pattenden, L. K.; Reid, R. C.; Tyssen, D. P.; Tyndall, J. D.; Birch, C. J.; Fairlie, D. P., "Beta-strand mimicking macrocyclic amino acids: templates for protease inhibitors with antiviral activity." *J. Med. Chem.* **2002,** 45, 371.

47. Marsault, E.; Peterson, M. L., "Macrocycles are great cycles: applications, opportunities, and challenges of synthetic macrocycles in drug discovery." *J. Med. Chem.* **2011,** 54, 1961-2004.

48. Mandadapu, S. R.; Weerawarna, P. M.; Prior, A. M.; Uy, R. A.; Aravapalli, S.; Alliston, K. R.; Lushington, G. H.; Kim, Y.; Hua, D. H.; Chang, K. O.; Groutas, W. C., "Macrocyclic inhibitors of 3C and 3C-like proteases of picornavirus, norovirus, and coronavirus." *Bioorg. Med. Chem. Lett.* 23, (13), 3709-12.

49. Mou, K.; Xu, B.; Ma, C.; Yang, X.; Zou, X.; Lu, Y.; Xu, P., "Novel CADD-based peptidyl vinyl ester derivatives as potential proteasome inhibitors." *Bioorg. & Med. Chem. Lett.* **2008,** 18, 2198–2202.

50. Hanessian, S.; Schaum, R., "1,3-Asymmetric Induction in Enolate Alkylation Reactions of N-Protected γ-Amino Acid Derivitives." *Tett. Lett.* **1997,** 38, (2), 163-166.

51. Narasaka, K.; Ukaji, Y., "Highly Stereoselective Alkylation Reaction of Ester Enolates Generated from δ-Hydroxy Carboxylic Acids." *Chem. Lett.* **1986**, 81-84.

52. Ukaji, Y.; Narasaka, K., "Stereoselective Alkylation of Lithium Enolates Generated from t-Butyl Esters of 4-Alkyl-Substituted 5-Hydroxypentanoic Acids." *Bull. Chem. Soc. Jpn.* **1988,** 61, 571-572.

53. Chalker, J. M.; Wood, C. S. C.; Davis, B. G., "A Convenient Catalyst for Aqueous and Protein Suzuki-Miyaura Cross-Coupling." *J. Am. Chem. Soc.* **2009,** 131, 16346–16347.

54. Song, K.; Zhao, X.; Xu, Y.; Liu, H., "Modification of graphene oxide via photo-initiated grafting polymerization. ." *J. Mater. Sci.* **2013**, (48), 5750–5755.

55. Brodie, B., *Ann. Chim. Phys.* **1855,** 45, 351.

56. Hummers, W. S.; Offeman, R. E., "Preparation of Graphitic Oxide." *J. Am. Chem. Soc.* **1958,** 80, 1339.

57. Huh, S.; Park, J.; Kim, Y. S.; Kim, K. S.; Hong, B. H.; Nam, J. M., "UV/ozone-oxidized large-scale graphene platform with large chemical enhancement in surface-enhanced Raman scattering." *ACS Nano* **2011,** 5, 9799-9806.

58. Dreyer, D. R.; Park, S.; Bielawski, C. W.; Ruoff, R. S., "The chemistry of graphene oxide." *Chem. Soc. Rev.* **2010,** 39, 228-240.

59. Jeong, H. K.; Jin, M. H.; So, K. P.; Lim, S. C.; Lee, Y. H., "Tailoring the characteristics of graphite oxides by different oxidation times." *J. Phys. D: Appl. Phys.* **2009,** 42, 065418.

60. Huang, H.; Li, Z.; Juncong She; Wang, W., "Oxygen density dependent band gap of reduced graphene oxide." *J. Appl. Phys.* **2012,** 111, 054317.

61. Bai, H.; Li, C.; Shi, G., "Functional composite materials based on chemically converted graphene." *Adv. Mater.* **2011**, 1089.

62. Mao, H. Y.; Laurent, S.; Chen, W.; Akhavan, O.; Imani, M.; Ashkarran, A. A.; Mahmoudi, M., "Graphene: promises, facts, opportunities, and challenges in nanomedicine." *Chem. Rev.* **2013,** 113, 3407-3424.

63. Chung, C.; Kim, Y.-K.; Shin, D.; Ryoo, S.-R.; Hong, B. H.; Min, D.-H., "Biomedical Applications of Graphene and Graphene Oxide." *Acc. Chem. Res.* **2013**, ahead of print.

64. Cui, L.; Song, Y.; Ke, G.; Guan, Z.; Zhang, H.; Lin, Y.; Huang, Y.; Zhu, Z.; Yang, C. J., "Graphene oxide protected nucleic acid probes for bioanalysis and biomedicine." *Chem. Eur. J.* **2013,** 19, 10442 – 10451.

65. Liu, Z.; Robinson, J. T.; Sun, X.; Dai, H., "PEGylated Nano-Graphene Oxide for Delivery of Water Insoluble Cancer Drugs." *J. Am. Chem. Soc.* **2008,** 130, 10876.

66. Rana, V. K.; Choi, M.-C.; Kong, J.-Y.; Kim, G. Y.; Kim, M. J.; Kim, S.-H.; Mishra, S.; Singh, R. P.; Ha, C.-S., "You have full text access to this content Synthesis and Drug-Delivery Behavior of Chitosan-Functionalized Graphene Oxide Hybrid Nanosheets. ." *Macromol. Mater. Eng.* **2011,** 296, 131-140.

67. Bao, H.; Pan, Y.; Ping, Y.; Sahoo, N. G.; Wu, T.; Li, L.; Li, J.; Gan, L. H., "Chitosan-functionalized graphene oxide as a nanocarrier for drug and gene delivery." *Small* **2011,** 11, 1569-1578.

68. Avinash, M. B.; Subrahmanyam, K. S.; Sundarayya, Y.; Govindaraju, T., "Covalent modification and exfoliation of graphene oxide using ferrocene." *Nanoscale* **2010,** 2, 1762-1766.

69. Karousis, N.; Economopoulos, S. P.; Sarantopoulou, E.; Tagmatarchis, N., "Porphyrin counter anion in imidazolium-modified graphene-oxide." *Carbon* **2010,** 48, 854-860.

70. Wang, H.; Zhang, Q.; Chu, X.; Chen, T.; Ge, J.; Yu, R., "Graphene oxide-peptide conjugate as an intracellular protease sensor for caspase-3 activation imaging in live cells." *Angew. Chem. Int. Ed.* **2011,** 50, 7065-7069.

71. Zhuang, X.-D.; Chen, Y.; Liu, G.; Li, P.-P.; Zhu, C.-X.; Kang, E.-T.; Neoh, K.-G.; Zhang, B.; Zhu, J.-H.; Li, Y.-X., "Conjugated-Polymer-Functionalized Graphene Oxide: Synthesis and Nonvolatile Rewritable Memory Effect." *Adv. Mater.* **2010,** 22, 1731-1735.

72. Depan, D.; Shah, J.; Misra, R. D. K., "Controlled release of drug from folate-decorated and graphene mediated drug delivery system: Synthesis, loading efficiency, and drug release response. ." *Mater. Sci. Eng.* **2011,** 31, 1305-1312.

73. Longqiang Xiao; Liqiong Liao; Liu, L., "Chemical modification of graphene oxide with carbethoxycarbene under microwave irradiation." *Chem. Phys. Lett.* **2013,** 556, 376-379.

74. Jahan, M.; Bao, Q.; Yang, J.-X.; Loh, K. P., "Structure-Directing Role of Graphene in the Synthesis of Metal-Organic Framework Nanowire." *J. Am. Chem. Soc.* **2010,** 132, 14487-14495.

75. Yang, W.; Ratinac, K. R.; Ringer, S. P.; Thordarson, P.; Gooding, J. J.; Braet, F., "Carbon nanomaterials in biosensors: should you use nanotubes or graphene?" *Angew. Chem.* **2010,** 122, 2160-2185.

76. Rao, C. N.; Sood, A. K.; Subrahmanyam, K. S.; Govindaraj, A., "Graphene: The New Two-Dimensional Nanomaterial." *Angew. Chem.* **2009,** 121, 7890-7916.

77. Shen, H.; Zhang, L.; Liu, M.; Zhang, Z., "Biomedical Applications of Graphene." *Theranostics* **2012,** 2, 283-294.

78. Malarda, L. M.; Pimentaa, M. A.; Dresselhaus, G.; Dresselhaus, M. S., "Raman spectroscopy in graphene." *Physics Reports* **2009,** 473, 51-87.

79. Shen, J.; Shi, M.; Ma, H.; Yan, B.; Li, N.; Hu, Y.; Ye, M., "Synthesis of hydrophilic and organophilic chemically modified graphene oxide sheets." *Journal of Colloid and Interface Science* **2010,** 351, 366-370.

80. Kudin, K. N.; Ozbas, B.; Schniepp, H. C.; Prud'homme, R. K.; Aksay, I. A.; Car, R., "Raman spectra of graphite oxide and functionalized graphene sheets." *Nano Lett.* **2008,** 8, 36-41.

81. Zhu, Y.; Murali, S.; Cai, W.; Li, X.; Suk, J. W.; Potts, J. R.; Ruoff, R. S., "Graphene and Graphene Oxide: Synthesis, Properties, and Applications." *Adv. Mater.* **2010,** 22, 3906-3924.

82. Cai, W.; Piner, R. D.; Stadermann, F. J.; Park, S.; Shaibat, M. A.; Ishii, Y.; Yang, D.; Velamakanni, A.; An, S. J.; Stoller, M.; An, J.; Chen, D.; Ruoff, R. S., "Synthesis and solid-state NMR structural characterization of 13C-labeled graphite oxide." *Science* **2008,** 321, 1815-1817.

83. Mantsch, H. H.; Chapman, D., *Infrared Spectroscopy of Biomolecules*. Wiley-Liss, Inc.: New York, 1996.

84. Lu, C. H.; Yang, H. H.; Zhu, C. L.; Chen, X.; Chen, G. N., "A graphene platform for sensing biomolecules." *Angew. Chem. Int. Ed.* **2009,** 48, 4785-4787.

85. Lu, C. H.; Yang, H. H.; Zhu, C. L.; Chen, X.; Chen, G. N., "A graphene platform for sensing biomolecules." *Angew. Chem.* **2009,** 121, 4879-4881.

86. Jemal, A.; Bray, F.; Center, M.; Ferlay, J.; Ward, E.; Forman, D., *a cancer journal for clinicians* **2011,** 61, 69–90.

87. Hanahan, D.; Weinberg, R. A., "The hallmarks of cancer." *Cell* **2000,** 100, 57-70.

88. Qin, X.-J.; Ling, B. X., "Proteomic studies in breast cancer." *Oncology Lett.* **2012,** 3, 735-743.

89. van der Werff, M. P. J.; Mertens, B.; de Noo, M. E.; Bladergroen, M. R.; Dalebout, H. C.; Tollenaar, R. A. E. M.; Deelder, A. M., "Case-control breast cancer study of MALDI-TOF proteomic mass spectrometry data on serum samples. ." *Statistical Applications in Genetics and Molecular Biology* **2008,** 7, 1-12.

90. Drukteinis, J. S.; Mooney, B. P.; Flowers, C. I.; Gatenby, R. A., "Beyond Mammography: New Frontiers in Breast Cancer Screening. ." *The American Journal of Medicine* **2013,** 126, 472-479.

91. Swisher, L. Z.; Syed, L. U.; Prior, A. M.; Madiyar, F. R.; Carlson, K. R.; Nguyen, T. A.; Hua, D. H.; Li, J., "Electrochemical Protease Biosensor Based on Enhanced AC Voltammetry Using Carbon Nanofiber Nanoelectrode Arrays." *J. Phys. Chem. C:* **2013,** 117, 4268-4277.

92. Kandalaft, P. L.; Chang, K. L.; Ahn, C. W.; Traweek, S. T.; Mehta, P.; Battifora, H., "Prognostic significance of immunohistochemical analysis of cathepsin D in low-stage breast cancer." *Cancer* **1993,** 71, (9), 2756-63.

93. Hirai, K.; Yokoyama, M.; Asano, G.; Tanaka, S., "Expression of cathepsin B and cystatin C in human colorectal cancer." *Hum. Pathol.* **1999,** 30, (6), 680-6.

94. Macabeo-Ong, M.; Shiboski, C. H.; Silverman, S.; Ginzinger, D. G.; Dekker, N.; Wong, D. T.; Jordan, R. C., "Quantitative analysis of cathepsin L mRNA and protein expression during oral cancer progression." *Oral Oncol.* **2003,** 39, (7), 638-47.

95. Syed, L. U.; Liu, J.; Prior, A. M.; Hua, D. H.; Li, J., "Enhanced Electron Transfer Rates by AC Voltammetry for Ferrocenes Attached to the End of Embedded Carbon Nanofiber Nanoelectrode Arrays." *Electroanalysis* **2011,** 23, 1709-1717.

96. Ishii, S., "Legumain: asparaginyl endopeptidase." *Methods Enzymol.* **1994,** 244, 604-15.

97. Stern, L.; Perry, R.; Ofek, P.; Many, A.; Shabat, D.; Satchi-Fainaro, R., "A novel antitumor prodrug platform designed to be cleaved by the endoprotease legumain." *Bioconjug. Chem.* **2009,** 20, (3), 500-10.

98. Chen, J. M.; Dando, P. M.; Rawlings, N. D.; Brown, M. A.; Young, N. E.; Stevens, R. A.; Hewitt, E.; Watts, C.; Barrett, A. J., "Cloning, isolation, and characterization of mammalian legumain, an asparaginyl endopeptidase." *J. Biol. Chem.* **1997,** 272, (12), 8090-8.

99. Choe, Y.; Leonetti, F.; Greenbaum, D. C.; Lecaille, F.; Bogyo, M.; Bromme, D.; Ellman, J. A.; Craik, C. S., "Substrate profiling of cysteine proteases using a combinatorial peptide library identifies functionally unique specificities." *J. Biol. Chem.* **2006,** 281, (18), 12824-32.

100. Gutierrez, O. A.; Chavez, M.; Lissi, E., "A theoretical approach to some analytical properties of heterogeneous enzymatic assays." *Anal. Chem.* **2004,** 76, (9), 2664-8.

101. Almeida, P. C.; Oliveira, V.; Chagas, J. R.; Meldal, M.; Juliano, M. A.; Juliano, L., "Hydrolysis by cathepsin B of fluorescent peptides derived from human prorenin." *Hypertension* **2000,** 35, (6), 1278-83.

102. Nagler, D. K.; Storer, A. C.; Portaro, F. C.; Carmona, E.; Juliano, L.; Menard, R., "Major increase in endopeptidase activity of human cathepsin B upon removal of occluding loop contacts." *Biochemistry* **1997,** 36, (41), 12608-15.

103. Schogl, K.; Mechtler, H., *Monatsh. Chem.* **1966,** 97, 150-167.

VI. Appendices: Compound Spectral Data

AP13-17-FR24-AGAIN

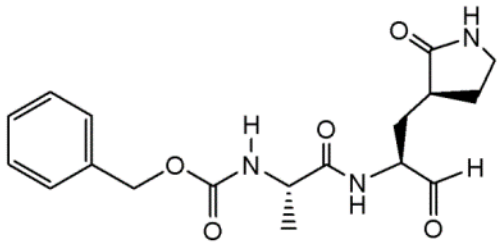

1

AP13-17-FR24-C13

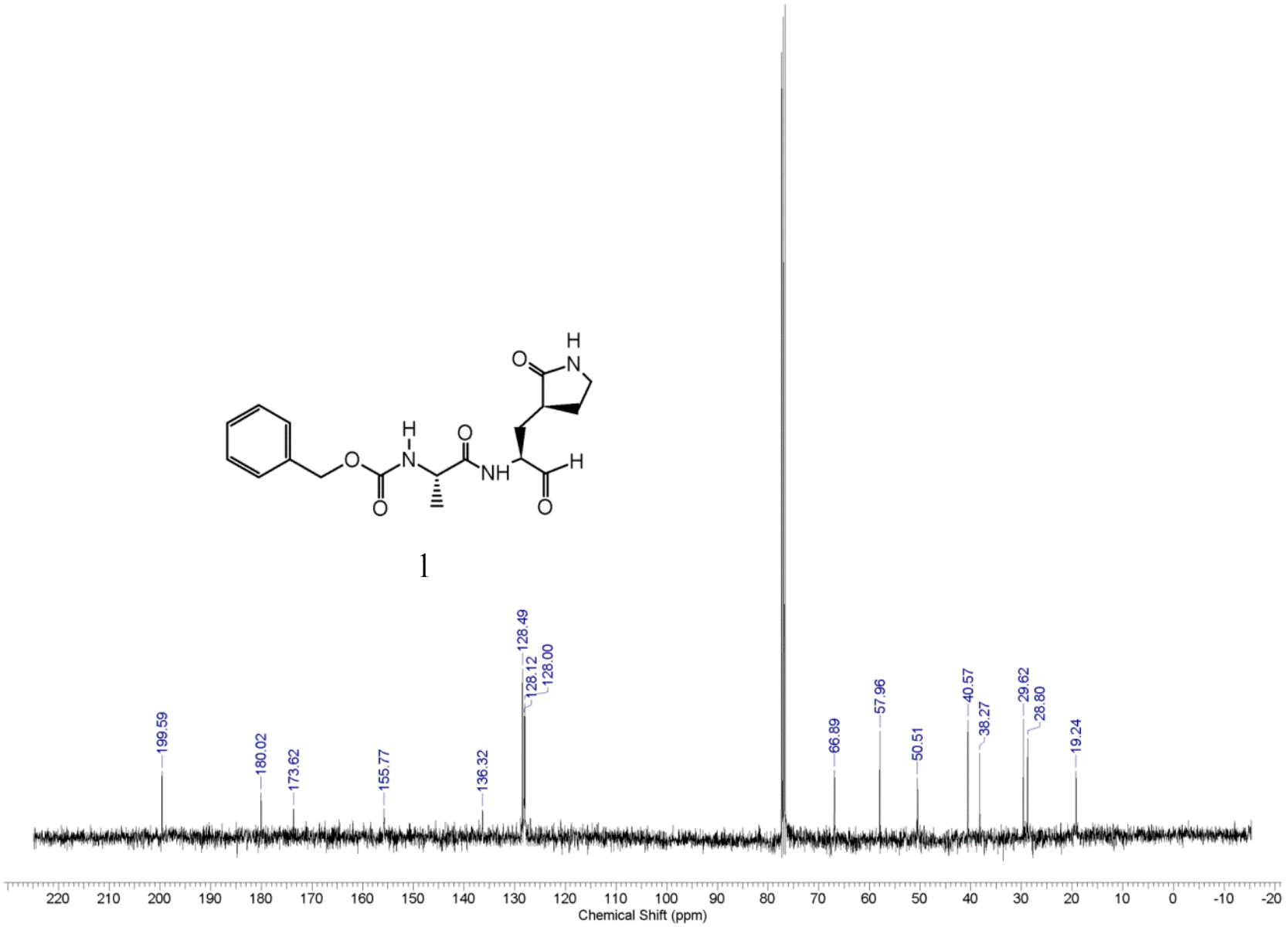

1

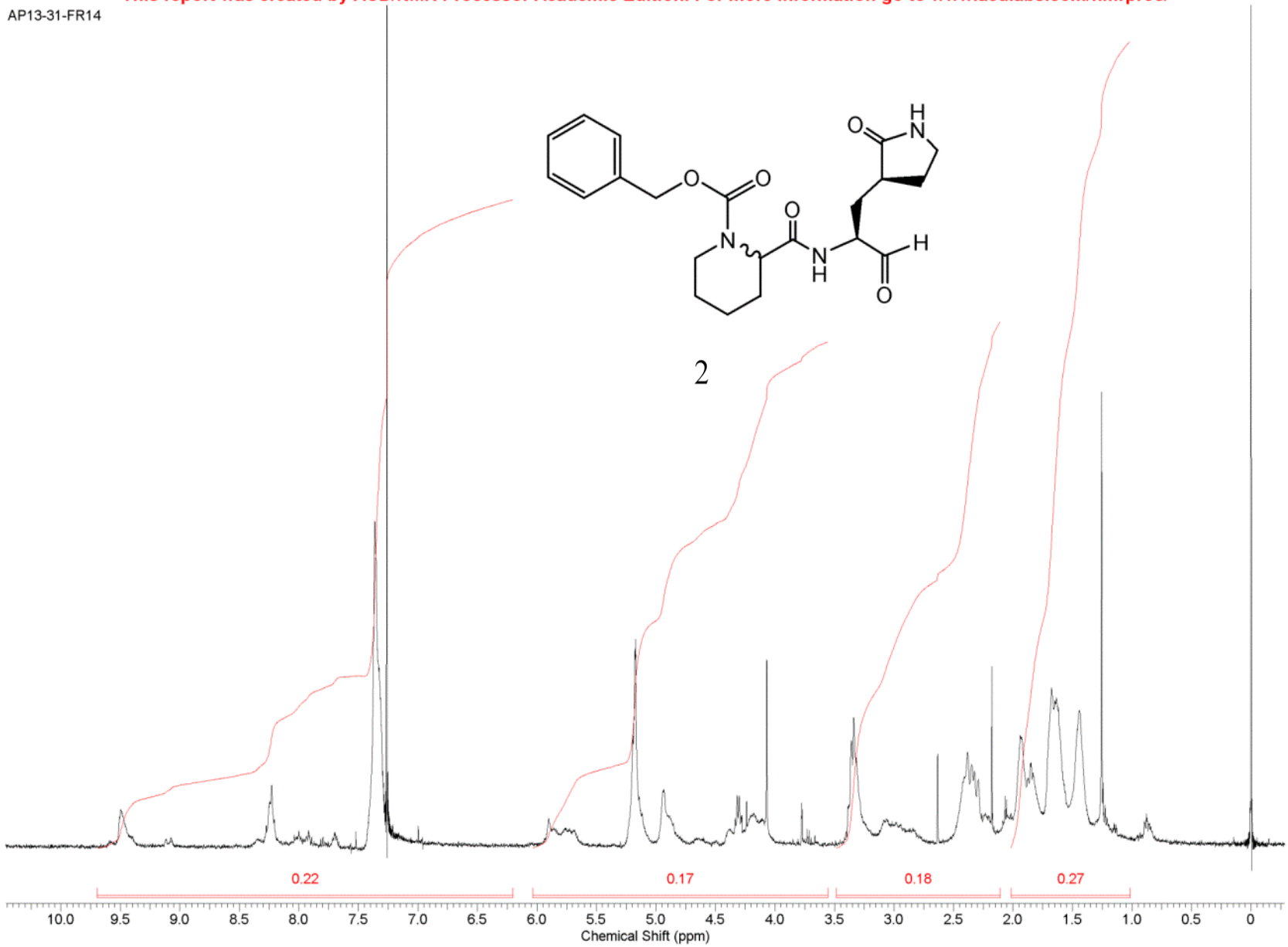

2

8/20/2013 6:05:54 PM

AP13-25-FR22

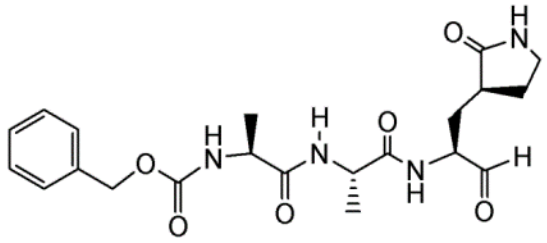

3

8/20/2013 6:24:54 PM

AP13-25-FR22-C13

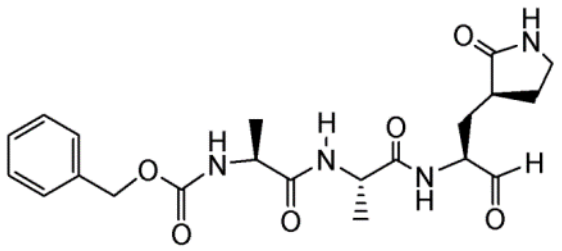

3

AP13-90-FR16-18

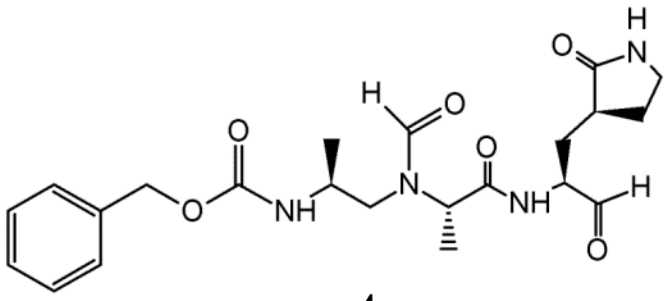

4

AP14-21-FR26-1H

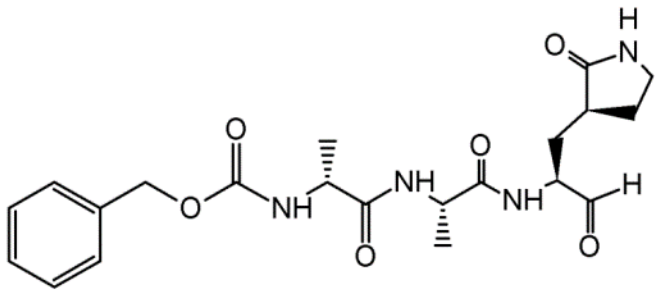

5

AP14-21-FR26-C13

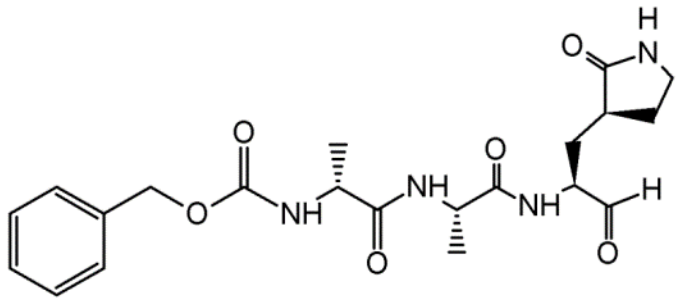

5

AP14-19-FR35-37

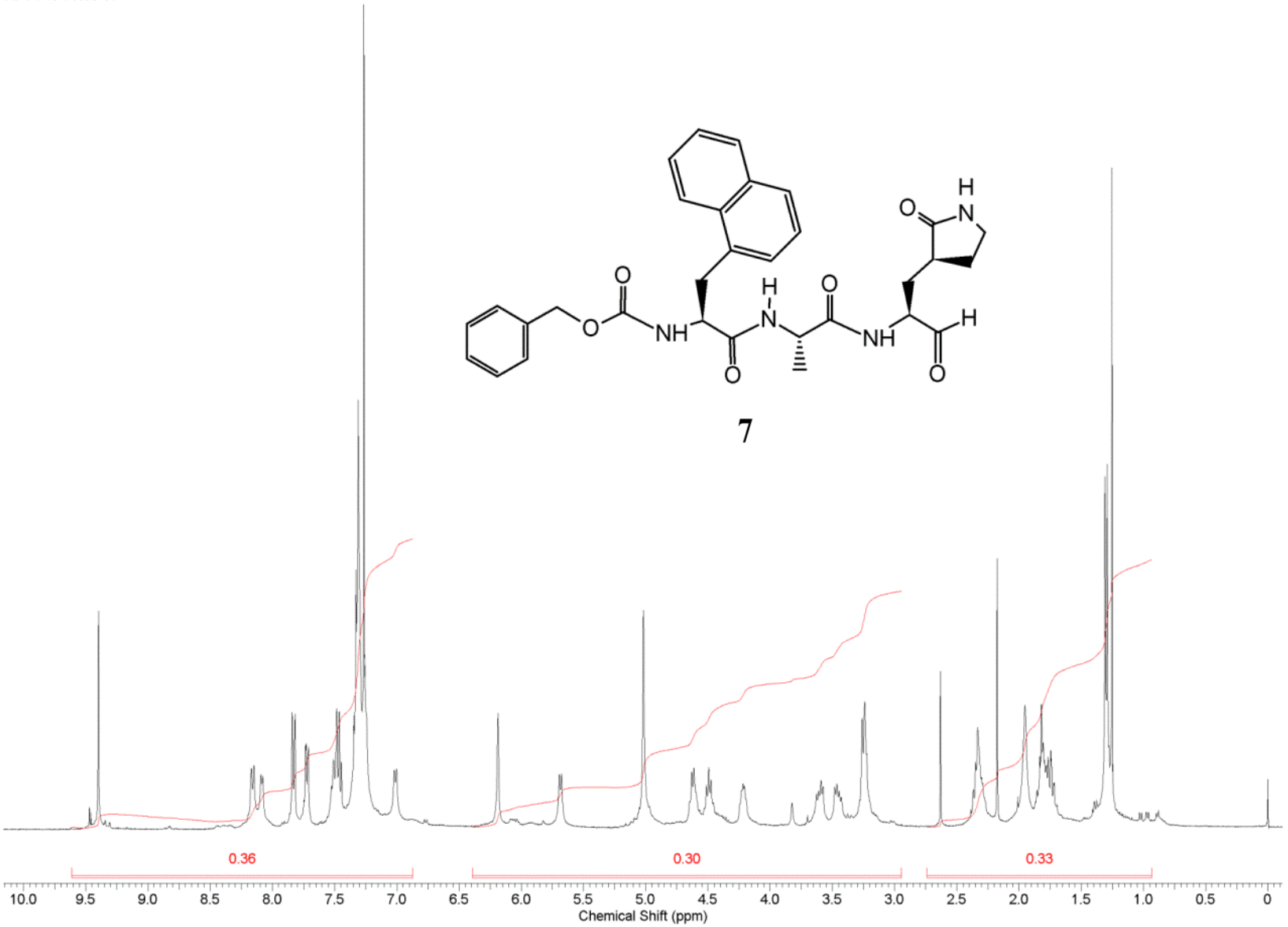

7

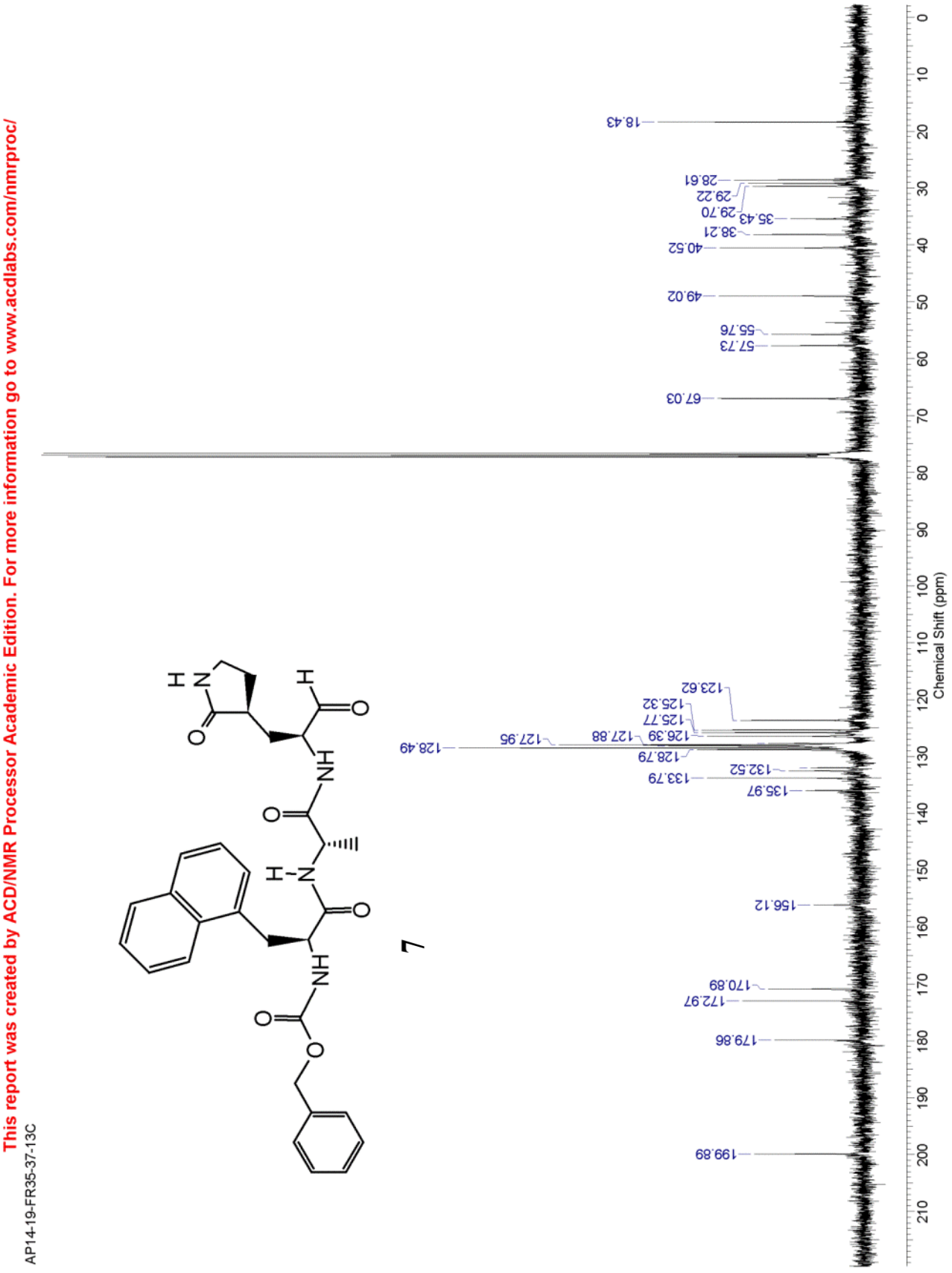
This report was created by ACD/NMR Processor Academic Edition. For more information go to www.acdlabs.com/nmrproc/
AP14-19-FR35-37-13C
7
18.43
28.61
29.22
29.70
35.43
38.21
40.52
49.02
55.76
57.73
67.03
123.62
125.32
125.77
126.39
127.88
127.95
128.49
128.79
132.52
133.79
135.97
156.12
170.89
172.97
179.86
199.89
Chemical Shift (ppm)

AP14-36-FR9

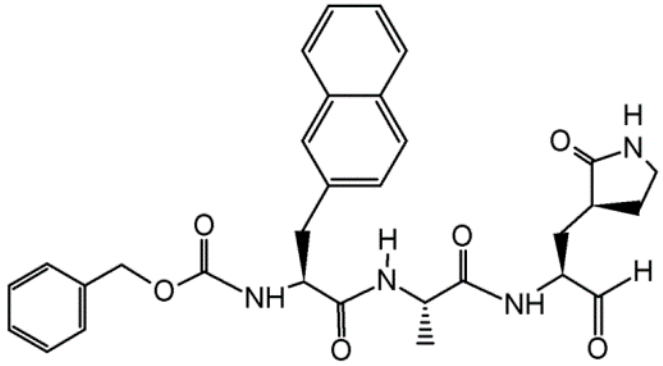

8

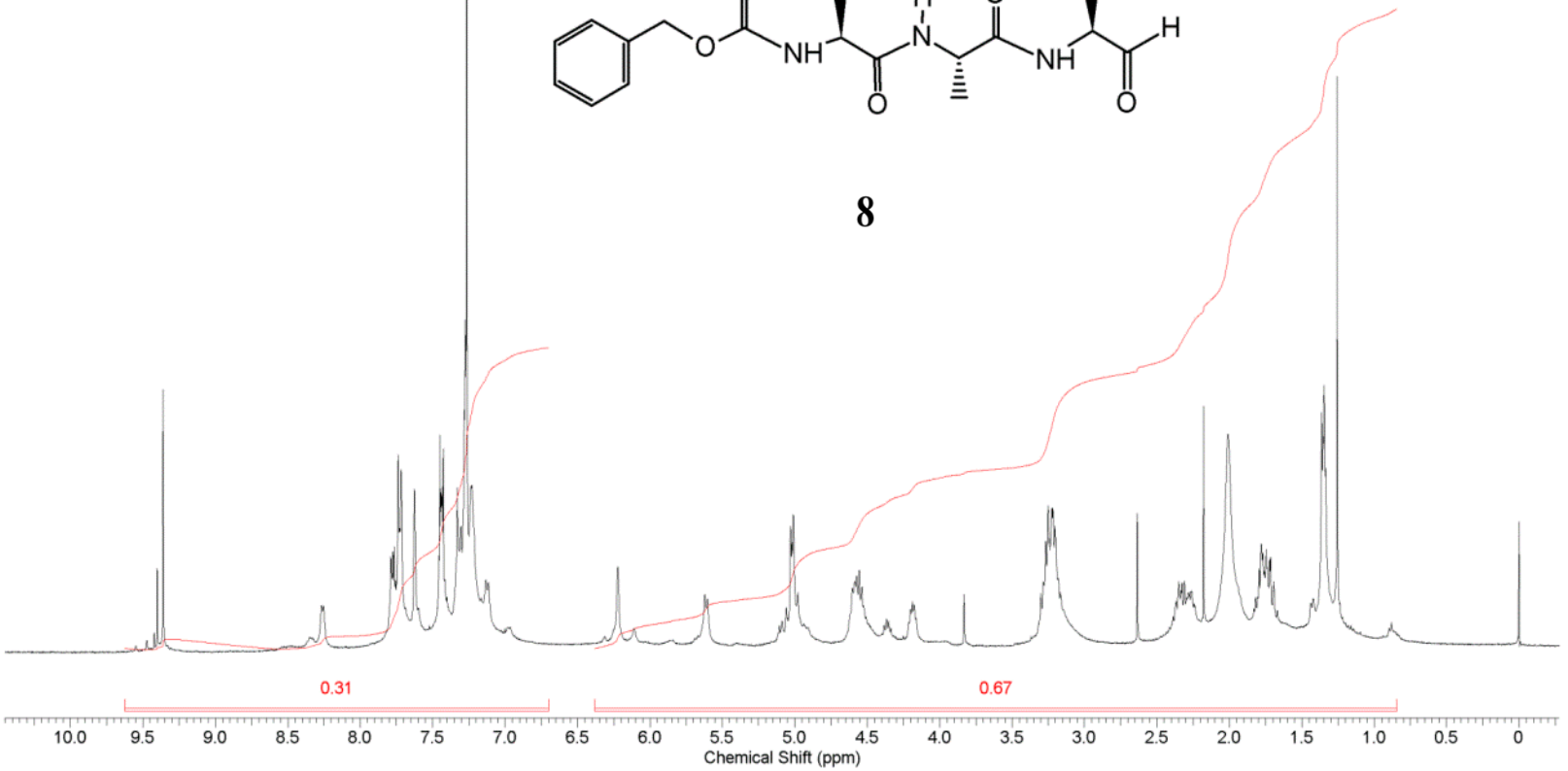

AP14-36-FR9-C13

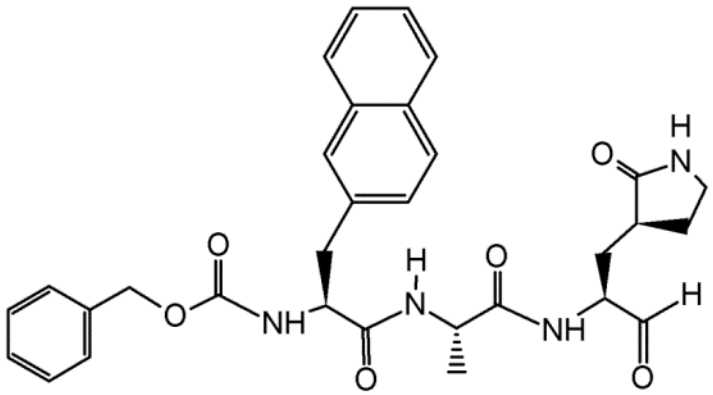

8

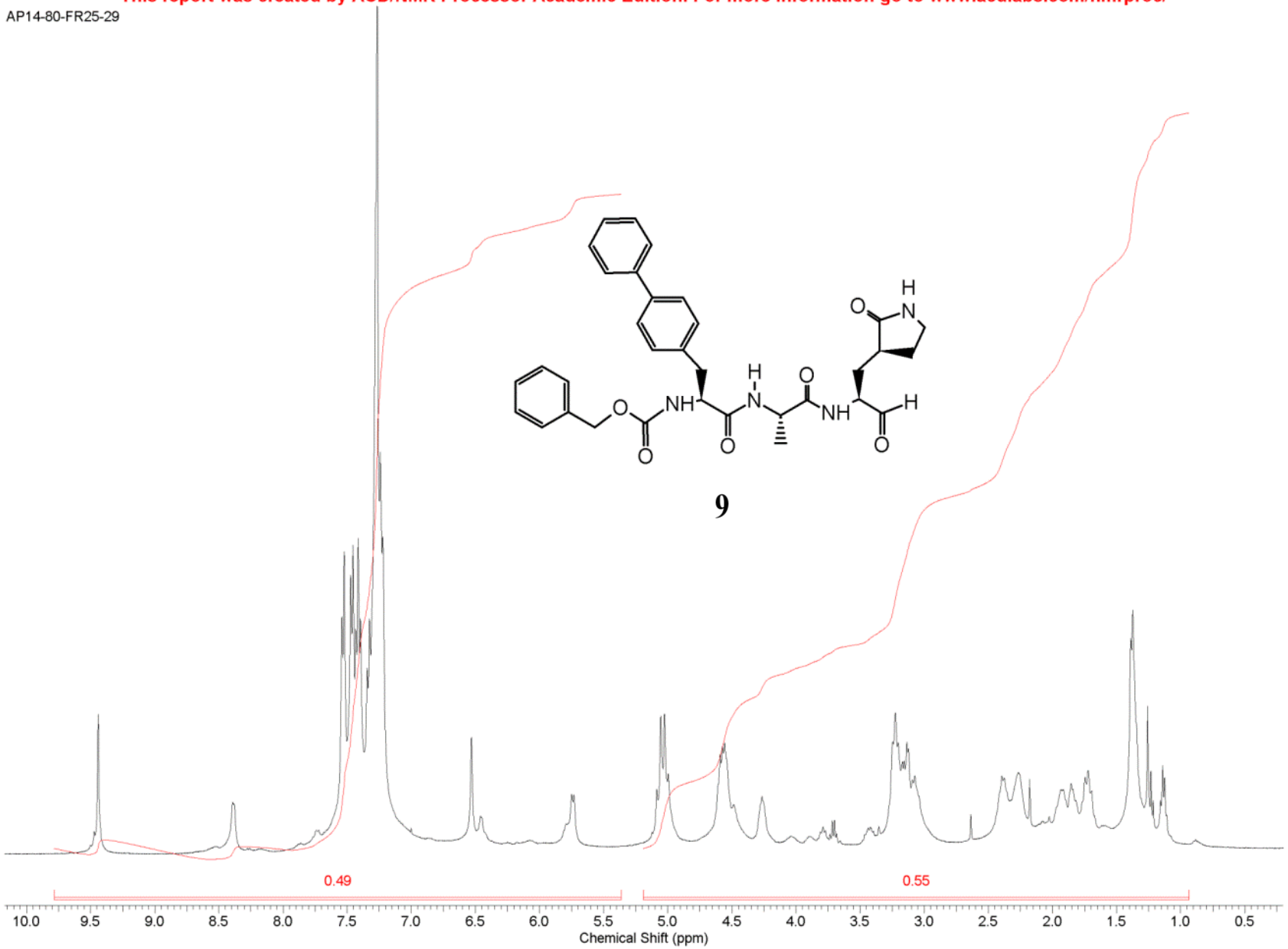

9

AP14-80-FR25-29-13C-AGAIN

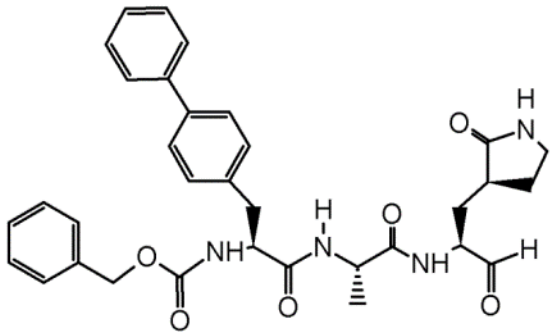

9

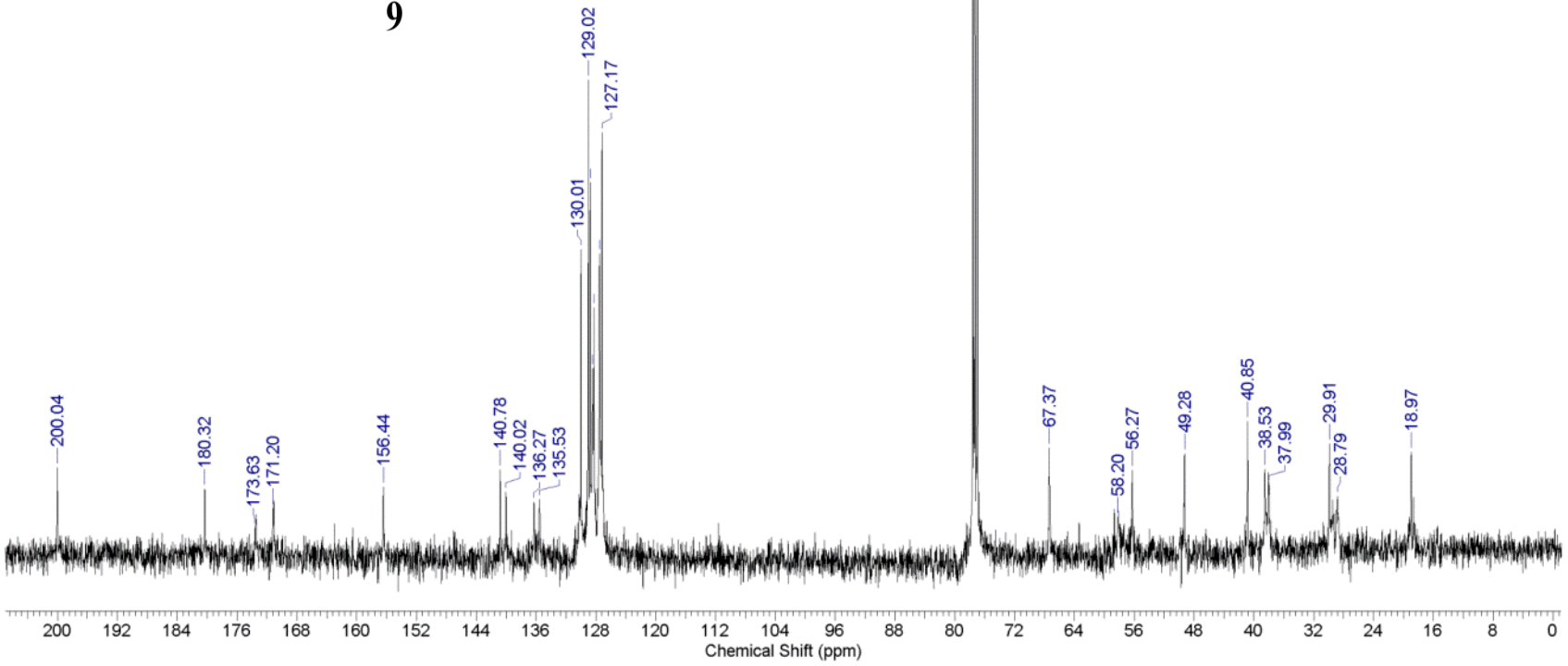

AP14-48-FR7

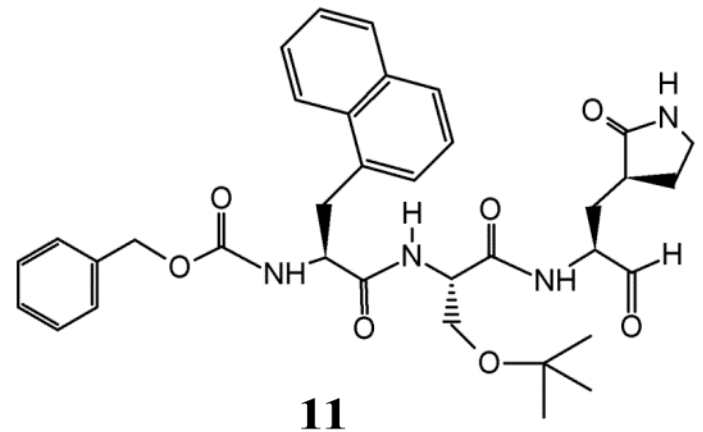

11

CQT

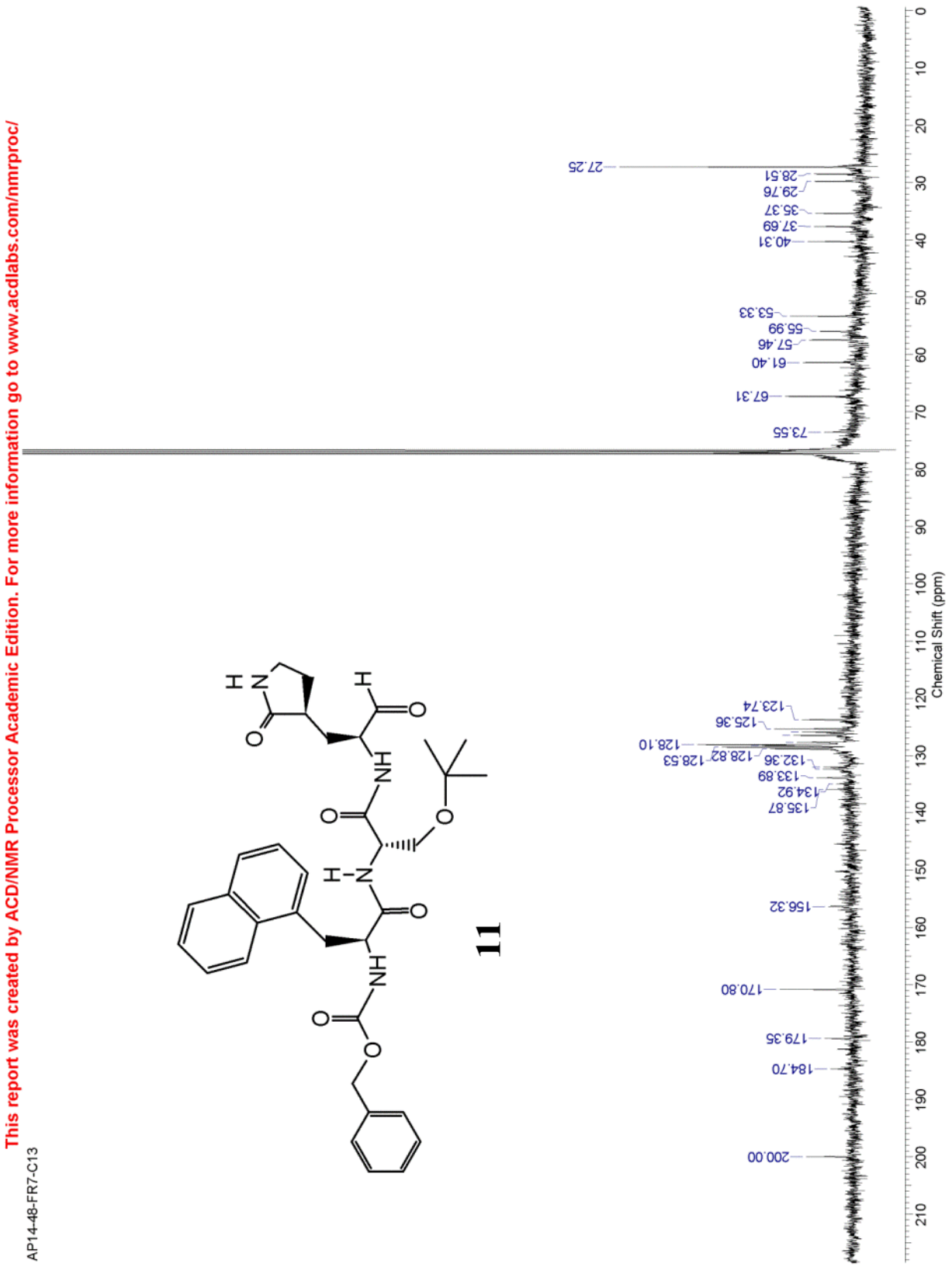
This report was created by ACD/NMR Processor Academic Edition. For more information go to www.acdlabs.com/nmrproc/
AP14-48-FR7-C13
27.25
28.51
29.76
35.37
37.69
40.31
53.33
55.99
57.46
61.40
67.31
73.55
123.74
125.36
128.10
128.53
128.82
132.36
133.89
134.92
135.87
156.32
170.80
179.35
184.70
200.00
Chemical Shift (ppm)
11

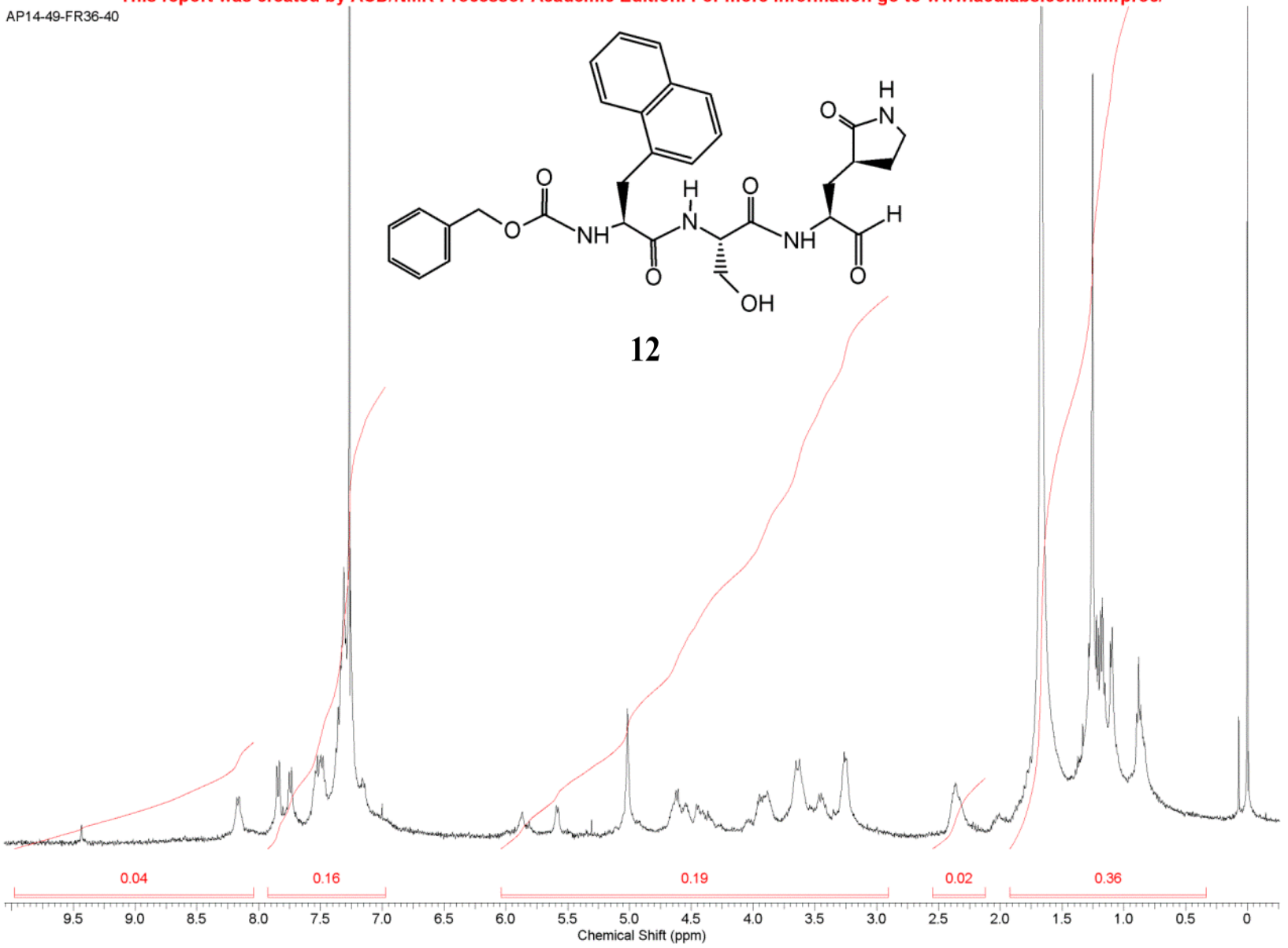

12

AP13-27-FR19

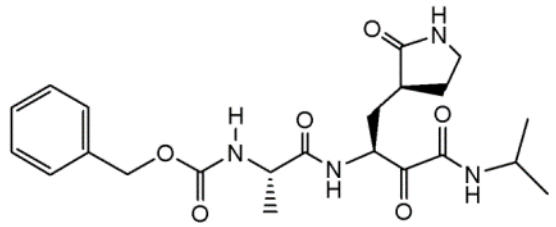

13

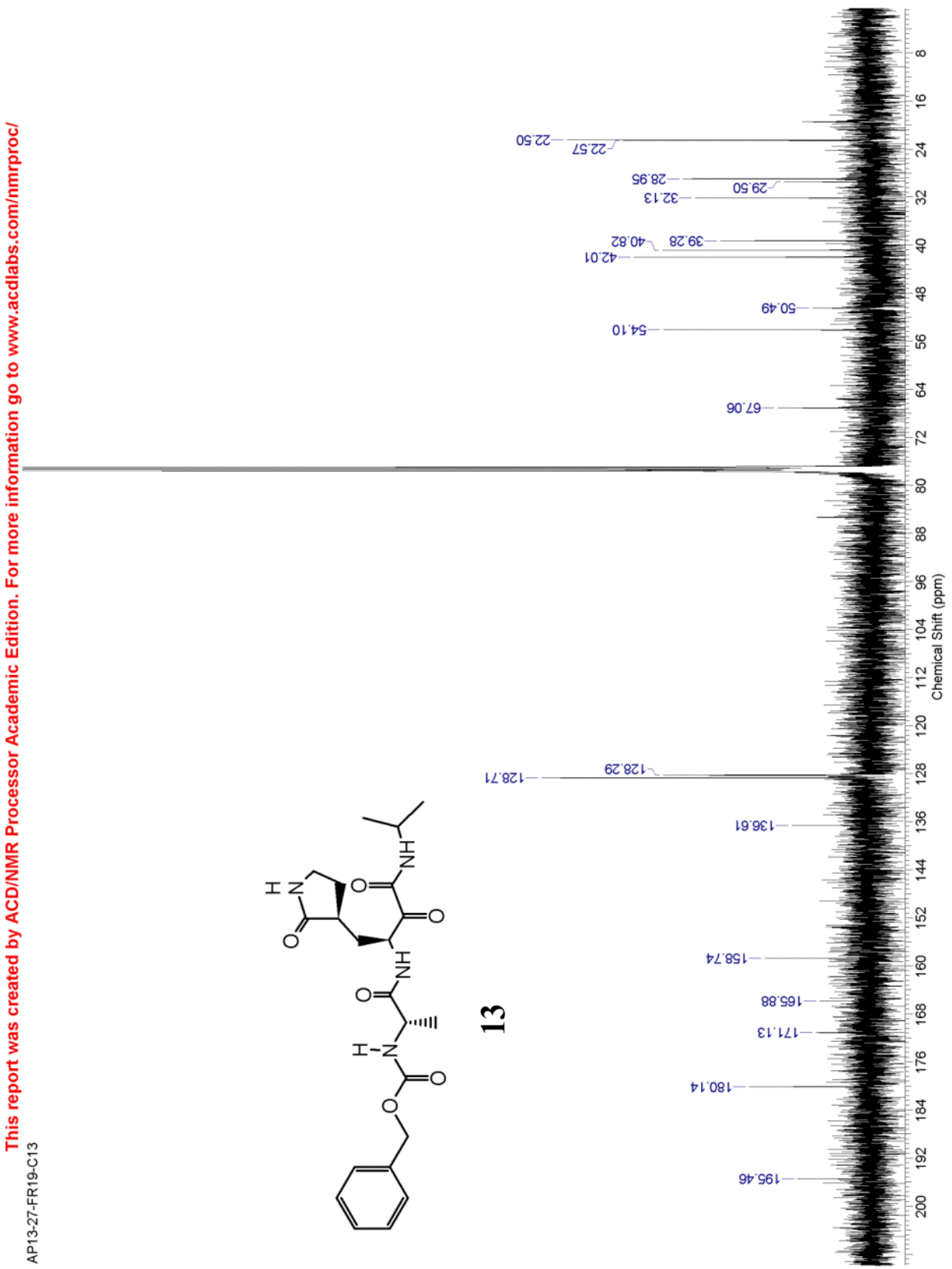
This report was created by ACD/NMR Processor Academic Edition. For more information go to www.acdlabs.com/nmrproc/
AP13-27-FR19-C13
13
22.50
22.57
28.95
29.50
32.13
39.28
40.82
42.01
50.49
54.10
67.06
128.29
128.71
136.61
158.74
165.88
171.13
180.14
195.46
Chemical Shift (ppm)

AP13-35-FR21

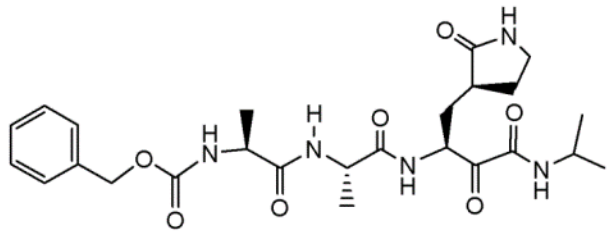

14

AP13-35-FR21-C13

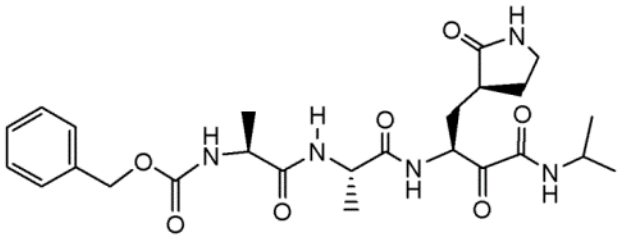

14

AP13-98-FR20-22

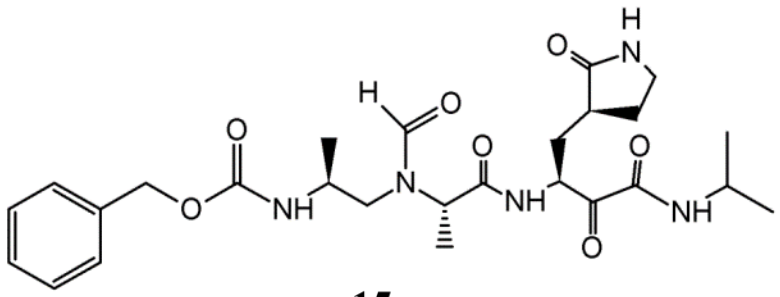

15

AP14-26-FR15

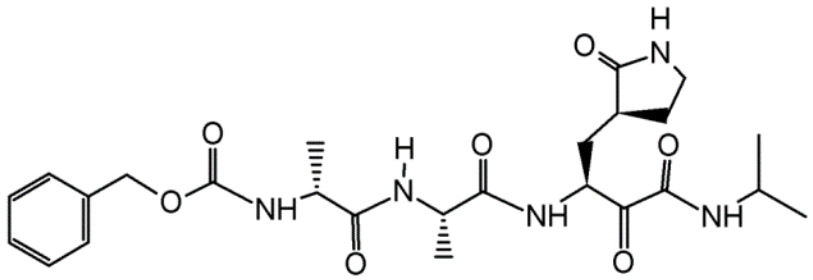

16

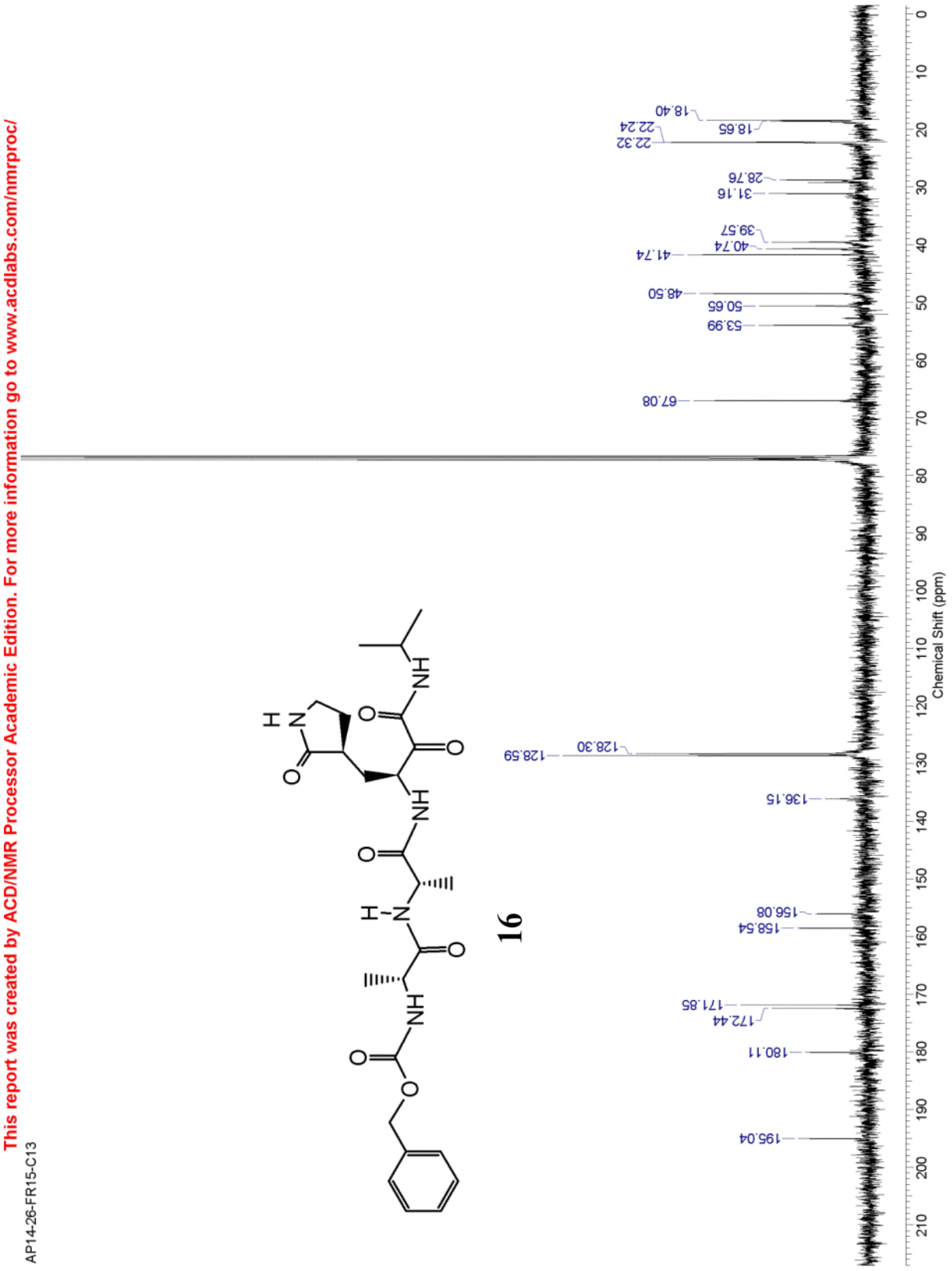
This report was created by ACD/NMR Processor Academic Edition. For more information go to www.acdlabs.com/nmrproc/
AP14-26-FR15-C13
16
18.40
18.65
22.24
22.32
28.76
31.16
39.57
40.74
41.74
48.50
50.65
53.99
67.08
128.30
128.59
136.15
156.08
158.54
171.85
172.44
180.11
195.04
Chemical Shift (ppm)

AP14-25-FR18

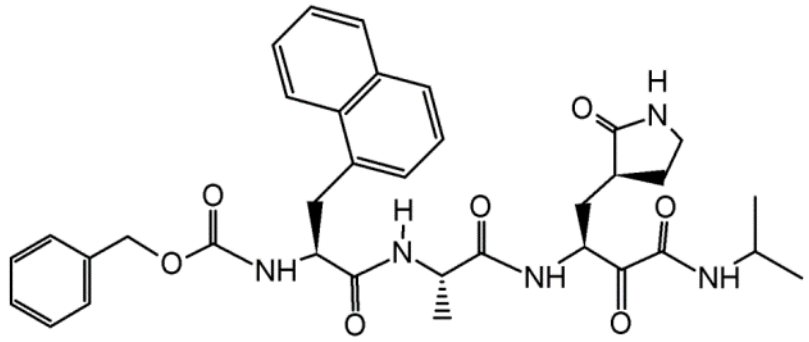

17

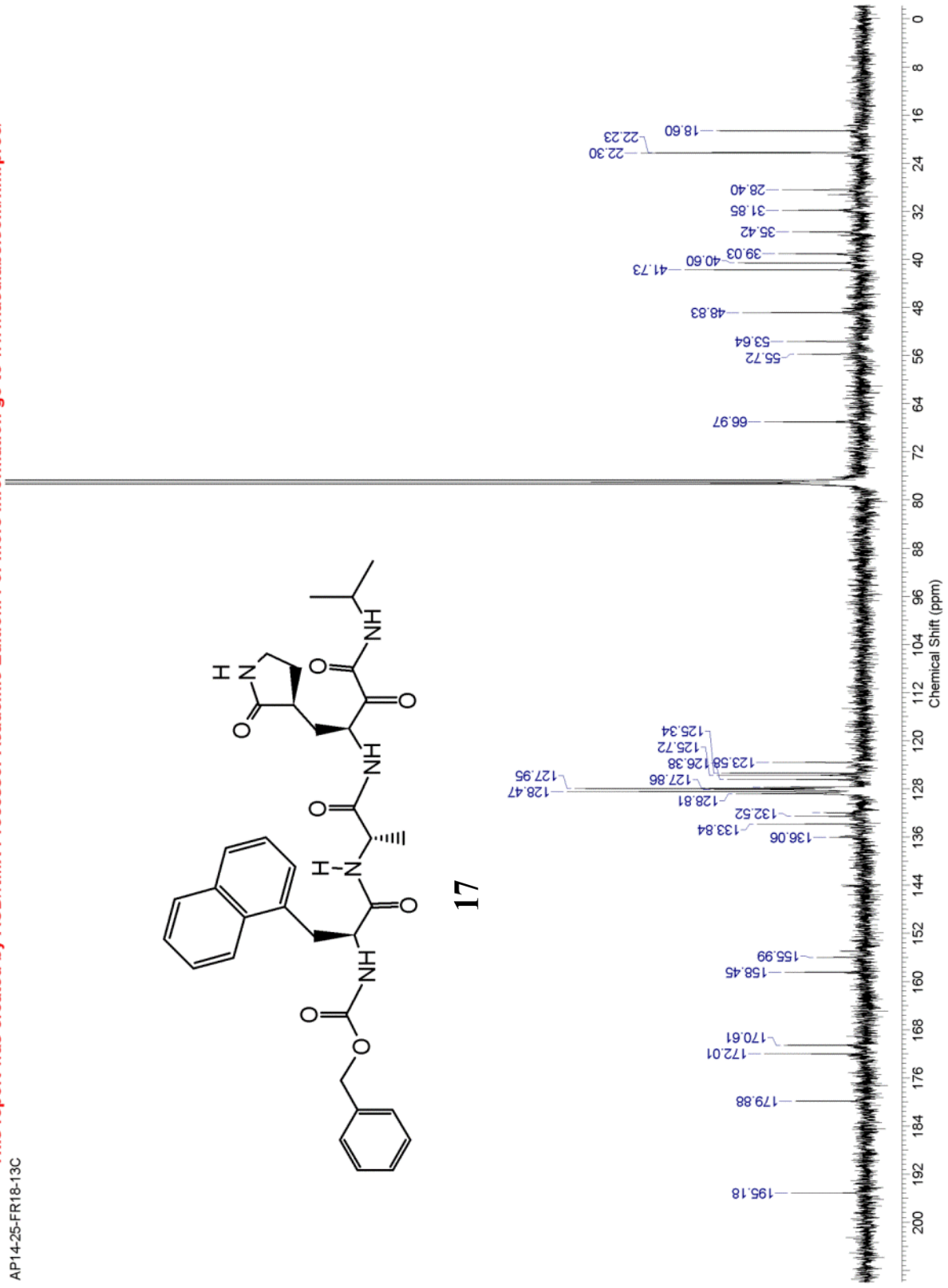
This report was created by ACD/NMR Processor Academic Edition. For more information go to www.acdlabs.com/nmrproc/
AP14-25-FR18-13C
18.60
22.23
22.30
28.40
31.85
35.42
39.03
40.60
41.73
48.83
53.64
55.72
66.97
123.58
125.34
125.72
126.38
127.86
127.95
128.47
128.81
132.52
133.84
136.06
155.99
158.45
170.61
172.01
179.88
195.18
Chemical Shift (ppm)

17

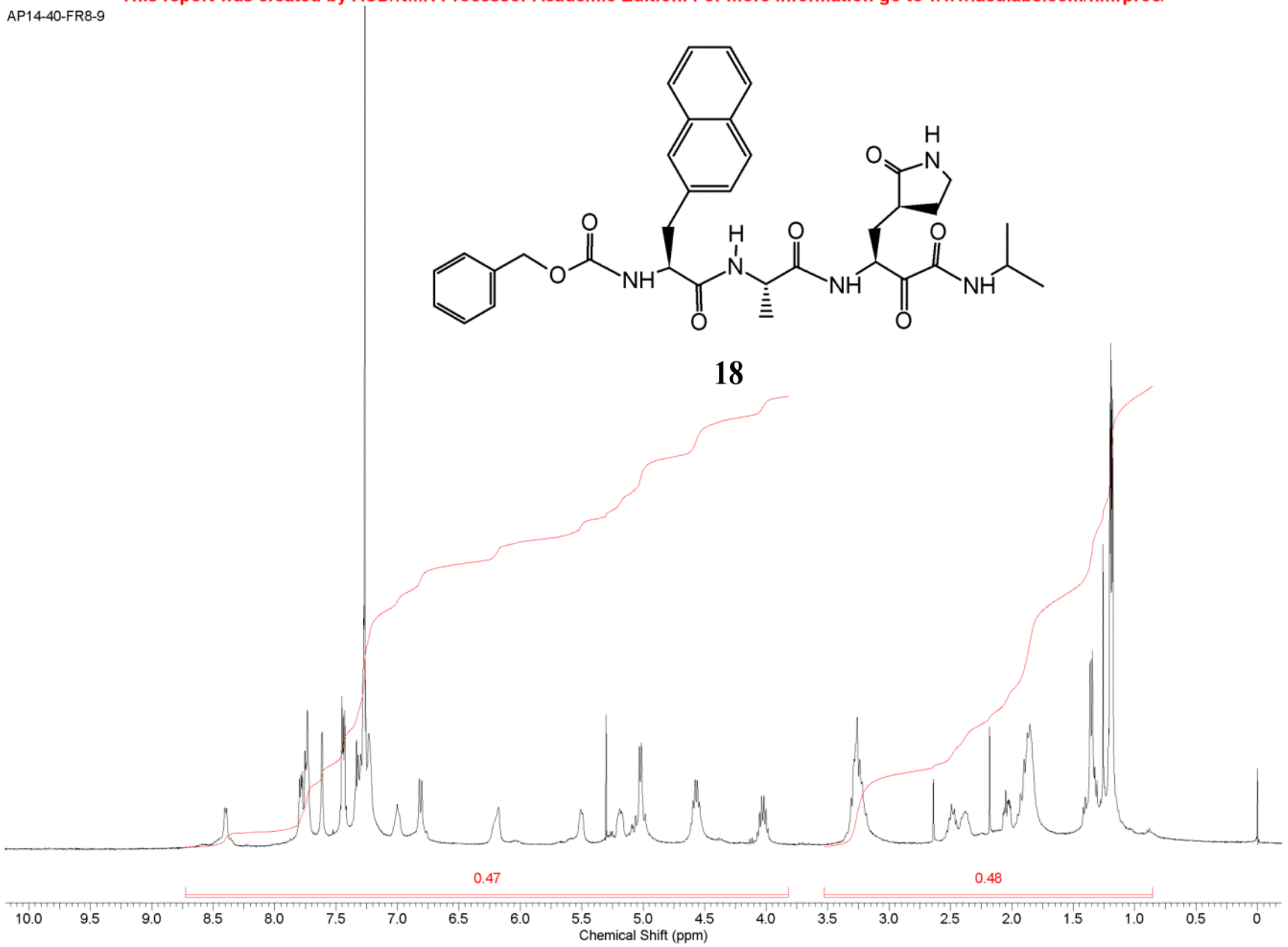

18

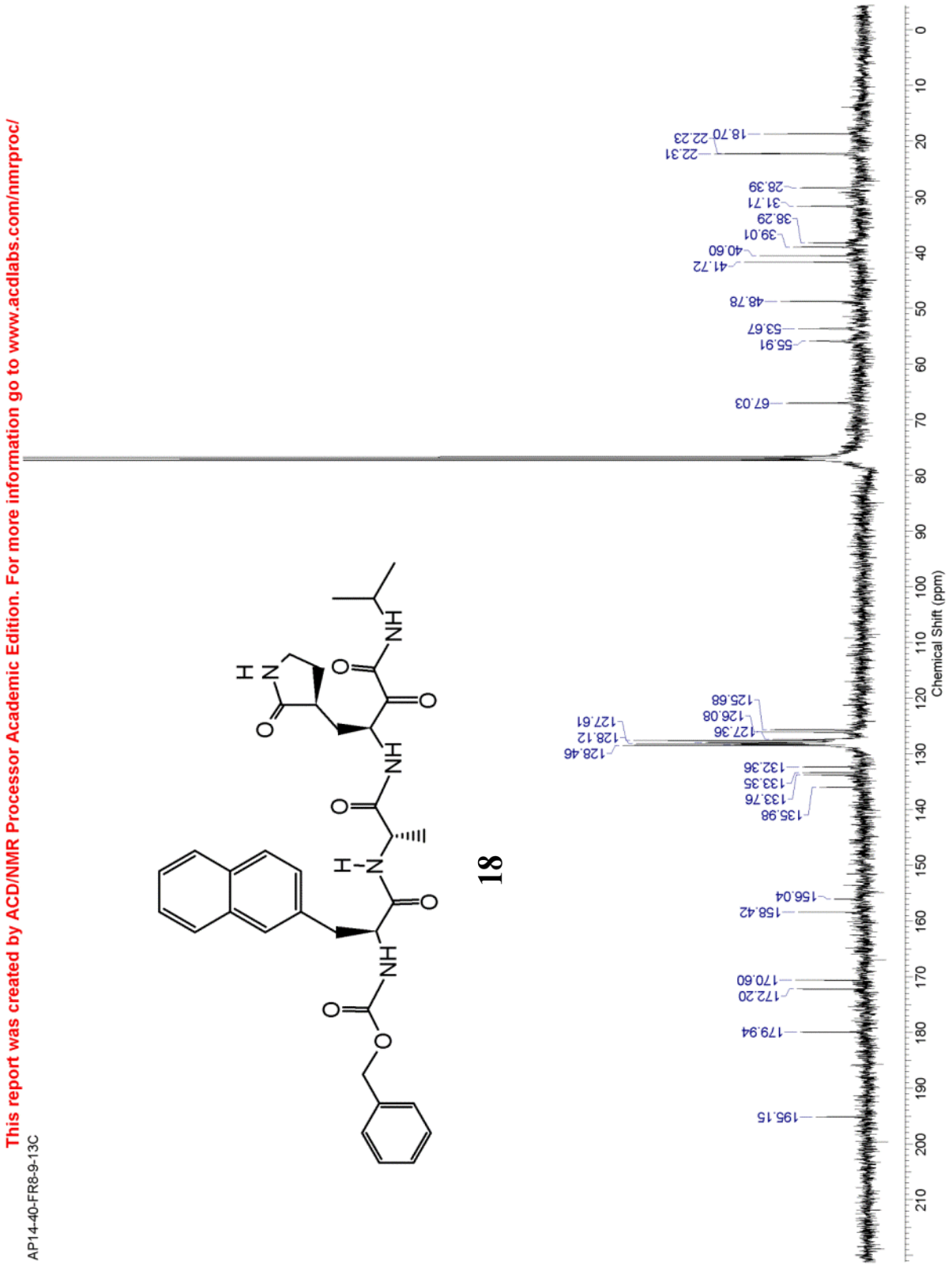
This report was created by ACD/NMR Processor Academic Edition. For more information go to www.acdlabs.com/nmrproc/
AP14-40-FR8-9-13C
18.70
22.23
22.31
28.39
31.71
38.29
39.01
40.60
41.72
48.78
53.67
55.91
67.03
125.68
126.08
127.36
127.61
128.12
128.46
132.36
133.35
133.76
135.98
156.04
158.42
170.60
172.20
179.94
195.15
Chemical Shift (ppm)

18

AP14-54-FR6-20

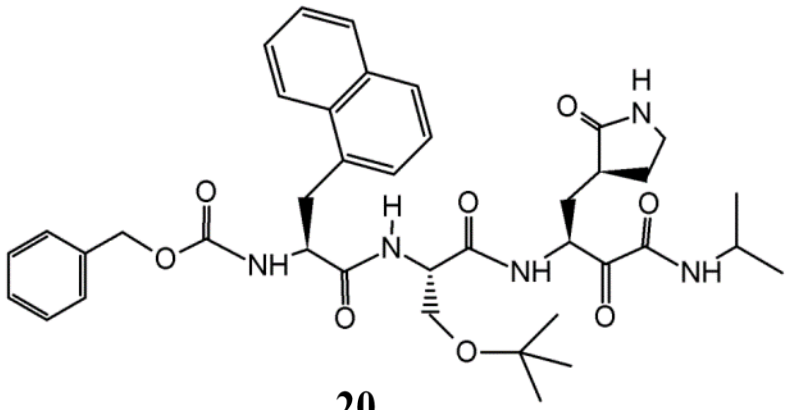

20

AP14-84-FR54-60

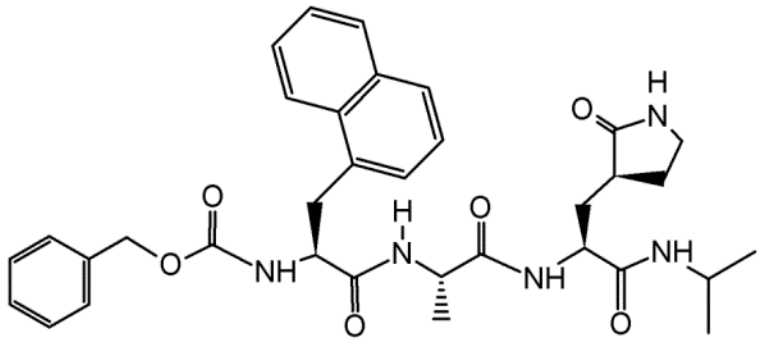

21

AP14-91-FR46-51

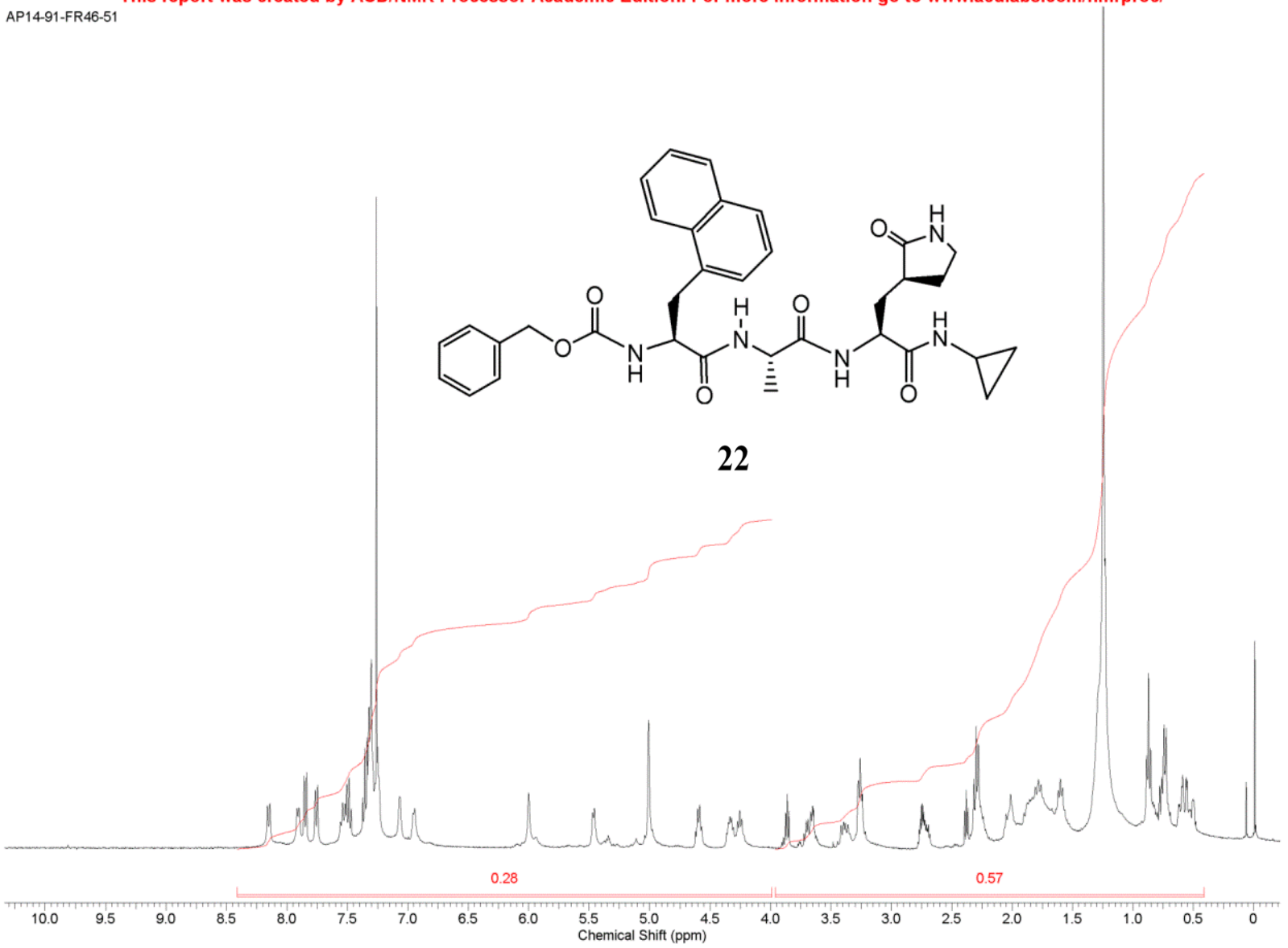

22

AP14-11-FR24-25

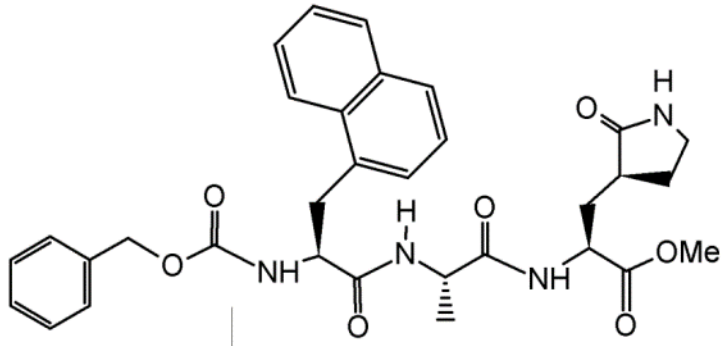

23

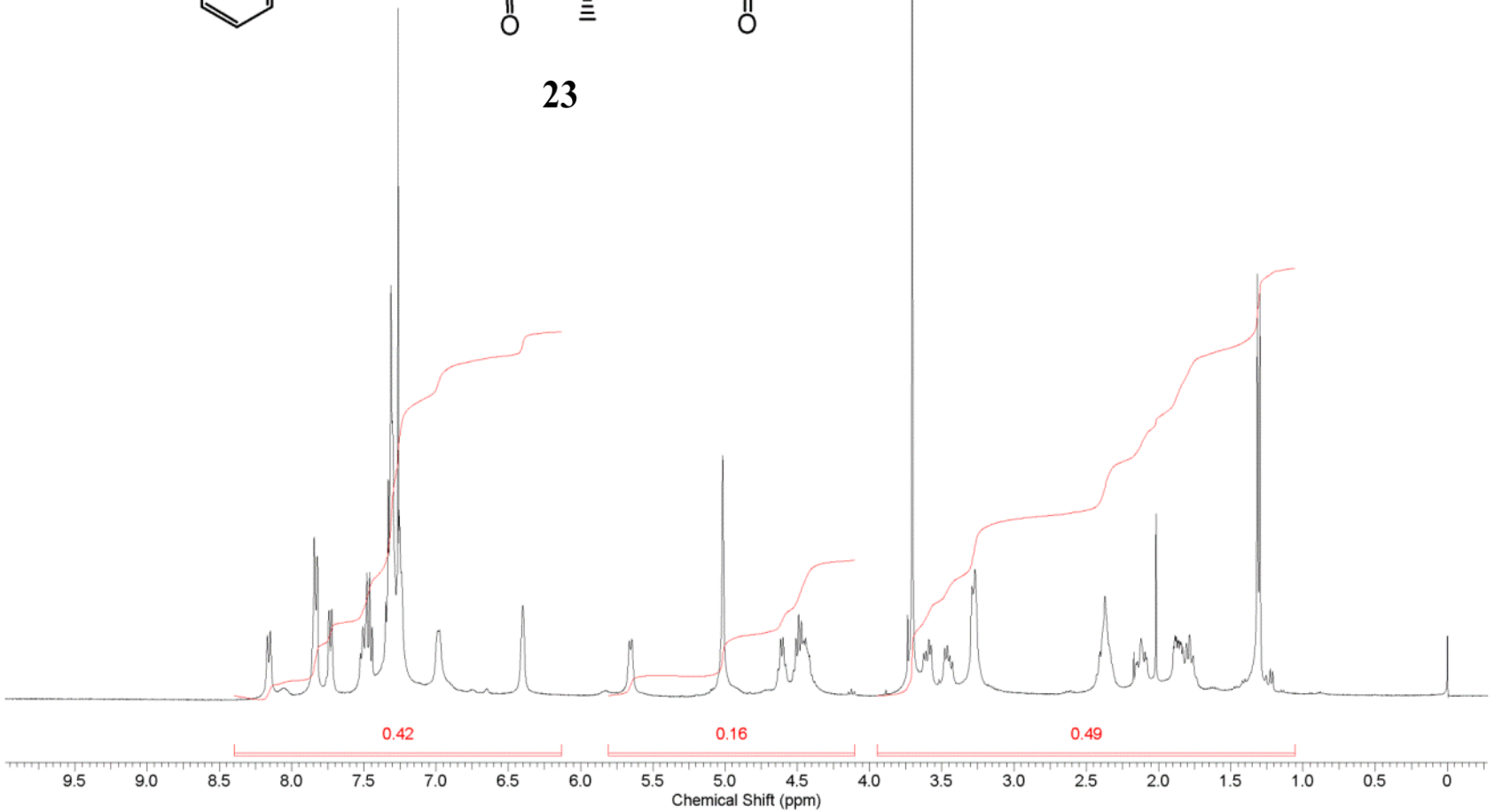

AP14-11-FR24-25-13C

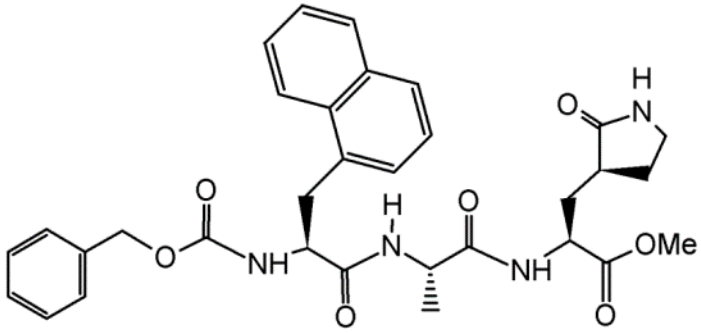

23

AP14-81-SOLID

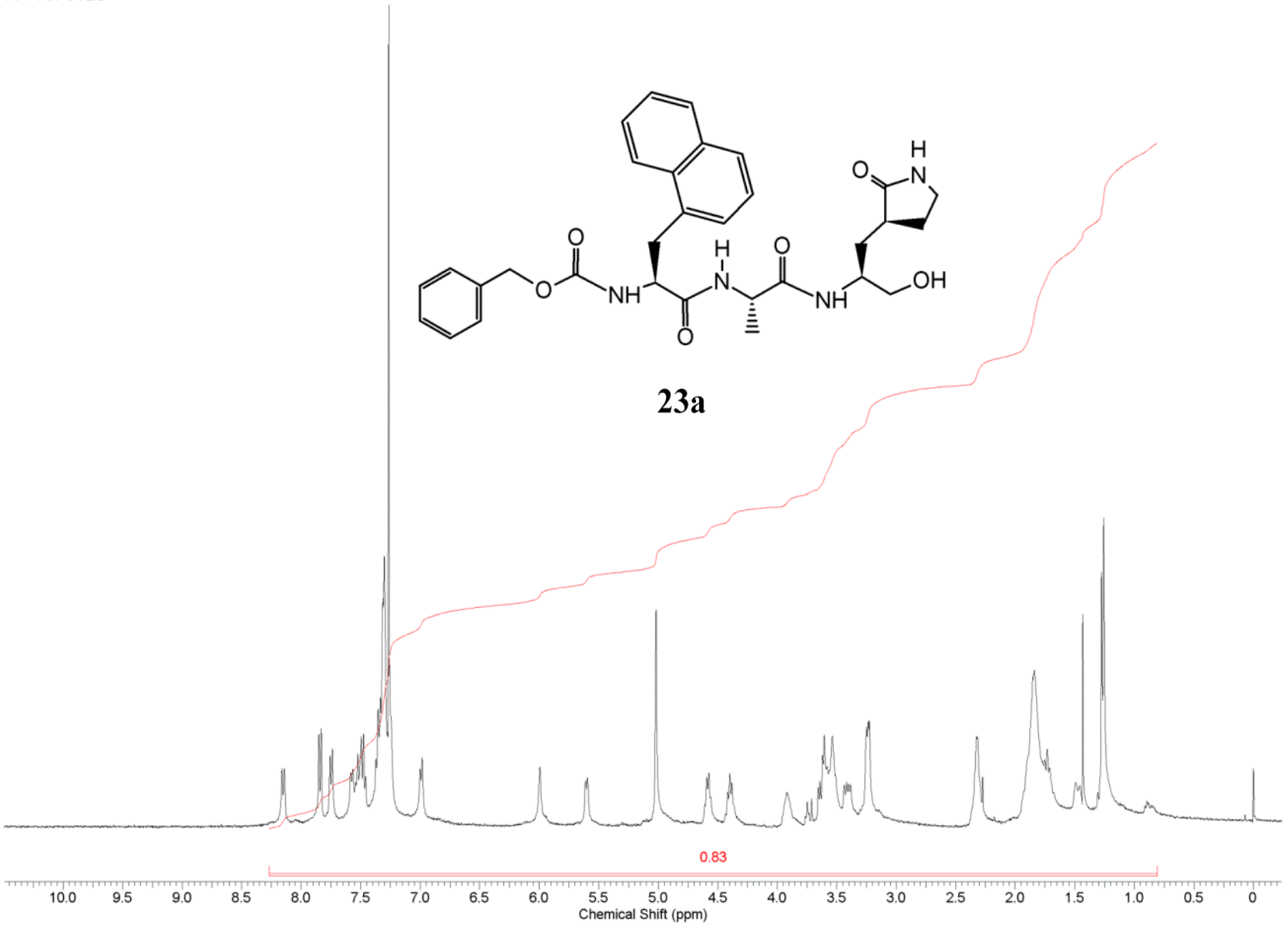

23a

AP14-62-FR28

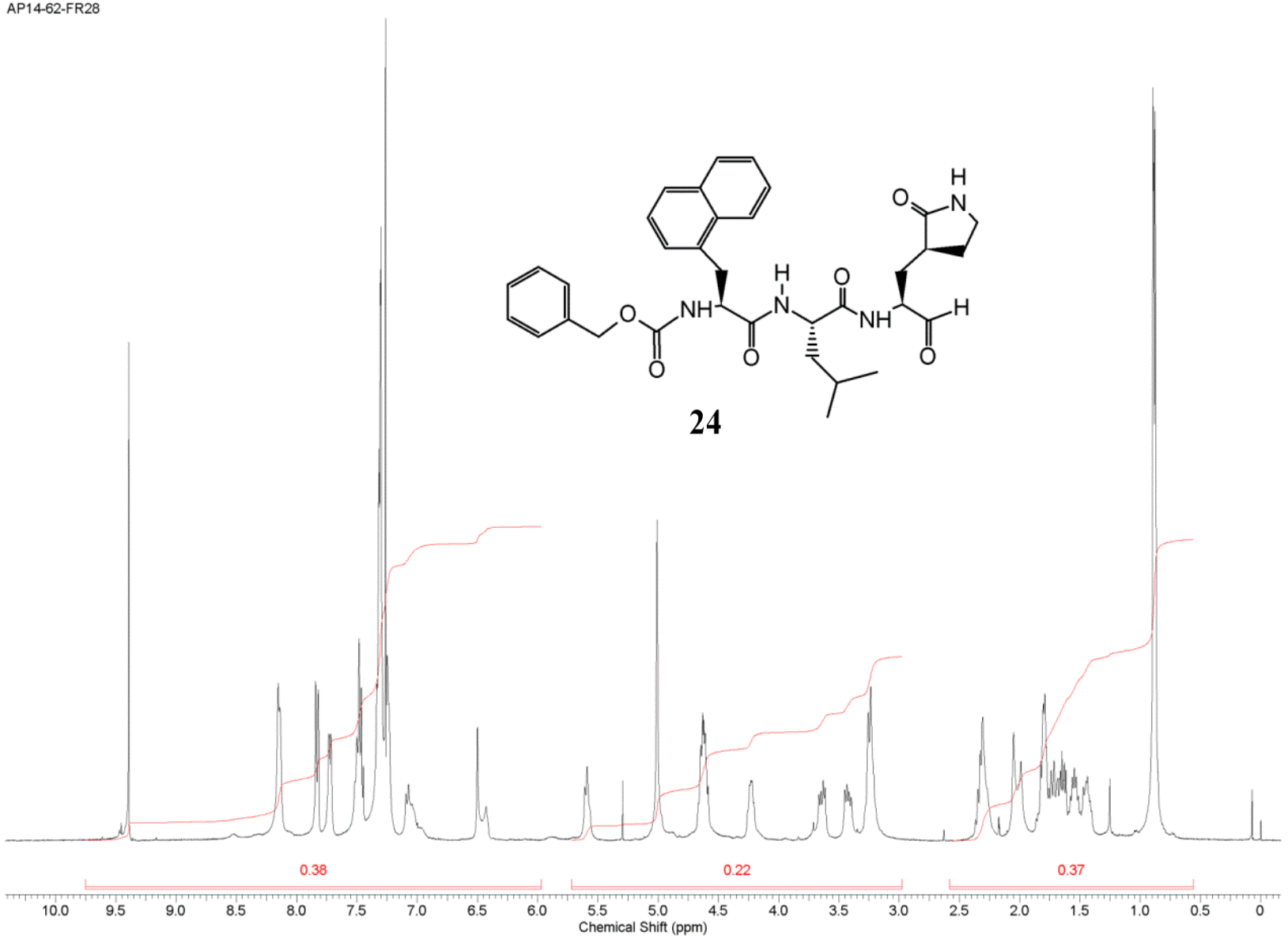

24

AP14-62-FR28-13C

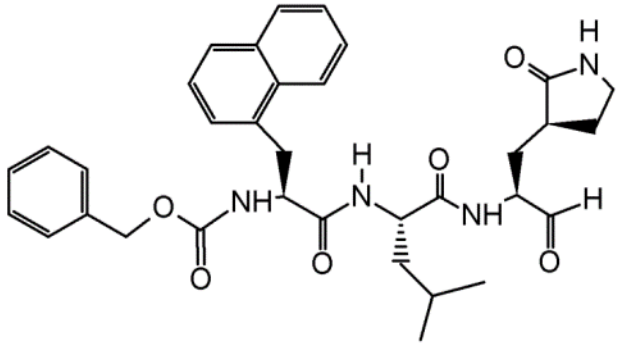

24

AP15-46-FR23

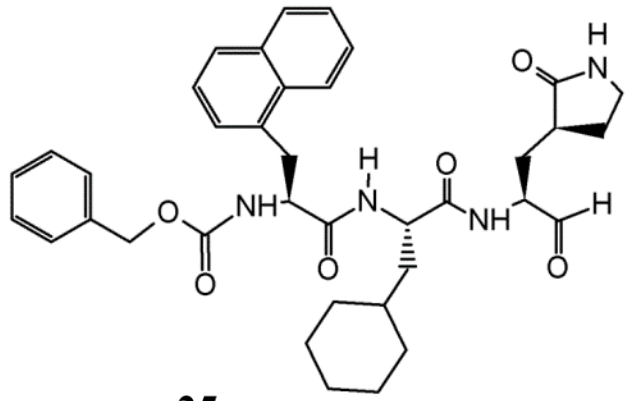

25

AP15-46-FR23-13C

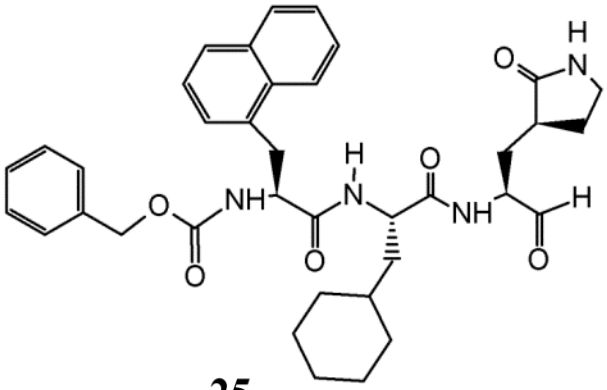

25

AP17-88-FR21-22

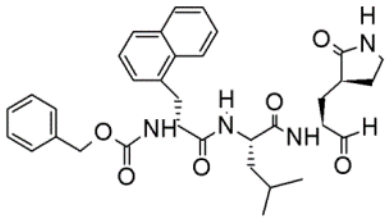

27

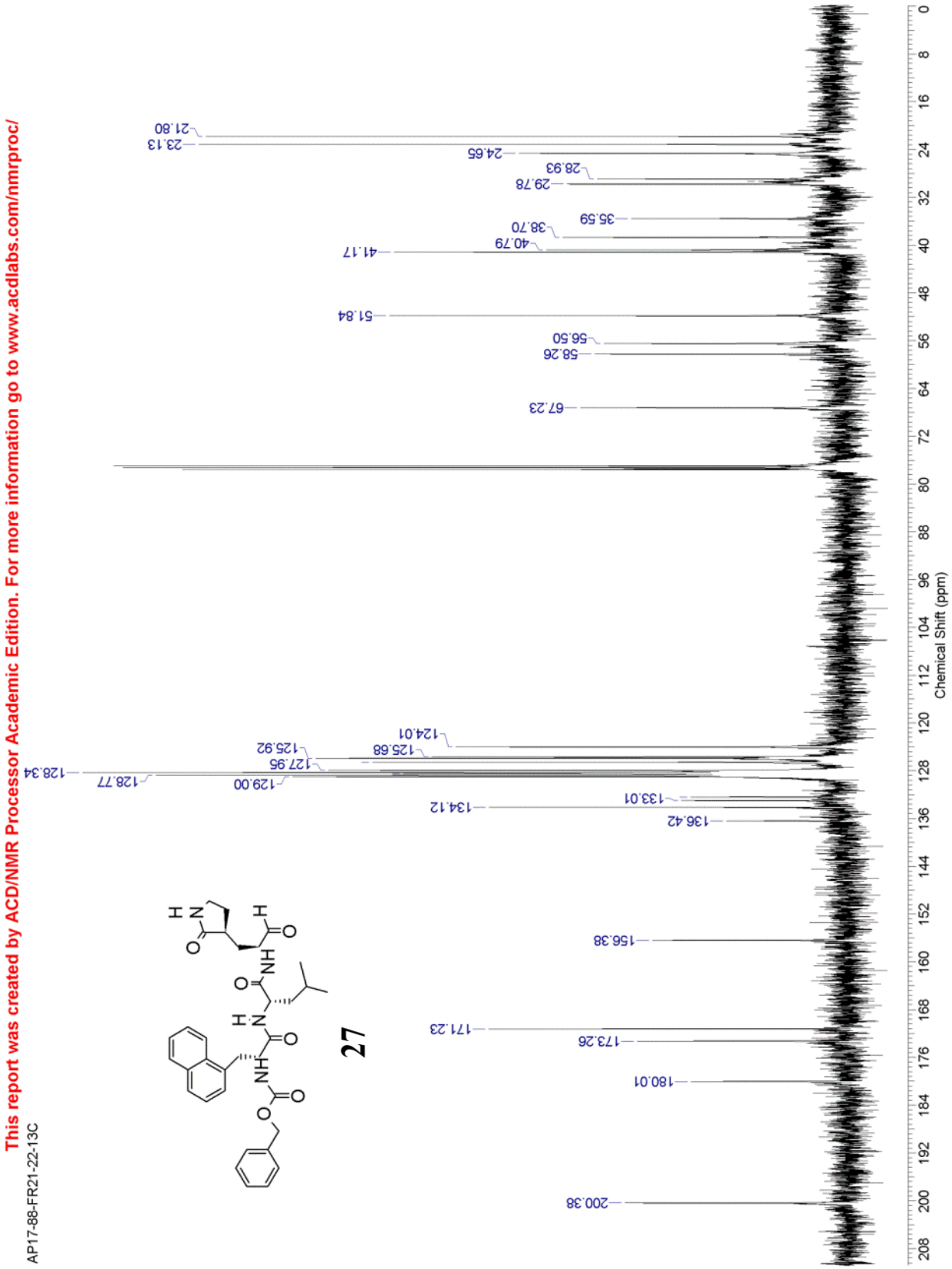
This report was created by ACD/NMR Processor Academic Edition. For more information go to www.acdlabs.com/nmrproc/
AP17-88-FR21-22-13C
27
Chemical Shift (ppm)
200.38
180.01
173.26
171.23
156.38
136.42
134.12
133.01
129.00
128.77
128.34
127.95
125.92
125.68
124.01
67.23
58.26
56.50
51.84
41.17
40.79
38.70
35.59
29.78
28.93
24.65
23.13
21.80

AP17-87-FR20-21

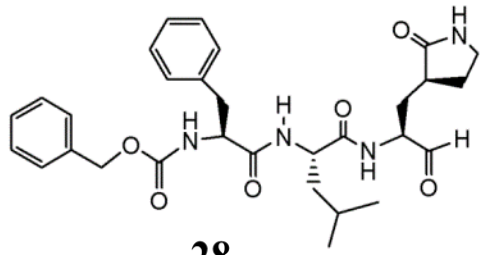

28

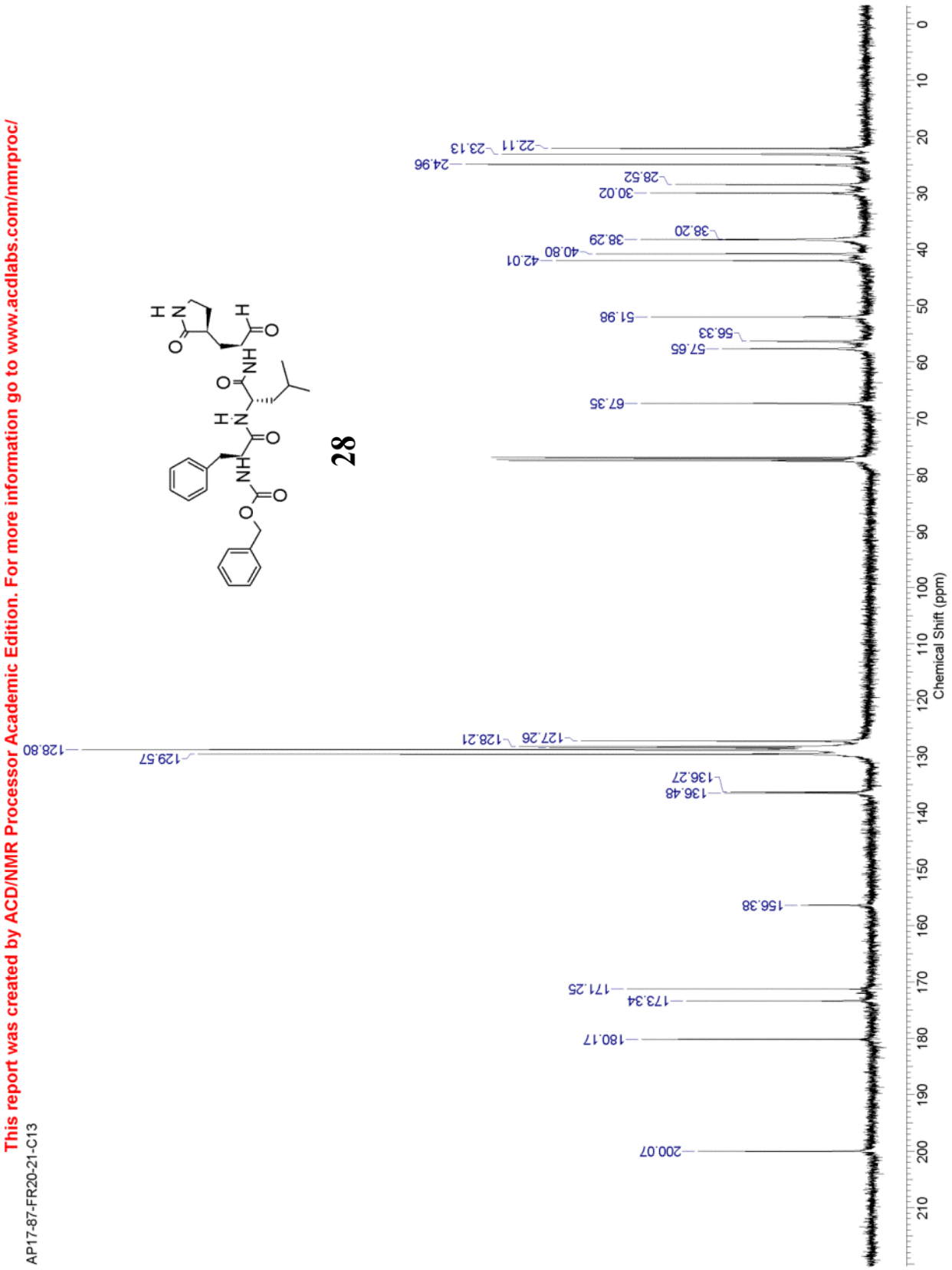
This report was created by ACD/NMR Processor Academic Edition. For more information go to www.acdlabs.com/nmrproc/
AP17-87-FR20-21-C13
28
200.07
180.17
173.34
171.25
156.38
136.48
136.27
129.57
128.80
128.21
127.26
67.35
57.65
56.33
51.98
42.01
40.80
38.29
38.20
30.02
28.52
24.96
23.13
22.11
Chemical Shift (ppm)

AP17-90-FR30-31

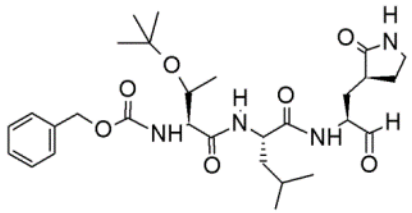

29

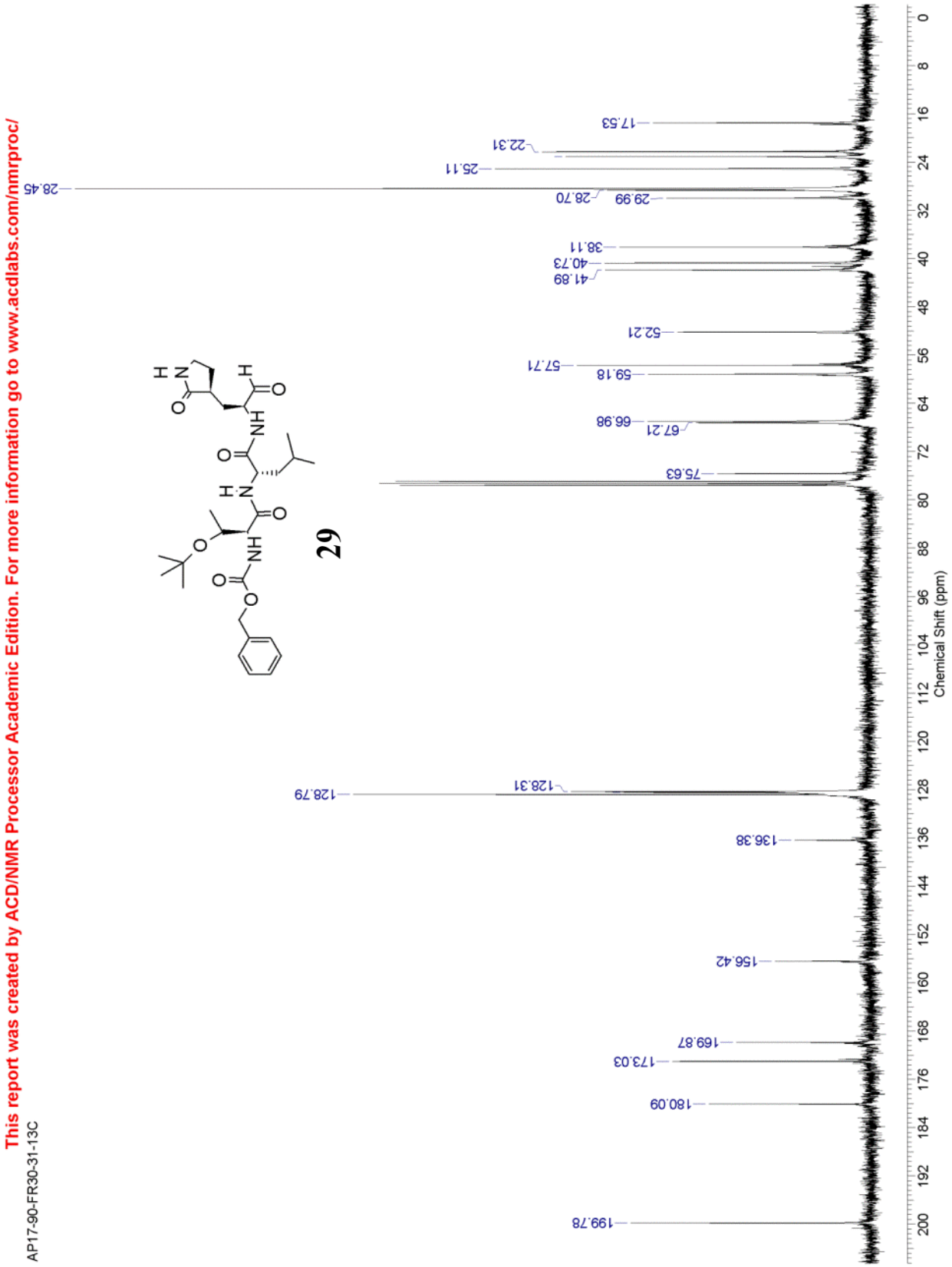
This report was created by ACD/NMR Processor Academic Edition. For more information go to www.acdlabs.com/nmrproc/
AP17-90-FR30-31-13C
29
199.78
180.09
173.03
169.87
156.42
136.38
128.79
128.31
75.63
67.21
66.98
59.18
57.71
52.21
41.89
40.73
38.11
29.99
28.70
28.45
25.11
22.31
17.53
Chemical Shift (ppm)

AP17-89-FR28

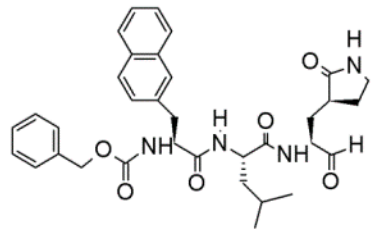

30

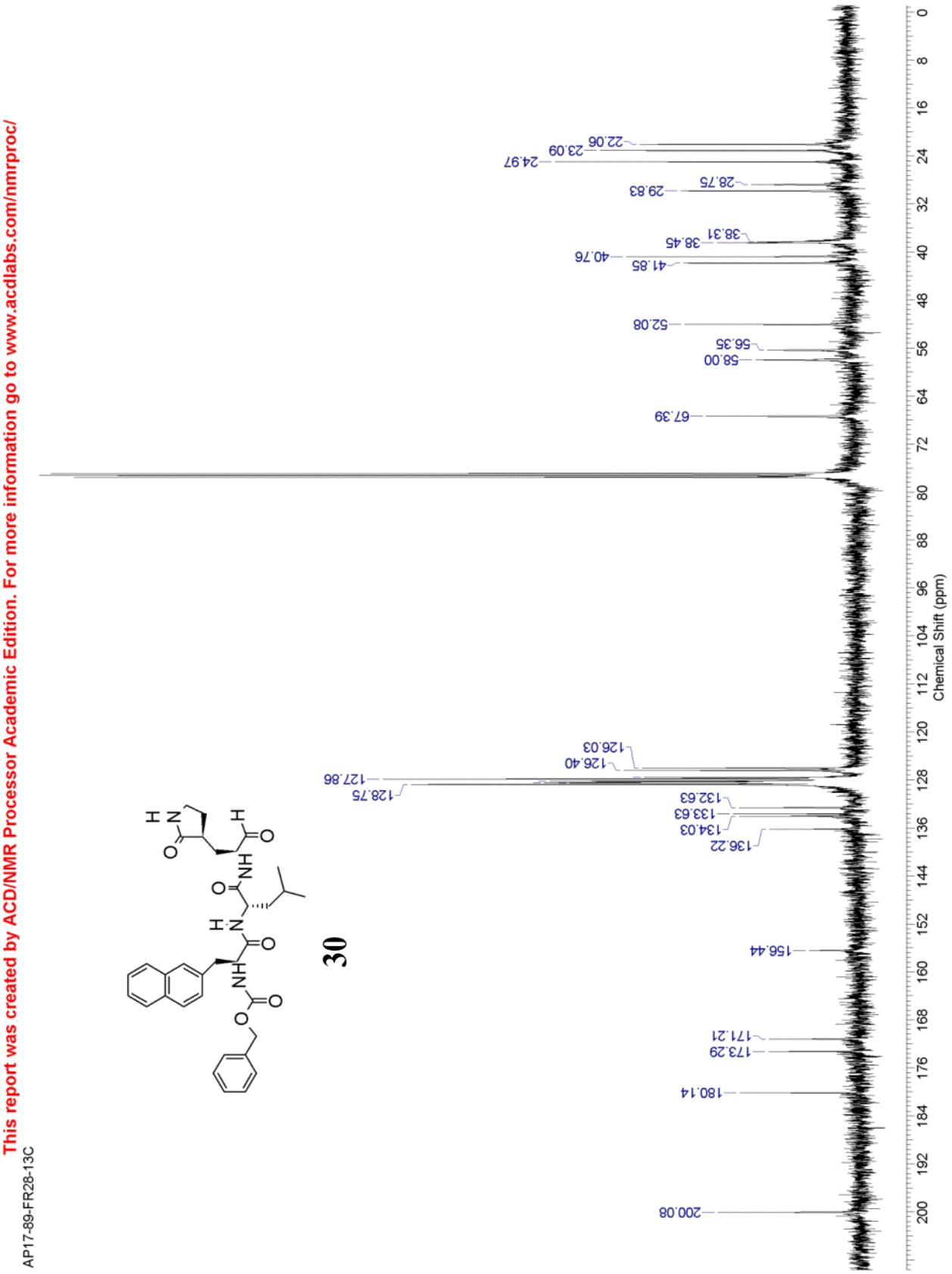
This report was created by ACD/NMR Processor Academic Edition. For more information go to www.acdlabs.com/nmrproc/
AP17-89-FR28-13C
30
22.06
23.09
24.97
28.75
29.83
38.31
38.45
40.76
41.85
52.08
56.35
58.00
67.39
126.03
126.40
127.86
128.75
132.63
133.63
134.03
136.22
156.44
171.21
173.29
180.14
200.08
Chemical Shift (ppm)

AP17-91-FR23-24

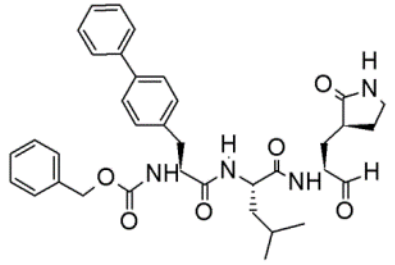

31

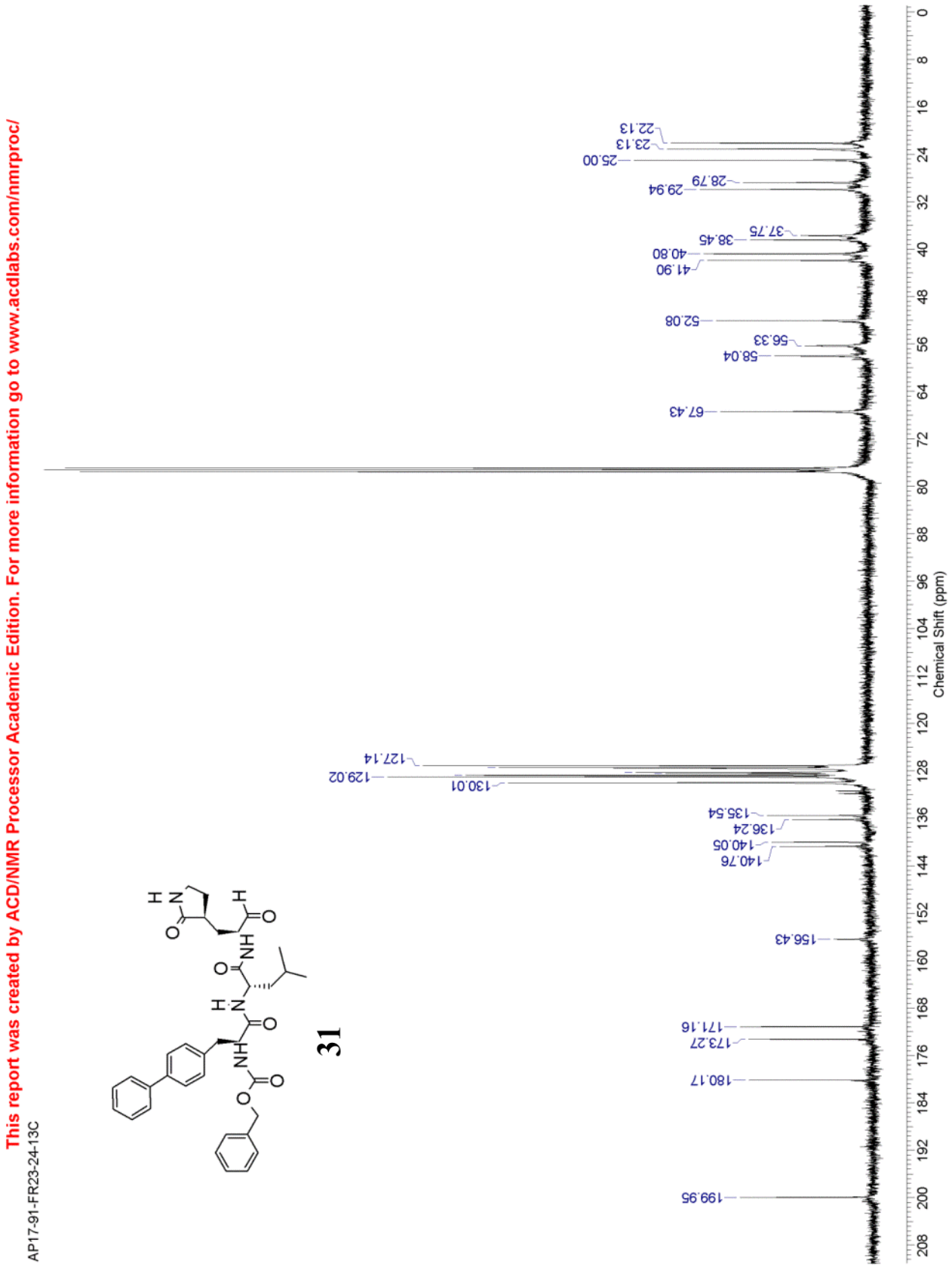
This report was created by ACD/NMR Processor Academic Edition. For more information go to www.acdlabs.com/nmrproc/
AP17-91-FR23-24-13C
22.13
23.13
25.00
28.79
29.94
37.75
38.45
40.80
41.90
52.08
56.33
58.04
67.43
127.14
129.02
130.01
135.54
136.24
140.05
140.76
156.43
171.16
173.27
180.17
199.95
Chemical Shift (ppm)

31

AP14-90-FR14-15

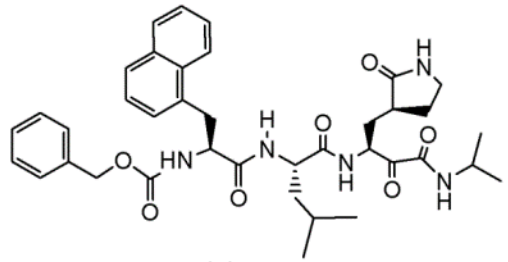

32

AP14-90-FR14-15-C13

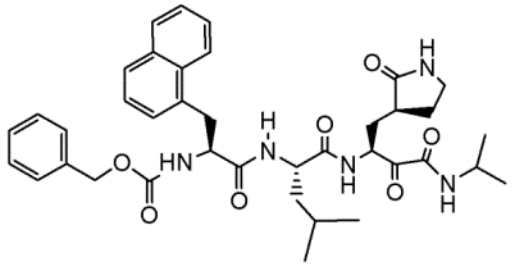

32

AP15-11-FR13

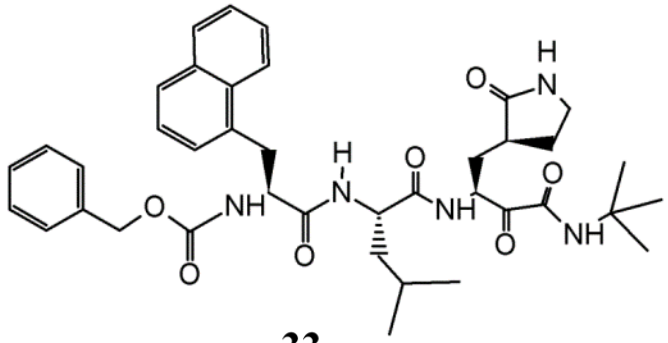

33

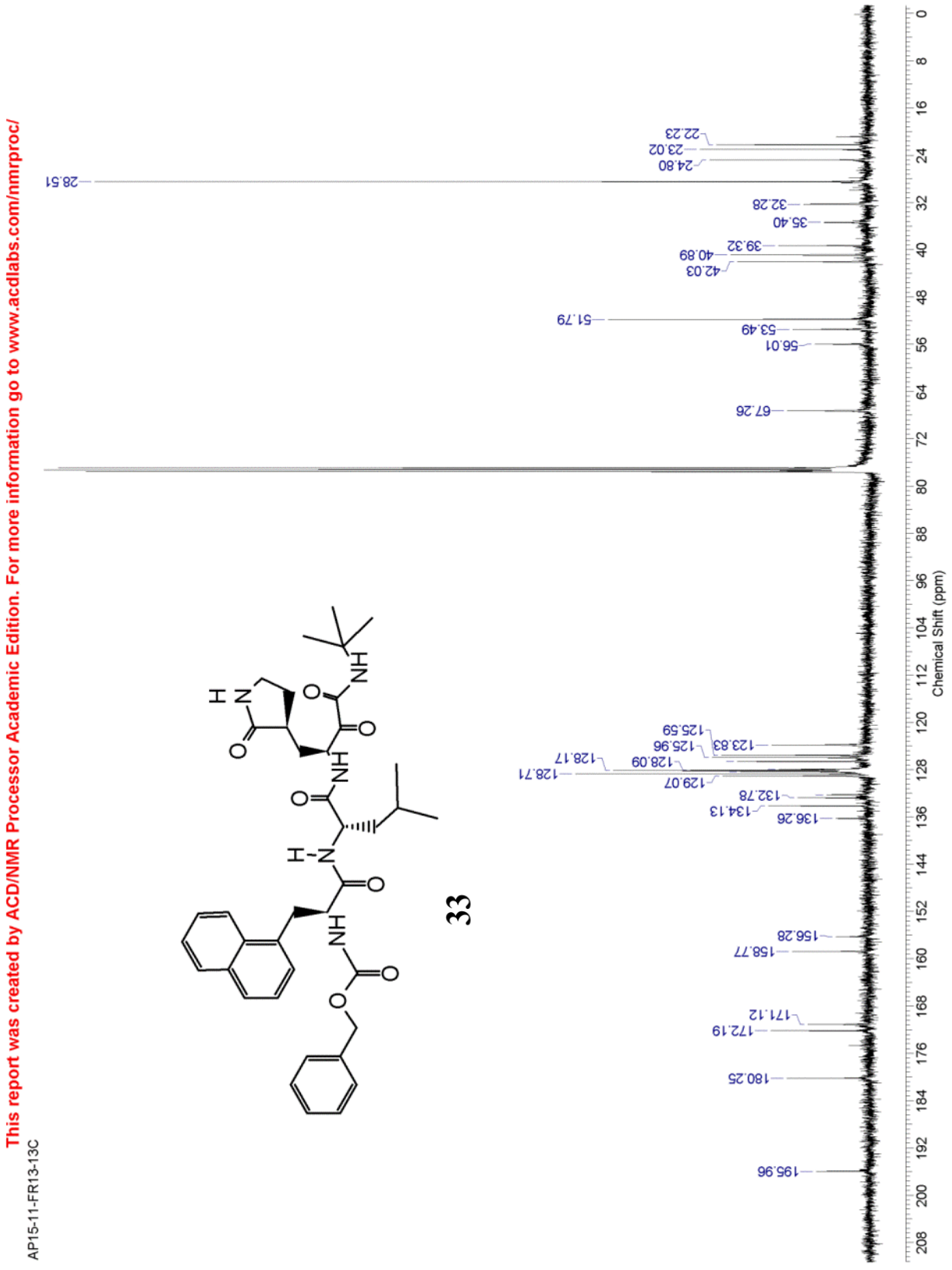
This report was created by ACD/NMR Processor Academic Edition. For more information go to www.acdlabs.com/nmrproc/
AP15-11-FR13-13C
22.23
23.02
24.80
28.51
32.28
35.40
39.32
40.89
42.03
51.79
53.49
56.01
67.26
123.83
125.96
125.59
128.09
128.17
128.71
129.07
132.78
134.13
136.26
156.28
158.77
171.12
172.19
180.25
195.96
Chemical Shift (ppm)

33

AP14-113-FR13

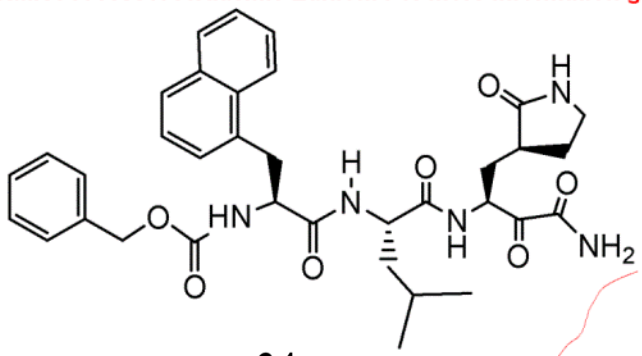

34

AP17-94-SOLID-AGAIN

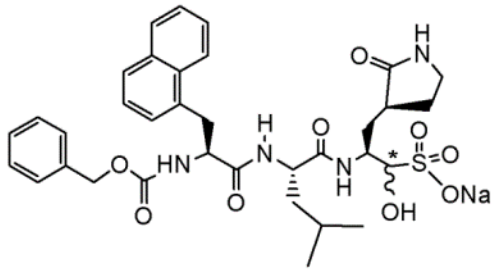

35

AP17-94-SOLID-AGAIN-13C

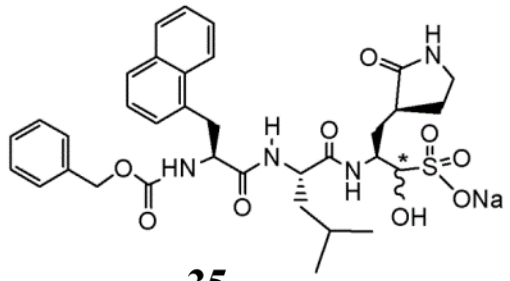

35

AP17-93-FR12-13

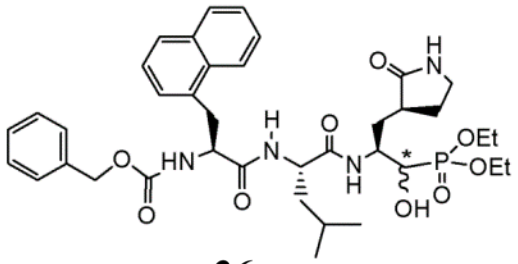

36

AP17-93-FR12-13-13C

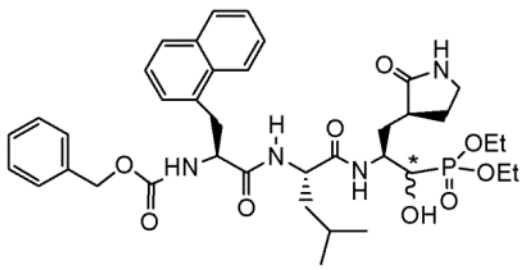

36

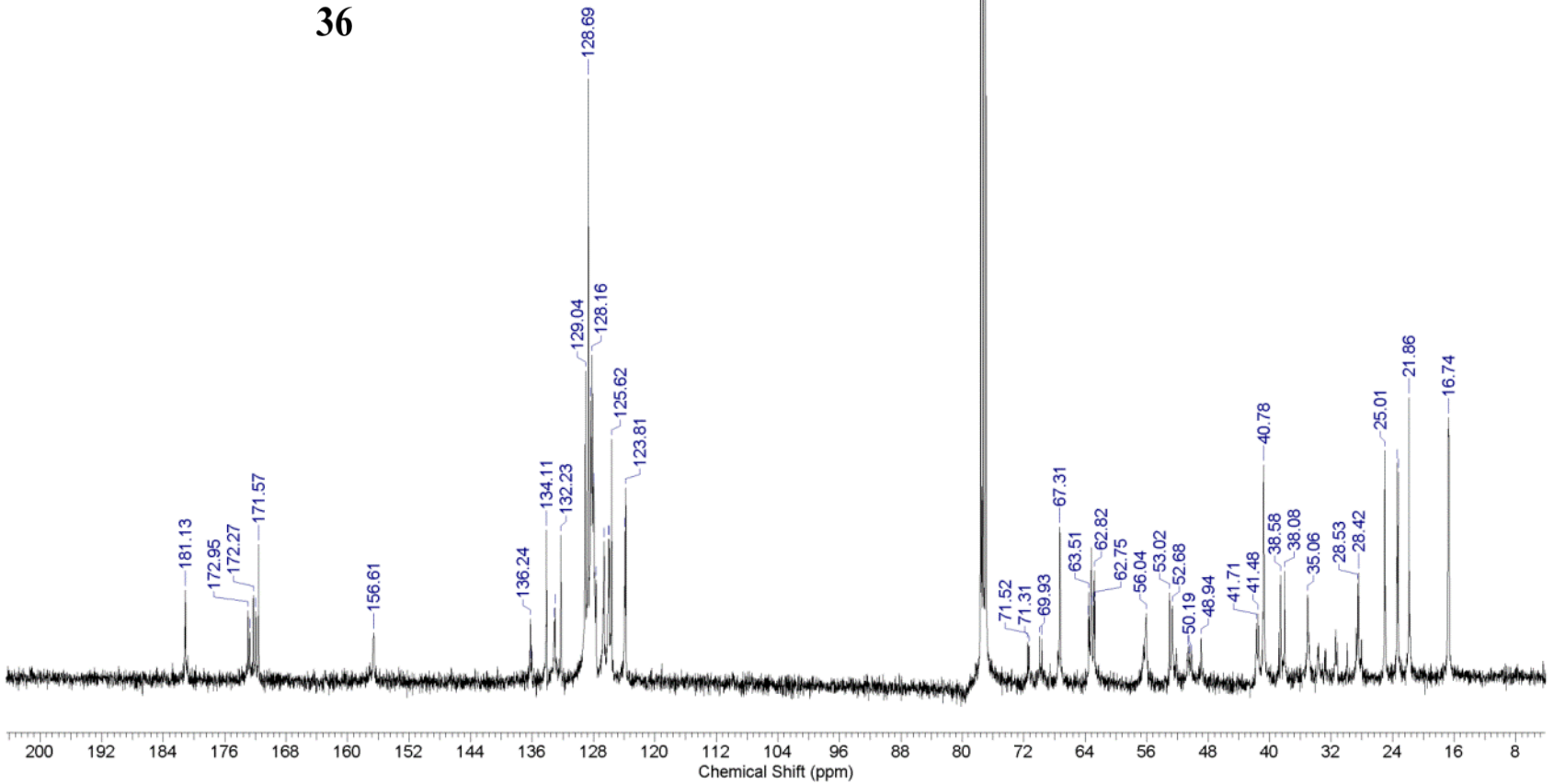

AP17-24-FR18

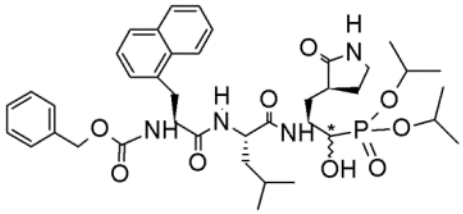

37

AP15-109-FR13-17

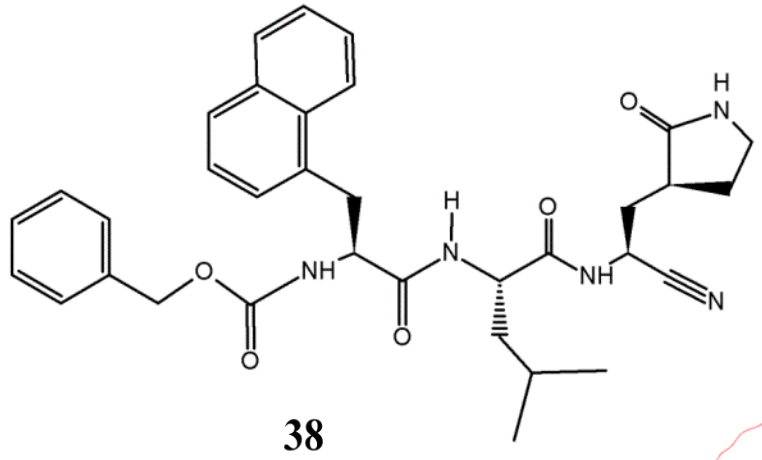

38

AP15-109-FR13-17-13C

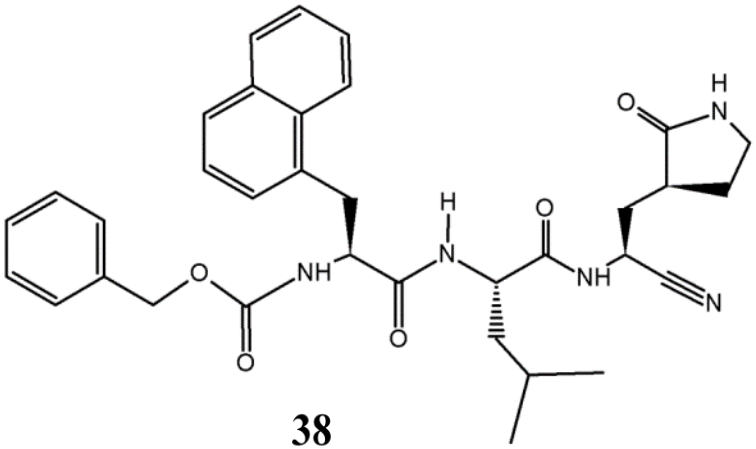

38

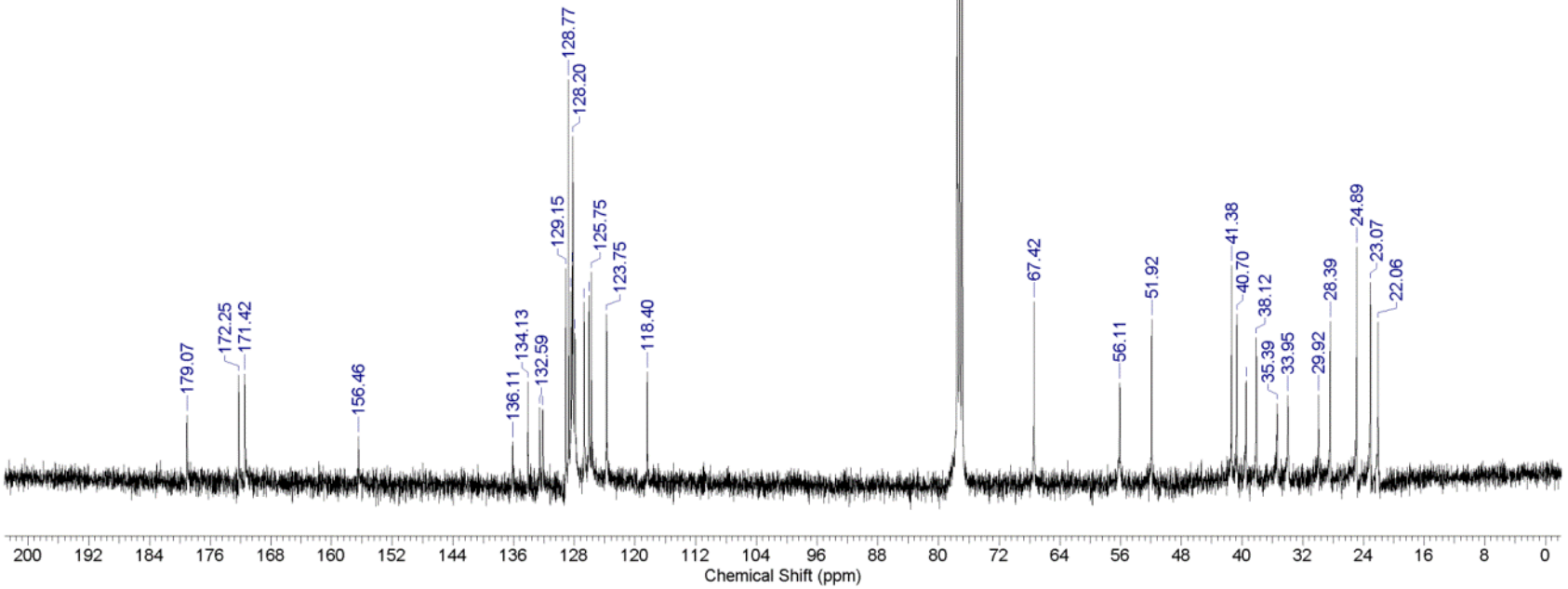

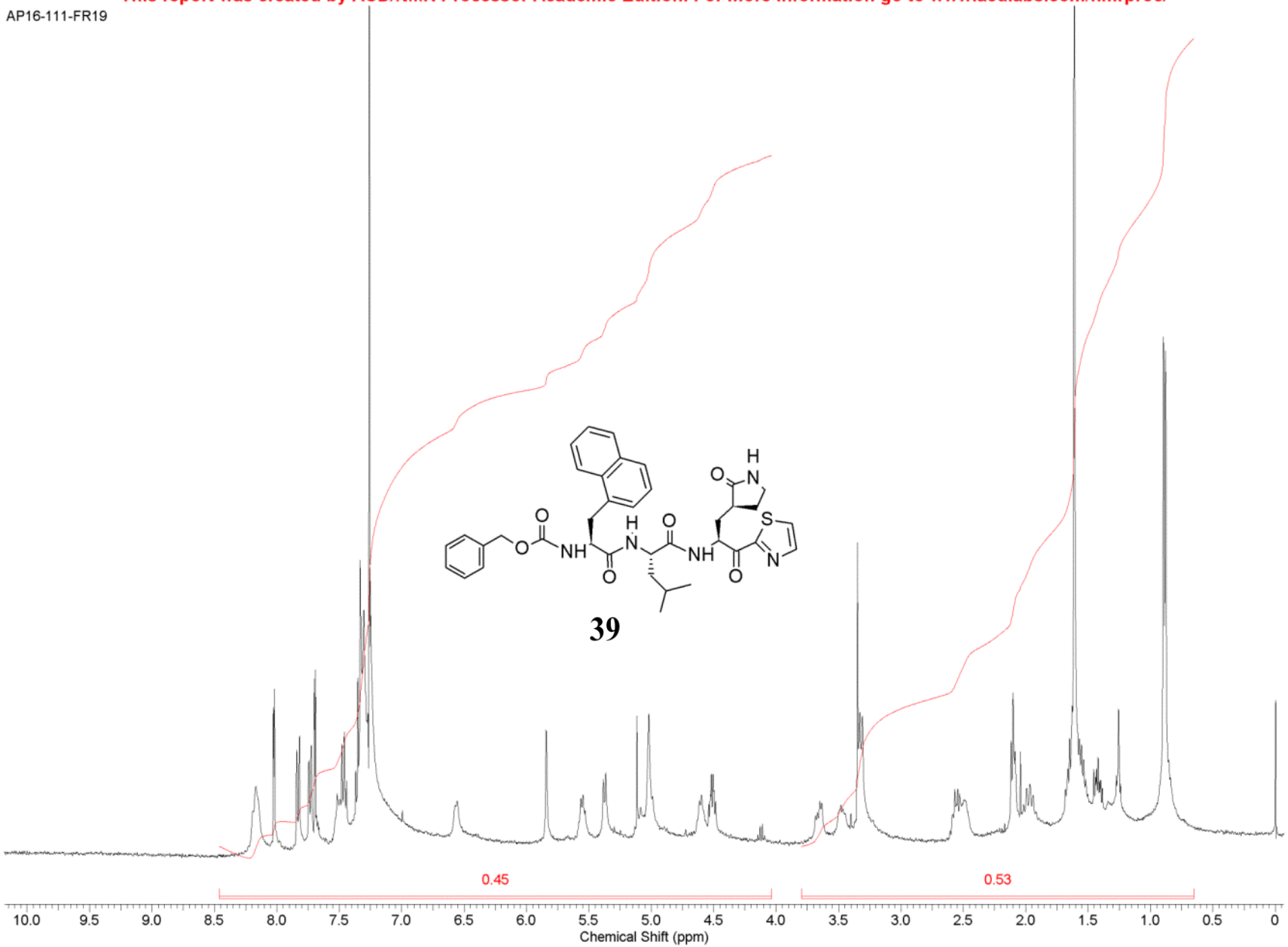

39

AP16-111-FR19-C13

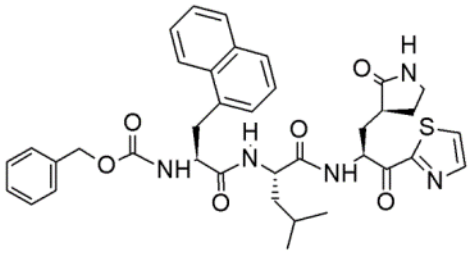

39

AP16-84-FR11-12

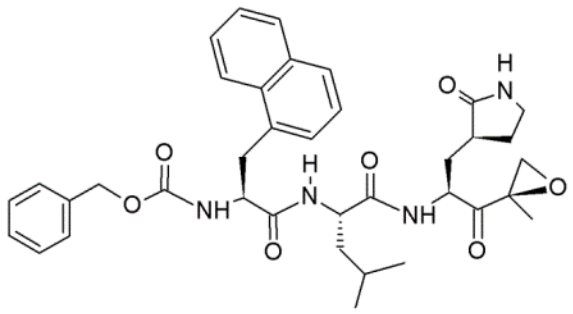

40

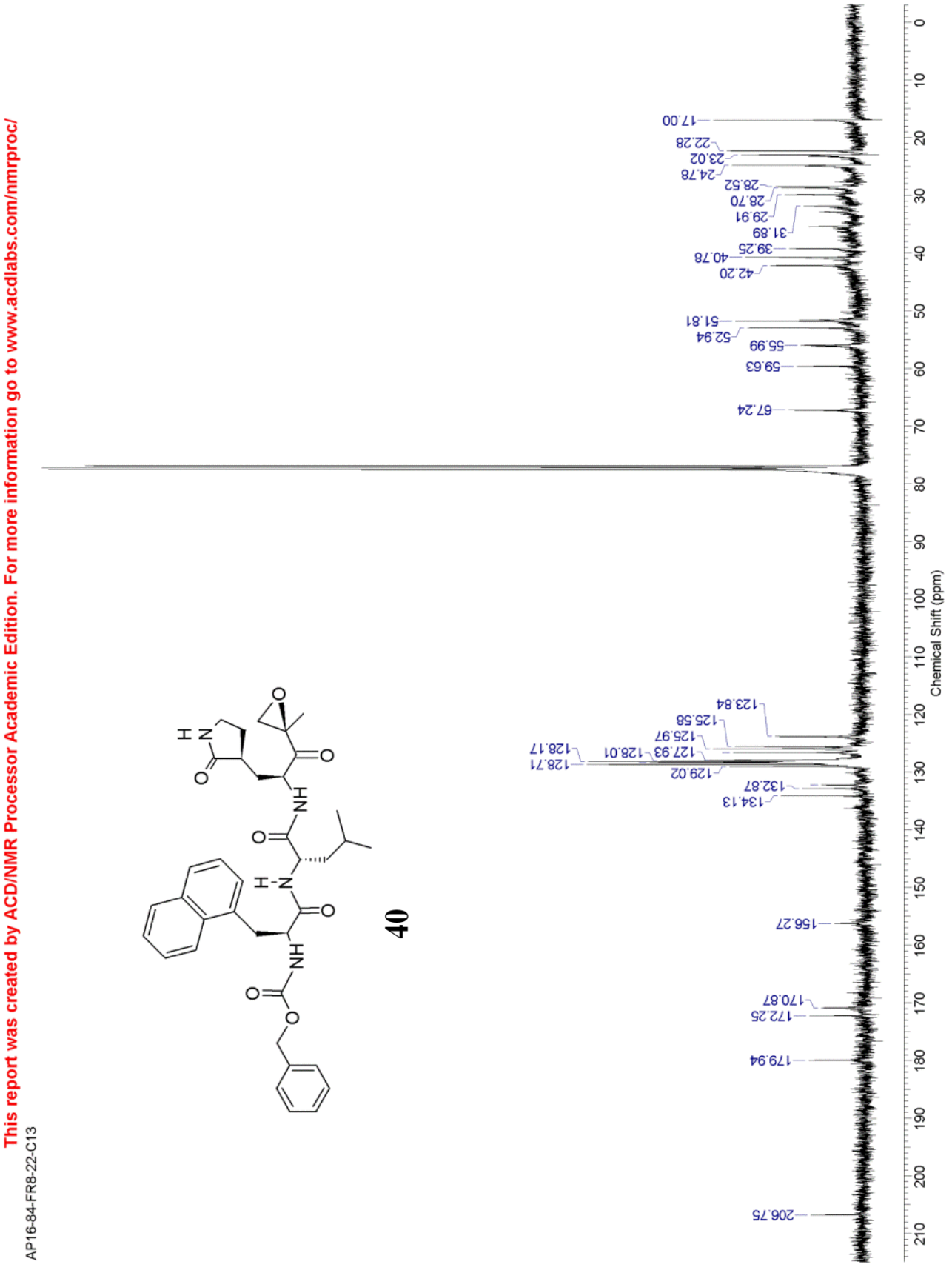
This report was created by ACD/NMR Processor Academic Edition. For more information go to www.acdlabs.com/nmrproc/
AP16-84-FR8-22-C13
40
17.00
22.28
23.02
24.78
28.52
28.70
29.91
31.89
39.25
40.78
42.20
51.81
52.94
55.99
59.63
67.24
123.84
125.58
125.97
127.93
128.01
128.17
128.71
129.02
132.87
134.13
156.27
170.87
172.25
179.94
206.75
Chemical Shift (ppm)

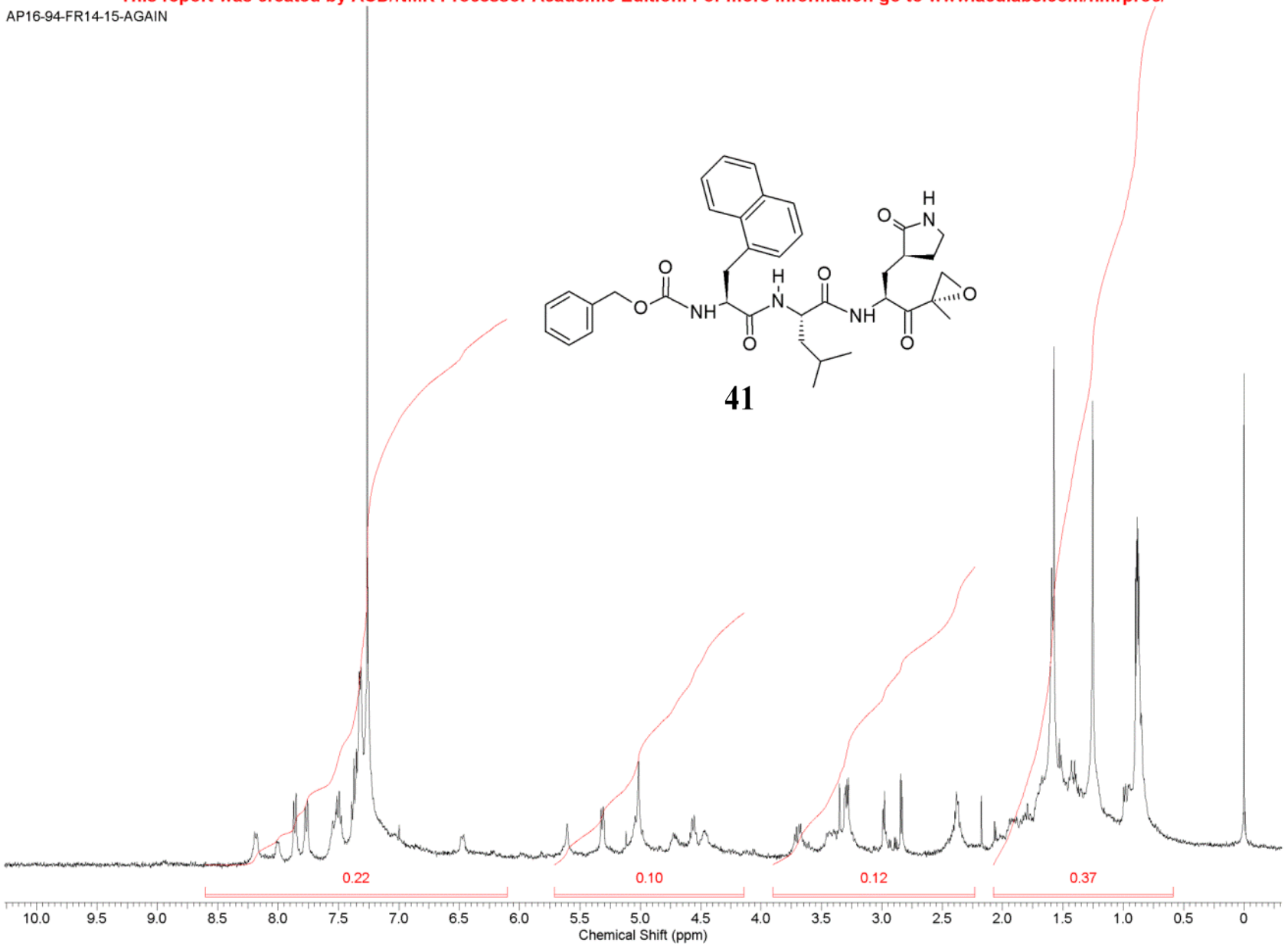

41

AP15-51-FR23

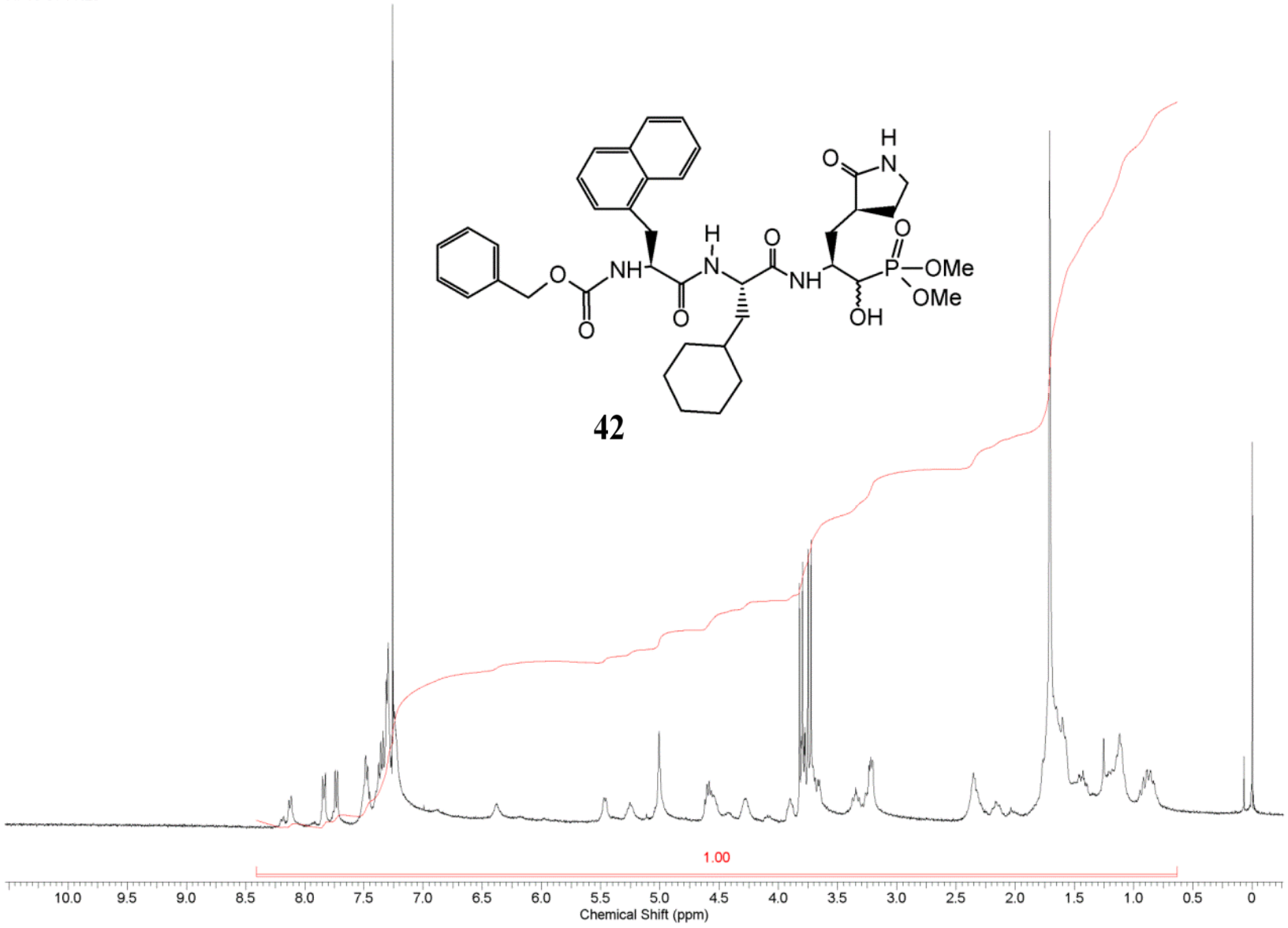

42

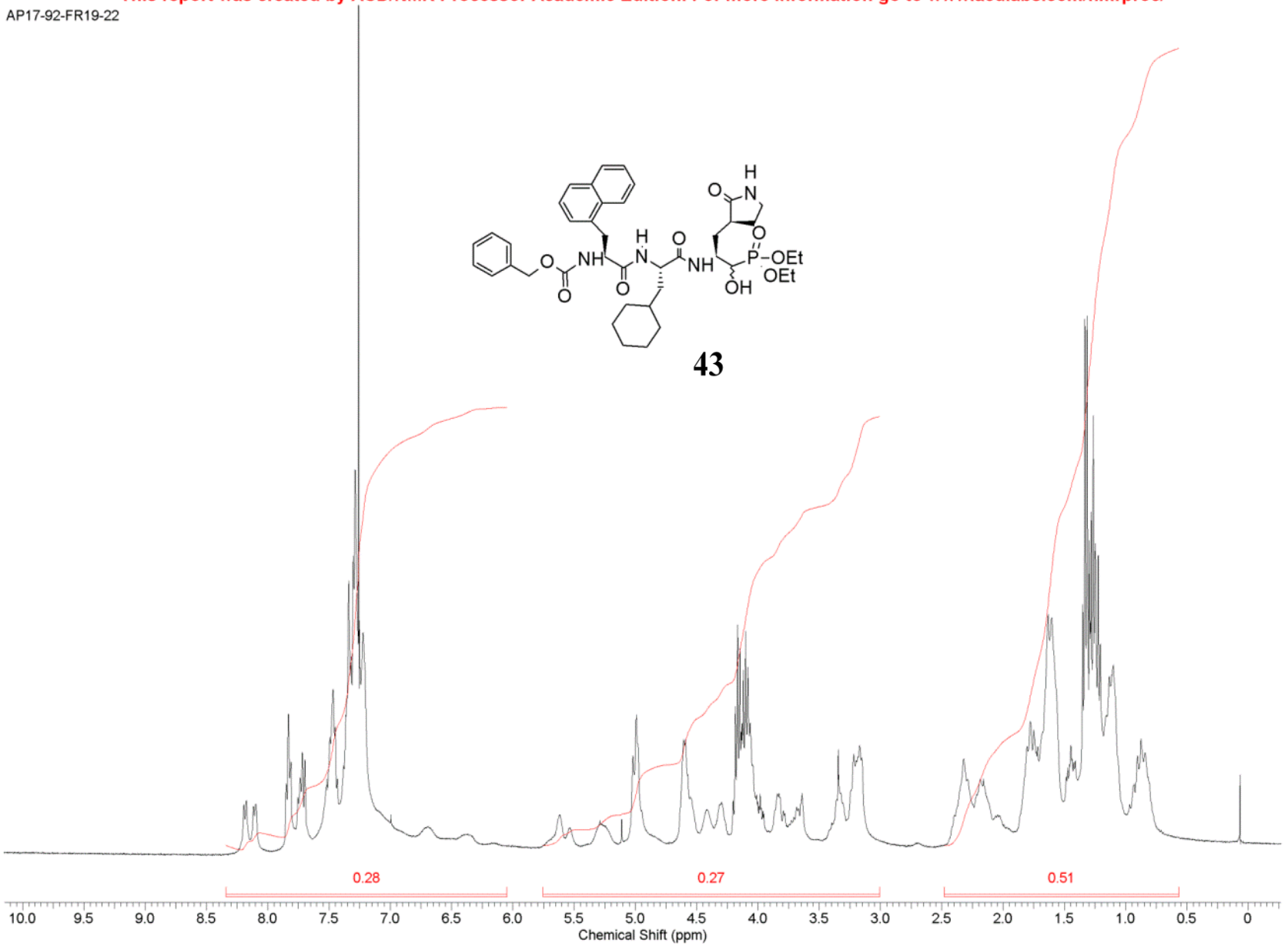

43

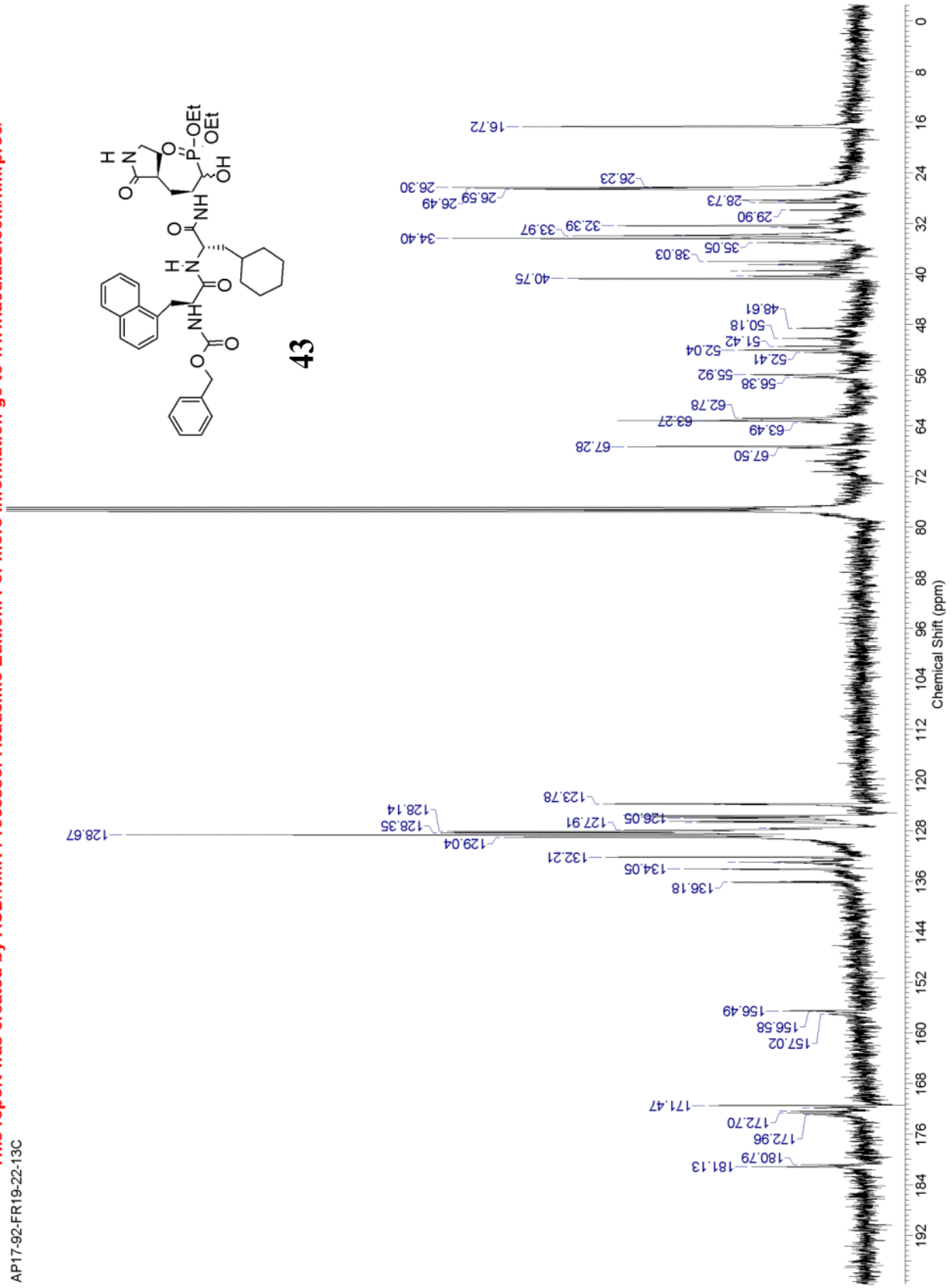
This report was created by ACD/NMR Processor Academic Edition. For more information go to www.acdlabs.com/nmrproc/
AP17-92-FR19-22-13C
43
16.72
26.23
26.30
26.59
26.49
28.73
29.90
32.39
33.97
34.40
35.05
38.03
40.75
48.61
50.18
51.42
52.04
52.41
55.92
56.38
62.78
63.27
63.49
67.28
67.50
123.78
126.05
127.91
128.14
128.35
128.67
129.04
132.21
134.05
136.18
156.49
156.58
157.02
171.47
172.70
172.96
180.79
181.13
Chemical Shift (ppm)

AP16-36-FR24-25

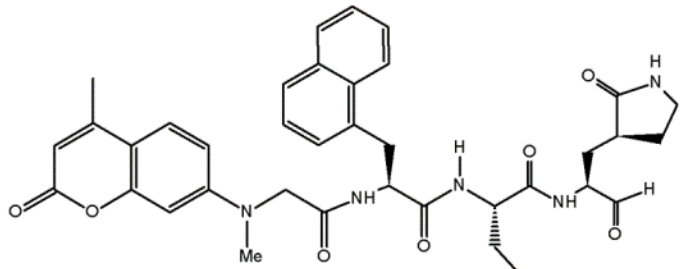

44

AP16-37-FR20

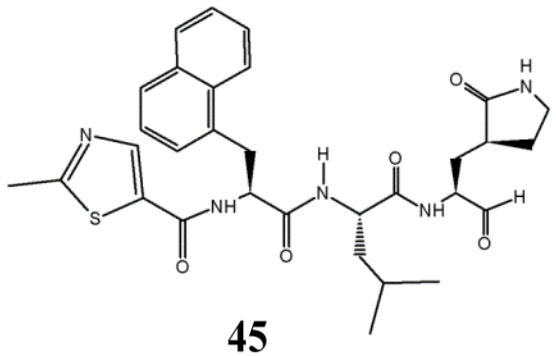

45

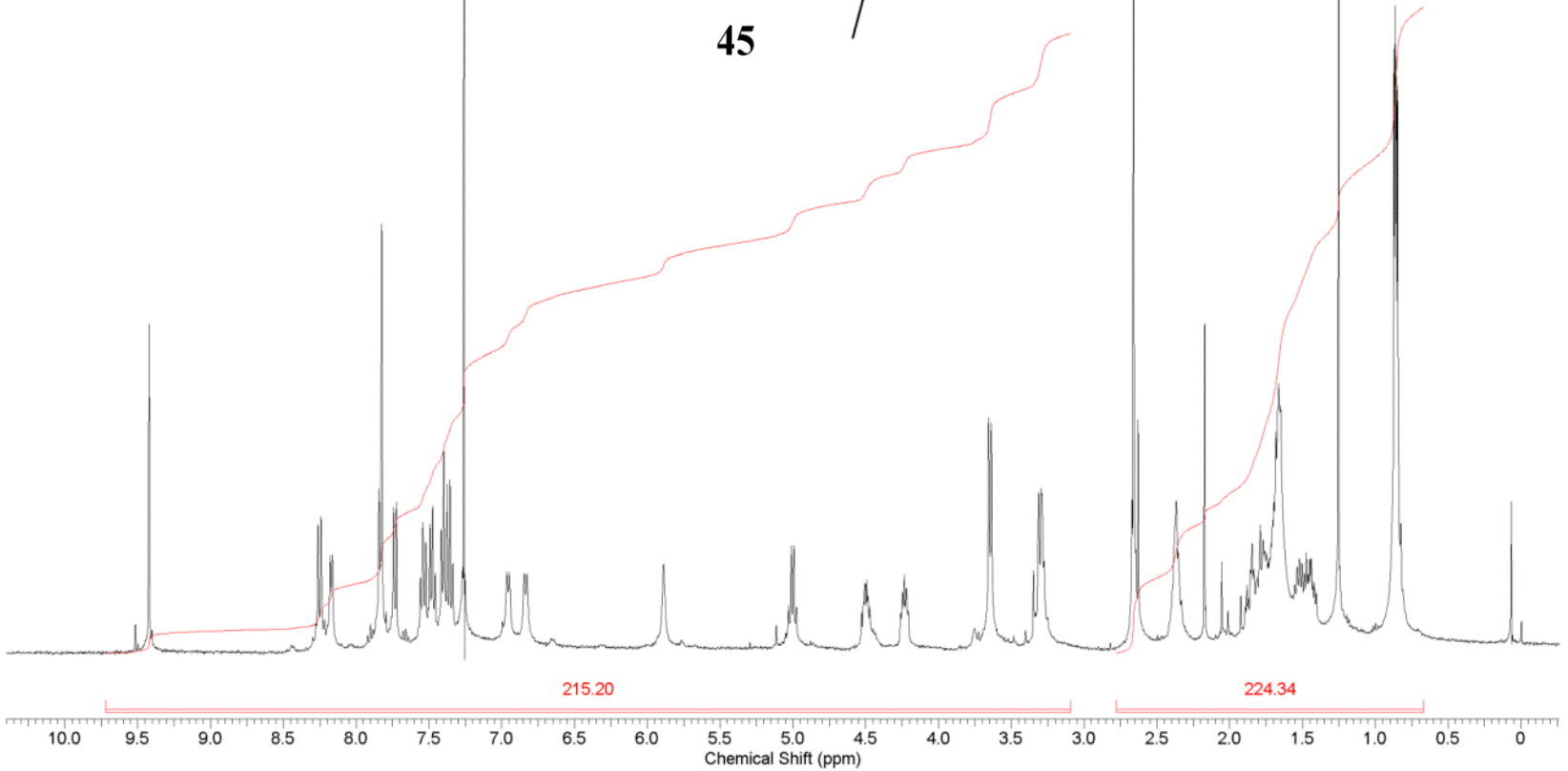

AP16-37-FR20-13C

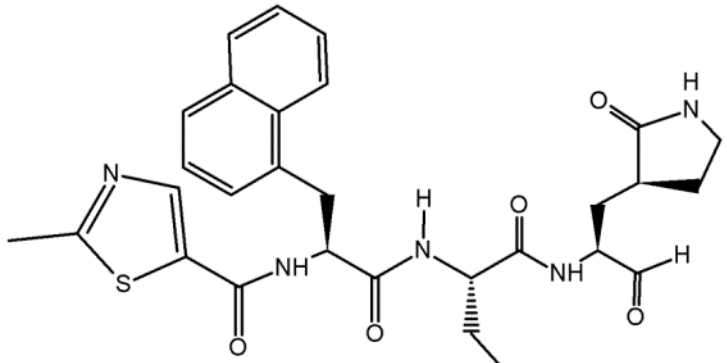

45

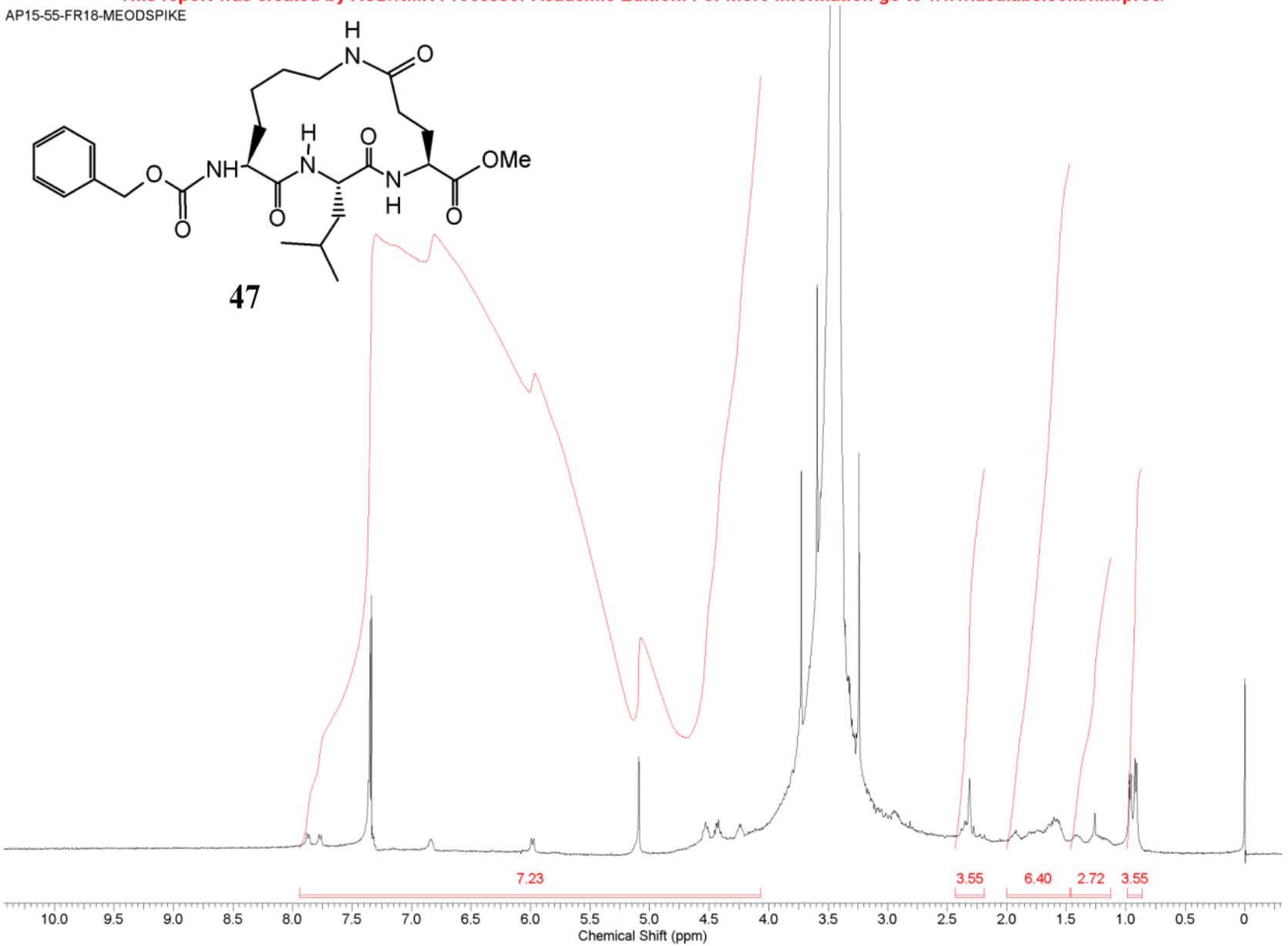

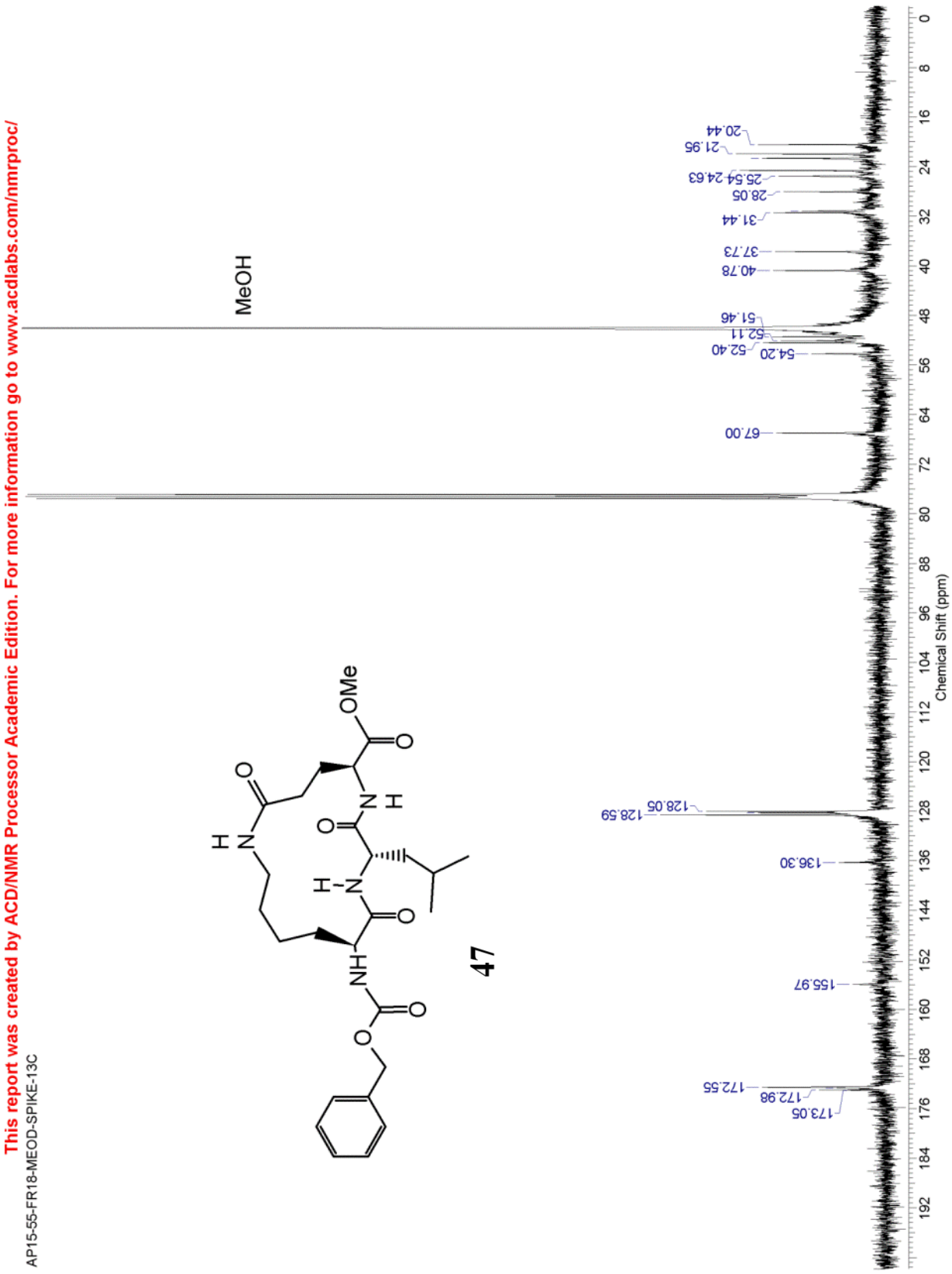
This report was created by ACD/NMR Processor Academic Edition. For more information go to www.acdlabs.com/nmrproc/
AP15-55-FR18-MEOD-SPIKE-13C
MeOH
OMe
47
20.44
21.95
25.54
24.63
28.05
31.44
37.73
40.78
51.46
52.11
54.20
52.40
67.00
128.05
128.59
136.30
155.97
172.55
172.98
173.05
Chemical Shift (ppm)

AP15-63-FR17-22

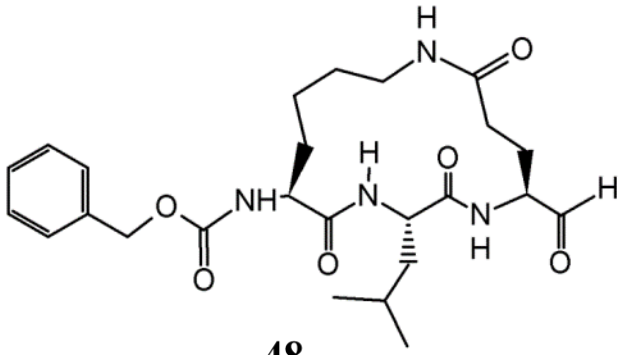

48

AP16-27-FR25

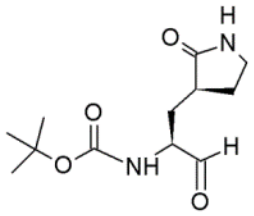

53a

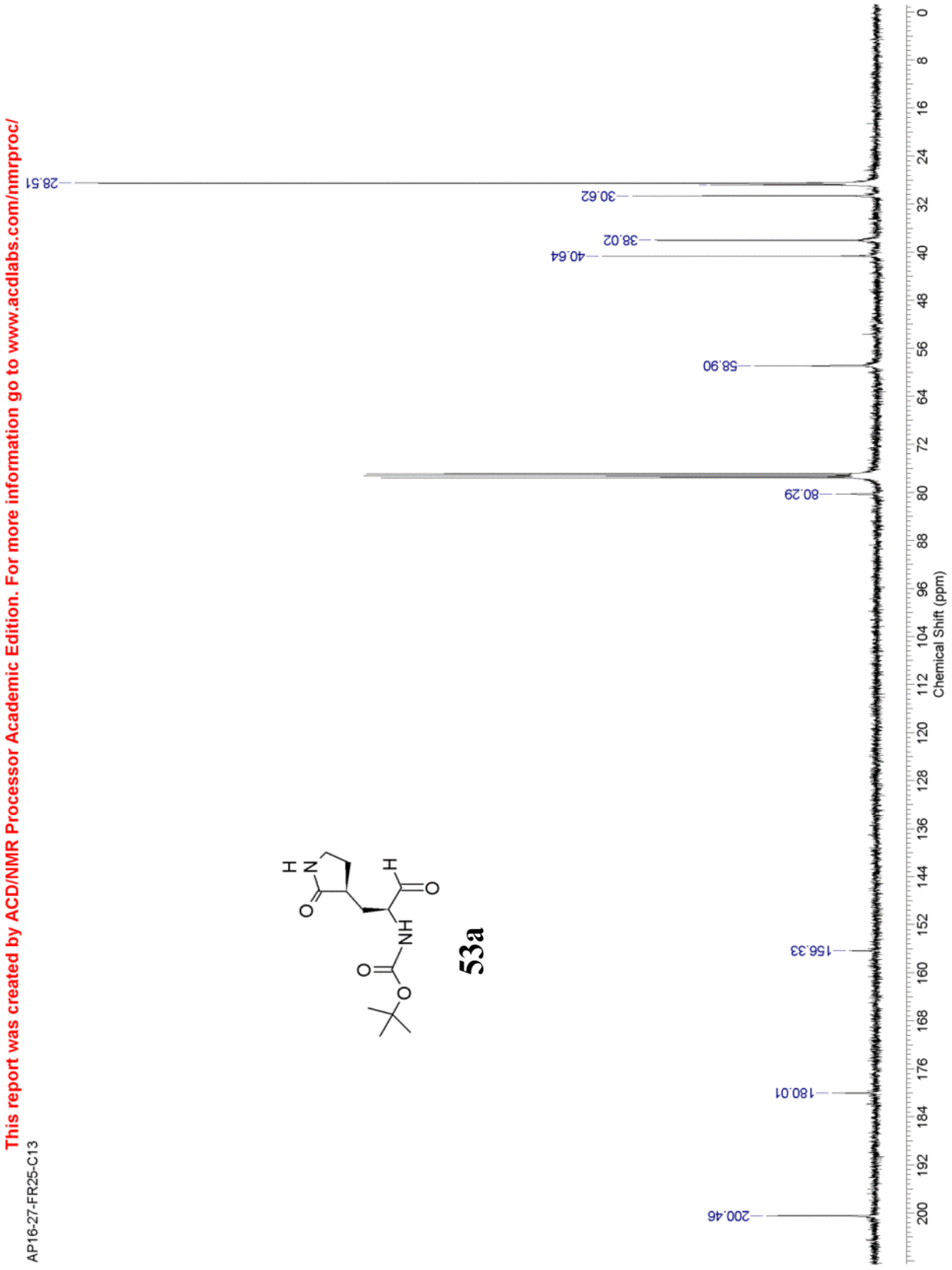
This report was created by ACD/NMR Processor Academic Edition. For more information go to www.acdlabs.com/nmrproc/
AP16-27-FR25-C13
28.51
30.62
38.02
40.64
58.90
80.29
156.33
180.01
200.46
Chemical Shift (ppm)
53a

AP12-117-FR12

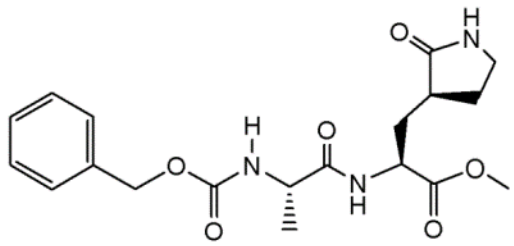

54

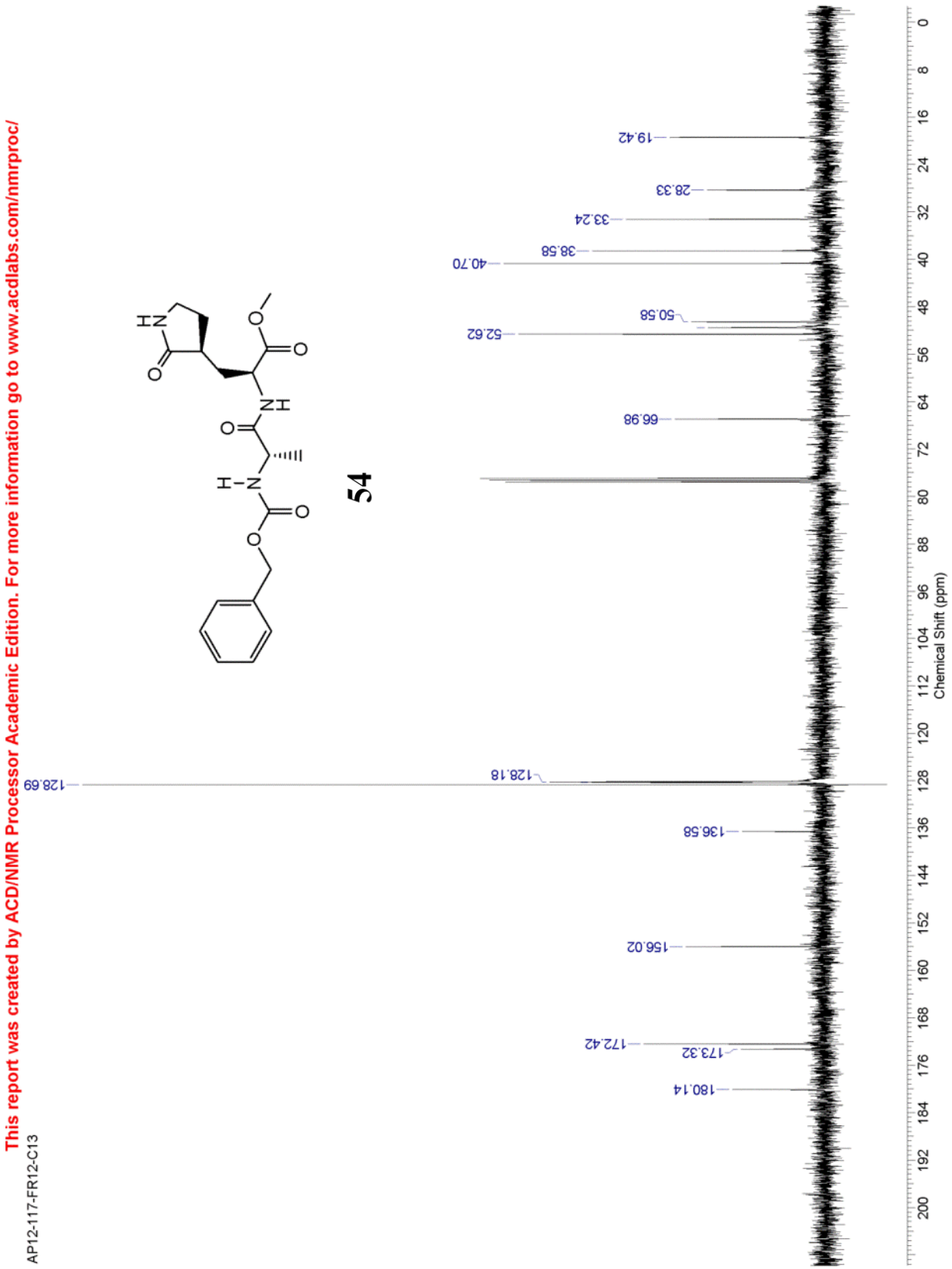
This report was created by ACD/NMR Processor Academic Edition. For more information go to www.acdlabs.com/nmrproc/
AP12-117-FR12-C13
54
19.42
28.33
33.24
38.58
40.70
50.58
52.62
66.98
128.18
128.69
136.58
156.02
172.42
173.32
180.14
Chemical Shift (ppm)

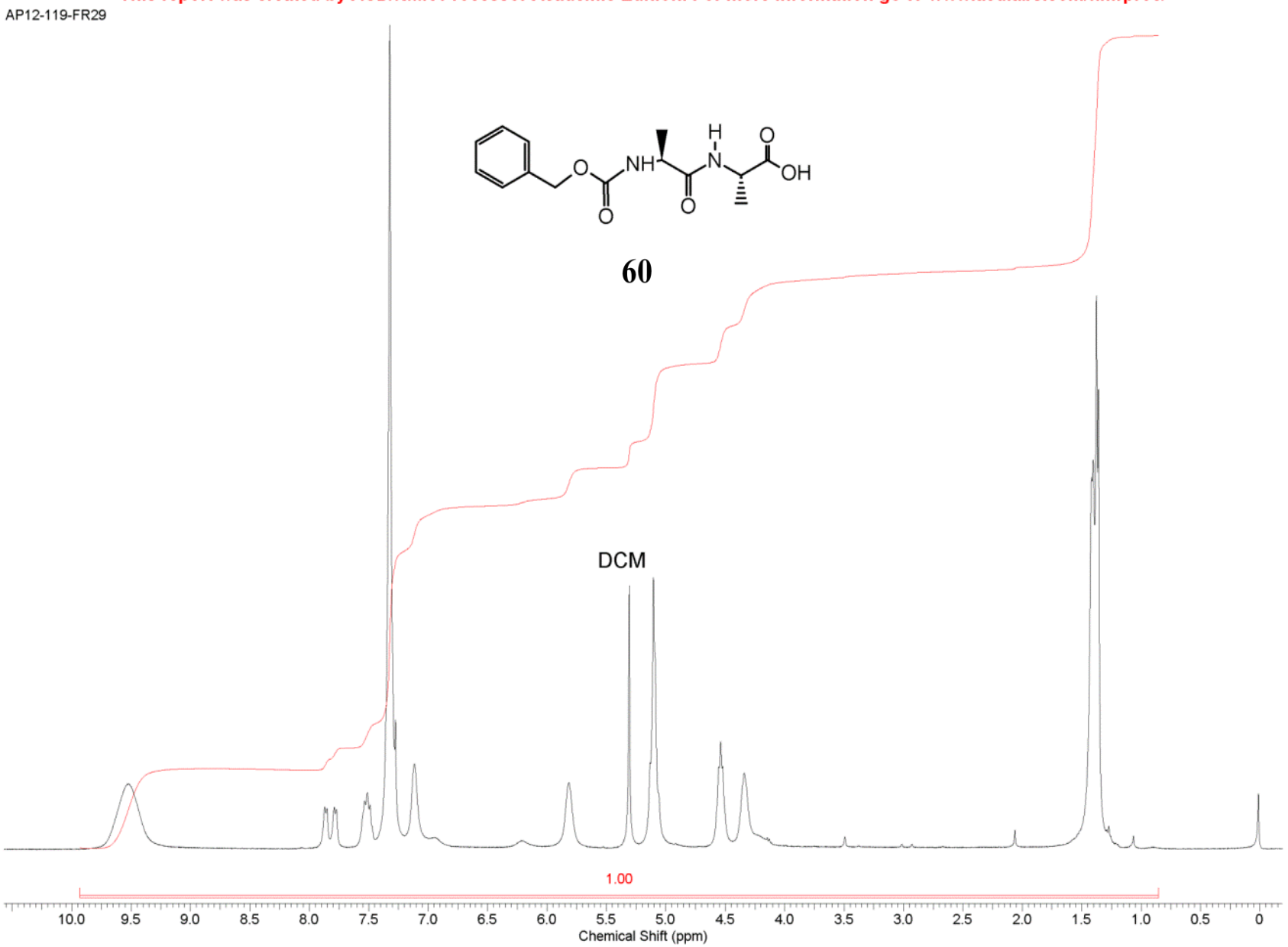

60

AP13-119-COLUMNFLUSH

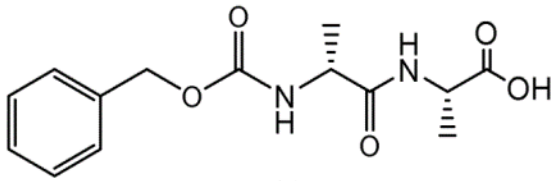

61

NAPTHYL-ALA-ALA-FR21-AGAIN

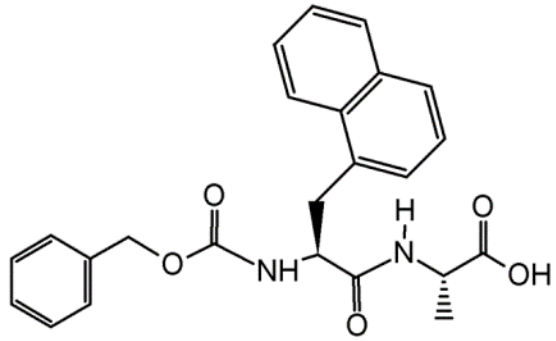

62

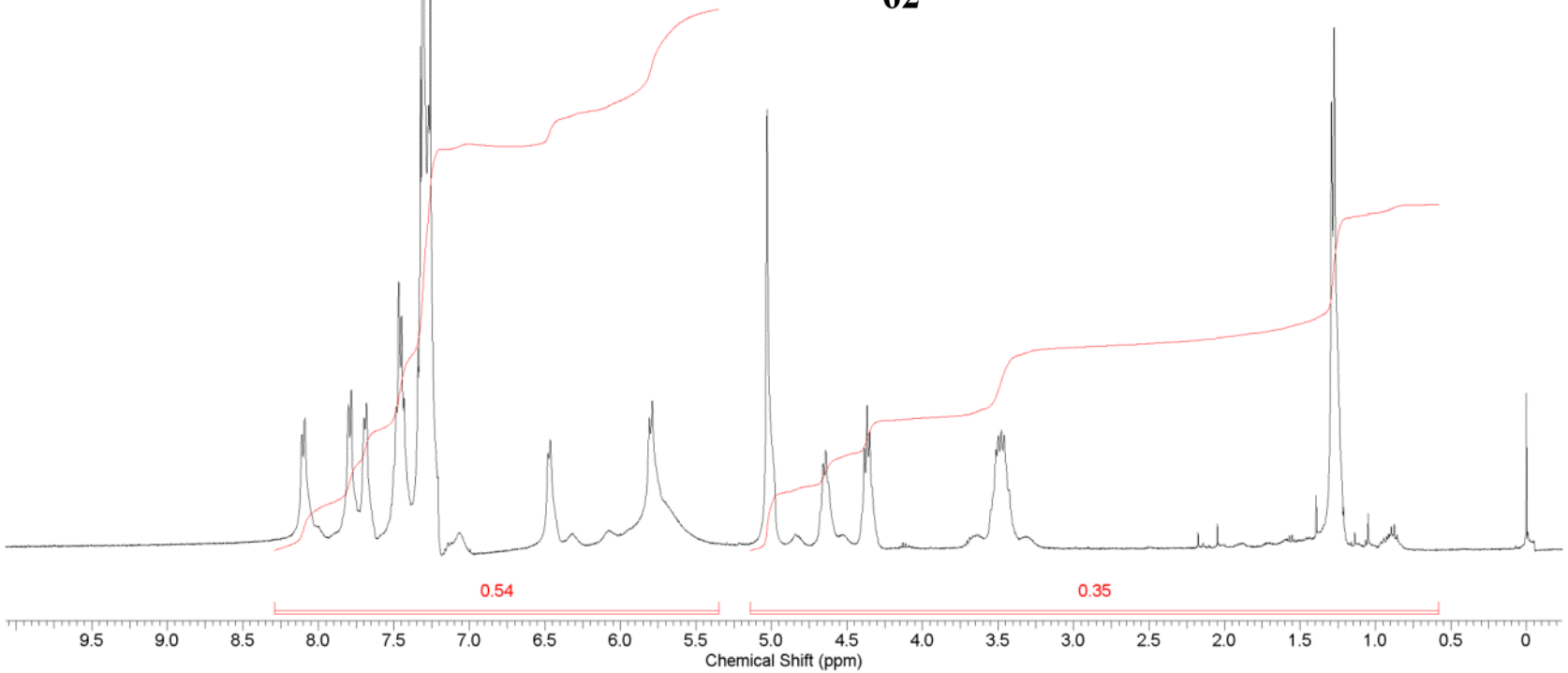

AP13-116-NAPTHYL-ALA-ALA-13C

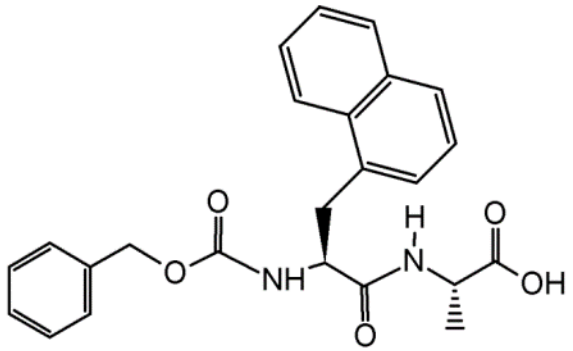

62

AP12-97-FR31

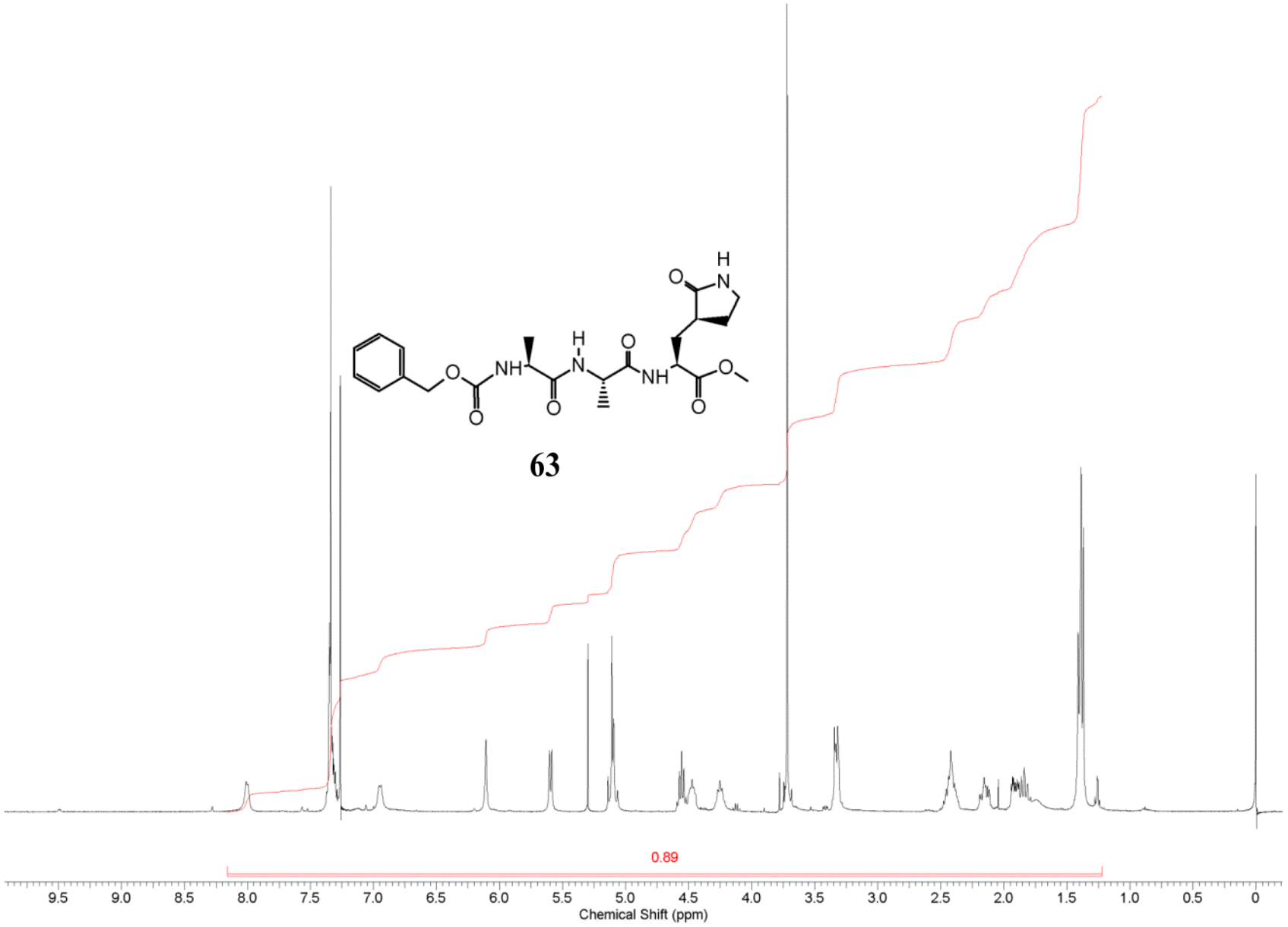

63

AP12-97-FR28-33-C13

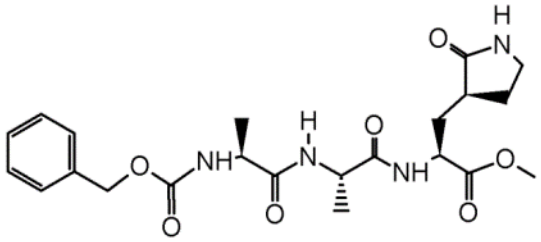

63

AP14-15-FR24

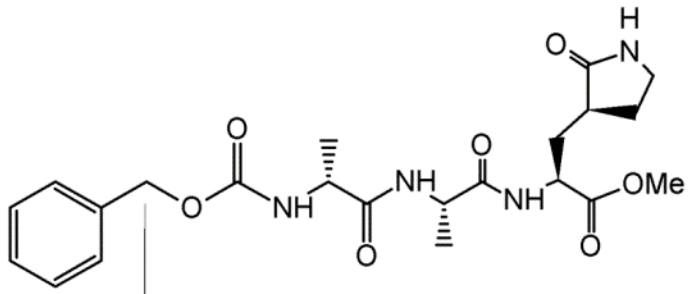

64

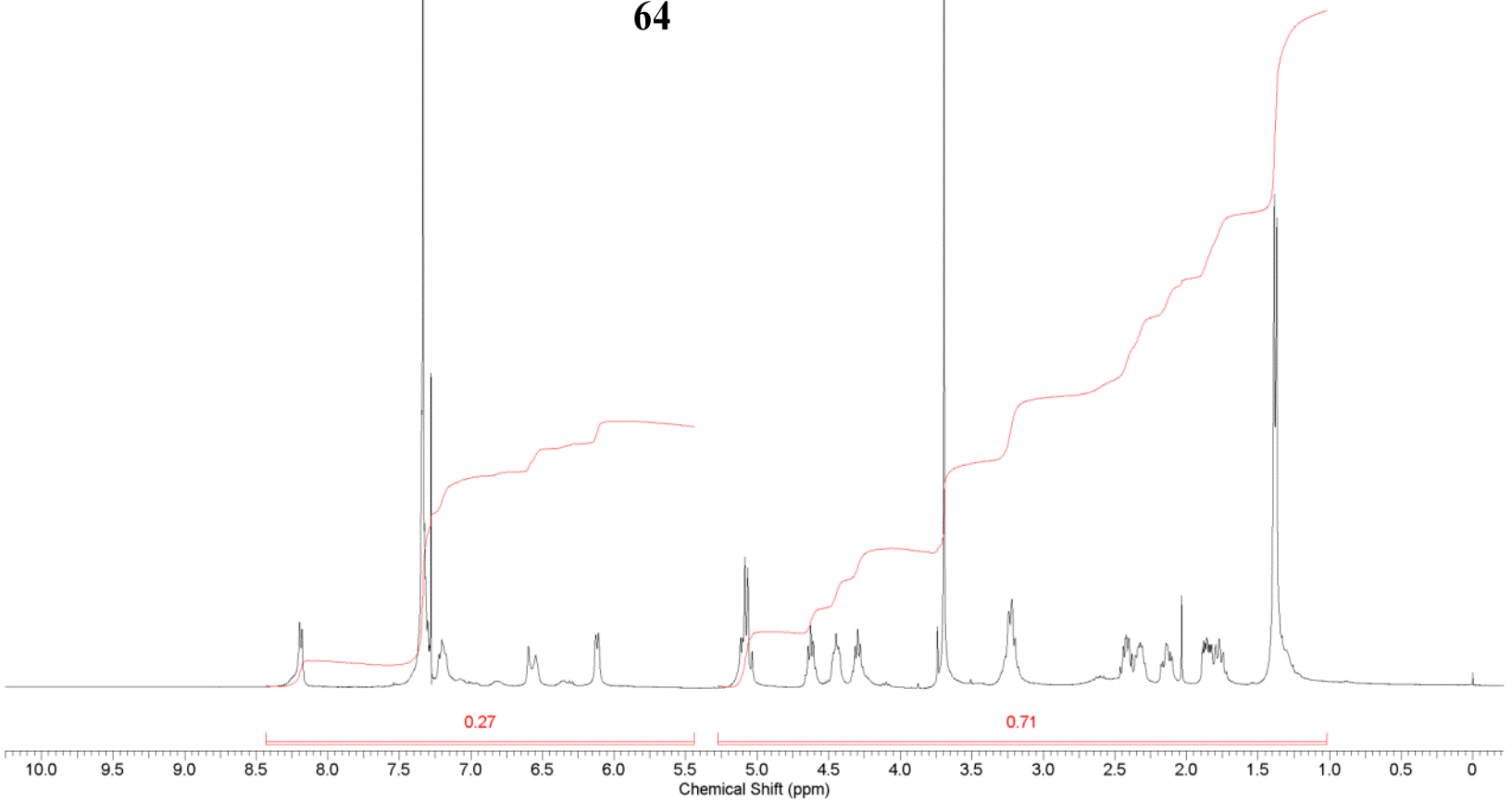

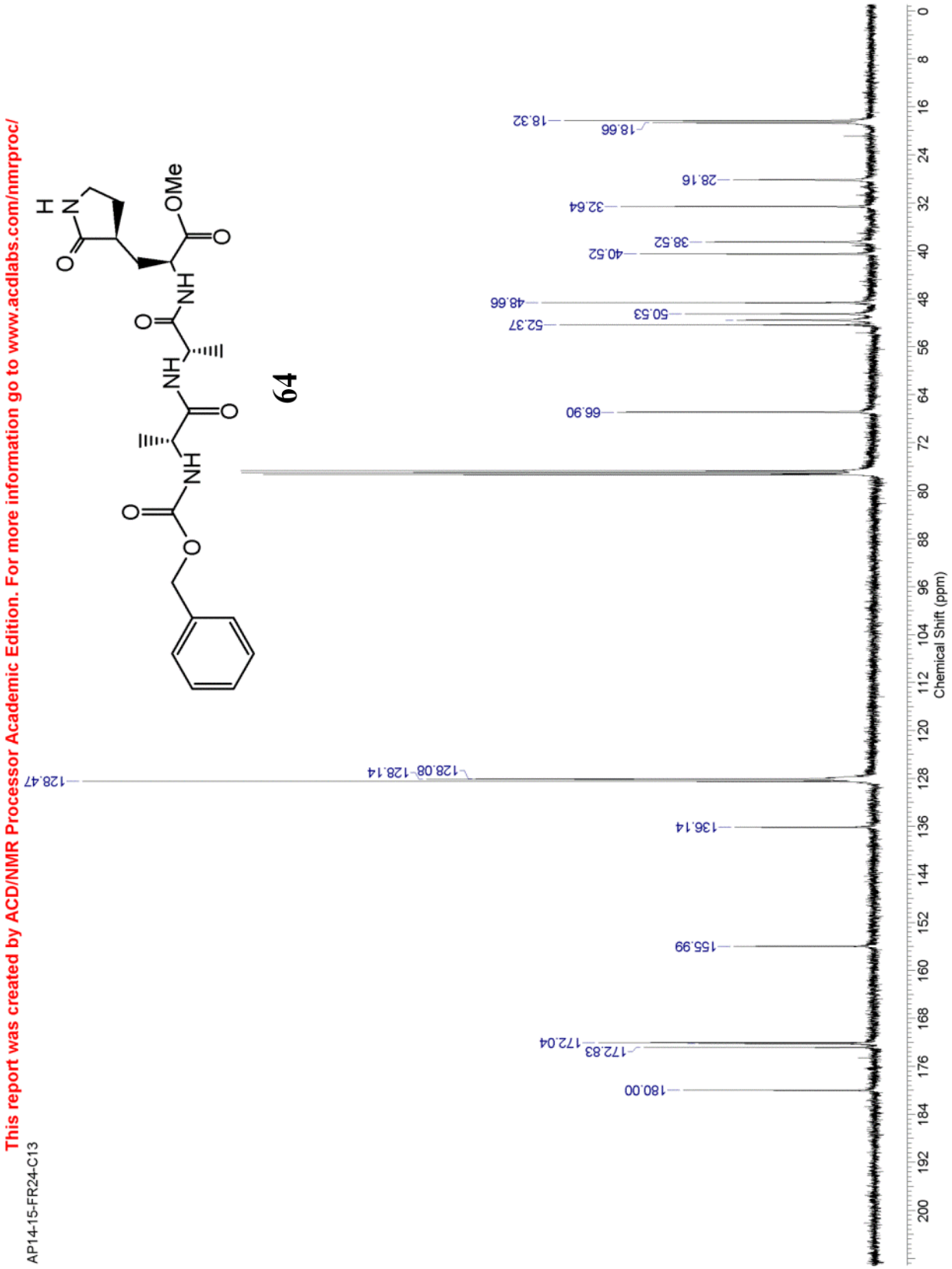
This report was created by ACD/NMR Processor Academic Edition. For more information go to www.acdlabs.com/nmrproc/
AP14-15-FR24-C13
64
OMe
NH
NH
NH
O
O
O
O
O
O
O
N
H
128.47
128.08
128.14
136.14
155.99
172.83
172.04
180.00
66.90
52.37
50.53
48.66
40.52
38.52
32.64
28.16
18.66
18.32
Chemical Shift (ppm)

AP13-39-CRUDE

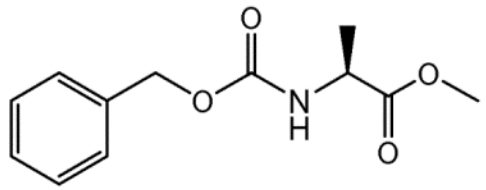

66

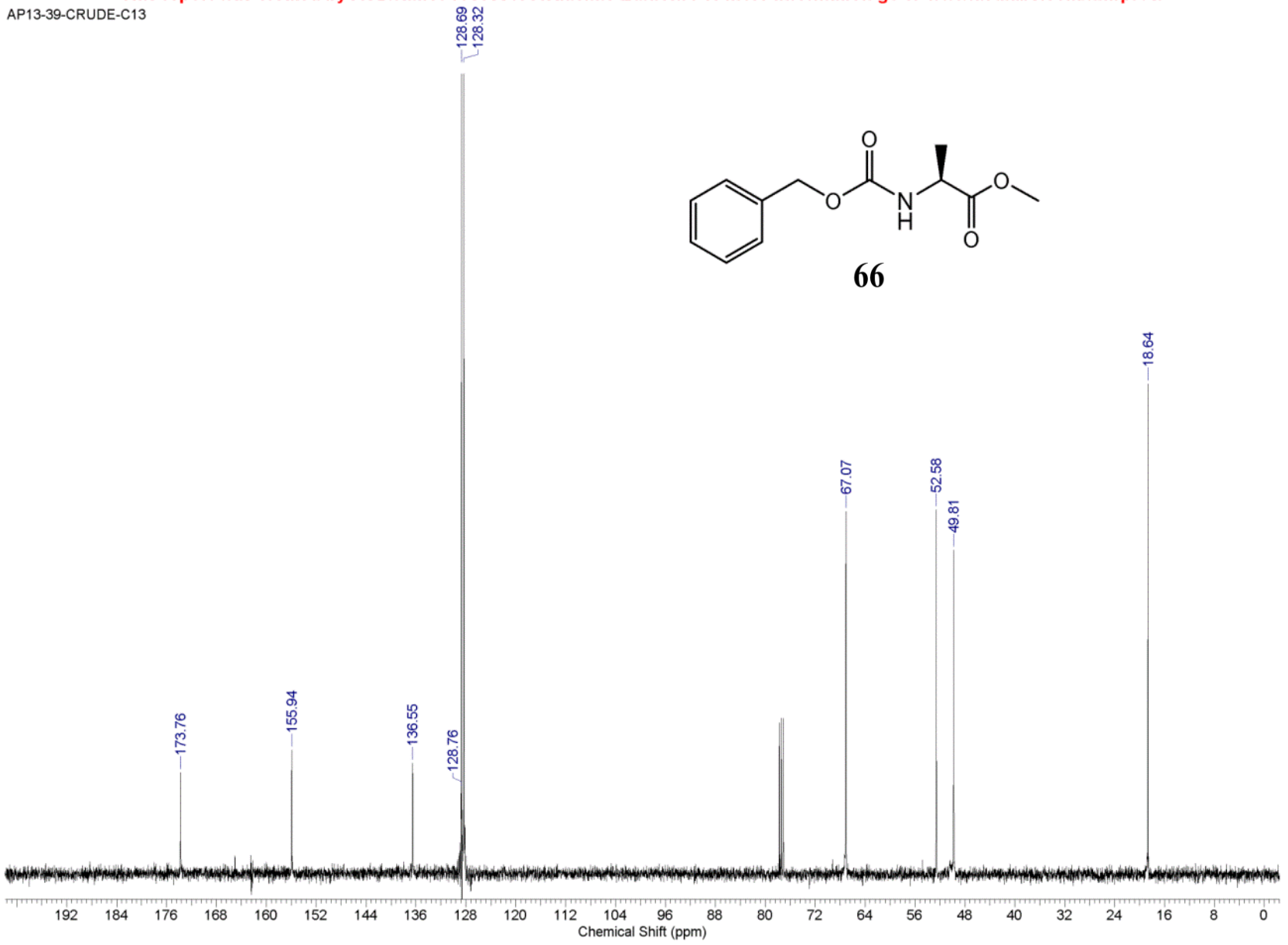

AP13-45-FR21

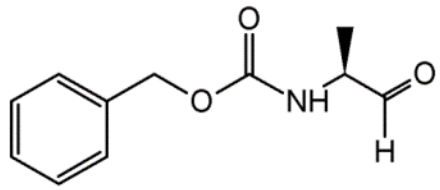

67

AP13-45-FR21-C13

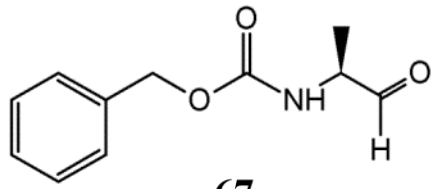

67

AP13-49-FR24-1H

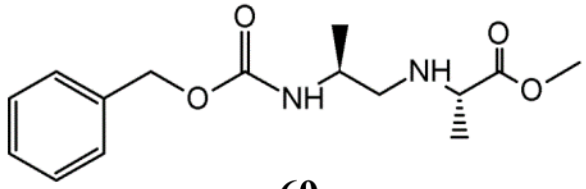

69

AP13-49-FR24-C13

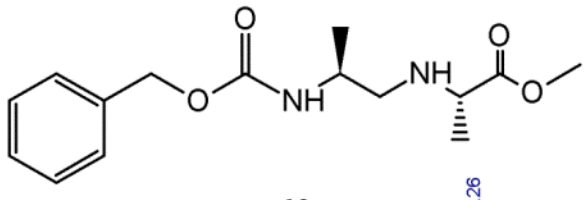

69

AP13-51-FR36-1H

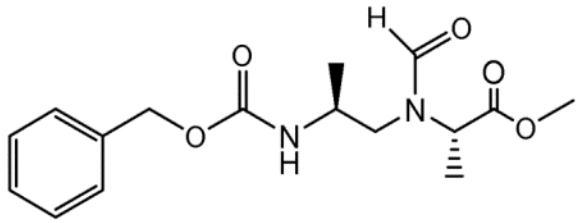

71

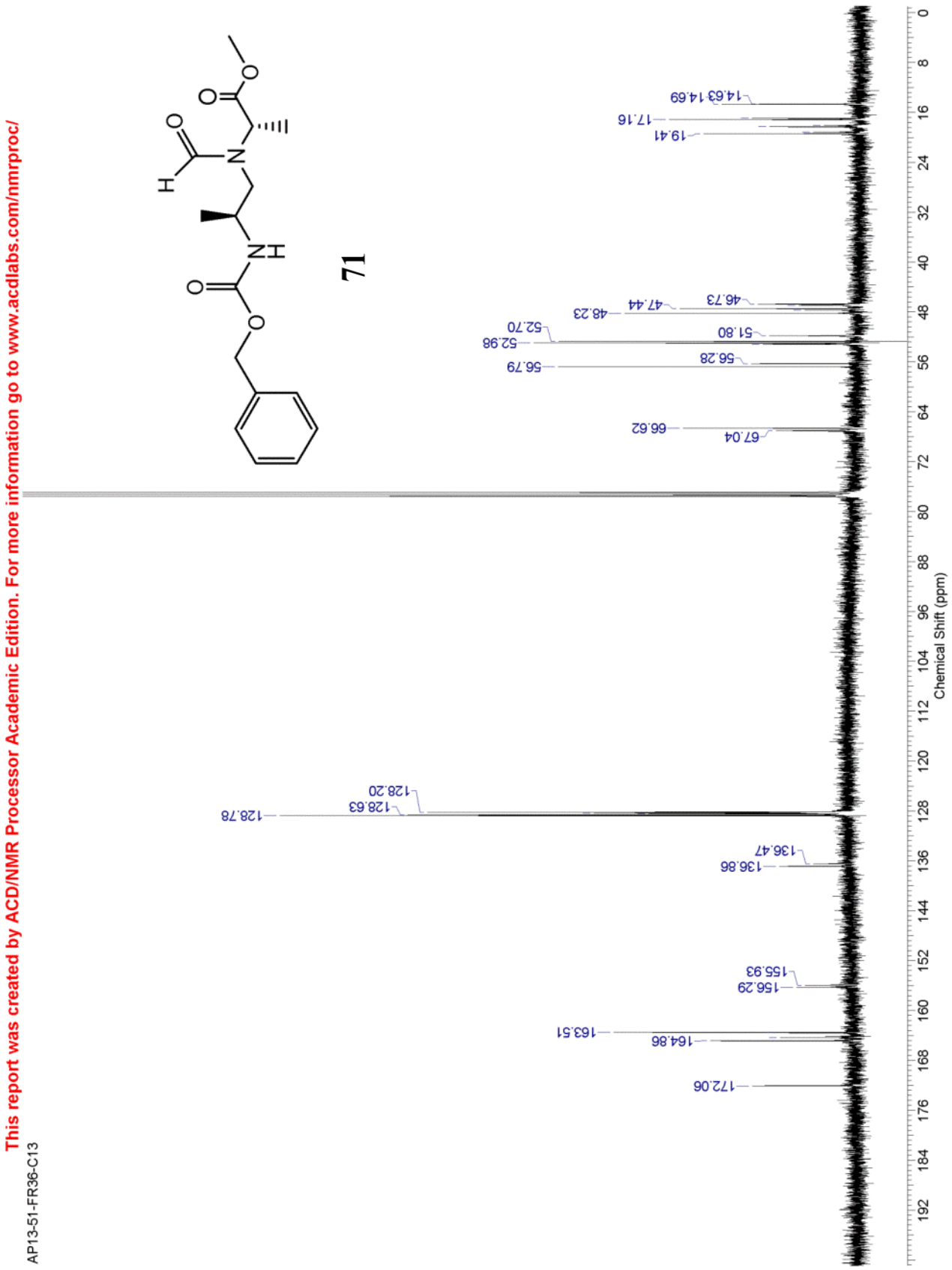
This report was created by ACD/NMR Processor Academic Edition. For more information go to www.acdlabs.com/nmrproc/
AP13-51-FR36-C13
71
14.63
14.69
17.16
19.41
46.73
47.44
48.23
51.80
52.70
52.98
56.28
56.79
66.62
67.04
128.20
128.63
128.78
136.47
136.86
155.93
156.29
163.51
164.86
172.06
Chemical Shift (ppm)

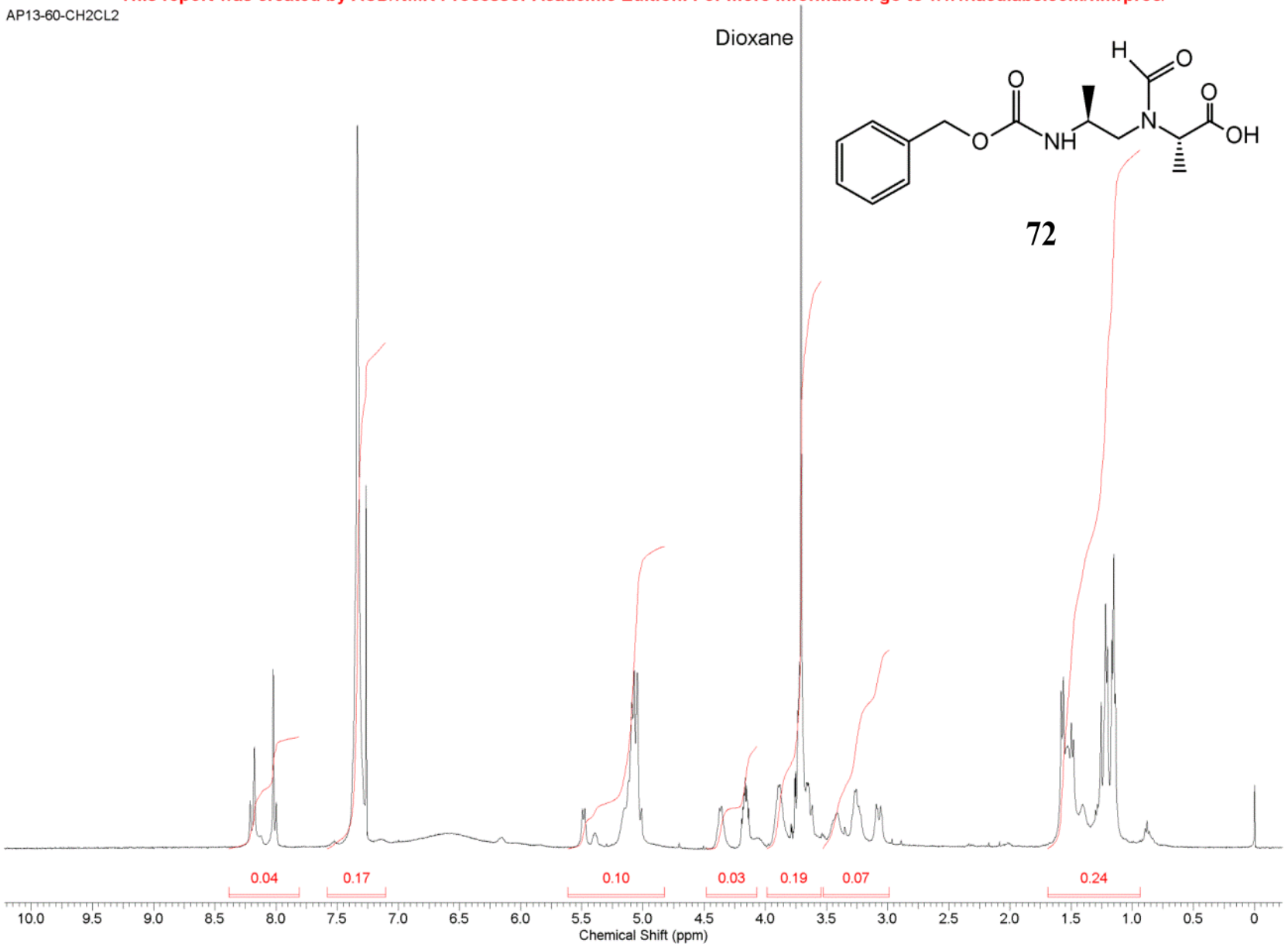

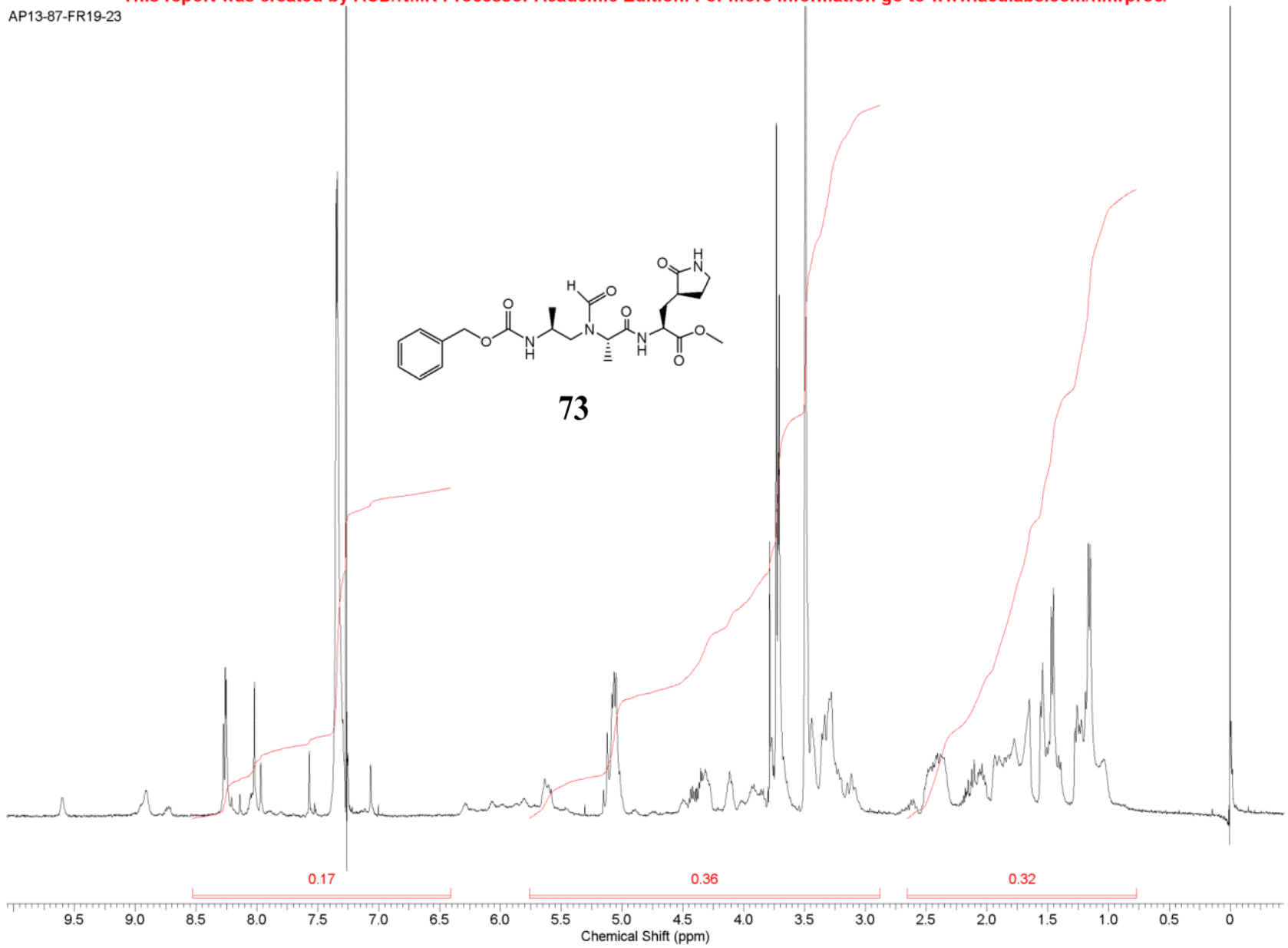

73

AP14-69-FR22

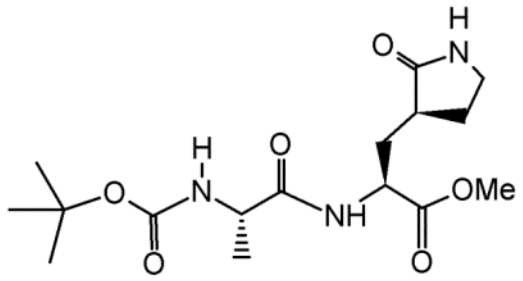

74

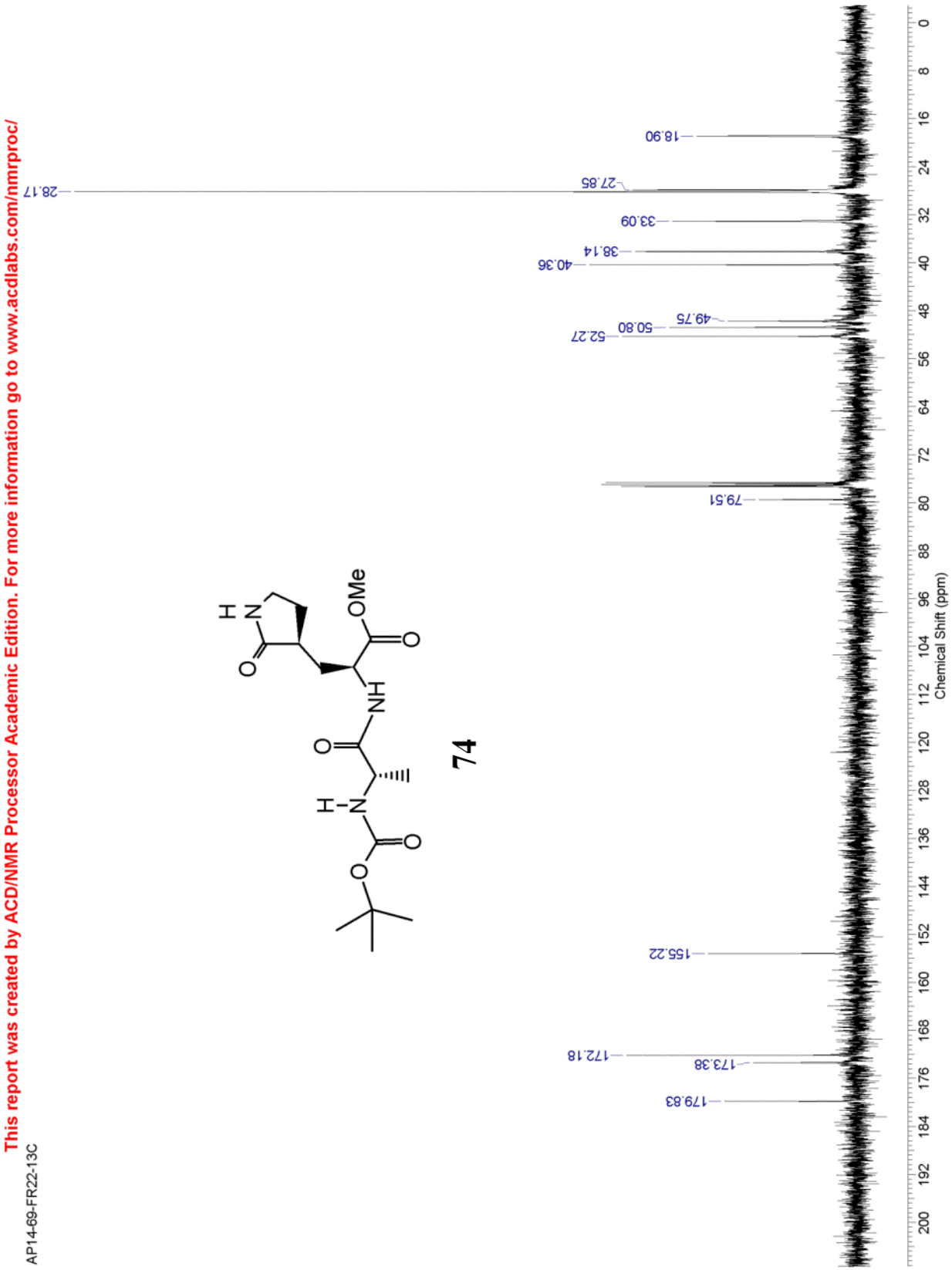
This report was created by ACD/NMR Processor Academic Edition. For more information go to www.acdlabs.com/nmrproc/
AP14-69-FR22-13C
74
28.17
27.85
18.90
33.09
38.14
40.36
49.75
50.80
52.27
79.51
155.22
172.18
173.38
179.83
Chemical Shift (ppm)

AP14-34-FR16

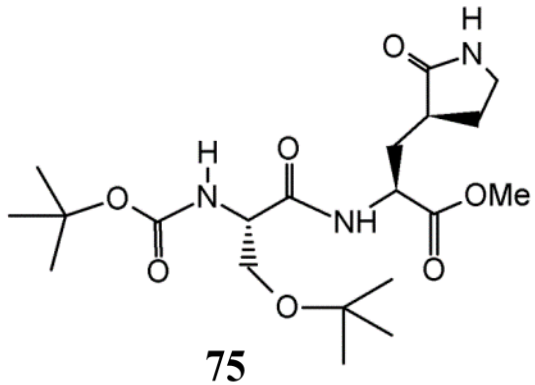

75

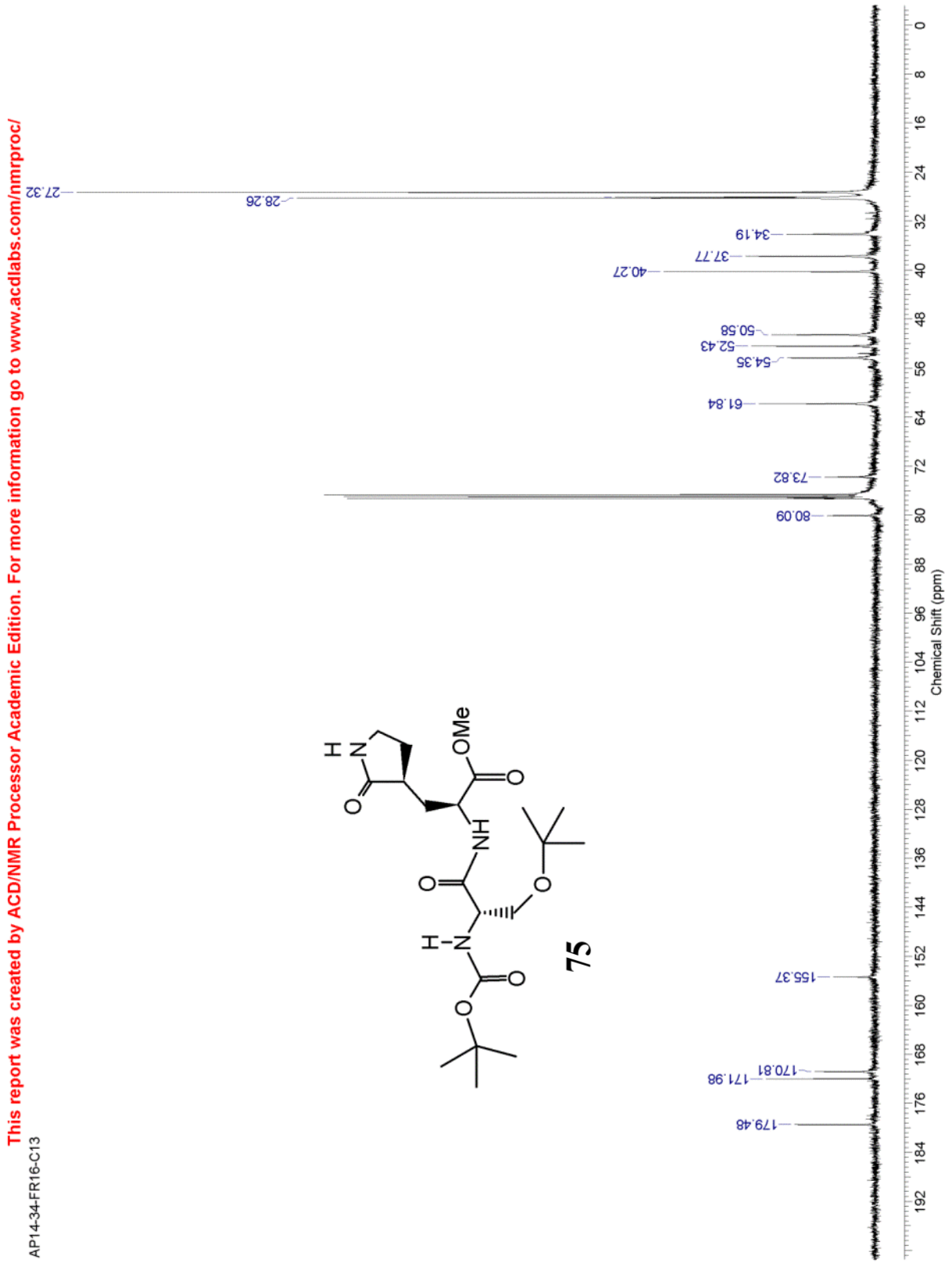
This report was created by ACD/NMR Processor Academic Edition. For more information go to www.acdlabs.com/nmrproc/
AP14-34-FR16-C13
27.32
28.26
34.19
37.77
40.27
50.58
52.43
54.35
61.84
73.82
80.09
155.37
170.81
171.98
179.48
Chemical Shift (ppm)
75

AP14-56-FR23-25

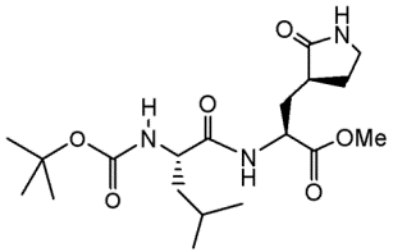

76

AP14-56-FR23-25-13C

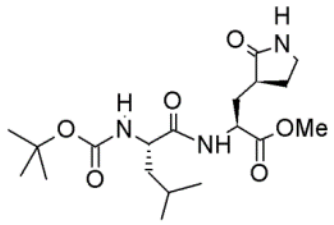

76

AP15-37-FR2-6

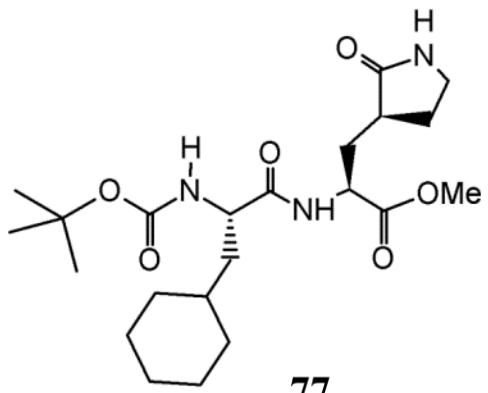

77

AP15-37-FR2-6-13C

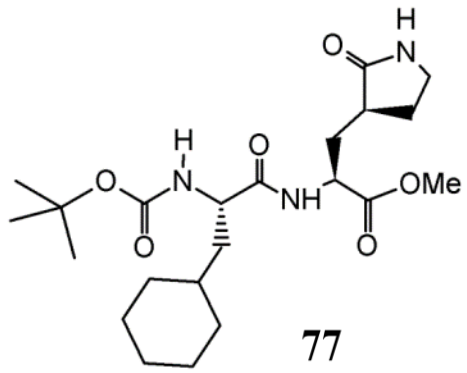

77

AP14-31-FR17

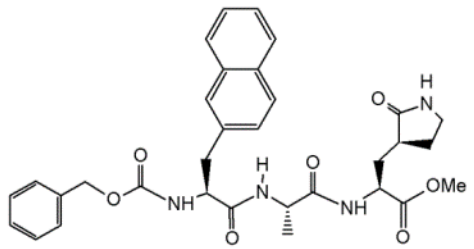

80

AP14-31-FR17-13C

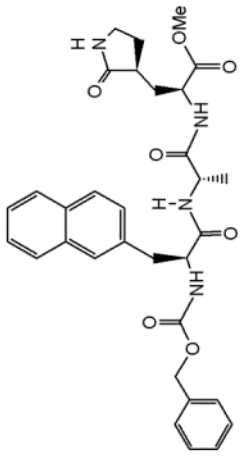

80

AP14-73-FR35-37

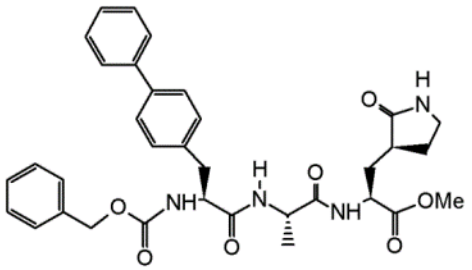

81

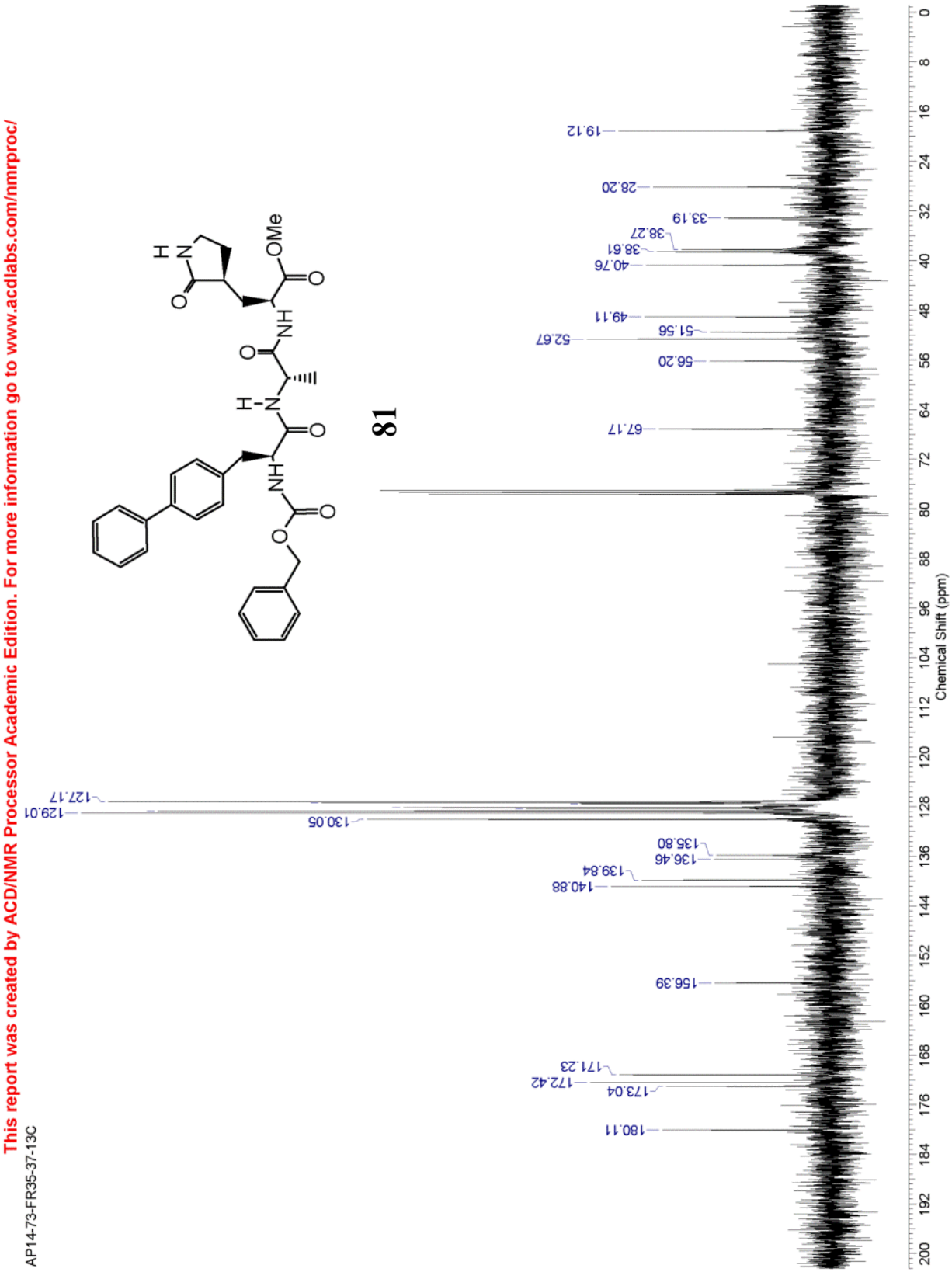
This report was created by ACD/NMR Processor Academic Edition. For more information go to www.acdlabs.com/nmrproc/
AP14-73-FR35-37-13C
81
19.12
28.20
33.19
38.27
38.61
40.76
49.11
51.56
52.67
56.20
67.17
127.17
129.01
130.05
135.80
136.46
139.84
140.88
156.39
171.23
172.42
173.04
180.11
Chemical Shift (ppm)

AP14-43-FR29

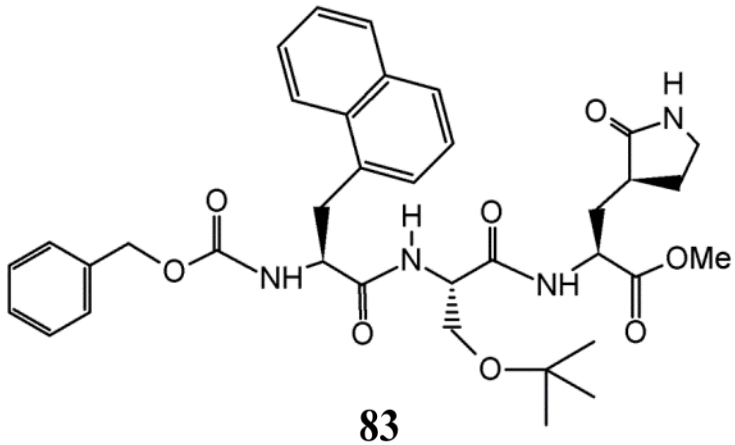

83

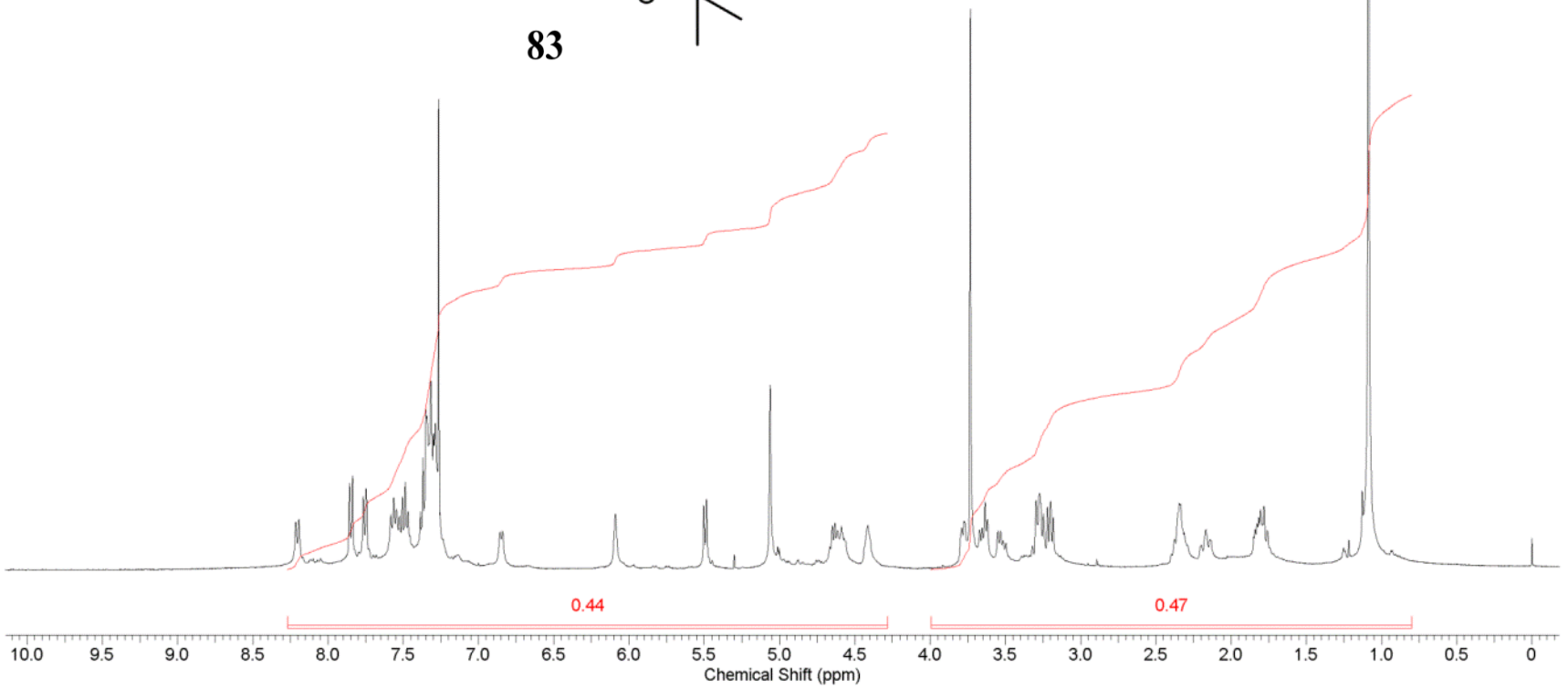

AP14-43-FR29-13C

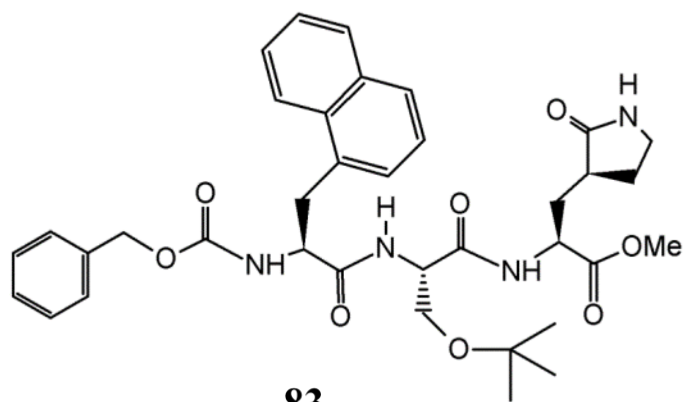

83

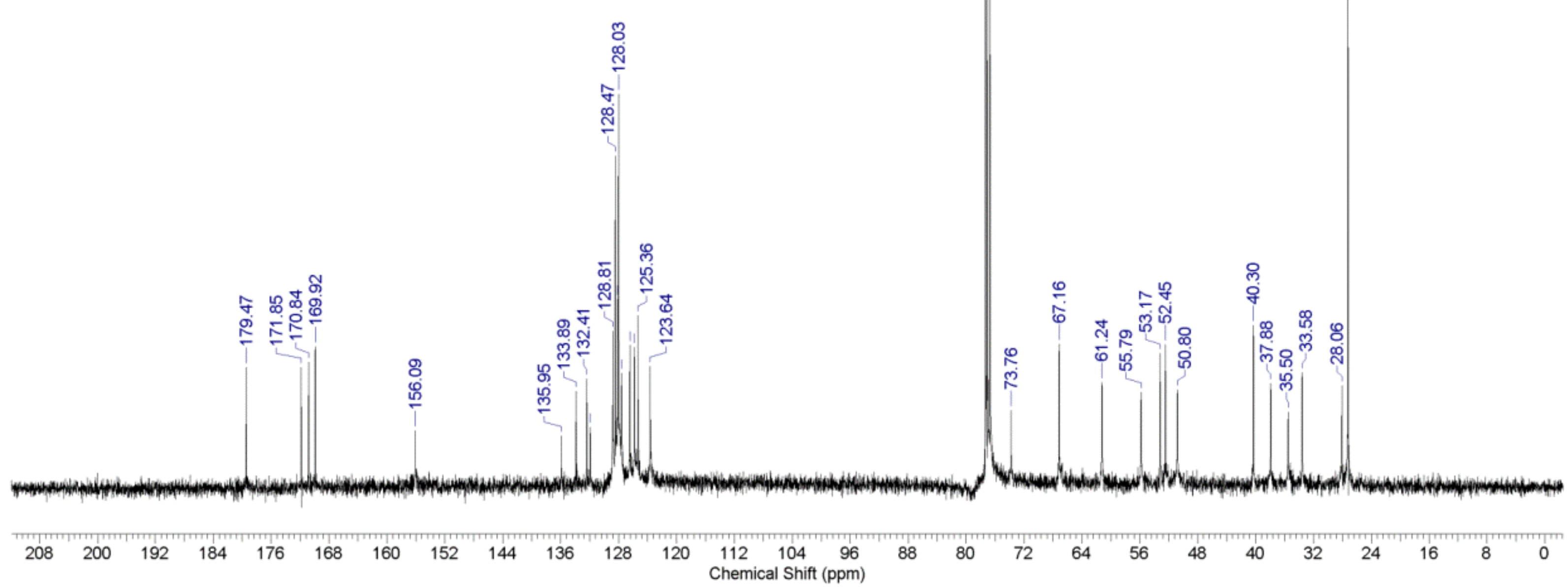

AP14-59-FR16-17

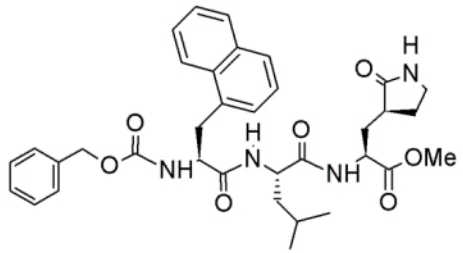

84

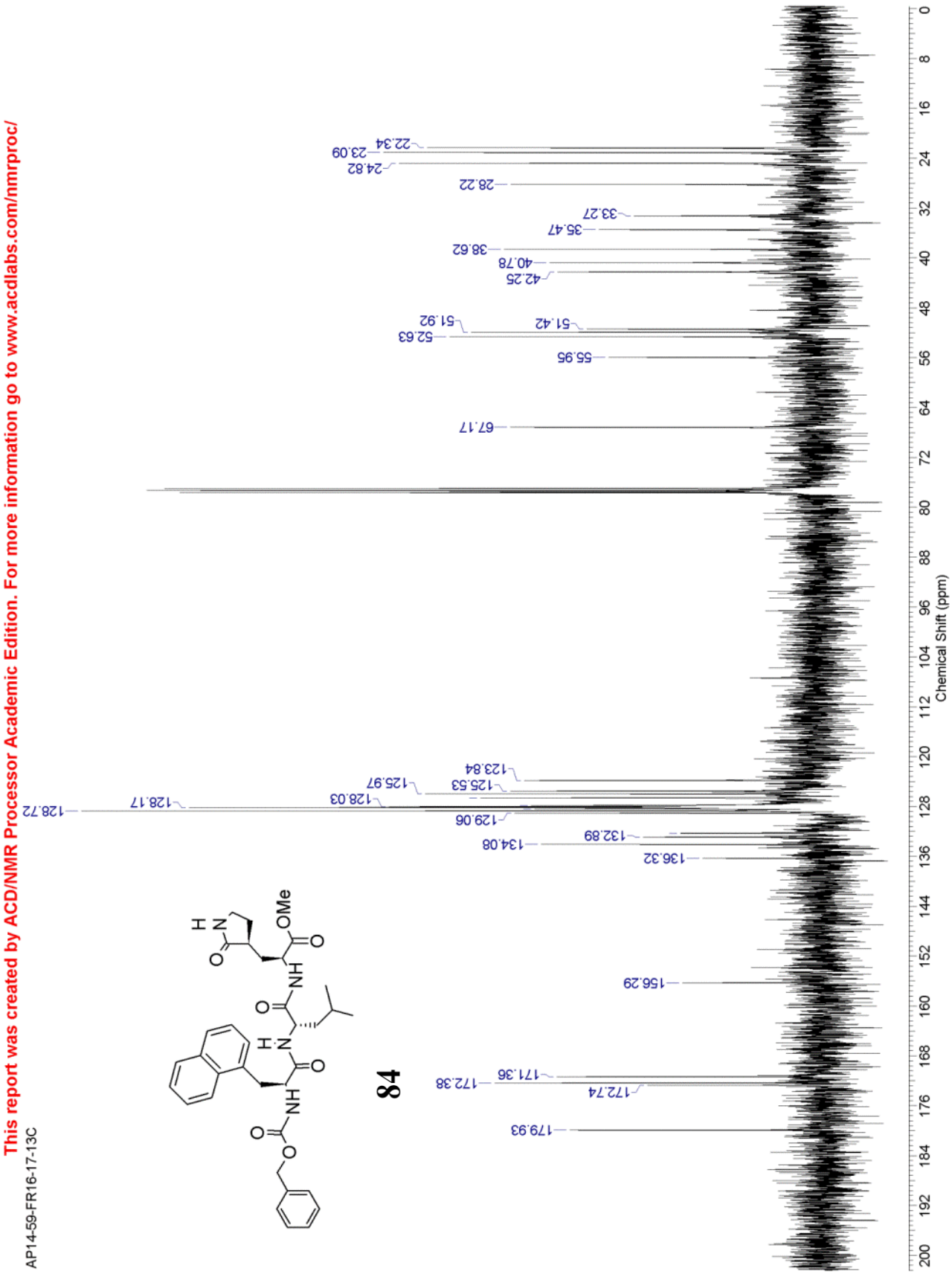
This report was created by ACD/NMR Processor Academic Edition. For more information go to www.acdlabs.com/nmrproc/
AP14-59-FR16-17-13C
84
22.34
23.09
24.82
28.22
33.27
35.47
38.62
40.78
42.25
51.42
51.92
52.63
55.95
67.17
123.84
125.53
125.97
128.03
128.17
128.72
129.06
132.89
134.08
136.32
156.29
171.36
172.38
172.74
179.93
Chemical Shift (ppm)

AP15-41-FR8

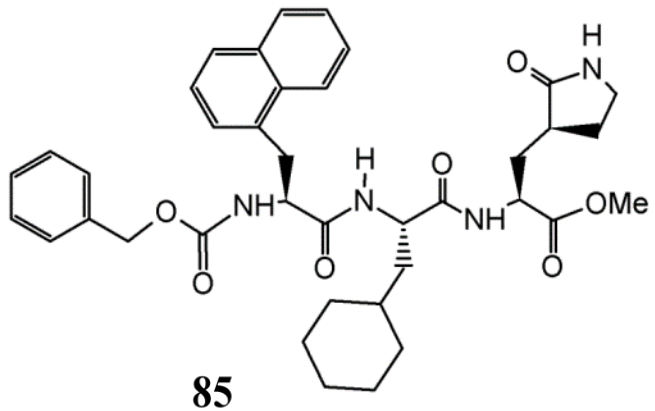

85

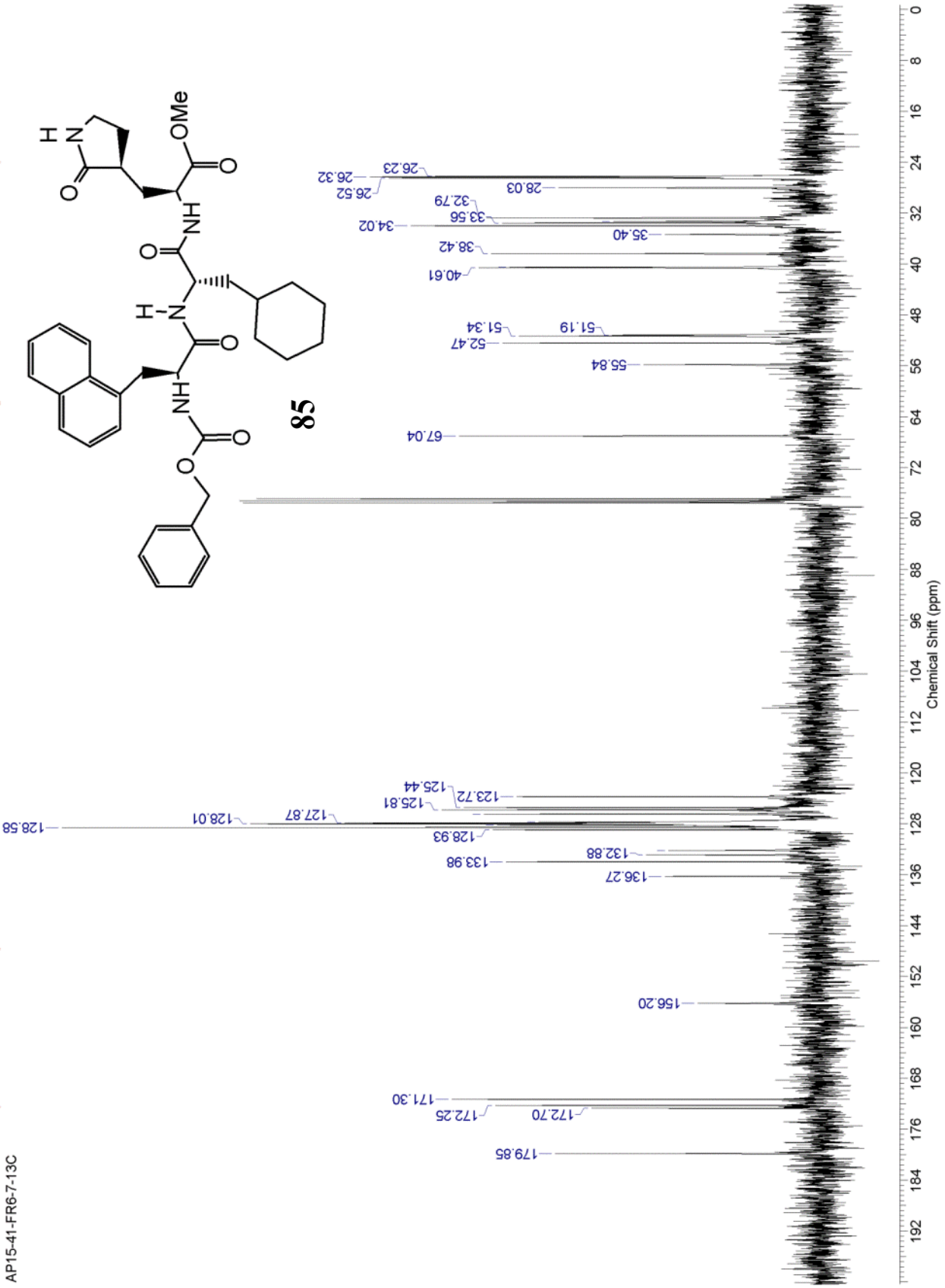
This report was created by ACD/NMR Processor Academic Edition. For more information go to www.acdlabs.com/nmrproc/
AP15-41-FR6-7-13C
85
179.85
172.70
172.25
171.30
156.20
136.27
133.98
132.88
128.93
128.58
128.01
127.87
125.81
125.44
123.72
67.04
55.84
52.47
51.19
51.34
40.61
38.42
35.40
34.02
33.56
32.79
28.03
26.52
26.32
26.23
Chemical Shift (ppm)

AP17-77-FR23

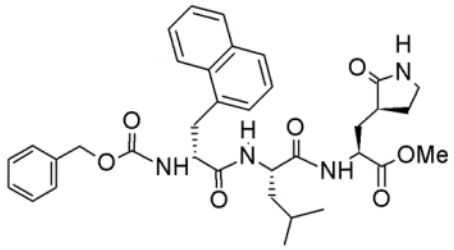

87

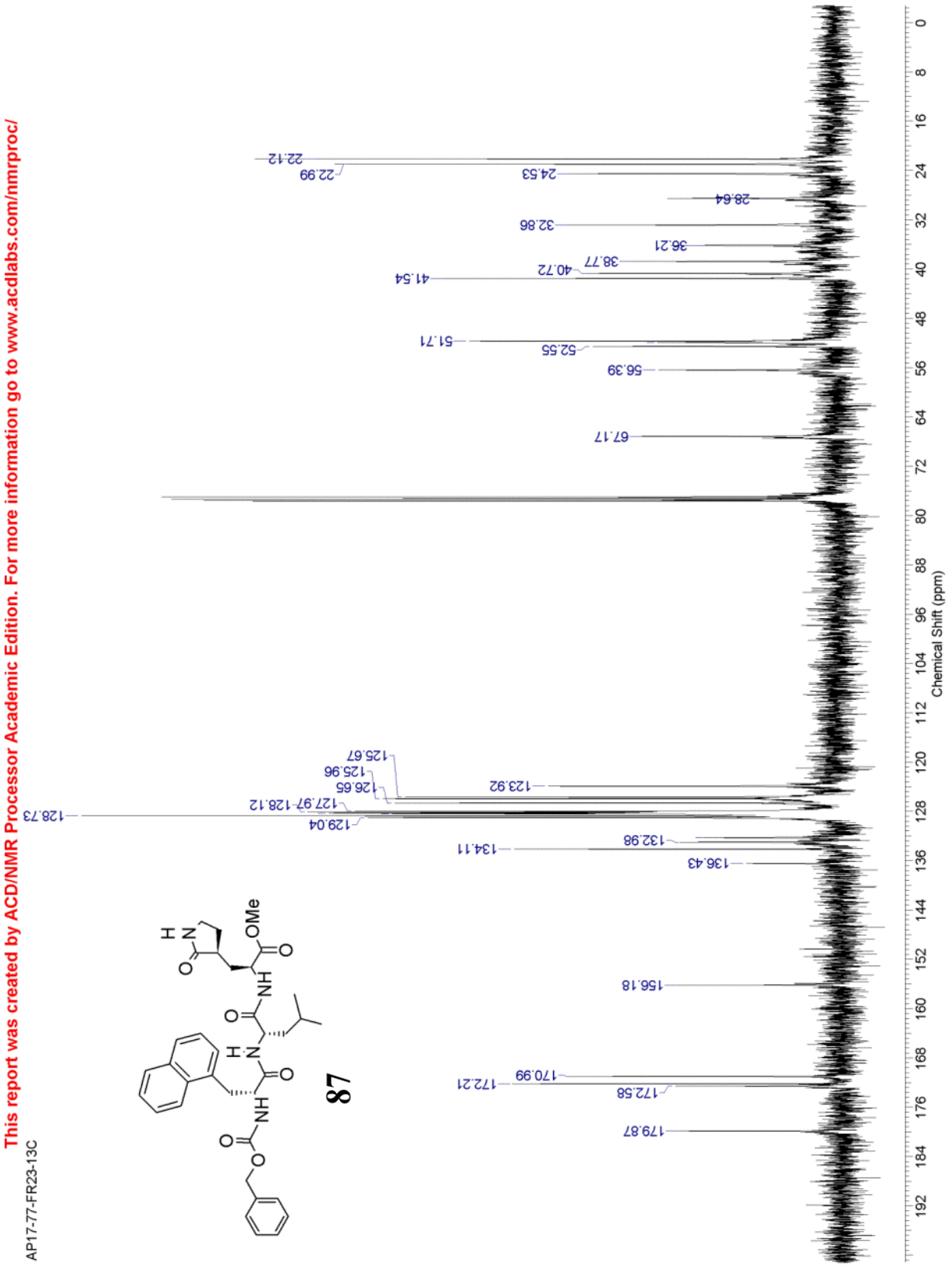
This report was created by ACD/NMR Processor Academic Edition. For more information go to www.acdlabs.com/nmrproc/
AP17-77-FR23-13C
87
Chemical Shift (ppm)
179.87
172.58
172.21
170.99
156.18
136.43
134.11
132.98
129.04
128.73
127.97
128.12
126.65
125.96
125.67
123.92
67.17
56.39
52.55
51.71
41.54
40.72
38.77
36.21
32.86
28.64
24.53
22.99
22.12

AP17-76-FR29

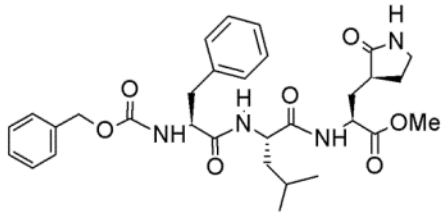

88

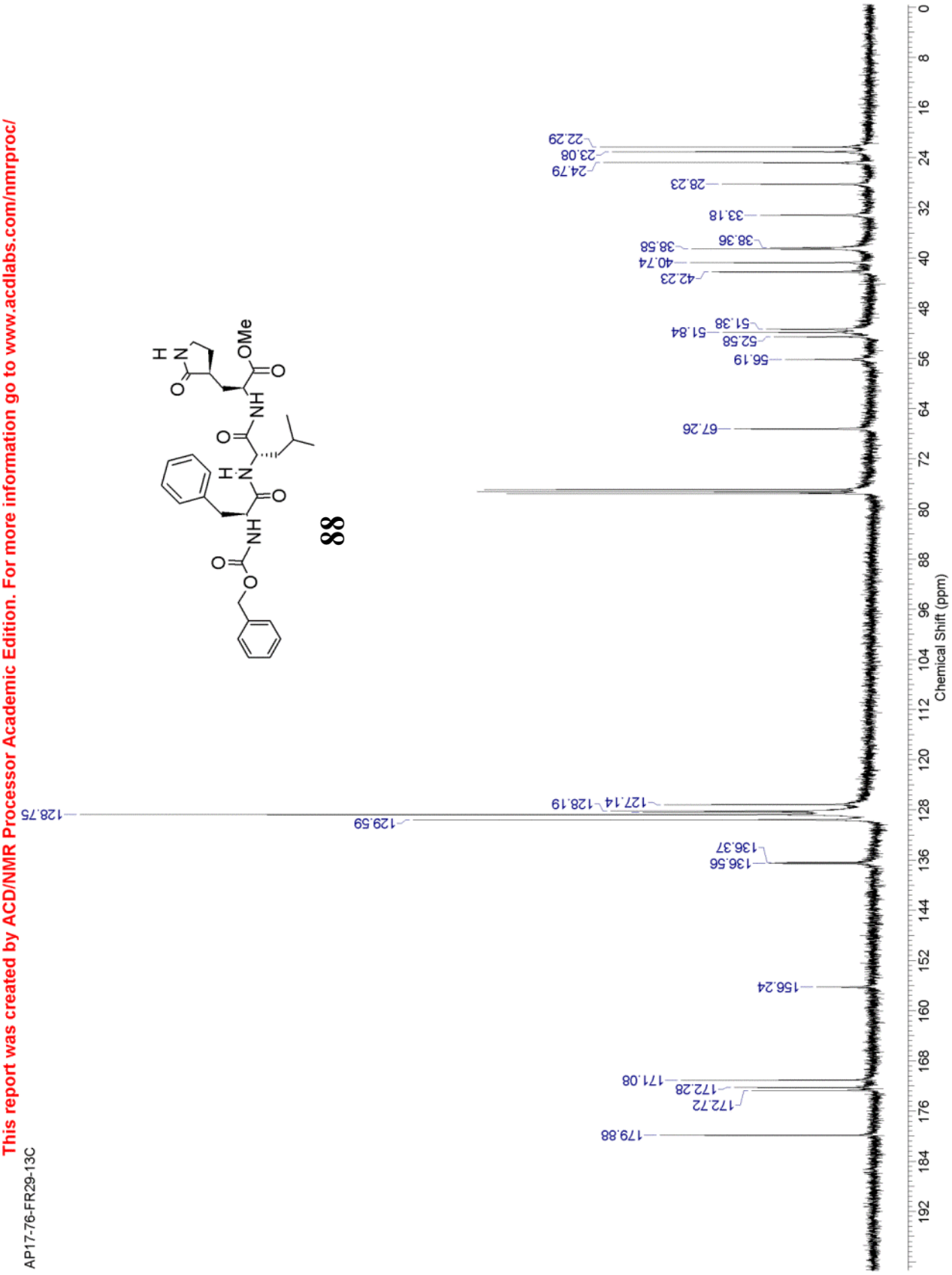
This report was created by ACD/NMR Processor Academic Edition. For more information go to www.acdlabs.com/nmrproc/
AP17-76-FR29-13C
88
179.88
172.72
172.28
171.08
156.24
136.56
136.37
129.59
128.75
127.14
128.19
67.26
56.19
52.58
51.84
51.38
42.23
40.74
38.58
38.36
33.18
28.23
24.79
23.08
22.29
Chemical Shift (ppm)

AP17-79-FR22

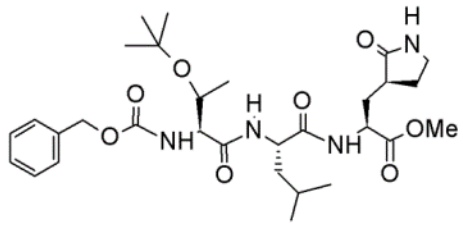

89

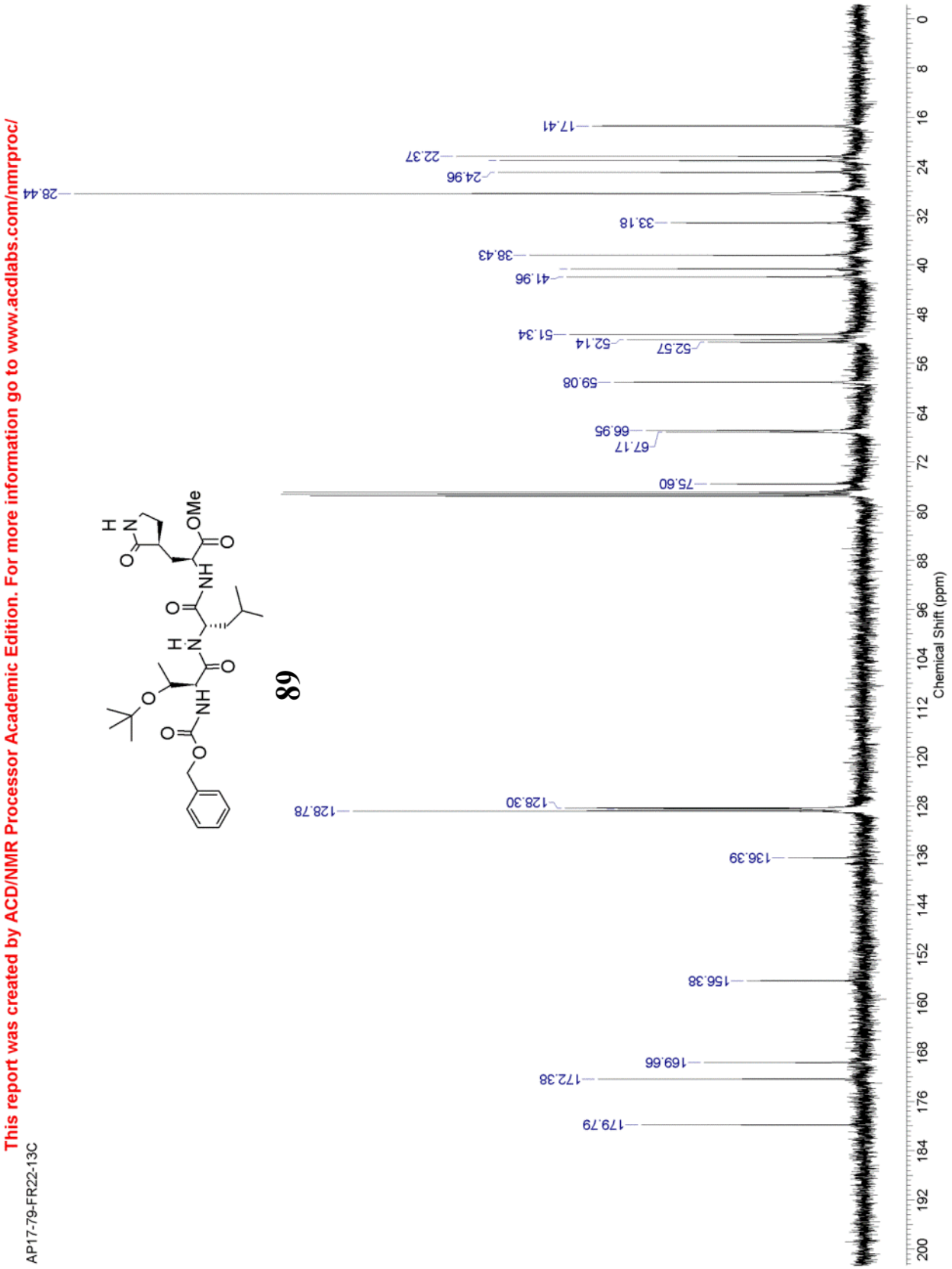
This report was created by ACD/NMR Processor Academic Edition. For more information go to www.acdlabs.com/nmrproc/
AP17-79-FR22-13C
89
17.41
22.37
24.96
28.44
33.18
38.43
41.96
51.34
52.14
52.57
59.08
66.95
67.17
75.60
128.30
128.78
136.39
156.38
169.66
172.38
179.79
Chemical Shift (ppm)

AP17-78-FR27

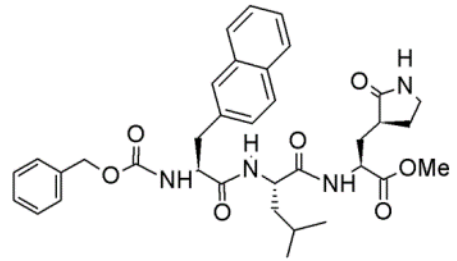

90

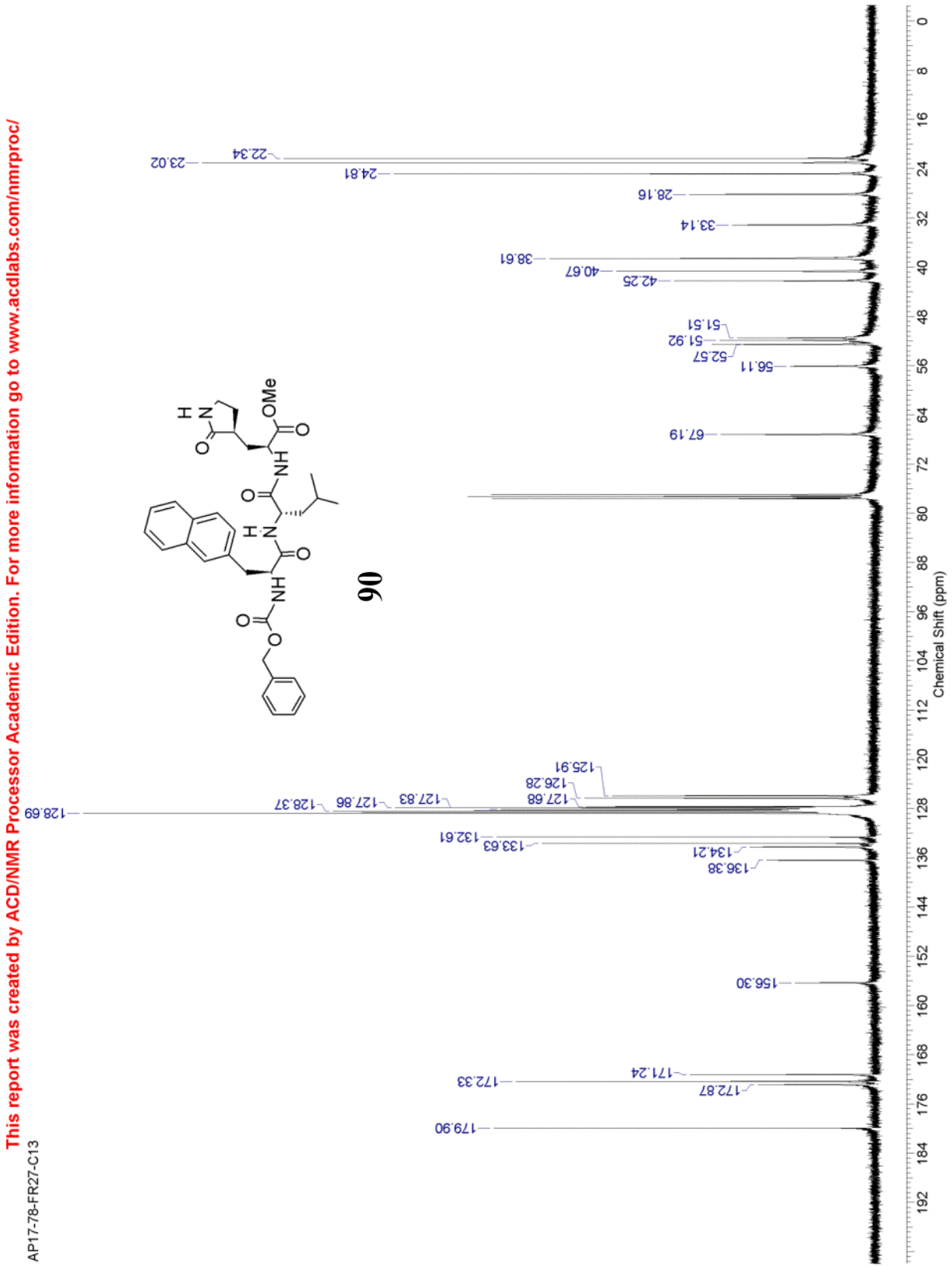
This report was created by ACD/NMR Processor Academic Edition. For more information go to www.acdlabs.com/nmrproc/
AP17-78-FR27-C13
90
Chemical Shift (ppm)
23.02
22.34
24.81
28.16
33.14
38.61
40.67
42.25
51.51
51.92
52.57
56.11
67.19
125.91
126.28
127.68
127.83
127.86
128.37
128.69
132.61
133.63
134.21
136.38
156.30
171.24
172.33
172.87
179.90

AP17-80-FR18

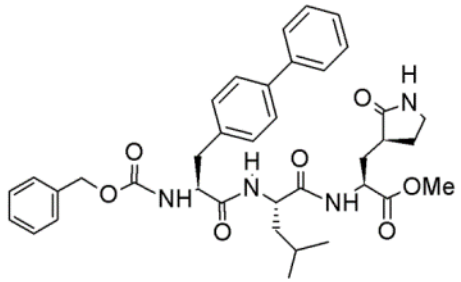

91

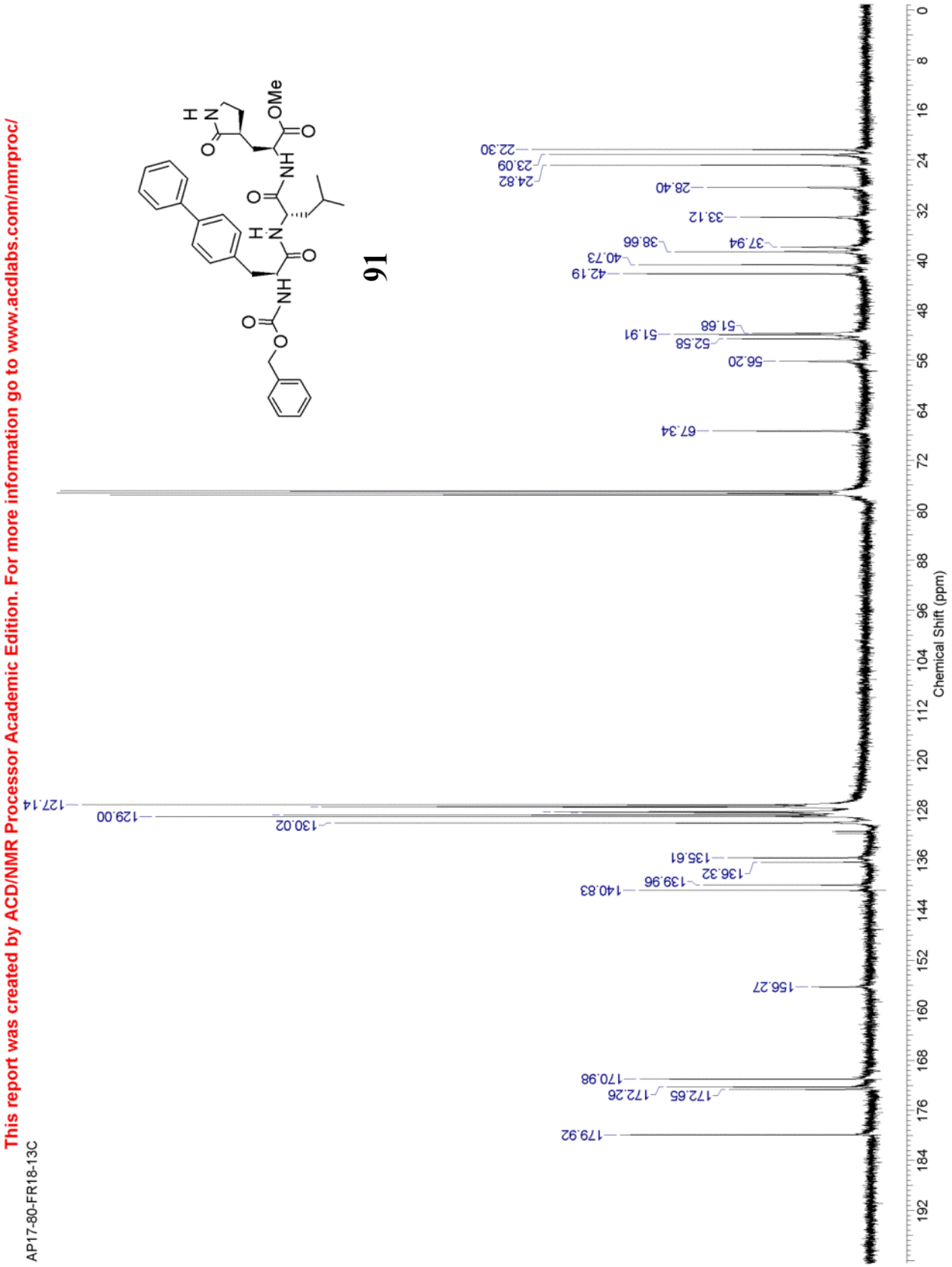
This report was created by ACD/NMR Processor Academic Edition. For more information go to www.acdlabs.com/nmrproc/
AP17-80-FR18-13C
91
22.30
23.09
24.82
28.40
33.12
37.94
38.66
40.73
42.19
51.68
51.91
52.58
56.20
67.34
127.14
129.00
130.02
135.61
136.32
139.96
140.83
156.27
170.98
172.26
172.65
179.92
Chemical Shift (ppm)

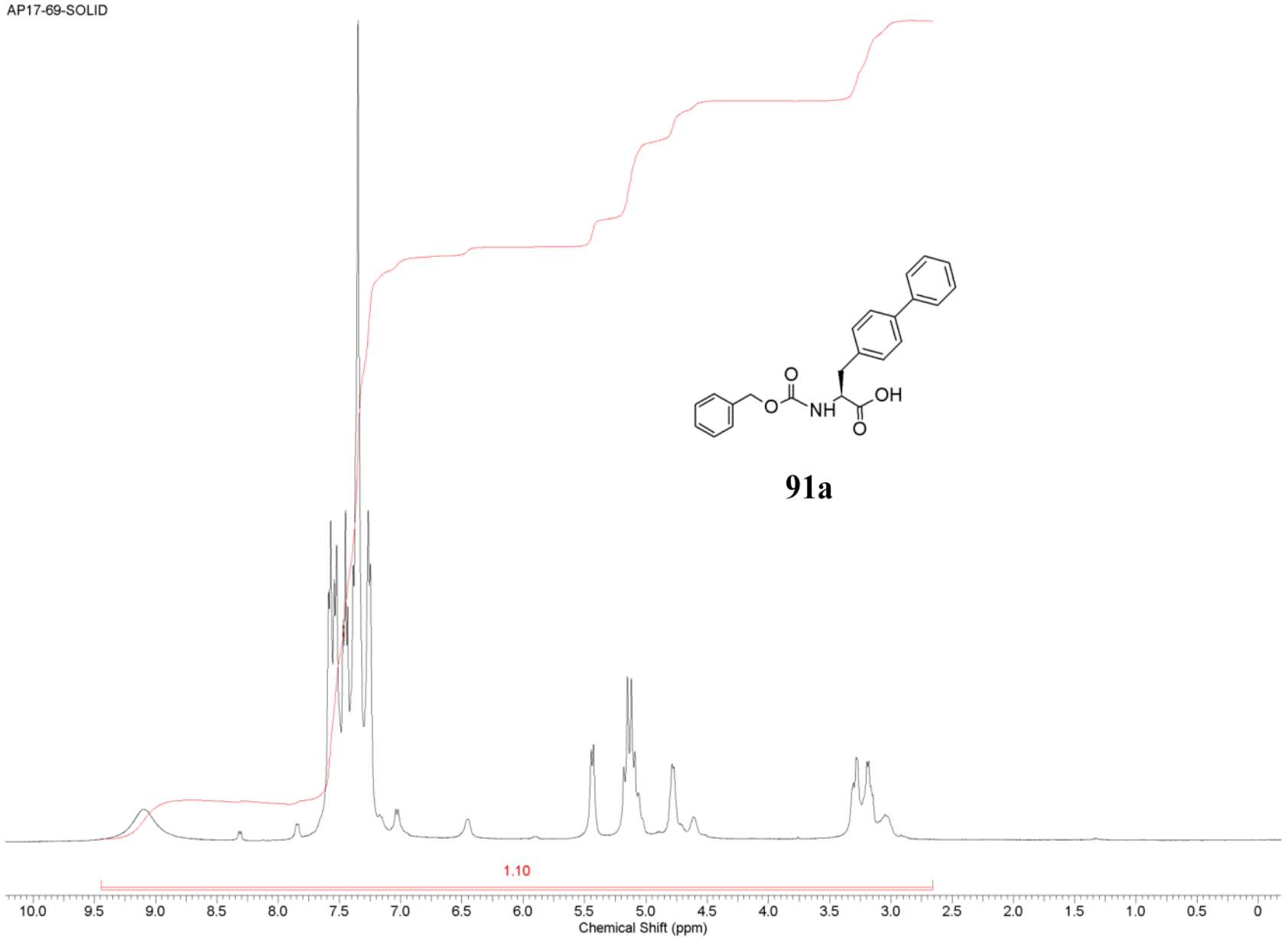

91a

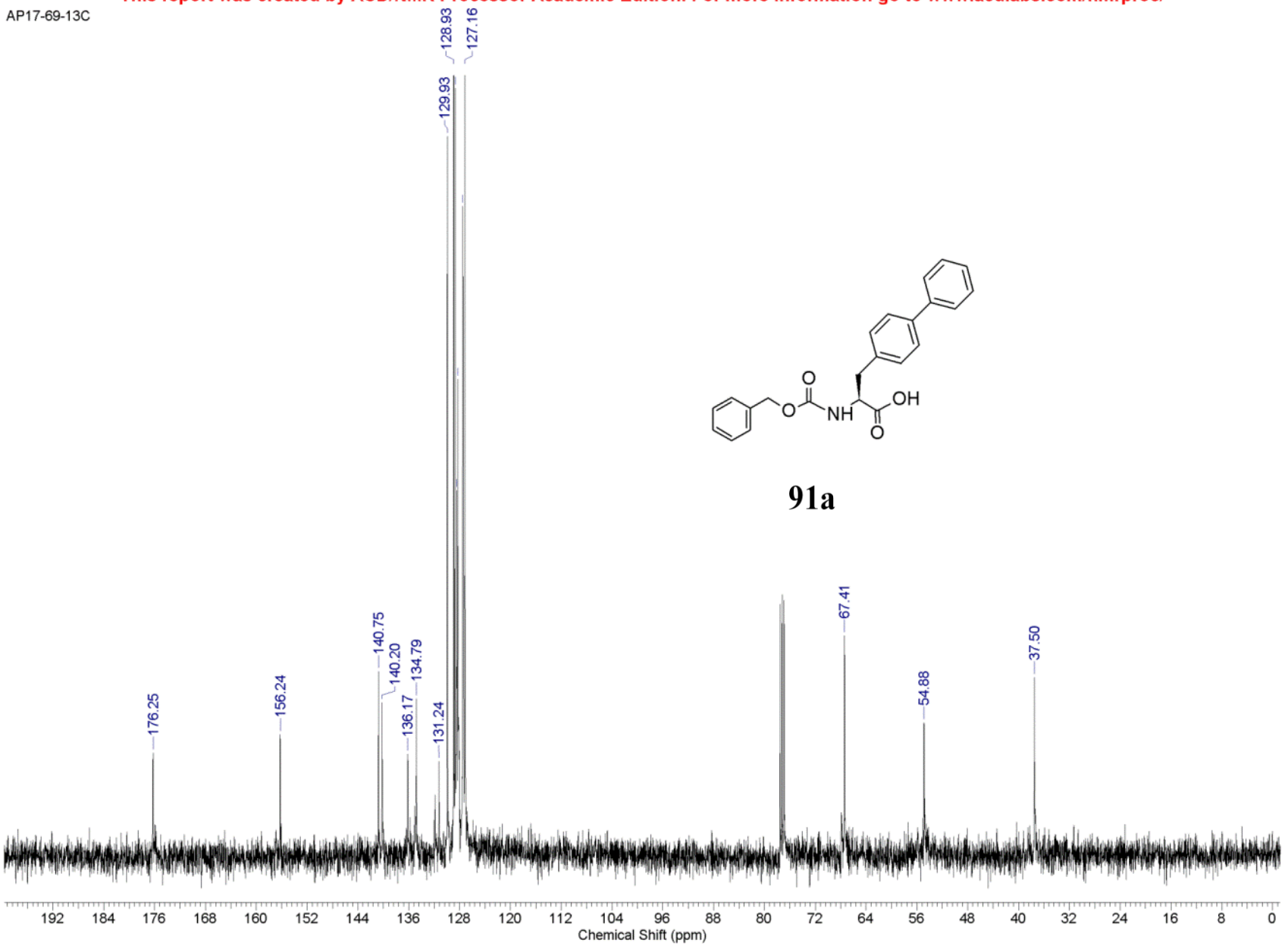

91a

AP16-105-FR39

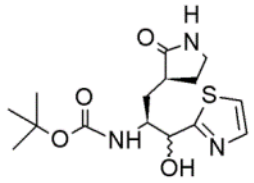

less polar

92-lp

AP16-105-FR50-52

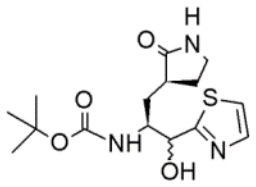

more polar

92-mp

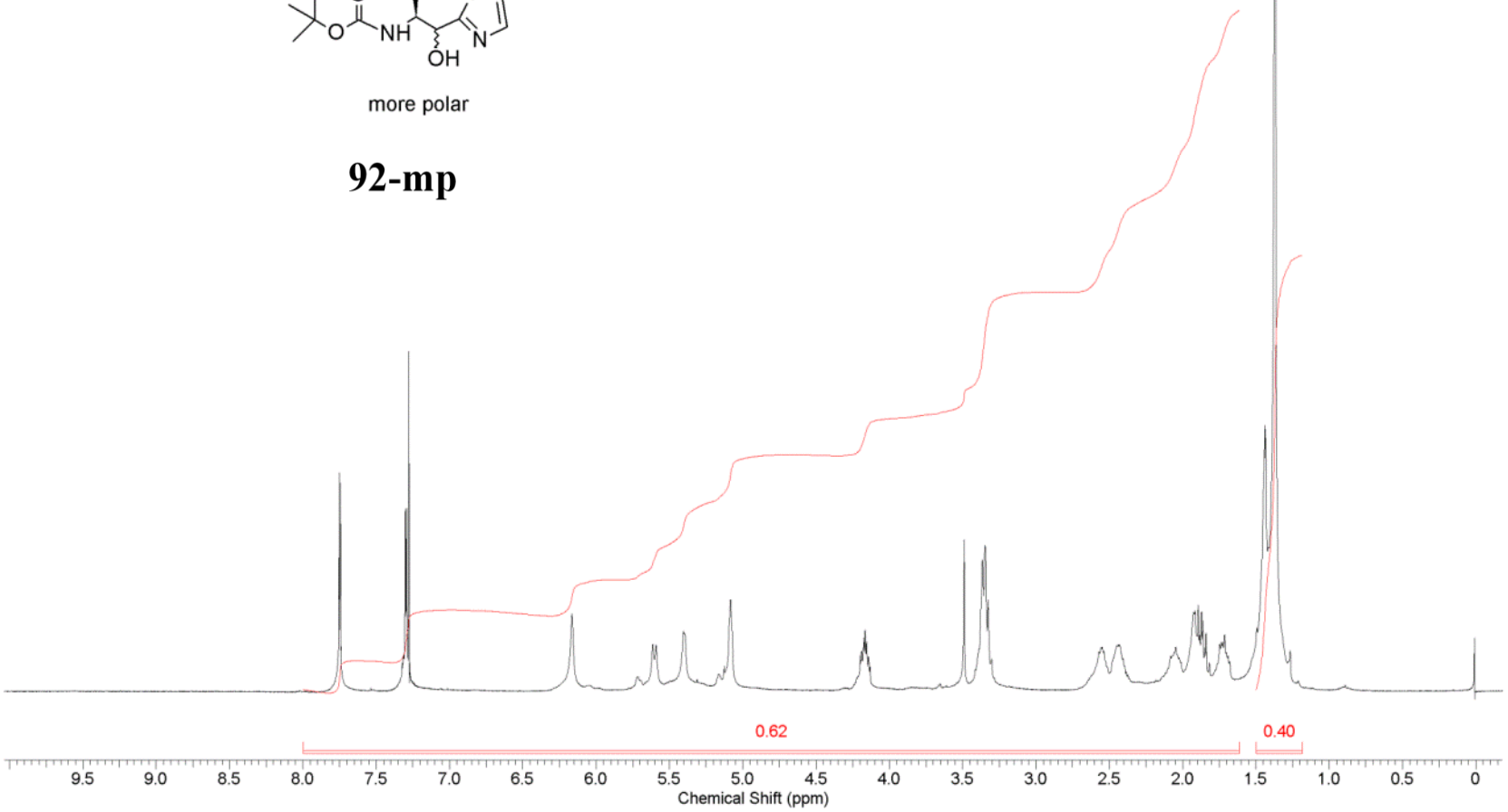

AP16-107-FR17

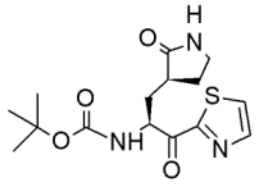

93

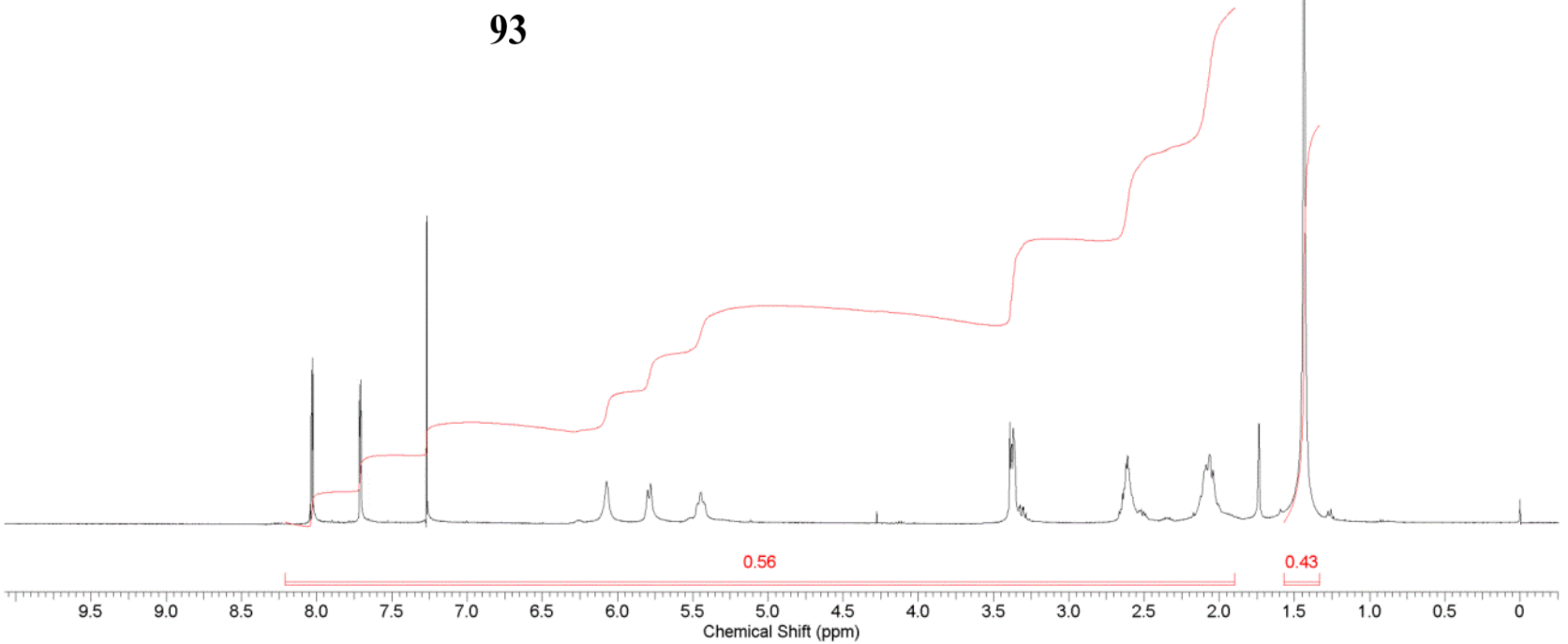

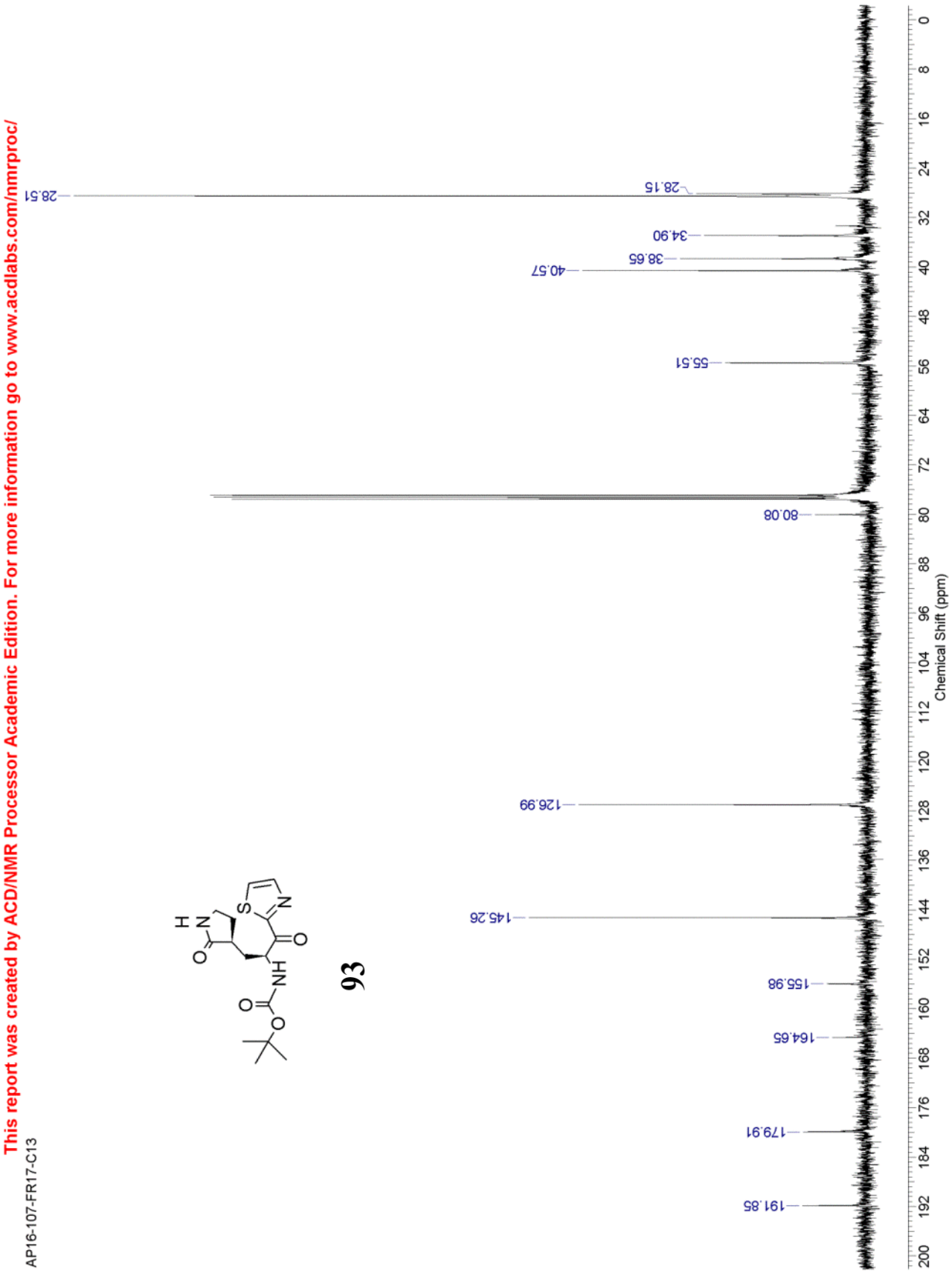
This report was created by ACD/NMR Processor Academic Edition. For more information go to www.acdlabs.com/nmrproc/
AP16-107-FR17-C13
28.51
28.15
34.90
38.65
40.57
55.51
80.08
126.99
145.26
155.98
164.65
179.91
191.85
Chemical Shift (ppm)

93

AP16-109-FR13

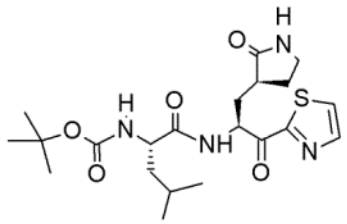

94

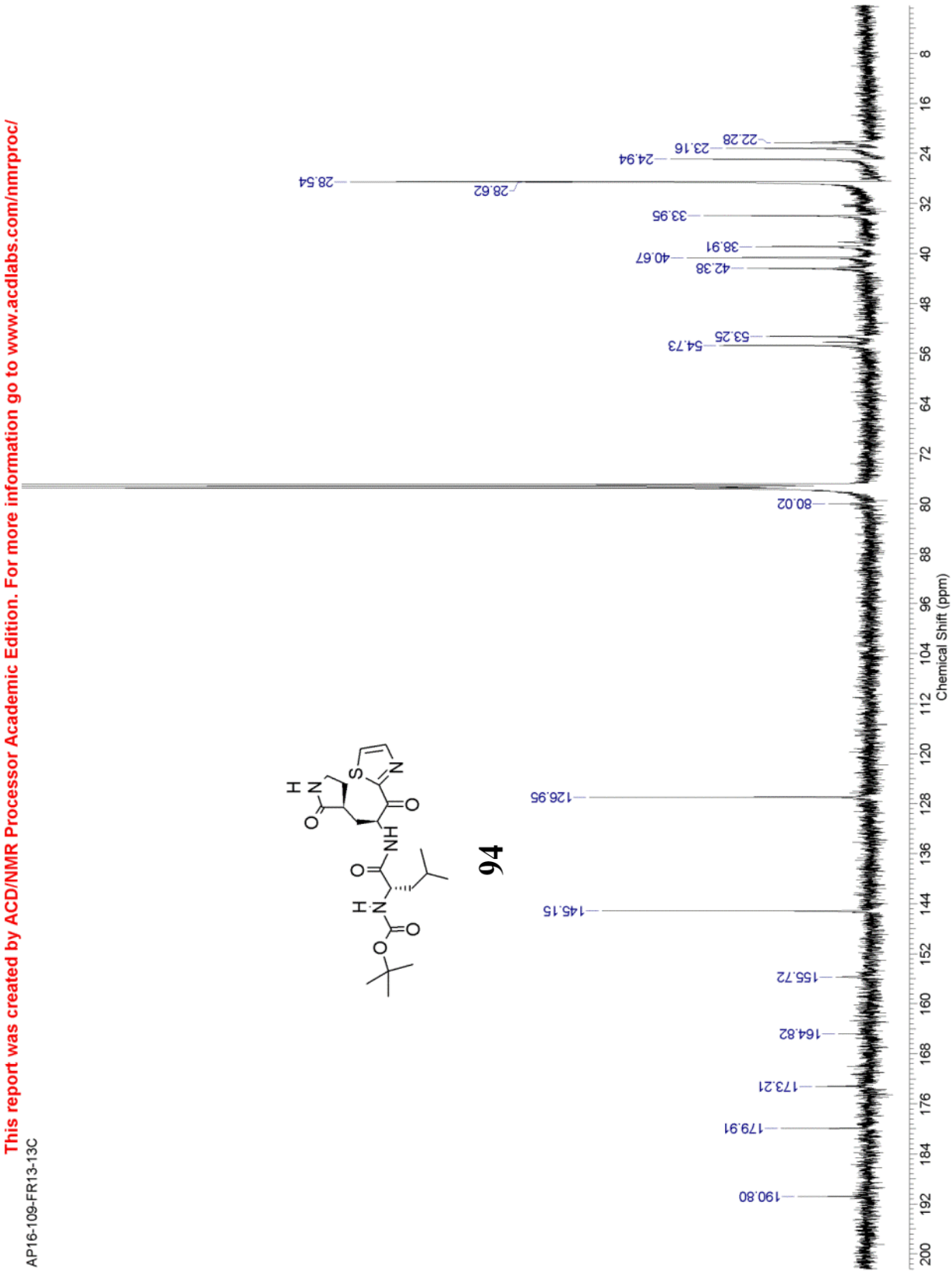
This report was created by ACD/NMR Processor Academic Edition. For more information go to www.acdlabs.com/nmrproc/
AP16-109-FR13-13C
94
190.80
179.91
173.21
164.82
155.72
145.15
126.95
80.02
53.25
54.73
42.38
40.67
38.91
33.95
28.62
28.54
24.94
23.16
22.28
Chemical Shift (ppm)

AP16-71-FR14

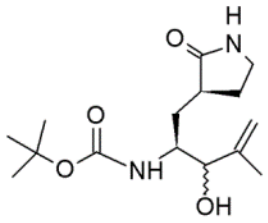

95

AP16-75-FR29-30

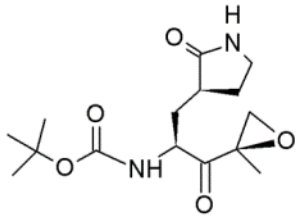

96-lp

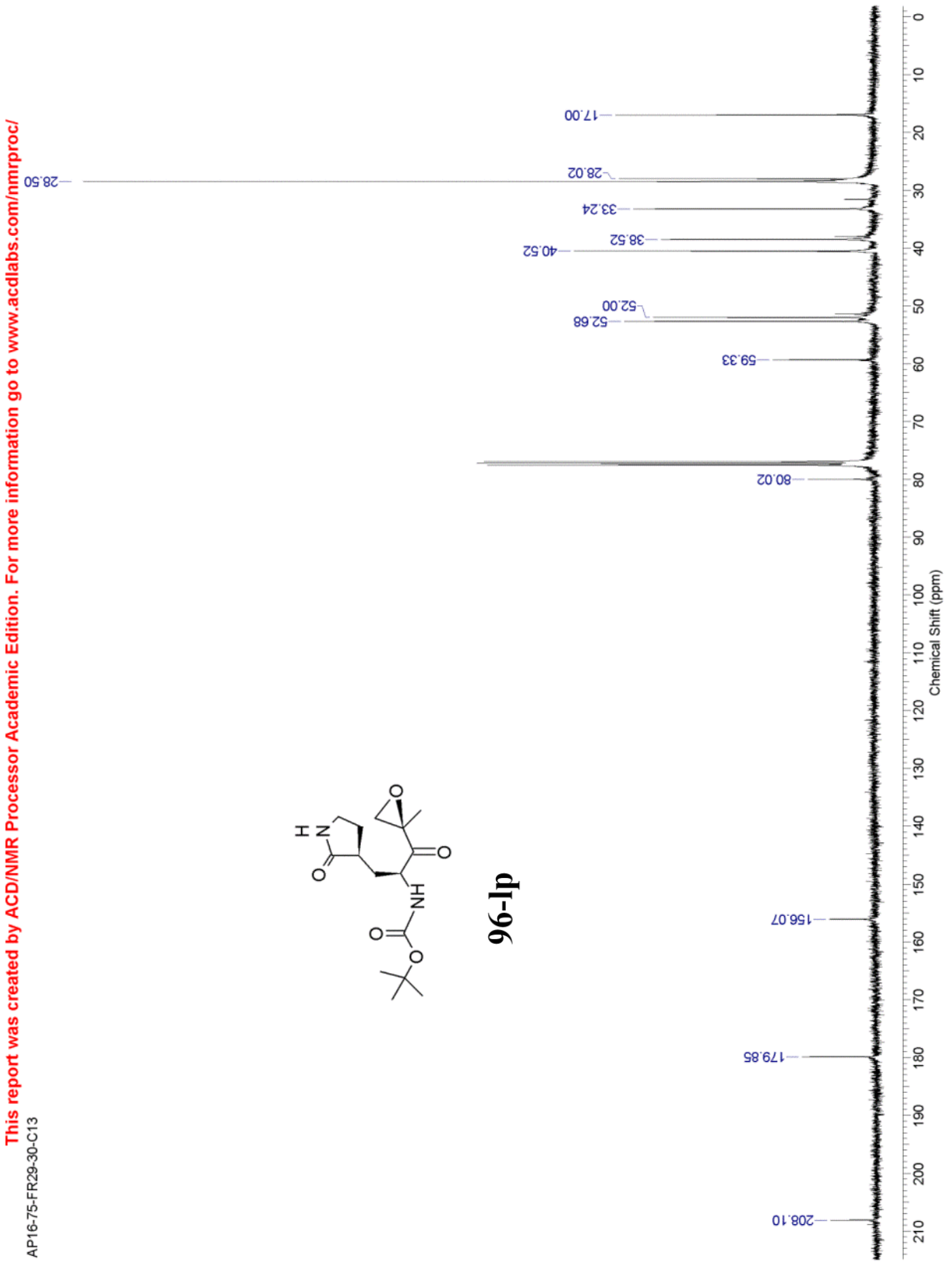
This report was created by ACD/NMR Processor Academic Edition. For more information go to www.acdlabs.com/nmrproc/
AP16-75-FR29-30-C13
96-Ip
17.00
28.02
28.50
33.24
38.52
40.52
52.00
52.68
59.33
80.02
156.07
179.85
208.10
Chemical Shift (ppm)

AP16-75-FR41-43

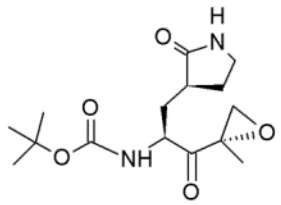

96-mp

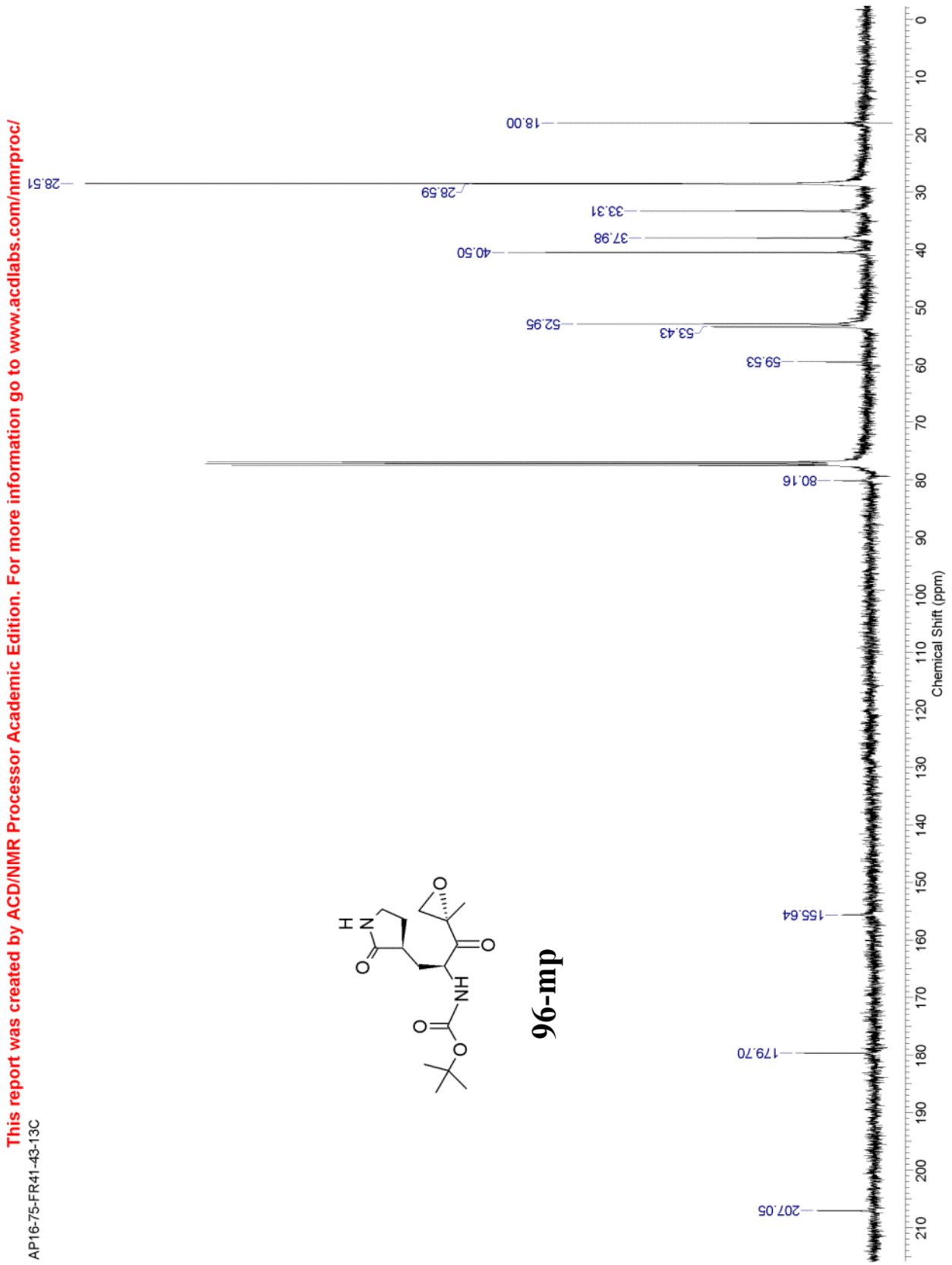
This report was created by ACD/NMR Processor Academic Edition. For more information go to www.acdlabs.com/nmrproc/
AP16-75-FR41-43-13C
96-mp
18.00
28.51
28.59
33.31
37.98
40.50
52.95
53.43
59.53
80.16
155.64
179.70
207.05
Chemical Shift (ppm)

AP16-79-FR19-21

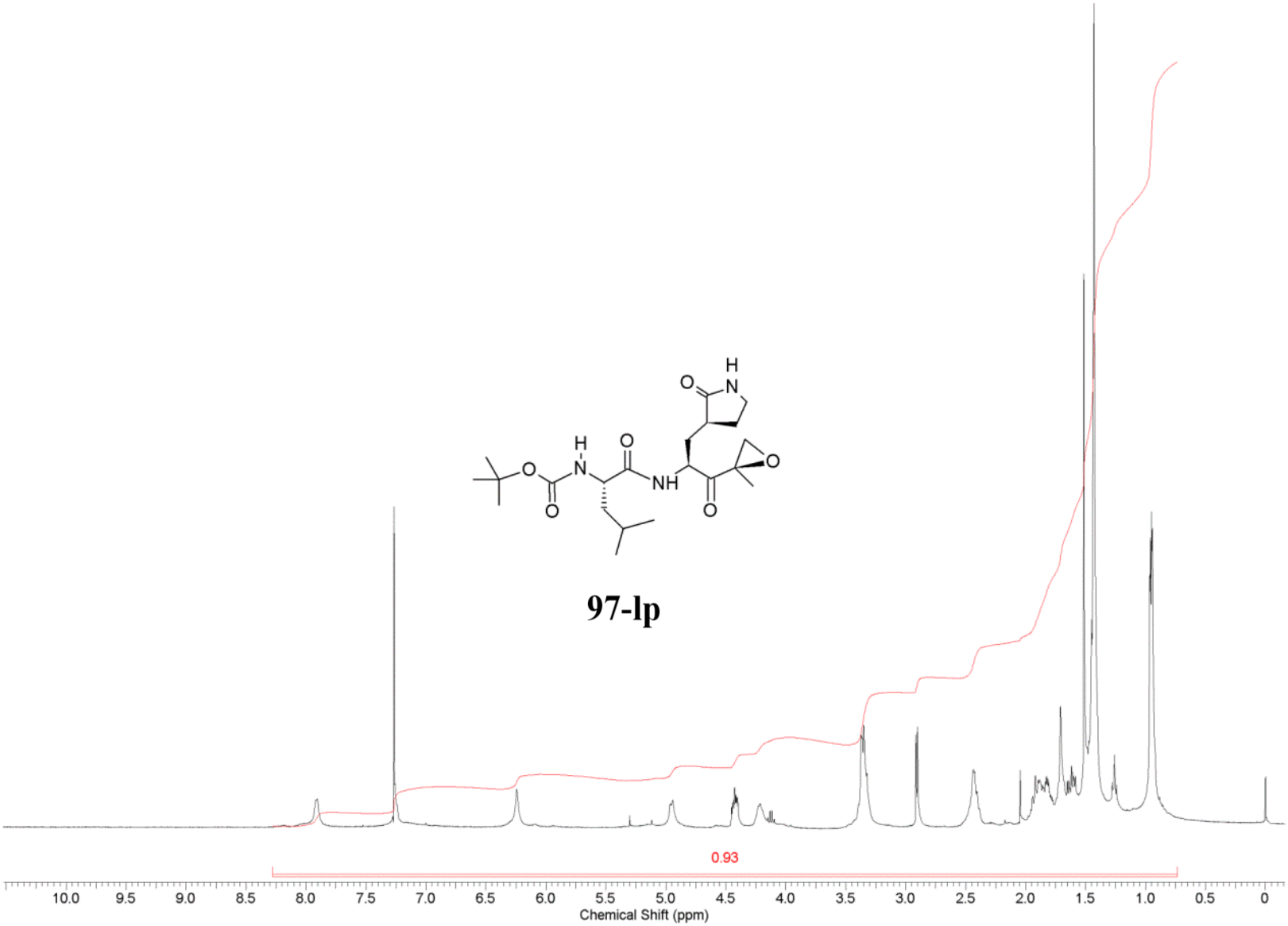

97-lp

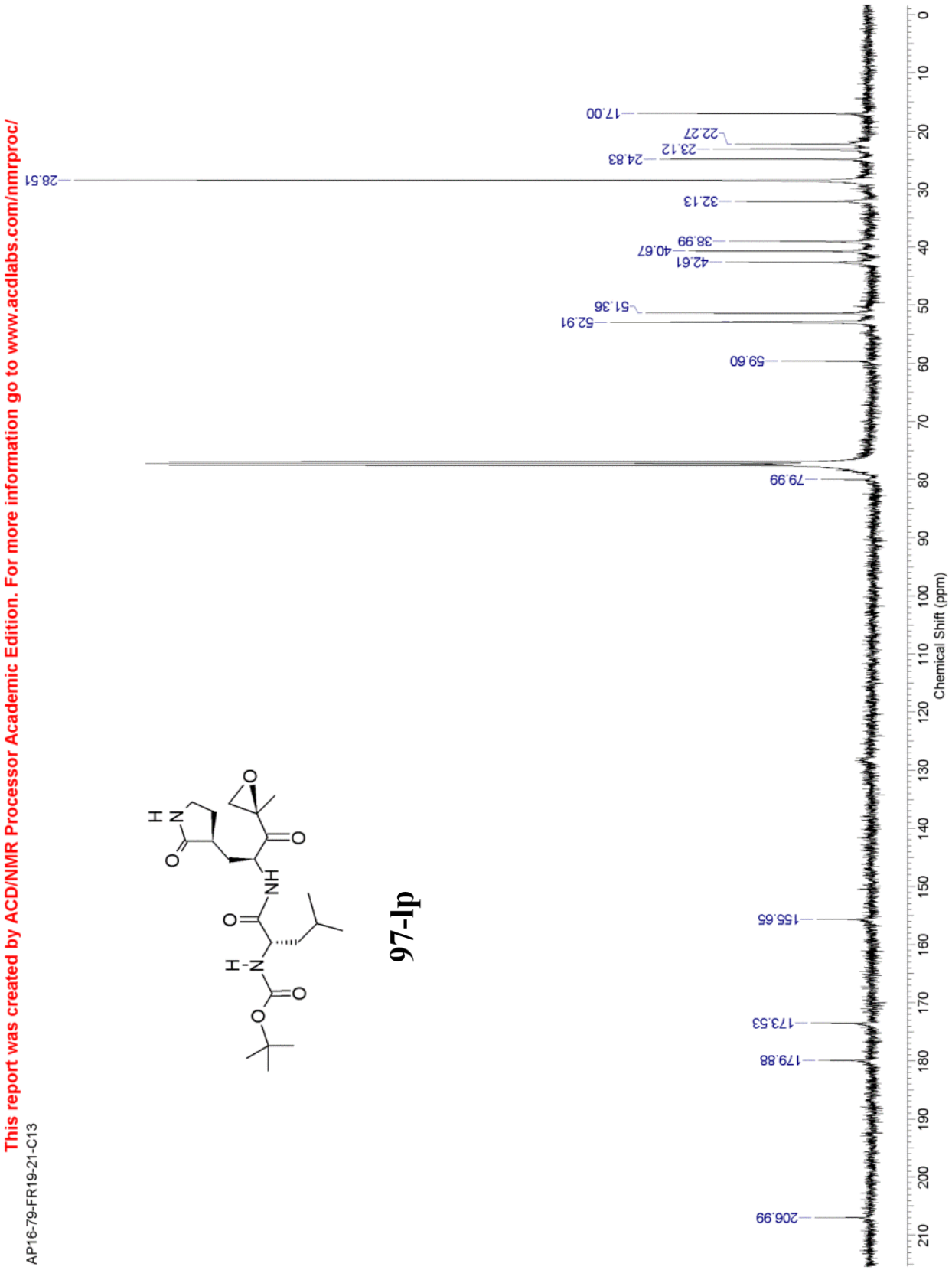
This report was created by ACD/NMR Processor Academic Edition. For more information go to www.acdlabs.com/nmrproc/
AP16-79-FR19-21-C13
97-lp
206.99
179.88
173.53
155.65
79.99
59.60
52.91
51.36
42.61
40.67
38.99
32.13
28.51
24.83
23.12
22.27
17.00
Chemical Shift (ppm)

AP16-92-FR12

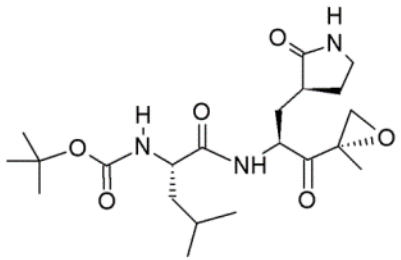

97-mp

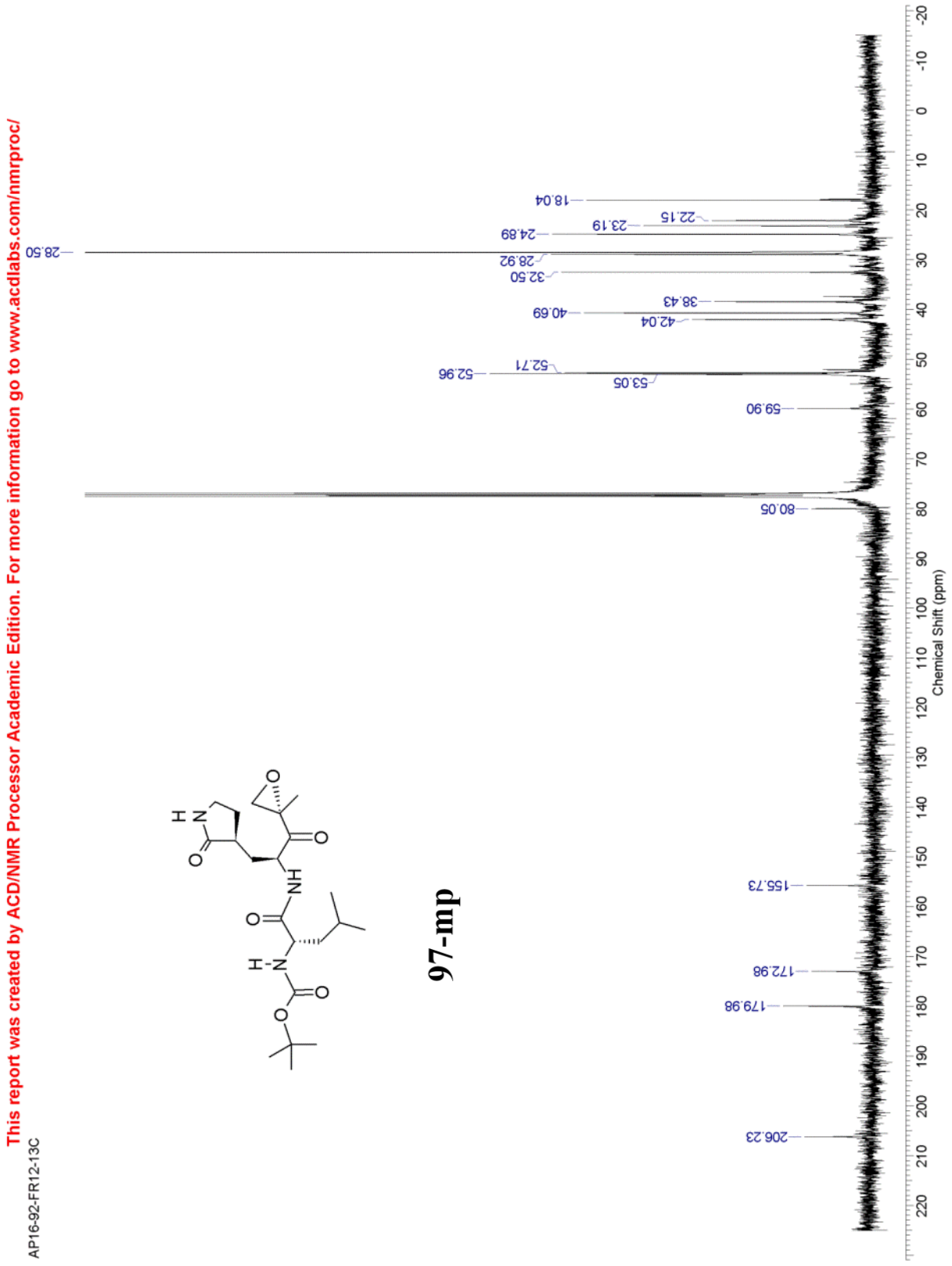
This report was created by ACD/NMR Processor Academic Edition. For more information go to www.acdlabs.com/nmrproc/
AP16-92-FR12-13C
97-mp
Chemical Shift (ppm)
18.04
22.15
23.19
24.89
28.50
28.92
32.50
38.43
40.69
42.04
52.71
52.96
53.05
59.90
80.05
155.73
172.98
179.98
206.23

AP16-29-CRUDE

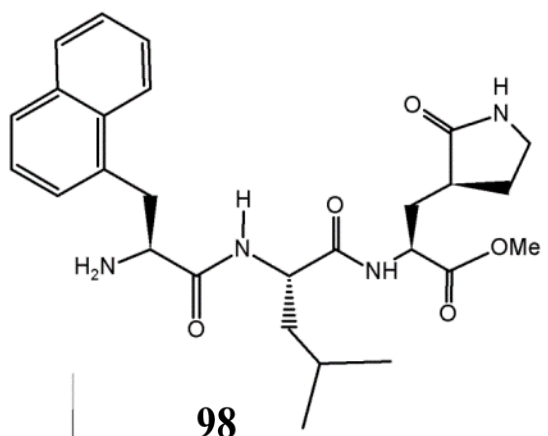

98

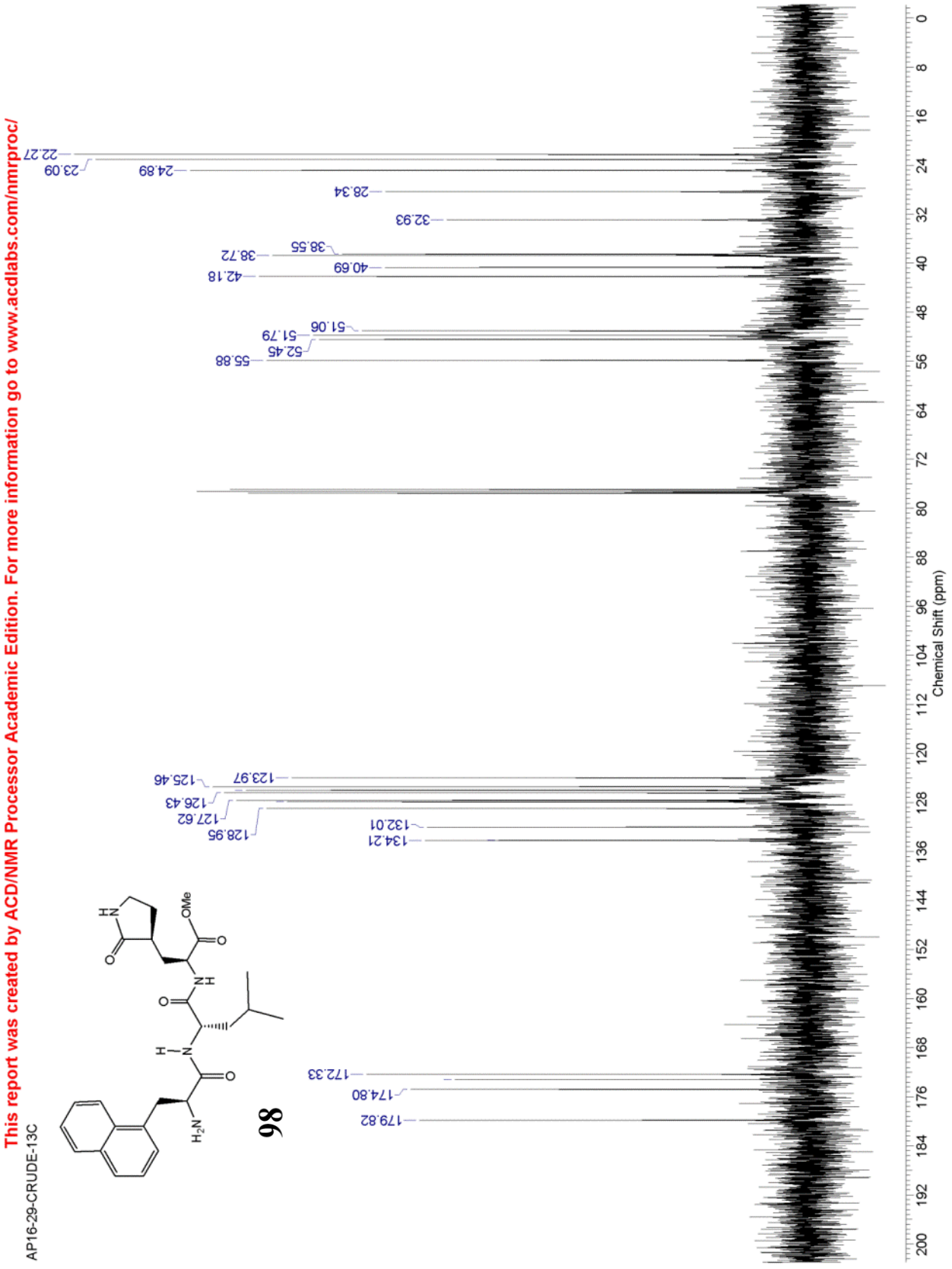
This report was created by ACD/NMR Processor Academic Edition. For more information go to www.acdlabs.com/nmrproc/
AP16-29-CRUDE-13C
98
22.27
23.09
24.89
28.34
32.93
38.55
38.72
40.69
42.18
51.06
51.79
52.45
55.88
123.97
125.46
126.43
127.62
128.95
132.01
134.21
172.33
174.80
179.82
Chemical Shift (ppm)

AP16-33-FR47

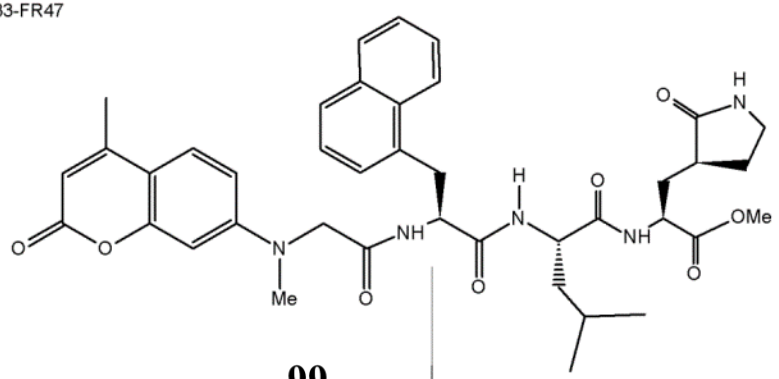

99

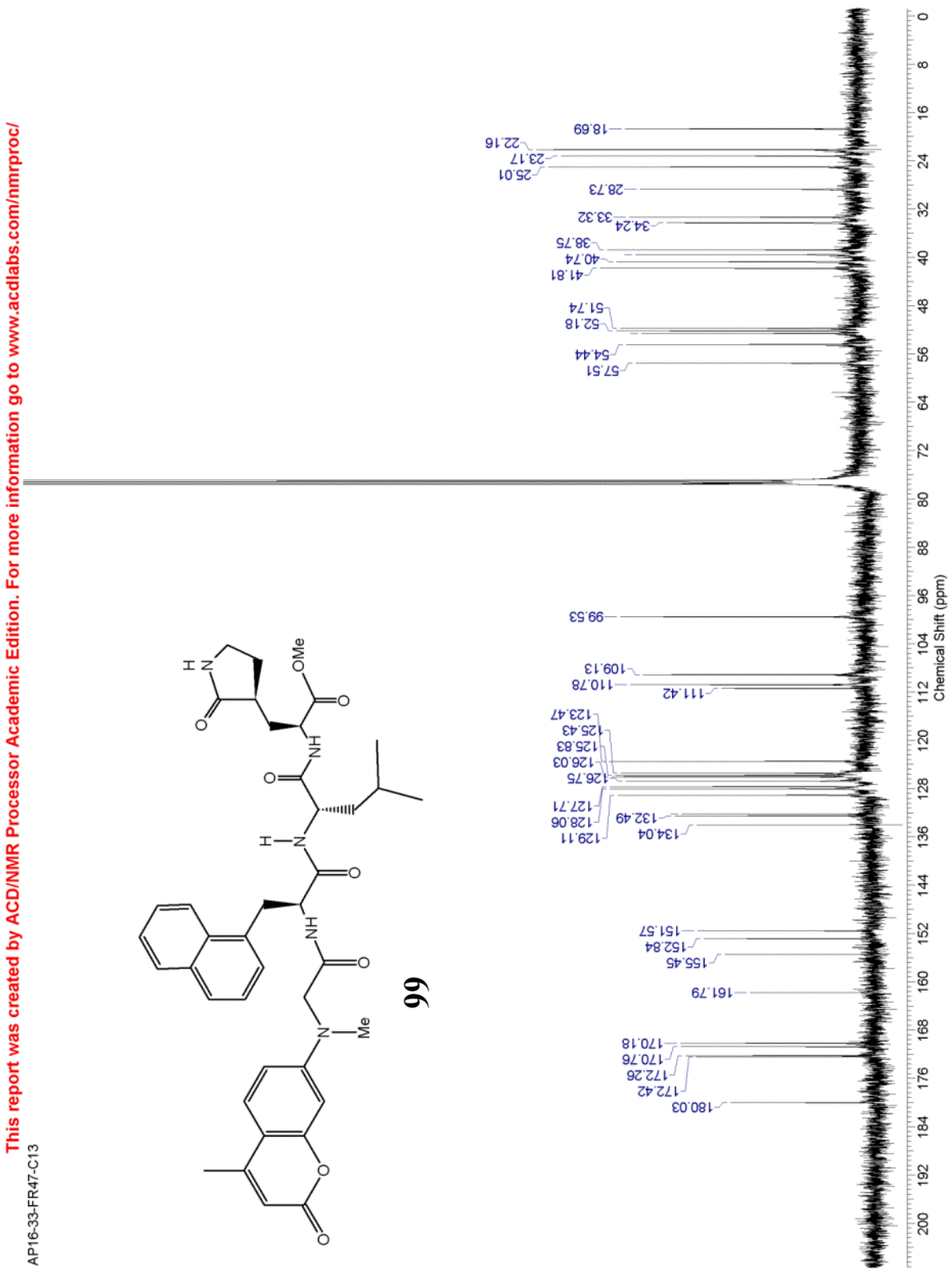
This report was created by ACD/NMR Processor Academic Edition. For more information go to www.acdlabs.com/nmrproc/
AP16-33-FR47-C13
99
18.69
22.16
23.17
25.01
28.73
33.32
34.24
38.75
40.74
41.81
51.74
52.18
54.44
57.51
99.53
109.13
110.78
111.42
123.47
125.43
125.83
126.03
126.75
127.71
128.06
129.11
132.49
134.04
151.57
152.84
155.45
161.79
170.18
170.76
172.26
172.42
180.03
Chemical Shift (ppm)

AP16-31-FR28-30

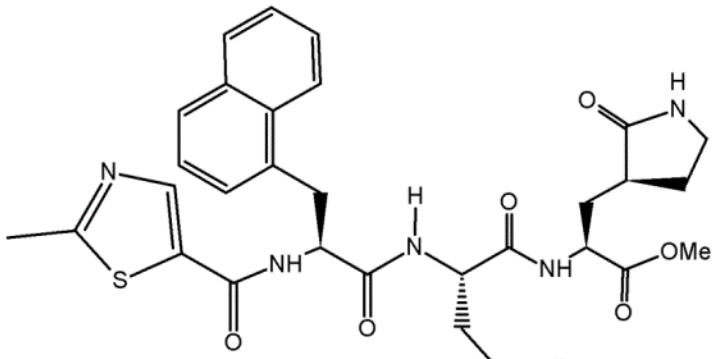

100

AP16-31-FR23-35-13C

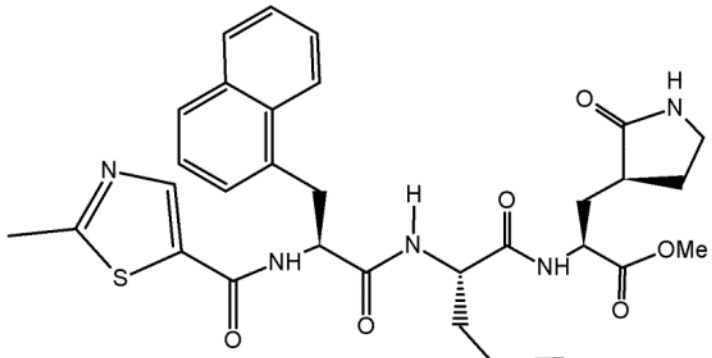

100

AP16-23-FR3

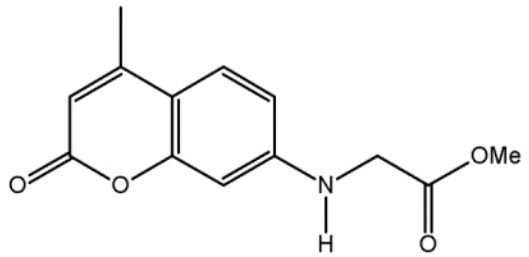

102

AP16-23-FR3-13C

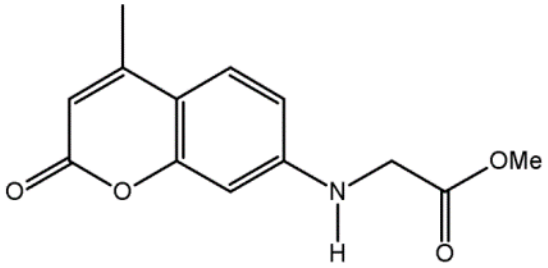

102

AP16-24-FR25

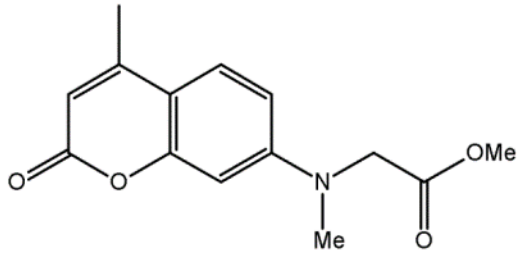

103

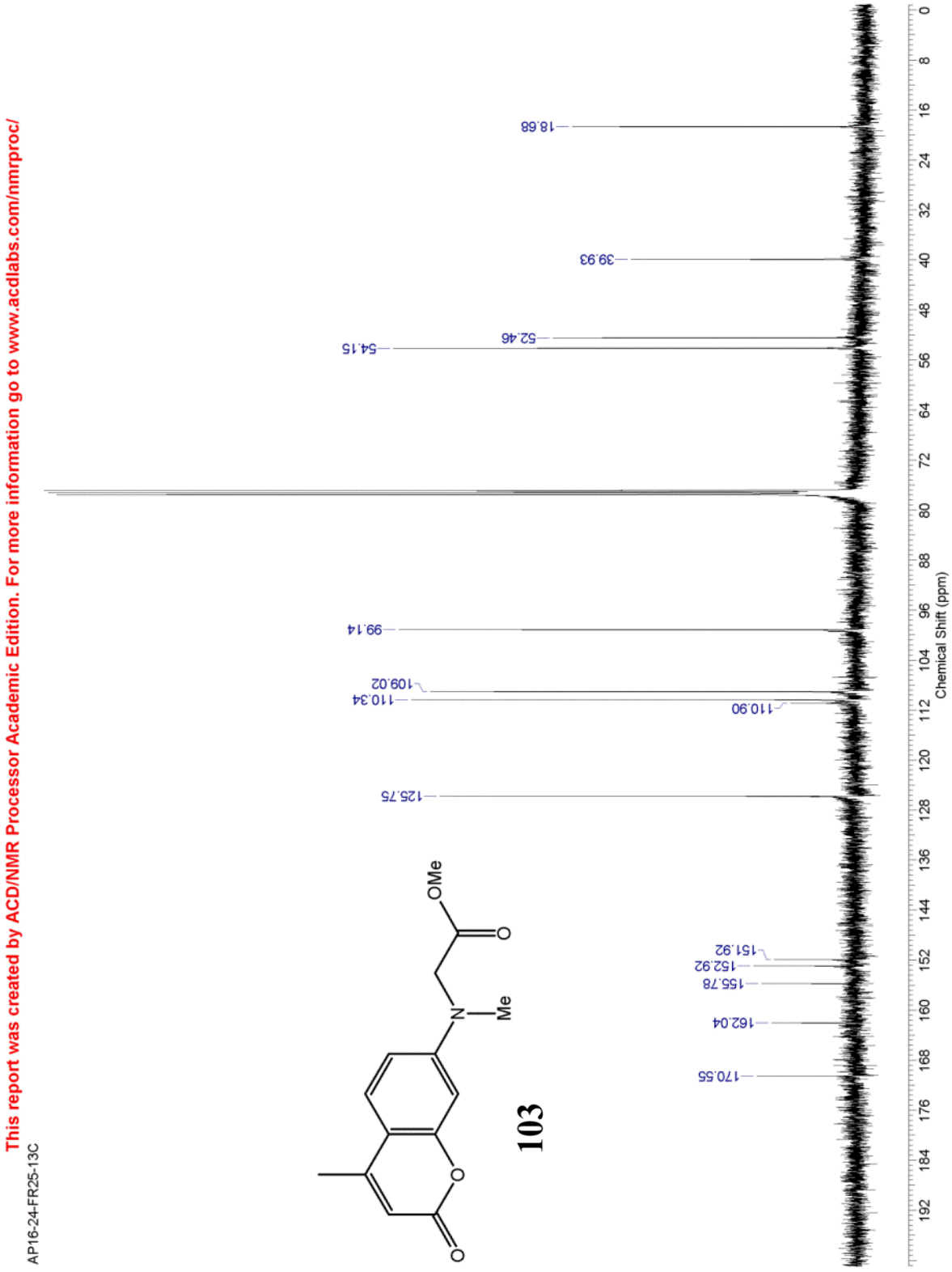
This report was created by ACD/NMR Processor Academic Edition. For more information go to www.acdlabs.com/nmrproc/
AP16-24-FR25-13C
18.68
39.93
52.46
54.15
99.14
109.02
110.34
110.90
125.75
151.92
152.92
155.78
162.04
170.55
OMe
O
N
Me
O
O
103
Chemical Shift (ppm)

AP16-30-CRUDE

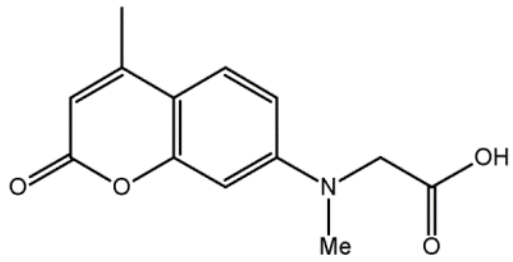

104

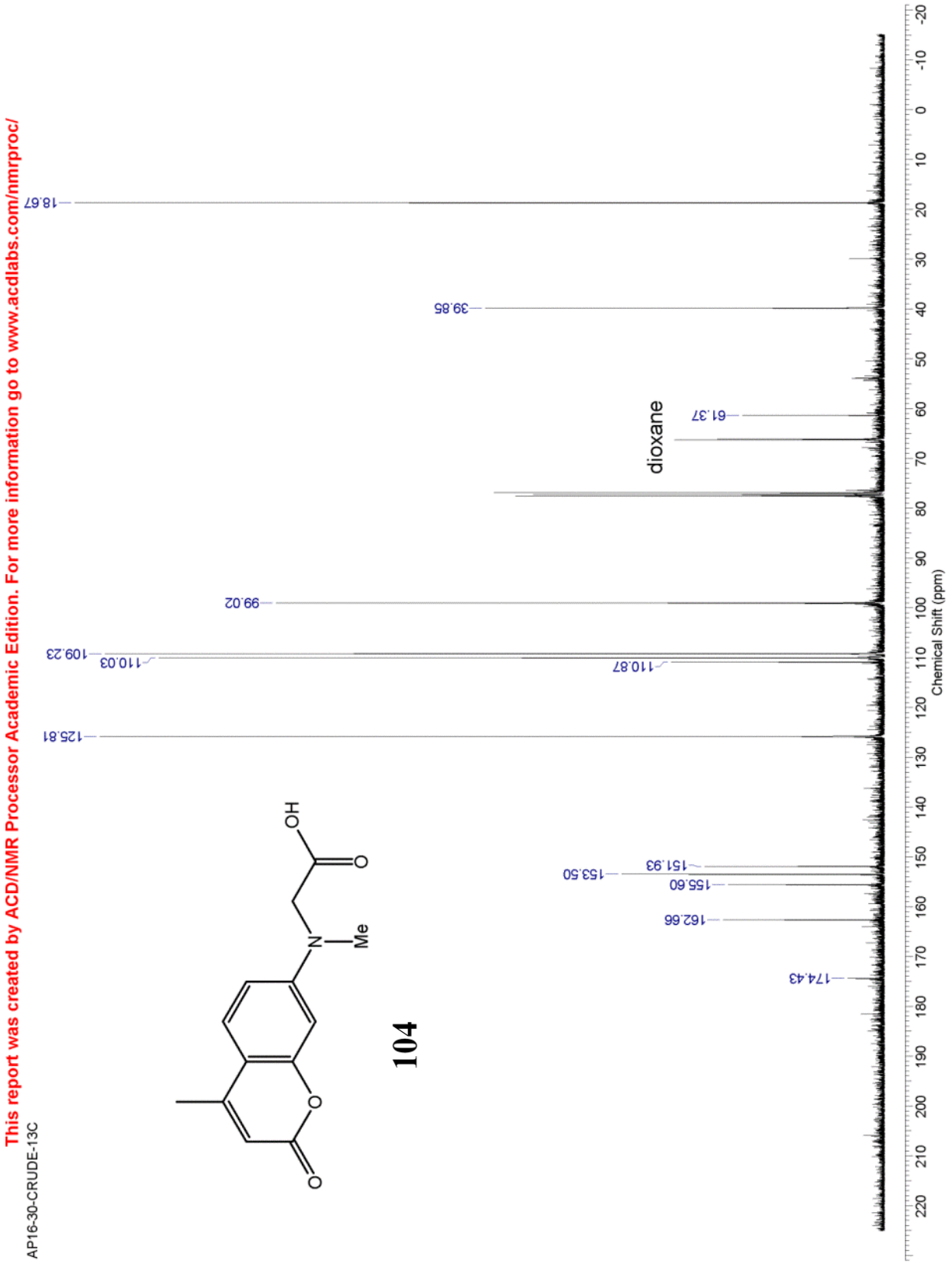
This report was created by ACD/NMR Processor Academic Edition. For more information go to www.acdlabs.com/nmrproc/
AP16-30-CRUDE-13C
18.67
39.85
61.37
dioxane
99.02
109.23
110.03
110.87
125.81
151.93
153.50
155.60
162.66
174.43
Chemical Shift (ppm)
104

AP15-49-FR58-60

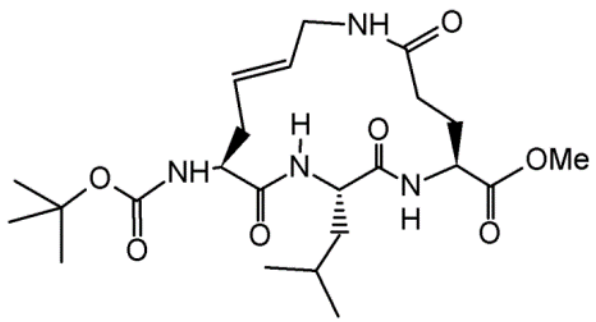

106

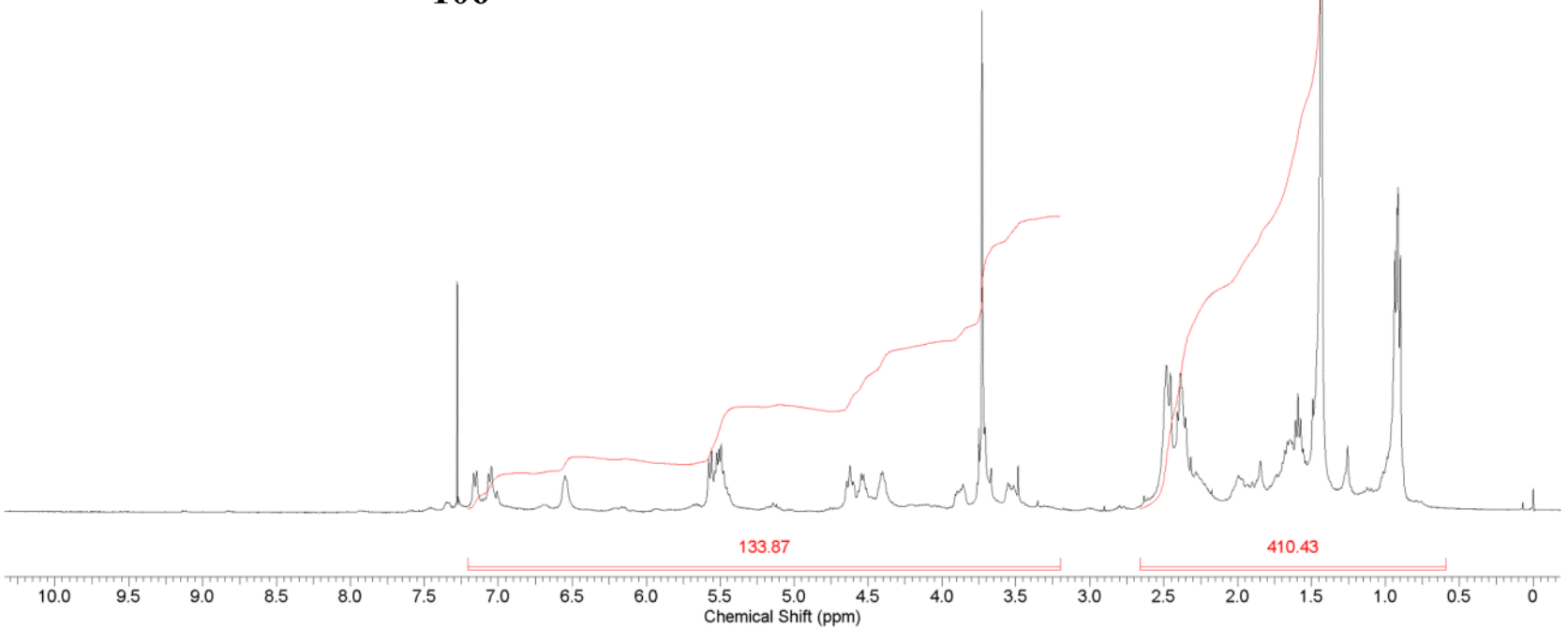

AP15-53-CRUDE

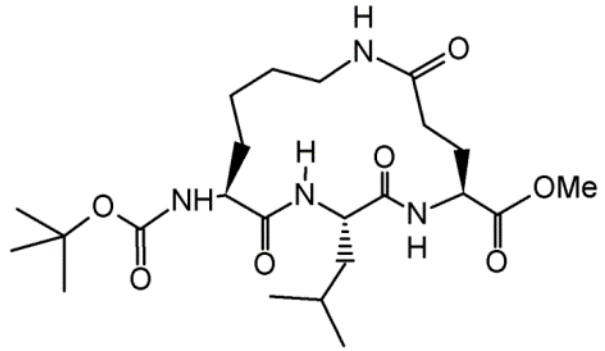

107

AP15-53-CRUDE-C13

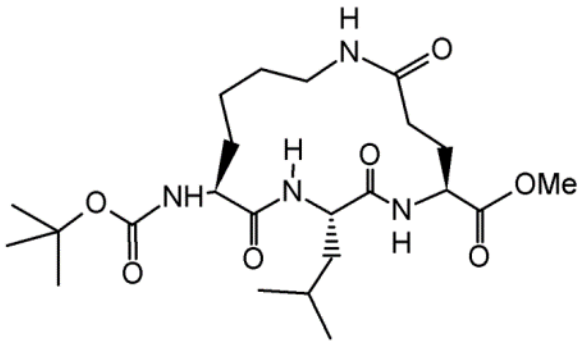

107

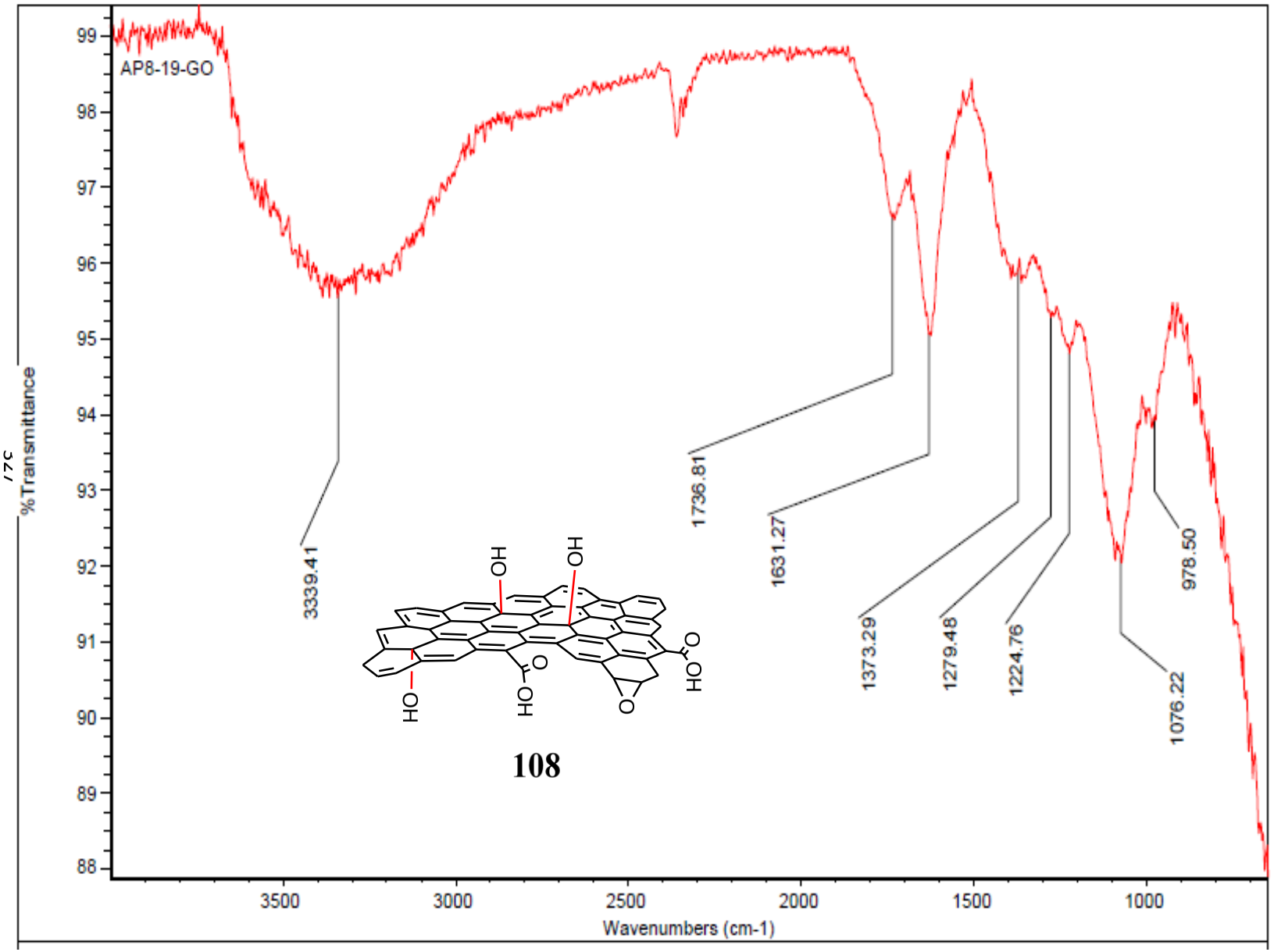
AP8-19-GO
%Transmittance
Wavenumbers (cm-1)
3339.41
1736.81
1631.27
1373.29
1279.48
1224.76
1076.22
978.50
OH
OH
HO
HO
O
HO
O

108

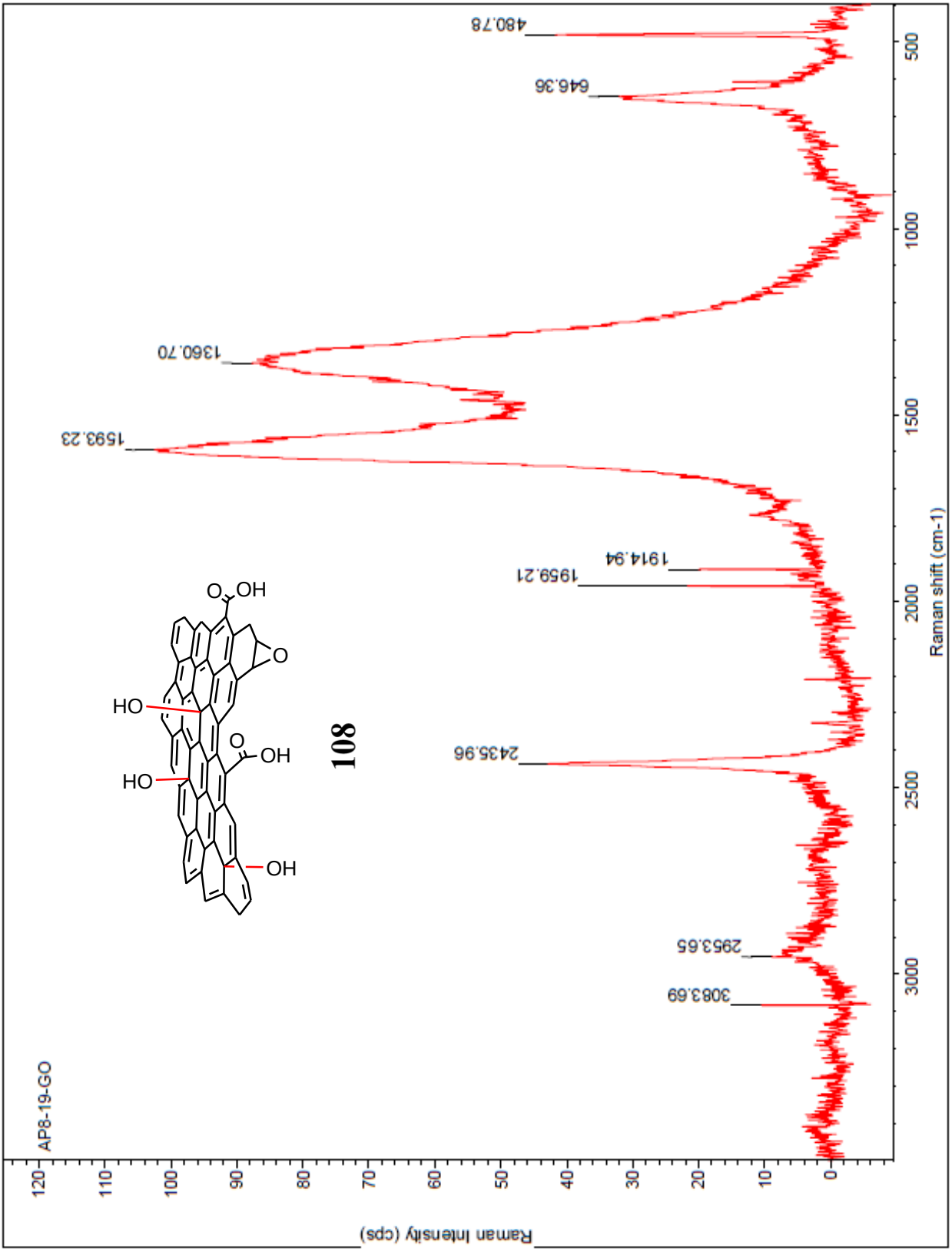
AP8-19-GO
Raman Intensity (cps)
Raman shift (cm-1)
480.78
646.36
1360.70
1593.23
1914.94
1959.21
2435.96
2953.65
3083.69
108
OH
O
HO
HO
OH
OH

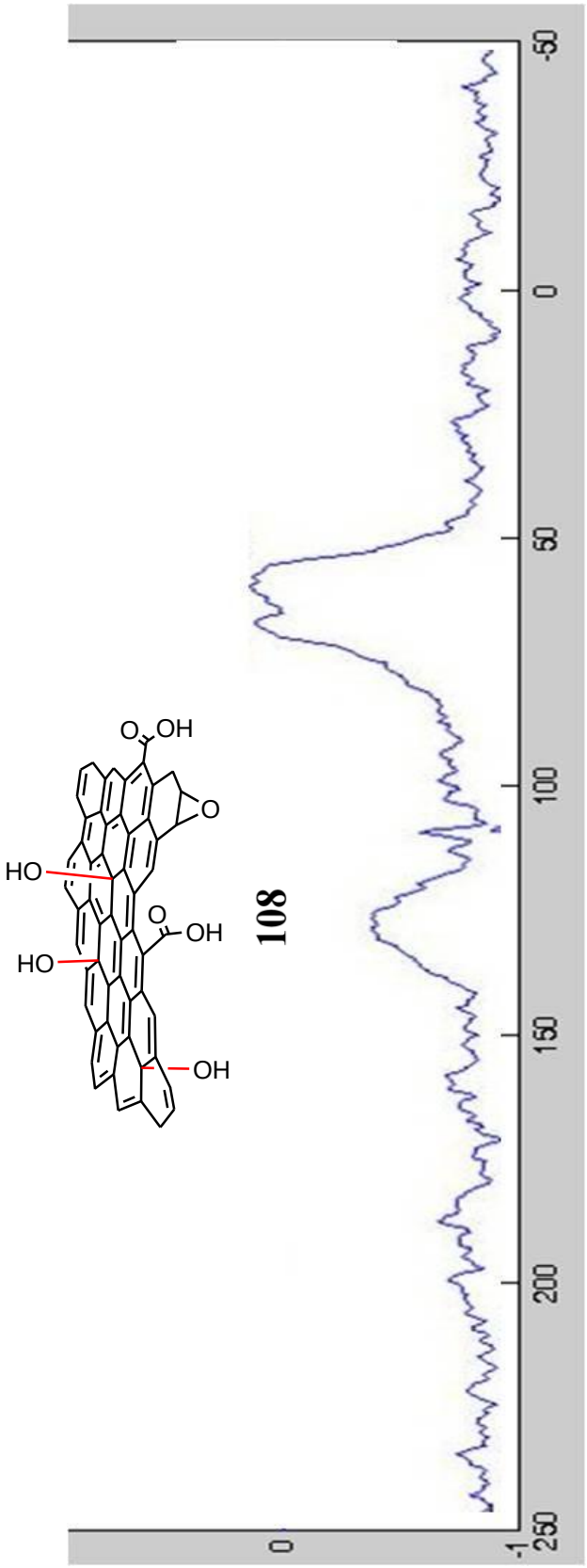
O
OH
O
HO
O
OH
HO
OH
108
-50
0
50
100
150
200
250
-1
0

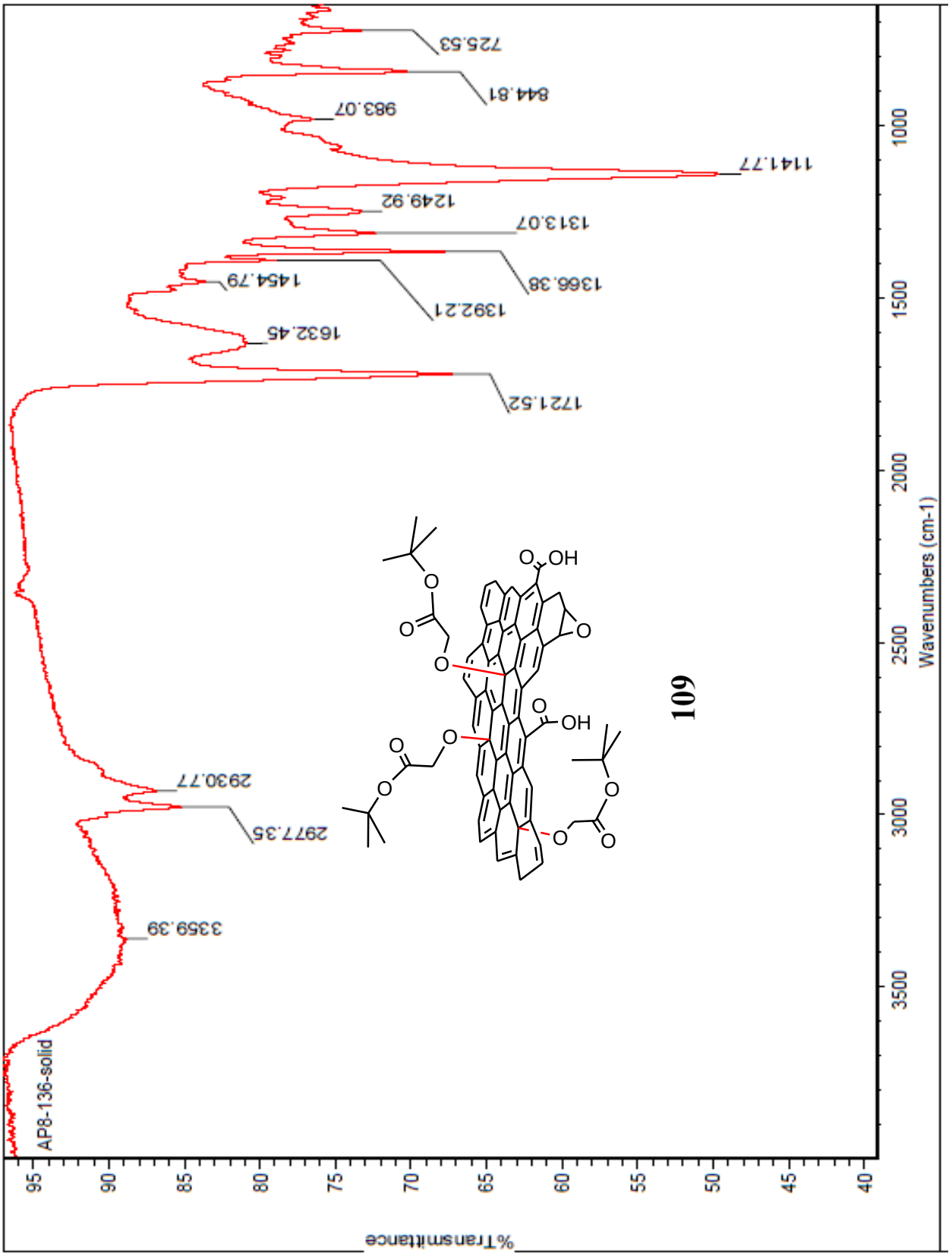
AP8-136-solid
%Transmittance
Wavenumbers (cm-1)
3359.39
2977.35
2930.77
1721.52
1632.45
1454.79
1392.21
1366.38
1313.07
1249.92
1141.77
983.07
844.81
725.53
109

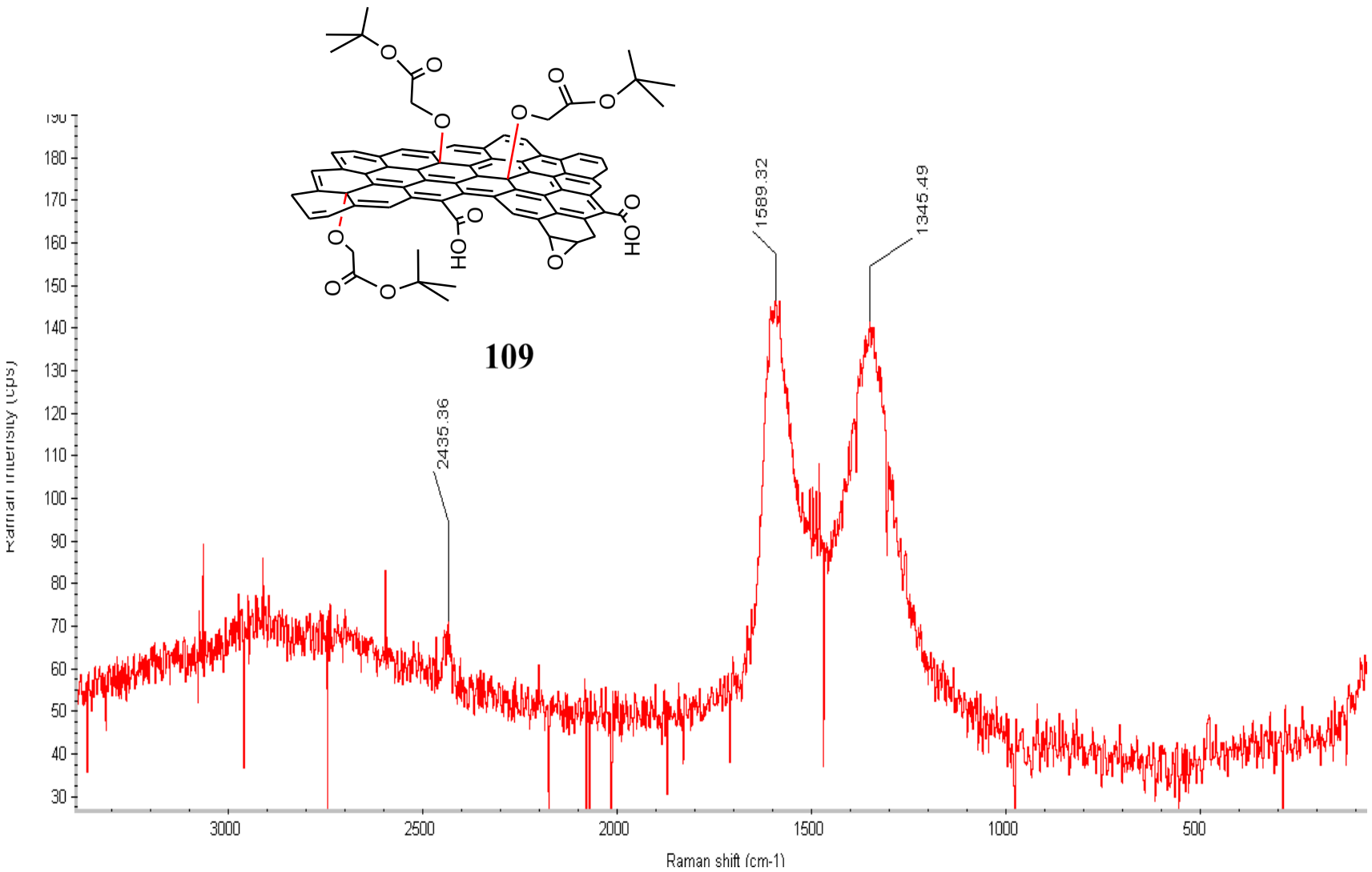
1589.32
1345.49
2435.36
Raman shift (cm-1)
3000
2500
2000
1500
1000
500

109

AP9-73-FR20-21

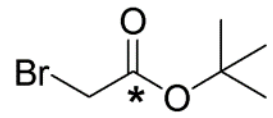

112

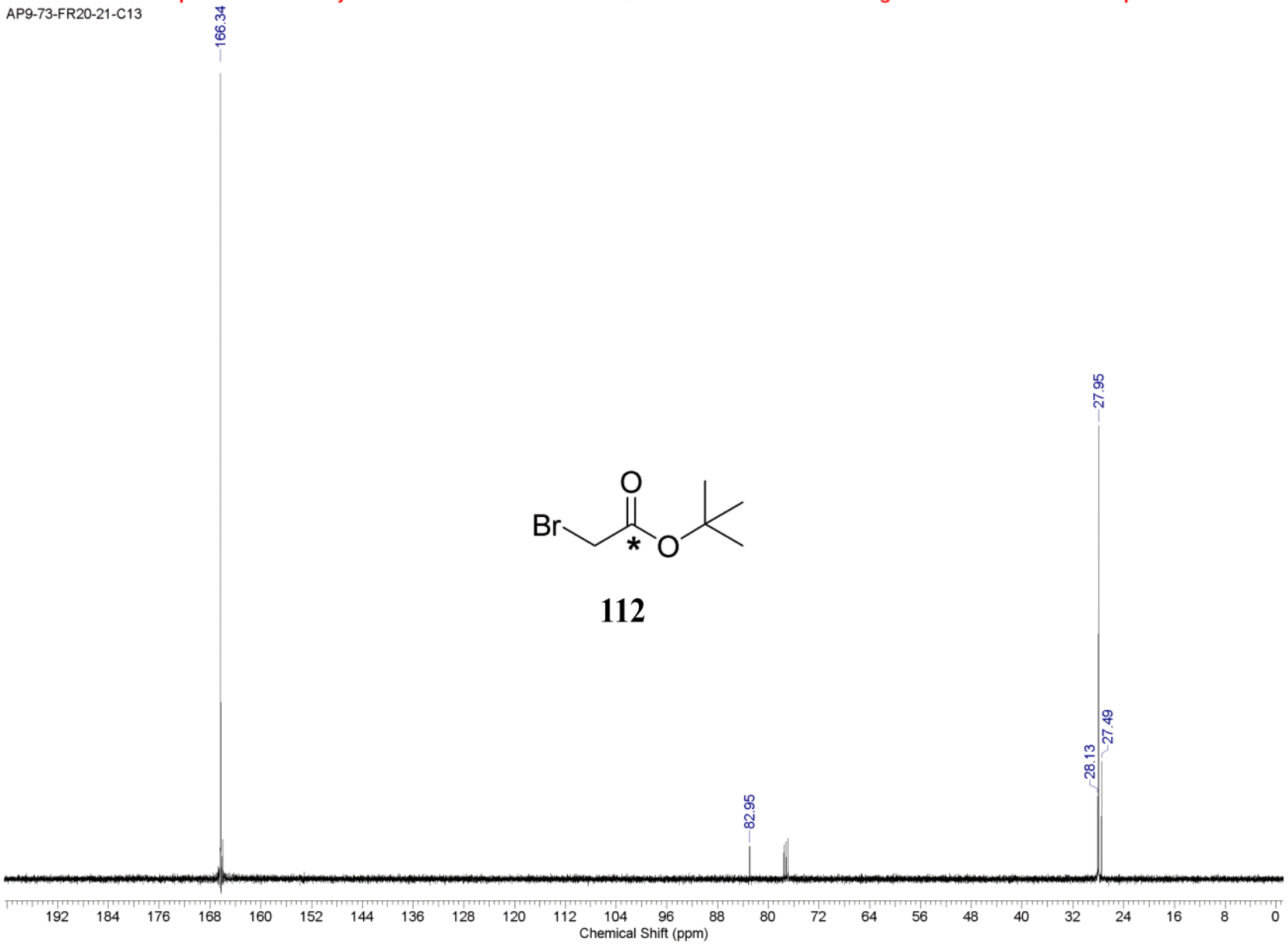

112

3284.69
2975.90
2932.90
1646.91
1439.74
1412.38
1385.02
1365.47
1248.21
1142.67
1095.77
1060.59
845.60
661.89
113
% Transmittance
Wavenumbers (cm-1)

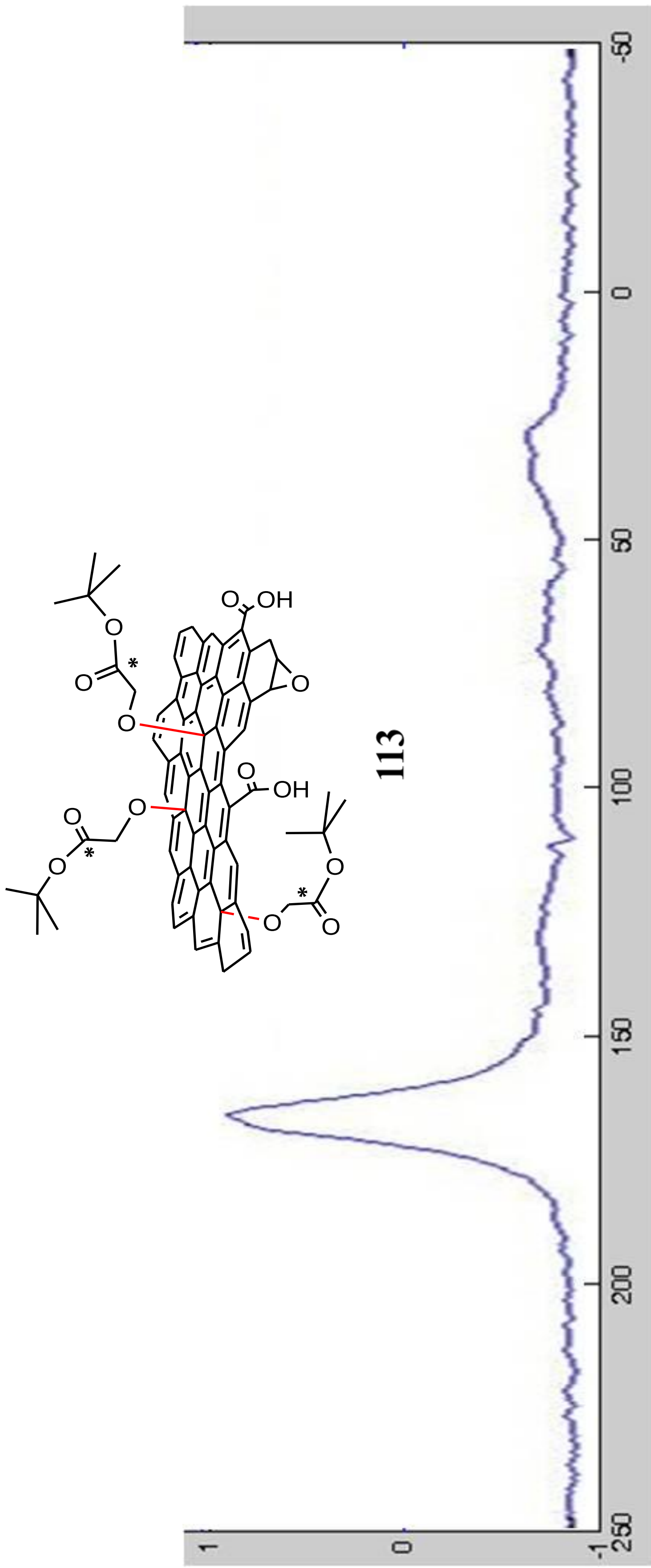

113

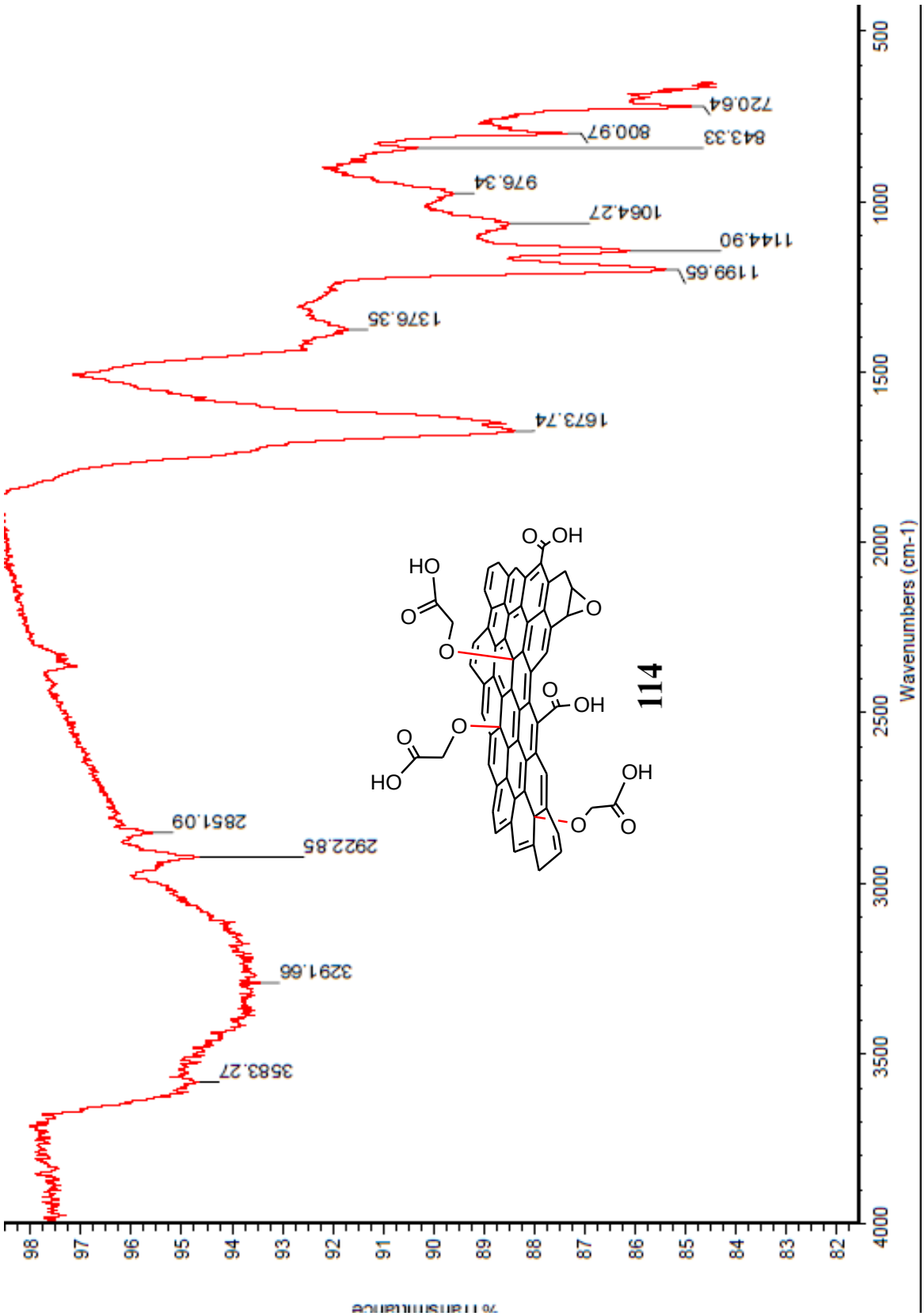
3583.27
3291.66
2922.85
2851.09
1673.74
1376.35
1199.65
1144.90
1064.27
976.34
843.33
800.97
720.64
Wavenumbers (cm-1)
114

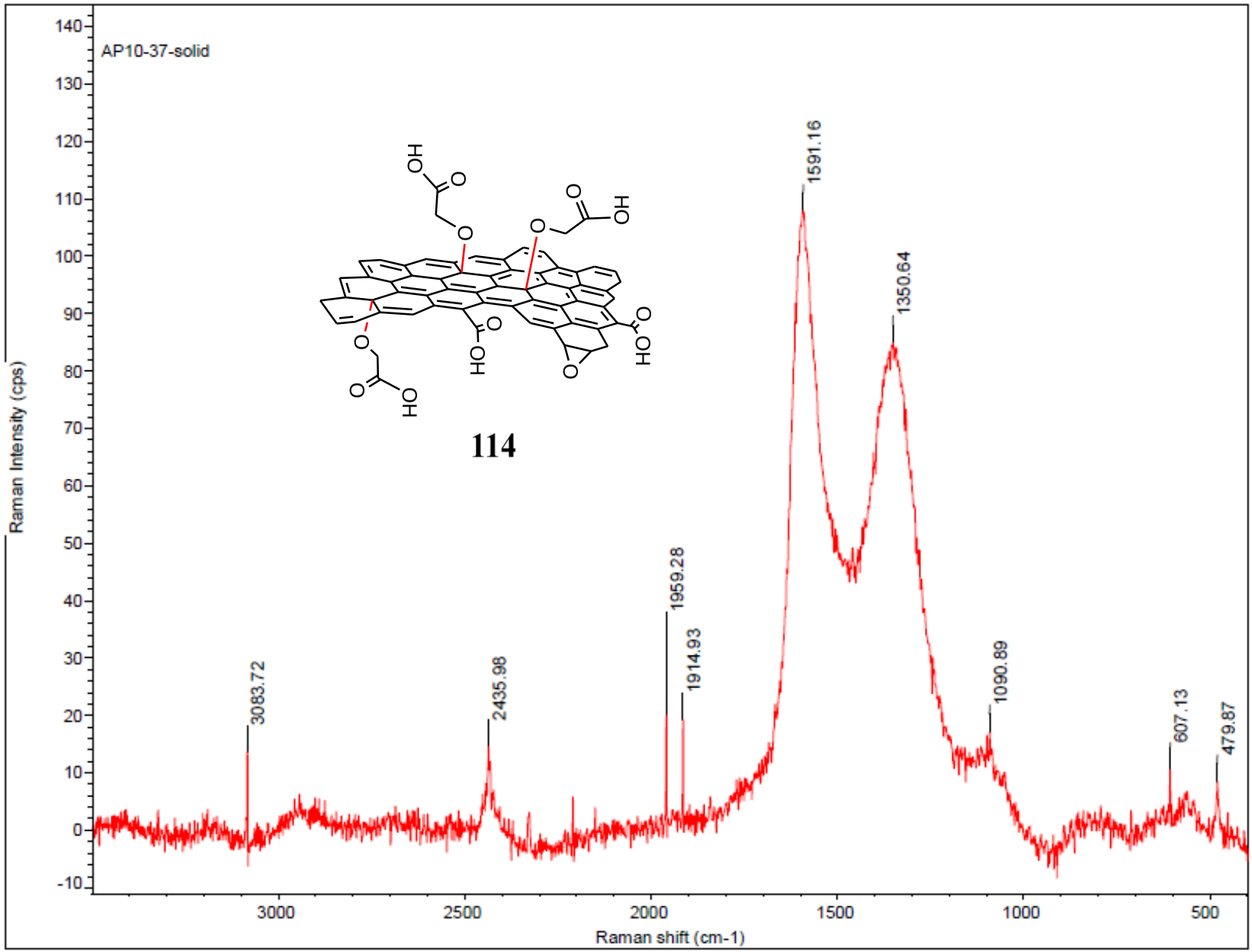
AP10-37-solid
Raman Intensity (cps)
Raman shift (cm-1)
3083.72
2435.98
1959.28
1914.93
1591.16
1350.64
1090.89
607.13
479.87

114

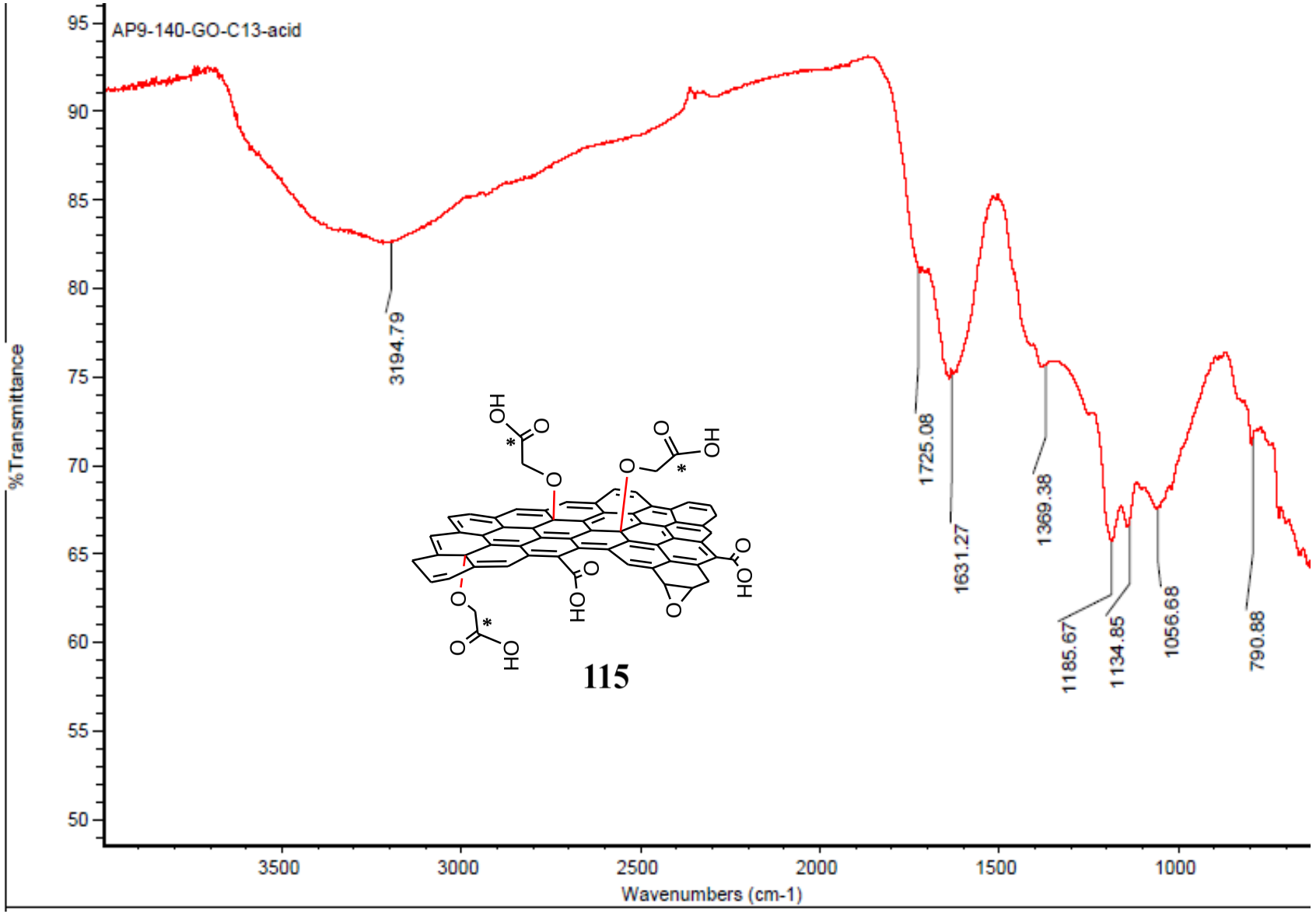
AP9-140-GO-C13-acid
%Transmittance
Wavenumbers (cm-1)
3194.79
1725.08
1631.27
1369.38
1185.67
1134.85
1056.68
790.88

115

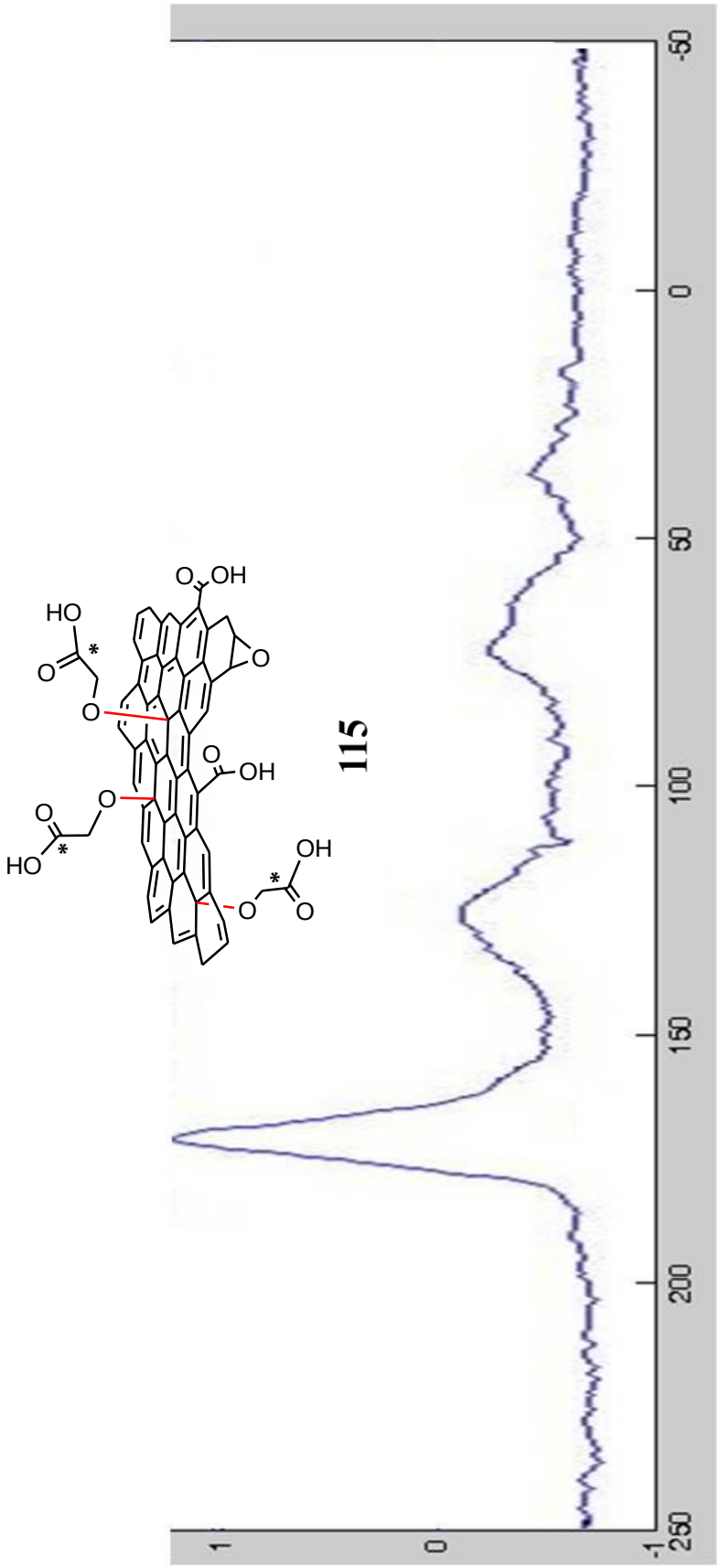
115
HO
O
O
O
O
OH
O
O
HO
O
O
OH
O
O
OH
1
0
-1
250
200
150
100
50
0
-50

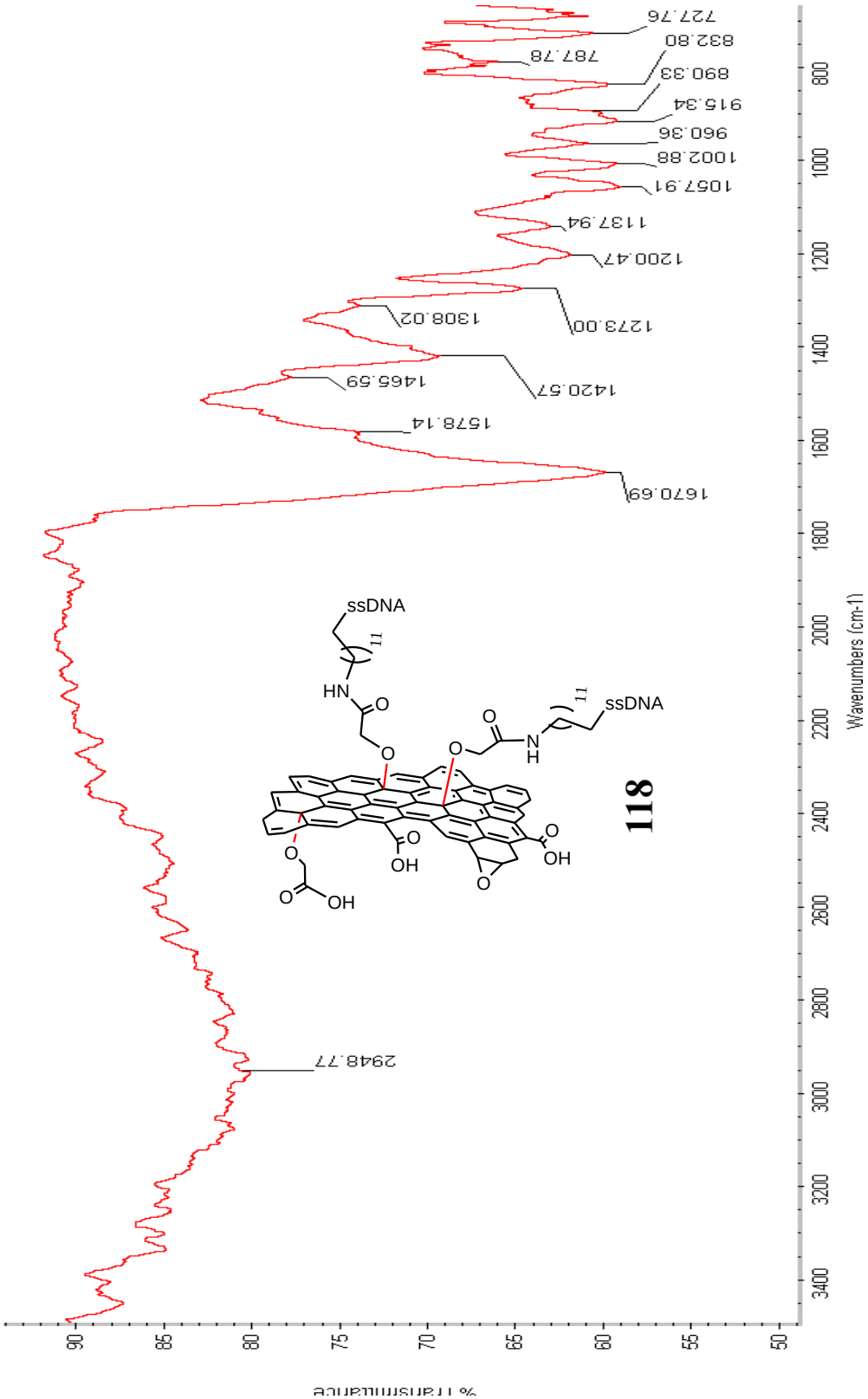
727.76
832.80
787.78
890.33
915.34
960.36
1002.88
1057.91
1137.94
1200.47
1273.00
1308.02
1420.57
1465.59
1578.14
1670.69
2948.77
ssDNA
11
HN
O
O
O
O
OH
O
OH
O
O
11
ssDNA
N
H
O
O
OH
O
118
% Transmittance
Wavenumbers (cm-1)

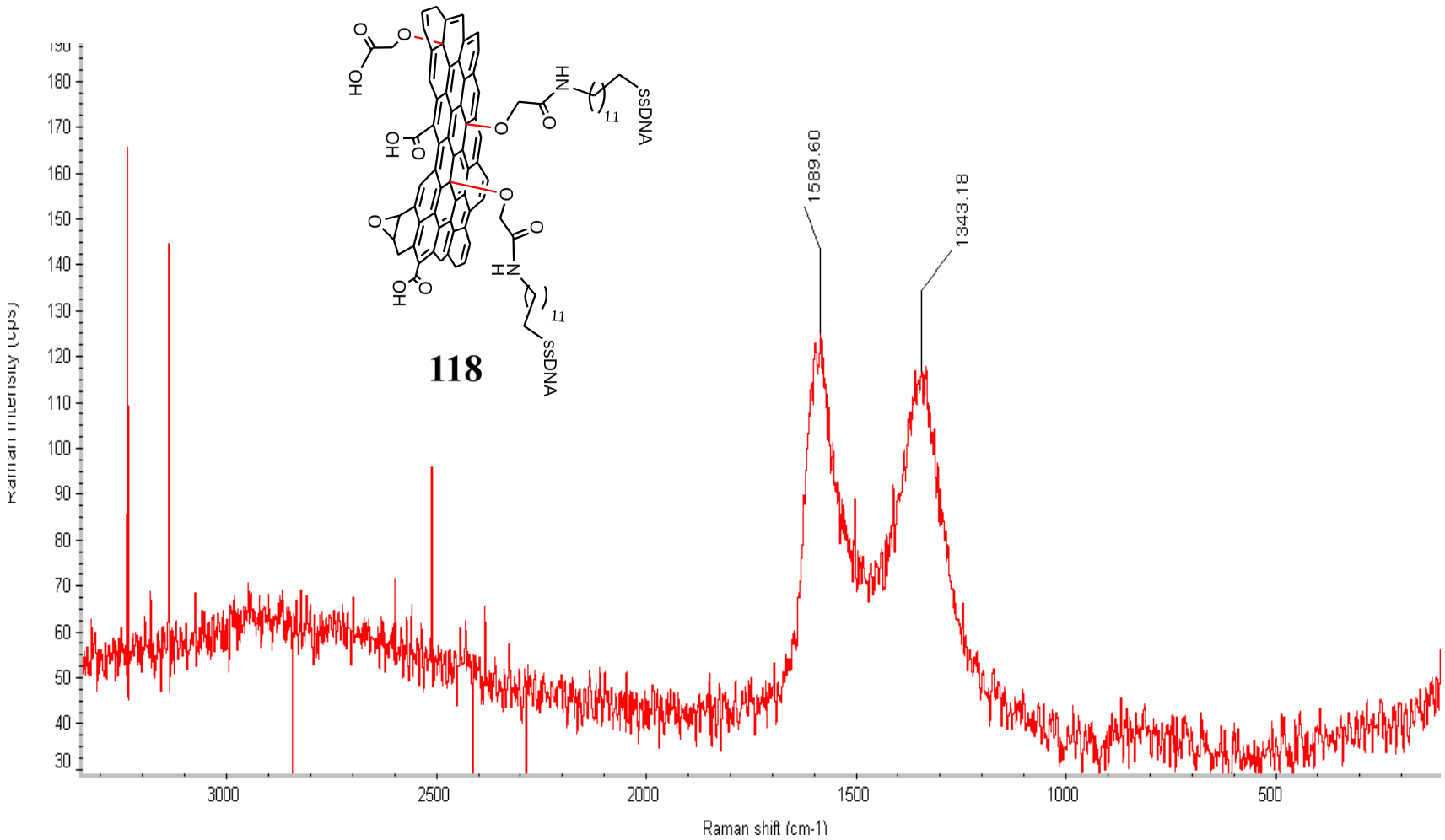
1589.60
1343.18
Raman shift (cm-1)
3000
2500
2000
1500
1000
500
ssDNA
ssDNA
11
11
HO
HO
HO
O
HN

118

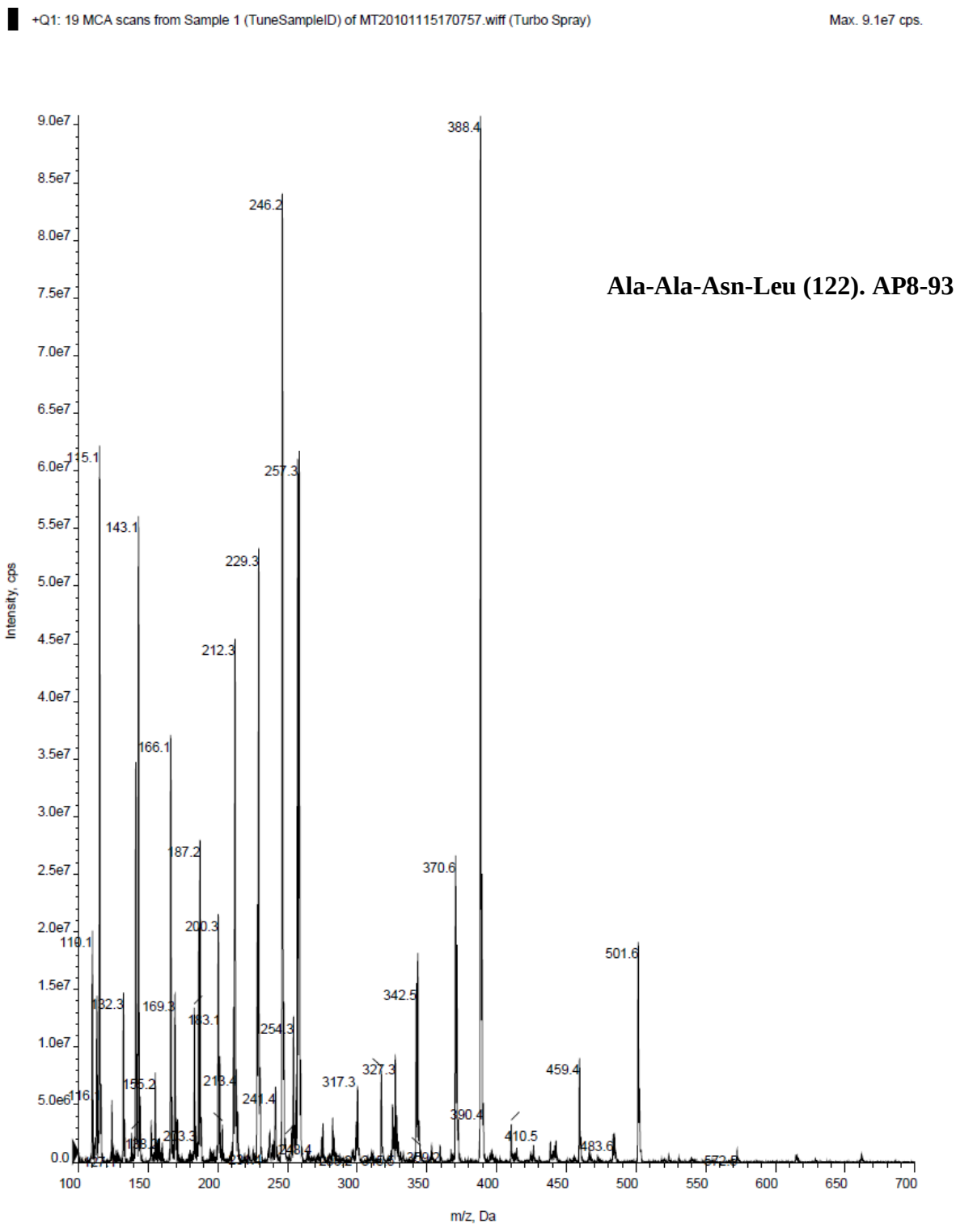

Ala-Ala-Asn-Leu (122). AP8-93

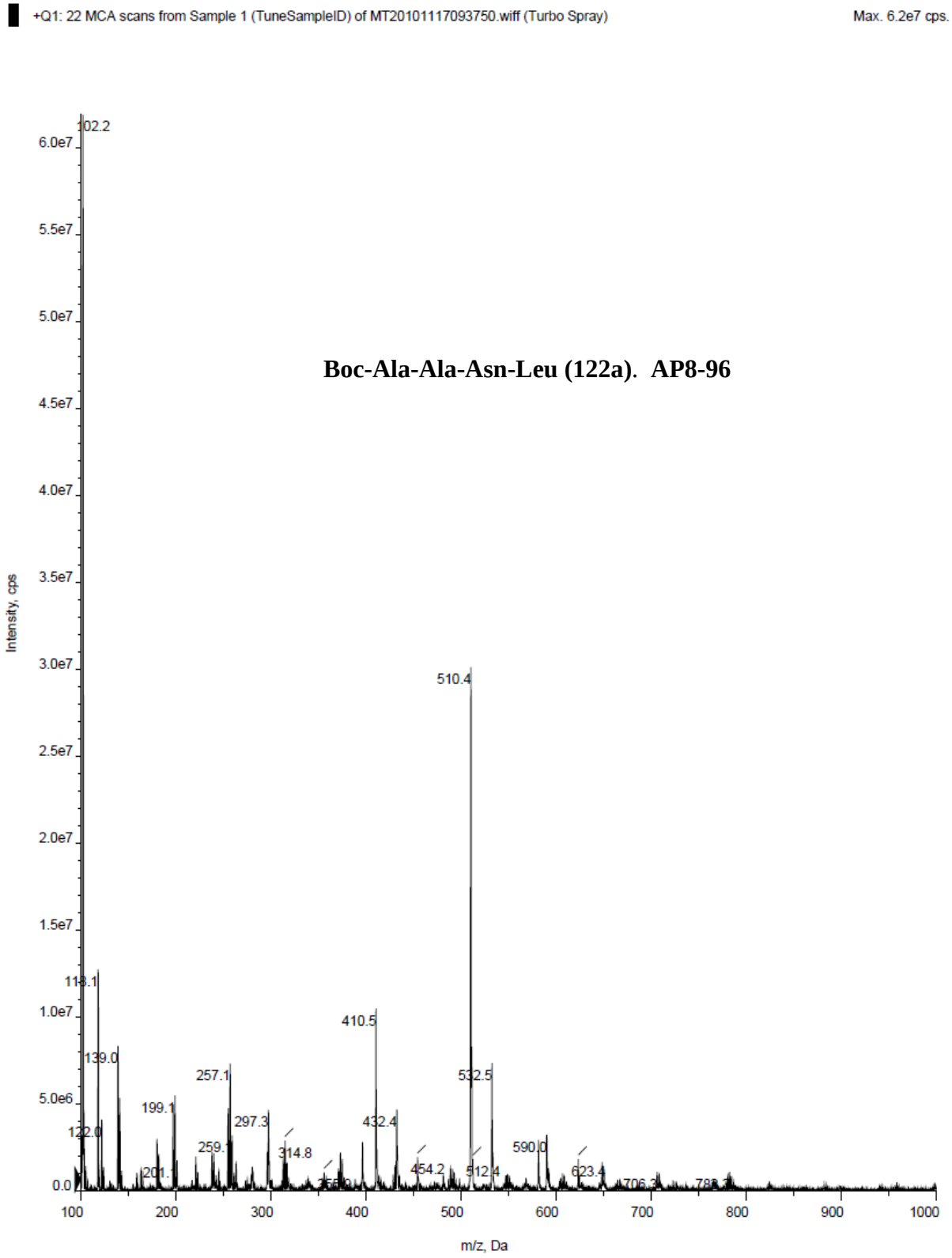
+Q1: 22 MCA scans from Sample 1 (TuneSampleID) of MT20101117093750.wiff (Turbo Spray)
Max. 6.2e7 cps.
Boc-Ala-Ala-Asn-Leu (122a). AP8-96
Intensity, cps
m/z, Da
102.2
510.4
410.5
532.5
257.1
139.0
199.1
297.3
432.4
590.0
314.8
454.2
512.4
623.4
259.1
201.1
122.0
6.0e7
5.5e7
5.0e7
4.5e7
4.0e7
3.5e7
3.0e7
2.5e7
2.0e7
1.5e7
1.0e7
5.0e6
0.0
100
200
300
400
500
600
700
800
900
1000

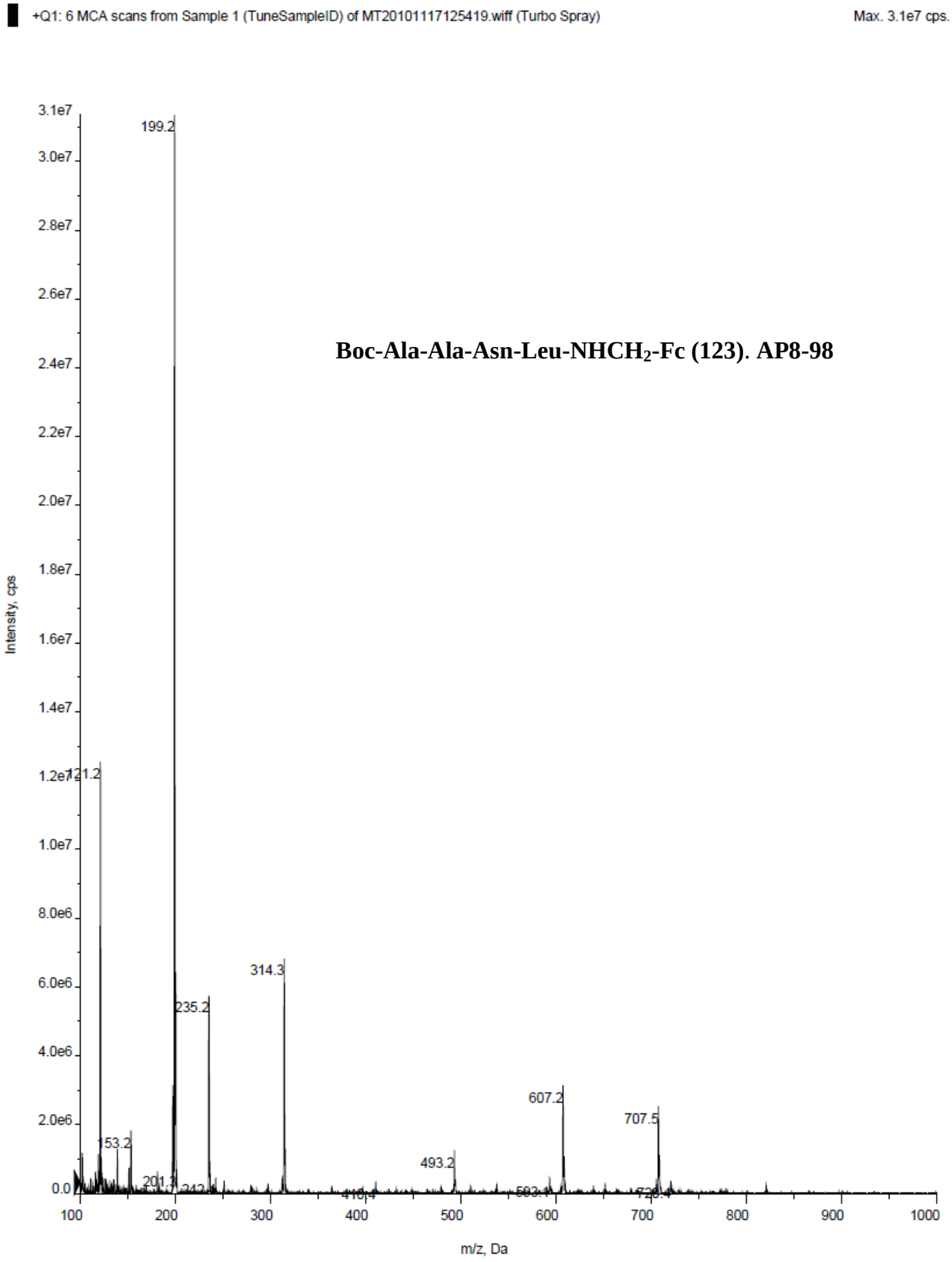
+Q1: 6 MCA scans from Sample 1 (TuneSampleID) of MT20101117125419.wiff (Turbo Spray)
Max. 3.1e7 cps.
Boc-Ala-Ala-Asn-Leu-NHCH2-Fc (123). AP8-98
Intensity, cps
m/z, Da
199.2
121.2
314.3
235.2
607.2
707.5
153.2
493.2
201.1
242.1
416.4
503.4
728.4

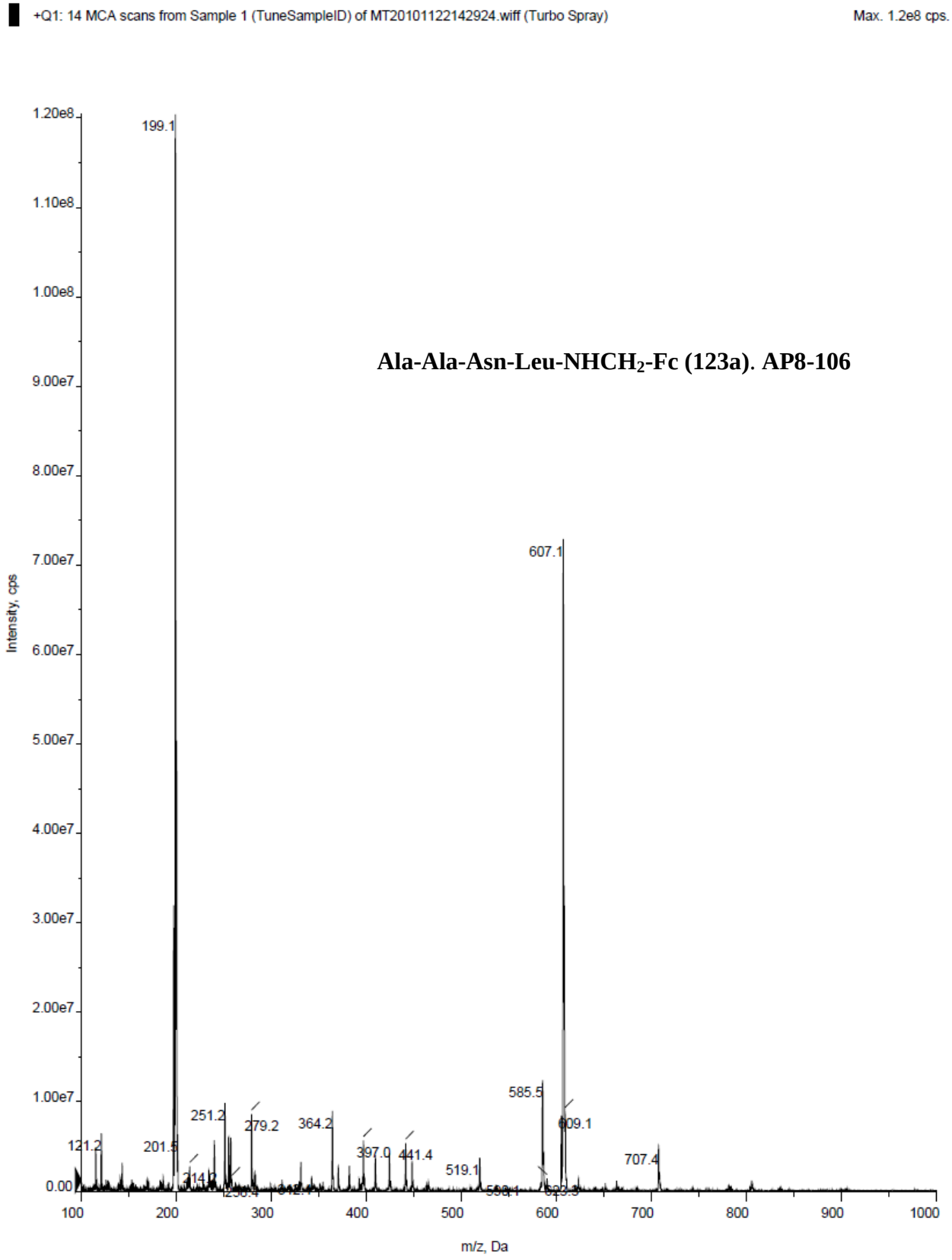
+Q1: 14 MCA scans from Sample 1 (TuneSampleID) of MT20101122142924.wiff (Turbo Spray)
Max. 1.2e8 cps.
Ala-Ala-Asn-Leu-NHCH2-Fc (123a). AP8-106
Intensity, cps
m/z, Da
199.1
607.1
585.5
609.1
251.2
279.2
364.2
397.0
441.4
519.1
707.4
121.2
201.5

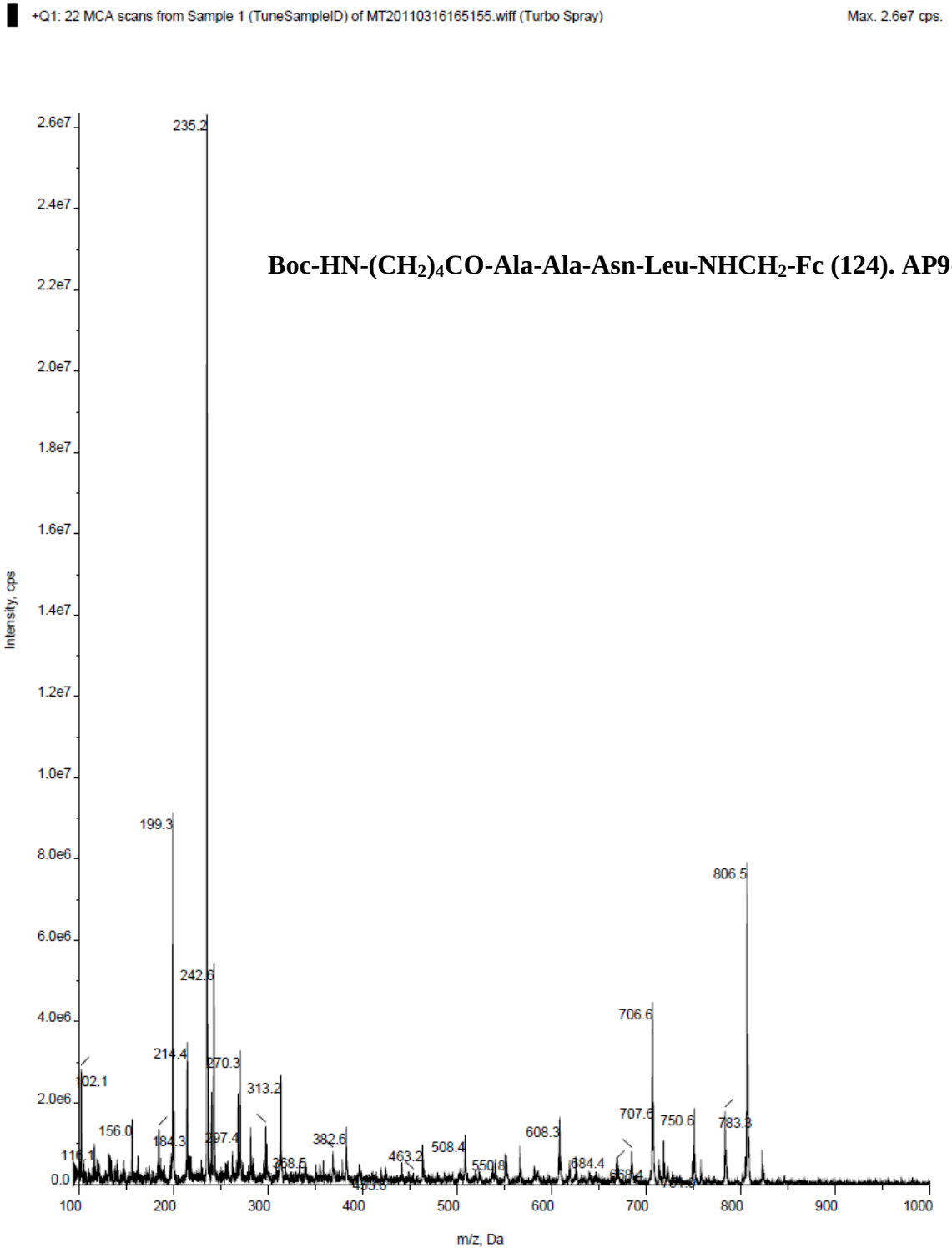
+Q1: 22 MCA scans from Sample 1 (TuneSampleID) of MT20110316165155.wiff (Turbo Spray)
Max. 2.6e7 cps.
Boc-HN-(CH2)4CO-Ala-Ala-Asn-Leu-NHCH2-Fc (124). AP9-85
Intensity, cps
m/z, Da
235.2
199.3
242.6
214.4
270.3
313.2
102.1
156.0
184.3
297.4
382.6
463.2
508.4
550.8
608.3
684.4
706.6
707.6
750.6
783.3
806.5

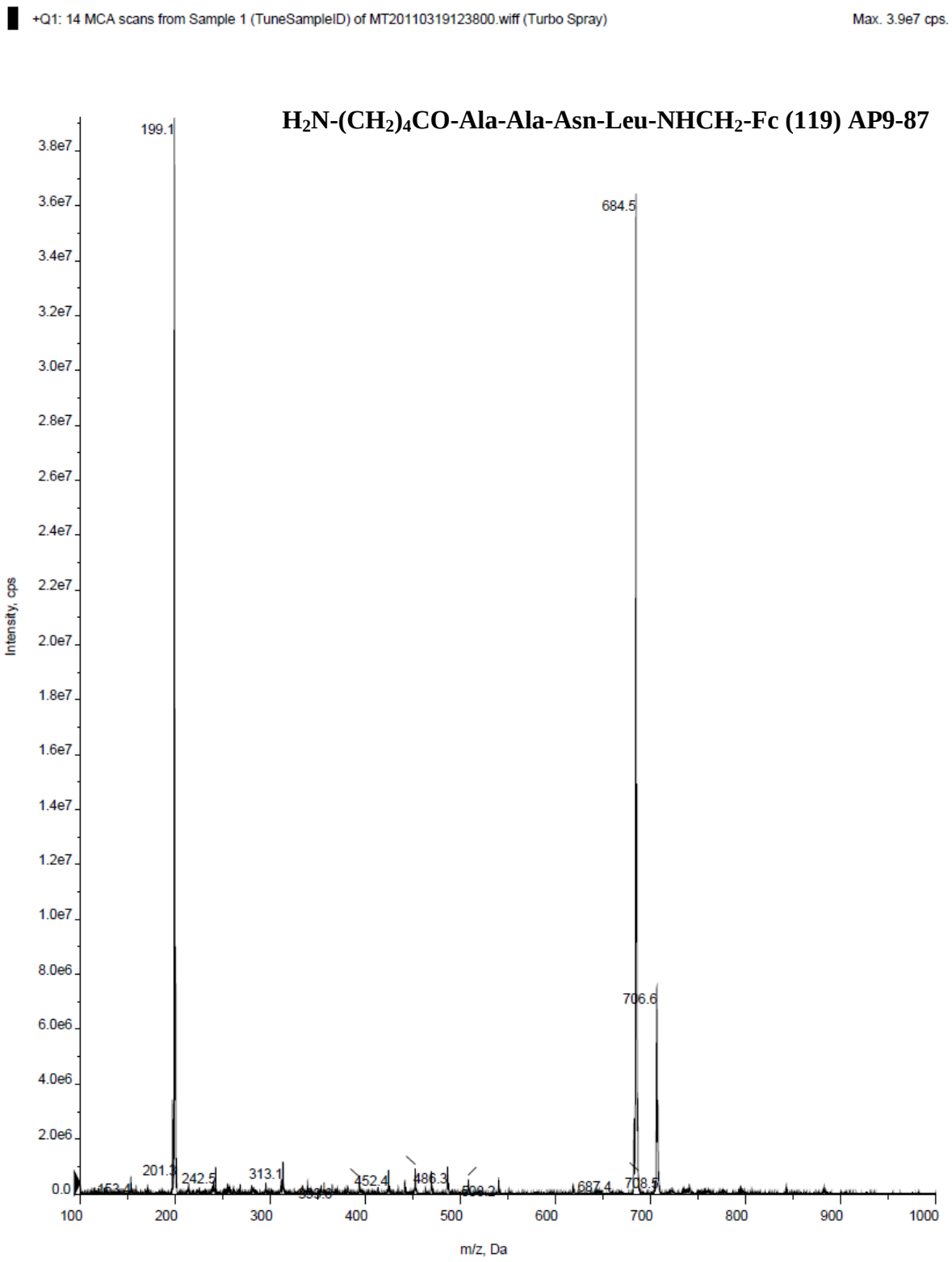
+Q1: 14 MCA scans from Sample 1 (TuneSampleID) of MT20110319123800.wiff (Turbo Spray)
Max. 3.9e7 cps.
H2N-(CH2)4CO-Ala-Ala-Asn-Leu-NHCH2-Fc (119) AP9-87
Intensity, cps
m/z, Da
199.1
684.5
706.6
201.3
242.5
313.1
452.4
486.3
687.4
708.5

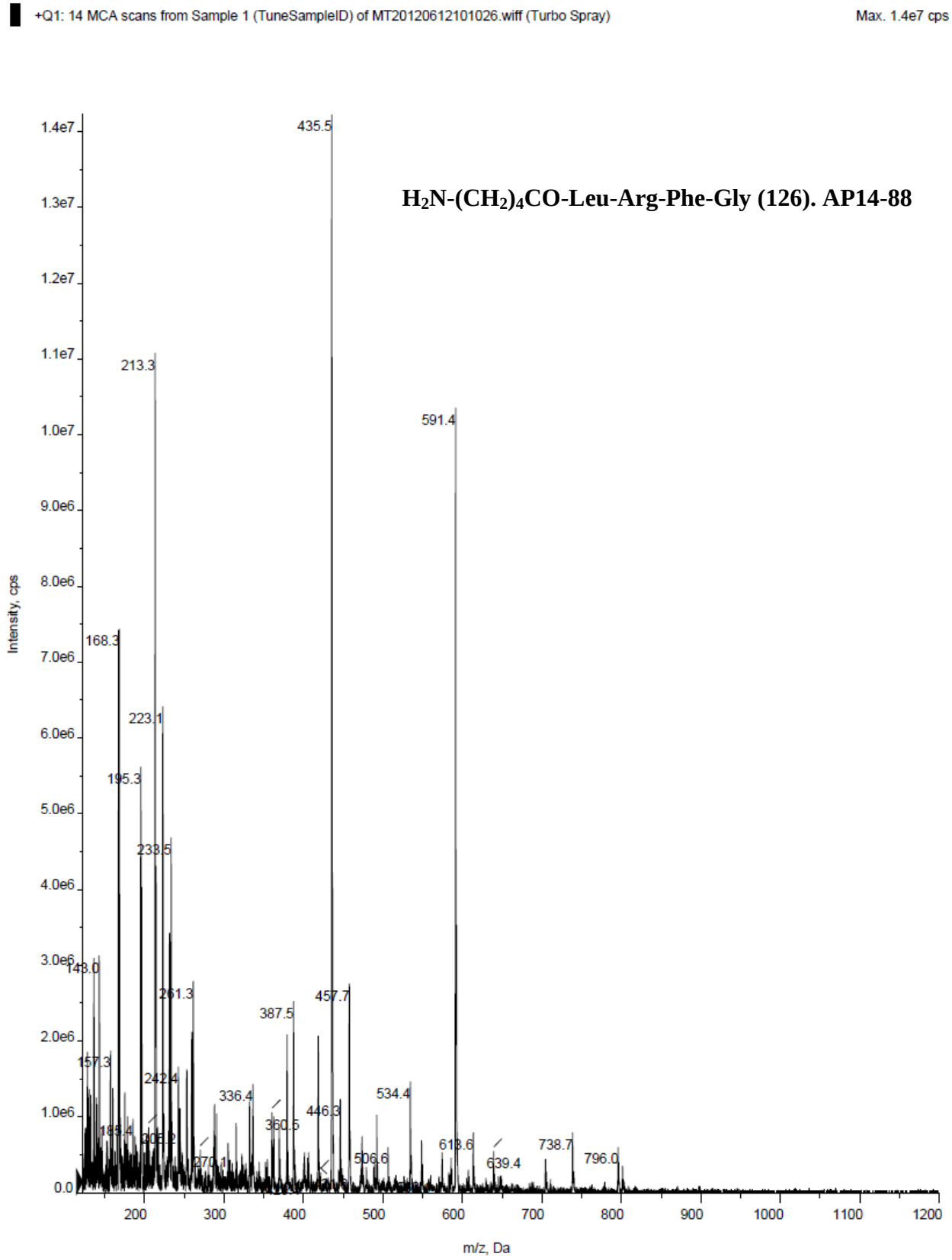
+Q1: 14 MCA scans from Sample 1 (TuneSampleID) of MT20120612101026.wiff (Turbo Spray)
Max. 1.4e7 cps
H2N-(CH2)4CO-Leu-Arg-Phe-Gly (126). AP14-88
Intensity, cps
m/z, Da
435.5
591.4
213.3
168.3
223.1
195.3
233.5
261.3
457.7
387.5
534.4
336.4
446.3
360.5
738.7
796.0
639.4
613.6
506.6
242.4
157.3
143.0
270.1

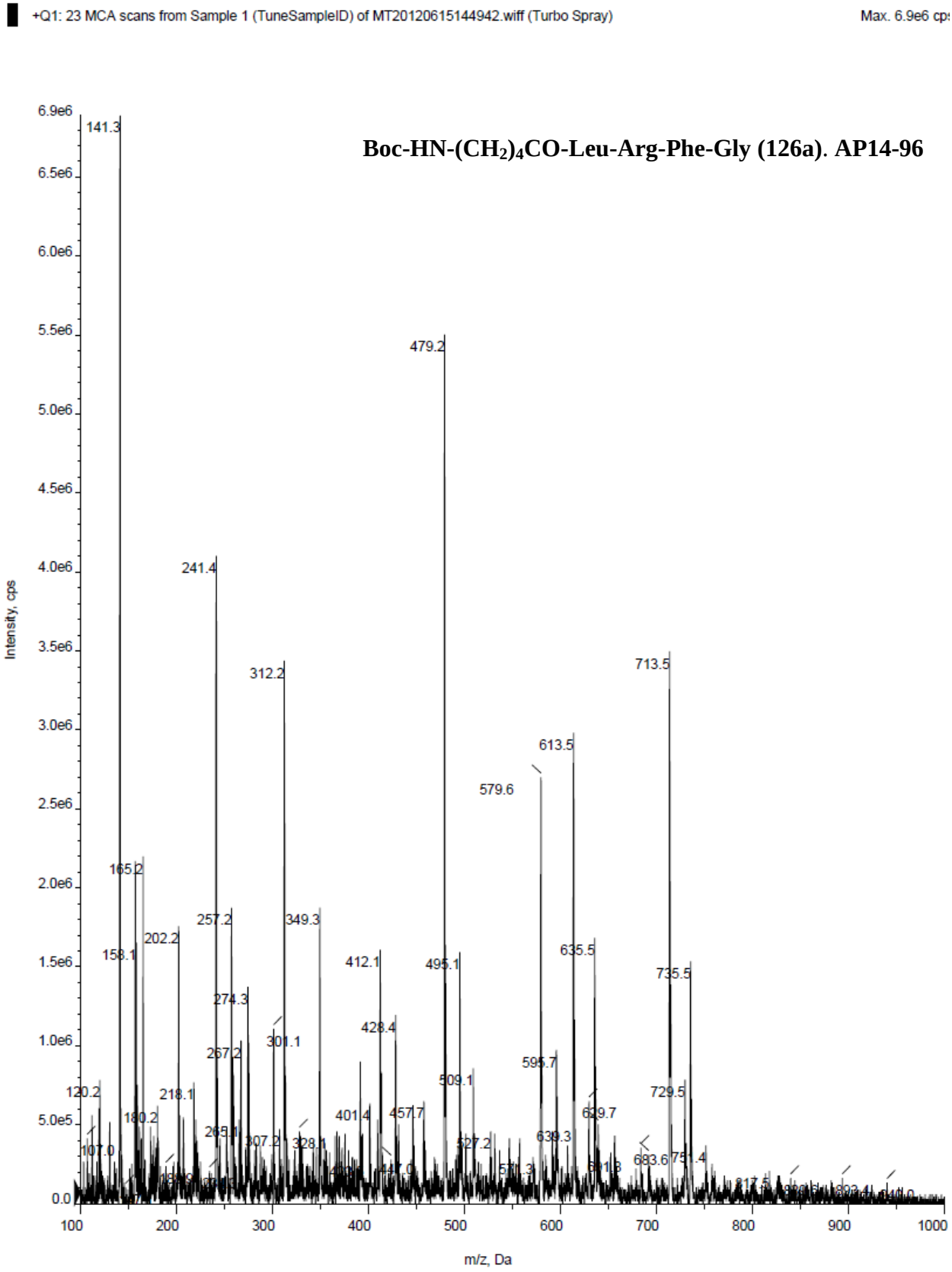
+Q1: 23 MCA scans from Sample 1 (TuneSampleID) of MT20120615144942.wiff (Turbo Spray)
Max. 6.9e6 cps
Boc-HN-(CH2)4CO-Leu-Arg-Phe-Gly (126a). AP14-96
Intensity, cps
m/z, Da
6.9e6
6.5e6
6.0e6
5.5e6
5.0e6
4.5e6
4.0e6
3.5e6
3.0e6
2.5e6
2.0e6
1.5e6
1.0e6
5.0e5
0.0
100
200
300
400
500
600
700
800
900
1000
141.3
479.2
241.4
312.2
713.5
613.5
579.6
165.2
257.2
349.3
202.2
158.1
412.1
495.1
635.5
735.5
274.3
428.4
301.1
267.2
595.7
509.1
120.2
218.1
729.5
180.2
401.4
457.7
629.7
265.1
307.2
328.1
527.2
639.3
107.0
683.6
751.4

+Q1: 19 MCA scans from Sample 1 (TuneSampleID) of MT20120617130602.wiff (Turbo Spray) Max. 3.2e6 cps

Boc-HN-$(CH_2)_4$CO-Leu-Arg-Phe-Gly-NHCH_2-Fc (127). AP14-97

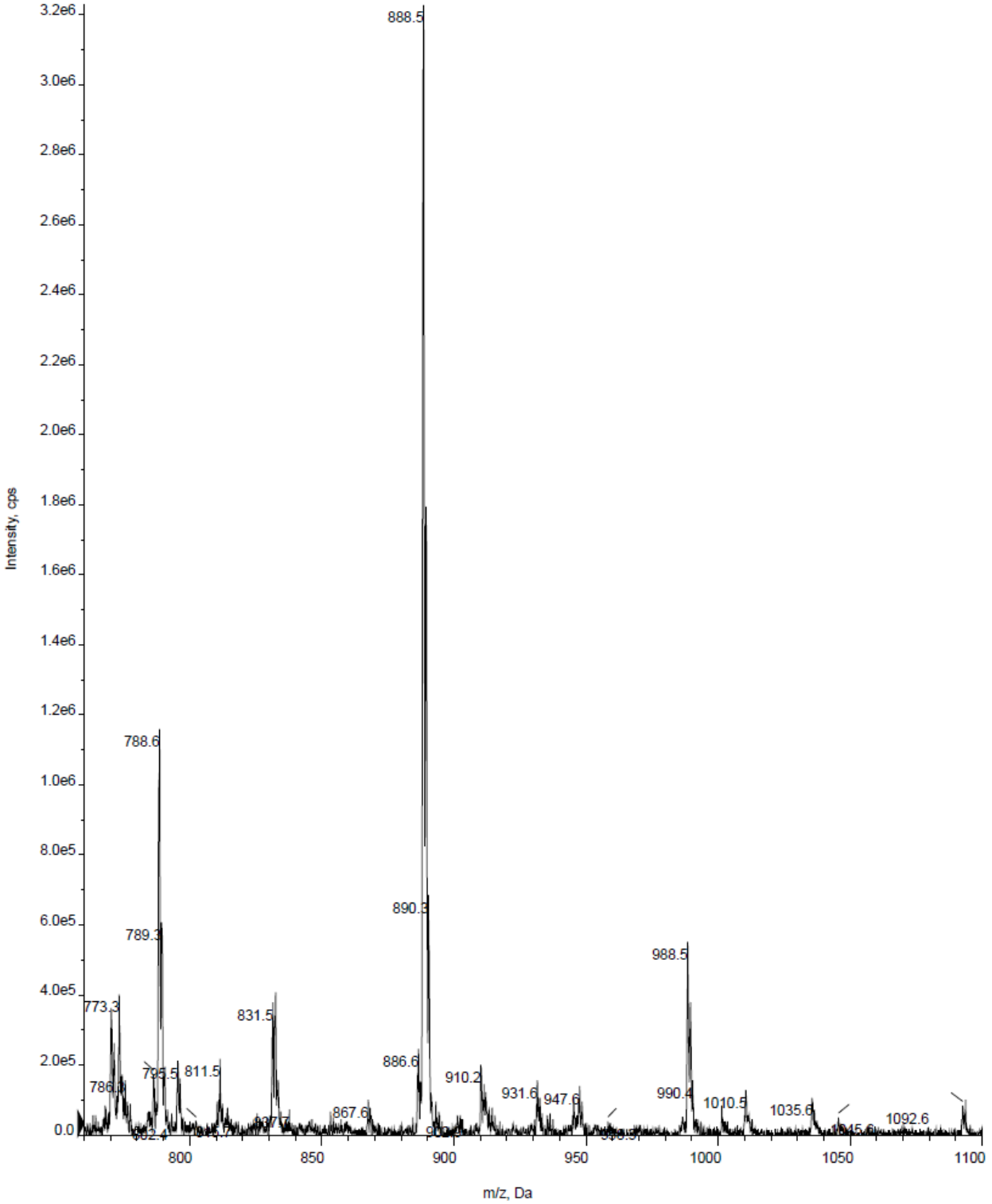

+Q1: 32 MCA scans from Sample 1 (TypeSampleID) of MT20120623193701.wiff (Turbo Spray)

H_2N-$(CH_2)_4$CO-Leu-Arg-Phe-Gly-$NHCH_2$-Fc (120). AP14-103

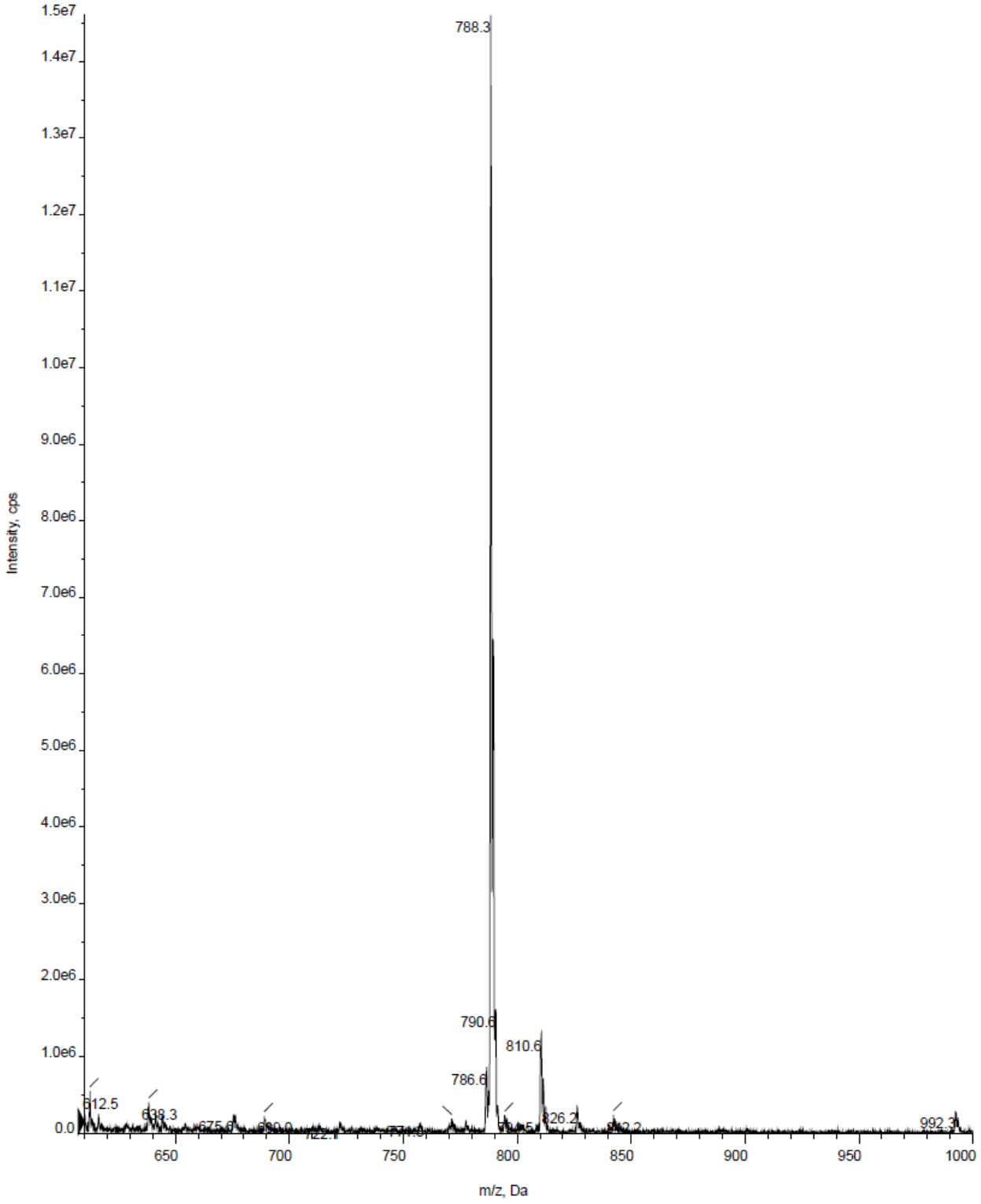

AP17-64-SOLID

H_2N-$(CH_2)_4$CO-Leu-Arg-Phe-Gly-$NHCH_2$-Fc (AP17-64)

120

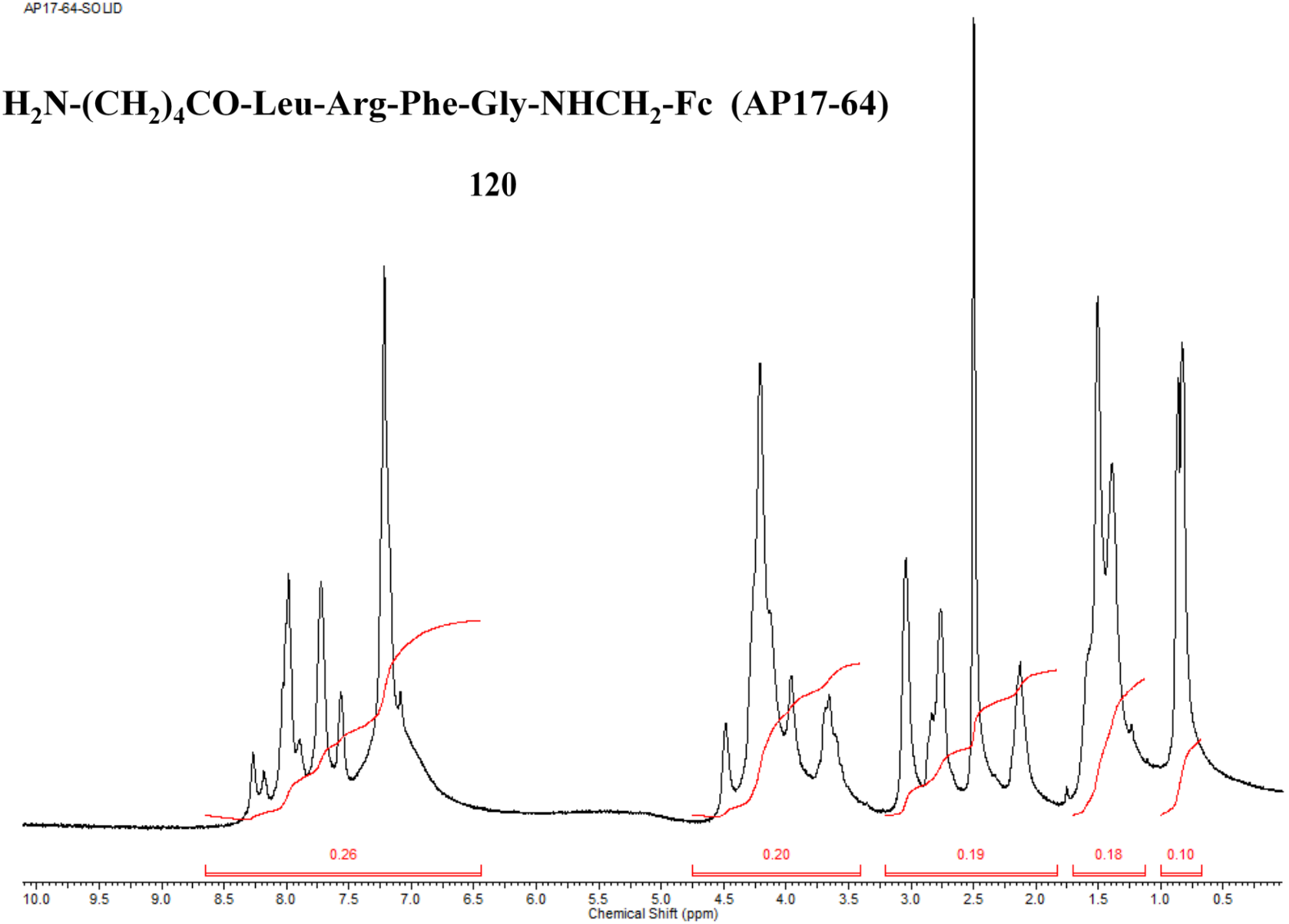

AP17-64-SOLID-13C

H_2N-$(CH_2)_4$CO-Leu-Arg-Phe-Gly-$NHCH_2$-Fc (AP17-64)

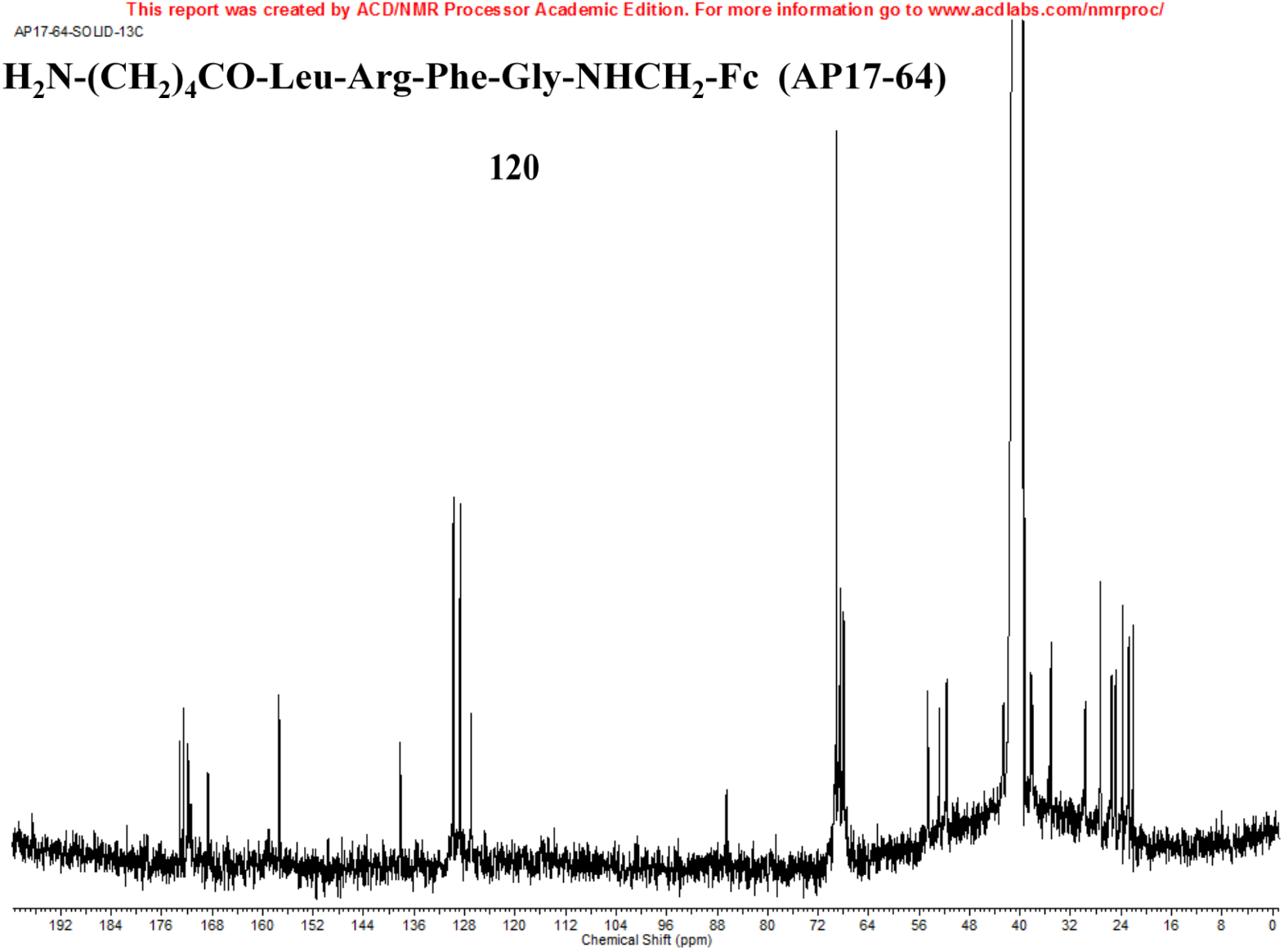

+Q1: 27 MCA scans from Sample 1 (TuneSampleID) of MT20130325111806.wiff (Turbo Spray) Max. 1.0e7 cps.

H_2N-$(CH_2)_4$CO-Leu-Asn-Phe-Gly (129). AP17-46

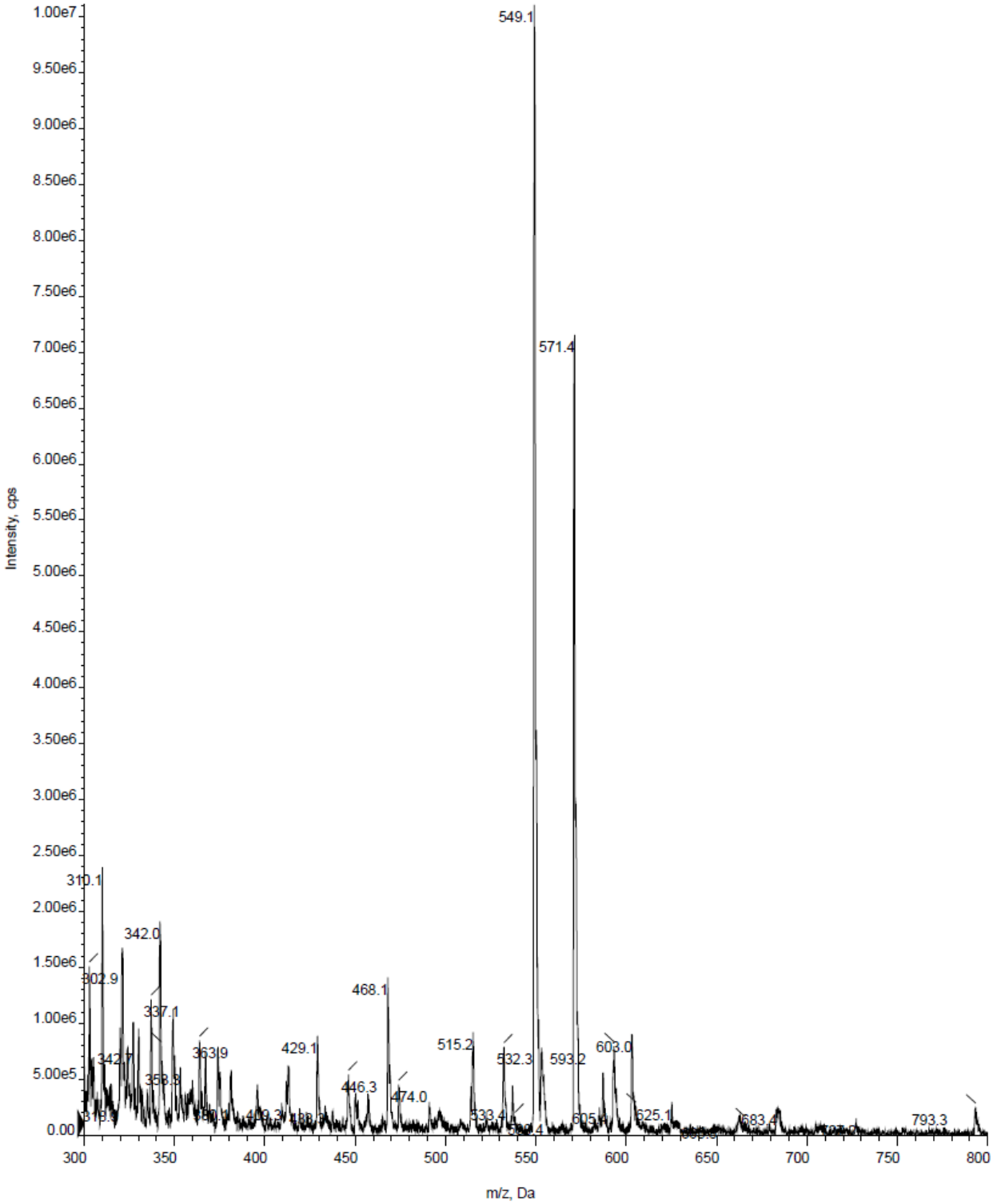

AP17-46-SOLID

H_2N-$(CH_2)_4$CO-Leu-Asn-Phe-Gly (AP17-46)

129

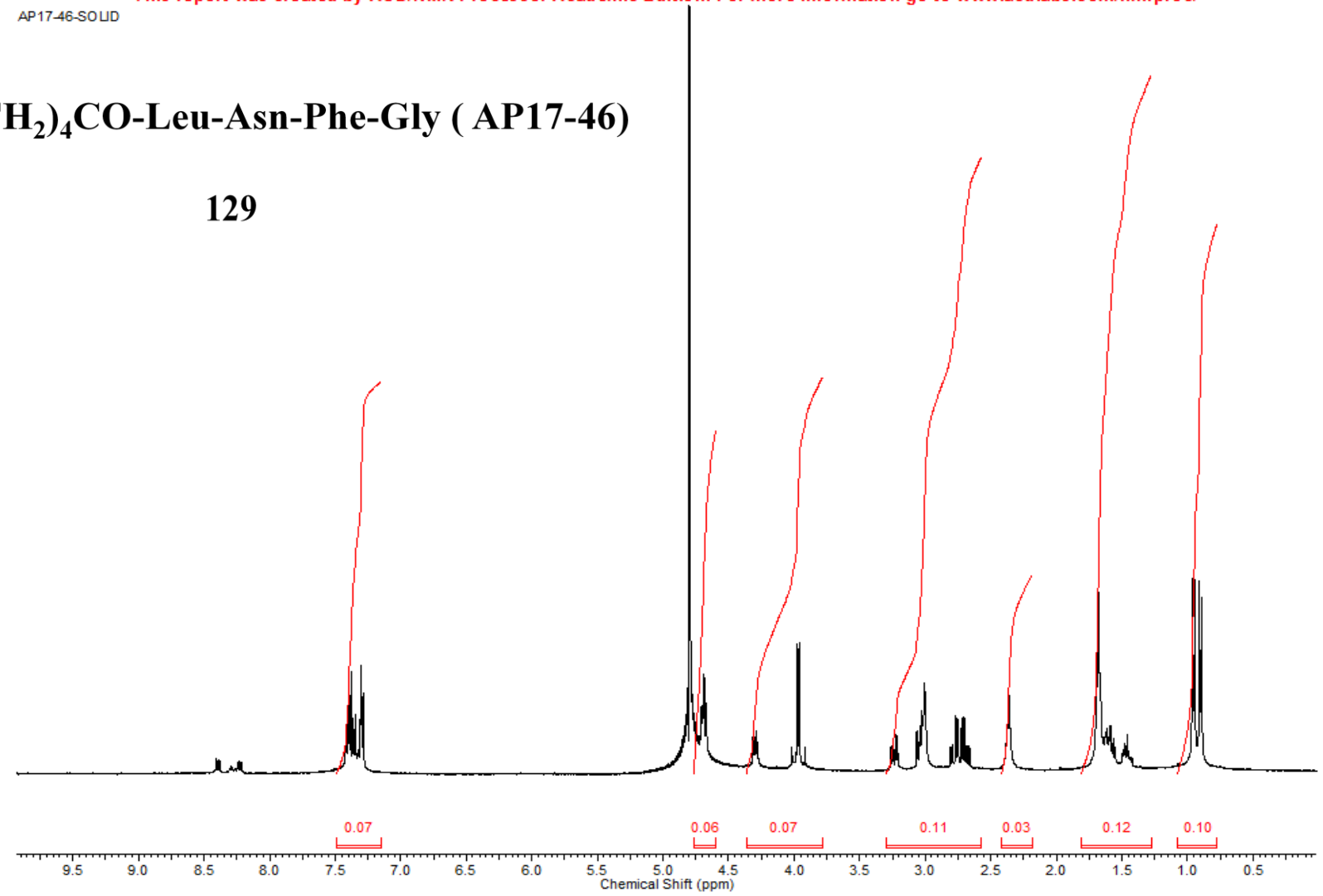

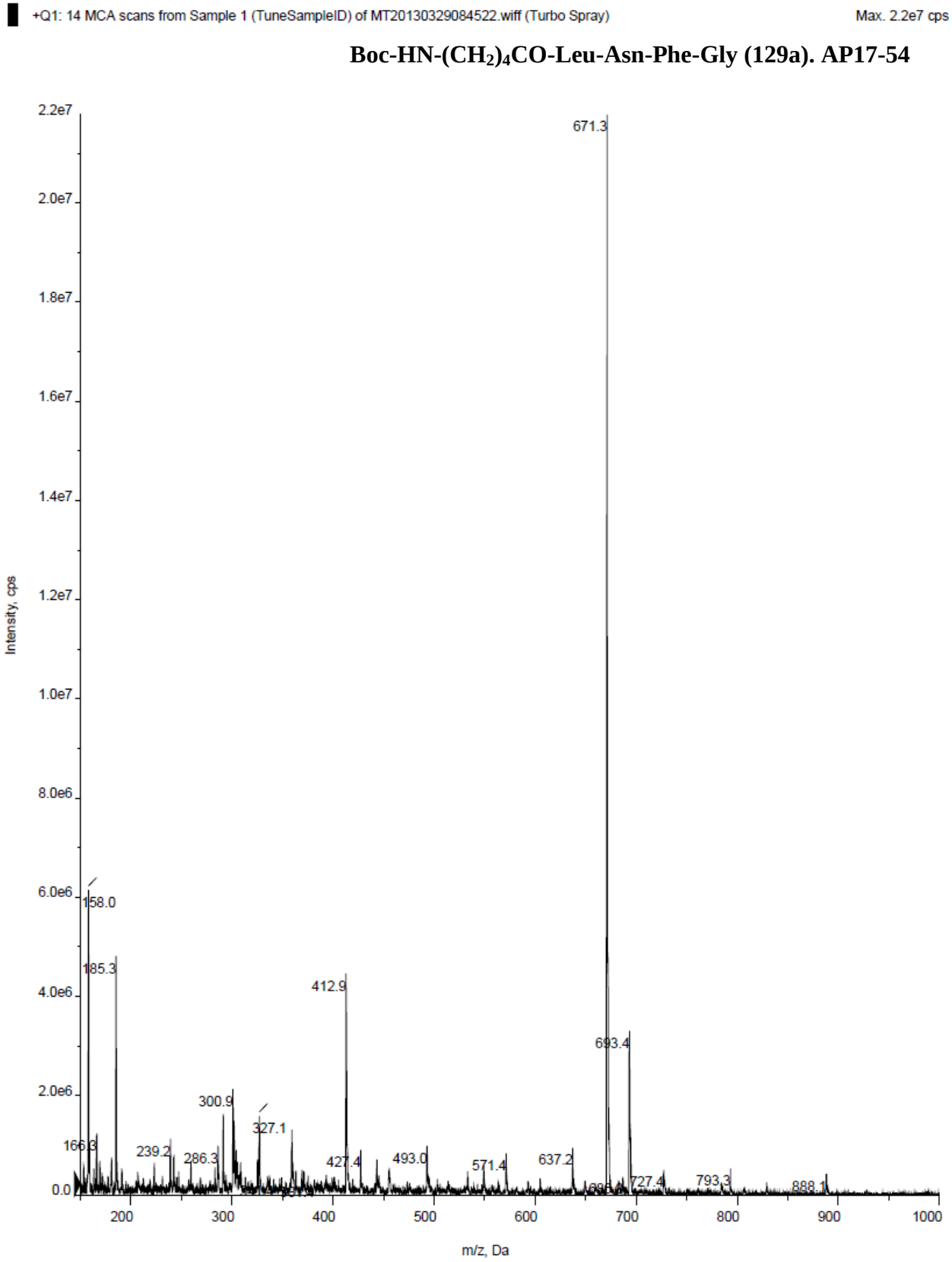
+Q1: 14 MCA scans from Sample 1 (TuneSampleID) of MT20130329084522.wiff (Turbo Spray)
Max. 2.2e7 cps
Boc-HN-(CH2)4CO-Leu-Asn-Phe-Gly (129a). AP17-54
Intensity, cps
m/z, Da
671.3
412.9
693.4
158.0
185.3
300.9
327.1
166.3
239.2
286.3
427.4
493.0
571.4
637.2
727.4
793.3
888.1

+Q1: 14 MCA scans from Sample 1 (TuneSampleID) of MT20130402085108.wiff (Turbo Spray) Max. 1.5e7 cps.

Boc-HN-$(CH_2)_4$CO-Leu-Asn-Phe-Gly-NHCH$_2$-Fc (130). AP17-65

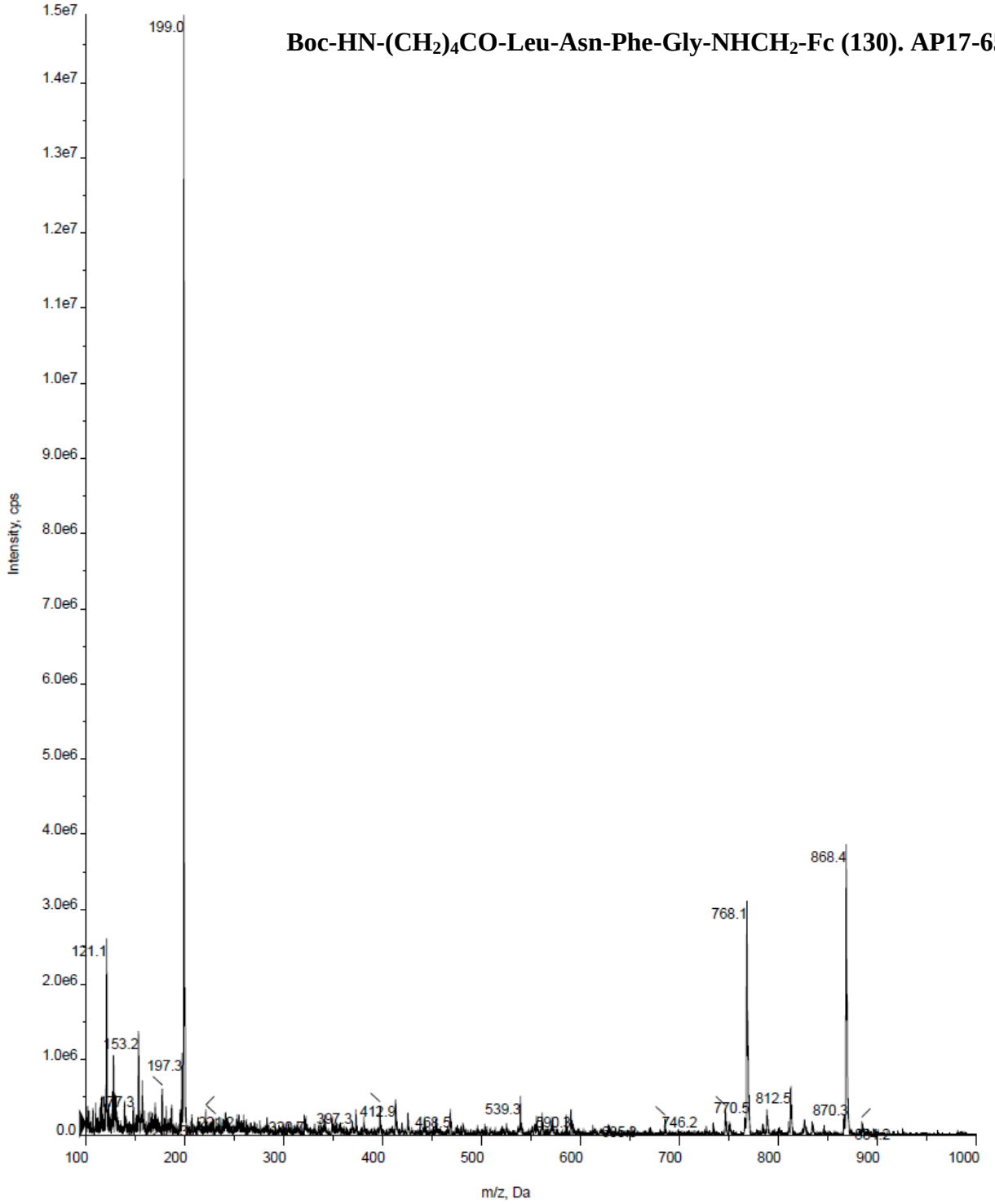

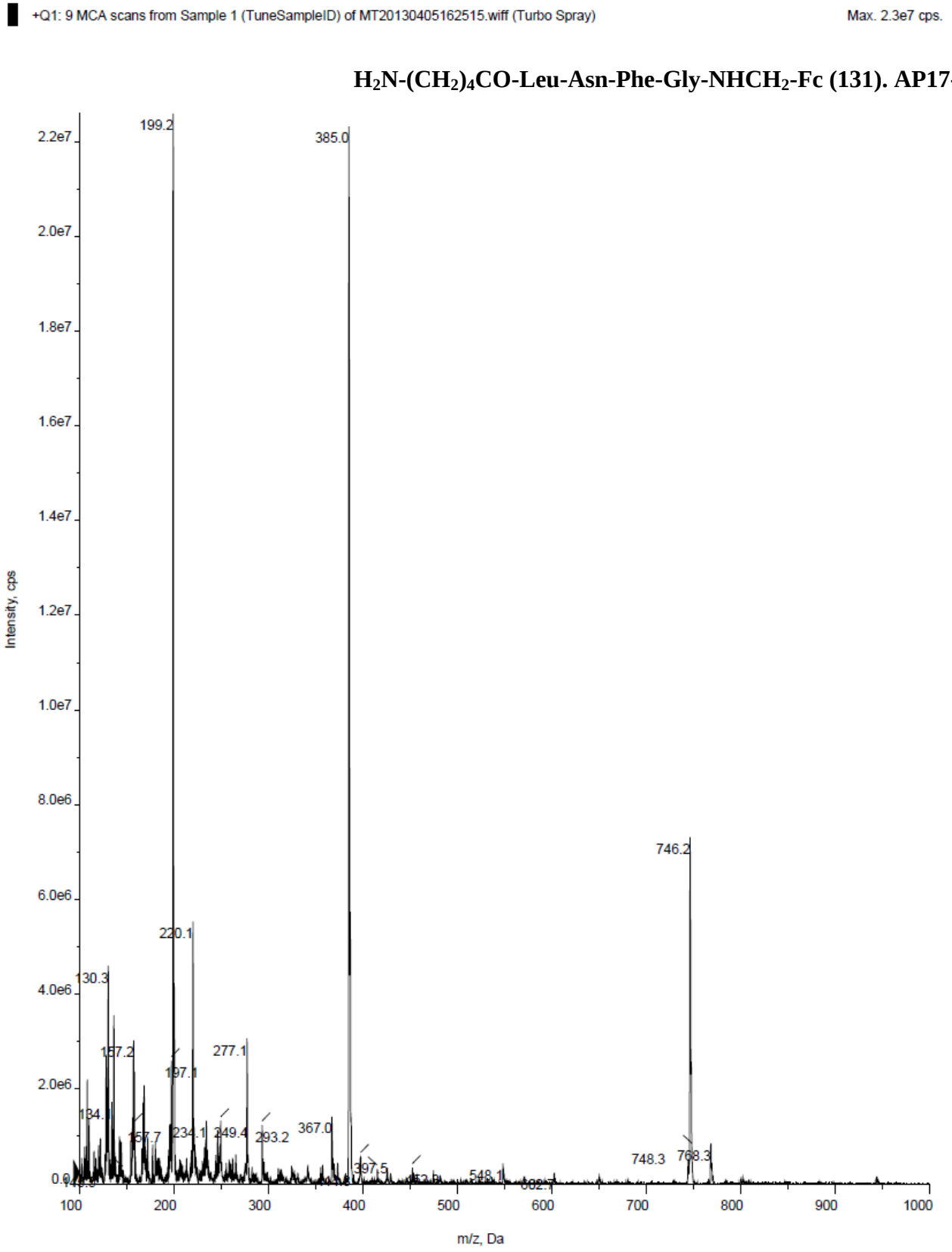
+Q1: 9 MCA scans from Sample 1 (TuneSampleID) of MT20130405162515.wiff (Turbo Spray)
Max. 2.3e7 cps.
H2N-(CH2)4CO-Leu-Asn-Phe-Gly-NHCH2-Fc (131). AP17-72
Intensity, cps
m/z, Da
199.2
385.0
746.2
220.1
130.3
157.2
277.1
197.1
184.1
157.7
234.1
249.4
293.2
367.0
397.5
548.1
748.3
768.3

AP17-72-SOLID-1H

H_2N-$(CH_2)_4$CO-Leu-Asn-Phe-Gly-$NHCH_2$-Fc (AP17-72)

131

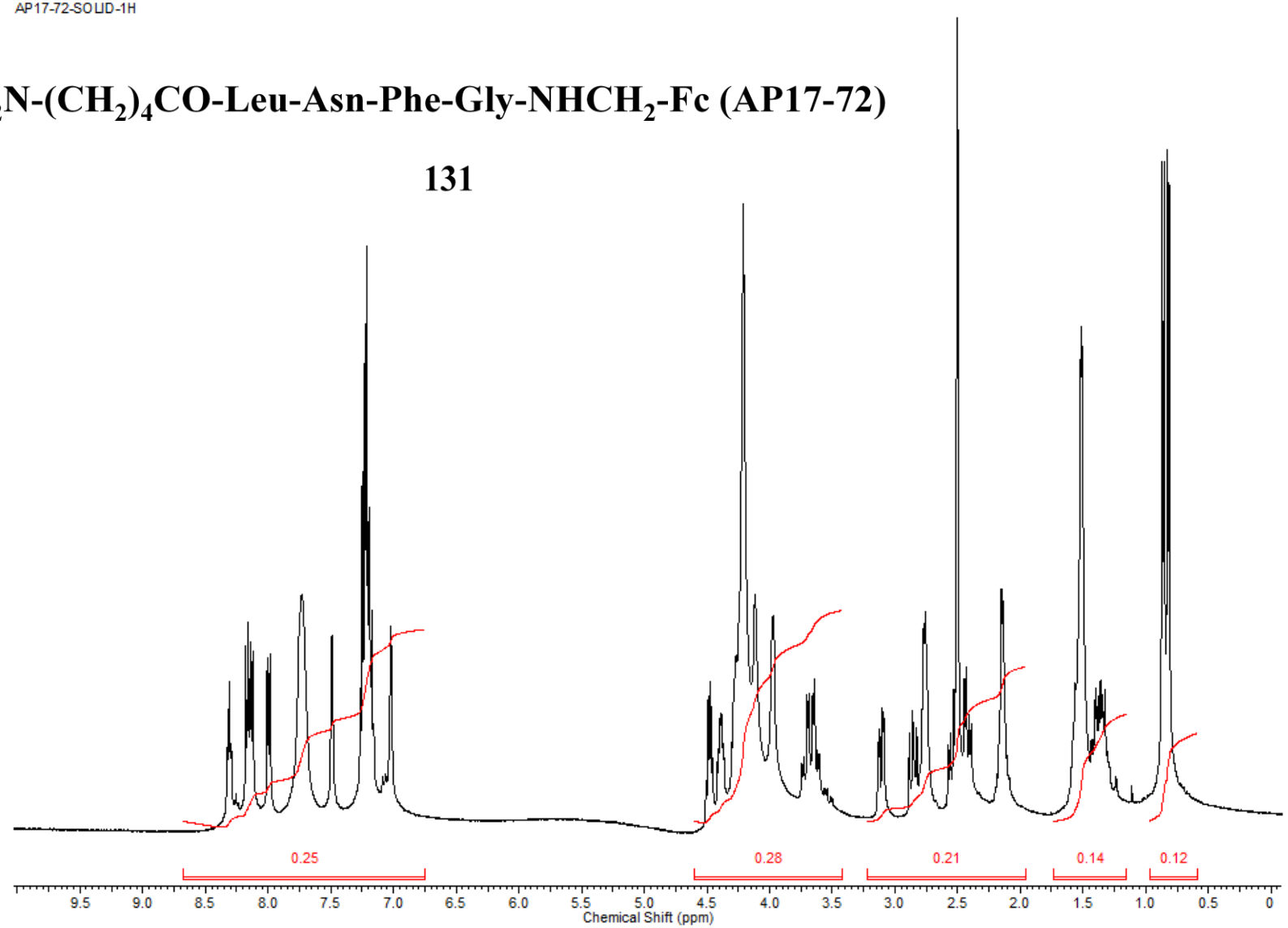

AP17-72-13C

H_2N-$(CH_2)_4$CO-Leu-Asn-Phe-Gly-$NHCH_2$-Fc (AP17-72)

131

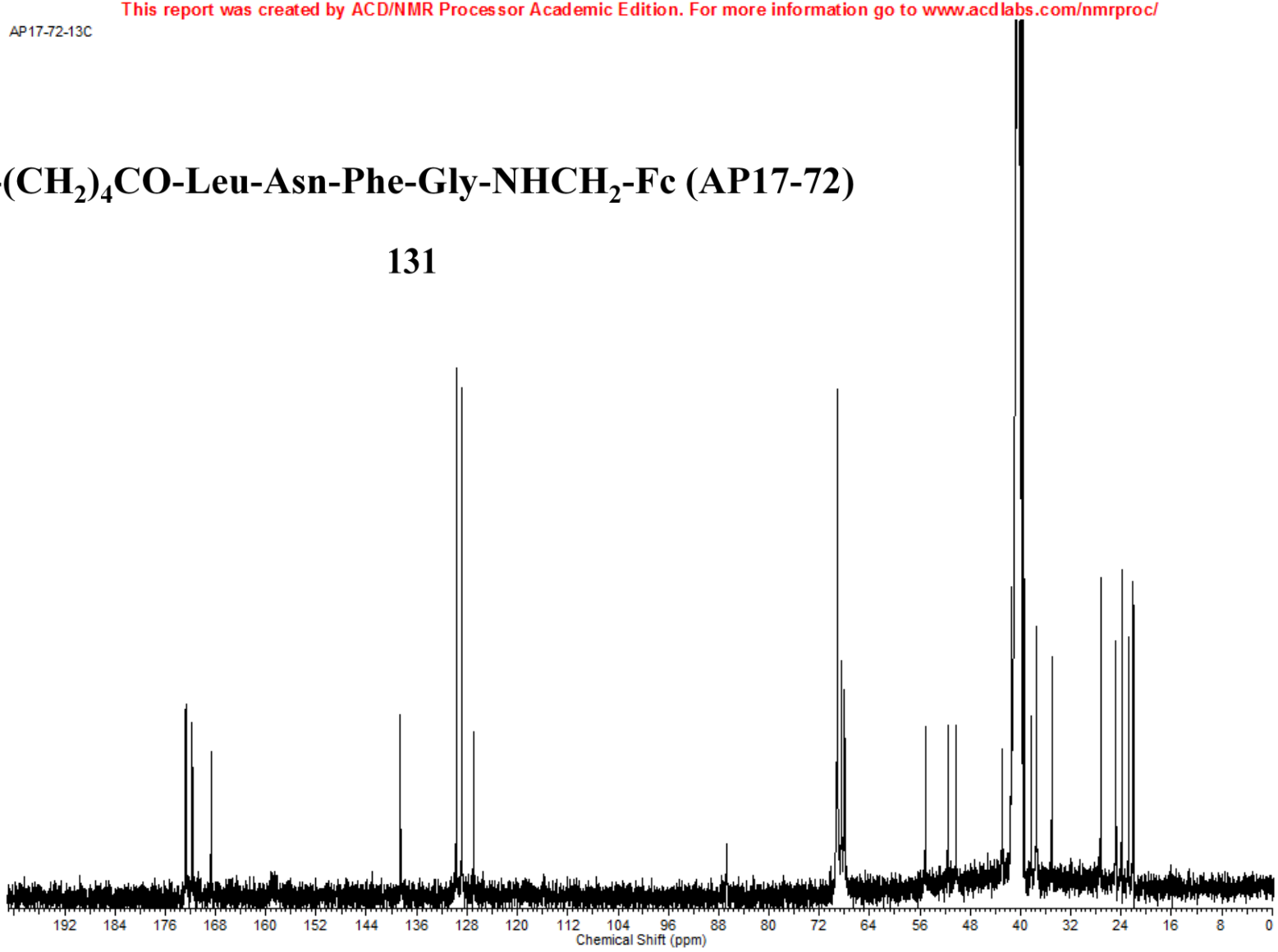

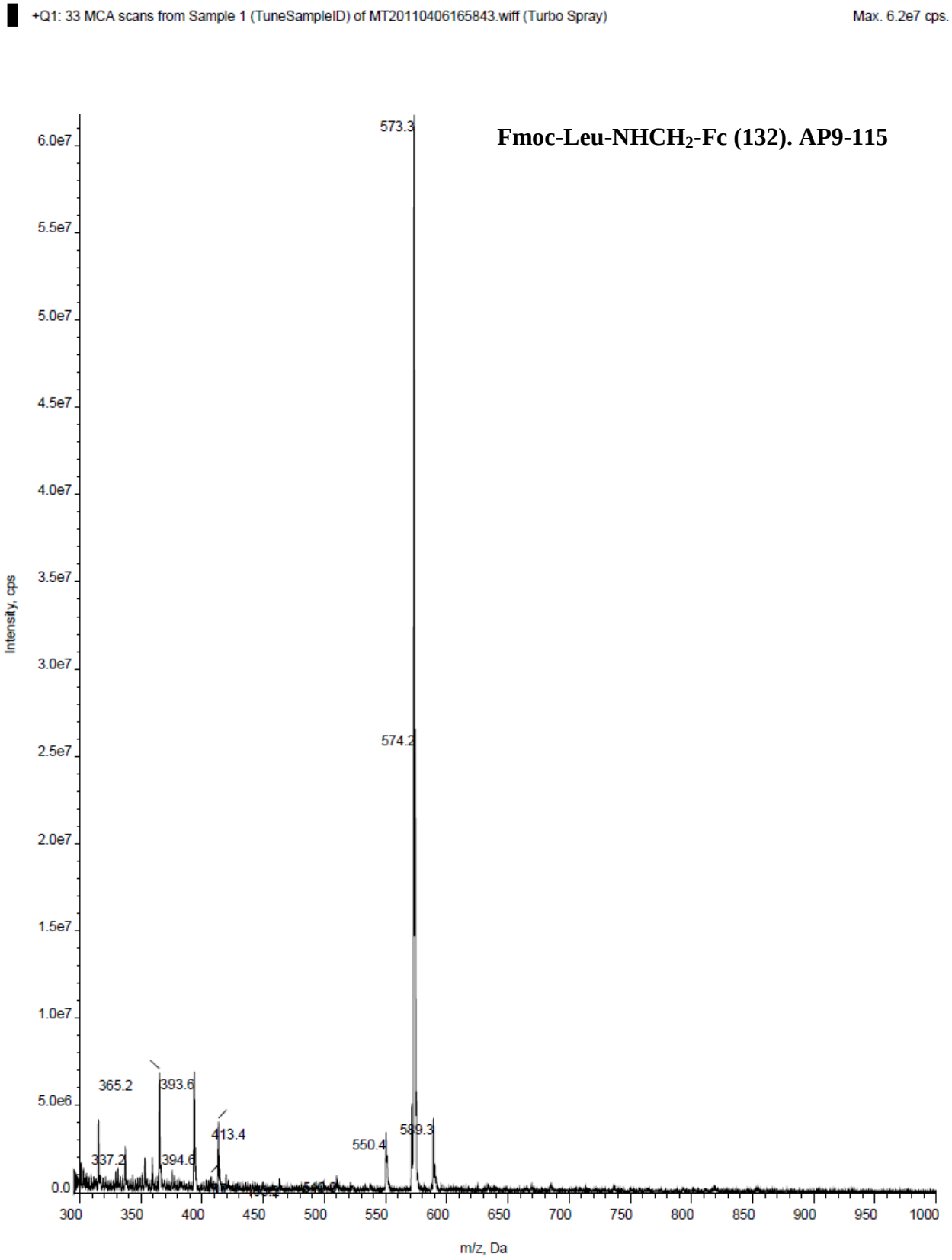
+Q1: 33 MCA scans from Sample 1 (TuneSampleID) of MT20110406165843.wiff (Turbo Spray)
Max. 6.2e7 cps.
Fmoc-Leu-NHCH2-Fc (132). AP9-115
Intensity, cps
m/z, Da
573.3
574.2
365.2
393.6
413.4
337.2
394.6
550.4
589.3

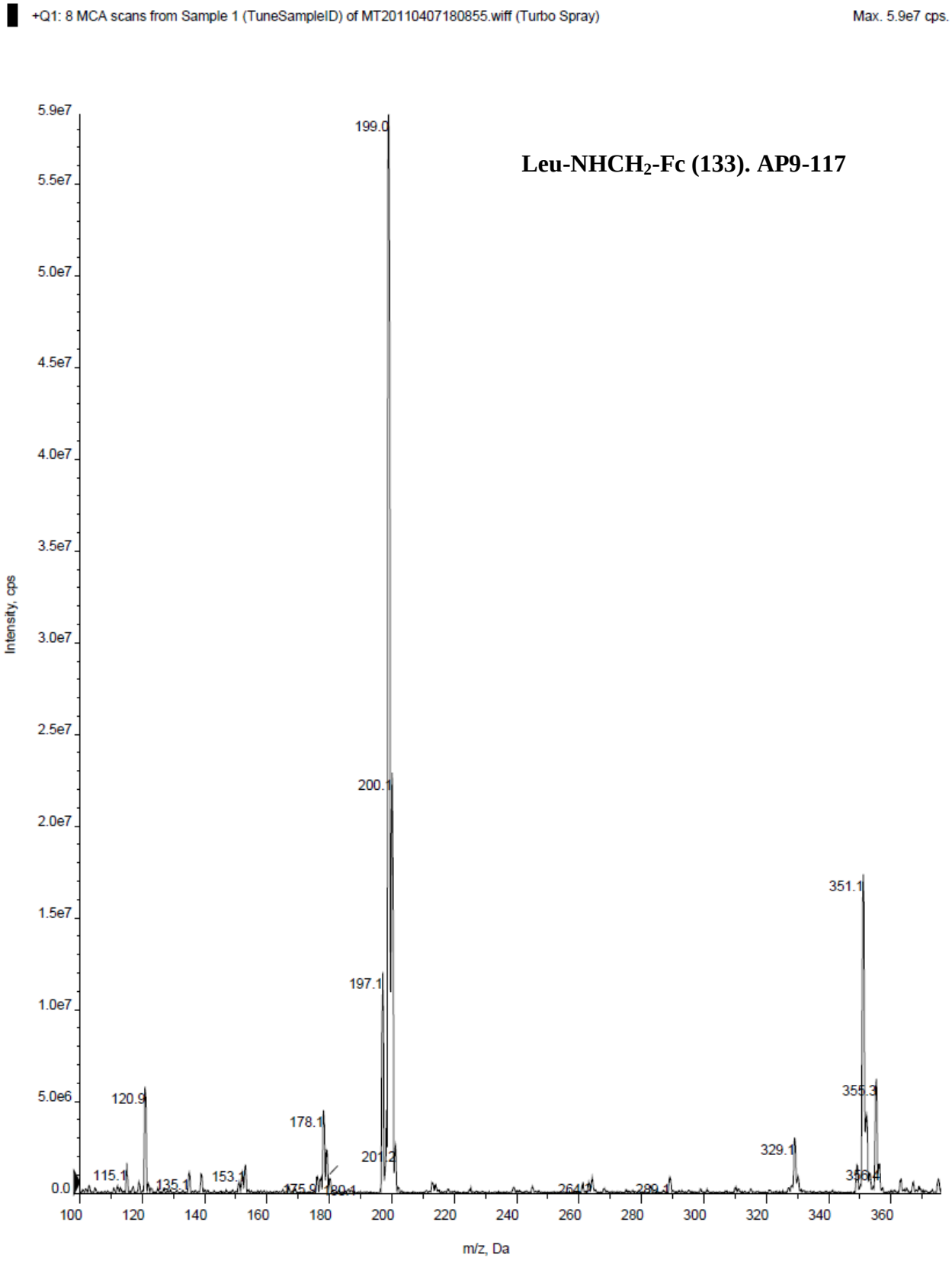
+Q1: 8 MCA scans from Sample 1 (TuneSampleID) of MT20110407180855.wiff (Turbo Spray)
Max. 5.9e7 cps.
Leu-NHCH2-Fc (133). AP9-117
Intensity, cps
m/z, Da
199.0
200.1
197.1
351.1
355.3
120.9
178.1
201.2
329.1
115.1
135.1
153.1
5.9e7
5.5e7
5.0e7
4.5e7
4.0e7
3.5e7
3.0e7
2.5e7
2.0e7
1.5e7
1.0e7
5.0e6
0.0
100
120
140
160
180
200
220
240
260
280
300
320
340
360

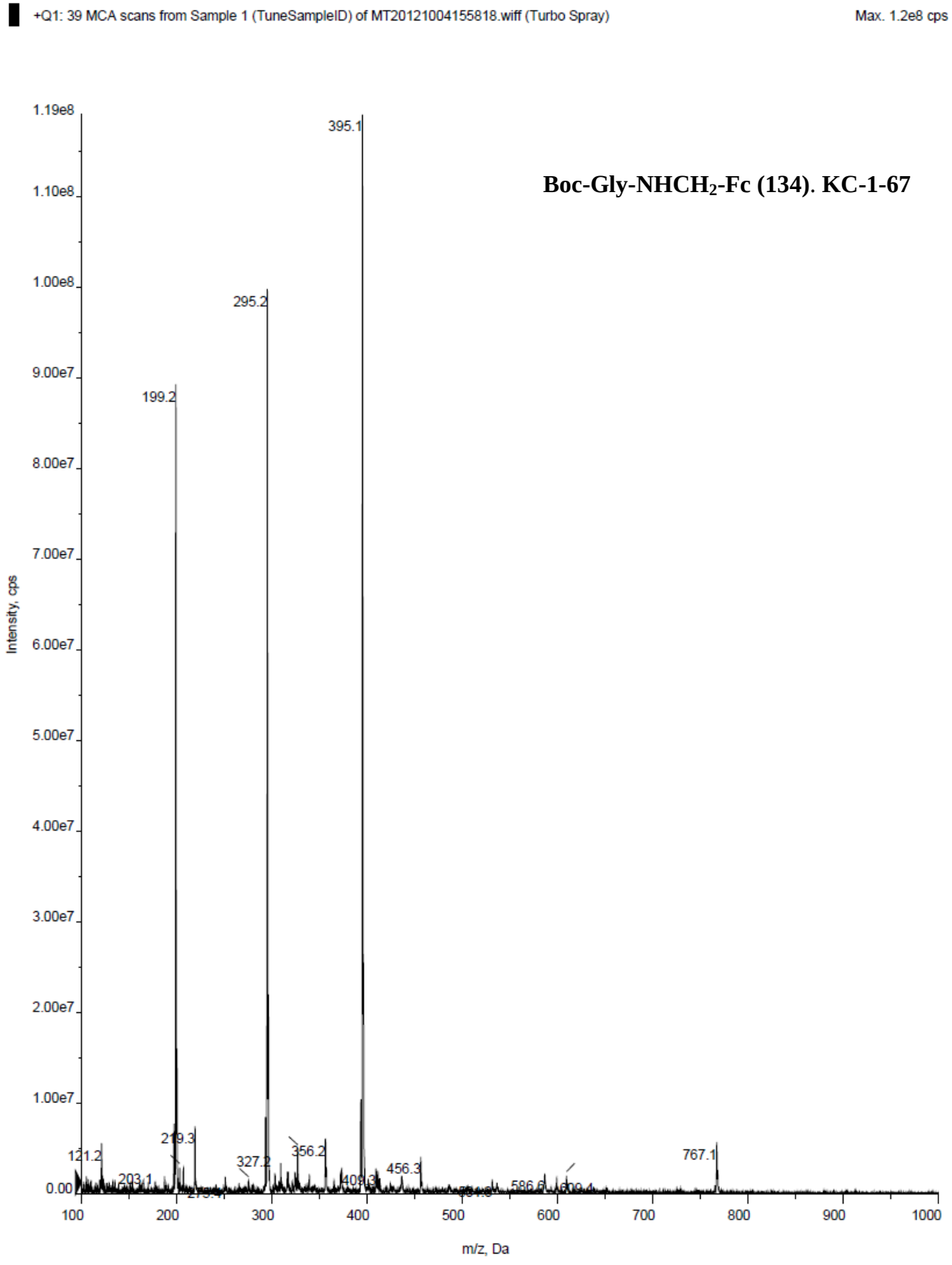
+Q1: 39 MCA scans from Sample 1 (TuneSampleID) of MT20121004155818.wiff (Turbo Spray)
Max. 1.2e8 cps
Boc-Gly-NHCH2-Fc (134). KC-1-67
Intensity, cps
m/z, Da
395.1
295.2
199.2
219.3
121.2
203.1
327.2
356.2
409.3
456.3
586.6
767.1

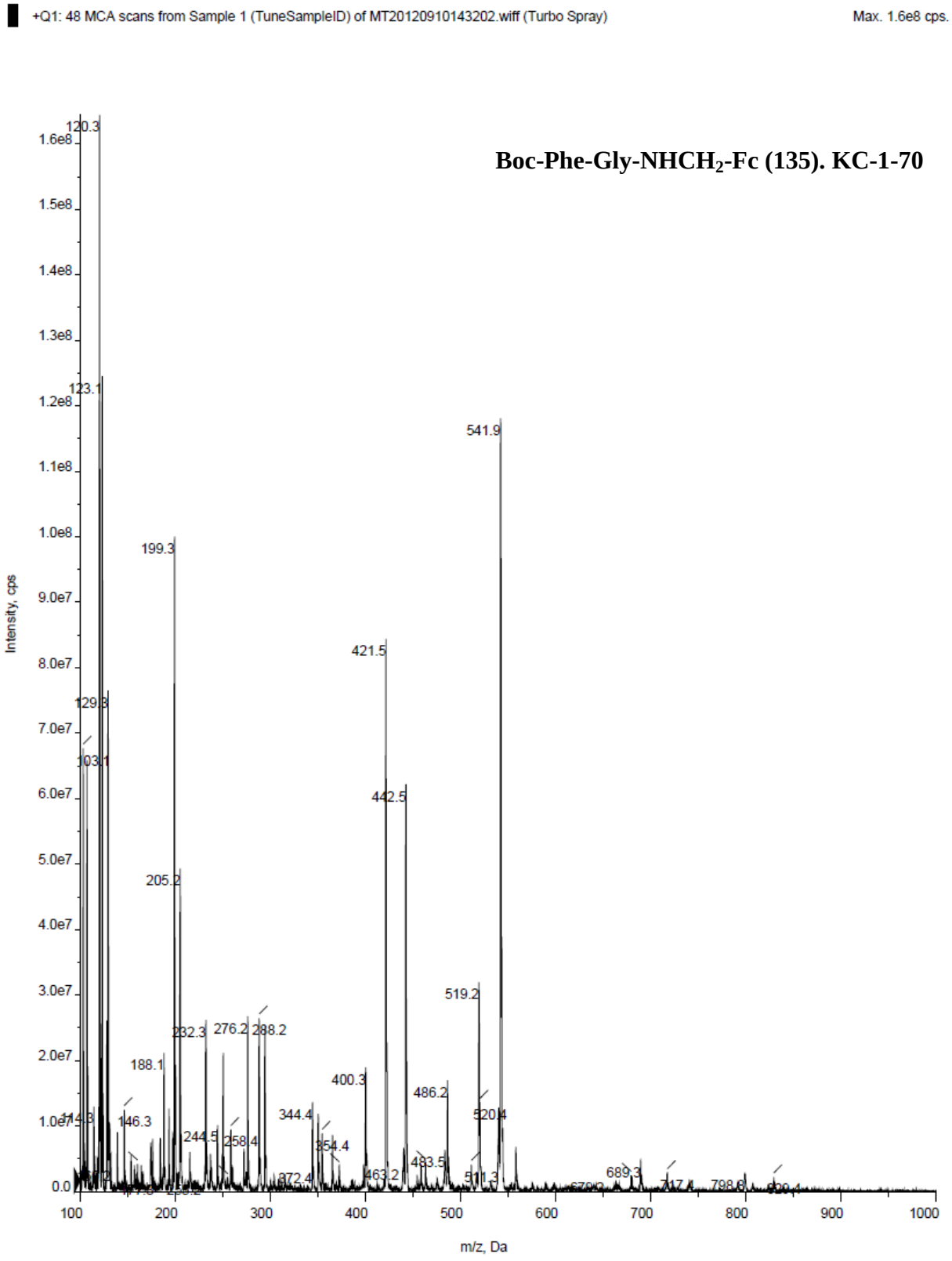
+Q1: 48 MCA scans from Sample 1 (TuneSampleID) of MT20120910143202.wiff (Turbo Spray)
Max. 1.6e8 cps.
Boc-Phe-Gly-NHCH2-Fc (135). KC-1-70
Intensity, cps
m/z, Da
120.3
123.1
541.9
199.3
421.5
442.5
205.2
519.2
232.3
276.2
288.2
188.1
400.3
486.2
344.4
354.4
146.3
244.5
258.4
463.2
483.5
689.3
717.4
798.6

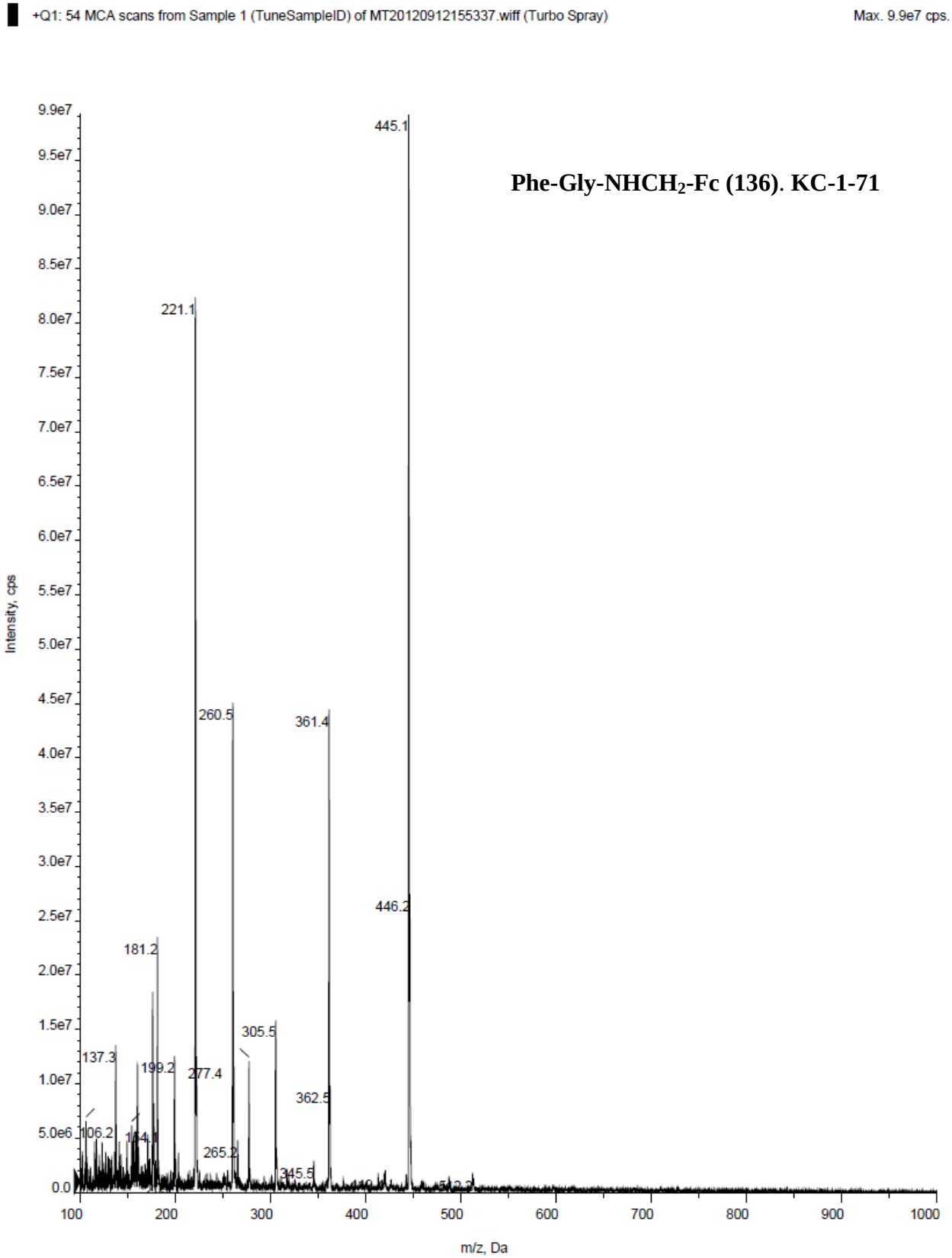
+Q1: 54 MCA scans from Sample 1 (TuneSampleID) of MT20120912155337.wiff (Turbo Spray)
Max. 9.9e7 cps.
Phe-Gly-NHCH2-Fc (136). KC-1-71
Intensity, cps
m/z, Da
445.1
221.1
260.5
361.4
446.2
181.2
305.5
137.3
199.2
277.4
362.5
106.2
265.2
345.5